ATOMIC AND PLASMA–MATERIAL INTERACTION DATA FOR FUSION

VOLUME 7 PART A

INTERNATIONAL
ATOMIC ENERGY AGENCY
VIENNA, 1998

The following States are Members of the International Atomic Energy Agency:

AFGHANISTAN
ALBANIA
ALGERIA
ARGENTINA
ARMENIA
AUSTRALIA
AUSTRIA
BANGLADESH
BELARUS
BELGIUM
BOLIVIA
BOSNIA AND HERZEGOVINA
BRAZIL
BULGARIA
BURKINA FASO
CAMBODIA
CAMEROON
CANADA
CHILE
CHINA
COLOMBIA
COSTA RICA
COTE D'IVOIRE
CROATIA
CUBA
CYPRUS
CZECH REPUBLIC
DEMOCRATIC REPUBLIC OF THE CONGO
DENMARK
DOMINICAN REPUBLIC
ECUADOR
EGYPT
EL SALVADOR
ESTONIA
ETHIOPIA
FINLAND
FRANCE
GABON
GEORGIA
GERMANY
GHANA
GREECE
GUATEMALA
HAITI
HOLY SEE
HUNGARY
ICELAND
INDIA
INDONESIA
IRAN, ISLAMIC REPUBLIC OF
IRAQ
IRELAND
ISRAEL
ITALY
JAMAICA
JAPAN
JORDAN
KAZAKHSTAN
KENYA
KOREA, REPUBLIC OF
KUWAIT
LATVIA
LEBANON
LIBERIA
LIBYAN ARAB JAMAHIRIYA
LIECHTENSTEIN
LITHUANIA
LUXEMBOURG
MADAGASCAR
MALAYSIA
MALI
MALTA
MARSHALL ISLANDS
MAURITIUS
MEXICO
MONACO
MONGOLIA
MOROCCO
MYANMAR
NAMIBIA
NETHERLANDS
NEW ZEALAND
NICARAGUA
NIGER
NIGERIA
NORWAY
PAKISTAN
PANAMA
PARAGUAY
PERU
PHILIPPINES
POLAND
PORTUGAL
QATAR
REPUBLIC OF MOLDOVA
ROMANIA
RUSSIAN FEDERATION
SAUDI ARABIA
SENEGAL
SIERRA LEONE
SINGAPORE
SLOVAKIA
SLOVENIA
SOUTH AFRICA
SPAIN
SRI LANKA
SUDAN
SWEDEN
SWITZERLAND
SYRIAN ARAB REPUBLIC
THAILAND
THE FORMER YUGOSLAV REPUBLIC OF MACEDONIA
TUNISIA
TURKEY
UGANDA
UKRAINE
UNITED ARAB EMIRATES
UNITED KINGDOM OF GREAT BRITAIN AND NORTHERN IRELAND
UNITED REPUBLIC OF TANZANIA
UNITED STATES OF AMERICA
URUGUAY
UZBEKISTAN
VENEZUELA
VIET NAM
YEMEN
YUGOSLAVIA
ZAMBIA
ZIMBABWE

The Agency's Statute was approved on 23 October 1956 by the Conference on the Statute of the IAEA held at United Nations Headquarters, New York; it entered into force on 29 July 1957. The Headquarters of the Agency are situated in Vienna. Its principal objective is "to accelerate and enlarge the contribution of atomic energy to peace, health and prosperity throughout the world".

Printed by the IAEA in Austria
December 1998

ATOMIC AND PLASMA–MATERIAL INTERACTION DATA FOR FUSION

VOLUME 7

PART A

INTERNATIONAL ATOMIC ENERGY AGENCY, VIENNA, 1998

The volumes of ATOMIC AND PLASMA–MATERIAL INTERACTION DATA FOR FUSION are published by the International Atomic Energy Agency normally once a year.

For these volumes, papers, letters and reviews are accepted which deal with the following topics:

- Elementary collision processes in fusion plasmas involving photons, electrons, ions, atoms and molecules;
- Collision processes of plasma particles with surfaces of fusion relevant materials;
- Plasma–material interaction phenomena, including the thermophysical response of materials.

Each submitted contribution should contain fusion relevant data and information in either of the above areas. Original contributions should provide new data, using well cstablishcd methods. Review articles should give a critical analysis or evaluation of a wider range of data. They are normally prepared on the invitation by the Editor or on prior mutual consent. Each submitted contribution is assessed by two independent referees.

Every manuscript submitted must be accompanied by a *disclaimer* stating that the paper has not been published and is not being considered for publication elsewhere. If no copyright is claimed by the authors, the IAEA automatically owns the copyright of the paper.

Guidelines for the preparation of manuscripts are given on the inside back cover. Manuscripts and correspondence should be addressed to: The Editor, ATOMIC AND PLASMA–MATERIAL INTERACTION DATA FOR FUSION, International Atomic Energy Agency, Wagramer Strasse 5, P.O. Box 100, A-1400 Vienna, Austria.

Publisher: International Atomic Energy Agency, Wagramer Strasse 5, P.O. Box 100, A-1400 Vienna, Austria

Editor: R.K. Janev, Atomic and Molecular Data Unit, Division of Physical and Chemical Sciences

---

ATOMIC AND PLASMA–MATERIAL INTERACTION DATA FOR FUSION, VOLUME 7
IAEA, VIENNA, 1998
STI/PUB/023/APID/07/A

EDITORIAL NOTE

The present volume of Atomic and Plasma-Material Interaction Data for Fusion is devoted to a critical review of the chemical erosion behaviour of fusion plasma-facing materials, in particular carbon, beryllium and tungsten. The present volume is intended to provide fusion reactor designers a detailed survey and parameterization of existing, critically assessed data for the chemical erosion of plasma-facing materials by particle impact. The survey and data compilation is presented for a variety of materials containing the elements C, Be and W (including dopants in carbon materials) and impacting plasma species. The dependencies of chemical erosion yields on the material temperature, incident projectile energy, and flux are considered. The main data compilation is presented as separate data sheets indicating the material, impacting plasma species, experimental conditions, and parameterizations in terms of analytic functions.

This volume of Atomic and Plasma-Material Interaction Data for Fusion is the result of a five year Co-ordinated Research Programme on "Plasma-Interaction Induced Erosion of Fusion Reactor Materials" in the period 1992-1997. A companion volume is in preparation, which will provide a critical review and data compilation for physical sputtering and radiation-enhanced sublimation induced by fusion plasma particle impact.

The International Atomic Energy Agency expresses its appreciation to the contributors to this volume for their dedicated effort and co-operation.

Vienna, April 1998

Particle Induced Erosion of Be, C and W in Fusion Plasmas.

Part A: Chemical Erosion of Carbon-Based Materials.

A. A. Haasz[a], J. A. Stephens[b], E. Vietzke[c], W. Eckstein[d], J. W. Davis[a] and Y. Hirooka[e]

[a] *Fusion Research Group, University of Toronto, Institute for Aerospace Studies, 4925 Dufferin Street, Toronto, Ontario, Canada, M3H 5T6*

[b] *Division of Physical and Chemical Sciences, Nuclear Data Section, International Atomic Energy Agency, P.O. Box 100, Wagramer Strasse 5, A-1400 Vienna, Austria*

[c] *Institut für Plasmaphysik, Forschungszentrum Jülich (KFA), EURATOM Association, D-52425 Jülich, Germany*

[d] *Max-Planck-Institut für Plasmaphysik, EURATOM Association, D-85748 Garching bei München, Germany*

[e] *Fusion Energy Research Program, Department of Applied Mechanics and Engineering Sciences, University of California, San Diego, La Jolla, CA 92093-0417*

CONTENTS

1 INTRODUCTION

1.1 Motivations and Scope

Extensive literature is available on the erosion of a wide spectrum of materials that have – over the years – been considered for plasma-facing applications in fusion reactors. The term 'erosion', in itself, encompasses processes such as physical sputtering, chemical reactions leading to the formation of volatile particles, radiation-enhanced sublimation (which occurs for carbon-based materials), and thermal sublimation. The major deleterious effects of erosion include: a reduced lifetime for the plasma-facing material, contamination of the fusion plasma, and tritium uptake due to codeposition of eroded material with the hydrogen fuel. Indeed, these issues are among the critical research and development challenges that need to be resolved for next-generation fusion devices such as the International Thermonuclear Experimental Reactor, ITER.

The preparation of this compendium results from an IAEA Coordinated Research Programme on "Plasma-Interaction Induced Erosion of Fusion Reactor Materials." The objective of the programme was to focus and coordinate the research activities of the participating institutions on the understanding of physical mechanisms of erosion processes and to undertake the compilation and critical assessment of a comprehensive erosion database for fusion research. We anticipate that the information so generated will be useful for the design of plasma-facing components, and also for modelling the transport of eroded particles in the fusion plasma, which in most cases leads to the redeposition of such particles on wall surfaces.

Due to the multifaceted nature of erosion and the broad spectrum of elements and compounds for which erosion data are available, an all-inclusive compendium would not only entail an immense task, but would also be cumbersome for the user community. Hence, in this document we focus on erosion due to **physical sputtering, chemical erosion** and **radiation-enhanced sublimation** induced by fusion plasma particle impact. Thermal sublimation is well understood and has been documented in standard handbooks.

Regarding target materials, we have selected Be, C and W, the three primary candidate materials being considered for ITER. Some relevant compounds of these elements (e.g., B_4C, TiC, SiC, etc.), as well as dopants used in conjunction with carbon, are also included. The impacting plasma species have also been selected on the basis of their fusion relevance. Here we included the hydrogenic species H, D, T, the He ash, O impurity, and elements that either result from the erosion process (such as C, Be, W, etc.) or are injected into the plasma for their effectiveness in dispersing power loading via enhanced radiation (e.g., Ne, Ar, N_2, etc.).

1.2 Basic Features of Particle-Induced Erosion Processes

Physical sputtering occurs via collisional interactions between impacting projectile atoms and atoms in the target, leading to the ejection of some of the target atoms. This process occurs for all materials for incident particle energies above a certain threshold, which is characteristic of the target-projectile combination; the

physical sputtering yield is not a function of temperature. The mechanisms associated with physical sputtering are well understood and are well-documented [1-5].

The occurrence of **chemical erosion** depends on the projectile-target combination and its mutual chemical reactivity. Chemical erosion can occur at all incident particle energies. For example, in the case of carbon, H impact leads to the formation of hydrocarbons, with yields peaking in the 500-1000 K temperature range; reactions occur even at sub-eV impact energies, with no evidence of an energy threshold. At present, the mechanisms associated with chemical erosion of carbon due to hydrogen impact are not fully understood. Recent modelling advances [6-10], however, have provided new insights into the complex physical/chemical interactions. Oxygen impact on carbon produces CO_2 and CO. Combined H and O also leads to the formation of some water. For Be and W, chemical erosion is also possible; e.g., O impact on W produces a variety of tungsten oxides, W_xO_y. Here, we shall concentrate on the chemical erosion of carbon and carbon-based materials.

Radiation-enhanced sublimation (RES) has only been observed in carbon-based materials, and is induced by energetic particle impact at temperatures above ~1200 K. The present understanding of RES is based on the formation of interstitial-vacancy pairs in the implantation zone by energetic incident atoms (chemically inert or otherwise). At sufficiently high temperatures the interstitial C atoms diffuse to the surface, and subsequently leave the surface with 'thermal' energy [11-14]. This model of RES agrees well with experimental observations, with the exception of flux-dependence predictions. The model predicts a decrease of RES yield with increasing incident particle flux to the power of (-0.25). Experimental results generally show a power of ~(-0.1) [15-18]. Since RES results from atom displacements, this process (like physical sputtering) only occurs above an incident particle energy threshold.

The contribution of these erosion processes to the total erosion yield depends on both target and projectile characteristics. For example, in Fig. 1.1 we show the relative role of physical sputtering [5], chemical erosion [19-22] and RES [13, 15] for protium and deuterium impact on carbon for different H [Fig. 1.1a] and D [Fig. 1.1b] energies, as a function of carbon temperature. For both H and D, we note that physical sputtering yields are only applicable for energies above the sputtering threshold (~40 eV for H and ~33 eV for D). Physical sputtering is a function of energy, and the yield for 1000 eV H and D are relatively higher than those at 100 eV. Chemical erosion becomes significant for temperatures below ~1000 K, with the chemical erosion yield being dependent on both the target temperature and projectile energy. The chemical erosion yield vs temperature curves are characterized by a maximum whose level (Y_m) and the temperature at which it occurs (T_m) also depend on the projectile energy. The monotonically increasing yield for temperatures above ~1000 K for the 100 and 1000 eV cases is due to radiation-enhanced sublimation. For the sub-eV and 10 eV cases only chemical erosion occurs, as these energies are below the thresholds for both physical sputtering and RES. We note that the physical sputtering and RES yields for D are relatively higher than for H. On the other hand, the chemical erosion yields for the two isotopes of hydrogen are not significantly different. In addition to the parameters noted above, the incident projectile flux density is also an important parameter. Unfortunately, the flux density range available with mass-analyzed accelerators is limited to $\sim 10^{16}/cm^2s$ which is 2 or 3 orders of magnitude

lower than the fluxes existing in the divertor and limiter regions of tokamaks. To explore the high tokamak-relevant fluxes, erosion yield measurements are also being performed in laboratory plasma devices and tokamaks.

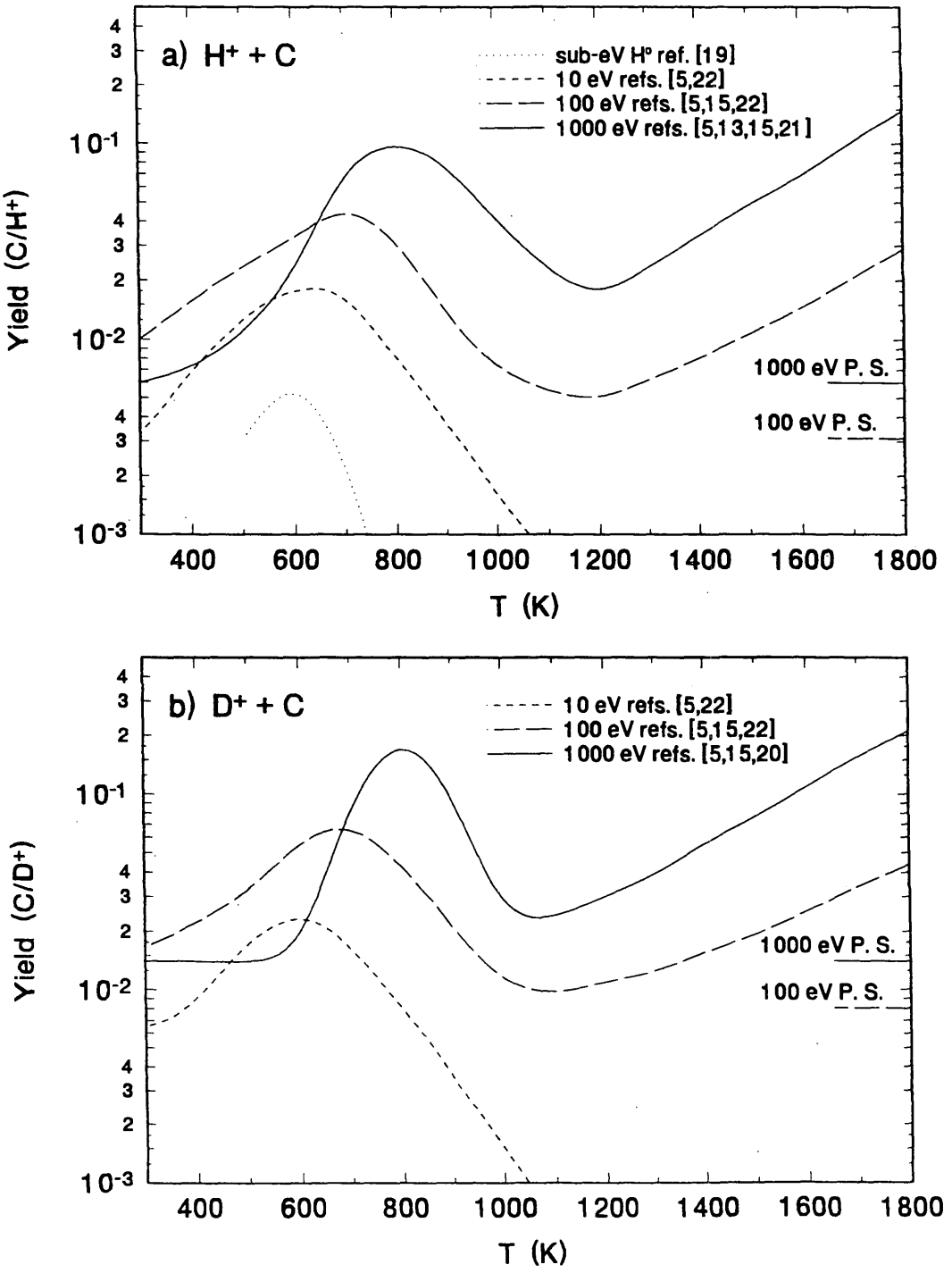

Figure 1.1: Erosion yields due to hydrogen and deuterium impact of carbon are presented at various energies, illustrating the characteristics of physical sputtering, radiation-enhanced sublimation and chemical erosion.

1.3 Organization and Presentation of the Compiled Erosion Data

The information in this compendium has been organized with two objectives in mind. First, selected collections of data obtained by various laboratories under specified parameter groupings have been compiled. In this process, the authors of the compendium exercised a degree of critical assessment. It is anticipated that the data so presented will be in a form that is transparent to the user community – for the design of plasma-facing components and the modelling of impurity transport and redeposition processes in tokamaks. The second objective was to be as inclusive as possible in presenting the available erosion data in order to provide access to information not contained in the 'selected collections'. Both sets of data, the **'selected collection'** and the **'individual sources'**, are included in this compendium.

On the most part, the experimental erosion data presented in this compendium were obtained from controlled laboratory experiments with mass-analyzed ion beams. Furthermore, only steady-state measurements are included. In the case of physical sputtering, the process is well understood and reliable model calculations are also available, and the experimental data have been fitted to the model. In cases where no experimental data are available, especially at low energies, only model calculations are given. Attempts at modelling chemical erosion and radiation-enhanced sublimation have also been made, with varying success, and work in this area is still continuing. Where applicable, models are fitted to the experimental data. However, for the most part, the chemical and RES data are fitted to polynomial or other appropriate analytic expressions. Therefore, users of the data presented here are cautioned that the **fitting equations only apply in the experimental parameter ranges indicated.**

The compendium is presented in two Volumes of *Atomic and Plasma-Material Interaction Data for Fusion.* In this Volume, Part A, we exclusively deal with 'chemical erosion' of carbon-based materials. In the following Volume, Part B, we present physical sputtering data for C, Be, and W, and RES data for carbon-based materials.

2 Erosion Data Derived from Tokamaks

Although it is evident that the most relevant erosion data for fusion applications should be available from tokamak experiments, the task associated with the derivation of such data is extremely difficult due to the complexity of the plasma-materials interaction processes and the structure of the tokamak devices themselves. Determination of erosion yields requires spatially resolved measurements of incident particle fluxes (and particle energies) and the fluxes of the released particles, formed via the various erosion processes. Notwithstanding these complexities, several attempts have been made to derive erosion yields from tokamak experiments. Here we shall present an overview of the various methods used. Reviews on this subject and a comparison of available results can be found elsewhere [10, 23-26].

To obtain and compare erosion data, knowledge of the conditions under which the data have been generated is required. In laboratory experiments, using ion or atom beams, control over the impacting particles, in terms of both fluxes and energies, is sufficiently good. Determination of the eroded particle fluxes is also

well in hand since recycling and redeposition do not occur. Thus, consistent results have been obtained in different laboratories, at least in the ion energy range above ~100 eV, as can be seen in the compiled collection of data in this compendium. In ion-beam experiments where deceleration is used to reach low energies, especially in the sub-100 eV range, some control is lost over the exact energy due to the possible formation of energetic neutrals via charge exchange. To overcome the flux limitations of ion-beam experiments, erosion studies are also being performed in laboratory plasma devices, with fusion-relevant fluxes ($\sim 10^{18}/cm^2s$) and energies. An inherent difficulty of this method is the determination of the impact parameters [flux density and energy] and the amount of released impurities. The diagnostic techniques used, e.g., Langmuir probes and H_α spectroscopy, pose interpretation problems and lead to uncertainties [27, 28]. Such plasma experiments can be operated without redeposition of the eroded particles, allowing for measurements of erosion yields.

The complexity of fusion devices makes it even more difficult to measure erosion yields in tokamaks. Indirect methods are used to determine the flux densities and energies of the impacting and eroded particles. The most advanced method is **emission spectroscopy in the plasma edge** as described in the review of Behringer et al. [29] and Pospieszczyk [30]. However, this method is also plagued with interpretation difficulties, some of which are listed below.

- In most cases the observation geometry is complex and the observed signals are the sum of events from different plasma regions.
- In the whole observation volume the local electron temperature (T_e) and density (n_e) have to be known in order to evaluate the photon efficiencies. For limiter experiments, the use of lithium and helium atomic beam diagnostics have improved considerably the determination of T_e and n_e [31].
- Much effort is being expended on the determination of photon efficiencies. As an example, the incident hydrogen flux is derived from the recycling hydrogen via H_α emission, whereas in the past, equal photon efficiencies were often assumed for a hydrogen atom and for the two atoms in the H_2 molecule. This assumption can lead to an underestimation of the molecular flux by a factor of up to four; this is especially important below 1100 K, where hydrogen recycles from graphite predominantly in the form of molecules [28].
- A principal question is the erosion and local redeposition (local transport) [26, 32] which may reduce the observed erosion yield. Another important factor is the condition of the surface and the influence of freshly redeposited impurities; e.g., the hydrocarbon formation from a metal test limiter was found to be similar to that from a graphite limiter under the same plasma edge conditions in carbonized machines [26].

Another in situ tokamak technique, especially used for the determination of chemical erosion, is the **sniffer probe** in TEXTOR [33]. This system acts as a small pump limiter in the scrape-off layer where a plasma column impinges on a heatable graphite strip. Detection is via partial pressure rise of the residual gas in the probe cavity. Uncertainties in the determination of yields arise from: changing surface

conditions due to redeposition; additional reaction products due to reflected hydrogen atoms at nearby walls; and the interaction of the plasma column with the residual gas. Taking these uncertainties into account, the measured yields should be an upper limit of the real value.

We wish to emphasize the difficulties associated with the derivation of erosion yields from tokamak measurements. We further note that when comparing yield results from different experiments, care must be taken to consider the conditions under which the measurements were made and which analysis method is applied. As an example, in reference [26] CD, CII and D_α emissions from a graphite test limiter at a flux density of 2×10^{18} D/m^{2}s were measured to determine the temperature dependence of the erosion yield. By using the usual photon efficiency, a maximum chemical erosion yield of 4% is obtained. A more indirect method, using the temperature-dependent CII and CD line intensities, allows one to distinguish between the contributions to the observed emissions due to physical sputtering and chemical erosion. From an estimate of the physical sputtering yield, a maximum chemical erosion yield of 1% is obtained. This value is 4 times smaller that that derived by the former method. At present, no explanation is available for this discrepancy. Some remarks will follow on the different erosion mechanisms occurring in tokamaks.

2.1 Physical Sputtering

Sputtering mechanisms observed in laboratory experiments also occur in fusion devices, and the yields measured in laboratory experiments can be used for impurity transport modelling in tokamaks. A discussion and comparison of some results is reviewed in [24] and [25].

2.2 Radiation-Enhanced Sublimation

Measurements of the RES effect in tokamaks are inconsistent. In both JET [34] and TFTR [35], large carbon influxes were observed which were partly attributed to RES. However, a clear identification of the carbon sources was not possible, and therefore, carbon influxes due to sublimation from local 'hot' spots could not be ruled out. More recently, spectroscopic measurements of the C influx above an inertial limiter in TORE SUPRA showed the characteristic temperature dependence associated with RES [36]. Yet another experiment, with a well defined test limiter in TEXTOR showed that RES may not occur under the high ion flux densities of tokamaks [37]. This is possibly due to a decrease in the RES yield above a certain flux density, as has been observed in a recent laboratory experiment [14]. Based on the TEXTOR results, it seems that RES may not be a serious problem in fusion devices. However, it must be acknowledged that this issue has not been fully resolved.

2.3 Chemical Erosion: Hydrocarbon formation

Evidence for the occurrence of chemical erosion in tokamaks, due to the interaction of the hydrogen fuel with carbon-based materials, includes the observation

of hydrocarbon formation in the TEXTOR **sniffer probe**, and the spectroscopic observations of CH bands in front of limiters and first-wall surfaces [10]. The importance of chemical erosion regarding component lifetime and impurity transport and redeposition is strongly influenced by plasma conditions and machine geometry. Pitcher and Stangeby [25] note that chemical erosion may have significant implications for the erosion of limiter and wall surfaces. However, based on experimental observations of CII line emissions and impurity transport modelling, they [25] conclude that at the divertor strike points of attached plasmas chemical sputtering is not important. This statement, however, cannot be viewed as being definitive as to whether chemical erosion does or does not occur at the strike points. Prompt redeposition of eroded hydrocarbons, or a reduced level of ionization and beak-up of hydrocarbons due to extremely low electron temperatures, could explain the absence of hydrocarbon contribution to the observed CII line emission. Indeed, under different plasma conditions, evidence of chemical erosion has been observed in the divertor region. From observations of CD band emissions at the divertor plate, Lieder et al. [38] derived a chemical erosion yield of ~3%; also, Pospieszczyk et al. [39] observed a dramatic increase in the C_2H_x formation for a detached plasma with a relatively low electron temperature at the plasma edge (~10 eV). Further evidence of chemical erosion is Poschenrieder's [23] observation of large quantities of hydrocarbons in the exhaust gas.

One of the outstanding issues regarding chemical erosion – and also RES – is the yield dependence on flux density, especially at low incident particle energies. Figures 2.1 and 2.2 contain a compilation of published chemical erosion yield data (mainly methane) for two incident energies of H and D, as a function of flux density. Although, a decreasing trend in the yield with increasing flux density is discernible, the large uncertainties in the determination of absolute yields, especially in the tokamak-generated data (due to the experimental difficulties discussed above), prevent us from drawing definitive conclusions to this effect.

2.4 Chemical Erosion due to Oxygen

The oxygen impurity in tokamak plasmas recycles on carbon in the form of CO and CO_2 [33]. It appears that yields obtained in laboratory ion-beam experiments can be directly applied to the tokamak plasma [40]. Since the oxygen ions impact on plasma-facing materials with relatively high energy (>100 eV), due to their multiple charge states, the reaction products CO and CO_2 are formed with a yield of nearly unity for the sum of the two species [10]. In addition, there is strong evidence that photons from tokamak plasmas impacting on plasma-facing surfaces lead to the release of CO_2, possibly due to photon-induced desorption from carbon-, oxygen- (and possibly water-) containing complexes on the surfaces [41]. At present, the mechanism responsible for this effect is not known.

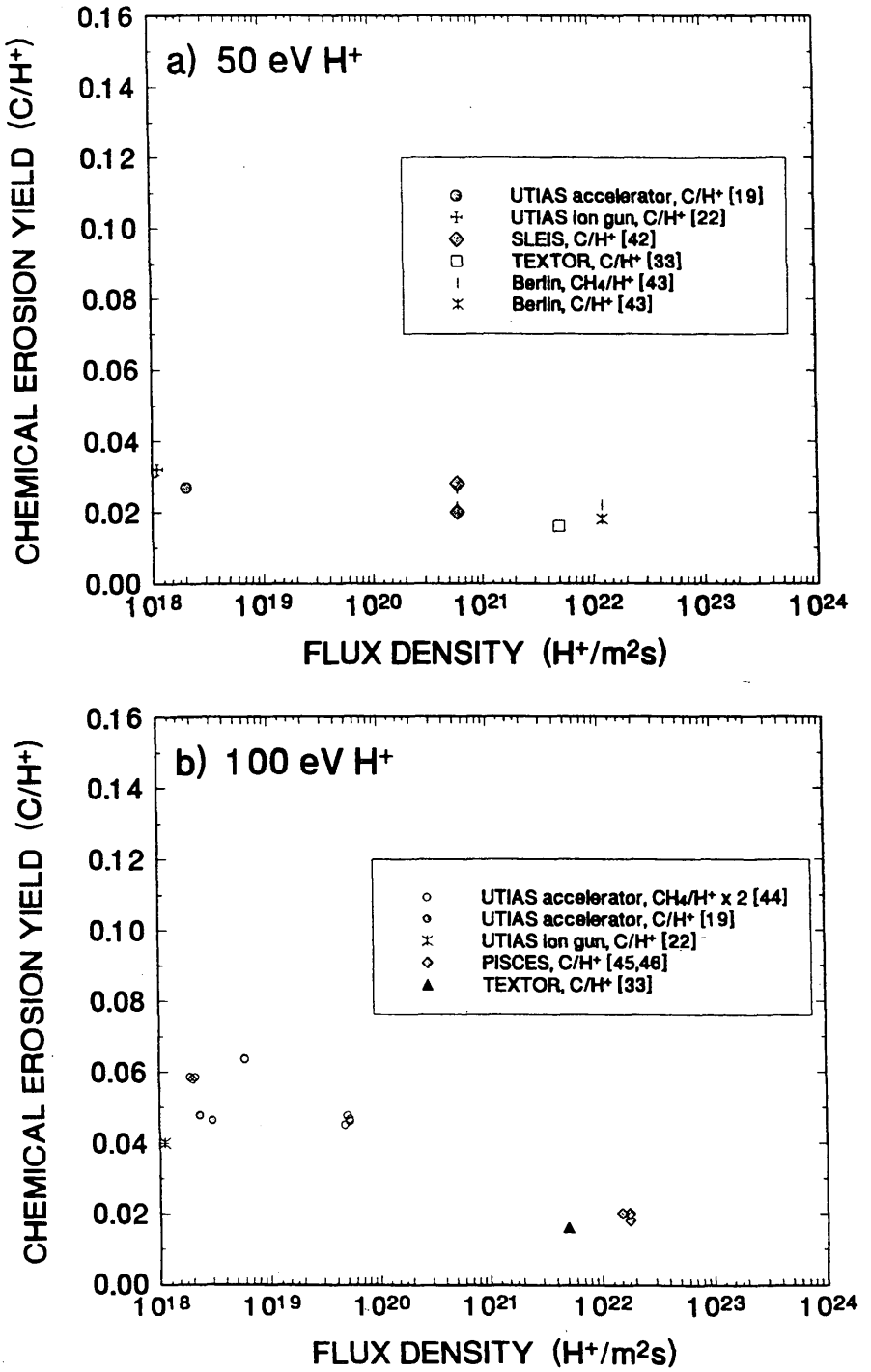

Figure 2.1: Chemical erosion yields obtained in ion-beam experiments and plasma devices, as a function flux density. Hydrogen data are shown for 50 and 100 eV energies. Experimental conditions are given separately for the two parts of the figure. 'PS' refers to physical sputtering.

(a) Ref. [19]: T_m = 750 K; Ref. [22]: T_m = 700 K; Ref. [42]: T= 473 – 573 K; Ref. [33]: T_m = 773 K (60-80 eV); Ref. [43]: for CH_4/H^+, T_m = 800 K (30 eV) and for C/H^+, T= 763 K (30 eV).

(b) Ref. [44]: T_m = 750 – 800 K; Ref. [19]: T_m = 650 – 800 K; Ref. [22]: T_m = 700 K; Ref. [45, 46]: T_m = 723 – 873 K (PS subtracted); Ref. [33]: T_m = 773 K (60-80 eV).

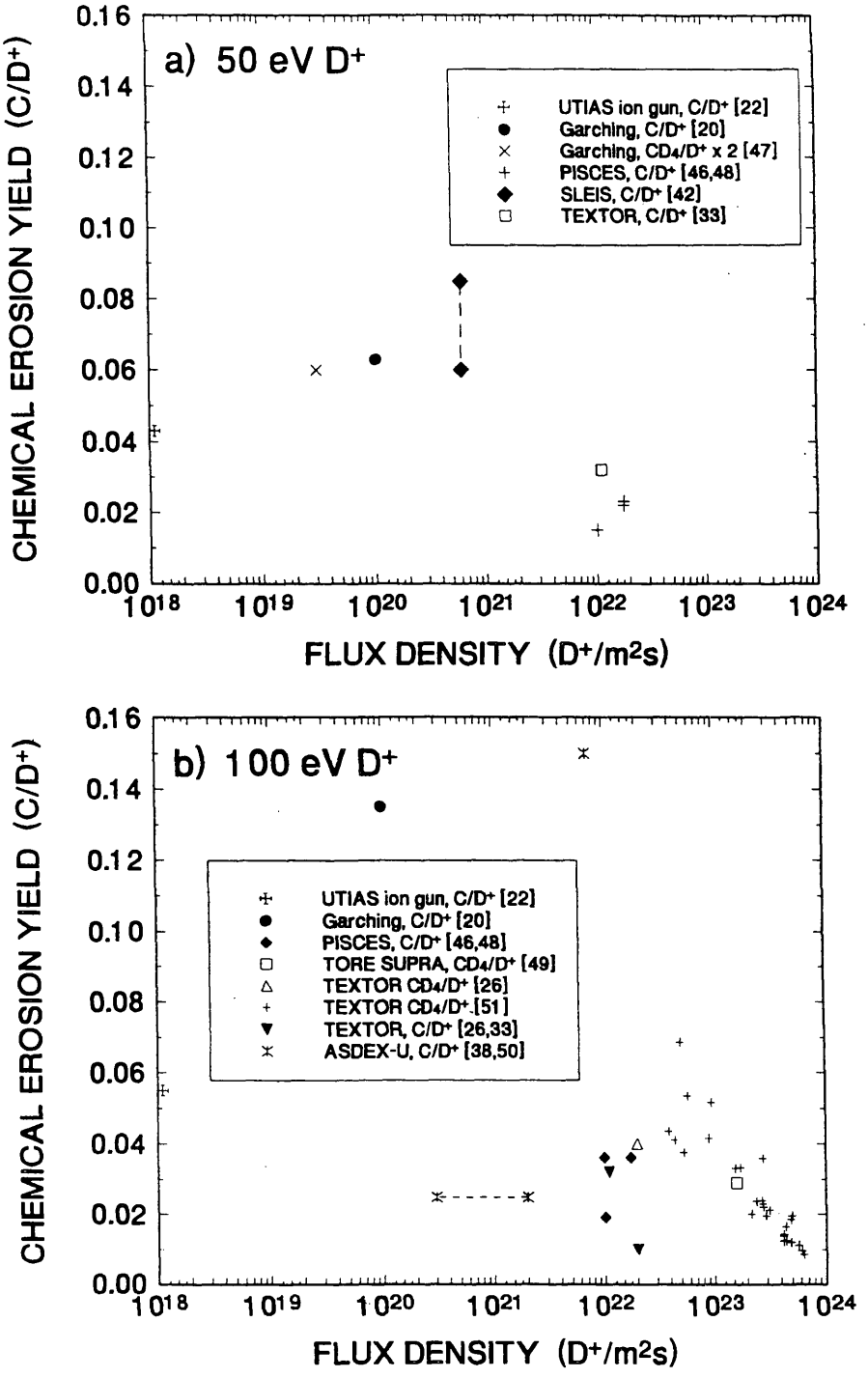

Figure 2.2: Chemical erosion yields obtained in ion-beam experiments and plasma devices, as a function flux density. Deuterium data are shown for 50 and 100 eV energies. Experimental conditions are given separately for the two parts of the figure. 'PS' refers to physical sputtering.

(a) Ref. [22]: T_m = 700 K; Ref. [20]: T= 823 K (PS subtracted); Ref. [47]: T_m = 800 K; Ref. [46, 48]: T_m = 723 – 873 K; Ref. [42]: T= 473 – 573 K; Ref. [33]: T_m = 773 K (60-80 eV).

(b) Ref. [22]: T_m = 700 K; Ref. [20]: T= 823 K (80 eV, PS subtracted); Ref. [46, 48]: T_m = 823 – 873 K (PS subtracted); Ref. [49]: T= 700 K (~135 eV); Ref. [26]: for CD_4/D^+, T= 700 – 1000 K (150 eV); Ref. [51]: T= 823 K (150 eV); Ref. [33]: T_m = 773 K (60-80 eV); Ref. [26]: for C/D^+, T= 700 – 1000 K (150 eV, lower limit); Ref. [38, 50]: T is not given.

References for Sections 1 and 2

[1] ECKSTEIN, W., PHILIPPS, V., "Physical Sputtering and Radiation Enhanced Sublimation", in *Physical Processes of the Interaction of Fusion Plasmas with Solids* (HOFER, W. O., J. ROTH, Eds.), Academic Press, San Diego (1996) 93.

[2] BEHRISCH, R. (Ed.), *Sputtering by Particle Bombardment I*, Topics in Applied Physics, Vol. **47**, Springer, Berlin (1981).

[3] BEHRISCH, R., (Ed.), *Sputtering by Particle Bombardment II*, Topics in Applied Physics, Vol. **52**, Springer, Berlin (1983).

[4] BEHRISCH, R., WITTMAACK, K. (Eds.), *Sputtering by Particle Bombardment III*, Topics in Applied Physics, Vol. **64**, Springer, Berlin (1991).

[5] ECKSTEIN, W., C. GARCIA-ROSALES, C., ROTH, J., OTTENBERGER, W., "Sputtering Data", Max-Planck-Institut für Plasmaphysik Report IPP 9/82 (1993).

[6] HORN, A., SCHENK, A., BEINER, J., WINTER, B., LUTTERLOH, C., WITTMANN, M., KÜPPERS, J., Chemical Physics Lett. **231** (1994) 193.

[7] WITTMANN, M., KÜPPERS, J., J. Nucl. Mater. **227** (1996) 186.

[8] ROTH, J., GARCIA-ROSALES, C., Nucl. Fusion **36** (1996) 1647.

[9] MECH, B. V., HAASZ, A. A., DAVIS, J. W., "A Model for Graphite Erosion Due to Low-energy H^+ and D^+", J. Appl. Phys., submitted.

[10] VIETZKE, E., HAASZ, A. A. "Chemical Erosion", in *Physical Processes of the Interaction of Fusion Plasmas with Solids* (HOFER, W. O., ROTH, J., Eds.), Academic Press, San Diego (1996) 135.

[11] ROTH, J., MÖLLER, W., Nucl. Instrum. and Meth. B **7/8** (1985) 788.

[12] VIETZKE, E., FLASKAMP, K., HENNES, M., PHILIPPS, V., Nucl. Instrum. and Meth. B **2** (1984) 617.

[13] FRANZEN, P., DAVIS, J. W., HAASZ, A. A., J. Appl. Phys. **78** (1995) 817.

[14] UEDA, Y., NAKANO, K., OHTSUKA, Y., ISOBE, M., GOTO, S., NISHIKAWA, M., J. Nucl. Mater. **227** (1996) 251.

[15] HAASZ, A. A., DAVIS, J. W., J. Nucl. Mater. **151** (1987) 77.

[16] PHILIPPS, V., VIETZKE, E., SCHORN, R. P., TRINKAUS, H., J. Nucl. Mater. **155-157** (1987) 319.

[17] HAASZ, A. A., DAVIS, J. W., CROESSMANN, C. D., DOYLE, B. L., NYGREN, R. E., WALSH, D. S., WATKINS, J. G., WHITLEY, J. B., J. Nucl. Mater. **173** (1990) 108.

[18] HAASZ, A. A., DAVIS, J. W., J. Nucl. Mater. **224** (1995) 141.

[19] DAVIS, J. W., HAASZ, A. A., STANGEBY, P. C., J. Nucl. Mater. **155-157** (1988) 234.

[20] ROTH, J., BOHDANSKY, J., Nucl. Instr. Meth. **B23** (1987) 549.

[21] HAASZ, A. A., DAVIS, J. W., J. Nucl. Mater. **175** (1990) 84.

[22] MECH, B. V., HAASZ, A. A., DAVIS, J. W., *"Isotopic effects in hydrocarbon formation due to low-energy H^+/D^+ impact on graphite"*, J. Nucl. Mater., in press.

[23] POSCHENRIEDER, W., BEHRINGER, K., BOSCH, H. ST., FIELD, A., KALLENBACK, A., KAUFMANN, M., KRIEGER, K., KÜPPERS, J., LIEDER, G., NAUJOKS, D., NEU, R., NEUHAUSER, J., GARCIA-ROSALES, C., ROTH, J., SCHNEIDER, R., and the ASDEX UPGRADE TEAM, J. Nucl. Mater. **220-222** (1995) 36.

[24] DAVIS, J. W., HAASZ, A. A., J. Nucl. Mater. **241-243** (1997) 37.

[25] PITCHER, C. S., STANGEBY, P. C., Plasma Phys. Contr. Fusion **39** (1997) 779.

[26] PHILIPPS, V., POSPIESZCZYK, A., ESSER, H. G., KÖGLER, U., MANK, G., SAMM, U., SCHWEER, B., VON SEGGERN, J., UNTERBERG, B., VIETZKE, E., WESCHENFELDER, F., WIENHOLD, P., WINTER, J., and the TEXTOR TEAM, J. Nucl. Mater. **241-243** (1997) 105.

[27] STANGEBY, P. C., Plasma. Phys. Contr. Fusion **37** (1995) 1031.

[28] POSPIESZCZYK, A., SERGIENKO, G., RUSBUELD, D., PHILIPPS, V., VIETZKE, E., *Proc. 24th EPS Conf. on Contr. Fusion and Plasma Phys.*, Bertesgaden (1997), Part IV, 1733.

[29] BEHRINGER, K. H., J. Nucl. Mater. **145-147** (1987) 145.

[30] POSPIESZCZYK, A., in *Atomic and Plasma-material Interaction Processes in Controlled Thermonuclear Fusion* (JANEV, R. K., DRAWIN, H. W., Eds.), Elsevier, Amsterdam (1993).

[31] SCHWEER, B., MANK, G., POSPIESZCZYK, A., BROSDA, B., POHLMEYER, B., J. Nucl. Mater. **196-198** (1992) 174.

[32] KÖGLER, U., WESCHENFELDER, F., WINTER, J., ESSER, H. G., PHILIPPS, V., POSPIESZCZYK, A., SCHWEER, B., VON SEGGERN, J., TOKAR, M. Z., WIENHOLD, P., J. Nucl. Mater. **241-243** (1997) 816.

[33] PHILIPPS, V., VIETZKE, E., ERDWEG, M., J. Nucl. Mater. **162-164** (1989) 550.

[34] REICHLE, R., SUMMERS, D. D. R., STAMP, M. F., J. Nucl. Mater. **176&177** (1990) 375.

[35] RAMSEY, A. T., BUSH, C. E., DYLLA, H. F., OWENS, D. K., PITCHER, C. S., ULRICKSON, M. A., Nucl. Fus. **3** (1991) 1811.

[36] TOBIN, S. J., HOGAN, J. T., DEMICHELIST, C., KLEPPER, C. C., MATTIOLI, M., MONIER-GARBET, P., GUILHEM, D., HESS, W. R., ISLER, R. C., Plasma Phys. Contr. Fusion **38** (1996) 251.

[37] PHILIPPS, V., POSPIESZCZYK, A., SCHWEER, B., UNTERBERG, B., VIETZKE, E., TRINKAUS, H., J. Nucl. Mater. **220-222** (1995) 467.

[38] LIEDER, G., BEHRINGER, K., FIELD, A. R., GARCIA-ROSALES, C., HIRSCH, S., KALLENBACH, A., NAPIONTEK, B., NAUJOKS, D., PITCHER, C. S., POSCHENRIEDER, W., RADTKE, R., ROTH, J., WEINLICH, M., and the ASDEX-UPGRADE TEAM, *Proc. 21st EPS Conf. on Contr. Fusion and Plasma Phys.*, Montpellier (1994), Part II, 722.

[39] POSPIESZCZYK, A., PHILIPPS, V., CASAROTTO, E., KÖGLER, U., SCHWEER, B., UNTERBERG, B., WESCHENFELDER, F., DIANO, G. Y., *Proc. 22nd EPS Conf. on Contr. Fusion and Plasma Phys.*, Bournemouth (1995), Part II, 309.

[40] PHILIPPS, V., VIETZKE, E., ERDWEG, M., Plasma Phys. Contr. Fusion **31** (1989) 1685.

[41] PHILIPPS, V., VIETZKE, E., ERDWEG, M., WINTER, J., J. Nucl. Mater. **200** (1993) 355.

[42] NAKAMURA, K., NAGASE, A., DAIRAKU, M., AKIBA, M., ARAKI, M., OKUMURA, Y., J. Nucl. Mater. **220-222** (1995) 890.

[43] GROTE, H. BOHMEYER, W., REINER, H. D., FUCHS, T. KORNEJEW, P., STEINBRINK, J., J. Nucl. Mater. **241-243** (1997) 1152.

[44] DAVIS, J. W., HAASZ, A. A., STANGEBY, P. C., J. Nucl. Mater. **145-147** (1987) 417.

[45] GOEBEL, D. M., HIROOKA, Y., CONN, R. W., LEUNG, W. K.,CAMPBELL, G. A., BOHDANSKY, J., WILSON, K. L., BAUER, W., CAUSEY, R. A., PONTEAU, A. E., KRAUSS, A. R., GRUEN, D. N., MENDELSOHN, M. H., J. Nucl. Mater. **145-147** (1987) 61.

[46] GOEBEL, D. M., BOHDANSKY, J., CONN, R. W., HIROOKA, Y., LEUNG, W. K., NYGREN, R. E., TYNAN, G. R., Fusion Technology **15** (1989) 102.

[47] GARCIA-ROSALES, C., ROTH, J., J. Nucl. Mater. **196-198** (1992) 573.

[48] FRANCONI, E., HIROOKA, Y., CONN, R. W., LEUNG, W. K., LABOMBARD, B., NYGREN, R. E., J. Nucl. Mater. **162-164** (1989) 892.

[49] KLEPPER, C. C., HOGAN, J. T., OWEN, L. W., HUCKAN, T., HESS, W. R., GUILHEM, D., GUIRLET, R., LOARER, T. *Proc. 20th EPS Conf. on Contr. Fusion and Plasma Phys.*, Lisbon (1993), Part II, 599.

[50] KALLENBACH, A., NEU, R., POSCHENRIEDER, W., and the ASDEX UPGRADE TEAM, Nucl. Fus. **34** (1994) 1557.

[51] POSPIESZCZYK, A., PHILIPPS, V., CASAROTTO, E., KÖGLER, U., SCHWEER, B., UNTERBERG, B., WESCHENFELDER, F., J. Nucl. Mater. **241-243** (1997) 833.

3 Carbon-Based Materials: Selected Collection of Chemical Erosion Data

The data presented here are limited to graphite and some carbon-containing materials, such as carbides and mixtures of carbon and dopant elements. In the context of fusion plasma-materials interactions, chemical erosion occurs when chemically reactive plasma species come into contact with plasma-facing components. The dominant plasma species are the hydrogen fuel (deuterium and tritium) and the He ash. Impurities such as O and elements resulting from wall erosion are present in small concentrations, typically two orders of magnitude lower than the fuel concentration. Chemical erosion of carbon-based materials in tokamaks is dominated by hydrogen and oxygen impact. However, through synergistic effects, non-reactive plasma species, in combination with the reactive ones, also play a role in the chemical erosion process.

The relative importance of the various erosion processes associated with H impact on carbon is schematically presented in Fig. 1.1 of the Introduction for three H^+ and D^+ impact energies. Here we shall focus on chemical erosion, which dominates at temperatures in the range 600-1000 K. We note that as the energy decreases, the absolute value of the chemical erosion yield decreases, and also the temperature at which the maximum occurs (T_m) shifts from ~750 K at 1 keV to ~650 K at 100 eV. In addition, a broadening of the temperature profile is observed, in comparison with the 1 keV case. At 10 eV, which is below the threshold for both physical sputtering and RES, only chemical erosion occurs. Again, we note a further decrease in the yield, as well as a further shift of T_m to ~600 K, and extended broadening of the temperature profile. Also shown in Fig. 1.1a, is the chemical erosion curve due to sub-eV H^0 atoms. Compared to the 10 eV H^+ curve, we note that Y_m is lower by about a factor of four, while T_m remains essentially the same.

In addition to the target temperature and particle impact energy dependence of the chemical erosion yield of graphite and other carbon-based materials due to H impact, the yield is also a function of the impacting species flux density.

In this section we present selected collections of chemical erosion data as functions of experimental variables which include target temperature, incident particle energy, incident particle flux, and in the case of two-species impact, flux ratio. The selected sets are organized by impacting particles according to sub-eV neutral hydrogen and deuterium (H^0, D^0), energetic hydrogen and deuterium ions (H^+, D^+), and oxygen atoms and ions (O^0, O^+). Also included are synergistic reactions involving neutral hydrogen atoms and hydrogen ions (H^0, H^+), as well as other combinations of hydrogen atoms/ions with some heavier atomic ions (He^+, C^+, Ne^+, O^+ and Ar^+). Associated with each set of incident particles, selected data are plotted to illustrate the general dependence of chemical erosion on the experimental variables. Comparisons of data sets from different laboratories are made where available relevant data exist. The figures are accompanied with brief comments providing experimental details where appropriate and observations of trends and significance of the collected data. For some of the figures (Figs. 3.6-3.11, 3.13-3.15, and 3.25) we have also included 'global fits' to selected groupings of data (e.g. methane erosion yields and total chemical yields). This is intended to help guide the eye, and also to be of

possible use for a parameterization of the data. Fitting coefficients and the analytic functions used for these global fits are indicated as needed in the comments below each figure. The lines drawn through the data in the rest of the figures in Section 3 are the analytic fits produced for the individual data sets compiled in Section 4. Fitting parameters for the individual curves and further experimental details are provided in Section 4.

List of Reactions for Section 3[1]

Figure	Reaction	Yield dependence
3.1	H^0(sub-eV) + C(PyG) $\rightarrow$ $CH_{3,4}$, $C_{chem-total}$	temperature
3.2	H^0(sub-eV) + C(PyG) $\rightarrow$ $CH_{3,4}$	temperature
3.3	H^0(sub-eV) + C(PyG) $\rightarrow$ $CH_{3,4}$	H^0 flux density
3.4	H^0(sub-eV), D^0(sub-eV) + a-C:H film, C(PyG) $\rightarrow$ $CH_{3,4}$, $C_{chem-total}$	temperature
	H^0(sub-eV) + redeposited film $\rightarrow$ $C_{chem-total}$	temperature
3.5	H^0(sub-eV) + a-C:H film, a-C/B:H film $\rightarrow$ CH_3^+, BH_2^+	temperature
3.6	H^+(1 keV), D^+(1 keV) + C(PyG) $\rightarrow$ CH_4, CD_4, $C_{chem-total}$	temperature
3.7	H^+(200 eV), D^+(200 eV) + C(PyG) $\rightarrow$ CH_4, CD_4, $C_{chem-total}$	temperature
3.8	H^+(100 eV), D^+(100 eV) + C(PyG) $\rightarrow$ CH_4, CD_4, $C_{chem-total}$	temperature
3.9	H^+(50 eV), D^+(50 eV) + C(PyG) $\rightarrow$ CH_4, CD_4, $C_{chem-total}$	temperature
3.10	H^+(20-30 eV), D^+(20-30 eV) + C(PyG) $\rightarrow$ CH_4, CD_4, $C_{chem-total}$	temperature
3.11	H^+(10 eV), D^+(10 eV) + C(PyG) $\rightarrow$ CH_4, CD_4, $C_{chem-total}$	temperature
3.12	H^+(100 eV) + C(PyG) $\rightarrow$ CH_4	H^+ flux density
	H^+(1 keV), D^+(1 keV) + C(PyG) $\rightarrow$ CH_4, CD_4, $C_{chem-total}$	H^+, D^+ flux density
3.13	H^+, D^+ + C(PyG) $\rightarrow$ CH_4, CD_4, $C_{chem-total}$	H^+, D^+ energy
3.14	H^+, D^+ + C(PyG) $\rightarrow$ CH_4, CD_4, $C_{chem-total}$	H^+, D^+ energy
3.15	H^+, D^+ + C(PyG) $\rightarrow$ CH_4, CD_4, $C_{chem-total}$	H^+, D^+ energy
3.16	H^+, D^+ + a-C:H film $\rightarrow$ CH_4, CD_4	temperature
3.17	H^+, D^+ + B_4C $\rightarrow$ CH_4, CD_4	temperature
3.18	H_3^+, D_2^+ + TiC $\rightarrow$ CH_4, CD_4	temperature
3.19	O^0(sub-eV), O_2(sub-eV) + C(PyG) $\rightarrow$ CO	temperature
3.20	O^+ + C(PyG) $\rightarrow$ CO, CO_2	temperature
3.21	O^0(<5 eV), O^+ + C(PyG) $\rightarrow$ C_{total} = [$C_{chemical}$ + $C_{physical}$]	O^+ energy
3.22	O^+ + B_4C $\rightarrow$ CO, BO, B_2O_2, [C+B]	temperature
3.23	[H^0(sub-eV), Ar^+] + C(PyG) $\rightarrow$ $CH_{3,4}$	temperature
3.24	H^+, [H^0(sub-eV), H^+] + C(PyG) $\rightarrow$ CH_4	temperature
3.25	[H^0(sub-eV), H^+] + C(PyG) $\rightarrow$ CH_4, $C_{chem-total}$	flux ratio [H^+]/[H^0]
3.26	[H^0(sub-eV), C^+(1 keV)] + C(PyG) $\rightarrow$ C_{total}	temperature
3.27	[H^0(sub-eV), C^+(1 keV)] + C(PyG) $\rightarrow$ C_{total}	flux ratio [C^+]/[H^0]
3.28	[H^0(sub-eV), O^+(2 keV)] + C(PyG) $\rightarrow$ C_{total}	flux ratio [O^+]/[H^0]
3.29	[H^+(100 eV), C^+(1 keV)] + C(PyG) $\rightarrow$ $C_{chem-total}$	temperature
	[H^+(300 eV), C^+(1 keV)] + C(PyG) $\rightarrow$ $C_{chem-total}$	temperature
3.30	[H^+(100 eV), X^+(1 keV)](X=He, C, Ne, Ar) + C(PyG) $\rightarrow$ $C_{chem-total}$	flux ratio [X^+]/[H^+]
3.31	[H^+(1 keV), O^+(5 keV)] + C(PyG) $\rightarrow$ CO, CO_2, H_2O, O_{total}	temperature
3.32	[Ar^+(5 keV), O_2(sub-eV)] + C(PyG) $\rightarrow$ CO, CO_2	temperature

[1]Due to difficulties in distinguishing which ion species were used in some experiments, for the purposes of this index, we shall use the notation H^+ and D^+ to represent atomic as well as molecular ions. Where available, the distinction is made on the figures.

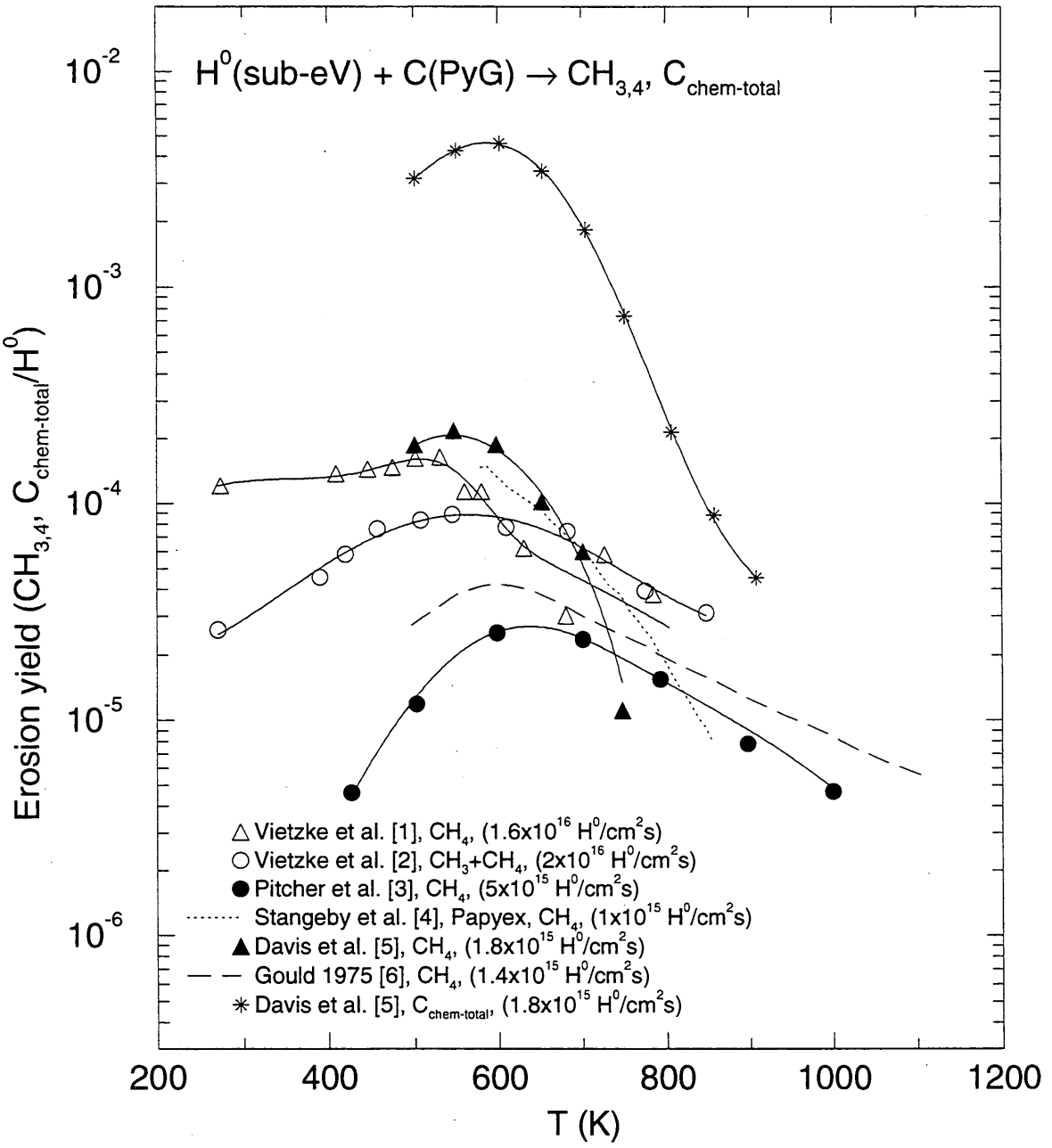

Figure 3.1: Hydrocarbon yield due to sub-eV H^0 impact on graphite as a function of temperature.

Results from various research groups indicate an uncertainty in the methane ($CH_{3,4}$) erosion yield of greater than an order of magnitude: maximum erosion yields vary from 2×10^{-5} to 2×10^{-4} $CH_{3,4}/H^0$. The maximum erosion yield occurs consistently at 500-600 K. As indicated by the data by Davis et al. [5], heavier hydrocarbons dominate the erosion yield, with $Y_{chem-total}$ being equal to $\sim 20 \times Y_{CH_4}$.

The total chemical erosion yield, $Y_{chem-total}$, is found from summing the contributions: $[CH_4] + 2 \times \{[C_2H_2] + [C_2H_4] + [C_2H_6]\} + 3 \times \{[C_3H_6] + [C_3H_8]\}$, and dividing by $[H^0]$.

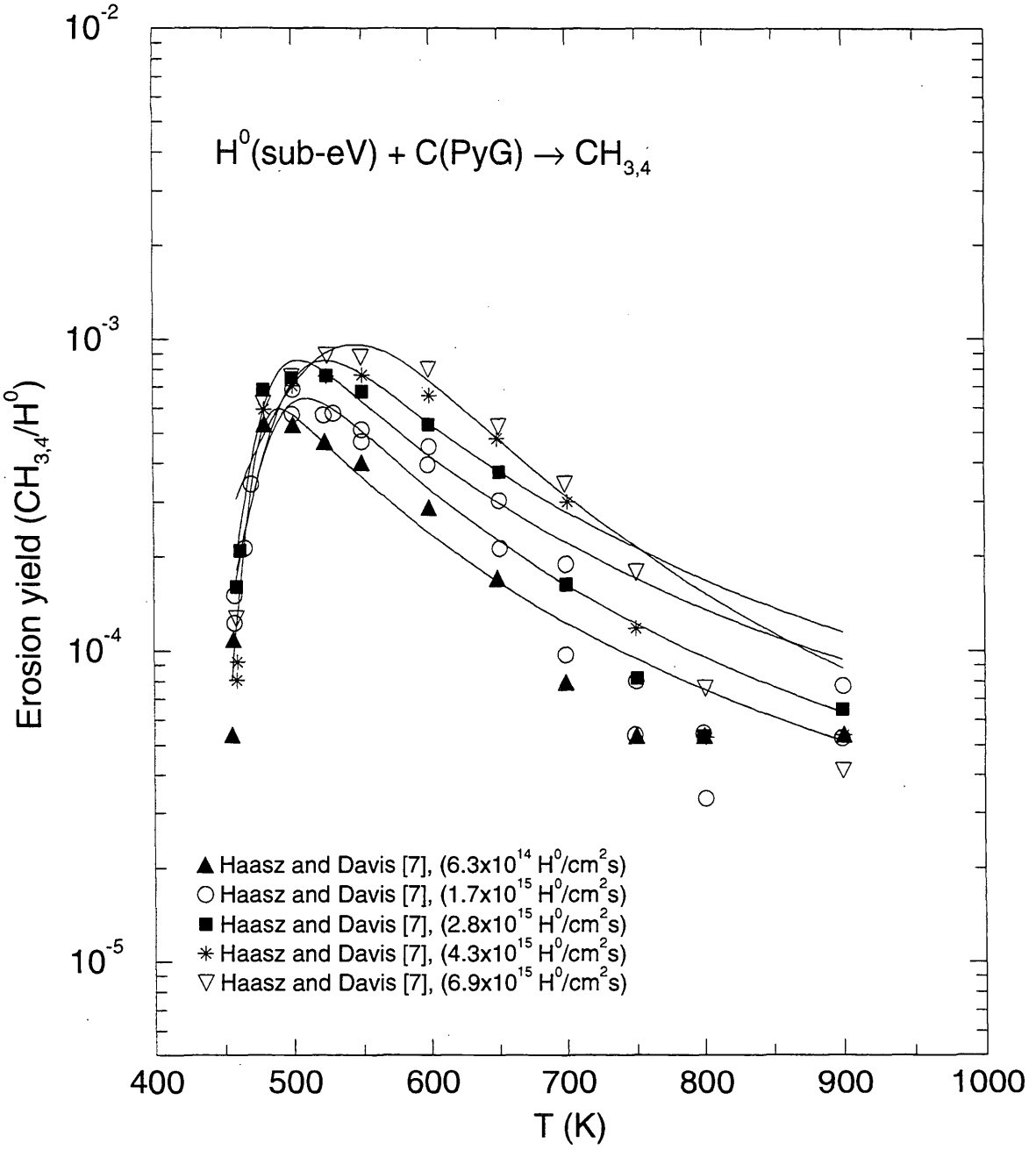

Figure 3.2: Methane yield due to sub-eV H^0 impact on graphite as a function of temperature for different flux densities.

In the flux range of the experiment, both Y_m and T_m increase with flux density. T_m increases from <500 K to ~550 K with increasing flux density. Y_m is plotted as a function of flux on Fig. 3.3.

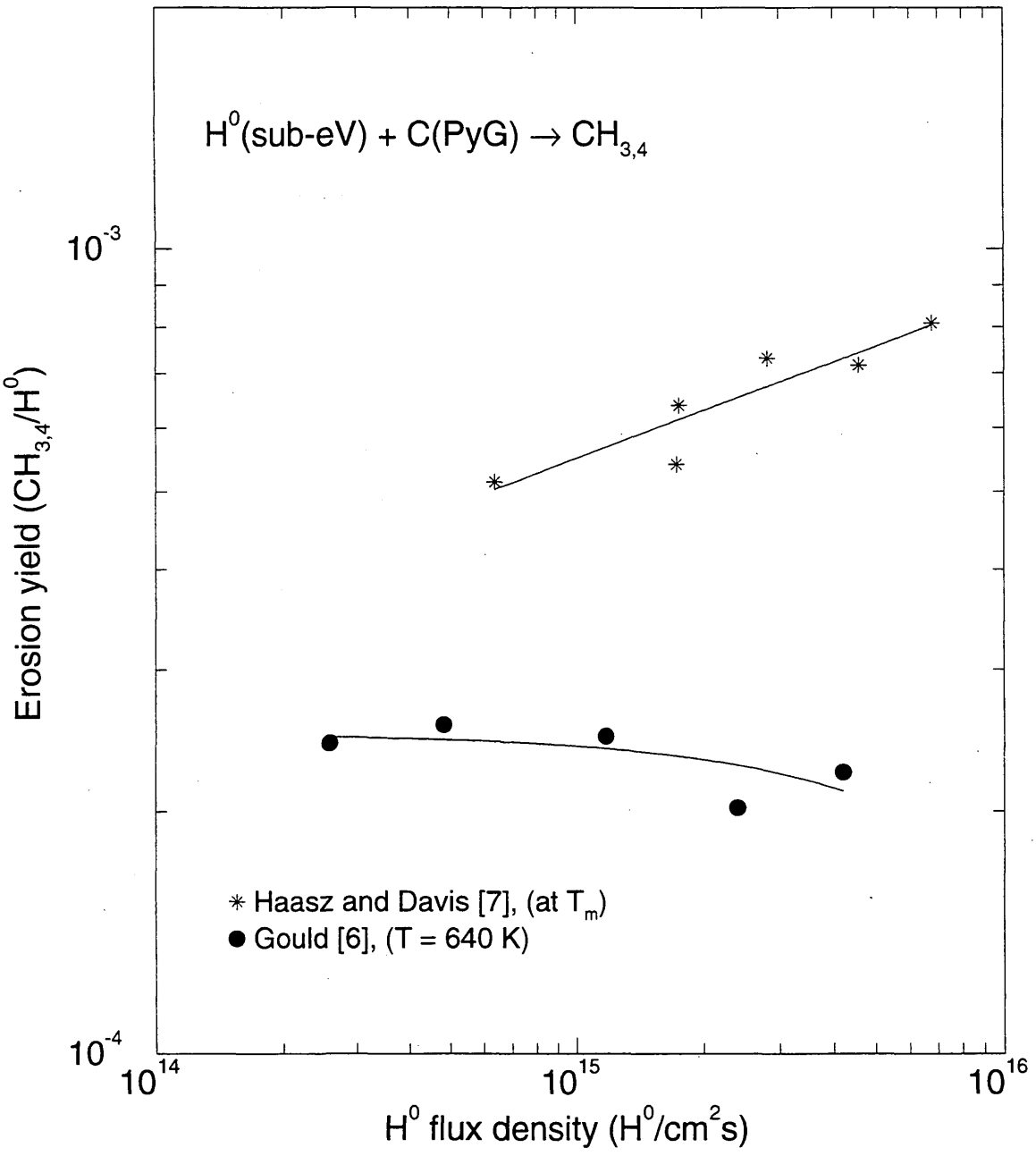

Figure 3.3: Flux density dependence of peak erosion yield due to sub-eV H^0 impact on graphite.

In the results of Haasz and Davis [7], the maximum erosion yield, Y_m, was observed to increase with increasing flux density; these data are from Fig. 3.2. Results from Gould [6] show no flux dependence, however, Gould's results are at constant temperature (640 K) not at T_m.

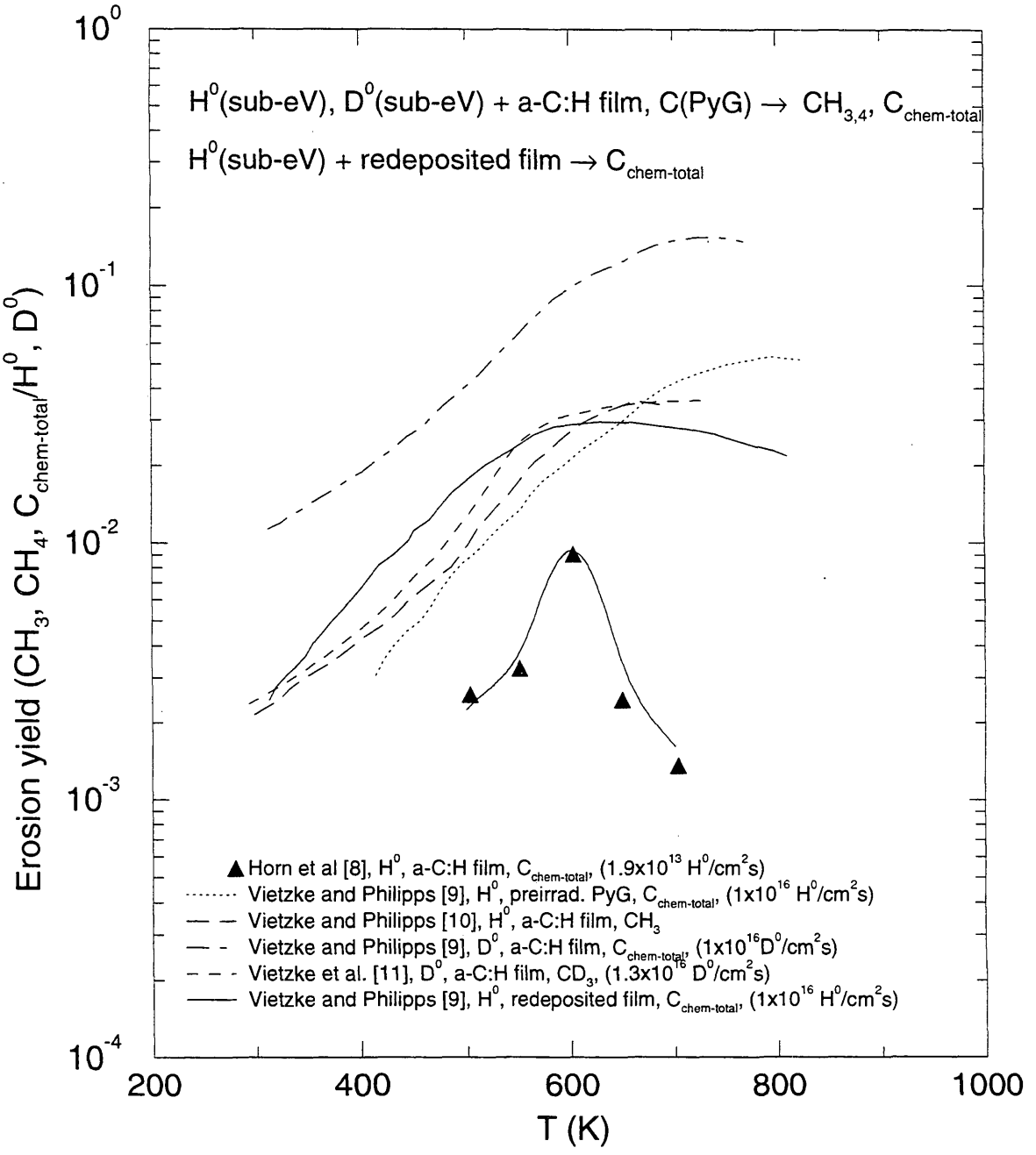

Figure 3.4: Chemical erosion of a-C:H films, ion-damaged graphite and tokamak films due to sub-eV H^0 impact, shown as a function of temperature.

The erosion of plasma-deposited a-C:H films due to sub-eV H^0 impact is found to be significantly larger than the erosion of graphite with a temperature dependence more characteristic of energetic ion-induced erosion. (The disappearance of the films prevents the measurements at >800 K.) The erosion of ion-damaged graphite is similar to the deposited films, but lower by a factor of 3, indicating that the ion-induced amorphous structure is similar to that of the plasma-deposited films. A tokamak-deposited layer is also similar. For the a-C:H film, the erosion is dominated by methane; the importance of heavier hydrocarbons is less than in the case of sub-eV H^0 on graphite. H^0 and D^0 have similar erosion yields. D^0 atoms on a-C:H films produce few mixed molecules, mostly deuterated methane. The erosion rates of Horn et al. [8] were determined by monitoring film thickness (initially 6 monolayers) via Auger Electron Spectroscopy, and thus reaction products were not directly measured as was the case for the other measurements; it is not evident why the results of Horn et al. [8] are much lower than the other film results.

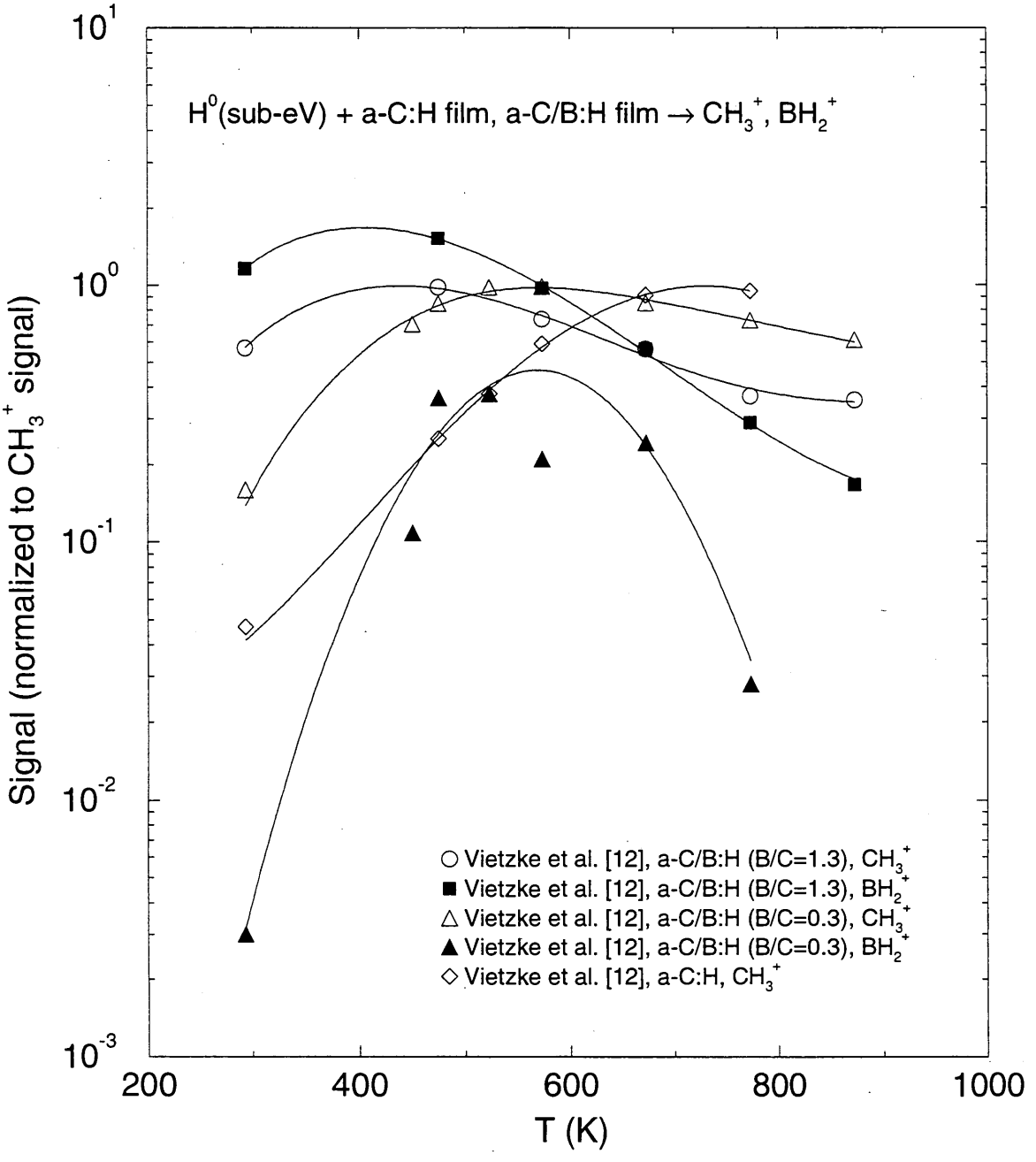

Figure 3.5: The erosion of boron-containing films due to sub-eV H^0 impact.

The release of various reaction products as a function of temperature was measured by line-of-sight mass spectrometry. Signals are normalized to the maximum CH_3^+ signal for each material. The maximum CH_3 yield occurs at progressively lower temperatures as the boron content of the film increases. Also, the relative production of BH_2 with respect to CH_3 increases with B content.

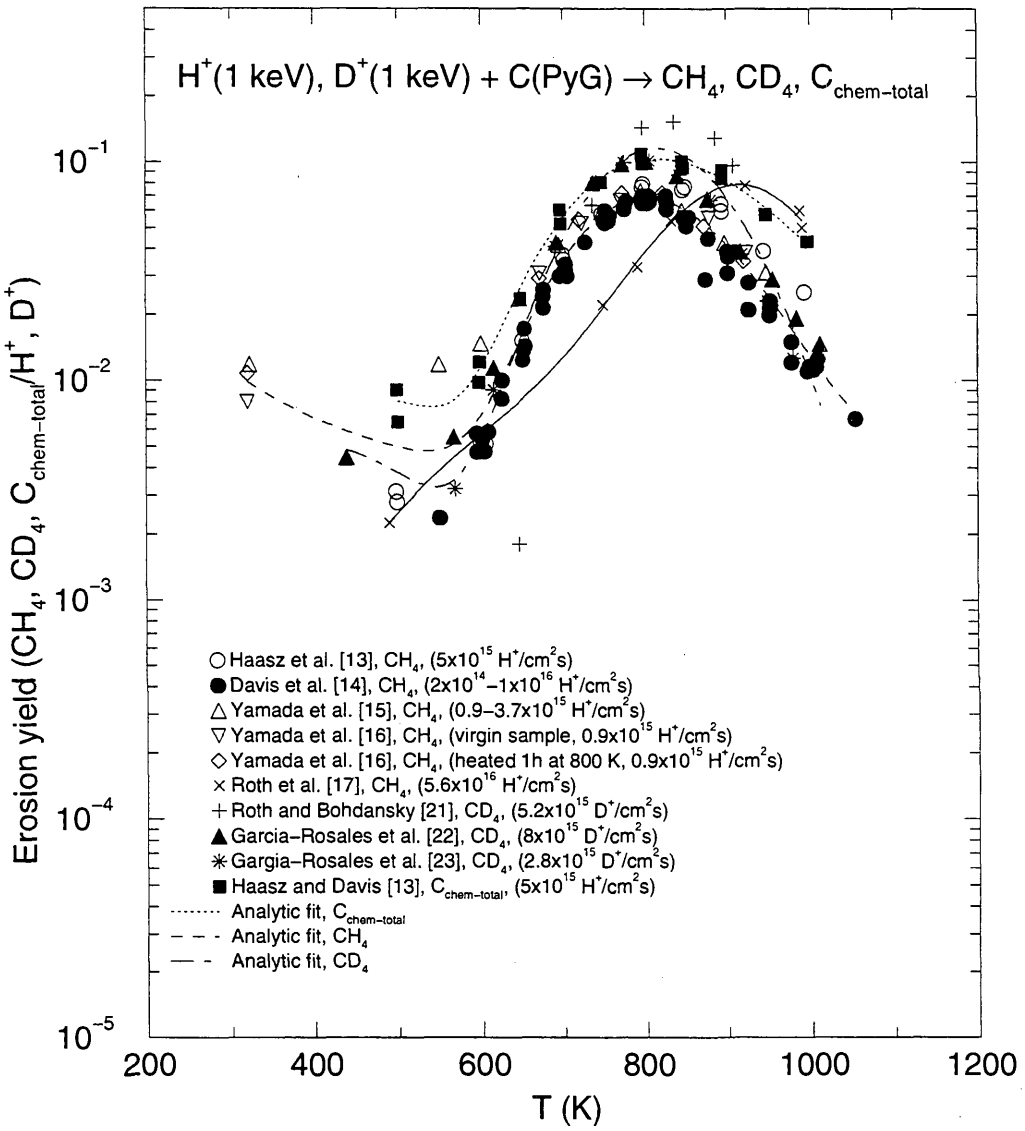

Figure 3.6: Chemical erosion of graphite yield due to 1 keV H^+ and D^+ impact, as a function of temperature.

The results from various research groups are much more consistent than for the case of sub-eV H^0 (Fig. 3.1). A peak in the erosion yield is observed at T_m ~800 K, with Y_m for methane being ~0.08, and Y_m for total hydrocarbon production ~0.1. Deuterium bombardment leads to somewhat higher yields. The spread in H^+ yields is <20% at T_m, while the spread in D^+ yields is about a factor of 2. One of the data sets [17] appears to be temperature shifted with respect to the others, having T_m ~900 K. Heavier hydrocarbons contribute ~20% to the total erosion yield.

The total chemical erosion yield, $Y_{chem-total}$, is found from summing the contributions: $[CH_4] + 2 \times \{[C_2H_2] + [C_2H_4] + [C_2H_6]\} + 3 \times \{[C_3H_6] + [C_3H_8]\}$, and dividing by $[H^+]$.

The data are divided into three groups, $C_{chem-total}$ (H^+), CH_4 and CD_4, and fitted separately with EYIELD8A. Fitting coefficients A_1-A_8:

$C_{chem-total}$ (H^+): [6.56215e-03, 8.09472e+02, 3.87984e-03, 1.50264e+03, 4.10935e-01, 1.2456e-33, 2.97967e-02, 1.38120e+01]

CH_4: [2.31140e-03, 7.96725e+02, 9.32705e-04, 5.34492e+03, 4.99014e-01, 9.52996e+04, -3.57652e-03, -2.98627e+00]

CD_4: [6.78366e-03, 8.10898e+02, 8.80847e-05, 1.20858e+04, 4.23316e-01, 1.90674e-25, 2.63156e-02, 10.3769e+01]

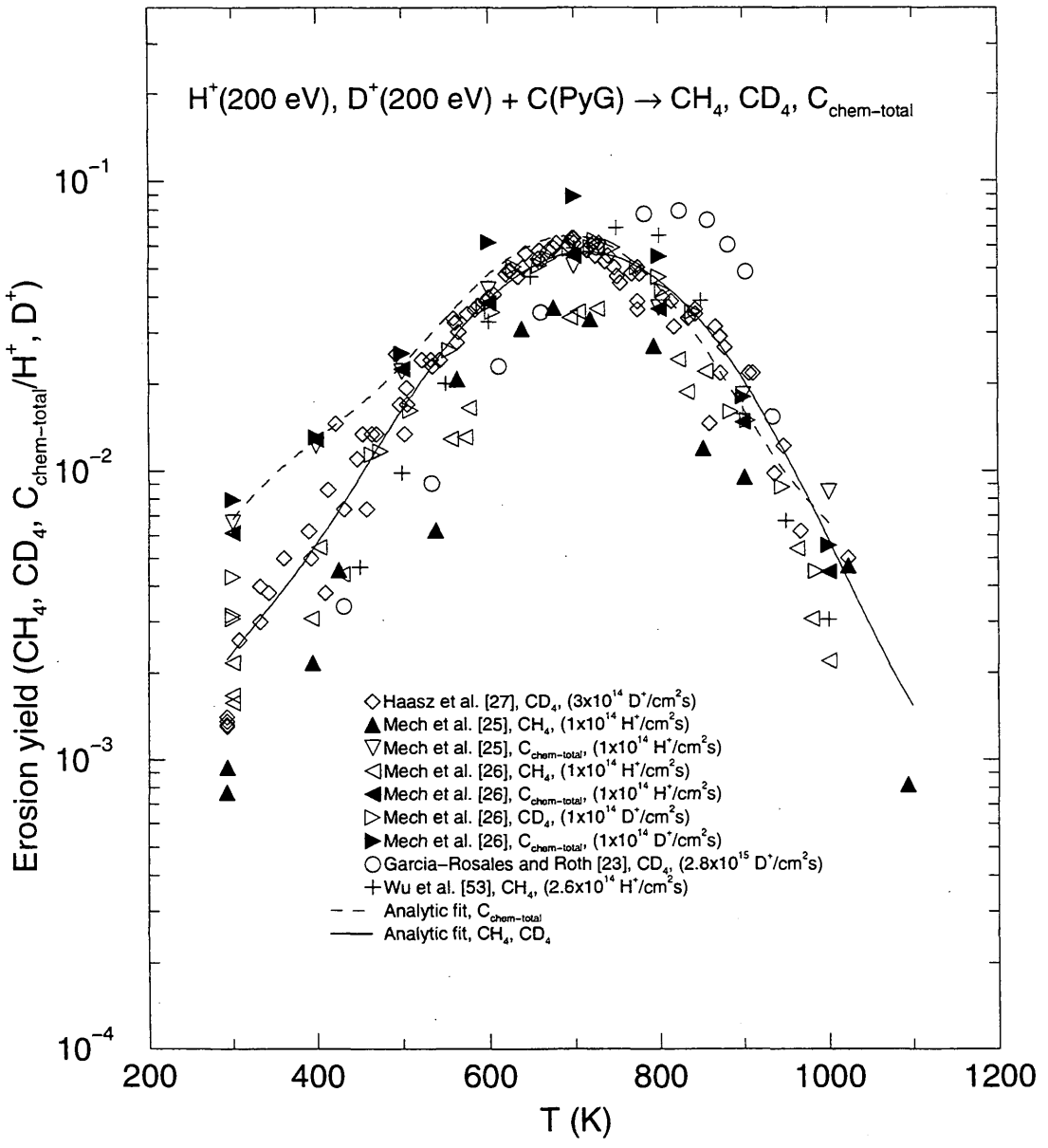

Figure 3.7: Chemical erosion yield of graphite due to 200 eV H^+ and D^+ impact, as a function of temperature.

When compared to the 1 keV case (Fig. 3.6), at 200 eV, a reduction in Y_m and T_m is observed, and the temperature profiles are somewhat broader. The data by Garcia-Rosales and Roth [23] are at a higher flux density, and this may be the reason why a higher T_m is observed. Agreement between data sets with the same ion species and energy is within ~20%. A comparison of methane and total chemical erosion yields indicates that the contribution of heavier hydrocarbons to the total erosion yield can be significant at 300 K.

The total chemical erosion yield, $Y_{chem-total}$, is found from summing the contributions: $[CH_4] + 2 \times \{[C_2H_2] + [C_2H_4] + [C_2H_6]\} + 3 \times \{[C_3H_6] + [C_3H_8]\}$, and dividing by $[H^+]$; for D^+ impact, substitute D for H.

The data are divided into two groups, $C_{chem-total}$ (H^+ and D^+) and methane (CH_4 and CD_4), and fitted separately with EYIELD7A. Fitting coefficients A_1-A_7:

$C_{chem-total}$ (H^+, D^+): [5.01070e-03, 6.94559e+02, 2.16981e+04, 3.53713e-01, 1.73319e-14, 9.09652e-03, 5.15871e+00]

CH_4, CD_4: [7.12225e-05, 6.92077e+02, 3.29118e+04, 1.01048e+00, 5.25702e-13, 7.94529e-03, 4.29824e+00]

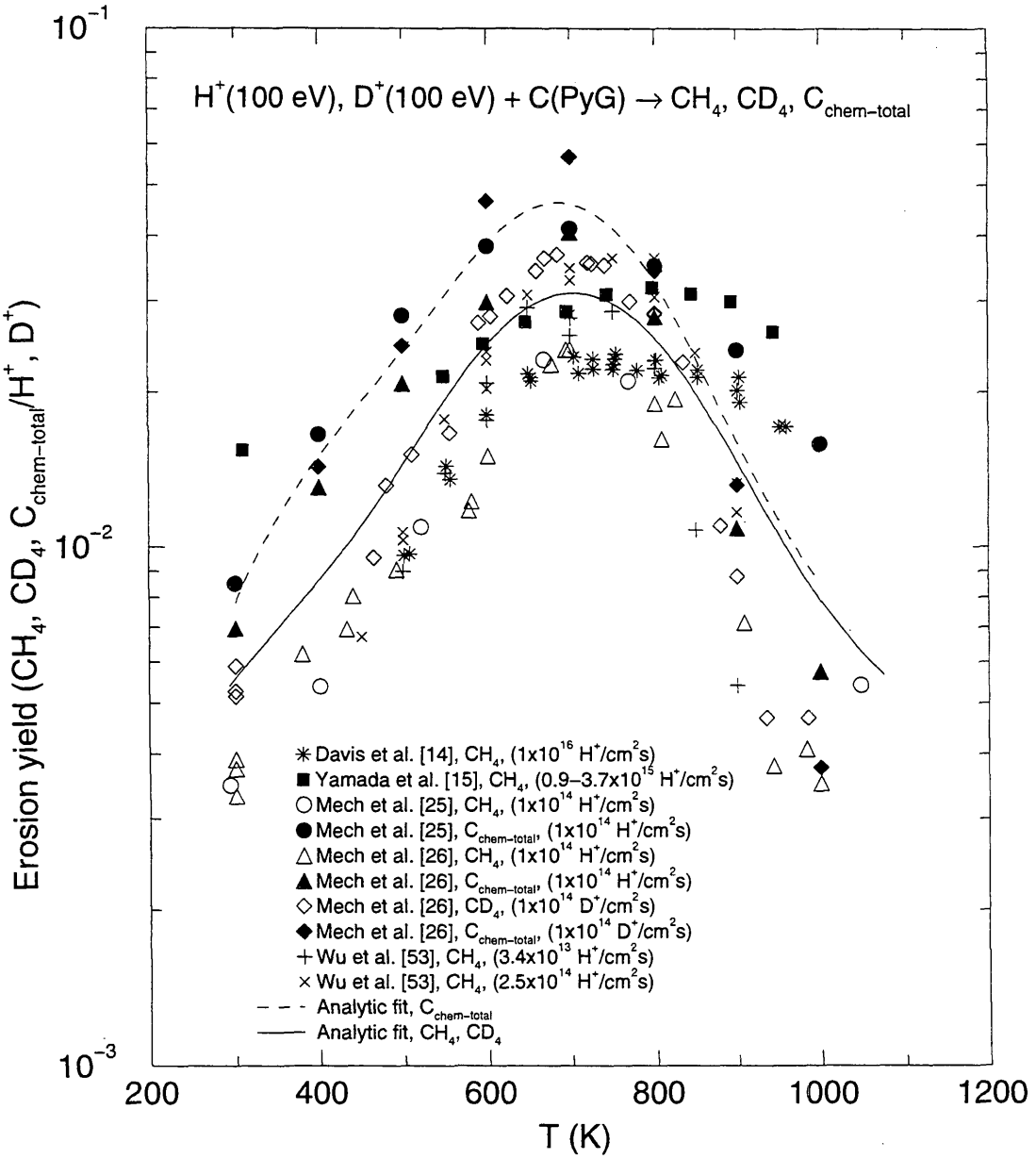

Figure 3.8: Chemical erosion yield of graphite due to 100 eV H^+ and D^+ impact, as a function of temperature.

A continued decrease in both T_m and Y_m is observed, as compared to 200 eV H^+/D^+ (Fig. 3.7). Maximum total chemical erosion yields are: Y_m~0.04 at T_m ~650-700 K. It is noted that there is a general increase in the room temperature erosion yields as compared to higher energy impact. The contribution of C_2 and C_3 hydrocarbons is about 40% of the total chemical erosion yield, with the relative contribution being dependent on temperature.

The total chemical erosion yield, $Y_{chem-total}$, is found from summing the contributions: $[CH_4] + 2 \times \{[C_2H_2] + [C_2H_4] + [C_2H_6]\} + 3 \times \{[C_3H_6] + [C_3H_8]\}$, and dividing by $[H^+]$; for D^+ impact, substitute D for H.

The data are divided into two groups, $C_{chem-total}$ (H^+ and D^+) and methane (CH_4 and CD_4), and fitted separately with EYIELD7A. Fitting coefficients A_1-A_7:

$C_{chem-total}$ (H^+, D^+): [3.99327e-02, 6.98044e+02, 2.30345e+04, -5.61363e-02, 9.10029e-15, 9.06712e-03, 5.29365e+00]

CH_4, CD_4: [1.46434e-14, 589.521e+02, 38917.9e+04, 4.32914e+00, 5.79037e-09, 0.00442034e-03, 2.64508e+00]

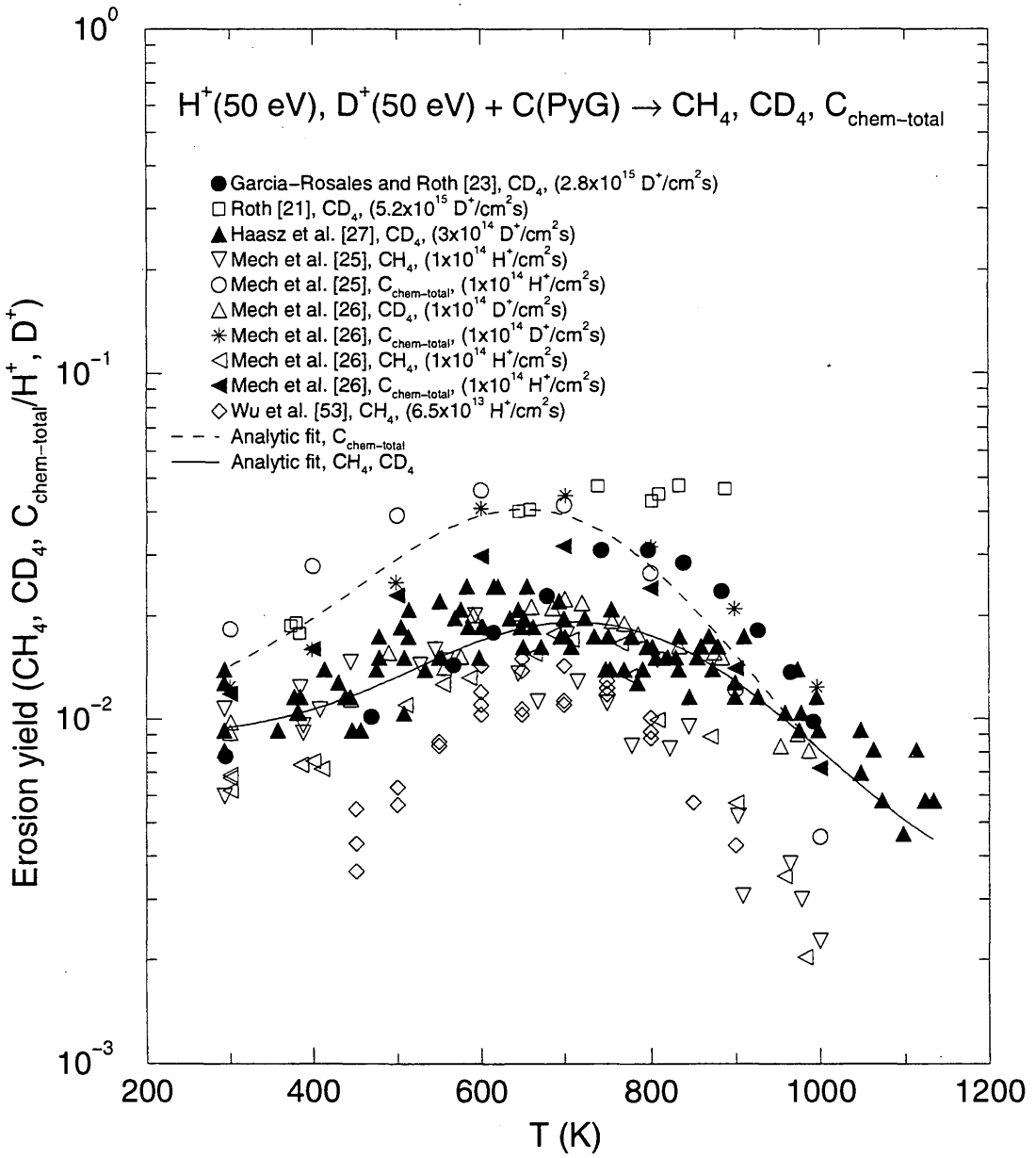

Figure 3.9: Chemical erosion yield of graphite due to 50 eV H^+ and D^+ impact, as a function of temperature.

At this ion energy (and lower energies), significantly different erosion patterns are observed, leading to uncertainties in the results of a factor of 2-3. Maximum erosion yields are: Y_m~0.03-0.05, at T_m~600 K or 800 K (depending on the data set). D^+ erosion yields are not significantly larger than H^+. Room temperature total chemical erosion yields are increased over more energetic ion bombardment to Y~0.01-0.02; these yields are a factor of 2-3 smaller than the peak erosion yields. Heavier hydrocarbons contribute ~50% to the total erosion yield.

The total chemical erosion yield, $Y_{chem-total}$, is found from summing the contributions: $[CH_4] + 2 \times \{[C_2H_2] + [C_2H_4] + [C_2H_6]\} + 3 \times \{[C_3H_6] + [C_3H_8]\}$, and dividing by $[H^+]$; for D^+ impact, substitute D for H.

The data are divided into two groups, $C_{chem-total}$ (H^+ and D^+) and methane (CH_4 and CD_4), and fitted separately with EYIELD7A. Fitting coefficients A_1-A_7:

$C_{chem-total}$ (H^+, D^+): [2.27401e-03, 6.50347e+02, 4.31717e+04, 3.93147e-01, 4.23820e-06, 3.86650e-03, 1.61146e+00]

CH_4, CD_4: [1.47344e-03, 7.16531e+02, 5.87093e+04, 3.25764e-01, 3.56546e-04, 2.14365e-03, 6.7817e-01]

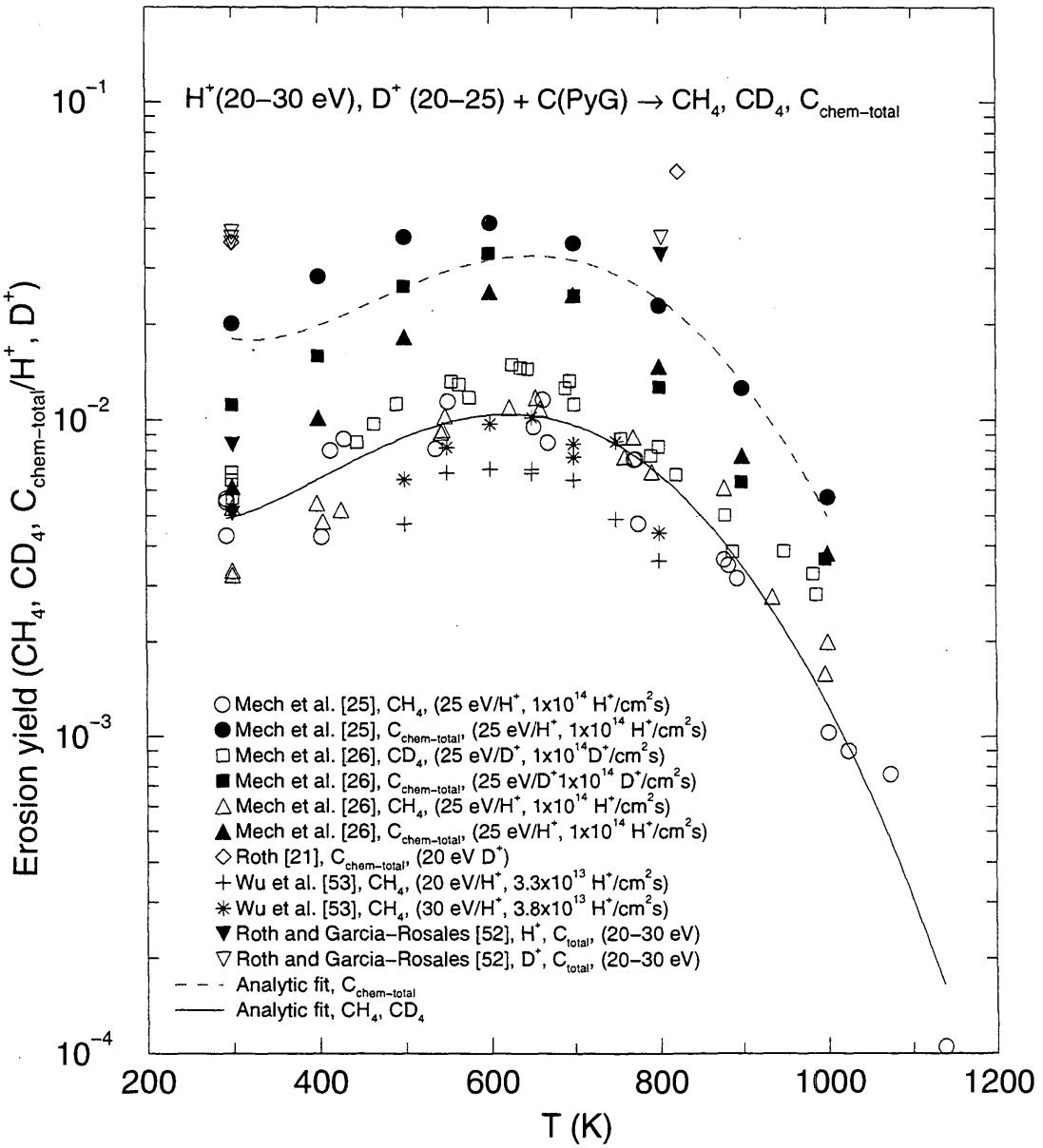

Figure 3.10: Chemical erosion yield of graphite due to 20-30 eV H^+ and D^+ impact, as a function of temperature.

Maximum total chemical erosion yields of Y_m~0.03-0.04 are observed at ~600 K. Total chemical erosion yields at room temperature are: Y_m~0.01-0.04. Heavier hydrocarbons contribute > 50% to the total chemical erosion yield.

The total chemical erosion yield, $Y_{chem-total}$, is found from summing the contributions: $[CH_4] + 2 \times \{[C_2H_2] + [C_2H_4] + [C_2H_6]\} + 3 \times \{[C_3H_6] + [C_3H_8]\}$, and dividing by $[H^+]$; for D^+ impact, substitute D for H.

The data are divided into two groups, $C_{chem-total}$ (H^+ and D^+) and methane (CH_4 and CD_4), and fitted separately with EYIELD7A. Fitting coefficients A_1-A_7:

$C_{chem-total}$ (H^+, D^+): [8.57284e+28, 9.75243e+02, 4.05067e+04, -1.04098e+01, -8.00000e-24, -9.00000e-02, -3.80000e+01]

CH_4, CD_4: [5.46490e+18, 8.88294e+02, 4.60076e+04, -7.17606e+00, -8.80348e-24, -9.46521e-02, -3.86175e+01]

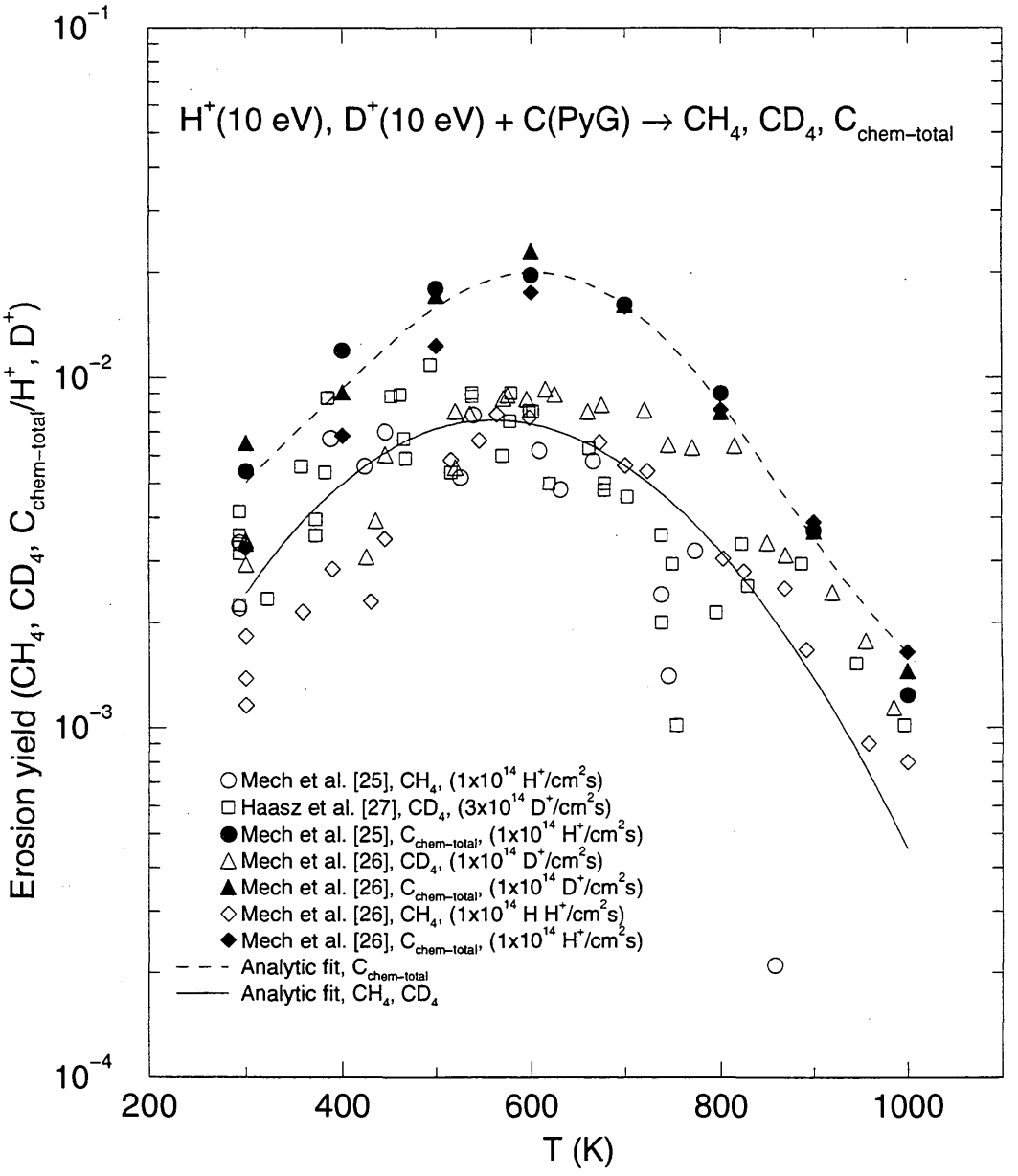

Figure 3.11: Chemical erosion yield of graphite due to 10 eV H^+ and D^+ impact, as a function of temperature.

Only one source of data is available for erosion at this ion energy. Even so, there is a scatter in the data of a factor of 3-4. Maximum total chemical erosion yields are: $Y_m \sim 0.2$, with no significant differences observed between H^+ and D^+. As at 20-30 and 50 eV/H^+, room temperature yields are ~2-3 times smaller than Y_m. Heavier hydrocarbons contribute >50% to the total chemical erosion yield.

The total chemical erosion yield, $Y_{chem-total}$, is found from summing the contributions: $[CH_4] + 2 \times \{[C_2H_2] + [C_2H_4] + [C_2H_6]\} + 3 \times \{[C_3H_6] + [C_3H_8]\}$, and dividing by $[H^+]$; for D^+ impact, substitute D for H.

The data are divided into two groups, $C_{chem-total}$ (H^+ and D^+) and methane (CH_4 and CD_4), and fitted separately with EYIELD7A. Fitting coefficients A_1-A_7:

$C_{chem-total}$ (H^+, D^+): [1.52689e-04, 5.9293e+02, 3.49716e+04, 7.17836e-01, 1.17349e-10, 7.46550e-03, 3.44444e+00]

CH_4, CD_4: [3.49511e-08, 4.16245e+00, 8.07690e+04, 1.98156e+00, 6.83914e+05, 5.80466e-01, 2.63443e+01]

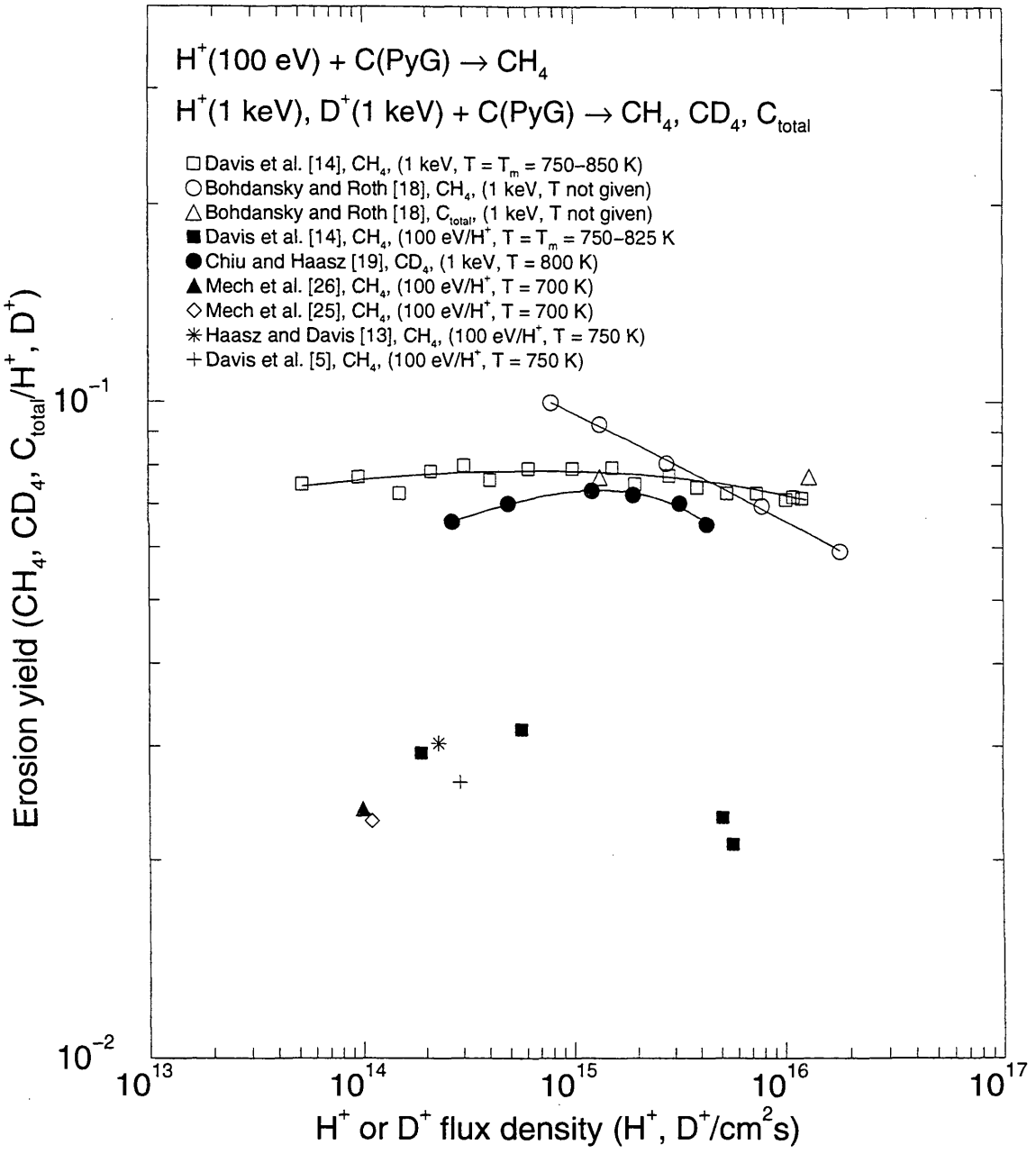

Figure 3.12: Methane yield due to 100 eV H^+, 1 keV H^+ and 1 keV D^+ impact on graphite, as a function of flux density.

The flux dependence of the erosion yield is very sensitive to the target temperature at which the measurement is made. Because the temperature, T_m, at which the maximum erosion yield, Y_m, occurs is dependent on flux density, flux-dependent measurements at constant temperature have a much larger variation in yield than measurements which follow Y_m. At 1 keV, there appears to be a shallow maximum in Y_m at $\sim 10^{15}$ $H^+(D^+)/cm^2s$. At 100 eV/H^+, uncertainties in the data are somewhat larger, and it is difficult to determine a flux density dependence.

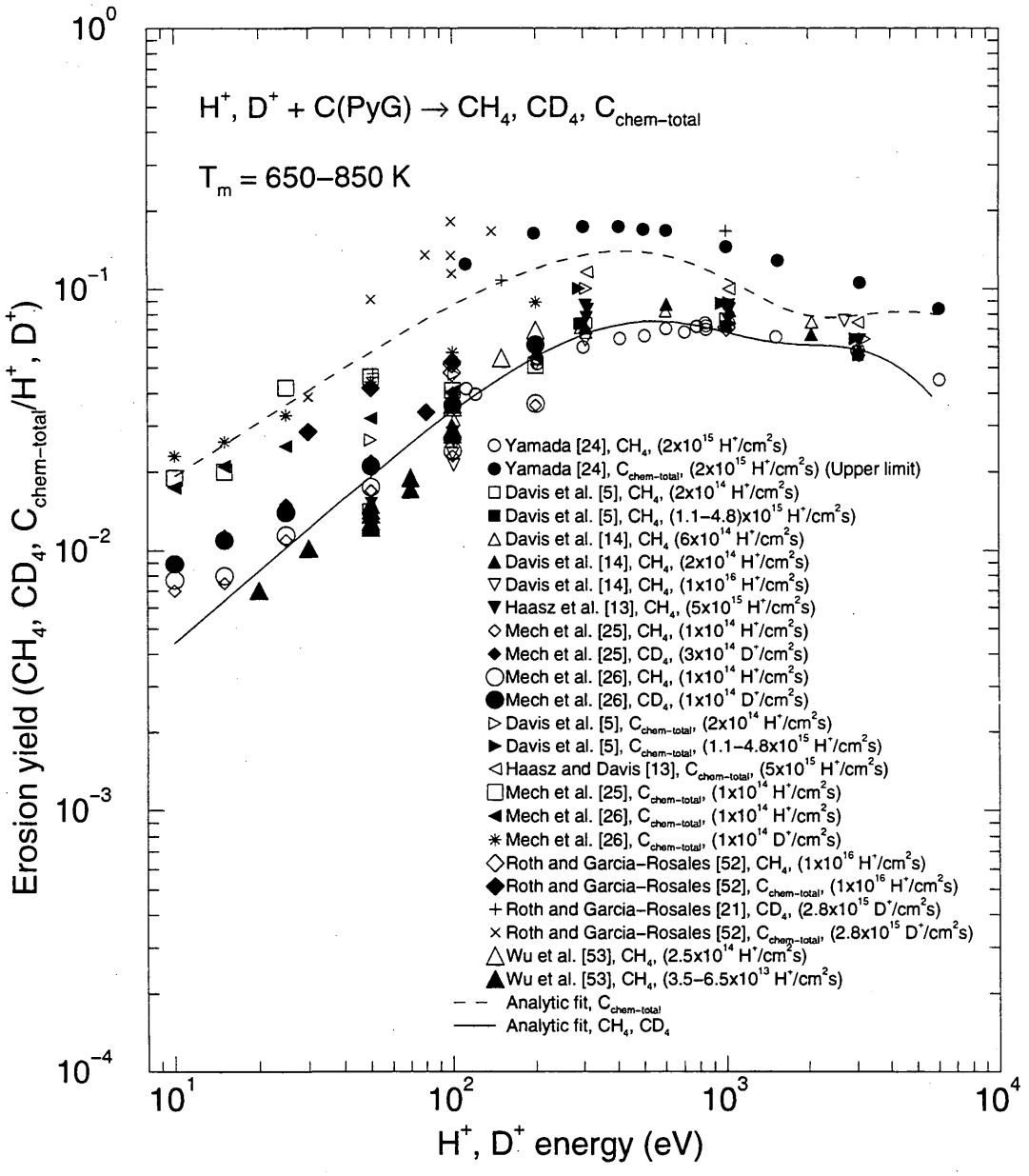

Figure 3.13: Energy dependence of Y_m for H^+ and D^+ impact on graphite.

The chemical erosion yield has a maximum at 300-1000 eV. Above this energy there is a gradual decrease in yield, while there is a steeper decrease at lower energies. T_m is varying with both energy and flux density, from 650 K at low energy and low flux density to 850 K at high energy and high flux density. There is no evidence for a threshold in the erosion process down to 10 eV.

The total chemical erosion yield, $Y_{chem-total}$, is found from summing the contributions: $[CH_4] + 2 \times \{[C_2H_2] + [C_2H_4] + [C_2H_6]\} + 3 \times \{[C_3H_6] + [C_3H_8]\}$, and dividing by $[H^+]$; for D^+ impact, substitute D for H.

The data are divided into two groups, $C_{chem-total}$ (H^+ and D^+) and methane (CH_4 and CD_4), and fitted separately with EYIELD7A. Fitting coefficients A_1-A_7:

$C_{chem-total}$ (H^+, D^+): [2.98287e+07, -1.75200e+01, 1.71170e+01, 7.27649e-01, 5.79133e-02, 1.38486e-01, 6.41777e-01]

CH_4, CD_4: [3.90115e+03, -7.16921e+00, 5.49761e+00, 1.02596e+00, 6.68507e-02, 3.48429e-01, 0.829478e-01]

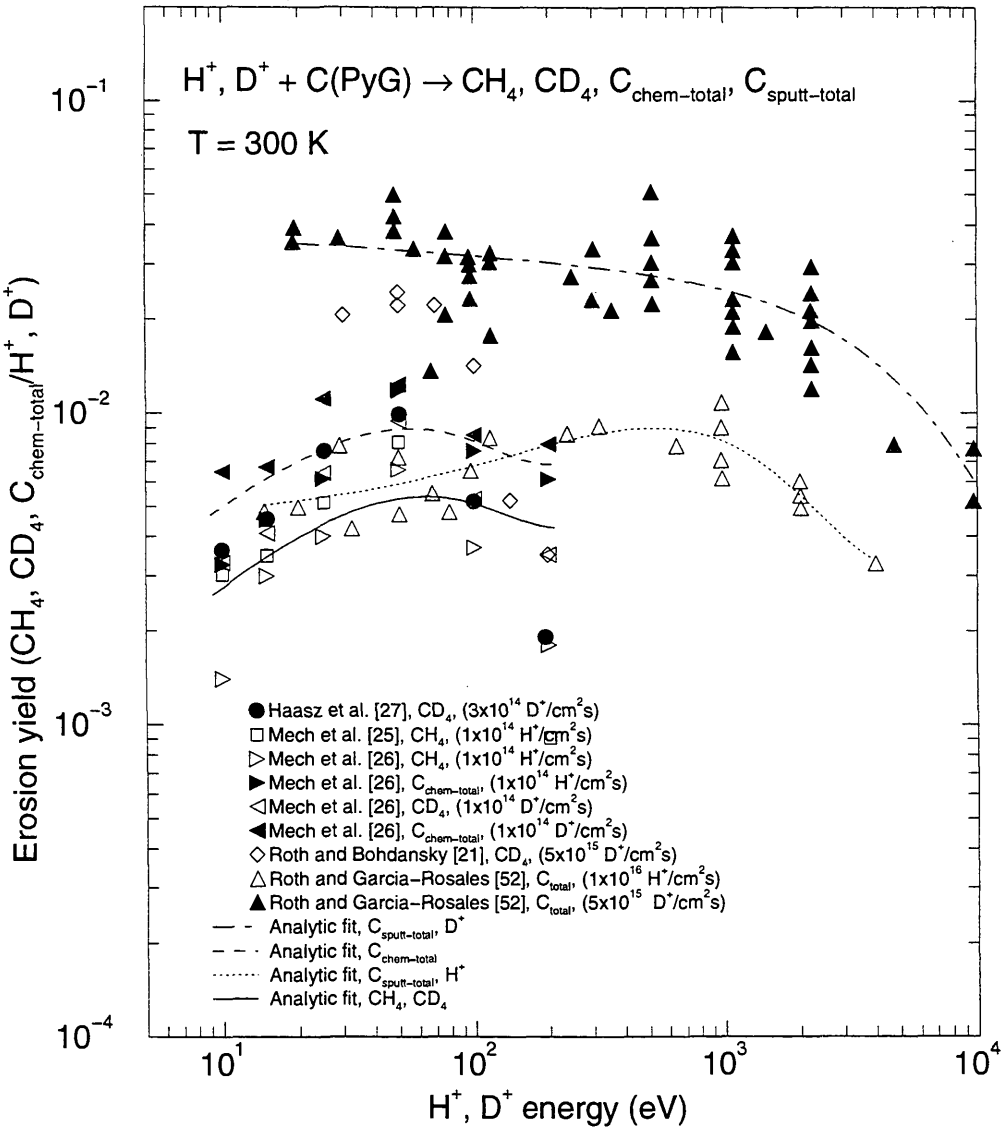

Figure 3.14: Energy dependence of the chemical erosion yield at 300 K for H^+ and D^+ impact on graphite in the 10 eV-10 keV energy range.

Room temperature total chemical erosion yields exhibit a minor energy dependence; Y_m~0.01-0.02 near 50 eV. Total sputtering yields tend to be nearly constant below ~1 keV. D^+ results from Garching [21] tend to be about 3-4 times larger than results from Toronto [25-27], while good agreement is seen for the H^+ data. The Garching results indicate a strong H^+/D^+ isotopic dependence, while the Toronto results show similar yields for both isotopes.

The total chemical erosion yield, $Y_{chem-total}$, is found from summing the contributions: $[CH_4] + 2 \times \{[C_2H_2] + [C_2H_4] + [C_2H_6]\} + 3 \times \{[C_3H_6] + [C_3H_8]\}$, and dividing by $[H^+]$; for D^+ impact, substitute D for H. $Y_{sputt-total}$ is the total sputtering yield as measured by mass loss, and includes chemical erosion and physical sputtering yields.

The data are divided into four groups, $C_{sputt-total}$ (D^+), $C_{sputt-total}$ (H^+), $C_{chem-total}$ (H^+ and D^+) and methane (CH_4 and CD_4), and fitted separately with EYIELD5A. Fitting coefficients A_1-A_5:
$C_{sputt-total}$ (D^+): [4.04526e-02, 1.65342e-04, -4.87384e-02, 4.04639e-05, 3.35005e-01]
$C_{sputt-total}$ (H^+): [1.63600e-04, 1.20490e-03, 6.64900e-01, 4.73300e-03, -5.41400e-02]
$C_{chem-total}$ (H^+, D^+): [9.45550e-04, 1.71528e-02, 7.14742e-01, 2.05177e-04, 6.20837e-01]
CH_4, CD_4: [4.78244e-04, 1.56349e-02, 7.37187e-01, 1.25311e-04, 6.14271e-01]

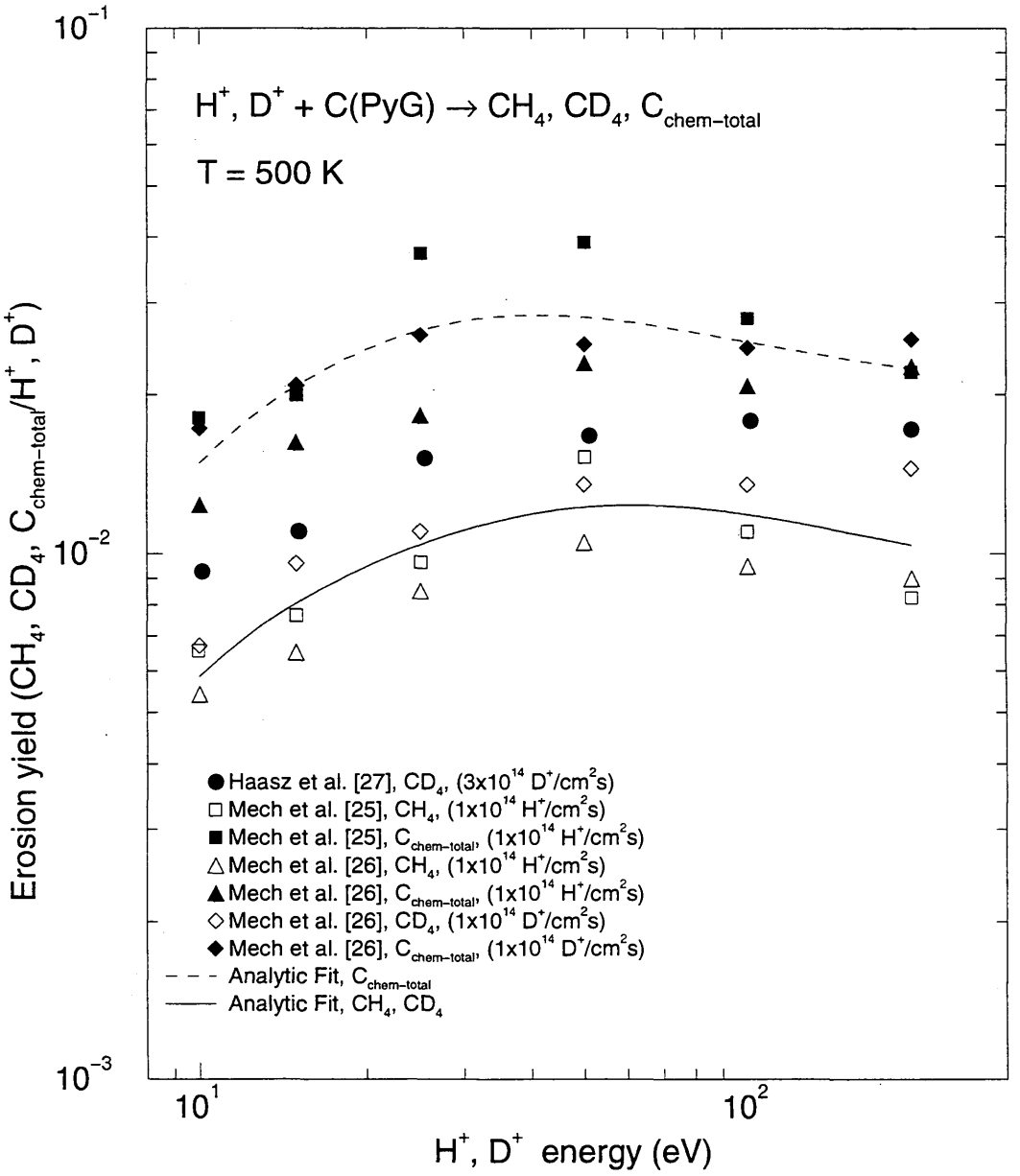

Figure 3.15: Energy dependence of the chemical erosion yields at 500 K for H^+ and D^+ impact on graphite in the 10-200 eV energy range.

At 500 K, there is a weaker energy dependence than observed at 300 K (Fig. 3.14), or at T_m (Fig. 3.13). The maximum erosion yield is found at ~50-100 eV.

The total chemical erosion yield, $Y_{chem-total}$, is found from summing the contributions: $[CH_4] + 2 \times \{[C_2H_2] + [C_2H_4] + [C_2H_6]\} + 3 \times \{[C_3H_6] + [C_3H_8]\}$, and dividing by $[H^+]$; for D^+ impact, substitute D for H.

The data are divided into two groups, $C_{chem-total}$ (H^+ and D^+) and methane (CH_4 and CD_4), and fitted separately with EYIELD4D. Fitting coefficients A_1-A_4:
$C_{chem-total}$ (H^+, D^+): [3.50786e-02, -8.13021e+01, 8.58146e-01, -9.14441e+01]
CH_4, CD_4: [1.62560e-02, -1.60275e+02, 1.06371e+00, -1.69863e+02]

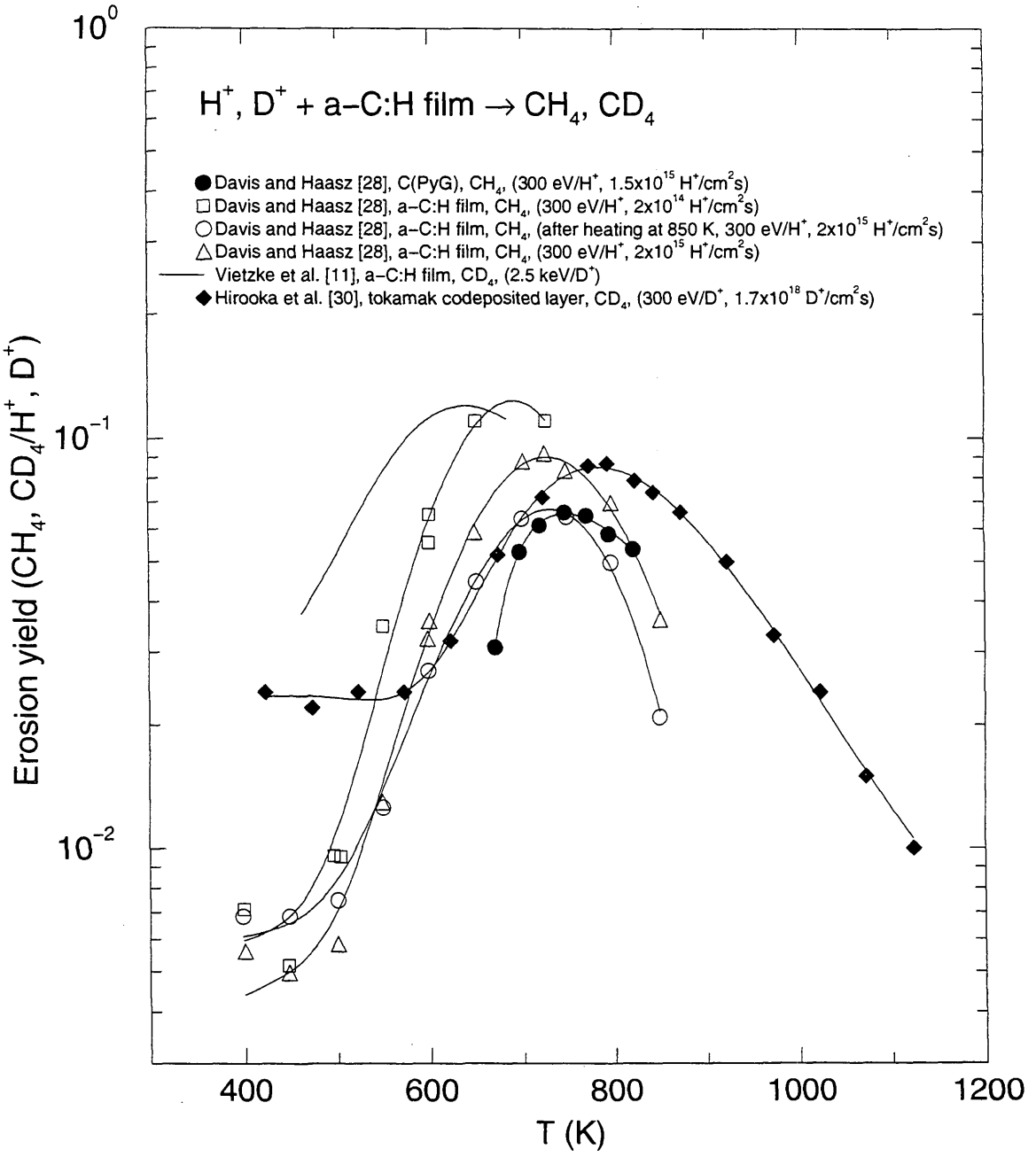

Figure 3.16: Methane yield due to 300 eV H^+ and 2.5 keV D^+ impact on a-C:H films, and D^+ impact on tokamak codeposited layers, as a function of temperature.

The temperature dependence of the erosion of a-C:H films is similar to pyrolytic graphite (shown for comparison), except that yields are somewhat higher, until the films are baked to drive off the hydrogen. In the 300 eV H^+ case, erosion with a lower flux density leads to a decrease in T_m and a small increase in Y_m, similar to the effect of flux density change on graphite (Fig. 3.12). The flux density is not available for the results of Vietzke et al. [11]. For the codeposited layer [30], the maximum erosion yield is similar to D^+ on graphite, however, the yield below ~600 K is much larger, and not characteristic of typical erosion patterns.

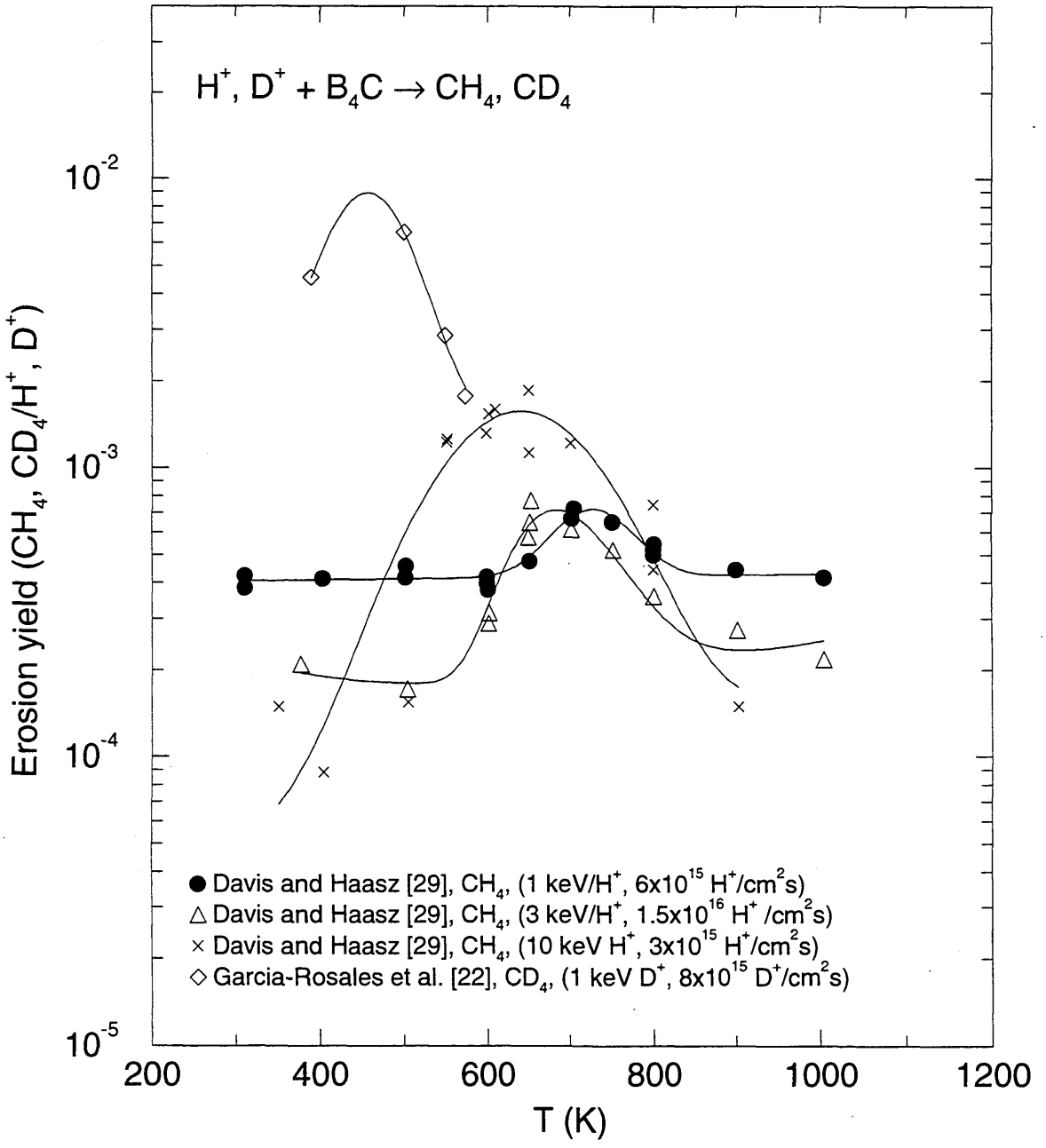

Figure 3.17: Methane yield due to H^+ and D^+ impact on B_4C, as a function of temperature.

Erosion yields were found to have long transient behaviour [29] which made determination of steady-state yields difficult. Generally, erosion yields are 1-2 orders of magnitude smaller than for graphite. Data from Garcia-Rosales et al. [22] at temperatures above 600 K have not been reproduced here due to the difficulty in extracting small signals from the linear plots in the original publication.

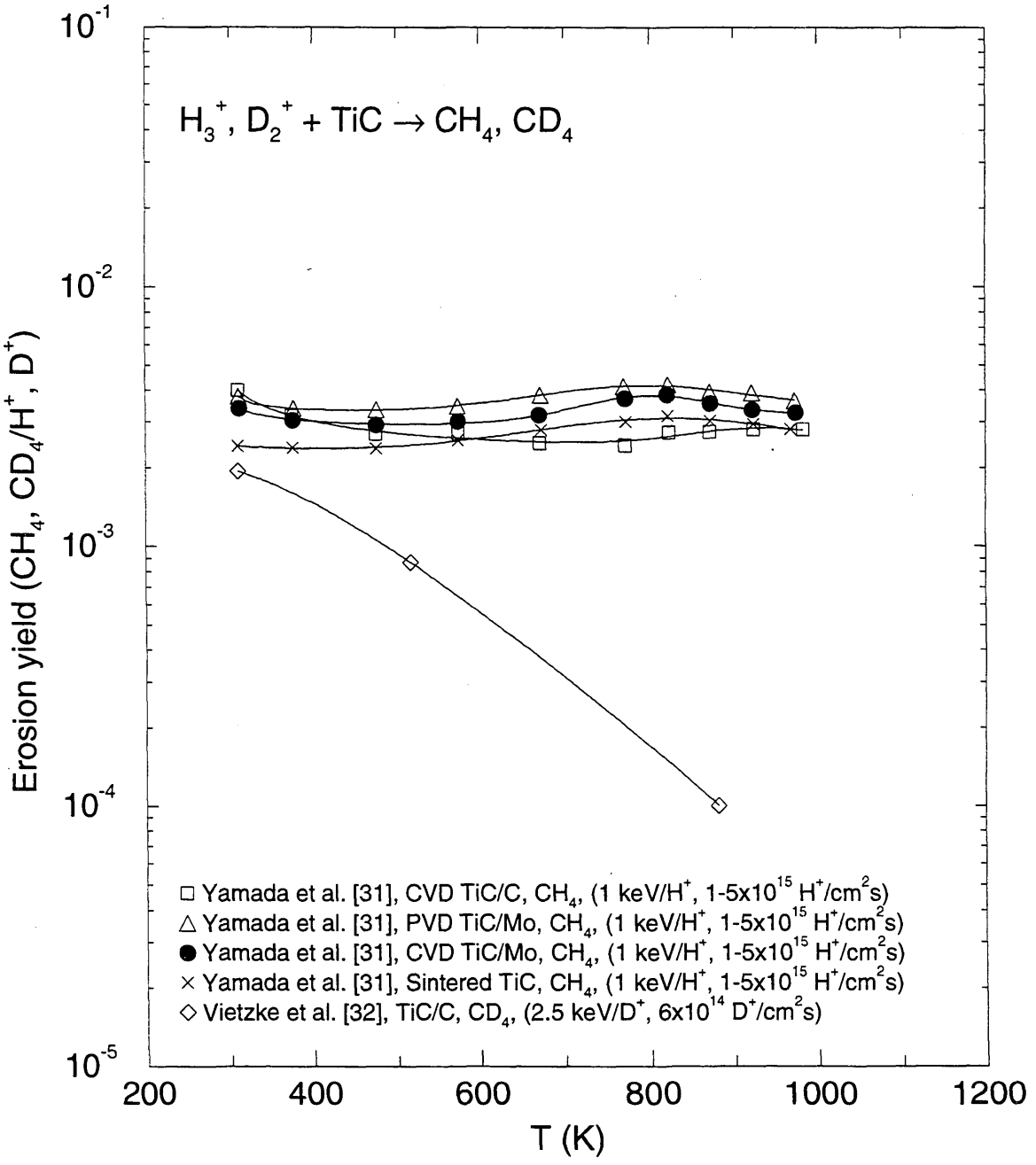

Figure 3.18: Methane yield due to 1 keV H^+ and 2.5 keV D^+ impact on TiC, as a function of temperature.

Erosion yields from different laboratories show markedly different behaviour. As in the case of B_4C (Fig. 3.17), strong transient effects are observed [32]. Different coating techniques studied by Yamada et al. [31] lead to TiC layers with similar erosion characteristics.

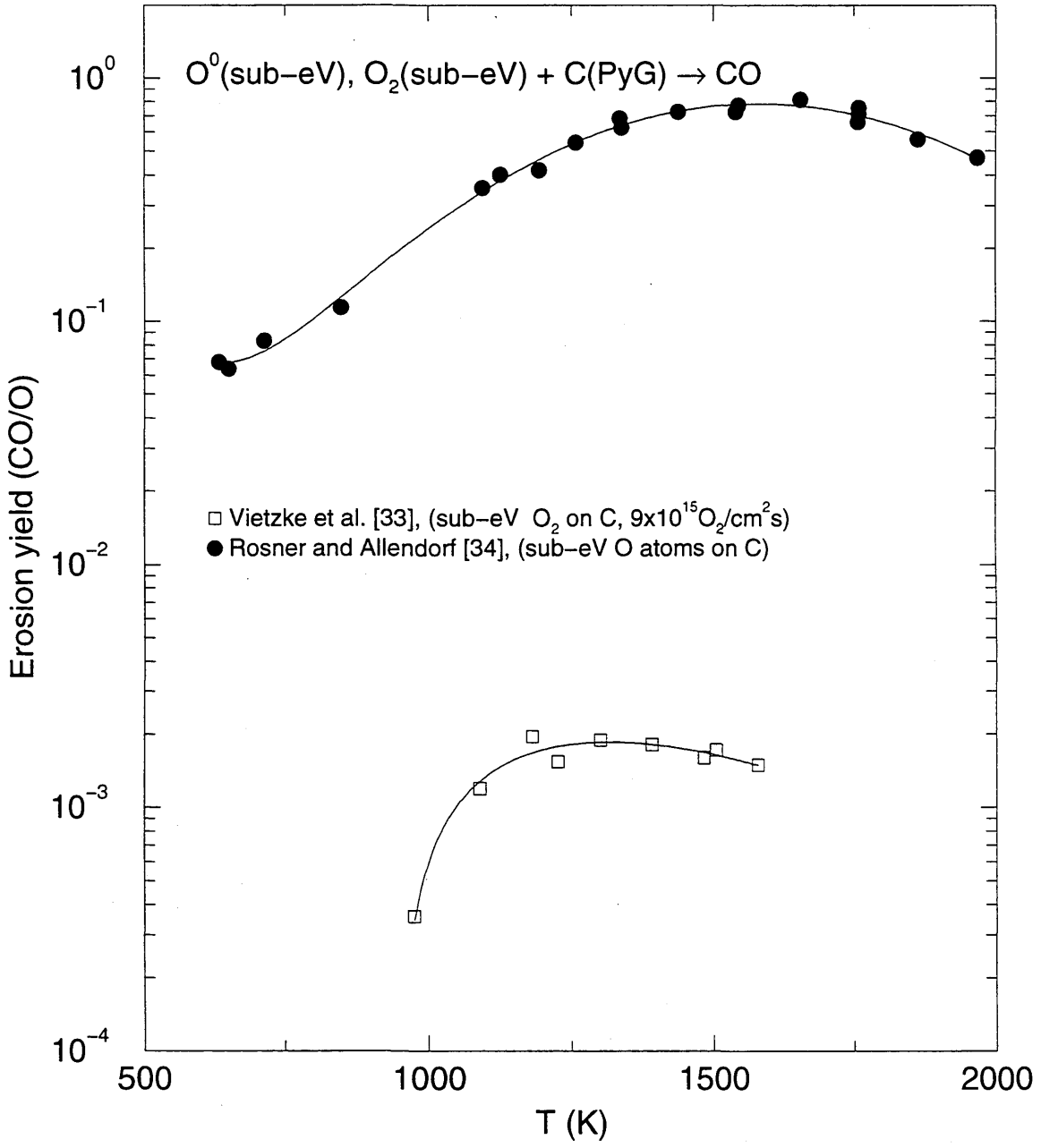

Figure 3.19: Temperature dependence of the erosion of graphite due to exposure to sub-eV oxygen atoms and molecules.

The maximum erosion yield is almost 3 orders of magnitude higher for O^0 than O_2. The temperature for maximum erosion, T_m, is much higher than that observed for H^0 or H^+-induced erosion: ~1400 K for O_2 and ~1600 K for O^0.

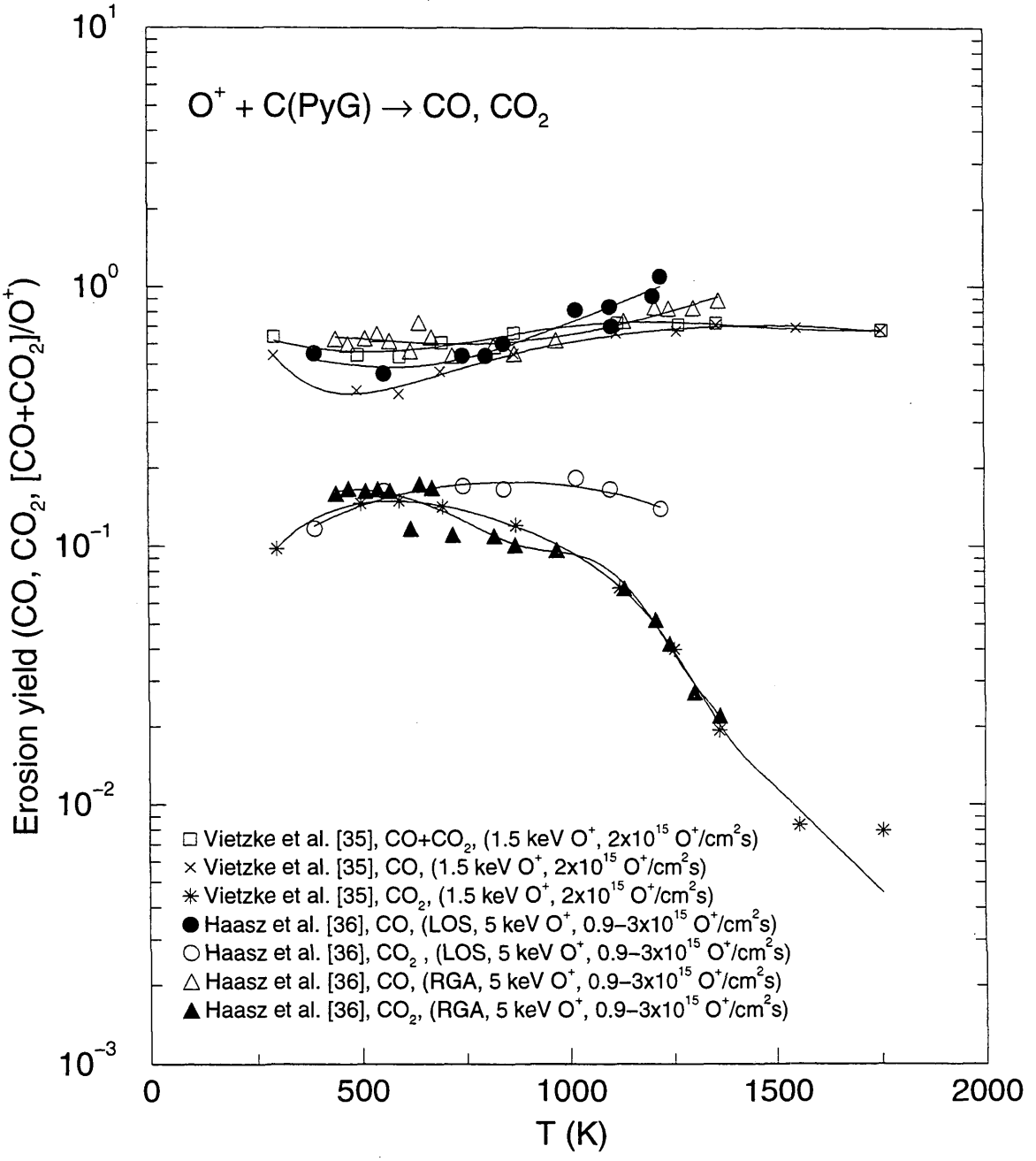

Figure 3.20: The erosion of graphite due to energetic O^+ impact as a function of temperature.

The total chemical erosion yields $\{[CO] + [CO_2]\}/[O^+]$~0.6-1.0 for temperatures in the range 300 to 1800 K. (Yields > 1 are due to difficulties in calibration of line-of-sight experiments [36].) CO_2 production is generally much smaller than CO, and has a more pronounced temperature dependence. No reemission of O_2, nor other oxygen-containing molecules are observed [36]. LOS refers to line-of-sight and RGA to residual gas analysis.

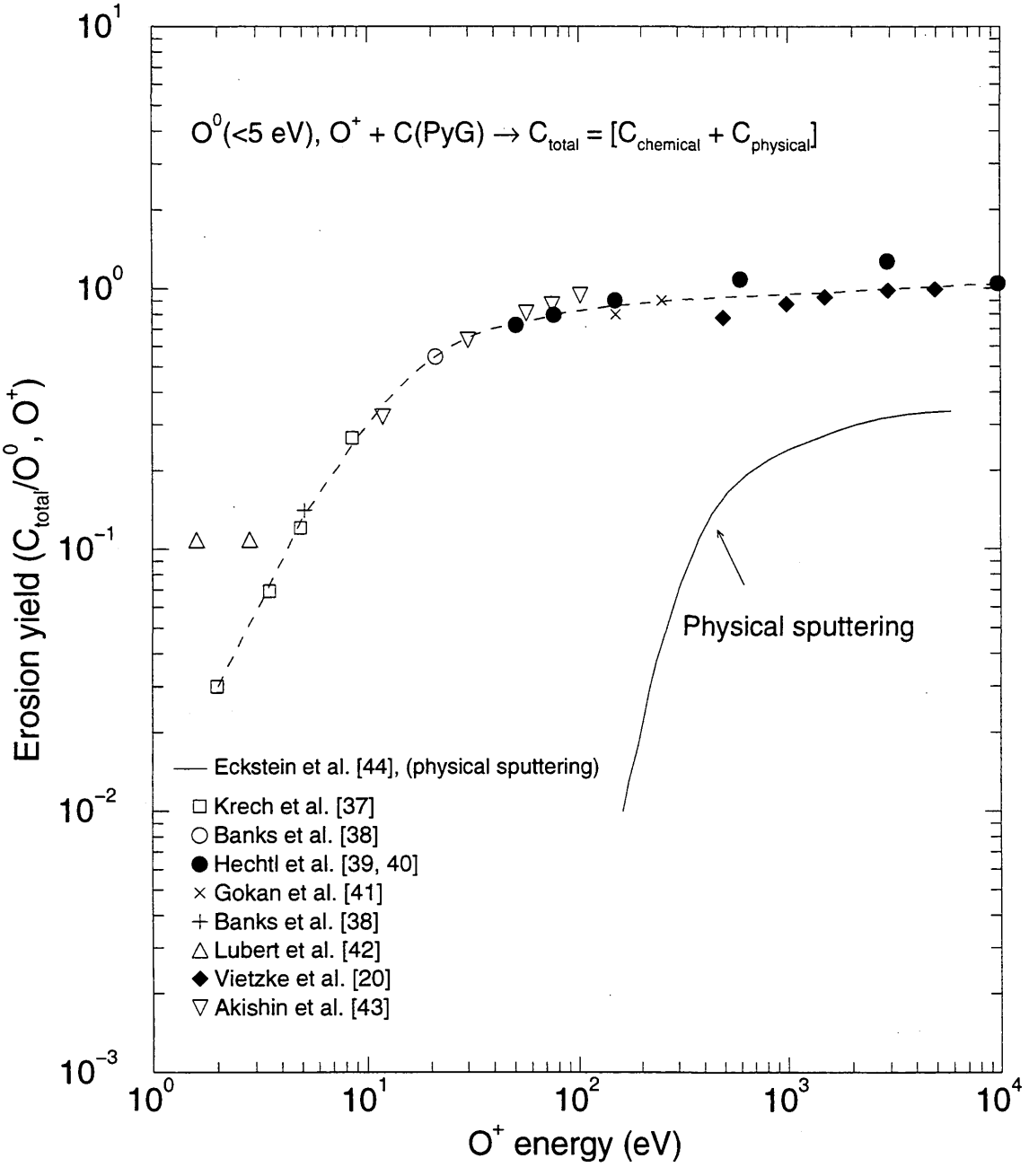

Figure 3.21: Energy dependence of the erosion yield of graphite due to O^+ and O^0 impact at 300 K, from 2 eV to 10 keV.

For O^+ energies > 100 eV, erosion yields are near unity. Below 100 eV, the erosion yield decreases sharply. At < 5 eV, there is a discrepancy in the results by different investigators; one shows a continued decrease in yield [37], while the other shows a leveling off at ~0.1 [42]. Physical sputtering levels are shown for comparison, and have been added to some chemical erosion results [20] in order to obtain a total erosion yield.

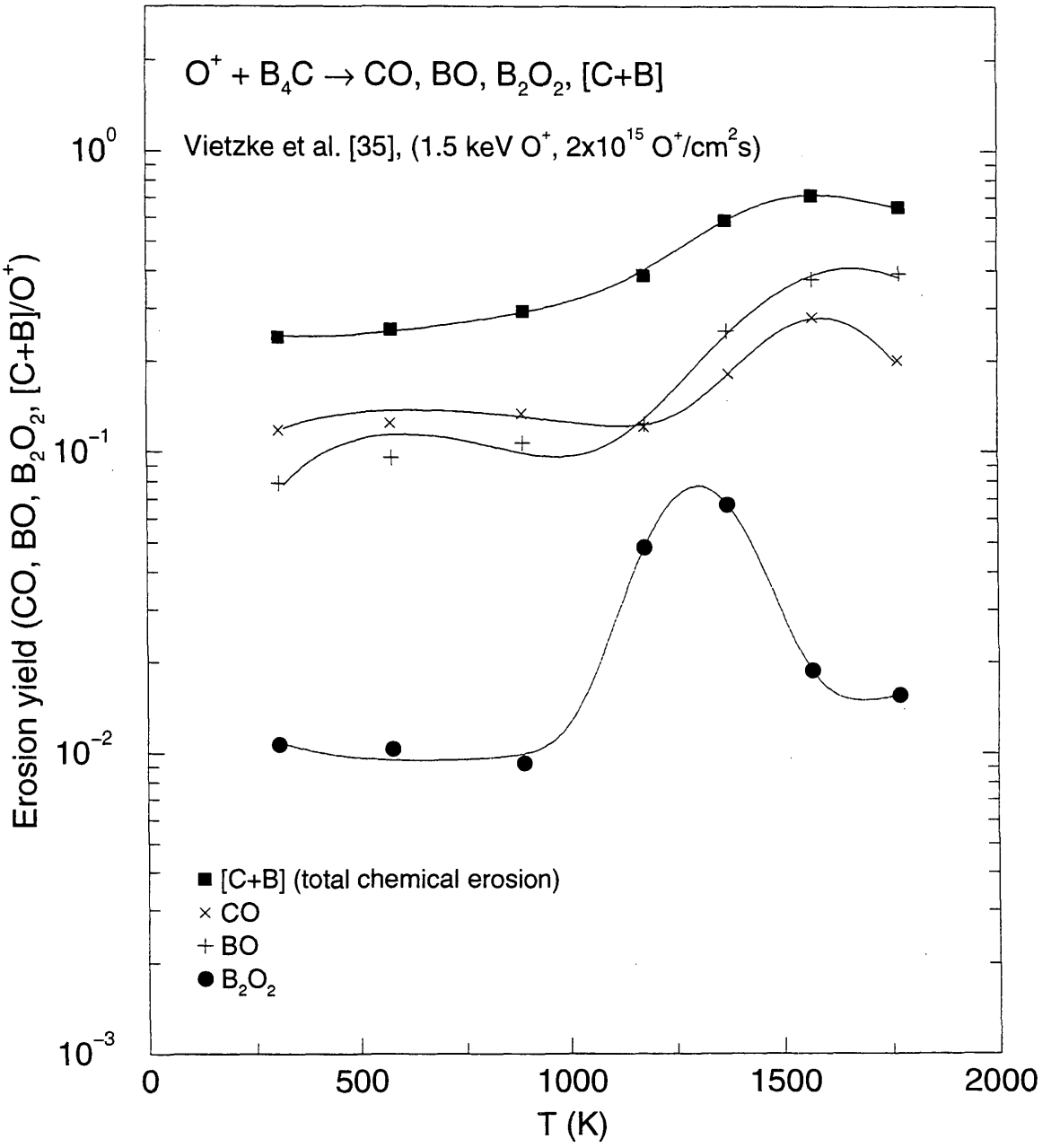

Figure 3.22: Chemical erosion of B_4C due to O^+ impact, as a function of temperature.

The primary species produced are BO and CO, with lesser amounts of more complex molecules. The maximum erosion yield is near 1600 K.

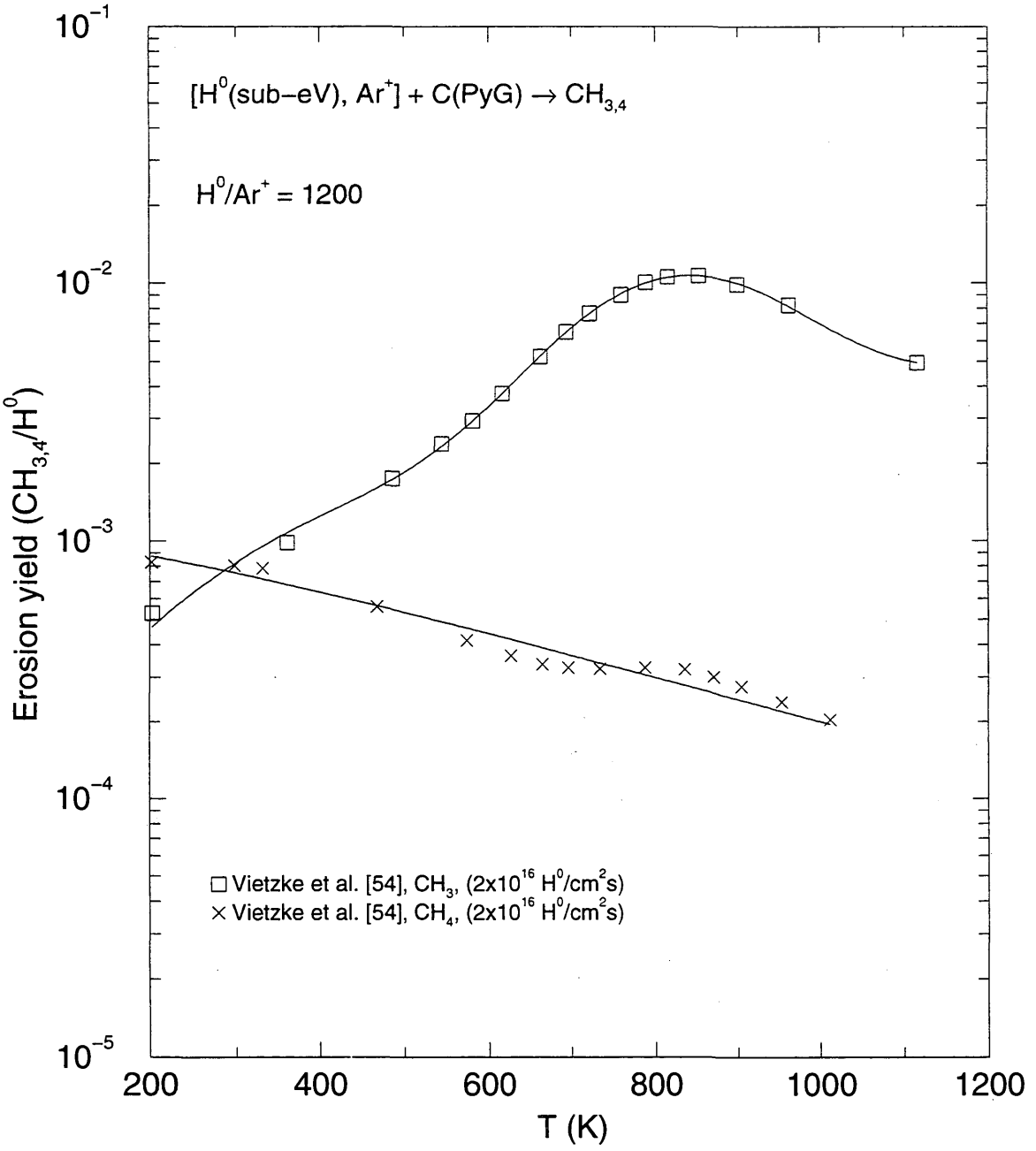

Figure 3.23: Synergistic chemical erosion of graphite due to combined sub-eV H^0 and 5 keV Ar^+, as a function of temperature.

Line-of-sight measurements indicate that the CH_3 radical is the dominant erosion product, with lesser amounts of CH_4.

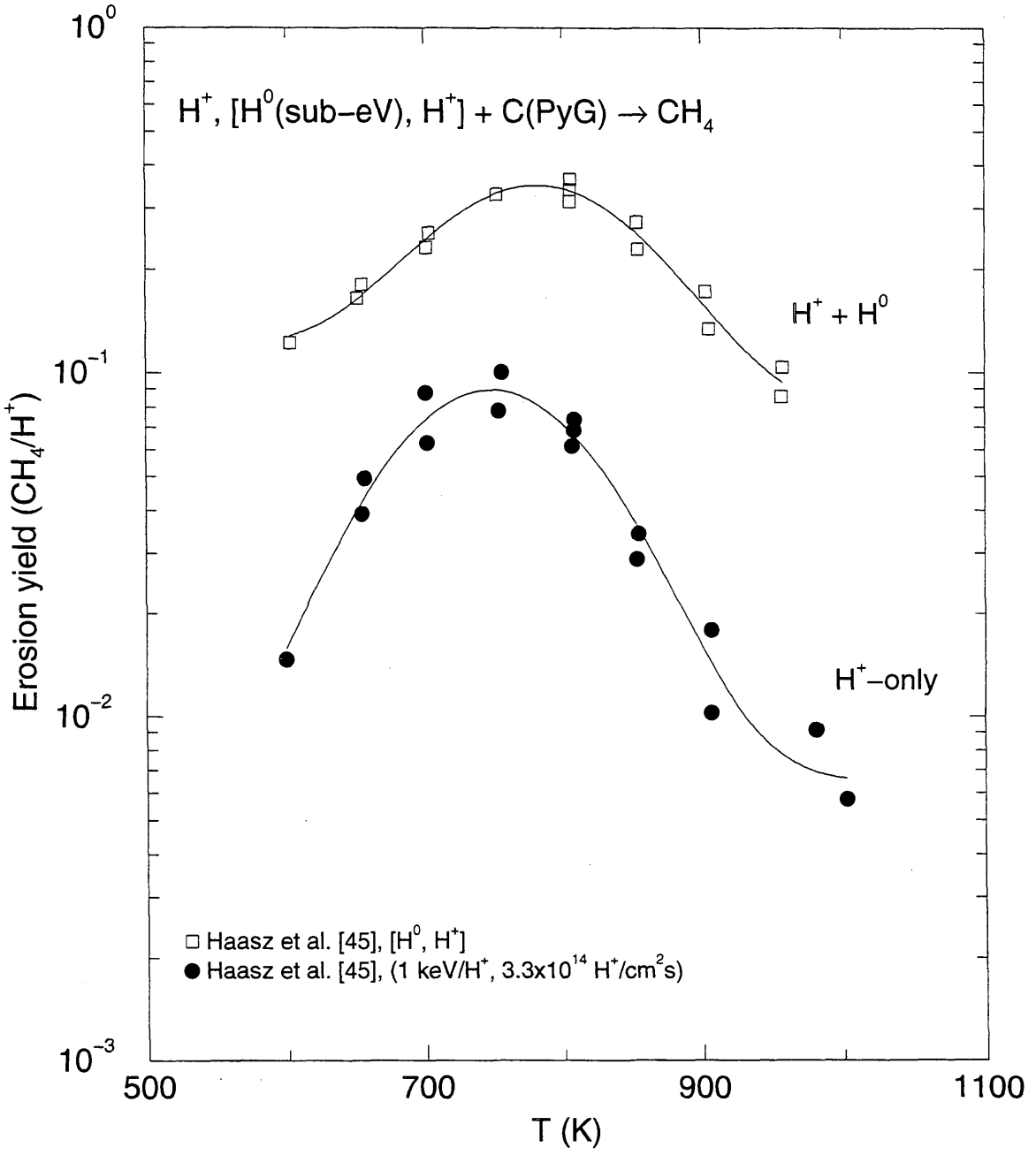

Figure 3.24: Synergistic chemical erosion of graphite due to combined sub-eV H^0 and 1 keV H^+, as a function of temperature.

Methane yield is shown for H^+-only impact and combined H^+ and H^0, with a flux ratio, $[H^+]/[H^0]$, of ~0.2. The addition of H^0, which on its own has a much smaller (100x) erosion yield, enhances the methane yield by a factor of 5-10.

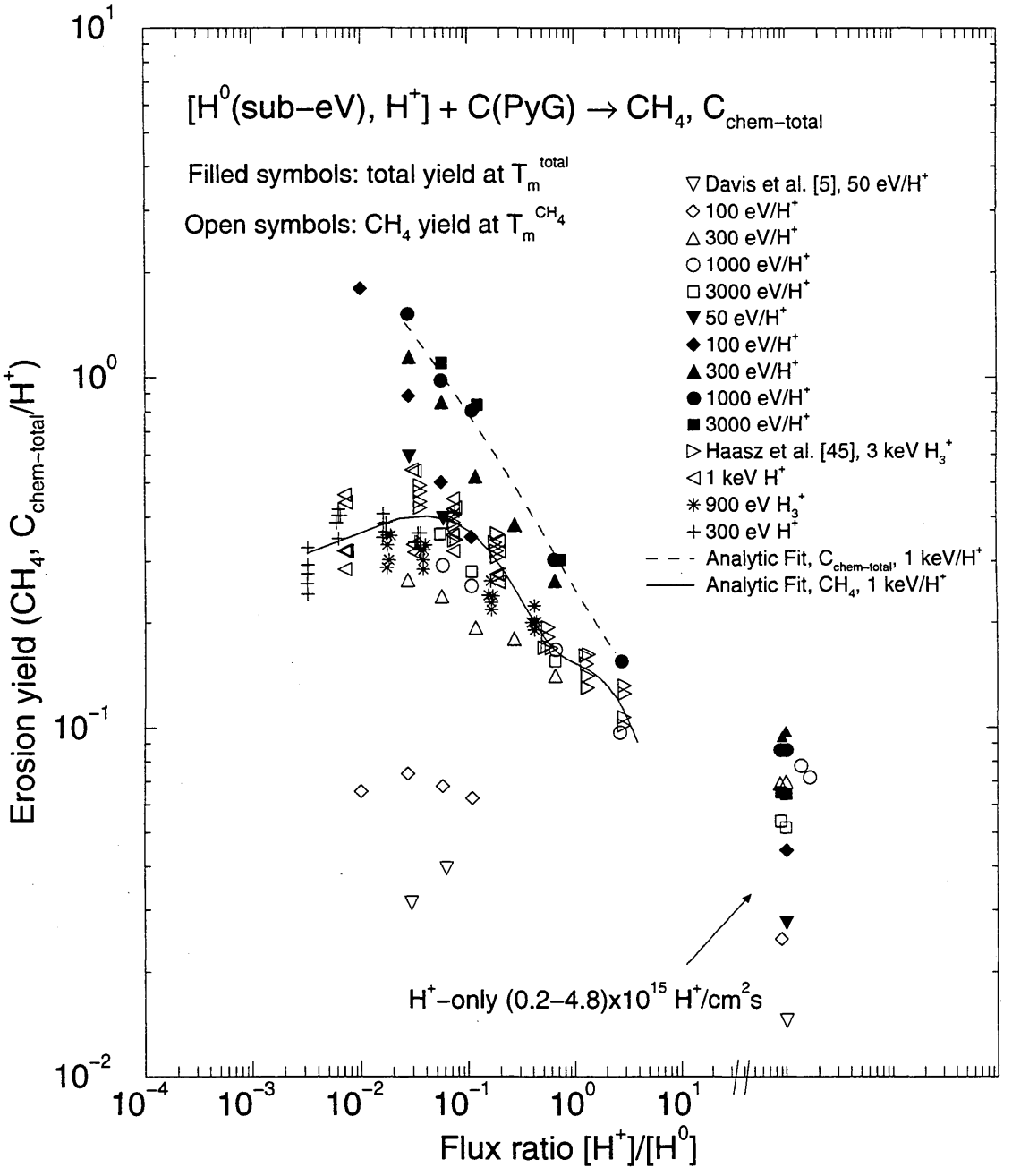

Figure 3.25: Synergistic chemical erosion of graphite due to combined sub-eV H^0 and energetic H^+, normalized by the H^+ flux, as a function of the $[H^+]/[H^0]$ flux ratio.

Yields are normalized by the H^+ flux only. The total yields increase to >1 during combined H^+ and H^0 impact for $[H^+]/[H^0]$ flux ratios of $\lesssim$0.1. Near-surface damage due to energy deposition from the energetic H^+ ions leads to enhanced reactivity of the graphite to the sub-eV H^0. Because the hydrocarbon production is normalized by the H^+ flux only, yields larger than those normally associated with H^+ erosion of graphite are observed.

The total chemical erosion yield, $Y_{chem-total}$, is found from summing the contributions: $[CH_4] + 2 \times \{[C_2H_2] + [C_2H_4] + [C_2H_6]\} + 3 \times \{[C_3H_6] + [C_3H_8]\}$, and dividing by $[H^+]$.

The data are divided into two groups, $C_{chem-total}$ (1 keV/H^+) and CH_4 (1 keV/H^+), and fitted separately with EYIELD7A and EYIELD5A, respectively. Fitting coefficients A_1-A_7:

$C_{chem-total}$ (H^+): [1.92300e+03, -3.80860e+01, 3.15170e+02, 1.74610e-01, 6.04770e+01, 5.66540e+00, 1.54630E-01]

CH_4: [8.04760e-02, 1.80890e+00, -3.96690e-01, 2.36840e-01, -4.20920e-01]

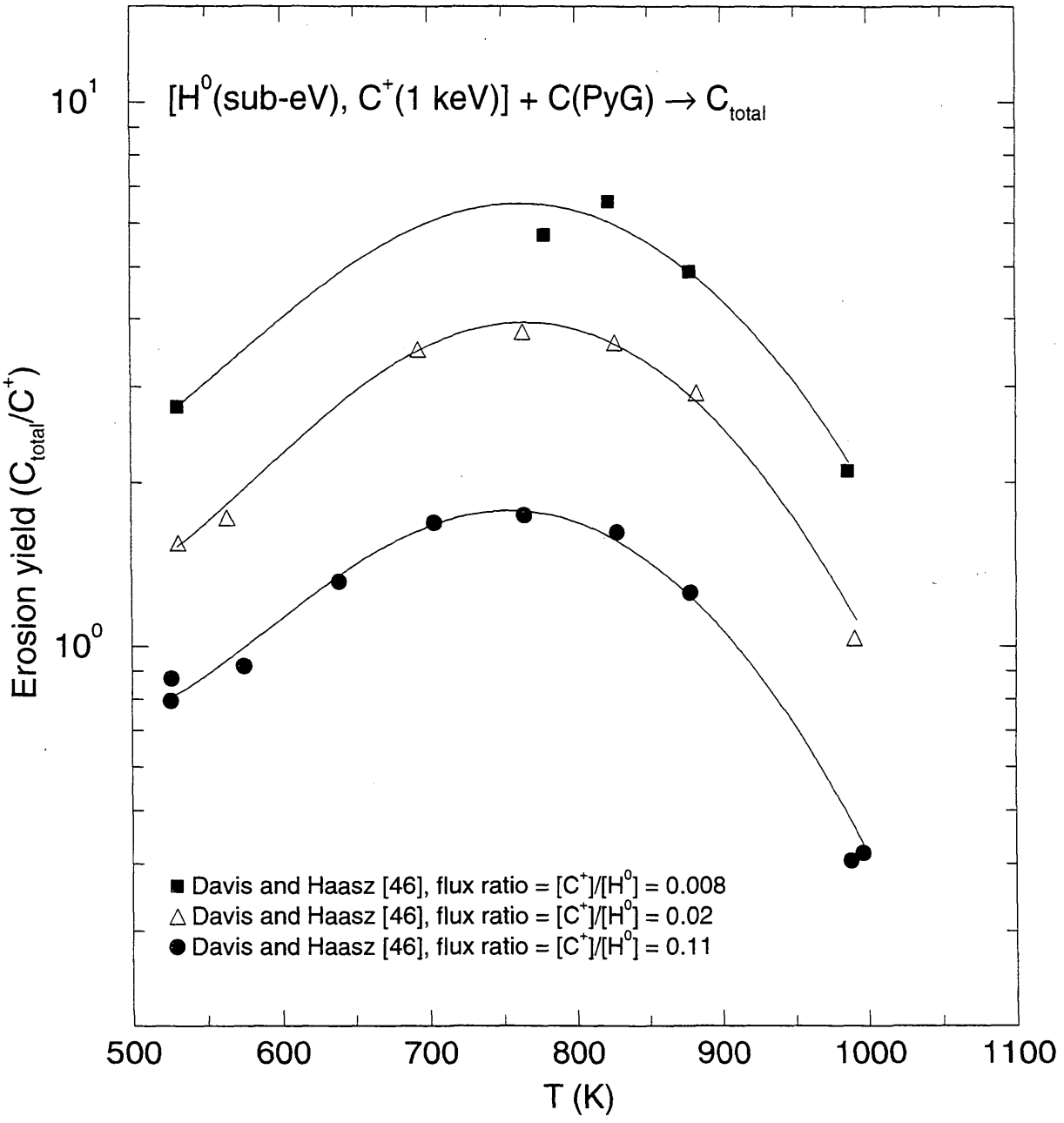

Figure 3.26: Synergistic chemical erosion of graphite due to sub-eV H^0 in combination with 1 keV C^+, normalized by the C^+ flux, as a function of temperature.

For a given C^+ flux, the total chemical erosion yield is found to increase with increasing H^0 flux, i.e., decreasing $[C^+]/[H^0]$ flux ratio. While it is the H^0 atoms which are reacting chemically, the C^+ ions enhance the reactions through the near-surface deposition of energy. It is assumed that physically sputtered carbon atoms react with H^0 on the test chamber walls, and thus the total yield $Y_{total} = Y_{chem-total} + Y_{physical}$ is measured. Erosion yields much larger than unity are observed for low flux ratios.

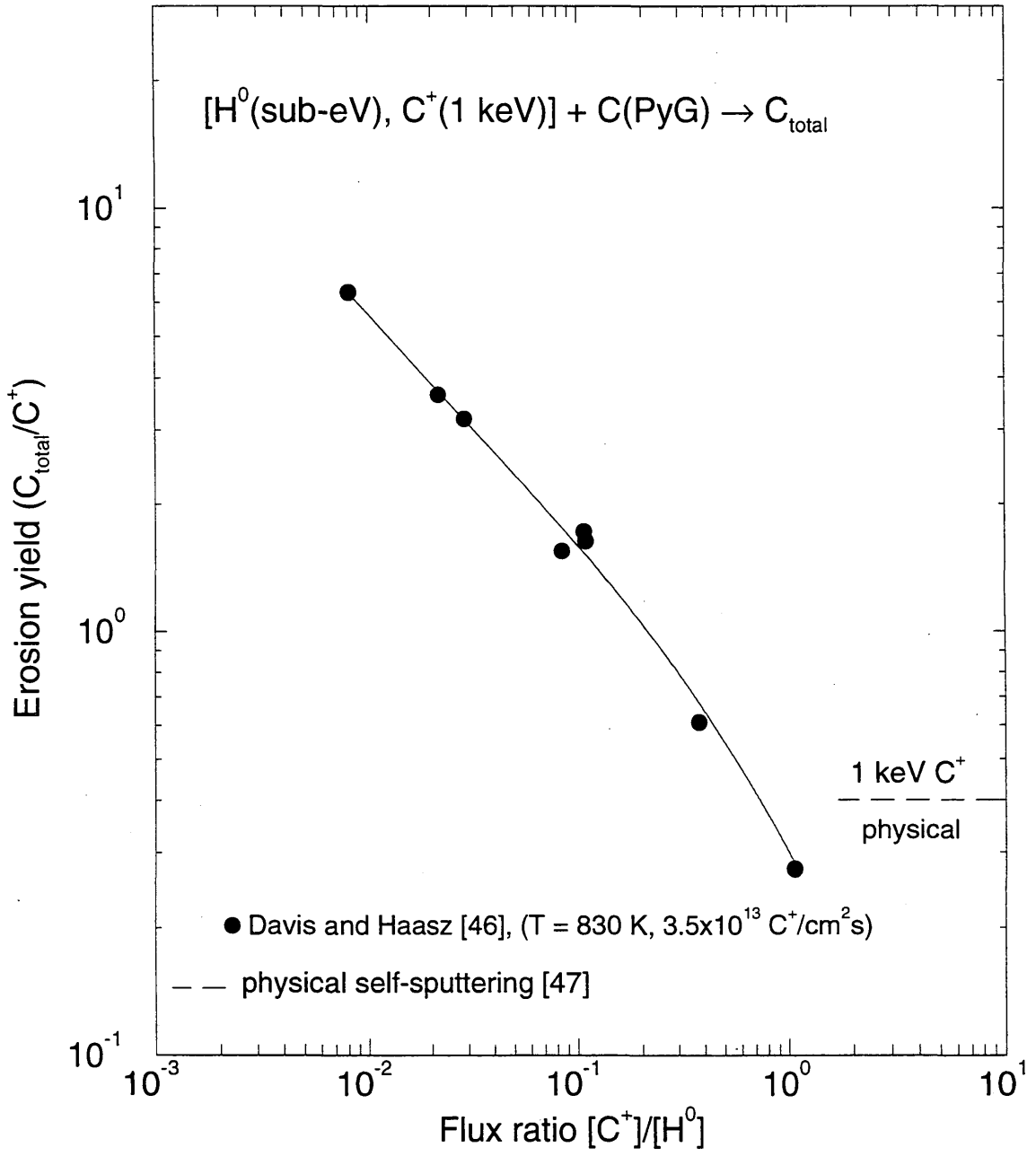

Figure 3.27: Synergistic chemical erosion of graphite due to simultaneous impact by sub-eV H^0 and 1 keV C^+, at 830 K, normalized by the C^+ flux, as a function of the $[C^+]/[H^0]$ flux ratio.

The effective yield attributed to each C^+ ion is enhanced by the addition of H^0. For a given C^+ flux density, the larger the H^0 flux, i.e., the smaller the $[C^+]/[H^0]$ flux ratio, the greater the effective yield. While it is the H^0 atoms which are reacting chemically, the C^+ ions enhance the reactions through the near-surface deposition of energy. It is assumed that physically sputtered carbon is included in the measurement due to reactions between C atoms and H^0 on the test chamber walls, however, at high $[C^+]/[H^0]$ flux ratios, the H^0 flux to the walls may not be sufficient to remove all of the physically sputtered C.

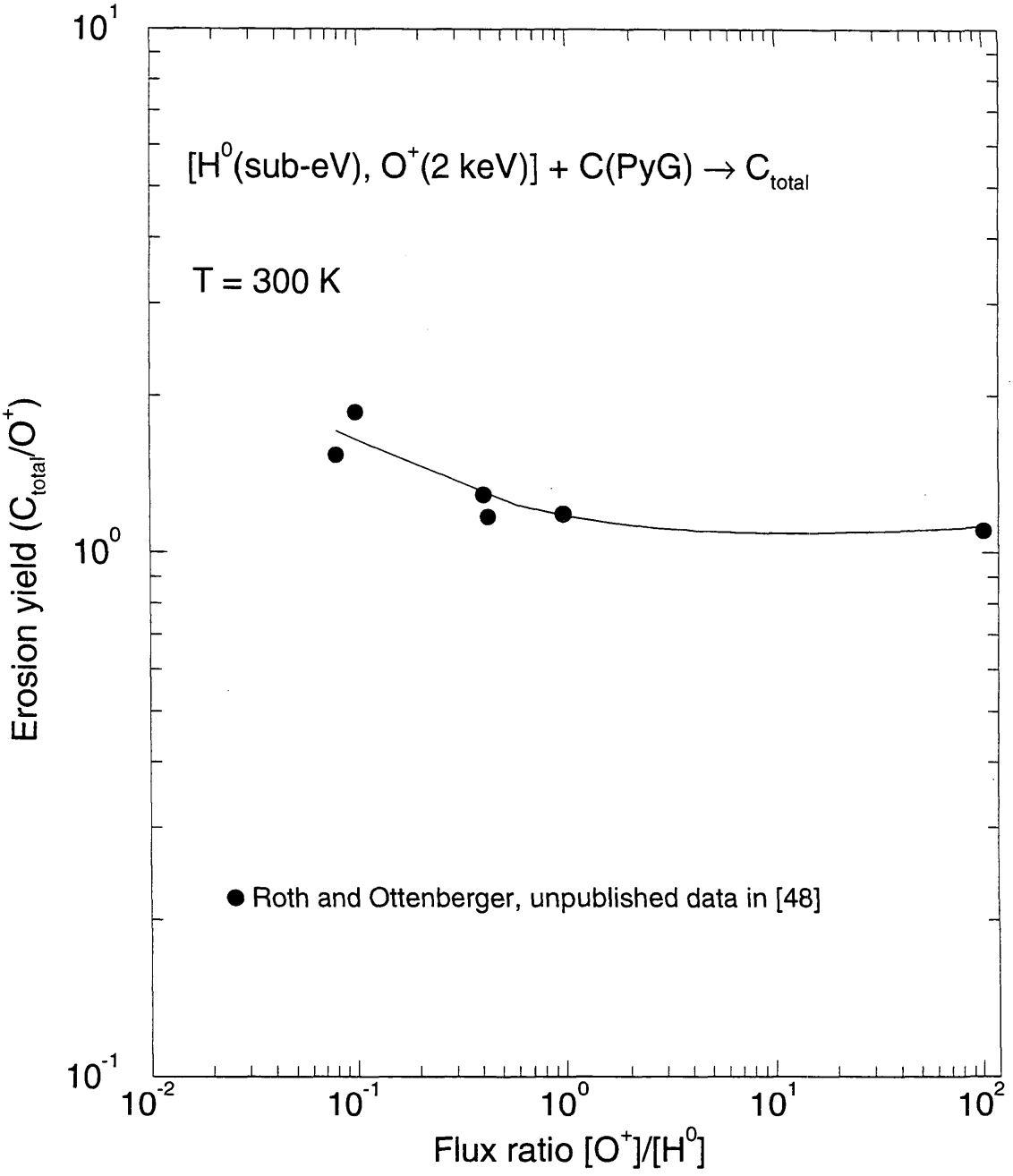

Figure 3.28: Synergistic erosion (measured by mass loss) due to combined sub-eV H^0 and 2 keV O^+ at 300 K, normalized by the O^+ flux, as a function of the $[O^+]/[H^0]$ flux ratio.

As in the cases of combined $[H^0, H^+]$ (Fig. 3.25) and $[H^0, C^+]$ impact (Fig. 3.27), simultaneous bombardment with O^+ and H^0 leads to enhanced erosion yields. The enhancements may not appear as significant as in the other cases, due to the high chemical erosion yield due to O^+ on its own. Also, the reaction temperature of 300 K is likely well below the temperature for maximum erosion.

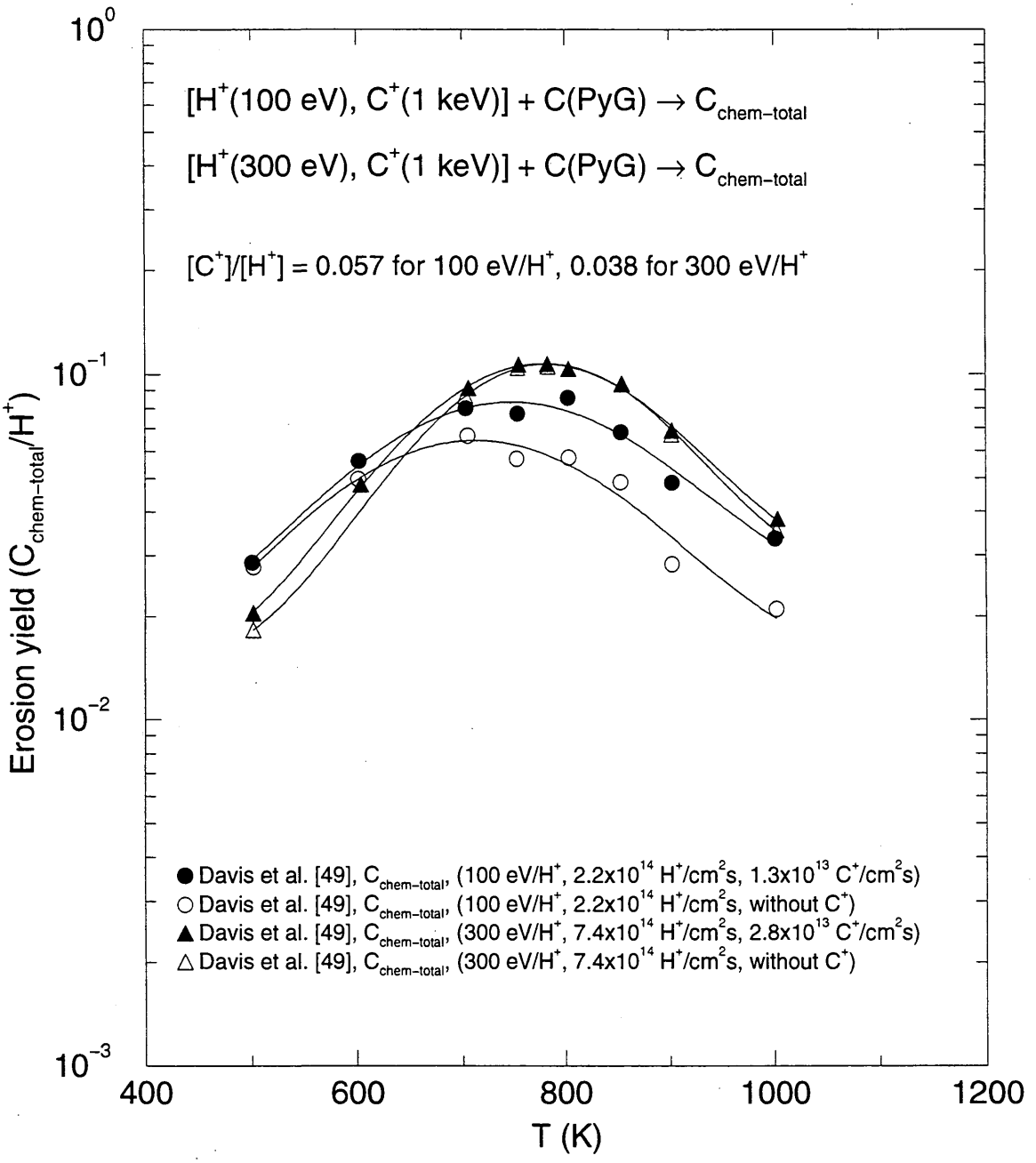

Figure 3.29: Synergistic chemical erosion due to combined 100 eV H^+ and 1 keV C^+ as a function of temperature for fixed flux ratios, normalized by the H^+ flux.

The temperature dependence of the 100 eV H^+ erosion yield is shown with and without simultaneous bombardment with 1 keV C^+ ions. The addition of C^+ to the H^+ flux leads to an enhancement of hydrocarbon yield, particularly at higher temperatures; the erosion yield due to 100 eV H^+ is somewhat lower than for 300 eV H^+ where the yield is at its maximum (see Fig. 3.13), such that the addition of greater near-surface ion damage leads to greater erosion. In the case of 300 eV H^+ in combination with 1 keV C^+, such an enhancement is not observed.

The total chemical erosion yield, $Y_{chem-total}$, is found from summing the contributions: $[CH_4] + 2 \times \{[C_2H_2] + [C_2H_4] + [C_2H_6]\} + 3 \times \{[C_3H_6] + [C_3H_8]\}$, and dividing by $[H^+]$.

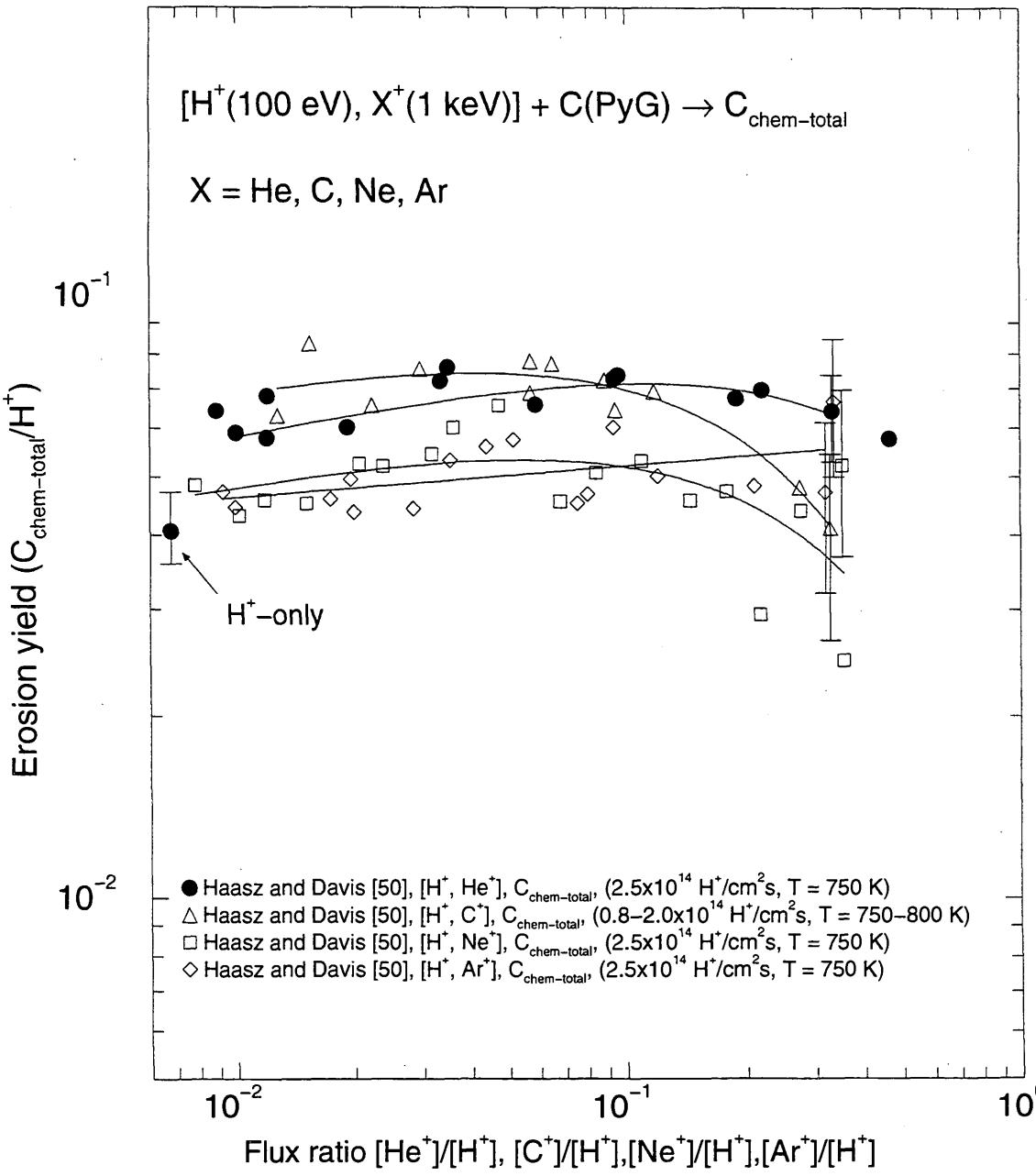

Figure 3.30: Synergistic chemical erosion due to combined 100 eV H^+ and 1 keV He^+, C^+, Ne^+ or Ar^+ ions as a function of incident particle flux ratio at 750 K (in one case 750-800 K).

The erosion yield due to H^+ ions alone at 100 eV is somewhat lower than at 300 eV (see Fig. 3.13), such that the addition of greater near-surface ion damage may lead to greater erosion. The creation of greater near-surface ion damage through the addition of a second ion species (in this case He^+, C^+, Ne^+ or Ar^+) leads to erosion yields which are enhanced by varying degrees over the range of flux ratios studied. In the case of He^+ and C^+, the enhancement is as large as ~50%, while for Ne^+ and Ar^+ the enhancement is very small. The decrease in yield for large $[C^+]/[H^+]$ or $[Ne^+]/[H^+]$ is possibly due to C^+ or Ne^+ ions breaking up hydrocarbon precursors in the implantation zone.

The total chemical erosion yield, $Y_{chem-total}$, is found from summing the contributions: $[CH_4] + 2 \times \{[C_2H_2] + [C_2H_4] + [C_2H_6]\} + 3 \times \{[C_3H_6] + [C_3H_8]\}$, and dividing by $[H^+]$.

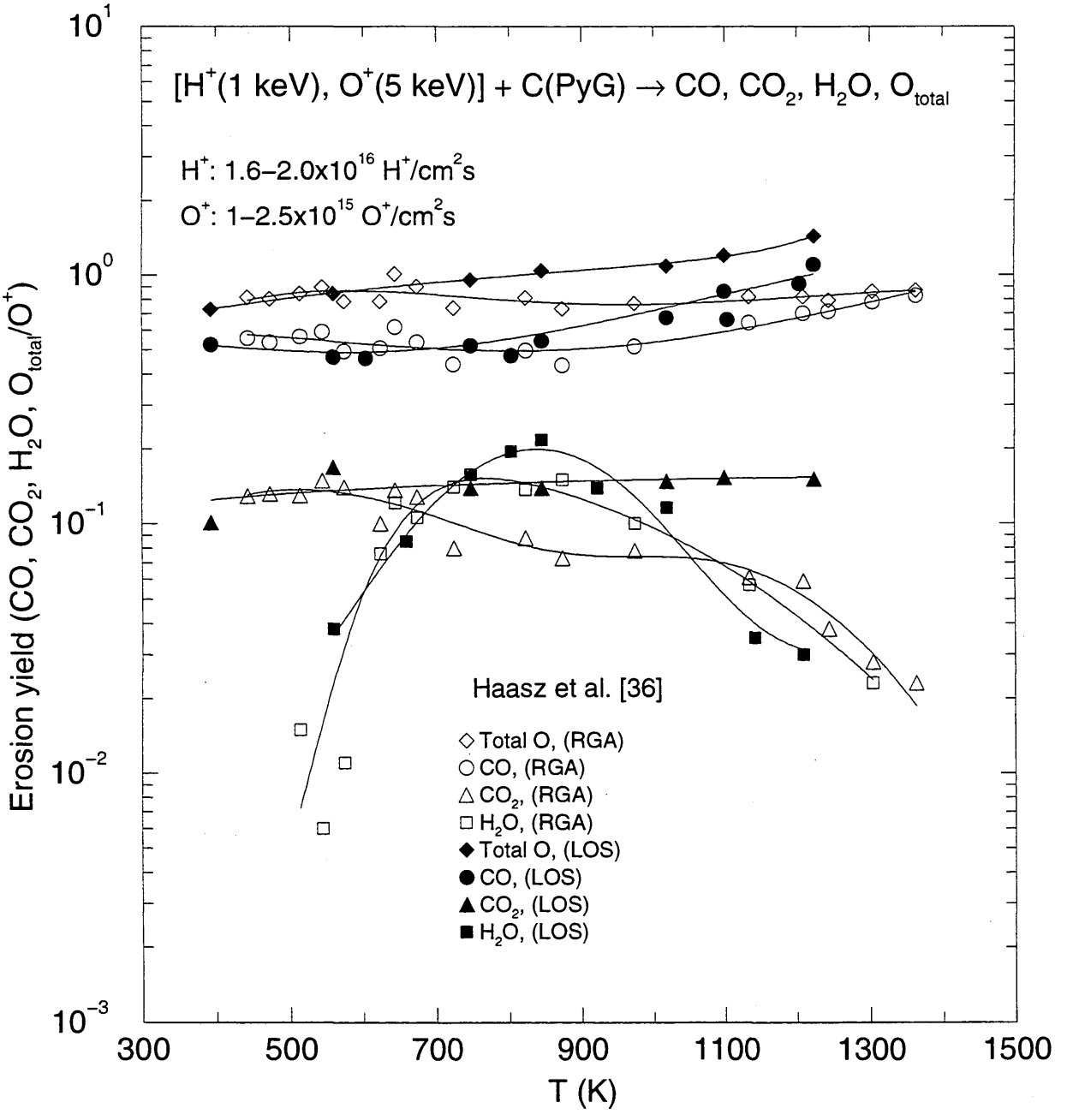

Figure 3.31: Synergistic chemical erosion due to combined 1 keV H^+ and 5 keV O^+ with incident flux ratios of $[O^+]/[H^+]$~0.05-0.2, as a function of temperature.

In contrast to other synergistic experiments reported in this compendium, the $[O^+, H^+]$ synergism leads to a reduction of the carbon erosion yield through the production of H_2O. O^+-only yields from the same experiment are shown on Fig. 3.20. The addition of H^+ to the O^+ flux leads to a small decrease in CO and CO_2 production, and the production of a small amount of H_2O. There is a strong temperature dependence to the H_2O production, with a peak of ~0.2 H_2O/O^+, near 800 K. A small decrease in CH_4 yield is found for the same case [36]. LOS refers to line-of-sight and RGA to residual gas analysis.

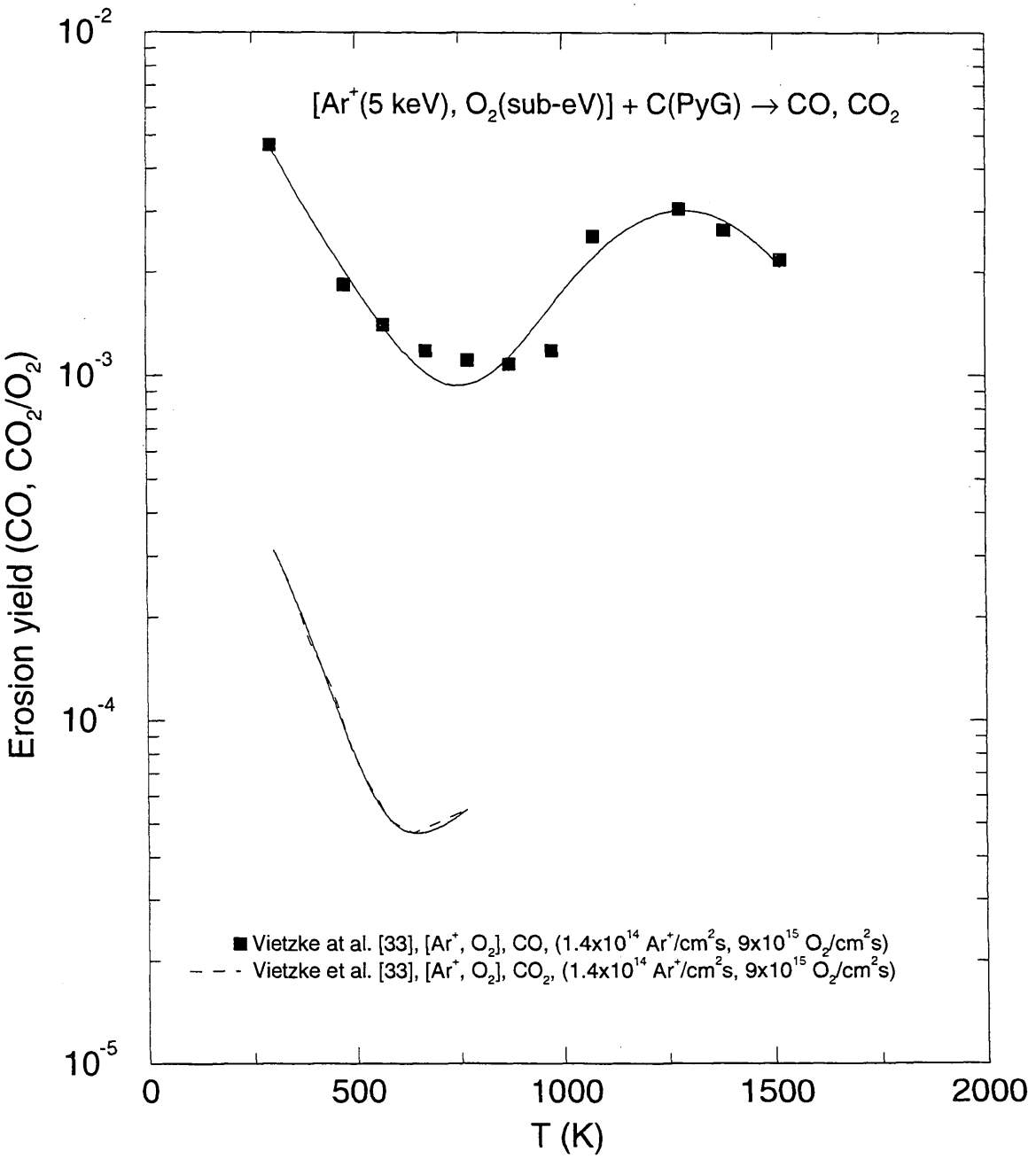

Figure 3.32: Combined thermal O_2 and 5 keV Ar^+ on graphite, as a function of temperature.

Above 1000 K, the addition of Ar^+ increases the O_2 erosion yield by ~50% (see Fig. 3.19). However, the Ar^+ ions lead to the creation of a low temperature branch to the reaction which is not observed for O_2 only, but which leads to larger erosion yields below room temperature. Both CO and CO_2 were observed for this low temperature branch, with CO being the dominant reaction product.

References for Section 3

[1] VIETZKE, E., FLASKAMP, K., PHILLIPS, V., J. Nucl. Mater. **111&112** (1982) 763.

[2] VIETZKE, E., FLASKAMP, K., PHILLIPS, V., J. Nucl. Mater. **128&129** (1984) 545.

[3] PITCHER, C. S., AUCIELLO, O., HAASZ, A. A., STANGEBY, P. C., J. Nucl. Mater. **128&129** (1984) 597.

[4] STANGEBY, P. C., AUCIELLO, O., HAASZ, A. A., J. Vac. Sci. Tech. A **1** (1983) 1425.

[5] DAVIS, J. W., HAASZ, A. A., STANGEBY, P. C., J. Nucl. Mater. **155-157** (1988) 234.

[6] GOULD, R. K., J. Chem. Phys. **63** (1975) 1825.

[7] HAASZ, A. A., DAVIS, J. W., J. Chem. Phys. **85** (1986) 3293.

[8] HORN, A., SCHENK, A., BIENER, J., WINTER, B., LUUTERLOH, C., WITTMANN, M., KÜPPERS, J., Chem. Phys. Lett. **231** (1994) 193.

[9] VIETZKE, E., PHILLIPS, V., Fusion Tech. **15** (1989) 108.

[10] VIETZKE, E., PHILLIPS, V., Radiochem. Acta **43** (1988) 75.

[11] VIETZKE, E., FLASKAMP, K., PHILIPPS, V., ESSER, G., WIENHOLD, P., WINTER, J., J. Nucl. Mater. **145-147** (1987) 443.

[12] VIETZKE, E., PHILIPPS, V., FLASKAMP, K., WINTER, J., VEPREK, S., KOIDL, P., *Symposium Proceedings, 10th International Symposium on Plasma Chemistry* (EHLEMANN, U., LERGON, H. G., WIESEMANN, K., Eds.), **3** (1991) 1.

[13] HAASZ, A. A., DAVIS, J. W., J. Nucl. Mater. **175** (1990) 84.

[14] DAVIS, J. W., HAASZ, A. A., STANGEBY, P. C., J. Nucl. Mater. **145-147** (1987) 417.

[15] YAMADA, R., NAKAMURA, K., SONE, K., SAIDOH, M., J. Nucl. Mater. **95** (1980) 278.

[16] YAMADA, R., NAKAMURA, K., SAIDOH, M., J. Nucl. Mater. **98** (1981) 167.

[17] ROTH, J., BOHDANSKY, J., POSCHENRIEDER, W., SINHA, M. K., J. Nucl. Mater. **63** (1976) 222.

[18] BOHDANSKY, J., ROTH, J., Rad. Eff. **89** (1985) 49.

[19] CHIU, S., HAASZ, A. A., J. Nucl. Mater. **208** (1994) 282.

[20] VIETZKE, E., HAASZ, A. A., "Chemical Erosion", in *Physical Processes of the Interaction of Fusion Plasmas with Solids*, Academic Press, Orlando (1996) 135-176.

[21] ROTH, J., BOHDANSKY, J., Nucl. Instr. Meth. B **23** (1987) 549.

[22] GARCÍA-ROSALES, C., GAUTHIER, E., ROTH, J., SCHWÖRER, R., ECKSTEIN, W., J. Nucl. Mater. **189** (1992) 1.

[23] GARCÍA-ROSALES, C., ROTH, J., J. Nucl. Mater. **196-198** (1992) 573.

[24] YAMADA, R., J. Nucl. Mater. **145-147** (1987) 359.

[25] MECH, B. V., HAASZ, A. A., DAVIS, J. W., J. Nucl. Mater. **241-243** (1997) 1147.

[26] MECH, B. V., Ph.D. Thesis, University of Toronto (1997); MECH, B. V., HAASZ, A. A., DAVIS, J. W., J. Nucl. Mater., in press.

[27] HAASZ, A. A., MECH, B. V., DAVIS, J. W., J. Nucl. Mater. **231** (1996) 170.

[28] DAVIS, J. W., HAASZ, A. A., J. Nucl. Mater. **149** (1987) 349.

[29] DAVIS, J. W., HAASZ, A. A., J. Nucl. Mater. **175** (1990) 117.

[30] HIROOKA, Y., POSPIESZCZYK, A., CONN, R. W., MILLS, B., NYGREN, R. E., RA, Y., J. Vac. Sci. Tech. A **7** (1989) 1070.

[31] YAMADA, R., NAKAMURA, K., SAIDOH, M., J. Nucl. Mater. **111&112** (1982) 744.

[32] VIETZKE, E., FLASKAMP, K., PHILLIPS, V., J. Nucl. Mater. **128&129** (1984) 564.

[33] VIETZKE, E., TANABE, T., PHILLIPS, V., ERDWES, M., FLASKAMP, K., J. Nucl. Mater. **145-147** (1987) 425.

[34] ROSNER, D., ALLENDORF, H. D., *Heterogeneous Kinetics at Elevated Temperatures*, Proc. Int. Conf. Univ. Pennsylvania 1969, Plenum, New York (1970) 231.

[35] VIETZKE, E., REFKE, A., PHILLIPS, V., HENNES, M., J. Nucl. Mater. **220-222** (1995) 249.

[36] HAASZ, A. A., CHEN, A. Y. K., DAVIS, J. W., VIETZKE, E., J. Nucl. Mater. **248** (1997) 19.

[37] KRECH, R. *et al.*, Proc. EOIM-3 BMDO Experiment Workshop, Arcadia, California (1993).

[38] BANKS, B. A., *et al.*, NAS TM 101971 (1989) and LDEF Materials Data Analysis Workshop, Florida (1990).

[39] HECHTL, E., BOHDANSKY, J., ROTH, J., J. Nucl. Mater. **103&104** (1981) 333.

[40] HECHTL, E., BOHDANSKY, J., J. Nucl. Mater. **122&123** (1984) 1431.

[41] GOKAN, H. *et al.*, J. Electrochem. Soc. Solid State Sci. Techn. **130** (1983) 143.

[42] LUBERT, L. *et al.*, Proc. 4th Eur. Symp. on Spacecraft Materials, CERT, Toulouse, France (1988), 393, Publ. CEPAD (1989).

[43] AKISHIN, A. I., *et al.*, Bull. Russ. Acad. Sci., Phys. **58** No. 3 (1994) 109.

[44] ECKSTEIN, W., GARCÍA-ROSALES, C., ROTH, J., Sputtering Dara, Report of IPP Garching, IPP9/82 (1993).

[45] HAASZ, A. A., DAVIS, J. W., AUCIELLO, O., STANGEBY, P. C., VIETZKE, E., FLASKAMP, K., PHILLIPS, V., J. Nucl. Mater. **145-147** (1987) 412.

[46] DAVIS, J. W., HAASZ, A. A., Appl. Phys. Lett. **57** (1990) 1976.

[47] ROTH, J., BOHDANSKY, J., OTTENBERGER, W., J. Nucl. Mater. **165** (1989) 193.

[48] ROTH, J., VIETZKE, E., HAASZ, A. A., Suppl. Nucl. Fusion **1** (1991) 63.

[49] DAVIS, J. W., HAASZ, A. A., Wu, C. H., J. Nucl. Mater. **196-198** (1992) 581.

[50] HAASZ, A. A., DAVIS, J. W., Nucl. Instr. Meth. B **83** (1993) 117.

[51] ROTH, J., J. Nucl. Mater. **145-147** (1987) 87.

[52] ROTH, J., GARCÍA-ROSALES, C., Nucl. Fusion **36** (1996) 1647.

[53] WU, C. H., DAVIS, J. W., HAASZ, A. A., in *15th European Conf. on Controlled Fusion and Plasma Heating*, Dubrovnik, Europhysics Conf. Abstracts Vol. 12B Part II, (1988) 691.

[54] VIETZKE, E., PHILIPPS, V., Nucl. Instr. Meth. B **23** (1987) 449.

4 Comprehensive Set of Chemical Erosion Data from Various Laboratories

In this section we present a list of individual reactions, followed by corresponding individual data sheets. The organization of the listing proceeds from lighter reactants (e.g. H^0, H^+, D^0..) and simple target materials (pyrolytic graphite) to heavier reactants (e.g. Ne^+, O^+, Ar^+..) and more complex targets (e.g. doped graphites, B_4C, TiC). In some cases data from a common source publication have been retained on adjacent sheets (e.g. reactions 4.2.1.73-4.2.1.86). The individual data sheets include the data source, accuracy when known, analytic fitting functions and coefficients used to parameterize the data, and brief comments on the relevant experimental conditions or parameters. The accuracies indicated are absolute unless otherwise indicated.

A list of abbreviations used in the comments (and on some graphs) are given in Appendix A. This includes abbreviations for the 'ALADDIN' hierarchical labels appearing on the data sheets, which specify a particular reactant, material, or type of erosion process. A list of the analytic functions used for fitting (ALADDIN evaluation functions) are given in Appendix B.

This information will be used in future (on-line) computer databasing of the erosion data included in this compendium. ALADDIN (**A** **L**abelled **A**tomic **D**ata **IN**terface) is the data format and database system currently utilized by the Atomic and Molecular Data Unit, IAEA, to provide on-line retrievals of numerical atomic, molecular and plasma-surface interaction data for fusion research.

List of Reactions for Section 4

4.1 Chemical erosion of graphite due to sub-eV hydrogen and deuterium atoms

4.1.1 H^0

4.1.1.1 H^0 + pyrolytic graphite → CH_4, C_2H_2

4.1.1.2 H^0 + pyrolytic graphite → CH_4

4.1.1.3 H^0 + pyrolytic graphite → CH_4, C_2-molecules

4.1.1.4 H^0 + pyrolytic graphite → CH_3, CH_4

4.1.1.5 H^0 + pyrolytic graphite → CH_4

4.1.1.6 H^0 + pyrolytic graphite → CH_4

4.1.1.7 H^0 + pyrolytic graphite → CH_3, CH_4

4.1.1.8 H^0 + pyrolytic graphite → C_xH_y, C

4.1.1.9 H^0 + pyrolytic graphite → CH_3

4.1.1.10 H^0 + Papyex graphite → CH_4

4.1.1.11 H^0 + Papyex graphite → CH_4

4.1.1.12 H^0 + Papyex graphite → CH_4

4.1.1.13 H^0 + CLOR, POCO, pyrolytic, Papyex graphite → CH_4

4.1.1.14 H^0, H^+ + pyrolytic graphite → C

4.1.1.15 H^0, H_3^+ + PG-A graphite → CH_4

4.1.1.16 H^0 + a-C:H film → CH_3

4.1.1.17 H^0 + a-C:H, a-C/B:H films → BH_2^+, CH_3^+

4.1.1.18 H^0 + diamond/Mo → C

4.1.2 D^0

4.1.2.1 D^0 + a-C:H film → CH_3, CD_3

4.1.2.2 D^0, D^+ + a-C:H film → C

4.1.2.3 D^0, D^+, H^+ + a-C:H film → CH_4, CD_3, CD_4

4.2 Chemical erosion of graphite due to energetic hydrogen and deuterium ions

4.2.1 H^+, H_2^+, H_3^+

4.2.1.1 H^+ + pyrolytic graphite → CH_4

4.2.1.2 H^+ + pyrolytic graphite → CH_4, C_2H_4, C

4.2.1.3 H^+ + pyrolytic graphite → CH_4, C

4.2.1.4 H^+ + pyrolytic graphite → CH_3, CH_4

4.2.1.5 H^+ + pyrolytic graphite → CH_3, CH_4

4.2.1.6 H^+ + pyrolytic graphite → CH_4

4.2.1.7 H^+ + pyrolytic graphite → C_xH_y, C

4.2.1.8 H^+ + pyrolytic graphite → C

4.2.1.9 H^+ + pyrolytic graphite → CH_4

4.2.1.10 H^+ + pyrolytic graphite → C

4.2.1.11 H^+ + PG-A graphite → C

4.2.1.12 H^+ + PG-A graphite → CH_4

4.2.1.13 H^+ + PG-A graphite → C_xH_y

4.2.1.14 H^+ + PG-A graphite → C_xH_y

4.2.1.15 H^+ + POCO graphite → C

4.2.1.16 H^+ + POCO, ATJ, pyrolytic graphite, carbon/carbon composite → C

4.2.1.17 H^+ + POCO graphite → C

4.2.1.18 H^+ + MPg-8 graphite → C

4.2.1.19 H^+ + carbon fiber composites → CH_4

4.2.1.20 H_3^+ + pyrolytic graphite → CH_4

4.2.1.21 H_3^+ + pyrolytic graphite → CH_4

4.2.1.22 H_3^+ + pyrolytic graphite → CH_4

4.2.1.23 H_3^+ + pyrolytic graphite → CH_4

4.2.1.24 H_3^+ + pyrolytic graphite → CH_4

4.2.1.25 H_3^+ + pyrolytic graphite → CH_4

4.2.1.26 H_3^+ + pyrolytic graphite → CH_4, CD_4, C_{heavy}, C

4.2.1.27 H_3^+ + pyrolytic graphite → CH_4, CD_4, C_{heavy}, C

4.2.1.28 H_3^+ + pyrolytic graphite → CH_4, CD_4, C_{heavy}, C

4.2.1.29 H_3^+ + pyrolytic graphite → CH_4, CD_4, C_{heavy}, C

4.2.1.30 H_3^+ + pyrolytic graphite → CH_4, C

4.2.1.31 H_3^+ + pyrolytic graphite → C_xH_y, C

4.2.1.32 H_3^+ + pyrolytic graphite → C_xH_y, C

4.2.1.33 H_3^+ + pyrolytic graphite → C_xH_y, C

4.2.1.34 H_3^+ + pyrolytic graphite → C_xH_y, C

4.2.1.35 H_3^+ + pyrolytic graphite → C_xH_y, C

4.2.1.36 H_3^+ + pyrolytic graphite → C_xH_y, C

4.2.1.37 H_3^+ + pyrolytic graphite → CH_4, C_{heavy}, C

4.2.1.38 H_3^+ + pyrolytic graphite → CH_4, C_{heavy}, C

4.2.1.39 H_3^+ + pyrolytic graphite → CH_4, C_{heavy}, C

4.2.1.40 H_3^+ + pyrolytic graphite → CH_4, C_{heavy}, C

4.2.1.41 H_3^+ + pyrolytic graphite → C_xH_y, C

4.2.1.42 H_3^+ + pyrolytic graphite → C_xH_y, C

4.2.1.43 H_3^+ + pyrolytic graphite → C_xH_y, C

4.2.1.44 H_3^+ + pyrolytic graphite → C_xH_y, C

4.2.1.45 H_3^+ + pyrolytic graphite → C_xH_y, C

4.2.1.46 H_3^+ + pyrolytic graphite → C_xH_y, C

4.2.1.47 H_3^+ + PG-A graphite → CH_4

4.2.1.48 H_3^+ + a-C:H film → CH_4

4.2.1.49 H_3^+ + pyrolytic graphite → C_xH_y, C

4.2.1.50 H_3^+ + pyrolytic graphite → C_xH_y, C

4.2.1.51 H_3^+ + pyrolytic graphite → C_xH_y, C

4.2.1.52 H_3^+ + pyrolytic graphite → C_xH_y, C

4.2.1.53 H^0, H^+, H_3^+ + pyrolytic graphite → C_xH_y, C

4.2.1.54 H_3^+ + AEROLOR carbon/carbon composite (end cut) → C_xH_y, C

4.2.1.55 H_3^+ + AEROLOR carbon/carbon composite (top cut) → C_xH_y, C

4.2.1.56 H_3^+ + AEROLOR carbon/carbon composite (end cut) → C_xH_y, C

4.2.1.57 H_3^+ + AEROLOR carbon/carbon composite (top cut) → C_xH_y, C

4.2.1.58 H_3^+ + ALCAN carbon/carbon composite → C_xH_y, C

4.2.1.59 H_3^+ + ALCAN carbon/carbon composite (B doped) → C_xH_y, C

4.2.1.60 H_3^+ + ALCAN carbon/carbon composite (Si doped) → C_xH_y, C

4.2.1.61 H_3^+ + ALCAN carbon/carbon composite (Si and B doped) → C_xH_y, C

4.2.1.62 H_3^+ + CKC graphite → CH_4

4.2.1.63 H_3^+ + CKC-B2 (B doped) graphite → CH_4

4.2.1.64 H_3^+ + CKC-B10 (B doped) graphite → CH_4

4.2.1.65 H_3^+ + CKC-B20 (B doped) graphite → CH_4

4.2.1.66 H_3^+ + CKC-Si3 (Si doped) graphite → CH_4

4.2.1.67 H_3^+ + CKC-Si8 (Si doped) graphite → CH_4

4.2.1.68 H_3^+ + CKC-Si14 (Si doped) graphite → CH_4

4.2.1.69 H_3^+ + CKC-Ti2 (Ti doped) graphite → CH_4

4.2.1.70 H_3^+ + CKC-Ti8 (Ti doped) graphite → CH_4

4.2.1.71 H_3^+ + CKC-Ti16 (Ti doped) graphite → CH_4

4.2.1.72 H_3^+ + CKC W doped graphite → CH_4

4.2.1.73 H_3^+ + pyrolytic graphite → CH_4

4.2.1.74 H_3^+ + pyrolytic graphite → C

4.2.1.75 H_3^+ + CKC graphite → CH_4

4.2.1.76 H_3^+ + CKC graphite → C

4.2.1.77 H_3^+ + CKC graphite → CH_4

4.2.1.78 H_3^+ + CKC graphite → C

4.2.1.79 H_3^+ + CKC (TiB_2 doped) graphite → CH_4

4.2.1.80 H_3^+ + CKC (TiB_2 doped) graphite → C

4.2.1.81 H_3^+ + CKC (TiB_2 doped) graphite → CH_4

4.2.1.82 H_3^+ + CKC (TiB_2 doped) graphite → C

4.2.1.83 H_3^+ + CKC (TiB_2 doped) graphite → CH_4

4.2.1.84 H_3^+ + CKC (TiB_2 doped) graphite → C

4.2.1.85 H_3^+ + CKC (TiB_2 doped) graphite → CH_4

4.2.1.86 H_3^+ + CKC (TiB_2 doped) graphite → C

4.2.1.87 H_3^+ + TiC(CVD)/Mo → C

4.2.1.88 H_3^+ + TiC(CVD)/Mo → CH_4

4.2.1.89 H_3^+ + TiC(CVD, PVD)/Mo, POCO graphite → CH_4

4.2.1.90 H_3^+ + isotropic graphite (B doped) → C

4.2.1.91 H_3^+ + isotropic graphite (V doped) → C

4.2.1.92 H_2^+, H_3^+ + pyrolytic graphite → C

4.2.1.93 H^+, H_3^+ + isotropic graphite → CH_4

4.2.1.94 H^+, H_2^+, H_3^+ + pyrolytic graphite → CH_4

4.2.1.95 H^+, H_2^+, H_3^+ + pyrolytic graphite → CH_4

4.2.1.96 H^+, H_3^+ + PG-A graphite → CH_4

4.2.1.97 H^+, H_3^+ + GC-30 glassy carbon → CH_4

4.2.1.98 H^+, H_3^+ + B_4C → CH_4

4.2.2 D^+, D_2^+, D_3^+

4.2.2.1 D^+ + pyrolytic graphite → CD_4

4.2.2.2 D^+ + pyrolytic graphite → CD_4

4.2.2.3 D^+ + pyrolytic graphite → CD_4, C_2D_2, C

4.2.2.4 D^+ + pyrolytic graphite → CD_4

4.2.2.5 D^+, H^+ + pyrolytic graphite →CD_4, C
4.2.2.6 D^+ + pyrolytic graphite → C
4.2.2.7 D^+ + pyrolytic graphite → CD_4
4.2.2.8 D^+ + pyrolytic graphite → C
4.2.2.9 D^+, D_3^+ + pyrolytic graphite → CD_4
4.2.2.10 D^+ + pyrolytic graphite → CD_4
4.2.2.11 D^+ + POCO graphite → C
4.2.2.12 D^+ + redeposited carbon, POCO graphite → C
4.2.2.13 D^+ + pyrolytic graphite, B-doped GB graphite → C
4.2.2.14 D^+ + C-SiC coated graphite → C
4.2.2.15 D^+ + pyrolytic, B-doped SEP-CFC, Ti-doped graphite, Be/C → CD_4
4.2.2.16 D^+ + B-doped S 2508, USB 15, GB graphite, B_4C → CD_4
4.2.2.17 D^+ + pure, B-doped graphite, B_4C → C
4.2.2.18 D^+ + pyrolytic graphite → CD_4
4.2.2.19 D^+ + USB15 graphite → CD_4
4.2.2.20 D^+ + USB15, B-doped graphite → C, CD_4
4.2.2.21 D_2^+ + TiC-coated graphite → CH_4
4.2.2.22 D_2^+ + pyrolytic graphite → CD_4
4.2.2.23 D_2^+ + pyrolytic graphite → CD_4
4.2.2.24 D_2^+ + pyrolytic graphite → CD_4, C_{heavy}, C
4.2.2.25 D_2^+ + pyrolytic graphite → CD_4, C_{heavy}, C
4.2.2.26 D_2^+ + pyrolytic graphite → CD_4, C_{heavy}, C
4.2.2.27 D_2^+ + pyrolytic graphite → CD_4, C_{heavy}, C
4.2.2.28 D_2^+ + pyrolytic graphite → C_xD_y, C
4.2.2.29 D_2^+ + pyrolytic graphite → C_xD_y, C
4.2.2.30 D_2^+ + pyrolytic graphite → C_xD_y, C
4.2.2.31 D_2^+ + pyrolytic graphite → C_xD_y, C
4.2.2.32 D_2^+ + pyrolytic graphite → C_xD_y, C
4.2.2.33 D_2^+ + pyrolytic graphite → C_xD_y, C
4.2.2.34 D_3^+ + pyrolytic graphite (Ti doped) → C
4.2.2.35 D_3^+ + graphite (pyrolytic, Ti, B doped) → CD_4

4.2.3 H^+, D^+

4.2.3.1 H^+, D^+ + pyrolytic graphite → CH_4, CD_4
4.2.3.2 H^+, D^+ + pyrolytic graphite → C
4.2.3.3 H^+, D^+ + POCO graphite → C

4.3 Chemical erosion of graphite due to multi-species impact

4.3.1 [H^0, H^+], H^0, H^+

4.3.1.1 [H^0, H^+] + pyrolytic graphite → CH_4
4.3.1.2 [H^0, H^+] + pyrolytic graphite → CH_4, C_2H_x, C_3H_x, C
4.3.1.3 [H^0, H^+] + pyrolytic graphite → C_xH_y, C
4.3.1.4 [H^0, H^+] + pyrolytic graphite → C_xH_y, C
4.3.1.5 [H^0, H^+] + pyrolytic graphite → C_xH_y, C

4.3.1.6 $[H^0, H^+]$, H^0, H_3^+ + pyrolytic graphite → CH_4

4.3.1.7 $[H^0, H^+]$, H^0, H_3^+ + pyrolytic graphite → CH_4

4.3.2 $[H^0, C^+]$

4.3.2.1 $[H^0, C^+]$ + pyrolytic graphite → C

4.3.2.2 $[H^0, C^+]$ + pyrolytic graphite → C

4.3.3 $[H^0, O^+]$

4.3.3.1 $[H^0, O^+]$ + pyrolytic graphite → C

4.3.4 $[H^0, Ar^+]$, H^0, H^+

4.3.4.1 $[H^0, Ar^+]$ + pyrolytic graphite → CH_3, CH_4, C_2-compounds

4.3.4.2 $[H^0, Ar^+]$ + pyrolytic graphite → CH_3

4.3.4.3 $[H^0, Ar^+]$ + pyrolytic graphite → CH_3, CH_4, C_2-compounds

4.3.4.4 $[H^0, Ar^+]$ + pyrolytic graphite → CH_3, CH_4

4.3.4.5 $[H^0, Ar^+]$ + pyrolytic graphite → CH_3, CH_4

4.3.4.6 $[H^0, Ar^+]$ + CLOR, POCO, pyrolytic, Papyex graphite → CH_3

4.3.4.7 $[H^0, Ar^+]$, H^0 + pyrolytic graphite → C_2H_3

4.3.4.8 $[H^0, Ar^+]$, H^0, H^+ + pyrolytic graphite → CH_3, CH_4

4.3.4.9 $[H^0, Ar^+]$, H^0, H^+ + pyrolytic graphite, a-C:H → CH_3, CH_4

4.3.5 $[H^+, He^+]$

4.3.5.1 $[H^+, He^+]$ + pyrolytic graphite → C_xH_y, C

4.3.6 $[H^+, C^+]$

4.3.6.1 $[H^+, C^+]$ + pyrolytic graphite → C_xH_y, C

4.3.6.2 $[H^+, C^+]$ + pyrolytic graphite → C_xH_y, C

4.3.6.3 $[H^+, C^+]$ + pyrolytic graphite → C_xH_y, C

4.3.6.4 $[H^+, C^+]$ + pyrolytic graphite → C_xH_y, C

4.3.6.5 $[H^+, C^+]$ + pyrolytic graphite → C_xH_y, C

4.3.6.6 $[H^+, C^+]$ + pyrolytic graphite → C_xH_y, C

4.3.6.7 $[H^+, C^+]$ + pyrolytic graphite → C_xH_y, C

4.3.6.8 $[H^+, C^+]$ + pyrolytic graphite → C_xH_y, C

4.3.6.9 $[H^+, C^+]$ + pyrolytic graphite → C_xH_y, C

4.3.6.10 $[H^+, C^+]$ + pyrolytic graphite → C_xH_y, C

4.3.7 $[H^+, O^+]$

4.3.7.1 $[H^+, O^+]$, O^+ + pyrolytic graphite → CO, CO_2

4.3.7.2 $[H^+, O^+]$, O^+ + pyrolytic graphite → CO, CO_2

4.3.7.3 $[H^+, O^+]$, O^+ + pyrolytic graphite → CH_4

4.3.8 $[H^+, Ne^+]$

4.3.8.1 $[H^+, Ne^+]$ + pyrolytic graphite → C_xH_y, C

4.3.9 [H^+, Ar^+]

4.3.9.1 [H^+, Ar^+] + pyrolytic graphite → C_xH_y, C

4.3.10 [D^+, He^+]

4.3.10.1 [D^+, He^+] + pyrolytic graphite → CD_4

4.4 Chemical erosion of graphite due to oxygen and oxygen ions

4.4.1 O^0, O_2

4.4.1.1 O^0 + pyrolytic graphite → CO

4.4.1.2 O_2 + pyrolytic graphite → CO, CO_2

4.4.2 O^+, O_2^+

4.4.2.1 O^+ + pyrolytic graphite → C

4.4.2.2 O^+ + pyrolytic graphite → CO, CO_2, C

4.4.2.3 O_2^+ + pyrolytic graphite, B_4C → BO, CO

4.4.2.4 O_2^+ + pyrolytic graphite → CO, CO_2

4.4.2.5 O_2^+ + B_4C → BO, CO, B_2O_2

4.4.2.6 O_2^+ + SiC/C/Si → CO, CO_2, SiO, O, O_2

4.4.2.7 O_2^+ + a-Si/C:H → C, CO, CO_2, SiO, O, O_2

4.1.1.1 H^0 + pyrolytic graphite → CH_4, C_2H_2

Source: M. Balooch and D. R. Olander, J. Chem. Phys. **63**, 4772 (1975).

Accuracy: Indeterminate.

Comments: (1) Reaction products are detected by line-of-sight mass spectrometry.
(2) Specimen: graphite (pyrolytic).
(3) The apparent reaction probability is the ratio of the product signal amplitude to that of the reflected hydrogen.
(4) The incident atomic hydrogen beam intensity is 8.5×10^{16} atoms/cm^{2}s.

Analytic fitting function:

Reaction probability:

$$Y = A_1 \exp(-A_2 X) X^{A_3} + A_4 X^{A_5} \quad [\text{signal amplitude/reflected } H^0]$$

where $X = 10^4/T_s$ is in Kelvin^{-1}. The rms deviation of analytic fits for reactions A (○), B (●), C (□, ◇) and D (△, ∗) are 1.0%, 10.8%, 7.4% and 14.5%, respectively.

Fitting parameters A_1-A_5

A	5.4771E+01	-2.1318E-01	-5.6857E+00	-3.9666E+01	-4.9352E+00
B	2.3417E+05	-3.3793E-01	-1.0421E+01	-6.9764E+04	-8.6333E+00
C	-1.2411E+01	1.1427E-02	-1.9918E+00	7.5393E+00	-1.8543E+00
D	-5.8531E-01	-2.9088E-06	2.1129E+00	5.8526E-01	2.1129E+00

ALADDIN evaluation function for reaction probability: EYIELD5A

ALADDIN hierarchical labelling:

A: SATM H [+0] GRAPHITE T=HPG O=PRISM-PL C{2}H{2} [+0]
B: SATM H [+0] GRAPHITE T=HPG O=BASAL-PL C{2}H{2} [+0]
C: SATM H [+0] GRAPHITE T=HPG O=PRISM-PL CH{4} [+0]
D: SATM H [+0] GRAPHITE T=HPG O=BASAL-PL CH{4} [+0]

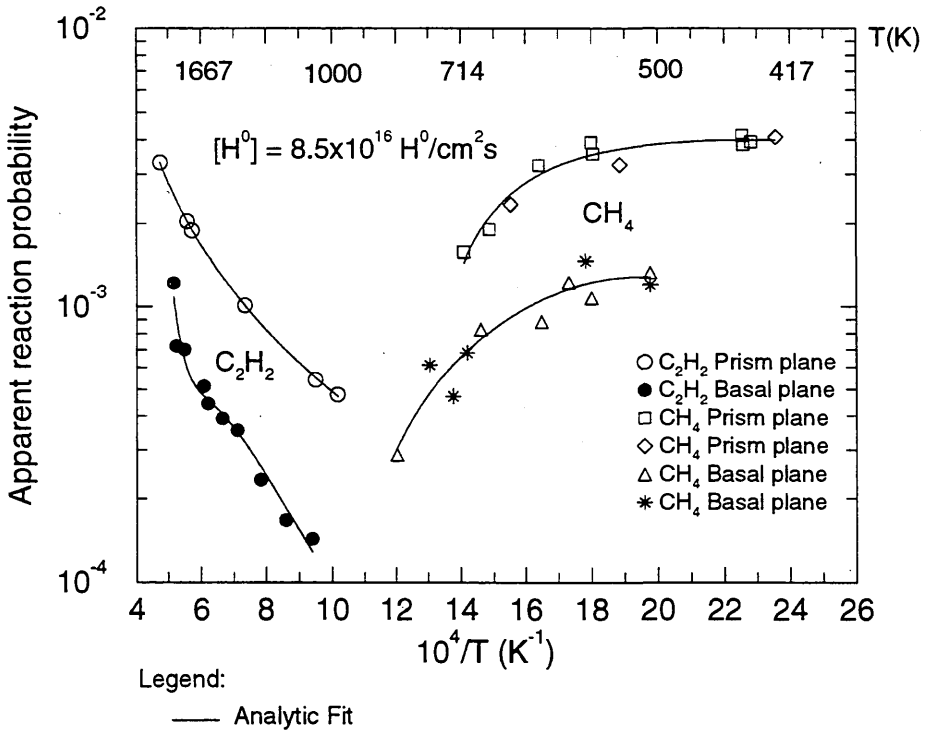

4.1.1.2 H^0 + pyrolytic graphite → CH_4

Source: R. K. Gould, J. Chem. Phys. **63**, 1825 (1975).

Accuracy: Indeterminate.

Comments: (1) Chemical erosion yield (CH_4 formation) due to H^0 impact.
(2) Specimen: graphite (pyrolytic, spectroscopic grade).
(3) H^0 produced by contact dissociation of H_2 on hot W filament.
(4) QMS measurement of CH_4, steady state.
(5) The formation rate of CH_4 was converted to a yield by dividing by the incident H^0 flux, and fitted to a straight line.

Analytic fitting function:

Erosion yield:

$$Y = A_1 F + A_2 \quad [CH_4/H^0]$$

where F is the flux density H^0/cm^2s. The rms deviation of the analytic fit is 6.3%.

Fitting parameters A_1-A_2

-9.0831E-21	2.5027E-04

ALADDIN evaluation function erosion yield: EYIELD2A

ALADDIN hierarchical labelling:

SATM H [+0] GRAPHITE T=HPG CH{4} [+0]

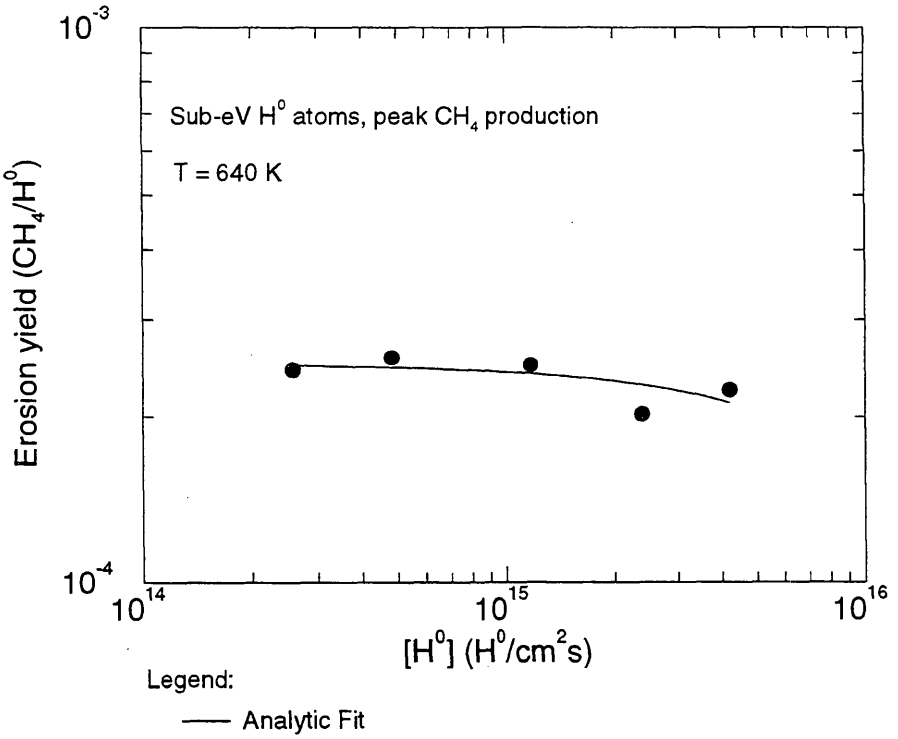

4.1.1.3 H^0 + pyrolytic graphite → CH_4, C_2-molecules

Source: E. Vietzke, K. Flaskamp, and V. Phillips, J. Nucl. Mater. **111&112**, 763 (1982).

Accuracy: Yield: 50%.

Comments: (1) H^0 atom reaction yield, H^0 beam produced in W oven at 2800 K.
(2) Specimen: machined pyrolytic graphite (HPG, Union Carbide).
(3) Line-of-sight detection by QMS.
(4) CH_3^+ signal assumed to originate only from cracking of CH_4 (see 4.1.1.4).
(5) Published data corrected for Maxwell-Boltzmann distributions with respect to specimen temperature.

Analytic fitting function:

Erosion yield:

$$Y = 1.0 \times 10^{-6}[A_1 \exp[-(\frac{T - A_2}{A_3 T + 1})^2 / A_4] T^{A_5} + A_6 \exp(-A_7 T) T^{A_8}] \quad [\text{molecules}/H^0]$$

where T is in Kelvin. The rms deviation of analytic fits for reactions A (△), B (•), C (○) and D (□) are 24.2%, 34.6%, 7.0% and 31.0%, respectively.

Fitting parameters A_1-A_8

A	9.3448E+01	-9.9400E+02	0.0	1.4535E+06	7.6376E-01	-5.8346E+02
	1.1498E-03	2.8891E-01				
B	1.2972E-01	5.2235E+02	-7.1864E-04	1.3165E+04	3.1117E-01	1.9521E-08
	9.3420E-03	3.6541E+00				
C	7.8246E-03	4.7071E+02	-1.3215E-03	1.7977E+05	7.8452E-01	1.8608E-08
	5.9017E-03	3.2298E+00				
D	3.9224E-02	5.6918E+02	-8.5146E-04	7.2402E+04	5.0928E-01	1.2166E-12
	1.0701E-02	5.0706E+00				

ALADDIN evaluation function for erosion yield: EYIELD8A

ALADDIN hierarchical labelling:

A: SATM H [+0] GRAPHITE T=HPG O=PRISM-PL-MI CH{4} [+0]
B: SATM H [+0] GRAPHITE T=HPG O=BASAL-PL-MI CH{4} [+0]
C: SATM H [+0] GRAPHITE T=HPG O=BASAL-PL-CL CH{4} [+0]
D: SATM H [+0] GRAPHITE T=HPG O=BASAL-PL-CL M26 [+0]

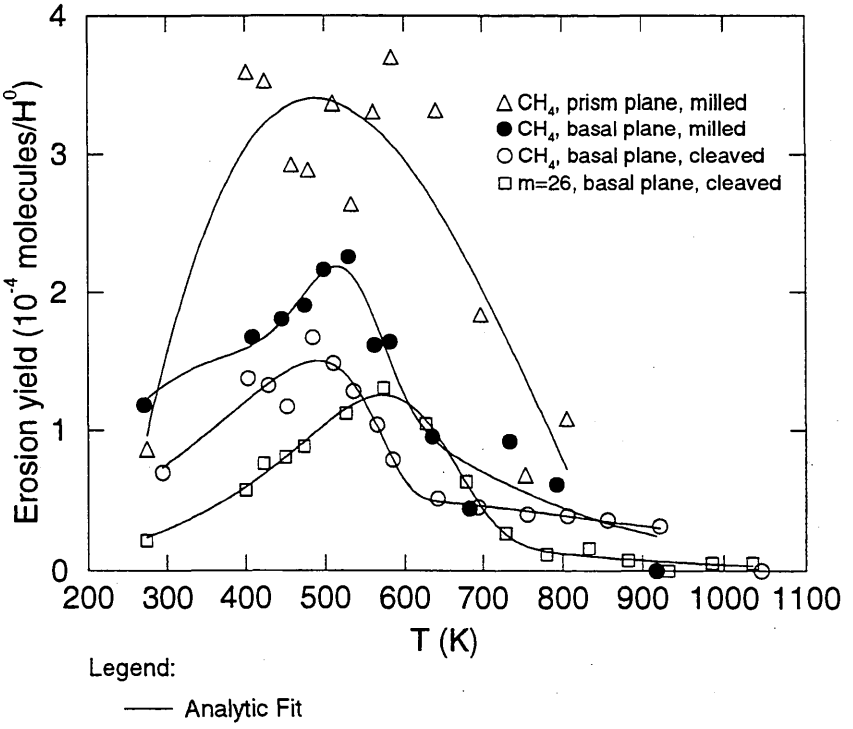

4.1.1.4 H^0 + pyrolytic graphite → CH_3, CH_4

Source: E. Vietzke, K. Flaskamp, and V. Philipps, J. Nucl. Mater. **128&129**, 545 (1984).

Accuracy: Yield: 50%.

Comments: (1) Steady-state CH_3 + CH_4 formation by H^0 atom impact.
(2) H beam formed in heated W tube at 2800 K.
(3) Specimen: machined pyrolytic graphite (HPG, Union Carbide).
(4) Published data corrected for thermal velocity distribution with respect to specimen temperature and for pumping of CH_4.

Analytic fitting function:

Erosion yield:

$$Y = 1.0 \times 10^{-2}[A_1 \exp(-(T - A_2)^2/A_3)T^{A_4} + A_5 \exp(-A_6 T)T^{A_7}] \quad [\text{molecules}/H^0]$$

where T is in Kelvin. The rms deviation of analytic fits for reactions A (□), B (•) and C (◇) are 26.8%, 21.7% and 6.5%, respectively.

Fitting parameters A_1-A_7

A	1.4315E-07	-3.2708E+03	7.7274E+05	4.5397E+00	-2.5490E+06	9.9793E+03
	-1.5861E+06					
B	2.3846E-03	5.8485E+02	5.1269E+04	1.5337E-01	9.7401E-03	-6.0278E-01
	-1.8696E+02					
C	3.8002E-03	5.5774E+02	3.9154E+04	9.6272E-02	3.4714E-03	-7.6730E-04
	-1.6596E-01					

ALADDIN evaluation function for erosion yield: EYIELD7A

ALADDIN hierarchical labelling:

A: SATM H [+0] GRAPHITE T=HPG CH{4} [+0]
B: SATM H [+0] GRAPHITE T=HPG CH{3} [+0]
C: SATM H [+0] GRAPHITE T=HPG CH{3} [+0] CH{4} [+0]

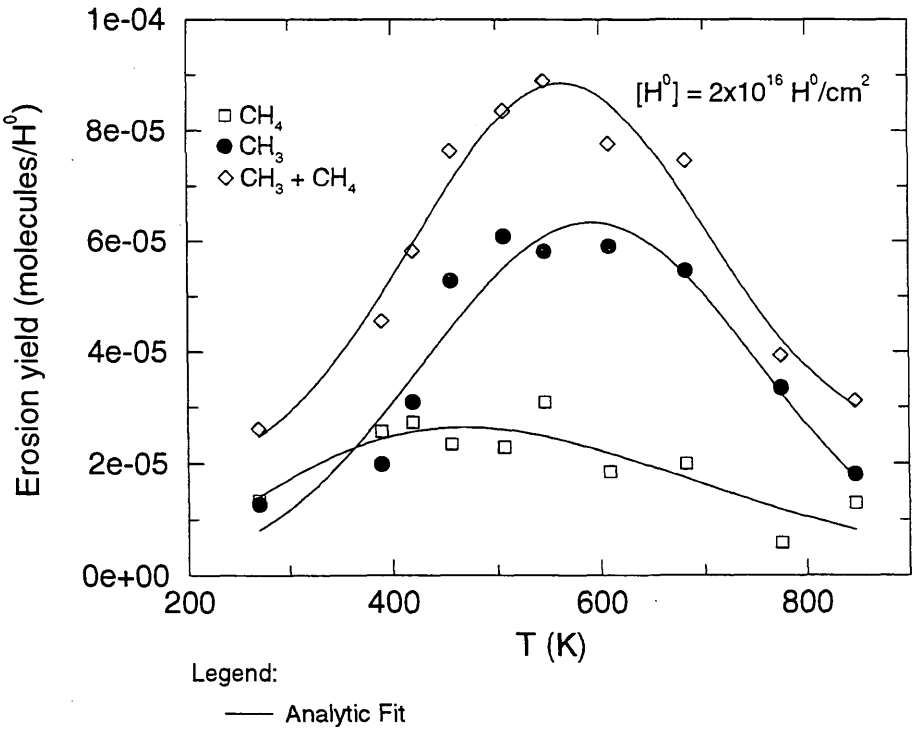

4.1.1.5 H^0 + pyrolytic graphite → CH_4

Source: C. S. Pitcher, A. O. Auciello, A. A. Haasz and P. C. Stangeby, J. Nucl. Mater. **128&129**, 597 (1984).

Accuracy: Yield: ±25%.

Comments: (1) Data on curve A correspond to the magnitude of prompt transient methane production subsequent to specimen "reactivation" by heating at 1250 K for 1 minute; data on curve B correspond to steady-state values.
(2) Specimen: graphite (pyrolytic).
(3) H^0 (sub-eV) beam produced by H_2 dissociation in a RF discharge tube; H^0 flux determined by QMS.
(4) Methane production is measured via QMS-RGA.

Analytic fitting function:

Methane yield:

$$Y = 1.0 \times 10^{-2}[A_1 \exp(-(T - A_2)^2/A_3)T^{A_4} + A_5 \exp(-A_6 T)T^{A_7}] \quad [CH_4/H^0]$$

where T is in Kelvin. The rms deviation of analytic fits for reactions A (o) and B (△) are 2.1% and 29.9%, respectively.

Fitting parameters A_1-A_7

A	6.8535E-10	5.8663E+02	1.6871E+04	2.2517E+00	2.2705E-41	2.2647E-02
	1.5720E+01					
B	2.9673E-02	7.9218E+02	3.3030E+04	3.8919E-02	-2.5371E-05	-5.6755E-03
	9.3366E-06					

ALADDIN evaluation function for methane yield: EYIELD7A

ALADDIN hierarchical labelling:

A, B: SATM H [+0] GRAPHITE T=HPG CH{4} [+0]

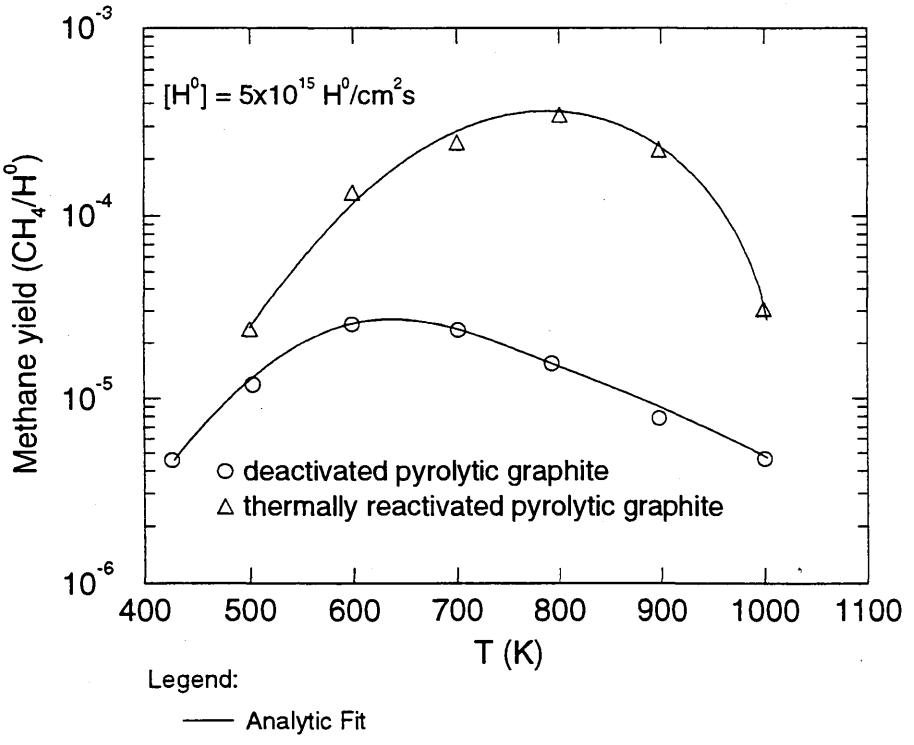

4.1.1.6 H^0 + pyrolytic graphite → CH_4

Source: A. A. Haasz and J. W. Davis, J. Chem. Phys. **85**, 3293 (1986).

Accuracy: Yield: ±35%; H^0 flux density: ±35%.

Comments: (1) Data correspond to steady-state methane yield at T_m.
(2) Specimen: graphite (pyrolytic).
(3) H^0 (sub-eV) is produced via dissociation of H_2 on a hot (1900 K) W ribbon; H^0 flux is varied by changing the H_2 backfill pressure.
(4) The rates from Fig. (2a) of the source paper were converted to erosion yields by dividing by the H^0 flux and a spot size of 0.2 cm^2.
(5) Methane production is measured by QMS-RGA.

Analytic fitting function:

Methane yield:

$$Y = A_1 \exp(-A_2 F) F^{A_3} \quad [\text{molecules}/H^0]$$

where hydrogen flux F is in H^0/cm^2s. The rms deviation of the analytic fit (*) is 6.7%.

Fitting parameters A_1-A_3

7.2745E-06	-1.8246E-17	1.1258E+00

ALADDIN evaluation function for methane yield: EYIELD3A

ALADDIN hierarchical labelling:

SATM H [+0] GRAPHITE T=HPG CH{4} [+0]

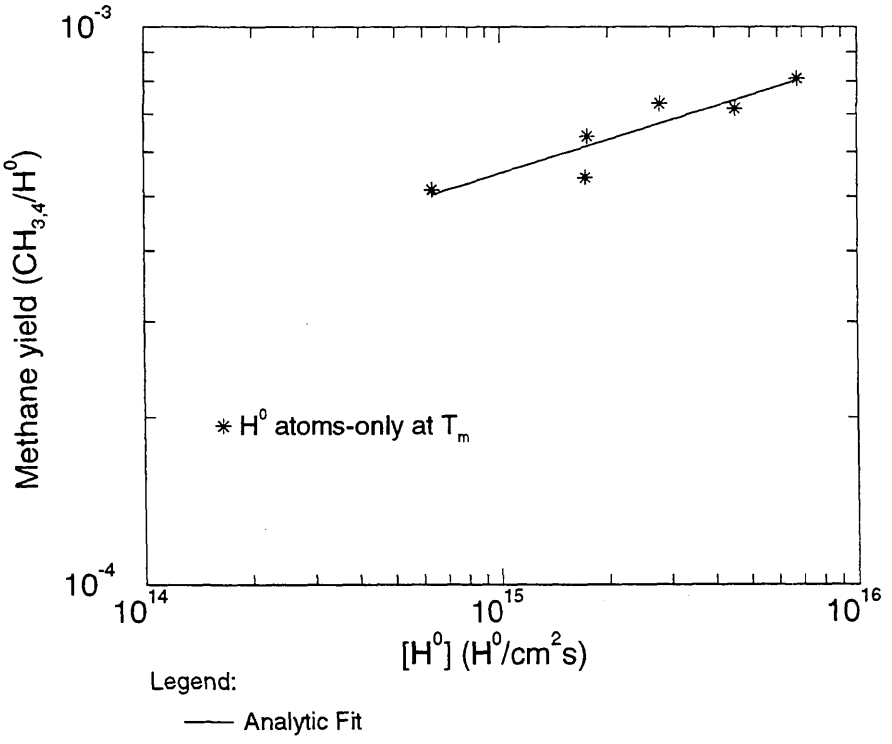

4.1.1.7 H^0 + pyrolytic graphite → CH_3, CH_4

Source: A. A. Haasz and J. W. Davis, J. Chem. Phys. **85**, 3293 (1986).

Accuracy: Yield: ±35%; T: $\pm 25K$.

Comments: (1) All data correspond to steady-state methane yields.
(2) Specimen: graphite (pyrolytic).
(3) H^0 (sub-eV) is produced via dissociation of H_2 on a hot (1900 K) W ribbon; H^0 flux is varied by changing the H_2 backfill pressure.
(4) Different symbols in the figure correspond to different H^0 fluxes.
(5) Methane production is measured via QMS-RGA.
(6) Production rate data was converted to a reaction yield and refitted to the kinetic equation provided in the source.

Analytic fitting function:

Methane yield:

$$Y = A_1 \exp(-A_2/T)/(1 + A_3 \exp(-A_4/T)) \quad [\text{molecules}/H^0]$$

where T is in Kelvin. The rms deviation of analytic fits for fluxes A (△), B (○), C (□), D (∗) and E (•) are 22.5%, 28.0%, 29.6%, 38.7% and 30.5%, respectively.

Fitting parameters A_1-A_4

A	1.3097E+22	2.7457E+04	5.3986E+27	3.0205E+04
B	8.0923E+08	1.3342E+04	3.4314E+14	1.6306E+04
C	2.3772E+12	1.6924E+04	5.0771E+17	1.9623E+04
D	1.9220E+07	1.1622E+04	3.6310E+12	1.4396E+04
E	8.7469E+01	5.7421E+03	8.8137E+07	9.7809E+03

ALADDIN evaluation function for methane yield: EYIELD4D

ALADDIN hierarchical labelling:

A-E: SATM H [+0] GRAPHITE T=HPG CH{3} [+0] CH{4} [+0]

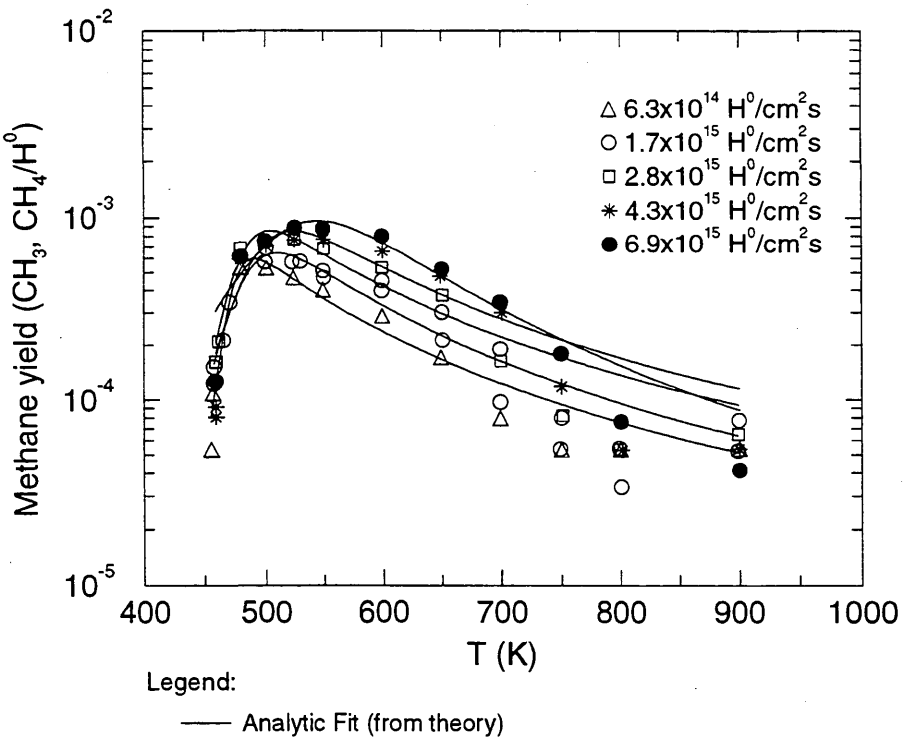

4.1.1.8 H^0 + pyrolytic graphite → C_xH_y, C

Source: J. W. Davis, A. A. Haasz, P. C. Stangeby, J. Nucl. Mater. **155-157**, 234 (1988).

Accuracy: Yield: ±35%; T: ±25K.

Comments: (1) Steady-state hydrocarbon yields.
(2) Specimen: graphite (pyrolytic).
(3) H^0 (sub-eV) is produced via dissociation of H_2 on a hot W ribbon.
(4) Methane measured via QMS-RGA.
(5) Yield for total chemical erosion, $Y_{chem-total} = [CH_4 + 2(C_2H_2 + C_2H_4 + C_2H_6) + 3(C_3H_6 + C_3H_8)]/H^0$.

Analytic fitting function:

Erosion yield:

$$Y = 1.0 \times 10^{-2}[A_1 \exp(-(T - A_2)^2/A_3)T^{A_4} + A_5 \exp(-A_6T)T^{A_7}] \quad [\text{molecules}/H^0]$$

where T is in Kelvin. The rms deviation of analytic fits for reactions A (∗), B (•), C (▽), D (◇), E (△), F (+) and G (○) are 2.5%, 5.9%, 0.7%, 4.2%, 3.9%, 0.5% and 2.2%, respectively.

Fitting parameters A_1-A_7

A	2.4170E-01	5.9226E+02	1.3128E+04	8.3944E-02	3.8173E+00	7.7385E-03	3.5123E-02
B	1.3318E-02	5.4363E+02	1.9684E+04	7.9927E-02	-1.6094E-03	3.7957E-04	-2.9008E-05
C	3.5087E-03	5.6082E+02	3.1741E+04	-2.7504E-02	3.4234E-04	5.5014E-05	-3.0104E-05
D	1.9425E-02	6.0937E+02	1.5342E+04	1.7463E-01	-9.1758E-01	5.7747E-03	5.1414E-03
E	1.5437E-01	6.0232E+02	1.3760E+04	-7.6963E-02	-1.7522E-05	-5.1159E-03	1.4221E-05
F	1.6308E-02	5.5489E+02	6.5404E+03	2.6716E-02	3.7271E-01	5.9112E-03	2.9745E-04
G	5.1028E-02	5.5710E+02	1.4674E+04	1.7707E-02	-1.8236E-01	5.2919E-03	1.0547E-04

ALADDIN evaluation function for erosion yield: EYIELD7A

ALADDIN hierarchical labelling:

A: SATM H [+0] GRAPHITE T=HPG C [+0]
B: SATM H [+0] GRAPHITE T=HPG CH{4} [+0]
C: SATM H [+0] GRAPHITE T=HPG C{2}H{2} [+0]
D: SATM H [+0] GRAPHITE T=HPG C{2}H{4} [+0]
E: SATM H [+0] GRAPHITE T=HPG C{2}H{6} [+0]
F: SATM H [+0] GRAPHITE T=HPG C{3}H{6} [+0]
G: SATM H [+0] GRAPHITE T=HPG C{3}H{8} [+0]

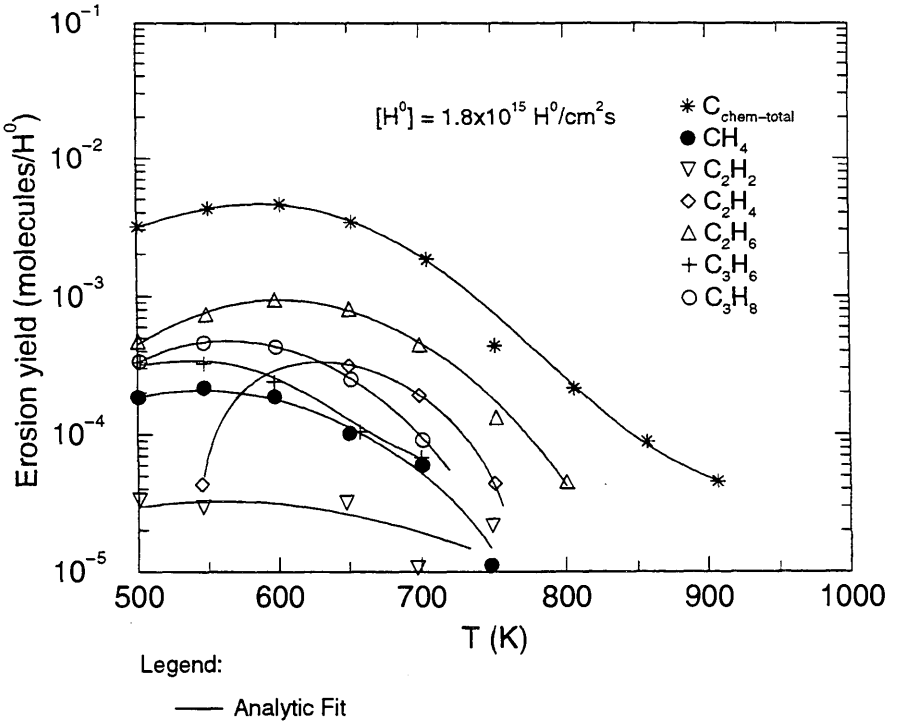

4.1.1.9 H^0 + pyrolytic graphite → CH_3

Source: E. Vietzke, V. Philipps and K. Flaskamp, J. Nucl. Mater. **162-164**, 898 (1989).

Accuracy: Yield: 50%.

Comments: (1) H^0 atom reaction on thermally annealed graphite, preirradiated by 5 keV D_2^+ (fluence: 5×10^{17} D^+/cm^2) at room temperature.
(2) Line-of-site QMS detection.
(3) Specimen: graphite (HPG).

Analytic fitting function:

Reaction yield:

$$Y = 1.0 \times 10^{-2}[A_1 \exp(-(T - A_2)^2/A_3)T^{A_4} + A_5 \exp(-A_6 T)T^{A_7}] \quad \text{[arb. units]}$$

where T is in Kelvin. The rms deviation of analytic fits for reactions A (○), B (●), C (△), D (□) and E (◇) are 9.6%, 5.0%, 10.0%, 3.7% and 2.0%, respectively.

Fitting parameters A_1-A_7

A	2.5691E-03	7.3403E+02	6.2702E+04	1.5955E+00	-6.9659E-06	1.2576E+00
	1.0000E+00					
B	5.2835E-03	6.7496E+02	5.3657E+04	1.3744E+00	-2.2036E-04	1.1759E+00
	1.0000E+00					
C	1.3666E-03	5.6627E+02	4.2074E+04	1.4759E+00	-2.2036E-04	1.1759E+00
	1.0000E+00					
D	1.0224E+01	5.7669E+02	7.7813E+03	-1.7874E-03	1.8325E-03	2.7727E-03
	1.4475E+00					
E	2.7949E+01	2.3490E+02	1.8809E+06	2.7604E-01	-2.4801E+01	4.0432E-04
	3.1649E-01					

ALADDIN evaluation function for reaction yield: EYIELD7A

ALADDIN hierarchical labelling:

A-E: SATM H [+0] GRAPHITE T=HPG CH{3} [+0]

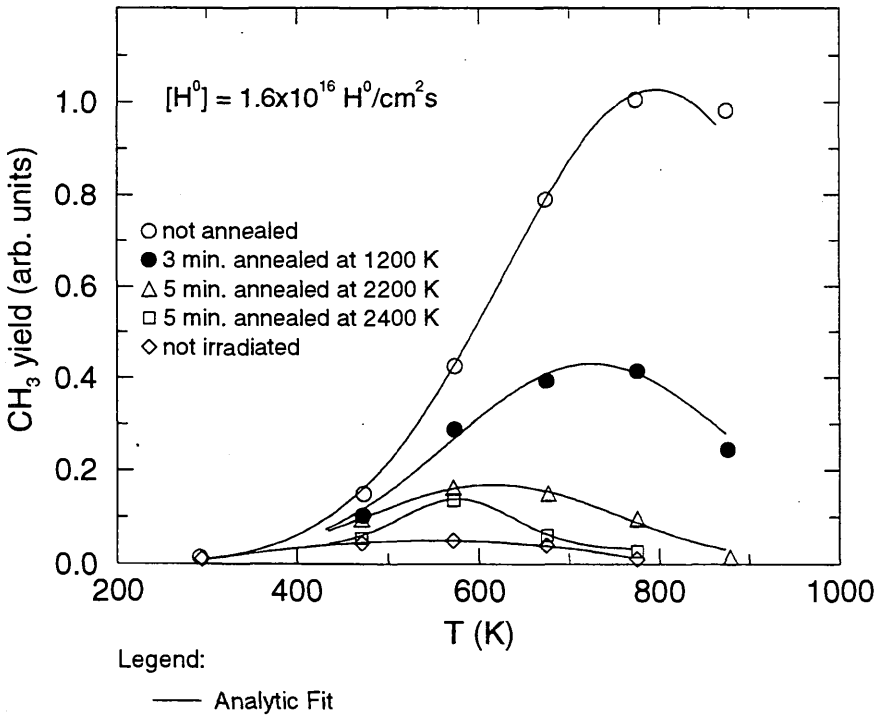

4.1.1.10 H^0 + Papyex graphite → CH_4

Source: C. Ashby, J. Nucl. Mater. **111&112**, 750 (1982).

Accuracy: Indeterminate.

Comments: (1) Data are for the dependence of thermal H^0 reaction rates on the reaction history of sample.
(2) Specimen: graphite (Papyex).
(3) Atomic hydrogen generated on a hot W film.
(4) Methane production rate is measured via QMS-RGA.
(5) The measurement sequence was from lower to higher temperatures for a given reaction set, and larger numbers indicate later reaction sets.

Analytic fitting function:

Production rate:

$$Y = 1.0 \times 10^{12}[A_1 \exp(-A_2 T)T^{A_3} + A_4 T^{A_5}] \quad \text{[molecules/s]}$$

where T is in Kelvin. The rms deviation of analytic fits for reactions A (2), B (3), C (4), D (5) and E (6) are 0.7%, 2.2%, 1.2%, 2.2% and 0.0%, respectively. The numbers 1-6 indicate different reaction histories. For reactions B and E the function $Y = A_1 T + A_2$ was used.

Fitting parameters A_1-A_5

A	7.6645E-08	-3.4119E-02	-1.1030E+00	1.1031E+00	3.7779E-01
B	1.1236E-02	-1.3357E-01			
C	1.8650E-13	-5.1714E-02	-1.2439E+00	1.5859E-02	8.9879E-01
D	1.5324E-15	-2.0688E-02	2.9201E+00	3.4006E-01	3.6197E-01
E	8.2118E-03	-1.7913E+00			

ALADDIN evaluation function for production rate: EYIELD2A, EYIELD5A

ALADDIN hierarchical labelling:

A-E: SATM H [+0] GRAPHITE T=PAPYEX CH{4} [+0]

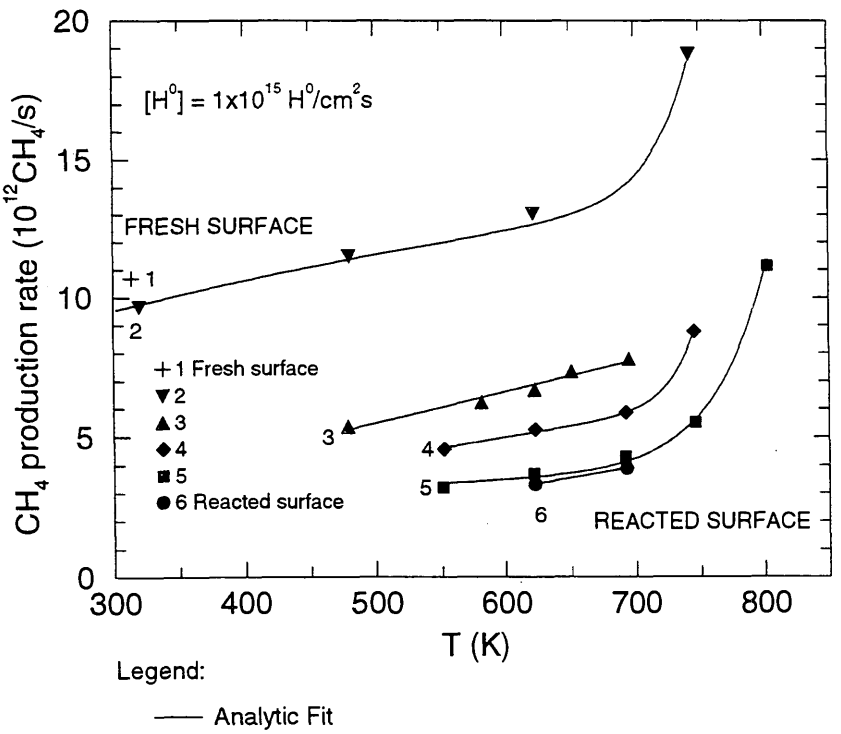

4.1.1.11 H^0 + Papyex graphite → CH_4

Source: A. A. Haasz, P. C. Stangeby, and O. Auciello, J. Nucl. Mater. **111&112**, 757 (1982).

Accuracy: Yield: ±35%; T: ±25K (The main uncertainty is in the H^0 flux density. "Absolute" yields are estimated to be within a factor of two; relative values: ±15%).

Comments: (1) The data correspond to the magnitude of prompt transient methane production, subsequent to specimen "reactivation" by heating at 1200 K for 1 minute.
(2) Specimen: graphite (Papyex).
(3) H^0 (sub-eV) is produced via dissociation of H_2 on a "hot" W ribbon.
(4) Methane production rate is measured via QMS-RGA.
(5) Different symbols in the figure correspond to different H^0 fluxes.
(6) The fact that the different symbols in the figure fall on the same curve indicates the absence of flux dependence in the flux range studied.

Analytic fitting function:

Methane yield:

$$Y = 1.0 \times 10^{-2}[A_1 \exp(-(T - A_2)^2/A_3)T^{A_4} + A_5 \exp(-A_6 T)T^{A_7}] \quad [CH_4/H^0]$$

where T is in Kelvin. The rms deviation of the analytic fit is 10.7%.

Fitting parameters A_1-A_7

5.1736E-03	8.2741E+02	2.6908E+04	3.5543E-01	-5.6130E-05	-2.7821E-04
7.0000E-01					

ALADDIN evaluation function for methane yield: EYIELD7A

ALADDIN hierarchical labelling:

SATM H [+0] GRAPHITE T=PAPYEX CH{4} [+0]

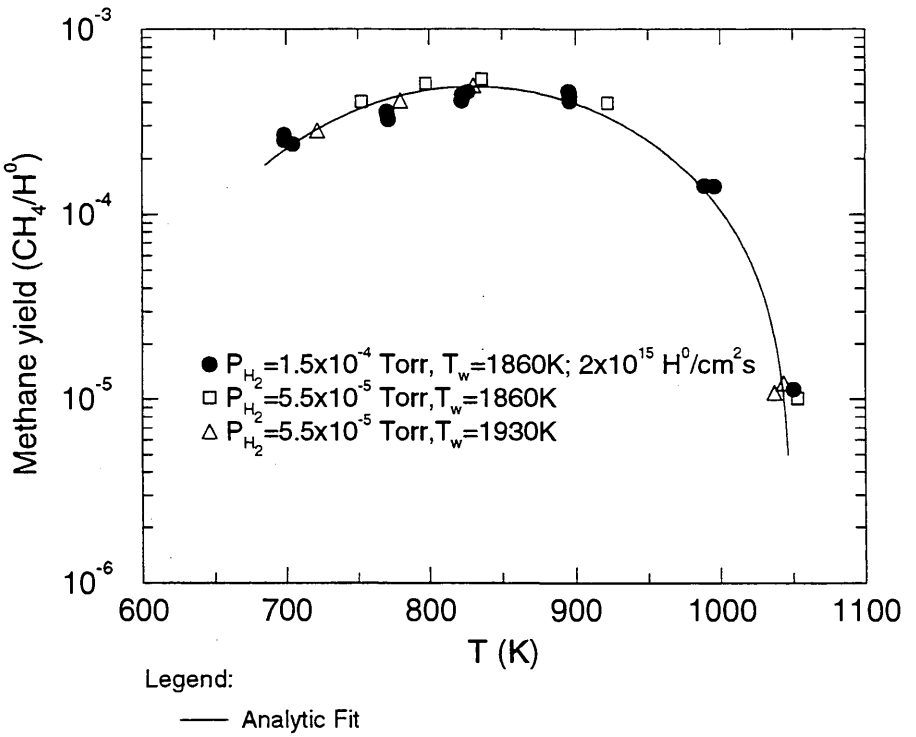

4.1.1.12 H^0 + Papyex graphite → CH_4

Source: P. C. Stangeby, A. O. Auciello, and A. A. Haasz, J. Vac. Sci. Technol. A **1** 1425 (1983).

Accuracy: Yield: ±25%; T: ±25K.

Comments: (1) Steady-state methane production for a "deactivated yield" resulting from preexposure of the sample to H^0 atoms.
(2) Specimen: graphite (Papyex).
(3) H^0 (sub-eV) is produced by H_2 dissociation on a hot W ribbon. H^0 flux determined by QMS.
(4) Methane production rate is measured via QMS-RGA.

Analytic fitting function:

Methane yield:

$$Y = A_1 \exp\left[-\left(\frac{T - A_2}{A_3 T + 1}\right)^2 / A_4\right] T^{A_5} + A_6 \exp(-A_7 T) T^{A_8} \quad [\text{molecules}/H^0]$$

where T is in Kelvin. The rms deviation of the analytic fit is 1.8%.

Fitting parameters A_1-A_8

9.5730e-03	5.7580e+02	-7.5973e-04	1.6584e+05	-8.3210e-01	5.3216e-05
1.1020e-02	1.1067e+00				

ALADDIN evaluation function for methane yield: EYIELD8A

ALADDIN hierarchical labelling:

SATM H [+0] GRAPHITE T=PAPYEX CH{4} [+0]

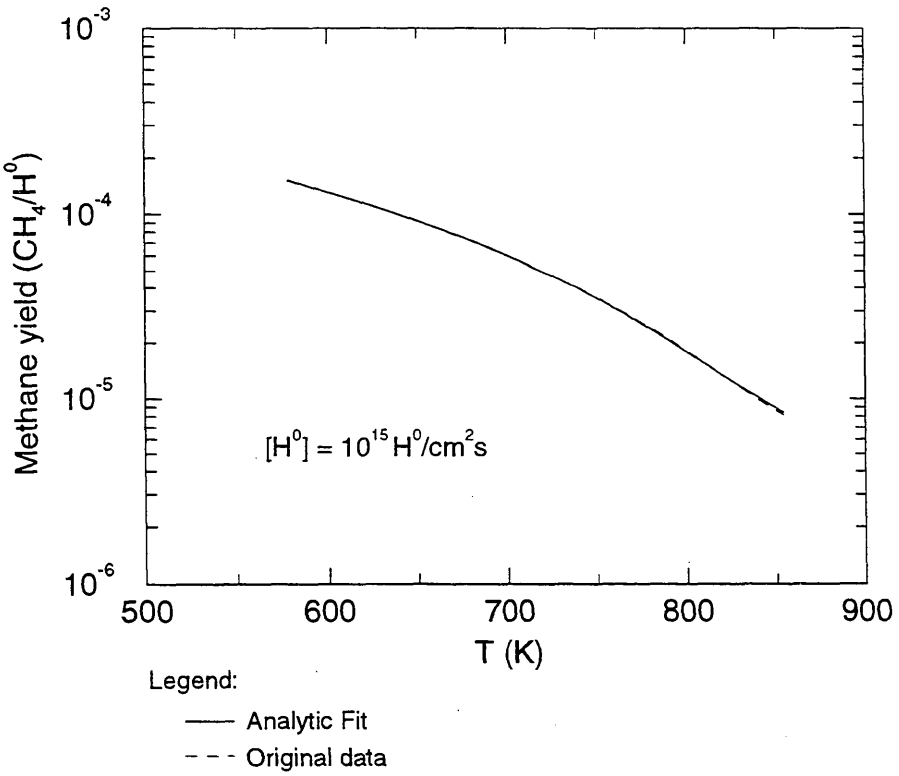

4.1.1.13 H^0 + CLOR, POCO, pyrolytic, Papyex graphite → CH_4

Source: V. Philipps, K. Flaskamp, and E. Vietzke, J. Nucl. Mater. **122&123**, 1440 (1984).

Accuracy: Yield: 50%.

Comments: (1) Comparison of H^0 atom reactions on different graphites.
(2) Line-of-sight detection by QMS.
(3) CH_3^+ assumed to originate only from cracking of CH_4.
(4) Measured yields were multiplied by $(280\ K/T)^{1/2}$ to obtain the "Relative yield".
(5) No correction concerning thermal distribution (sensitivity for RT used.)
(6) Specimens: pyrolytic graphite (HPG), POCO graphite (grain size 1 μm), Carbone Lorraine 5829, Papyex graphite.

Analytic fitting function:

Relative yield:

$$Y = 1.0 \times 10^{-2}[A_1 \exp(-(T - A_2)^2/A_3)T^{A_4} + A_5 \exp(-A_6 T)T^{A_7}] \quad \text{[arb. units]}$$

where T is in Kelvin. The rms deviation of analytic fits for reactions A (×), B (•), C (□) and D (△) are 16.9%, 31.4%, 2.4% and 22.3%, respectively. Data for curve C were fitted with EYIELD8A.

Fitting parameters A_1-A_8

A	5.5000E+02	0.0000E+00	2.5000E+03	0.0000E+00	7.3488E-08	9.0695E-03
	4.3488E+00					
B	3.9265E+02	4.8671E+02	4.2126E+03	-8.4216E-02	7.0625E-05	7.8066E-03
	3.0684E+00					
C	1.0219E+00	5.7192E+02	-9.9167E-04	5.6709E+04	1.7454E-02	1.5140E+00
	2.0071E-03	1.9403E-01				
D	4.7097E+02	5.2328E+02	8.1433E+03	-1.7281E-01	8.5201E-05	8.9981E-03
	3.1542E+00					

ALADDIN evaluation function for relative yield: EYIELD7A, EYIELD8A

ALADDIN hierarchical labelling:

A: SATM H [+0] GRAPHITE T=CLOR CH{4} [+0]
B: SATM H [+0] GRAPHITE T=POCO CH{4} [+0]
C: SATM H [+0] GRAPHITE T=PAPYEX CH{4} [+0]
D: SATM H [+0] GRAPHITE T=HPG CH{4} [+0]

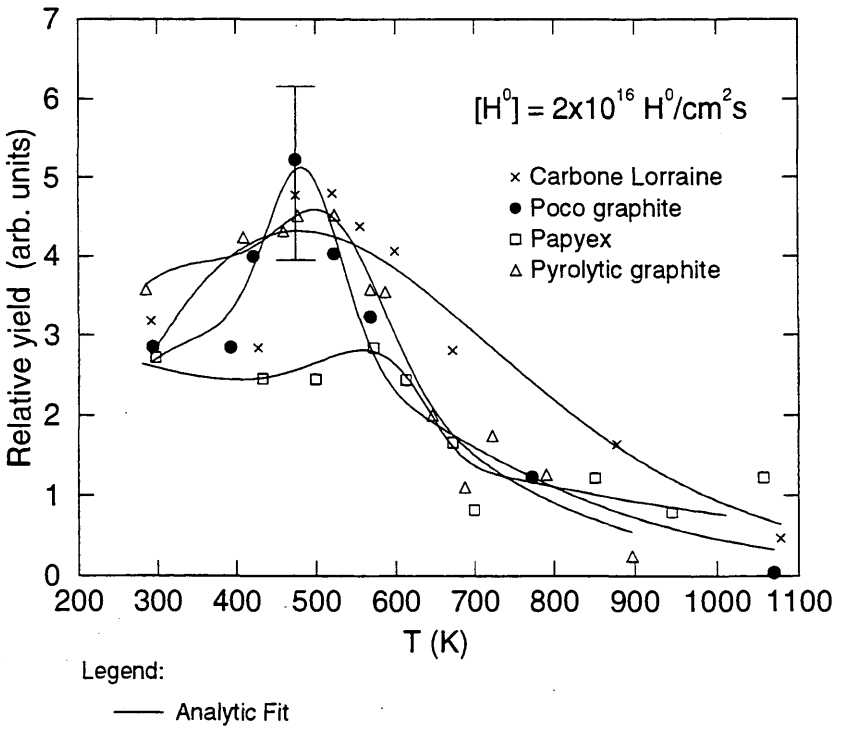

4.1.1.14 H^0, H^+ + pyrolytic graphite → C

Source: E. Vietzke and V. Philipps, Fusion Technol. **15**, 108 (1989).

Accuracy: Yield: 50%.

Comments: (1) Total chemical erosion yield due to H^0 impact.
(2) Specimen: graphite (Pyrolytic, redeposited carbon; pyrolytic pre-irradiated by D^+ at RT).
(3) D^+ fluence: $5 \times 10^{17}/cm^2$.
(4) Total chemical erosion yield = $[\sum x(C_xH_y)]/H^0$.
(5) H^+ data (shown for comparison) from R. Yamada, J. Nucl. Mater. **145-147**, 359 (1987).

Analytic fitting function:

Erosion yield:

$$Y = 1.0 \times 10^{-2}[A_1 \exp(-(T - A_2)^2/A_3)T^{A_4} + A_5 \exp(-A_6T)T^{A_7}] \quad [\text{eroded C}/H^0]$$

where T is in Kelvin. The rms deviation of analytic fits for reactions A (H^0, redeposited carbon), B (H^0, pre-irradiated by 2.5 keV D^+) and C (H^0, pyrolytic graphite) are 0.7%, 2.2% and 5.4%, respectively.

Fitting parameters A_1-A_7

A	1.4405E+00	6.1334E+02	3.5141E+04	8.7901E-02	1.3277E-02	-5.7348E-03
	-1.4980E-03					
B	5.5613E+00	7.9696E+02	4.4482E+04	-1.1261E-02	1.2763E-01	-8.6221E-04
	2.6136E-03					
C	2.3806E-01	5.9272E+02	2.5830E+04	-1.5841E-01	1.9940E-02	4.7640E-04
	9.8643E-04					

ALADDIN evaluation function for erosion yield: EYIELD7A

ALADDIN hierarchical labelling:

A: SATM H [+0] GRAPHITE T=HPG-REDEP C [+0]
B: SATM H [+0] GRAPHITE T=HPG-PI C [+0]
C: SATM H [+0] GRAPHITE T=HPG-PI C [+0]

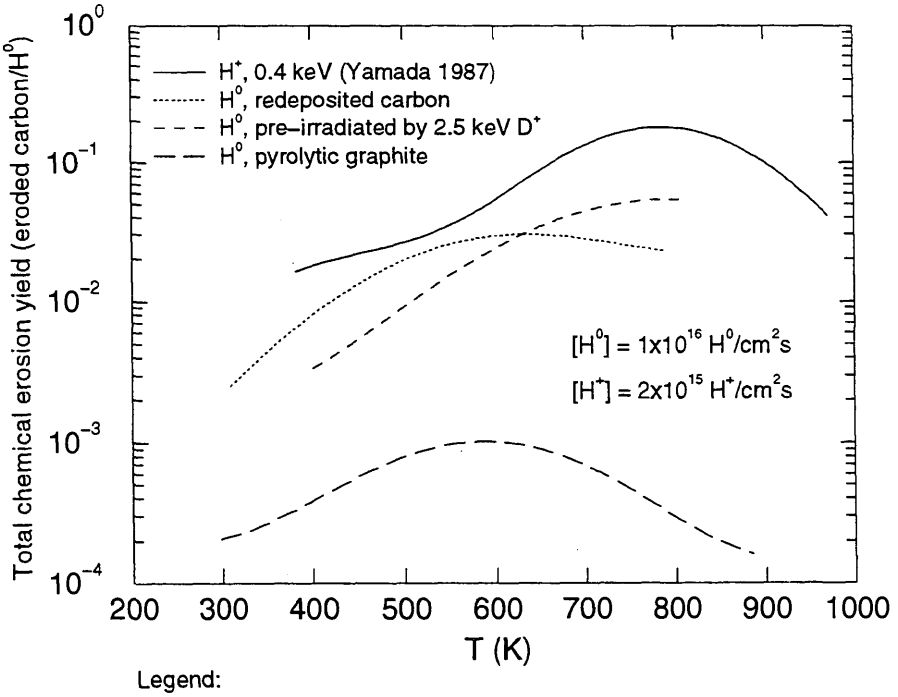

Legend:

All curves – Analytic Fits

4.1.1.15 H^0, H_3^+ + PG-A graphite → CH_4

Source: R. Yamada, K. Nakamura and M. Saidoh, J. Nucl. Mater. **98**, 167 (1981).

Accuracy: Indeterminate.

Comments: (1) Steady-state hydrocarbon yield.
(2) Specimen: graphite (pyrolytic, PG-A basal plane (Nippon Carbon)).
(3) H^+ ions: mass analyzed accelerator.
(4) Methane measured via QMS.
(5) Sub-eV H^0 produced on a hot (>1700 ^{0}C) Re filament, and conducted to specimen via teflon coated line. H^0 flux increases with increasing H_2 pressure.

Analytic fitting function:

Methane yield:

$$Y = 1.0 \times 10^{-4}[A_1 \exp(-(T - A_2)^2/A_3)T^{A_4} + A_5 \exp(-A_6 T)T^{A_7}] \quad [\text{molecules/H}^+]$$

where T is in ^{0}C. The rms deviation of the analytic fits for reactions A (•), B (×), C (△) and D (□) are 2.3%, 5.3%, 10.3% and 8.5%, respectively.

Fitting parameters A_1-A_7

A	5.5460E+02	5.2391E+02	1.0096E+04	1.4124E-04	1.4381E+02	-5.6460E-04
	-1.8231E-02					
B	5.3641E+02	5.2290E+02	1.3305E+04	3.9873E-04	2.2157E+02	-3.8529E-04
	-2.0532E-01					
C	5.9889E+02	5.1636E+02	8.2264E+03	-1.7610E-02	7.9657E+00	1.2335E-03
	5.5509E-01					
D	5.0218E+02	5.1700E+02	9.4420E+03	8.0659E-03	6.5762E+01	-1.2764E-03
	-4.7986E-02					

ALADDIN evaluation function for methane yield: EYIELD7A

ALADDIN hierarchical labelling:

A-D: SATM H{3} [+1] GRAPHITE T=PGA O=BASAL-PL CH{4} [+0]

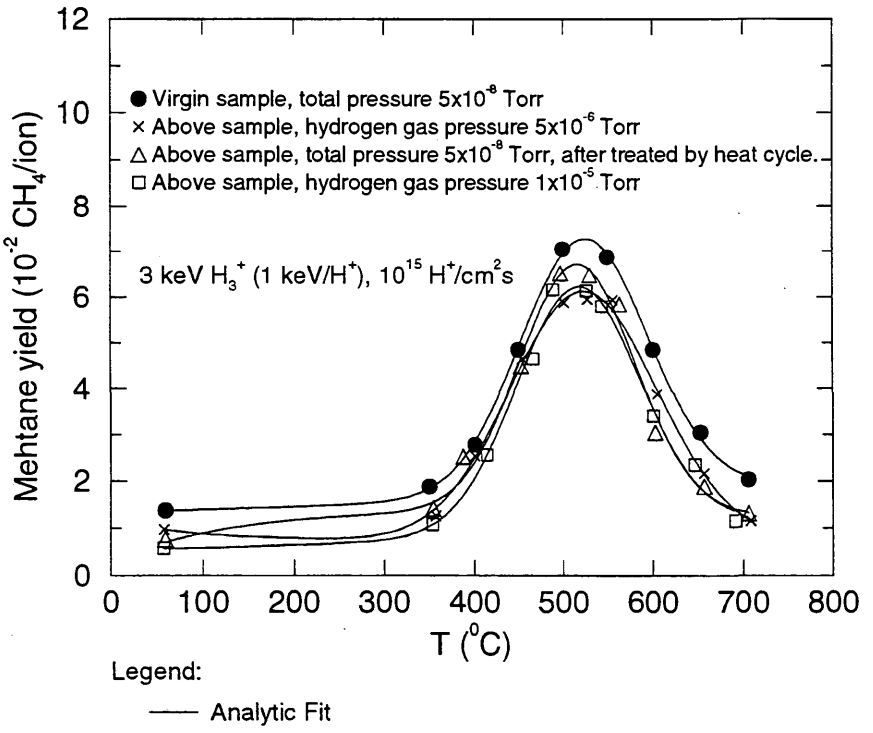

4.1.1.16 H^0 + a-C:H film → CH_3

Source: A. Horn, A. Schenk, J. Biener, B. Winter, C. Lutterloh, M. Wittmann, and J. Küppers, Chem. Phys. Lett. **231**, 193 (1994).

Accuracy: Indeterminate.

Comments: (1) Experiments were performed on several monolayers thick a-C:H films grown by ion beam desorption.
(2) a-C:H film surfaces subjected to thermal H^0 atoms from a heated Ta tube, with a flux of 1.9×10^{13} H^0/cm^2s.
(3) AES, HREELS and TDS were used to characterize film samples.

Analytic fitting function:

Erosion yield:

$$Y = 1.0 \times 10^{-5}[A_1 \exp(-(T - A_2)^2/A_3)T^{A_4} + A_5 \exp(-A_6 T)T^{A_7}] \quad [C/H^0]$$

where T is in Kelvin. The rms deviation of the analytic fit is 26.8%. The fit is to the theory analysis discussed in the source.

Fitting parameters A_1-A_7

	7.4705E+02	6.0034E+02	1.8015E+03	-2.8017E-03	1.1646E-08	6.8073E-03
	4.3068E+00					

ALADDIN evaluation function for erosion yield: EYIELD7A

ALADDIN hierarchical labelling:

SATM H [+0] GRAPHITE T=A-CH-FILM D=H CH{4} [+0]

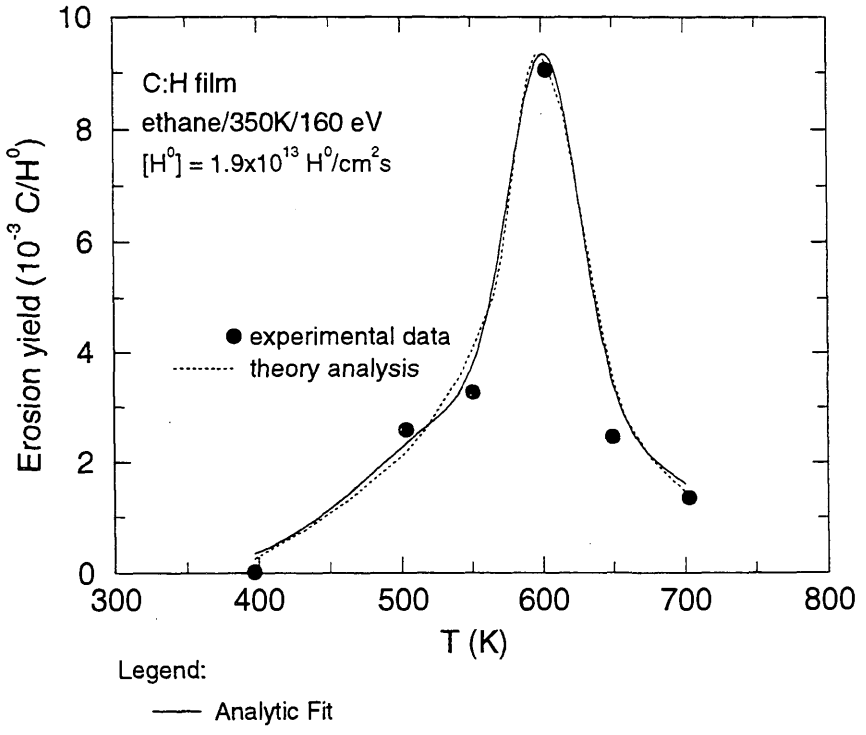

4.1.1.17 H^0 + a-C:H, a-C/B:H films → BH_2^+, CH_3^+

Source: E. Vietzke, V. Philipps, K. Flaskamp, J. Winter, S. Veprek and P. Koidl, in *10th International Symposium on Plasma Chemistry, Symposium Proceedings* (Editors: U. Ehlemann, H. G. Lergon and K. Wiesemann) **3**, 1 (1991).

Accuracy: Yield: 50%.

Comments: (1) Thermal atomic hydrogen reaction with amorphous films.
(2) Specimen: amorphous carbon film (a-C:H) and boron containing carbon film (a-C/B:H). The film for B/C = 0.3 has had a temperature excursion to 1600 K.
(3) Products detected by line-of-sight QMS.
(4) Signals normalized to the correspondent maximum CH_3^+ signal.

Analytic fitting function:

Reaction signal:

$$Y = A_1 \exp(-(T - A_2)^2/A_3)T^{A_4} + A_5 \exp(-A_6 T)T^{A_7} \quad [\text{signal}/CH_3^+]$$

where T is in Kelvin. The rms deviation of analytic fits for reactions A (△), B (•), C (○), D (□) and E (◇) are 8.0%, 33.6%, 4.1%, 5.8% and 5.0%, respectively. Data for curves B and E were fitted with EYIELD4B; curve C: EYIELD4A; curve D: EYIELD4D.

Fitting parameters A_1-A_7

A	3.5123e-03	4.3410e+02	2.5505e+04	9.02046e-01	2.4272e-03	5.0600e-03
	1.2996e+00					
B	5.2460e-08	5.3161e+02	1.6844e+04	2.5344e+00		
C	1.2231e-20	2.0955e-02	9.0193e+00	3.4619e-04		
D	2.6392e+01	1.5363e+03	3.3401e+02	3.4242e+03		
E	1.9573e+32	9.4669e+02	2.8731e+04	-1.1031e+01		

ALADDIN evaluation function for reaction signal: EYIELD7A, EYIELD4A, EYIELD4B, EYIELD4D

ALADDIN hierarchical labelling:

A, B: SATM H [+0] C T=A-CB-FILM BH{2} [+1]
C, D: SATM H [+0] C T=A-CB-FILM CH{3} [+1]
E: SATM H [+0] C T=A-CH-FILM CH{3} [+1]

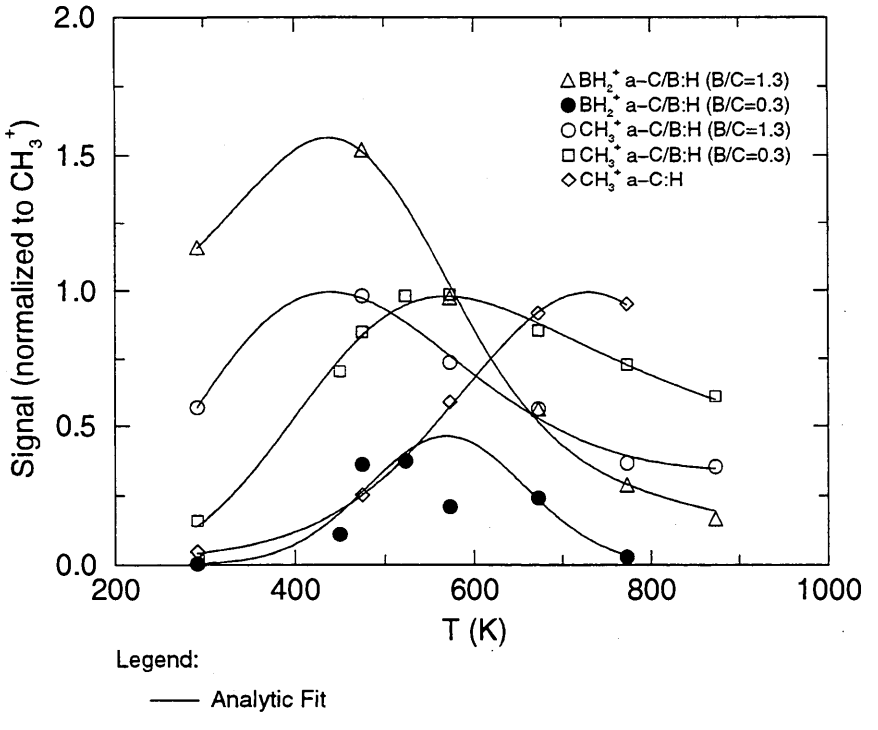

4.1.1.18 H^0 + diamond/Mo → C

Source: E. Vietzke, V. Philipps, K. Flaskamp, P. Koidl and Ch. Wild, Surf. Coatings Technol. **47**, 156 (1991).

Accuracy: Yield: 50%.

Comments: (1) Total chemical erosion yield measured for surface reaction of thermal atomic hydrogen with polycrystalline diamond film.
(2) Specimen: Film of 5 μm thickness prepared by hot-filament assisted CVD on Mo substrate.
(3) Reaction products detected using differentially pumped line-of-sight QMS.

Analytic fitting function:

Erosion yield:

$$Y = A_1 \exp(-(T - A_2)^2/A_3)T^{A_4} + A_5 \exp(-A_6 T/(A_7 T + 1.0))T^{A_8} \quad [\text{eroded C/H}^0]$$

where T is in Kelvin. The rms deviation of the analytic fit is 0.9%.

Fitting parameters A_1-A_8

1.5631e-05	6.2270e+02	1.8466e+04	1.5208e-01	6.0883e-08	6.2969e-04
-1.3030e-03	1.2175e+00				

ALADDIN evaluation function for erosion yield: EYIELD8B

ALADDIN hierarchical labelling:

SATM H [+0] Mo T=DIAM-FILM C [+0]

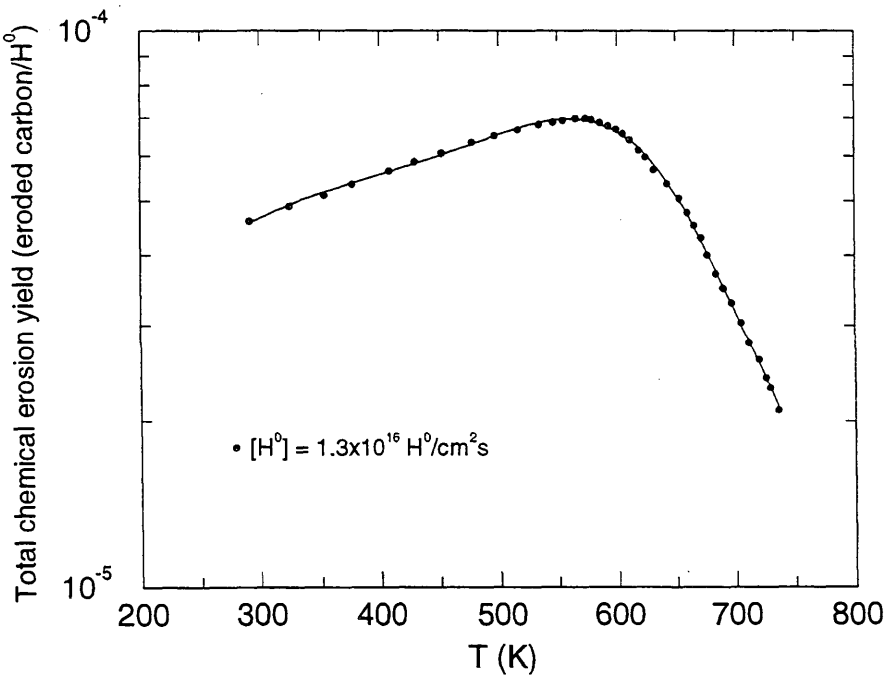

4.1.2.1 D^0 + a-C:H film → CH_3, CD_3

Source: E. Vietzke and V. Philipps, Nucl. Instr. and Meth. B **23**, 449 (1987).

Accuracy: Yield: 50%.

Comments: (1) Steady-state methyl radical formation by D^0 or H^0.
(2) H, D atom beam produced by thermal dissociation in W tube at 2800 K.
(3) Specimen: a-C:H film, graphite pre-irradiated with 5 keV D_2^+ (fluence 5×10^{17} D^+/cm^2).
(4) Line-of-sight QMS detection, Maxwell-Boltzmann distributions assumed.
(5) Results for the reaction H^0 + C (pre-irradiated by D^+) → CH_3 are included for comparison.

Analytic fitting function:

Erosion yield:

$$Y = 1.0 \times 10^{-2}[A_1 \exp(-(T - A_2)^2/A_3)T^{A_4} + A_5 \exp(-A_6 T)T^{A_7}] \quad [\text{molecules}/H^0, D^0]$$

where T is in Kelvin. The rms deviation of analytic fits for reactions A (×) and B (○) are 2.1% and 5.5%, respectively.

Fitting parameters A_1-A_7

A	1.8126E+00	6.0994E+02	5.4801E+03	-7.3302E-02	1.2678E-02	-6.6125E-03
	1.4699E-01					
B	-6.5969E-02	2.3870E+03	-1.9162E+06	5.7268E-01	7.9265E+00	1.0850E-03
	1.8974E-01					

ALADDIN evaluation function for erosion yield: EYIELD7A

ALADDIN hierarchical labelling:

A: SATM D [+0] GRAPHITE T=A-CH-FILM CD{3} [+0]
B: SATM H [+0] GRAPHITE T=A-CH-FILM CH{3} [+0]

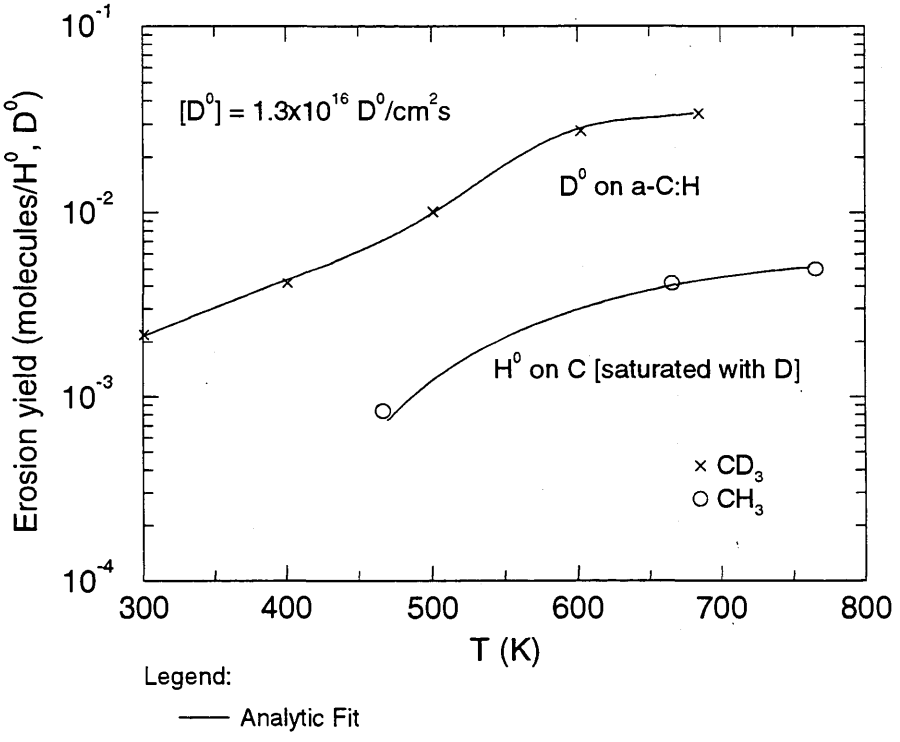

4.1.2.2 D^0, D^+ + a-C:H film → C

Source: E. Vietzke and V. Philipps, Fusion Technol. **15**, 108 (1989).

Accuracy: Yield: 50%.

Comments: (1) Total chemical erosion due to D^0 or D^+ impact.
(2) Specimen: a-C:H film.
(3) Reaction of H^0 on other amorphous surfaces: see 4.1.1.13.
(4) Original (continuous) data curves are not shown on the graph.
(5) Total chemical erosion yield = $[\sum x(C_xD_y)]/(D^+ \text{ or } D^0)$.

Analytic fitting function:

Erosion yield:

$$Y = 1.0 \times 10^{-2}[A_1 \exp(-(T - A_2)^2/A_3)T^{A_4} + A_5 \exp(-A_6T)T^{A_7}] \quad [\text{eroded C/D}^0]$$

where T is in Kelvin. The rms deviation of analytic fits for reactions A (D^0) and B (D^+) are 0.5% and 1.0%, respectively.

Fitting parameters A_1-A_7

A	1.4168E+01	6.6363E+02	1.9361E+04	3.8330E-02	2.4982E+00	-2.3101E-04
	7.5257E-02					
B	1.2762E+00	7.0901E+02	3.1289E+04	3.5389E-01	2.1038E-04	1.1857E-03
	1.5618E+00					

ALADDIN evaluation function for erosion yield: EYIELD7A

ALADDIN hierarchical labelling:

A: SATM D [+0] GRAPHITE T=A-CH-FILM C [+0]
B: SATM D [+1] GRAPHITE T=A-CH-FILM C [+0]

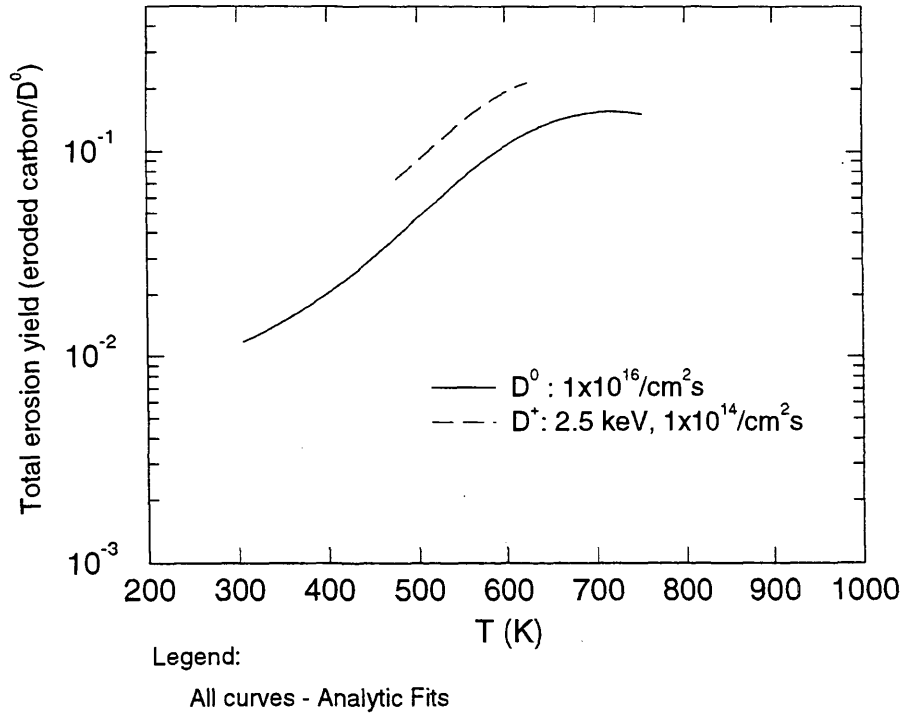

4.1.2.3 D^0, D^+, H^+ + a-C:H film → CH_4, CD_3, CD_4

Source: E. Vietzke, K. Flaskamp, V. Philipps, G. Esser, P. Wienhold and J. Winter, J. Nucl. Mater. **145-147**, 443 (1987).

Accuracy: Yield: 50%.

Comments: (1) Steady-state methane and methyl formation.
(2) Specimen: a-C:H film from TEXTOR (for D^+ and D^0); pyrolytic graphite (for H^+).
(3) Line-of-sight QMS detection.
(4) D^0 beam from thermal dissociation in W oven at 2800 K.
(5) Original (continuous curve) data are not shown.

Analytic fitting function:

Methane yield:

$$Y = 1.0 \times 10^{-2}[A_1 \exp(-(T - A_2)^2/A_3)T^{A_4} + A_5 \exp(-A_6 T)T^{A_7}] \quad \text{[molecules/H, D]}$$

where T is Kelvin. The rms deviation of analytic fits for reactions A (CD_4), B (CD_3) and C (CH_4) are 1.7%, 3.4% and 22.5%, respectively. Data for curve B were fitted with EYIELD8A.

Fitting parameters A_1-A_8

A	9.5655E+00	6.2413E+02	1.1442E+04	-5.5847E-02	5.8592E-03	-1.6653E-03
	8.9383E-01					
B	4.4519E-15	5.6815E+02	8.5621E+01	3.6600E-06	4.5431E+00	2.9675E-08
	-2.0727E-03	1.8623E+00				
C	4.4753E+02	7.4344E+02	1.2287E+04	-5.9207E-01	6.4277E-03	-1.6113E-02
	-1.5755E+00					

ALADDIN evaluation function for methane yield: EYIELD7A, EYIELD8A

ALADDIN hierarchical labelling:

A: SATM D [+1] GRAPHITE T=A-CH-FILM CD{4} [+0]
B: SATM D [+0] GRAPHITE T=A-CH-FILM CD{3} [+0]
C: SATM H [+1] GRAPHITE T=HPG CH{4} [+0]

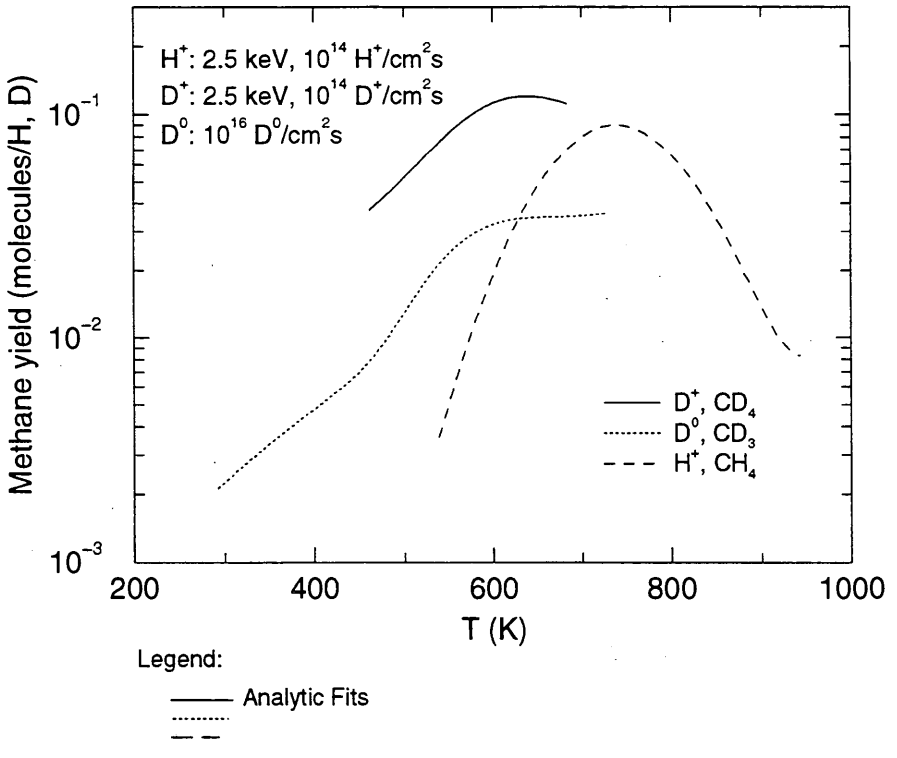

4.2.1.1 H^+ + pyrolytic graphite → CH_4

Source: S. K. Erents, C. M. Braganza and G. M. McCracken, J. Nucl. Mater. **63**, 399 (1976).

Accuracy: Indeterminate.

Comments: (1) Equilibrium hydrocarbon gas release.
(2) Specimen: graphite (pyrolytic).
(3) H^+ ions: mass analyzed accelerator.
(4) Methane measured via QMS-RGA.
(5) Original data were converted to yields using a beam spot area of 0.09 cm^2.

Analytic fitting function:

Methane yield:

$$Y = A_1 \exp[-(\frac{T - A_2}{A_3 T + 1})^2 / A_4] T^{A_5} + A_6 \exp(-A_7 T) T^{A_8} \quad [CH_4/H^+]$$

where T is in Kelvin. The rms deviation of the analytic fit is 14.5%.

Fitting parameters A_1-A_8

9.9840e-04	8.5078e+02	1.5010e+01	2.6035e-05	6.9725e-01	1.0910e-136
6.0534e-02	5.3621e+01				

ALADDIN evaluation function for methane yield: EYIELD8A

ALADDIN hierarchical labelling:

SATM H [+1] GRAPHITE T=HPG CH{4} [+0]

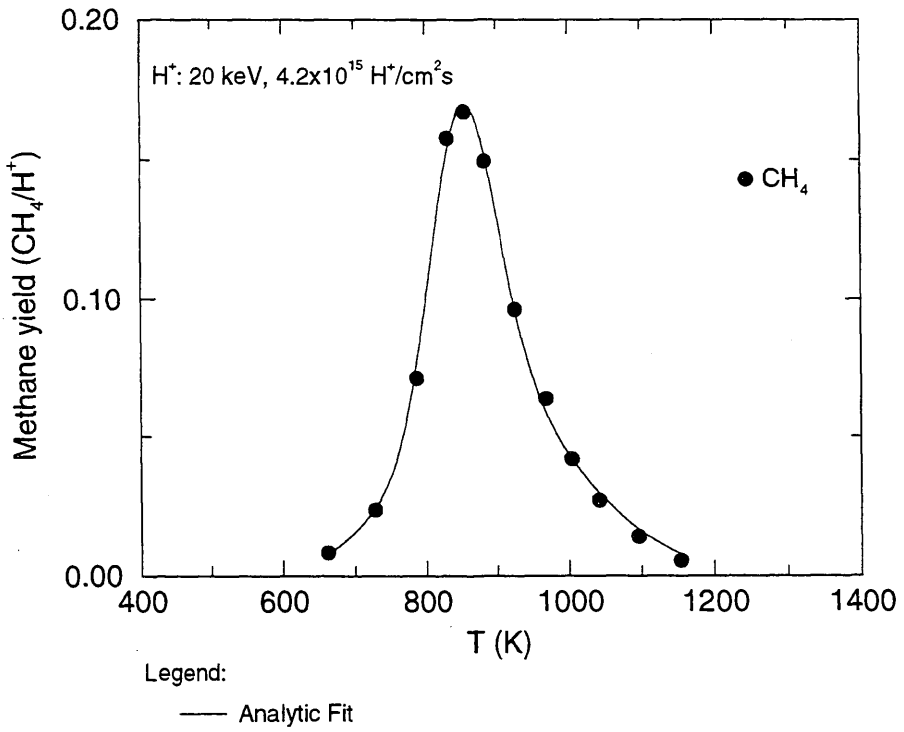

4.2.1.2 H^+ + pyrolytic graphite → CH_4, C_2H_4, C

Source: J. Roth and J. Bohdansky, "Graphite in High Power Fusion Reactors", IEA Workshop Rep., Federal Institute for Reactor Research, Würenlingen (1983).

Accuracy: Yield: Indeterminate.

Comments: (1) Total sputtering (chemical+physical) and chemical erosion yields compared at 580 ^{0}C and RT.
(2) Specimen: graphite (pyrolytic).
(3) $[H^+]$: 2×10^{15} H^+/cm^2s.

Analytic fitting function:

Sputtering yield:

$$Y = A_1 \exp(-A_2/E)/(1 + A_3 \exp(-A_4/E)) \quad [\text{particles}/H^+]$$

where E is in keV. The rms deviation of analytic fits for reactions A (•), B (◇), C (△) and D (□) are 1.7%, 10.5%, 5.7% and 2.6%, respectively. Data for curve D were fitted with EYIELD7A.

Fitting parameters A_1-A_7

A	9.0580e-02	-1.3767e+00	5.5049e-01	-1.4470e+00		
B	4.0850e-02	-1.3403e+00	3.6470e-01	-1.4376e+00		
C	1.6619e-03	-9.6101e+00	3.7030e-02	-9.7509e+00		
D	1.8463e-02	4.1293e+00	9.2616e+00	-1.1917e+00	-5.6320e-02	8.1333e+00
	-1.9544e-01					

ALADDIN evaluation function for sputtering yield: EYIELD4D, EYIELD7A

ALADDIN hierarchical labelling:

A: SAT H [+1] GRAPHITE T=HPG C [+0]
B: SATM H [+1] GRAPHITE T=HPG C{2}H{4} [+0]
C: SATM H [+1] GRAPHITE T=HPG CH{4} [+0]
D: SAT H [+1] GRAPHITE T=HPG C [+0]

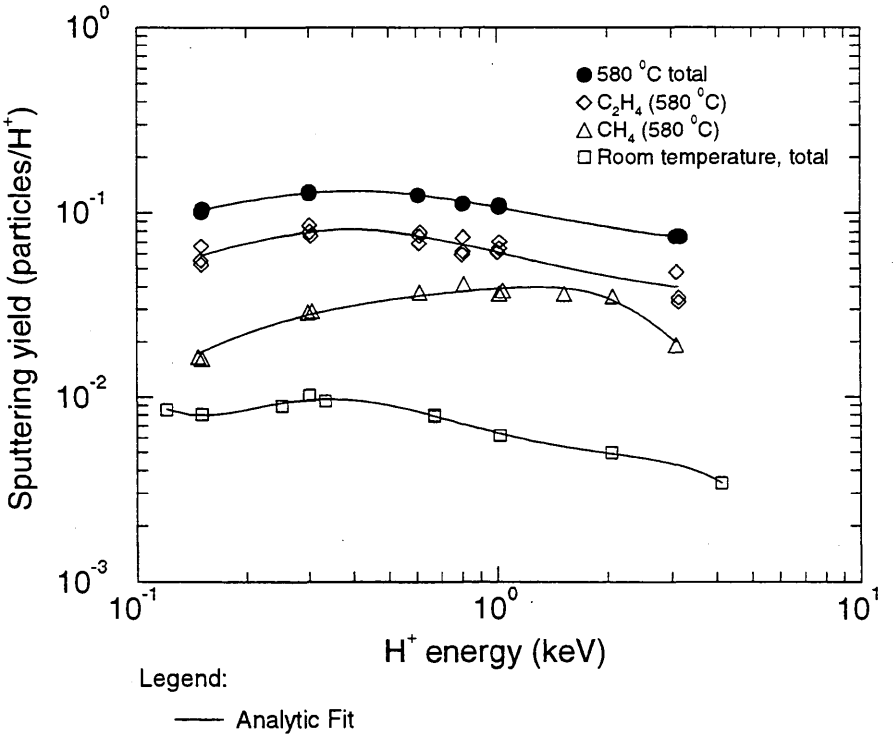

4.2.1.3 H^+ + pyrolytic graphite → CH_4, C

Source: J. Bohdansky and J. Roth, Rad. Effects **89**, 49 (1985).

Accuracy: Yield: ±20%.

Comments: (1) Chemical erosion yield due to CH_4 formation by impact of H^+ ions.
(2) Specimen: graphite (pyrolytic).
(3) QMS measurement of CH_4, steady state.
(4) Total C sputtering yield from same source shown for comparison.
(5) The temperature of the measurements is not given.

Analytic fitting function:

Erosion yield:

$$Y = A_1 \exp(-A_2 F) F^{A_3} + A_4 F \quad [CH_4/H^+]$$

where F is the flux density H^+/cm^2s. The rms deviation of the analytic fit is 0.8%.

Fitting parameters A_1-A_4

2.4409E+01	-6.8717E-18	-1.6035E-01	-4.9077E-19

ALADDIN evaluation function for erosion yield: EYIELD4A

ALADDIN hierarchical labelling:

SATM H [+1] GRAPHITE T=HPG CH{4} [+0]

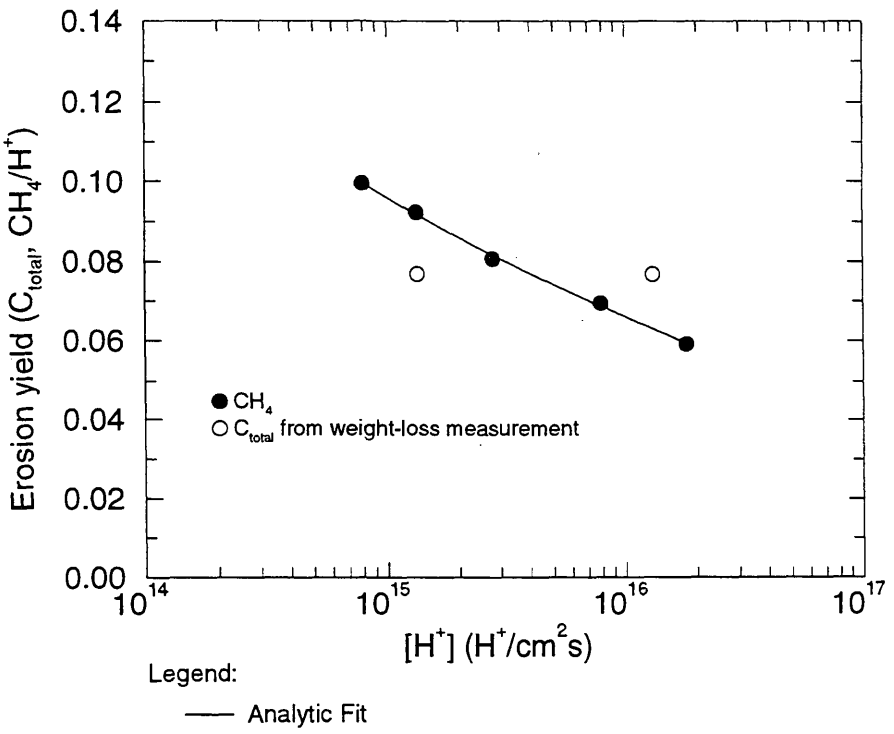

4.2.1.4 H^+ + pyrolytic graphite → CH_3, CH_4

Source: A. A. Haasz and J. W. Davis, J. Chem. Phys. **85**, 3293 (1986).

Accuracy: Rate: ±15%; H^0 flux density: ±5%.

Comments: (1) Steady-state methane production with the specimen at 750-800 K.
(2) Specimen: graphite (pyrolytic).
(3) H^+ ions are produced via a mass-analyzed accelerator.
(4) Methane is measured via QMS-RGA.
(5) Different sybols in the figure correspond to different H^+ energies.
(6) Prediction of flux dependence for 300eV/H^+ from model derived in original paper.

Analytic fitting function:

Methane yield:

$$Y = A_1 \exp(-A_2 F) F^{A_3} \quad [CH_{3,4}/H^+]$$

where F is in H/cm^2s. The rms deviation of the analytic fit (•) is 34.5%.

Fitting parameters A_1-A_3

1.0511E-06	1.6564E-16	1.3334E+00

ALADDIN evaluation function for methane yield: EYIELD3A

ALADDIN hierarchical labelling:

SATM H [+0] GRAPHITE T=HPG CH{3} [+0] CH{4} [+0]

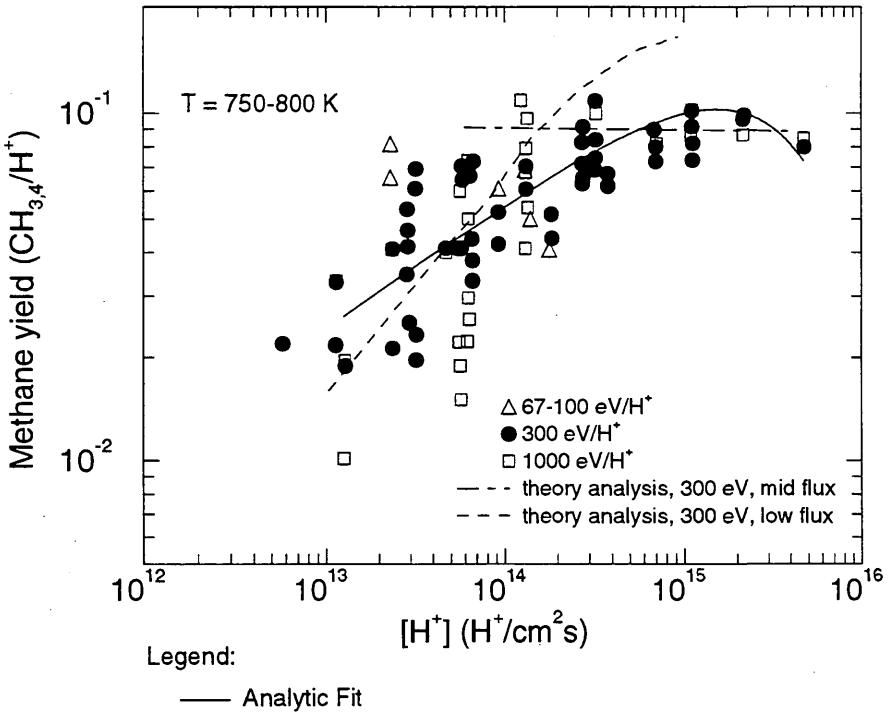

4.2.1.5 H^+ + pyrolytic graphite → CH_3, CH_4

Source: A. A. Haasz and J. W. Davis, J. Chem. Phys. **85**, 3293 (1986).

Accuracy: Yield: ±15%; T: ±25%.

Comments: (1) Steady-state methane yield.
(2) Specimen: graphite (pyrolytic).
(3) H^+ ions from mass-analyzed accelerator, all data at 300 eV/H^+.
(4) Methane measured via QMS-RGA.
(5) Different symbols in the figure correspond to different fluxes.

Analytic fitting function:

Methane yield:

$$Y = A_1 \exp(-(T - A_2)^2/A_3)T^{A_4} \quad [CH_{3,4}/H^+]$$

where T is in Kelvin. The rms deviation of analytic fits for reactions A (∗), B (+), C (○), D (•), E (□), F (◇) and G (△) are 12.6%, 17.5%, 109.0%, 120.0%, 50.6%, 57.8% and 12.7%, respectively.

Fitting parameters A_1-A_4

A	5.5140E+04	8.0410E+02	2.3555E+04	-2.0139E+00
B	6.2204E+04	7.8997E+02	2.2632E+04	-2.0526E+00
C	2.7373E+04	7.7264E+02	2.1349E+04	-1.9941E+00
D	3.7185E+04	7.7109E+02	1.7245E+04	-2.0372E+00
E	2.8242E+04	7.6948E+02	1.7834E+04	-2.0294E+00
F	2.1106E+04	7.5624E+02	1.2462E+04	-1.9720E+00
G	1.3091E+04	8.5437E+02	3.9938E+04	-1.9497E+00

ALADDIN evaluation function for methane yield: EYIELD4B

ALADDIN hierarchical labelling:

A-G: SATM H [+0] GRAPHITE T=HPG CH{3} [+0] CH{4} [+0]

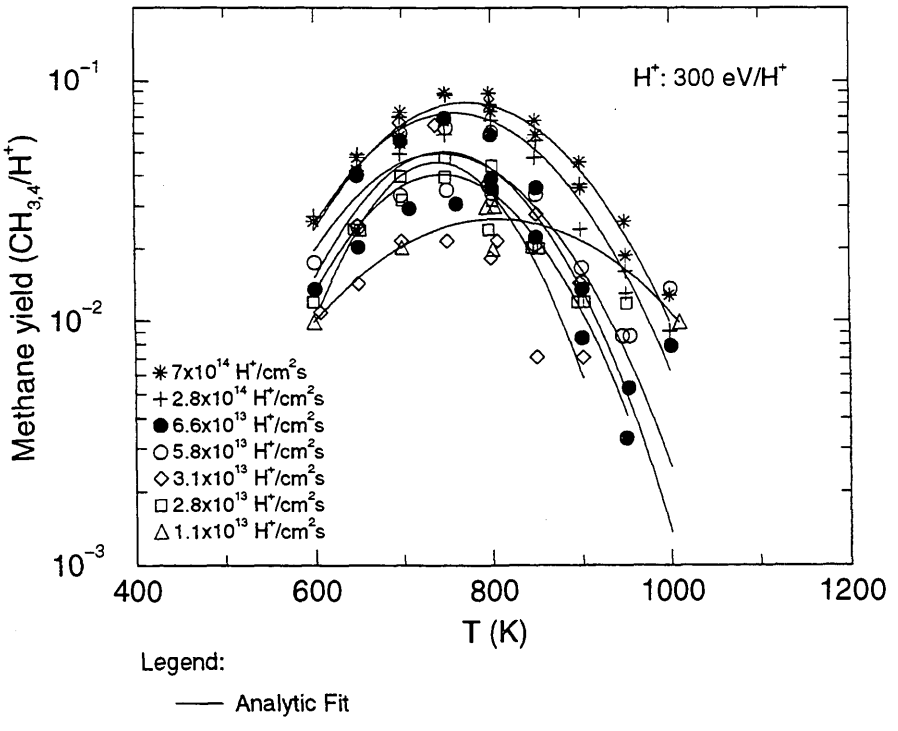

4.2.1.6 H^+ + pyrolytic graphite → CH_4

Source: J. W. Davis, A. A. Haasz and P. C. Stangeby, J. Nucl. Mater. **145-147**, 417 (1987).

Accuracy: Yield: ±15%; E: ±5eV.

Comments: (1) Steady-state methane yield.
(2) Specimen: graphite (pyrolytic).
(3) H^+ ions: mass analyzed accelerator.
(4) Methane measured via QMS-RGA.
(5) The energy dependence of the yield is affected by the specimen temperature.

Analytic fitting function:

Methane yield:

$$Y = A_1(\log E)^3 + A_2(\log E - A_3)^2 + A_4 \quad [\text{molecules}/H^+]$$

where E is in eV. The rms deviation of the analytic fits for reactions A (□), B (•), C (∗) and D (△) are 2.9%, 3.5%, 4.3% and 3.7%, respectively.

Fitting parameters A_1-A_4

A	-1.2929E-02	4.8371E-02	-5.6335E-01	-1.8388E-01
B	-1.6738E-03	-6.0300E-02	3.2278E+00	1.3141E-01
C	4.9330E-02	-4.6049E-01	1.5226E+00	-2.6749E-01
D	3.7215E-03	-9.4067E-02	2.3959E+00	7.0127E-03

ALADDIN evaluation function for methane yield: EYIELD4C

ALADDIN hierarchical labelling:

A-D: SATM H [+1] GRAPHITE T=HPG CH{4} [+0]

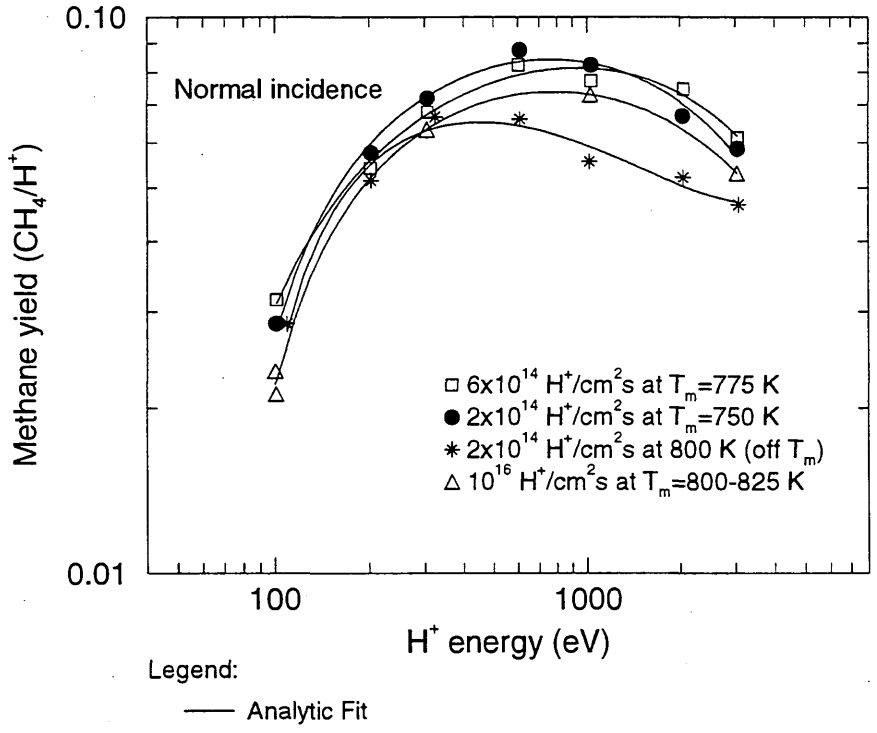

4.2.1.7 H^+ + pyrolytic graphite → C_xH_y, C

Source: J. W. Davis, A. A. Haasz and P. C. Stangeby, J. Nucl. Mater. **155-157**, 234 (1988).

Accuracy: Yield: ±15%; T: ±25K.

Comments: (1) Steady-state hydrocarbon yields.
(2) Specimen: graphite (pyrolytic).
(3) H^+ ions: mass analyzed accelerator.
(4) Methane measured via QMS-RGA.
(5) Yield for total chemical erosion, $Y_{chem-total} = [CH_4 + 2(C_2H_2 + C_2H_4 + C_2H_6) + 3(C_3H_6 + C_3H_8)]/H^+$.

Analytic fitting function:

Erosion yield:

$$Y = 1.0 \times 10^{-2}[A_1 \exp(-(T - A_2)^2/A_3)T^{A_4} + A_5 \exp(-A_6T)T^{A_7}] \quad [\text{molecules}/H^+]$$

where T is in Kelvin. The rms deviation of analytic fits for reactions A (∗), B (•), C (+), D (◇), E (△), F (□) and G (○) are 4.9%, 7.1%, 12.8%, 16.5%, 10.9%, 11.2% and 15.4%, respectively.

Fitting parameters A_1-A_7

A	2.2596E+00	7.7370E+02	3.7703E+04	2.1901E-01	2.3839E+01	4.5042E-02	2.9798E+00
B	8.3009E+00	7.9719E+02	2.9853E+04	-2.9174E-02	2.2319E+00	5.2058E-03	1.7283E-01
C	4.3891E-02	7.2540E+02	1.1878E+04	-2.2974E-02	3.1525E-05	-6.5280E-03	6.9062E-06
D	3.0914E-01	7.1281E+02	2.5664E+04	4.3476E-02	3.6880E-02	-1.7551E-03	7.9409E-04
E	5.2924E-02	7.0176E+02	8.6472E+03	3.2973E-02	6.7348E-02	-1.7909E-04	4.2995E-03
F	9.5564E-01	7.5014E+02	1.8879E+04	-6.0308E-02	1.6602E-02	-9.1407E-04	-1.0736E-02
G	1.3148E-01	7.1213E+02	1.4367E+04	-5.4467E-03	3.9673E-02	-1.0223E-03	8.9686E-04

ALADDIN evaluation function for erosion yield: EYIELD7A

ALADDIN hierarchical labelling:

A: SATM H [+0] GRAPHITE T=HPG C [+0]
B: SATM H [+0] GRAPHITE T=HPG CH{4} [+0]
C: SATM H [+0] GRAPHITE T=HPG C{2}H{2} [+0]
D: SATM H [+0] GRAPHITE T=HPG C{2}H{4} [+0]
E: SATM H [+0] GRAPHITE T=HPG C{2}H{6} [+0]
F: SATM H [+0] GRAPHITE T=HPG C{3}H{6} [+0]
G: SATM H [+0] GRAPHITE T=HPG C{3}H{8} [+0]

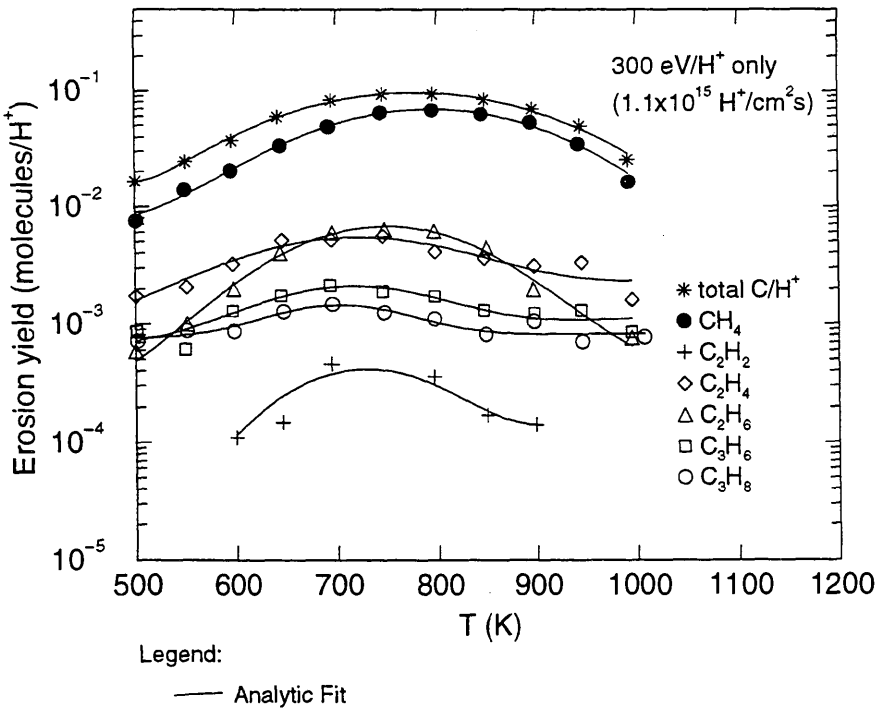

4.2.1.8 H^+ + pyrolytic graphite → C

Source: J. W. Davis, A. A. Haasz and P. C. Stangeby, J. Nucl. Mater. **155-157**, 234 (1988).

Accuracy: Yield: ±15%; Energy: ±5eV.

Comments: (1) Steady-state hydrocarbon yield at the maximum of the respective temperature dependencies.
(2) Specimen: graphite (pyrolytic).
(3) H^+ ions: mass analyzed accelerator.
(4) Hydrocarbon products measured via QMS-RGA.
(5) Yield for total chemical erosion, $Y_{chem-total} = [CH_4 + 2(C_2H_2 + C_2H_4 + C_2H_6) + 3(C_3H_6 + C_3H_8)]/H^+$.

Analytic fitting function:

Chemical erosion yield:

$$Y = A_1 \exp(-A_2/E)E^{A_3} + A_4 E^{A_5}] \quad [\text{molecules}/H^+]$$

where E is in keV. The rms deviation of analytic fits for reactions A (◇), B (□), C (○) and D (△) are 0.8%, 1.8%, 7.1% and 28.6%, respectively.

Fitting parameters A_1-A_5

A	7.4565E-02	3.3509E-01	-8.7801E-01	3.4745E-02	1.0785E-01
B	7.2165E-02	3.8771E-01	-8.3359E-01	2.5256E-02	1.9477E-01
C	8.6155E-03	4.3760E-01	-1.9592E+00	5.8489E-03	4.2135E-02
D	1.2347E-03	4.3095E-01	-2.5901E+00	3.3174E-03	2.3782E-01

ALADDIN evaluation function for chemical erosion yield: EYIELD5B

ALADDIN hierarchical labelling:

A: SATM H [+1] GRAPHITE T=HPG C [+0]
B: SATM H [+1] GRAPHITE T=HPG CH{4} [+0]
C: SATM H [+1] GRAPHITE T=HPG C{2}H{2} [+0] C{2}H{4} [+0] C{2}H{6} [+0]
D: SATM H [+1] GRAPHITE T=HPG C{3}H{6} [+0] C{3}H{8} [+0]

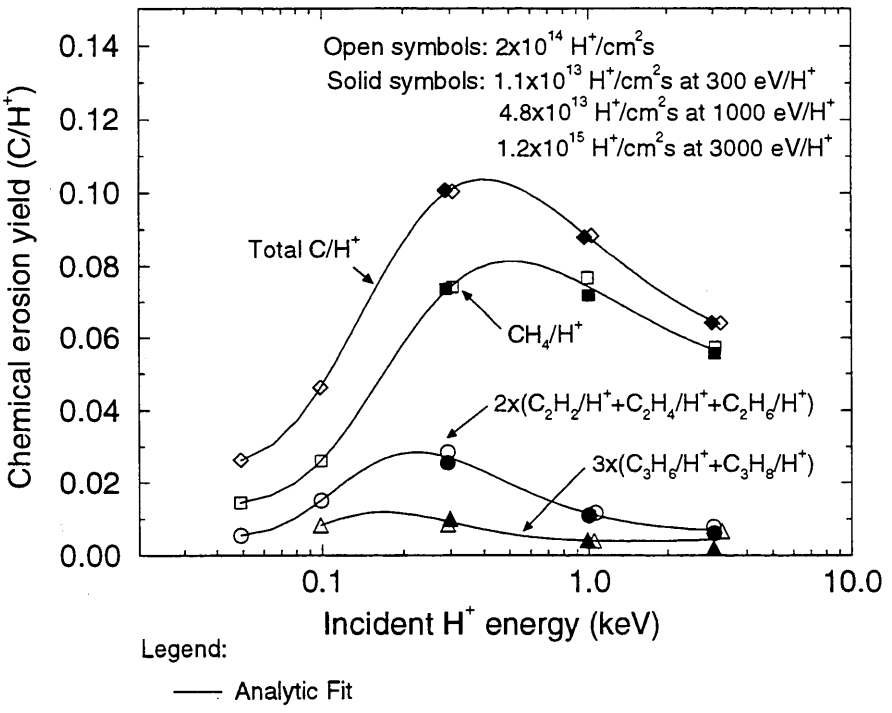

4.2.1.9 H^+ + pyrolytic graphite → CH_4

Source: J. Roth and C. García-Rosales, Nucl. Fusion **36**, 1647 (1996).

Accuracy: Yield: ±20%.

Comments: (1) Steady-state methane yield.
(2) Specimen: pyrolytic graphite.
(3) H^+ ions: mass-analyzed ion beam.
(4) Methane measured via QMS-RGA.

Analytic fitting function:

Methane yield:

$$Y = A_1 \exp(-(T - A_2)^2/A_3)T^{A_4} + A_5 \exp(-A_6 T)T^{A_7} \quad [CH_4/H^+]$$

where T is in Kelvin. The rms deviation of analytic fits for reactions A (•) and B (□) are 30.4% and 8.6%, respectively.

Fitting parameters A_1-A_7

A	8.5235e-04	8.7472e+02	7.3738e+04	6.5223e-01	3.2048e-03	1.6227e-02
	8.9293e-01					
B	8.2830e-03	7.9324e+02	1.8921e+04	3.5924e-01	-3.8416e-07	4.9100e-03
	1.6664e+00					

ALADDIN evaluation function for methane yield: EYIELD7A

ALADDIN hierarchical labelling:

A, B: SATM H [+1] GRAPHITE T=HPG CH{4} [+0]

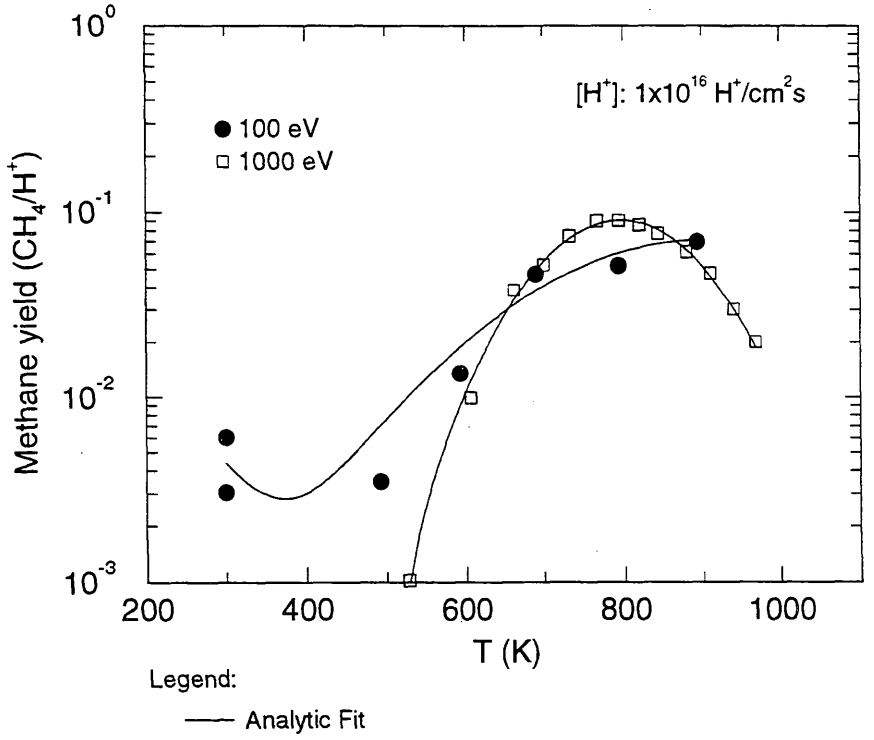

4.2.1.10 H^+ + pyrolytic graphite → C

Source: J. Roth and C. García-Rosales, Nucl. Fusion **36**, 1647 (1996).

Accuracy: Yield: ±20%.

Comments: (1) Weight loss measurement.
(2) Specimen: pyrolytic graphite.
(3) H^+ ions: mass-analyzed ion beam.
(4) Yield is for total (chemical+physical) sputtering.

Analytic fitting function:

Erosion yield:

$$Y = A_1 \exp(-A_2 E) E^{A_3} + A_4 E^{A_5} \quad [\mathrm{C/H^+}]$$

where E is in eV. The rms deviation of analytic fits for reactions A (•) and B (□) are 18.1% and 28.7%, respectively.

Fitting parameters A_1-A_5

A	1.6360e-04	1.2049e-03	6.6490e-01	4.7330e-03	-5.4140e-02
B	7.1405e-11	1.1317e-02	4.1858e+00	1.6364e-02	2.0512e-01

ALADDIN evaluation function for erosion yield: EYIELD5A

ALADDIN hierarchical labelling:

A, B: SATM H [+1] GRAPHITE T=HPG C [+0]

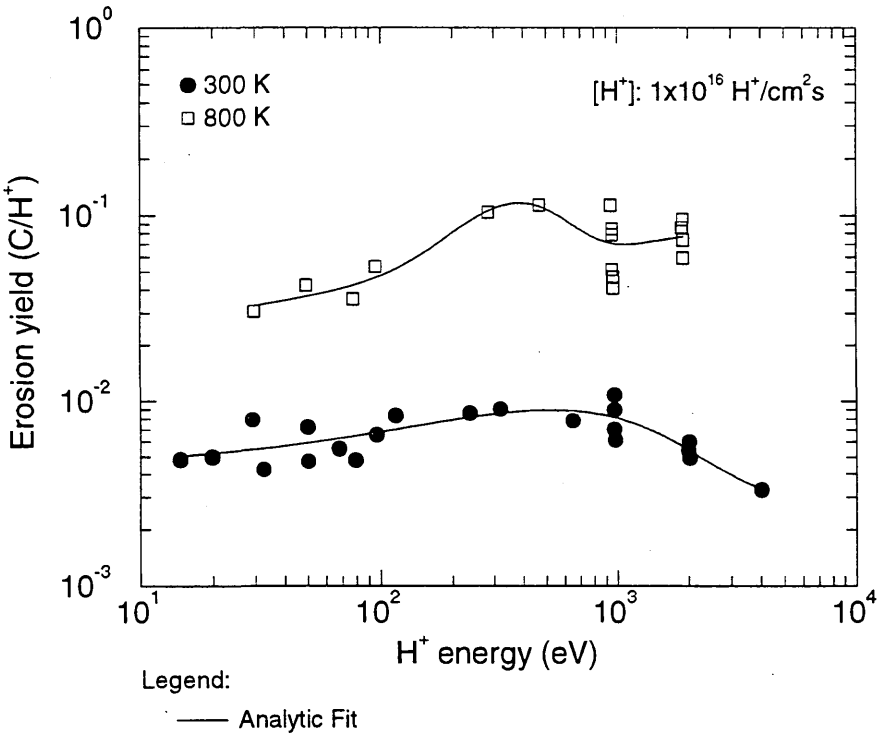

4.2.1.11 H^+ + PG-A graphite → C

Source: R. Yamada, K. Nakamura, K. Sone and M. Saidoh, J. Nucl. Mater. **95**, 278 (1980).

Accuracy: Yield (rel.): ±30%.

Comments: (1) Steady-state methane yield.
(2) Specimen: graphite (pyrolytic, PG-A basal plane (Nippon Carbon)).
(3) H^+ ions: mass analyzed accelerator.
(4) Metane measured via QMS-RGA.

Analytic fitting function:

Chemical sputtering yield:

$$Y = 1.0 \times 10^{-2}[A_1 \exp(-(E - A_2)^2/A_3)E^{A_4} + A_5 \exp(-A_6 E)E^{A_7}] \quad [\text{molecules/H}^+]$$

where E is in keV. The rms deviation of analytic fits for reactions A (•), B (□) and C (△) are 8.6%, 3.1% and 8.7%, respectively.

Fitting parameters A_1-A_7

A	1.2730E-02	-3.4217E-01	1.0899E-02	5.0892E-01	6.2935E+00	4.2240E-01
	4.6150E-01					
B	2.0241E+02	-3.3564E+01	3.1295E+02	4.5689E-01	2.5983E+01	2.3289E+00
	2.1041E+00					
C	7.7419E-06	-1.9795E+00	5.7636E+00	-4.9784E+00	2.4565E+00	4.8912E-01
	7.1733E-01					

ALADDIN evaluation function for chemical sputtering yield: EYIELD7A

ALADDIN hierarchical labelling:

A-C: SATM H [+1] GRAPHITE T=PGA O=BASAL-PL C [+0]

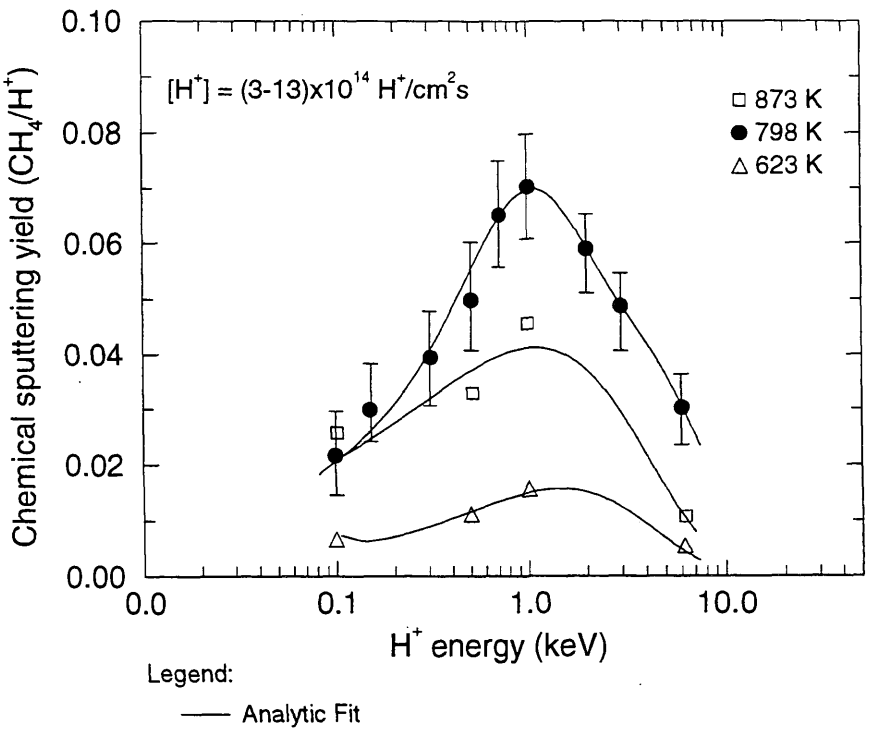

4.2.1.12 H^+ + PG-A graphite → CH_4

Source: R. Yamada, K. Nakamura, K. Sone and M. Saidoh, J. Nucl. Mater. **95**, 278 (1980).

Accuracy: Indeterminate.

Comments: (1) Steady-state methane yield.
(2) Specimen: graphite (pyrolytic, PG-A edge plane (Nippon Carbon)).
(3) H^+ ions: mass analyzed accelerator.
(4) Methane measured via QMS-RGA.

Analytic fitting function:

Methane yield:

$$Y = 1.0 \times 10^{-4}[A_1 \exp(-(T - A_2)^2/A_3)T^{A_4} + A_5 \exp(-A_6 T)T^{A_7}] \quad [CH_4/H^+]$$

where T is in ^{0}C. The rms deviation of analytic fits for reactions A (×), B (△), C (•) and D (□) are 1.9%, 3.6%, 7.3% and 7.5%, respectively.

Fitting parameters A_1-A_7

A	3.8003E+03	5.3009E+02	1.0909E+04	-2.9391E-01	2.1095E+02	-2.5971E-03
	-2.2758E-01					
B	8.6773E+02	5.4060E+02	1.5436E+04	-5.6799E-02	1.2402E+02	-4.4285E-04
	-1.5181E-02					
C	5.9541E+02	5.2734E+02	9.0774E+03	-1.0117E-01	9.9638E+00	3.3382E-04
	4.1170E-01					
D	3.7899E+02	5.3917E+02	3.6369E+04	-4.2074E-02	4.9031E+01	9.9437E-04
	1.2291E-01					

ALADDIN evaluation function for methane yield: EYIELD7A

ALADDIN hierarchical labelling:

A-D: SATM H [+1] GRAPHITE T=PGA O=EDGE-PL CH{4} [+0]

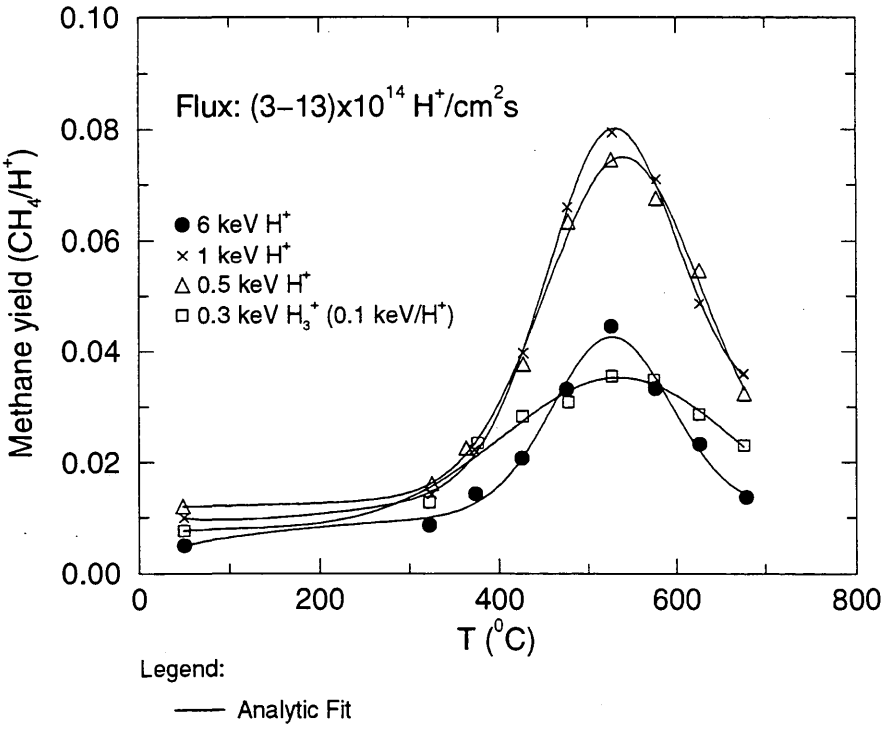

4.2.1.13 H^+ + PG-A graphite → C_xH_y

Source: R. Yamada, J. Nucl. Mater. **145-147**, 359 (1987).

Accuracy: Yield (rel.): ±30%.

Comments: (1) Steady-state hydrocarbon yield at the maximum of the respective temperature dependencies.
(2) Specimen: graphite (pyrolytic, PG-A (Nippon Carbon)).
(3) H^+ ions: mass analyzed accelerator.
(4) Hydrocarbon products measured via QMS-RGA.

Analytic fitting function:

Erosion yield:

$$Y = 1.0 \times 10^{-2}[A_1 \exp(-(E - A_2)^2/A_3)E^{A_4} + A_5 \exp(-A_6 E)E^{A_7}] \quad [C_xH_y/H^+]$$

where E is energy in keV. The rms deviation of analytic fits for reactions A (∗), B (×), C (○), D (•), E (◇), F (△) and G (□) are 0.5%, 2.3%, 4.3%, 11.2%, 4.1%, 7.6% and 10.6%, respectively.

Fitting parameters A_1-A_7

A	4.4773E+01	-2.7209E+00	4.8201E+00	5.3489E-01	5.4997E+00	2.2615E-01	5.9626E-01
B	3.3449E+03	-5.7057E+00	5.6692E+00	8.1909E-01	1.4534E+00	2.1445E-01	5.8351E-01
C	9.8150E+03	-1.5016E+00	4.3071E-01	1.8932E+00	9.5071E-01	2.0654E-01	-4.2763E-02
D	3.2008E+12	-3.5408E+00	5.7686E-01	3.6617E+00	2.2759E-01	2.9108E-01	8.6692E-02
E	1.6448E+00	1.3335E-04	1.0462E-01	1.2021E+00	1.4412E-01	1.1541E-01	-1.4983E-01
F	1.0177E-01	4.5978E+01	2.7675E+03	-2.8220E-01	1.7258E+01	1.0748E+01	1.7624E+00
G	6.8628E-02	-6.4329E+00	6.6573E+01	1.0167E+00	9.2872E-01	2.2449E+00	1.3059E+00

ALADDIN evaluation function for erosion yield: EYIELD7A

ALADDIN hierarchical labelling:

A: SATM H [+1] GRAPHITE T=PGA CH{4} [+0]
B: SATM H [+1] GRAPHITE T=PGA C{2}H{2} [+0]
C: SATM H [+1] GRAPHITE T=PGA C{2}H{4} [+0]
D: SATM H [+1] GRAPHITE T=PGA C{2}H{6} [+0]
E: SATM H [+1] GRAPHITE T=PGA C{3}H{6} [+0]
F: SATM H [+1] GRAPHITE T=PGA C{3}H{8} [+0]
G: SATM H [+1] GRAPHITE T=PGA C{3}H{4} [+0]

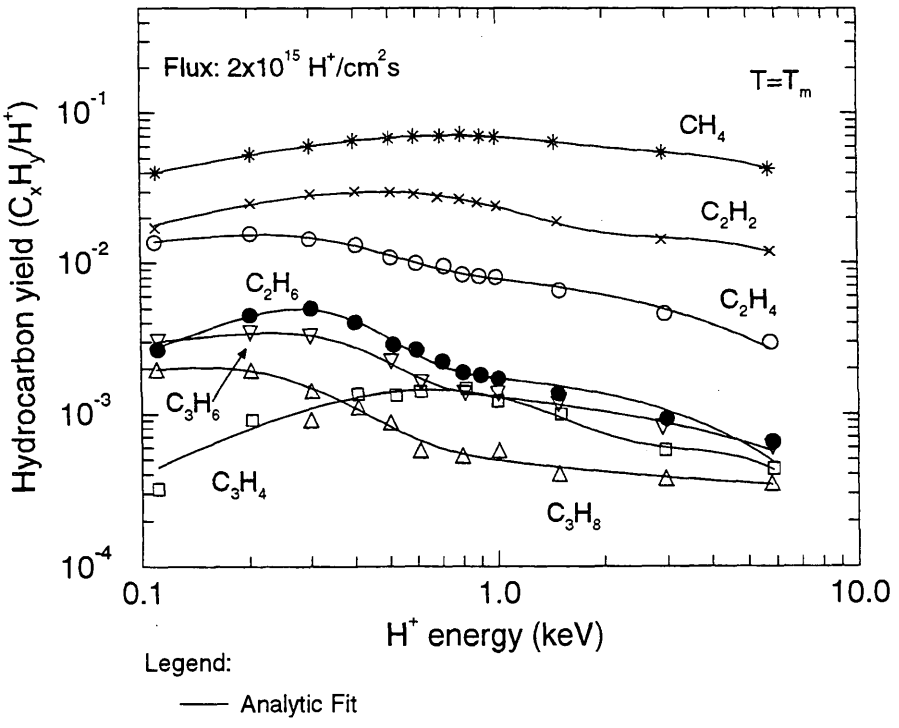

4.2.1.14 H^+ + PG-A graphite → C_xH_y

Source: R. Yamada, J. Nucl. Mater. **145-147**, 359 (1987).

Accuracy: Yield (rel.): ±30%.

Comments: (1) Steady-state hydrocarbon yield at the maximum of the respective temperature dependencies.
(2) Specimen: graphite (pyrolytic, PG-A (Nippon Carbon)).
(3) H^+ ions: mass analyzed accelerator.
(4) Hydrocarbon products measured via QMS-RGA.

Analytic fitting function:

Chemical sputtering yield:

$$Y = 1.0 \times 10^{-2}[A_1 \exp(-(E - A_2)^2/A_3)E^{A_4} + A_5 \exp(-A_6 E)E^{A_7}] \quad [C/H^+]$$

where E is energy in keV. The rms deviation of analytic fits for reactions A (•), B (□) and C (△) are 0.4%, 2.5% and 4.7%, respectively.

Fitting parameters A_1-A_7

A	-1.3695E+02	-3.2843E+00	1.4600E+00	-5.6206E-01	6.6605E-02	-5.7327E-02
	-5.8559E-01					
B	1.2910E+01	-1.5027E+00	3.7127E+00	4.5996E-01	5.7175E+00	1.9678E-01
	5.2996E-01					
C	1.5950E+01	-3.0849E-01	7.5022E-01	5.6261E-01	6.2877E+00	1.9362E-01
	2.4858E-01					

ALADDIN evaluation function for chemical sputtering yield: EYIELD7A

ALADDIN hierarchical labelling:

A: SATM H [+1] GRAPHITE T=PGA C{2}H{2} [+0] C{2}H{4} [+0] C{2}H{6} [+0]
B: SATM H [+1] GRAPHITE T=PGA CH{4} [+0]
C: SATM H [+1] GRAPHITE T=PGA C{3}H{4} [+0] C{3}H{6} [+0] C{3}H{8} [+0]

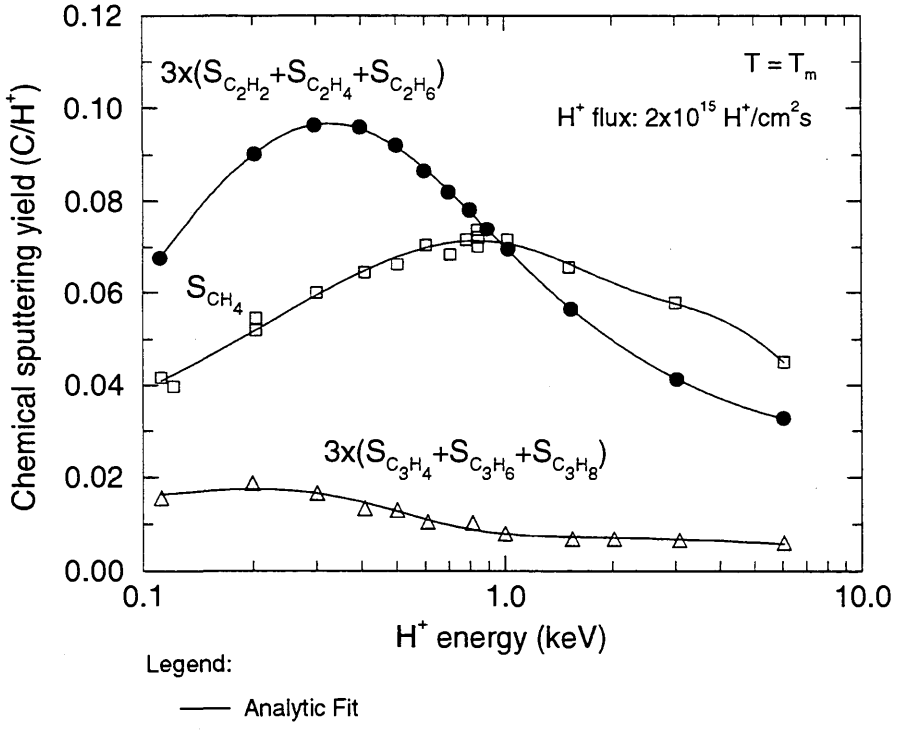

4.2.1.15 H^+ + POCO graphite → C

Source: D. M. Goebel, Y. Hirooka, R. W. Conn, W. K. Leung, G. A. Campbell, J. Bohdansky, K. L. Wilson, W. Bauer, R. A. Causey, A. E. Pontau, A. R. Krauss, D. M. Gruen and M. H. Mendelsohn, J. Nucl. Mater. **145-147**, 61 (1987).

Accuracy: Yield: ±20%; T: ±5%.

Comments: (1) High-flux (~10^{18} H^+/cm^2s), steady-state (>10 min.) plasma bombardment.
(2) Specimen: graphite (isotropic, POCO: AXF-5Q).
(3) Total erosion yield estimated from weight loss (>1 mg).
(4) Ionization mean free path calculated for $CH_4 + e \rightarrow CH_4^+ + 2e$.

Analytic fitting function:

Erosion yield:

$$Y = 1.0 \times 10^{-2}[A_1 \exp(-(T - A_2)^2/A_3)T^{A_4} + A_5 \exp(-A_6 T)T^{A_7}] \quad \text{[atoms/ion]}$$

where T is in ^{0}C. The rms deviation of the analytic fits for reactions A (•) and B (□) are 10.3% and 5.1%, respectively.

Fitting parameters A_1-A_7

A	1.1064E+01	5.8833E+02	7.4066E+04	-2.5537E-01	5.8230E-02	4.3067E-03
	6.2737E-01					
B	5.8824E-05	4.3032E+02	4.1400E+04	1.5427E+00	3.4868E-01	-1.6220E-03
	-1.9842E-01					

ALADDIN evaluation function for erosion yield: EYIELD7A

ALADDIN hierarchical labelling:

A, B: SAT H [+1] GRAPHITE T=POCO-AXF5Q C [+0]

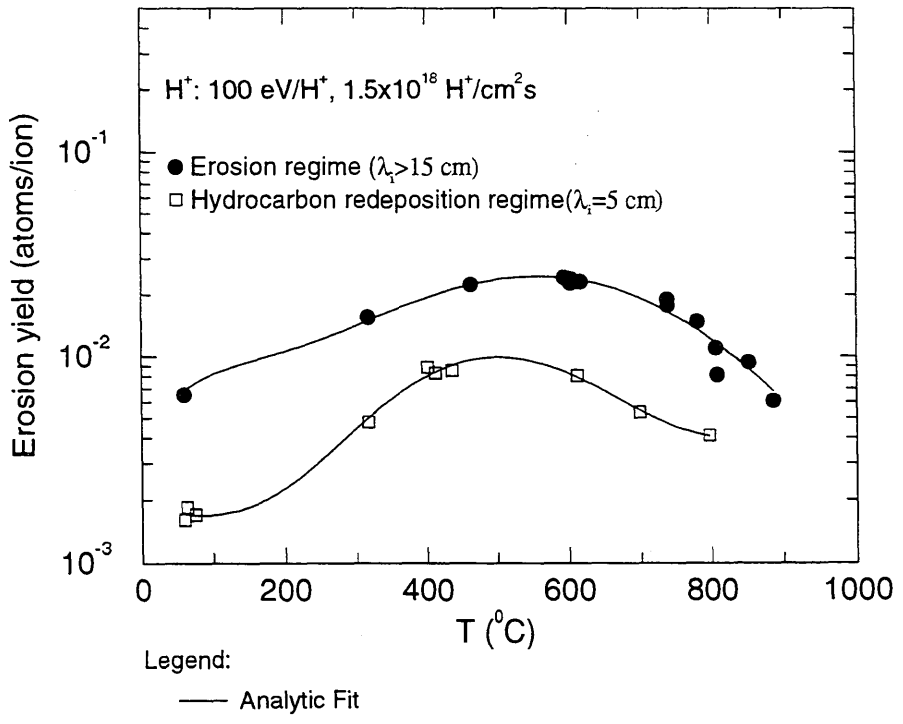

4.2.1.16 H^+ + POCO, ATJ, pyrolytic graphite, carbon/carbon composite → C

Source: D. M. Goebel, J. Bohdansky, R. W. Conn, Y. Hirooka, B. LaBombard, W. K. Leung, R. E. Nygren, J. Roth and G. R. Tynan, Nucl. Fusion **28**, 1041 (1988).

Accuracy: Yield: ±20%; T: ±5%.

Comments: (1) High-flux (~10^{18} H^+/cm^2s), steady-state (>10 min.) plasma bombardment.
(2) Specimen: isotropic graphite (POCO, ATJ), pyrolytic graphite (Union Carbide), a 4D C/C composite (FMI).
(3) Total erosion yield estimated from weight loss (>1 mg).
(4) Large ionization mean free path, i.e. no redeposition effect (see 4.2.1.15).

Analytic fitting function:

Erosion yield:

$$Y = A_1 \exp\left[-\left(\frac{T - A_2}{A_3 T + 1}\right)^2 / A_4\right] T^{A_5} + A_6 \exp(-A_7 T) T^{A_8} \quad [C/H^+]$$

where T is in ^{0}C. The rms deviation of analytic fits for reactions A (□) and B (○, •) are 10.2% and 8.2%, respectively.

Fitting parameters A_1-A_8

A	1.1867E-04	4.1624E+02	-1.2826E-03	4.2387E+05	7.6020E-01	4.7241e-46
	3.4420E-02	1.8851E+01				
B	2.5283E-02	5.9249E+02	-7.4742E-04	2.6748E+05	-5.6694E-02	1.0273E-09
	3.2171E-03	2.6383E+00				

ALADDIN evaluation function for erosion yield: EYIELD8A

ALADDIN hierarchical labelling:

A: SAT H [+1] GRAPHITE T=POCO C [+0]
B: SAT H [+1] GRAPHITE T=CC-COM-WE C [+0]

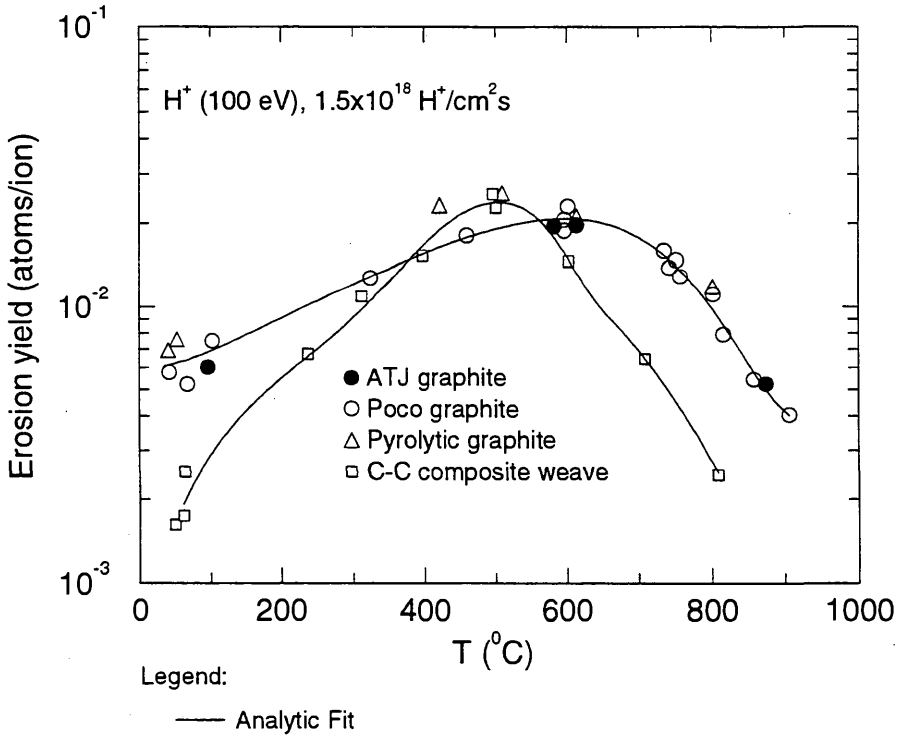

4.2.1.17 H^+ + POCO graphite → C

Source: D. M. Goebel, J. Bohdansky, R. W. Conn, Y. Hirooka, B. LaBombard, W. K. Leung, R. E. Nygren, J. Roth and G. R. Tynan, Nucl. Fusion **28**, 1041 (1988).

Accuracy: Yield: ±20%; T: ±5%.

Comments: (1) High-flux (~10^{18} H^+/cm^2s), steady-state (>10 min.) plasma bombardment.
(2) Specimen: isotropic graphite (POCO: AXF-5Q).
(3) Total erosion yield estimated from weight loss (>1 mg).
(4) Notice the effect of redeposition as a function of CH_4 ionization mean free path (λ_i).

Analytic fitting function:

Erosion yield:

$$Y = 1.0 \times 10^{-2}[A_1 \exp(-(T - A_2)^2/A_3)T^{A_4} + A_5 \exp(-A_6 T)T^{A_7}] \quad [C/H^+]$$

where T is in ^0C. The rms deviation of analytic fits for reactions A (•), B (□) and C (△) are 13.5%, 5.0% and 0.5%, respectively.

Fitting parameters A_1-A_7

A	3.4163E+01	6.0118E+02	6.5418E+04	-4.3152E-01	1.0482E-01	4.9230E-03
	4.6635E-01					
B	9.5249E-04	4.5051E+02	4.4423E+04	1.0417E+00	3.4254E-01	-6.5140E-04
	-1.0204E-01					
C	2.7204E-01	5.5148E+02	2.4285E+05	1.1304E-02	9.8609E-02	2.1408E-03
	-9.7756E-04					

ALADDIN evaluation function for erosion yield: EYIELD7A

ALADDIN hierarchical labelling:

A-C: SAT H [+1] GRAPHITE T=POCO-AXF5Q C [+0]

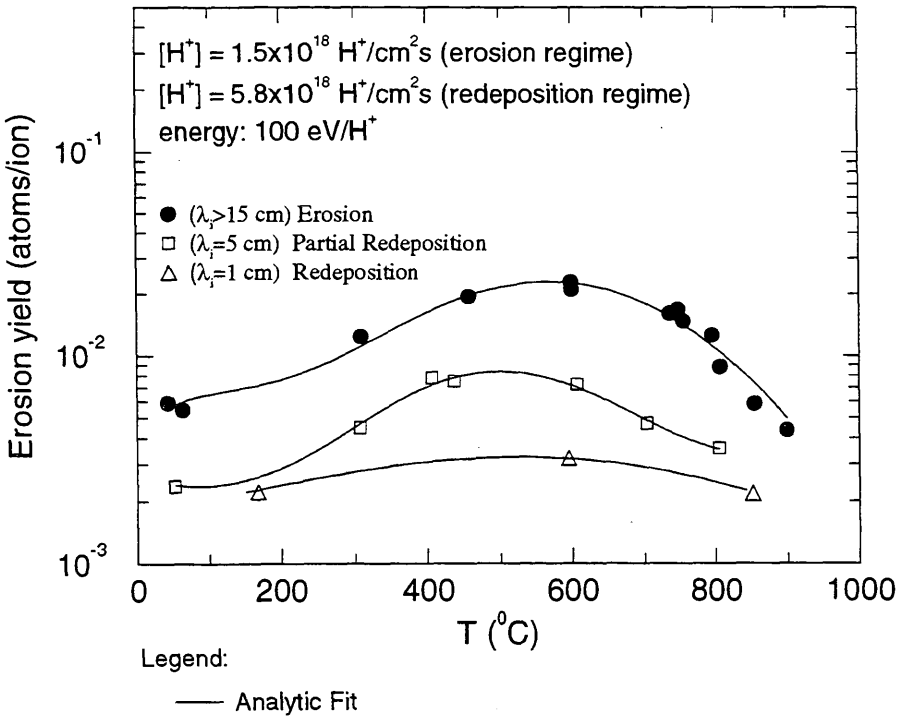

4.2.1.18 H^+ + MPg-8 graphite → C

Source: M. I. Guseva and Y. V. Martynenko, J. Nucl. Mater. **128&129**, 798 (1984).

Accuracy: Indeterminate.

Comments: (1) Weight loss measurement.
(2) Specimen: graphite (MPg-8).
(3) H^+ ions: mass-analyzed ion beams.

Analytic fitting function:

Sputtering yield:

$$Y = 1.0 \times 10^{-2}[A_1 \exp(-(T - A_2)^2/A_3)T^{A_4} + A_5 \exp(-A_6 T)T^{A_7}] \quad \text{[atoms/ion]}$$

where T is in ^{0}C. The rms deviation of the analytic fit is 7.9%.

Fitting parameters A_1-A_7

8.6054E+00	4.9828E+02	5.7139E+03	7.0882E-04	1.3311E-02	-1.0002E-03
7.6678E-01					

ALADDIN evaluation function for sputtering yield: EYIELD7A

ALADDIN hierarchical labelling:

SATM H [+1] GRAPHITE T=MPG-8 C [+0]

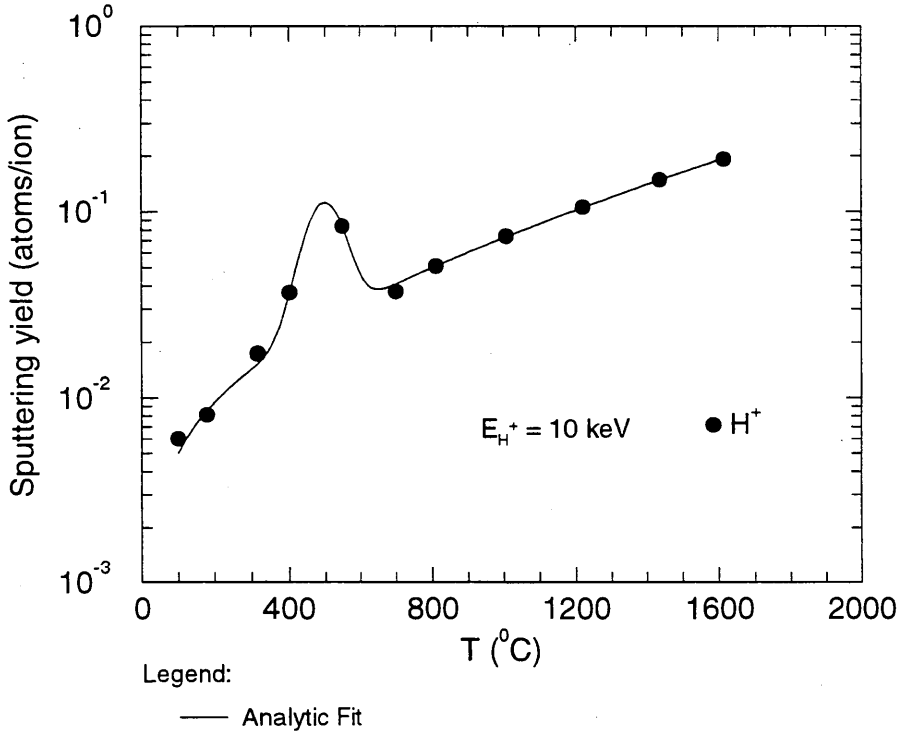

4.2.1.19 H^+ + carbon fiber composites → CH_4

Source: H. Grote, W. Bohmeyer. H.-D. Reiner, T. Fuchs, P. Kornejew and J. Steinbrink, J. Nucl. Mater. **241-243**, 1152 (1997).

Accuracy: Yield: 20%.

Comments: (1) Steady-state methane production measured via QMS and spectroscopically.
(2) Total erosion yield measured by mass loss.
(3) Experiments were performed in the plasma generator PSI-1 at the Max Planck Institute for Plasmaphysics (Berlin).
(4) Specimen: Advanced carbon fiber composites, including silicon-doped NS 31 (SEP).

Analytic fitting function:

Erosion yield:

$$Y = 1.0 \times 10^{-2}[A_1 \exp[-(\frac{T - A_2}{A_3 T + 1})^2 / A_4] T^{A_5} + A_6 \exp(-A_7 T) T^{A_8}] \quad [\mathrm{C/H^+}]$$

where T is in ^{0}C. The rms deviation of analytic fits for reactions A (△), B (◇) and C (•, ○) are 5.8%, 3.4% and 10.7%, respectively.

Fitting parameters A_1-A_8

A	1.2891e-01	3.8955e+04	7.3415e-02	2.9382e+06	6.3560e-01	-7.2101e-08
	1.3744e-03	2.9252e+00				
B	3.0329e-01	8.3766e+02	1.2720e-03	1.2729e+05	8.5210e-01	-1.6160e-08
	3.1513e-03	3.7389e+00				
C	1.8457e-02	4.8573e+02	6.0603e-04	1.3864e+04	6.1152e-01	1.3770e-10
	1.2098e-02	4.4985e+00				

ALADDIN evaluation function for erosion yield: EYIELD8A

ALADDIN hierarchical labelling:

A: SATM H [+1] GRAPHITE T=CFC CH{4} [+0]
B: SATM H [+1] GRAPHITE T=CFC CH{4} [+0]
C: SATM H [+1] GRAPHITE T=CFC D=Si CH{4} [+0]

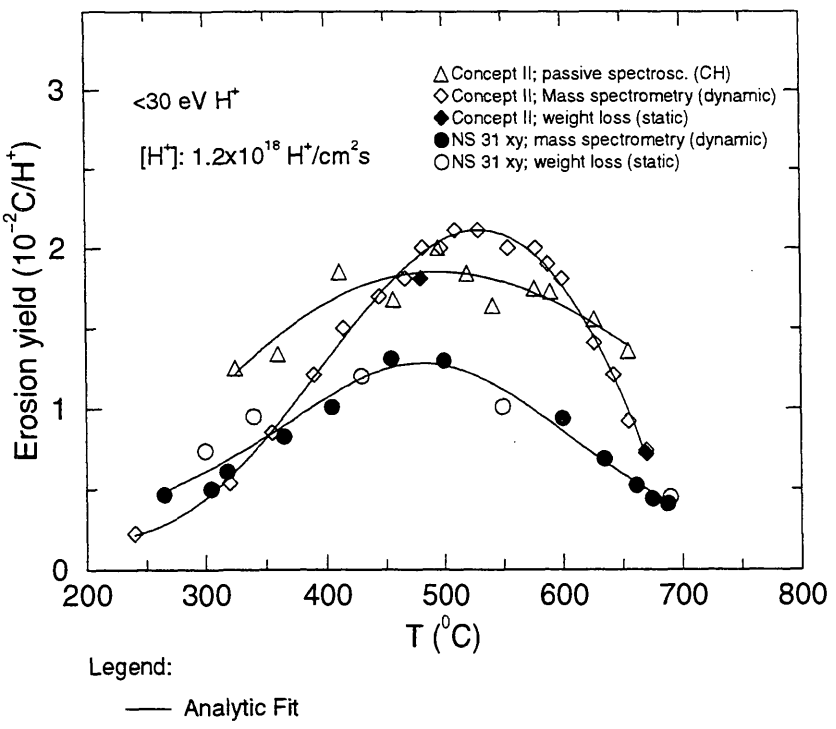

4.2.1.20 H_3^+ + pyrolytic graphite → CH_4

Source: C. H. Wu, J. W. Davis and A. A. Haasz, in *15th European Conf. on Controlled Fusion and Plasma Heating*, Dubrovnik, May 16-20, 1988, Europhysics Conf. Abstracts Vol. 12B Part II, p. 691.

Accuracy: Yield: ±20%; T:±25K.

Comments: (1) Steady-state methane yield.
(2) Specimen: pyrolytic graphite.
(3) Incident ions were mass-analyzed.
(4) Methane measured by QMS-RGA.

Analytic fitting function:

Methane yield:

$$Y = A_1 \exp(-(T - A_2)^2/A_3)T^{A_4} \quad [CH_4/H^+]$$

where T is in Kelvin. The rms deviation of analytic fits for reactions A (∗), B (○), C (•), D (□) and E (◇) are 4.0%, 9.9%, 12.3%, 4.2% and 10.2%, respectively. Data for curve E were fitted with EYIELD9A.

Fitting parameters A_1-A_9

A	3.7824e-06	5.8045e+02	4.6327e+04	1.1789e+00		
B	5.8662e-06	5.9048e+02	4.5106e+04	1.1565e+00		
C	4.6750e-03	6.7132e+02	4.4584e+04	1.5655e-01		
D	8.1540e-02	7.1178e+02	2.7038e+04	-2.3190e-01		
E	1.1410e+00	7.3459e+02	3.6485e+04	-5.1736e-01	-2.2932e-04	2.2545e-03
	1.1034e+00	-9.6278e+00	-3.6701e-01			

ALADDIN evaluation function for methane yield: EYIELD4B, EYIELD9A

ALADDIN hierarchical labelling:

A-E: SATM H{3} [+1] GRAPHITE T=HPG CH{4} [+0]

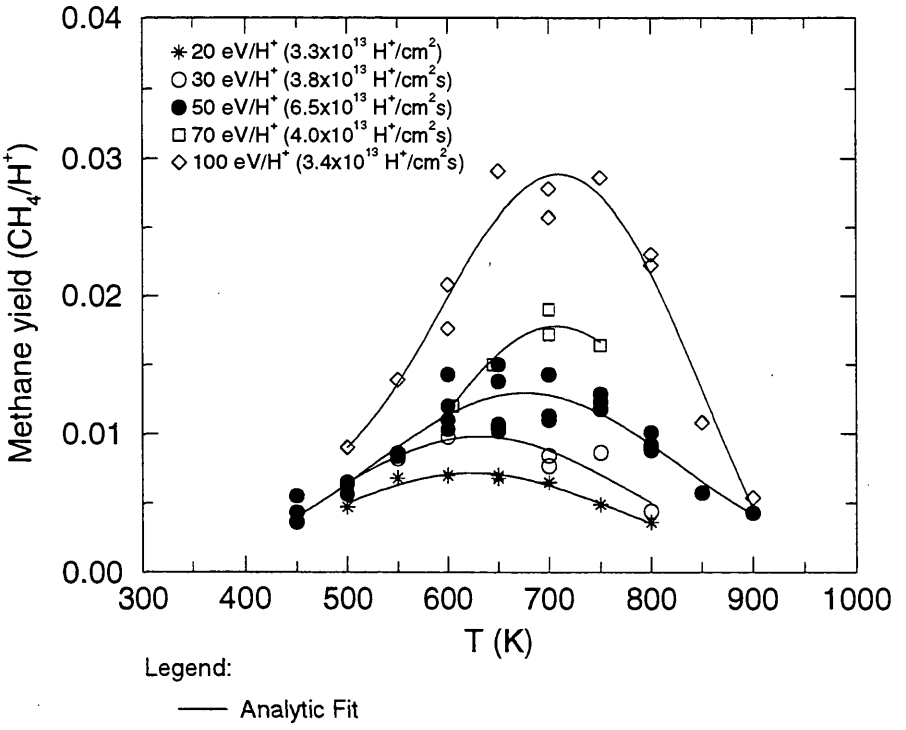

4.2.1.21 H_3^+ + pyrolytic graphite → CH_4

Source: C. H. Wu, J. W. Davis and A. A. Haasz, in *15th European Conf. on Controlled Fusion and Plasma Heating*, Dubrovnik, May 16-20, 1988, Europhysics Conf. Abstracts Vol. 12B Part II, p. 691.

Accuracy: Yield: ±20%; T: ±25K.

Comments: (1) Steady-state methane yield.
(2) Specimen: pyrolytic graphite.
(3) Incident ions were mass-analyzed.
(4) Methane measured by QMS-RGA.

Analytic fitting function:

Methane yield:

$$Y = A_1 \exp[-(\frac{T - A_2}{A_3 T + 1})^2 / A_4] T^{A_5} + A_6 \exp(-A_7 T) T^{A_8} \quad [CH_4/H^+]$$

where T is in Kelvin. The rms deviation of analytic fits for reactions A (∗), B (○), C (•) are 7.6%, 8.0% and 7.6%, respectively.

Fitting parameters A_1-A_8

A	-1.4548e-03	5.8859e+02	0.0	-1.2162e+06	1.0618e+00	1.6738e-02
	-8.4585e-04	6.0329e-01				
B	3.0486e-04	7.3755e+02	-6.0950e-04	7.7910e+04	7.7876e-01	6.4412e-10
	1.0589e-03	2.3996e+00				
C	3.9047e-04	7.3698e+02	-5.6793e-04	6.7293e+04	7.8241e-01	6.6166e-09
	-2.9134e-03	1.4582e+00				

ALADDIN evaluation function for methane yield: EYIELD8A

ALADDIN hierarchical labelling:

A-C: SATM H{3} [+1] GRAPHITE T=HPG CH{4} [+0]

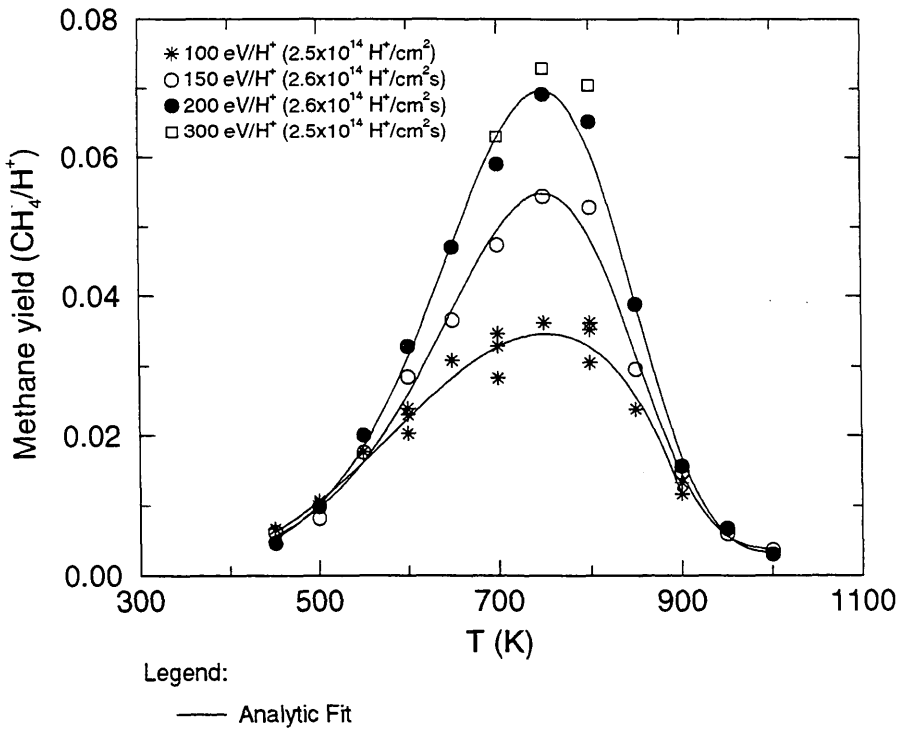

4.2.1.22 H_3^+ + pyrolytic graphite → CH_4

Source: C. H. Wu, J. W. Davis and A. A. Haasz, in *15th European Conf. on Controlled Fusion and Plasma Heating*, Dubrovnik, May 16-20, 1988, Europhysics Conf. Abstracts Vol. 12B Part II, p. 691.

Accuracy: Yield: ±20%; T: ±25K.

Comments: (1) Steady-state methane yield.
(2) Specimen: pyrolytic graphite.
(3) Incident ions were mass-analyzed.
(4) Methane measured by QMS-RGA.

Analytic fitting function:

Methane yield:

$$Y = A_1 \exp(-A_2 E) E^{A_3} + A_4 E^{A_5} \quad [CH_4/H^+]$$

where E is in eV. The rms deviation of analytic fits for reactions A (△) and B (•) are 1.3% and 5.7%, respectively.

Fitting parameters A_1-A_5

A	1.9272e-02	1.0871e-04	1.0147e+00	-2.0039e-02	1.0
B	2.1703e-06	-2.7961e-02	1.2126e+00	1.2065e-03	5.9902e-01

ALADDIN evaluation function for methane yield: EYIELD5A

ALADDIN hierarchical labelling:

A, B: SATM H{3} [+1] GRAPHITE T=HPG CH{4} [+0]

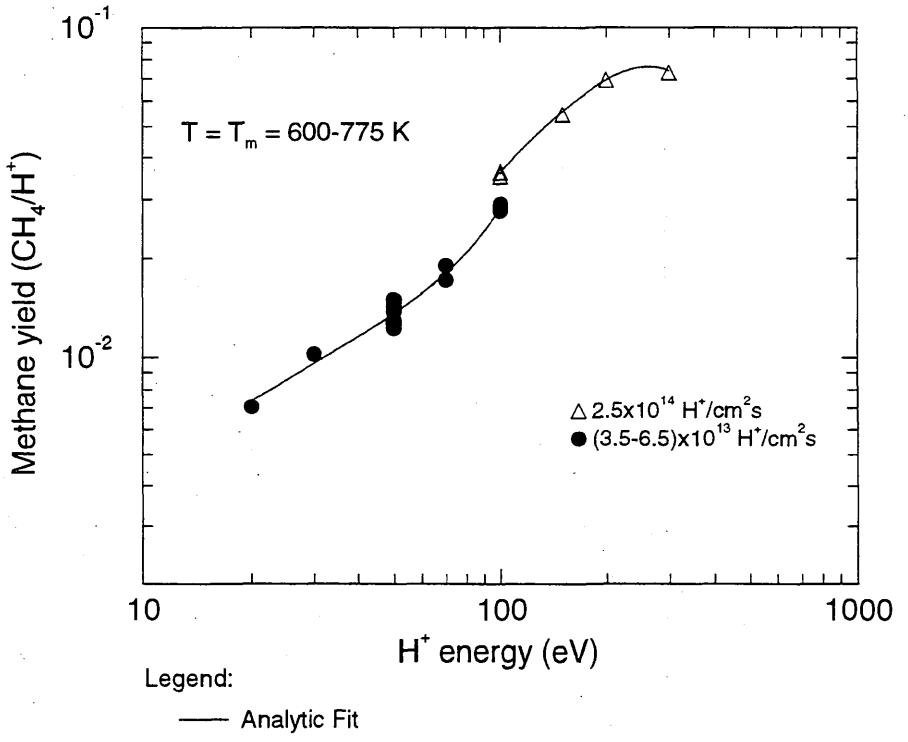

4.2.1.23 H_3^+ + pyrolytic graphite → CH_4

Source: J. W. Davis, A. A. Haasz and P. C. Stangeby, J. Nucl. Mater. **145-147**, 417 (1987).

Accuracy: Yield: ±15%.

Comments: (1) Steady-state methane yield at $T = T_m$.
(2) Specimen: graphite (pyrolytic).
(3) H^+ ions: mass analyzed accelerator.
(4) Methane measured via QMS-RGA.

Analytic fitting function:

Methane yield:

$$Y = A_1(\log F)^3 + A_2(\log F - A_3)^2 + A_4 \quad [CH_4/H^+]$$

where flux density F is in H^+/cm^2s. The rms deviation of the analytic fits for reactions A (•) and B (□) are 2.0% and 1.2%, respectively.

Fitting parameters A_1-A_4

A	-5.2208E-04	-1.0261E-03	4.4188E+00	8.8531E-02
B	4.0120E-03	-3.1265E-02	1.1364E+00	5.1185E-02

ALADDIN evaluation function for methane yield: EYIELD4C

ALADDIN hierarchical labelling:

A, B: SATM H{3} [+1] GRAPHITE T=HPG CH{4} [+0]

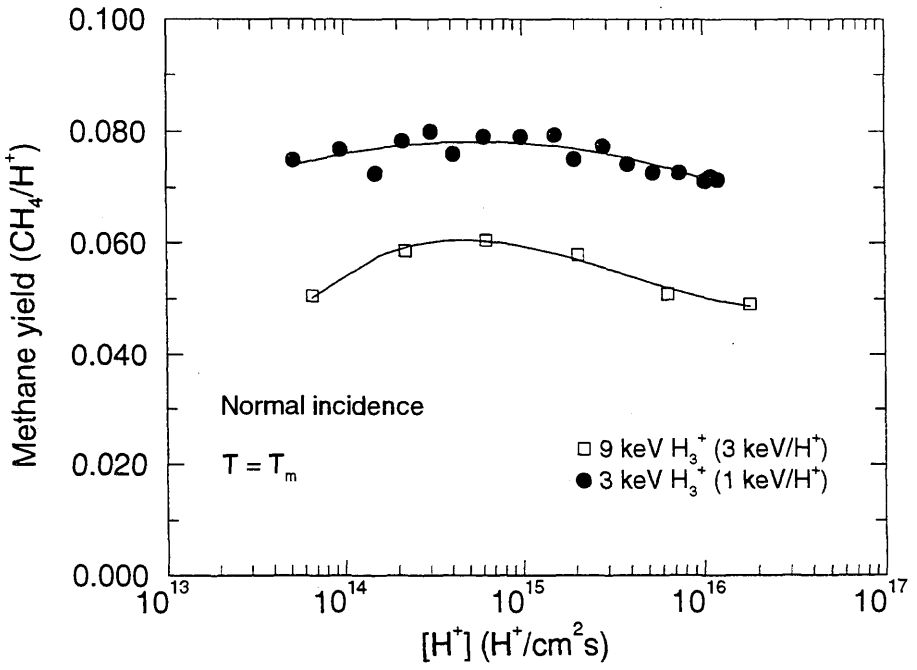

4.2.1.24 H_3^+ + pyrolytic graphite → CH_4

Source: J. W. Davis, A. A. Haasz and P. C. Stangeby, J. Nucl. Mater. **145-147**, 417 (1987).

Accuracy: Yield: ±15%.

Comments: (1) Steady-state methane yield.
(2) Specimen: graphite (pyrolytic).
(3) H^+ ions: mass analyzed accelerator.
(4) Methane measured via QMS-RGA.
(5) T_m varies with flux density.

Analytic fitting function:

Methane yield:

$$Y = A_1(\log F)^3 + A_2(\log F - A_3)^2 + A_4 \quad [CH_4/H^+]$$

where flux density F is in H^+/cm^2s. The rms deviation of the analytic fits for reactions A (□), B (•), C (▽) and D (△) are 5.0%, 4.0%, 4.8% and 3.1%, respectively.

Fitting parameters A_1-A_4

A	6.4769E-03	-3.0002E-01	7.7637E+00	-6.1087E+00
B	-2.6514E-04	-6.5368E-03	2.9558E+01	2.3540E+00
C	-5.1448E-05	-4.5646E-04	3.2206E+01	3.5601E-01
D	-1.9148E-04	-3.5140E-03	3.1443E+01	1.6709E+00

ALADDIN evaluation function for methane yield: EYIELD4C

ALADDIN hierarchical labelling:

A-D: SATM H{3} [+1] GRAPHITE T=HPG CH{4} [+0]

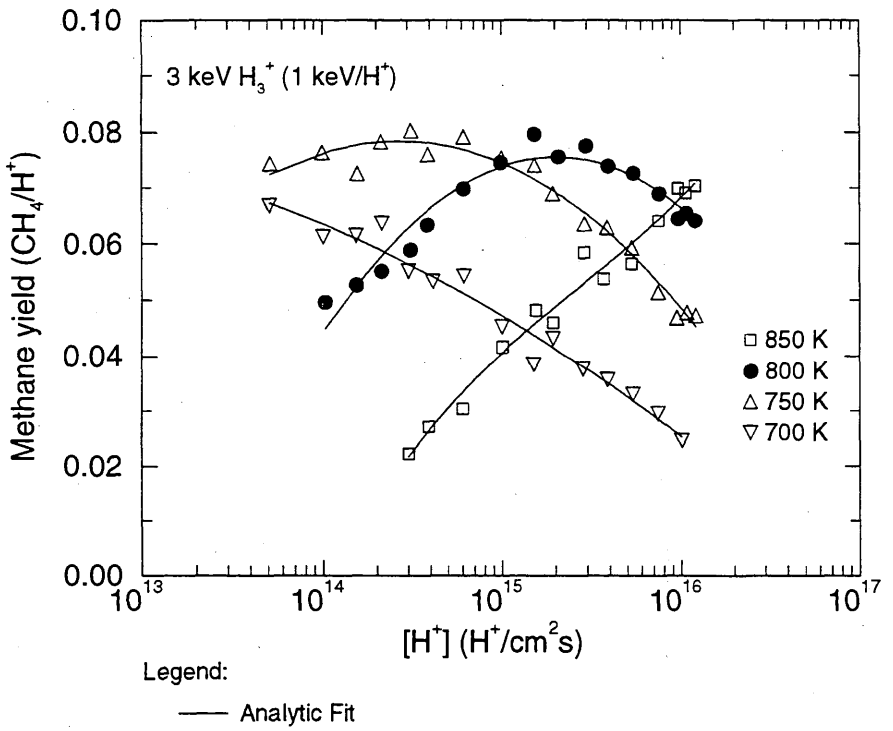

4.2.1.25 H_3^+ + pyrolytic graphite → CH_4

Source: J. W. Davis, A. A. Haasz and P. C. Stangeby, J. Nucl. Mater. **145-147**, 417 (1987).

Accuracy: Yield: ±15%; T: ±25K.

Comments: (1) Steady-state methane yield.
(2) Specimen: graphite (pyrolytic).
(3) H^+ ions: mass analyzed accelerator.
(4) Methane measured via QMS-RGA.
(5) The yield profile broadens with decreasing H^+ energy.

Analytic fitting function:

Methane yield:

$$Y = 1.0 \times 10^{-2}[A_1 \exp(-(T - A_2)^2/A_3)T^{A_4} + A_5 \exp(-A_6 T)T^{A_7}] \quad [CH_4/H^+]$$

where T is in Kelvin. The rms deviation of the analytic fits for reactions A (□), B (•), C (△) and D (∗) are 9.4%, 16.2%, 3.7% and 3.5%, respectively.

Fitting parameters A_1-A_7

A	1.8477E+00	8.0277E+02	9.3883E+03	1.4408E-01	1.1926E-01	-1.5480E-03
	6.5571E-02					
B	5.5314E+00	8.0253E+02	1.3733E+04	1.7511E-02	5.0406E-02	-2.4552E-03
	2.4187E-02					
C	2.8412E+00	7.8883E+02	2.4535E+04	9.7328E-02	7.7704E-02	-2.3344E-03
	9.1608E-04					
D	1.7650E+00	5.1567E+02	3.3606E+05	1.7160E-01	-5.2622E+00	2.5640E-03
	1.7083E-01					

ALADDIN evaluation function for methane yield: EYIELD7A

ALADDIN hierarchical labelling:

A-D: SATM H{3} [+1] GRAPHITE T=HPG CH{4} [+0]

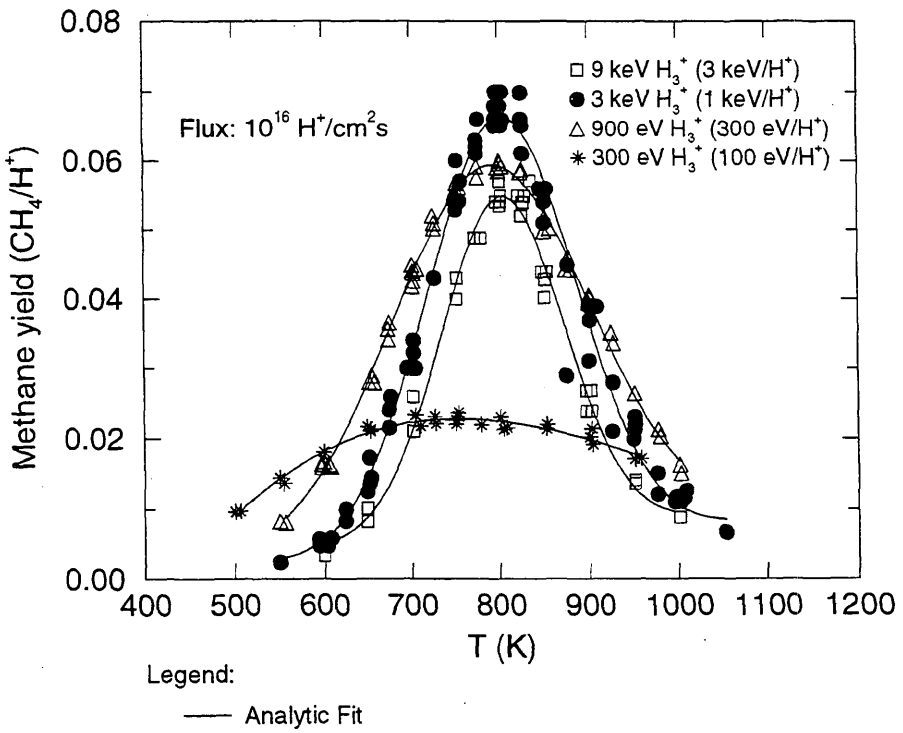

4.2.1.26 H_3^+ + pyrolytic graphite → CH_4, CD_4, C_{heavy}, C

Source: B. V. Mech, A. A. Haasz, and J. W. Davis, J. Nucl. Mater. **241-243**, 1147 (1997).

Accuracy: Yield: ±20%; T: ±25K.

Comments: (1) Steady-state hydrocarbon yield.
(2) Specimen: pyrolytic graphite (HPG99).
(3) Incident ions were mass-analyzed.
(4) Reaction products measured by QMS-RGA.
(5) Yield for total chemical erosion, $Y_{chem-total} = [CH_4 + 2(C_2H_2 + C_2H_4 + C_2H_6) + 3(C_3H_6 + C_3H_8)]/H^+$.
(6) Y_{heavy} is the hydrocarbon contribution excluding methane = $[2(C_2H_2 + C_2H_4 + C_2H_6) + 3(C_3H_6 + C_3H_8)]/H^+$.
(7) CD_4 data from A. A. Haasz, B. V. Mech and J. W. Davis, J. Nucl. Mater. **231**, 170 (1996).

Analytic fitting function:

Erosion yield:

$$Y = A_1 \exp[-(\frac{T - A_2}{A_3 T + 1})^2 / A_4] T^{A_5} + A_6 \exp(-A_7 T) T^{A_8} \quad [\text{molecules/H}^+]$$

where E is in eV. The rms deviation of analytic fits for reactions A (•), B (○), C (□) and D (◇) are 0.6%, 1.6%, 1.1% and 4.5%, respectively. Data for curve D were fitted with EYIELD7A.

Fitting parameters A_1-A_8

A	1.0188E-01	5.7089E+01	5.7600E-02	3.9753E+02	-4.5335E-01	4.4392E-07	2.0066E-01
	4.4162E+00						
B	1.4324E-03	4.1769E+01	1.7059E-02	4.5410E+02	4.4657E-01	9.5095E-05	2.3482E-01
	2.3627E+00						
C	5.3365E-03	2.8327E+01	3.0219E-01	8.0705E+00	1.9724E-01	4.0015E-07	2.0414E-01
	4.5131E+00						
D	1.5970E-01	3.3830E+01	1.4799E+03	3.6776E-01	1.4210E-03	2.2217E-02	1.7469E+00

ALADDIN evaluation function for erosion yield: EYIELD7A, EYIELD8A

ALADDIN hierarchical labelling:

A: SATM H{3} [+1] GRAPHITE T=HPG99 C [+0]
B: SATM H{3} [+1] GRAPHITE T=HPG99 CH{4} [+0]
C: SATM H{3} [+1] GRAPHITE T=HPG99 C{X}H{Y} [+0]
D: SATM D{3} [+1] GRAPHITE T=HPG99 CD{4} [+0]

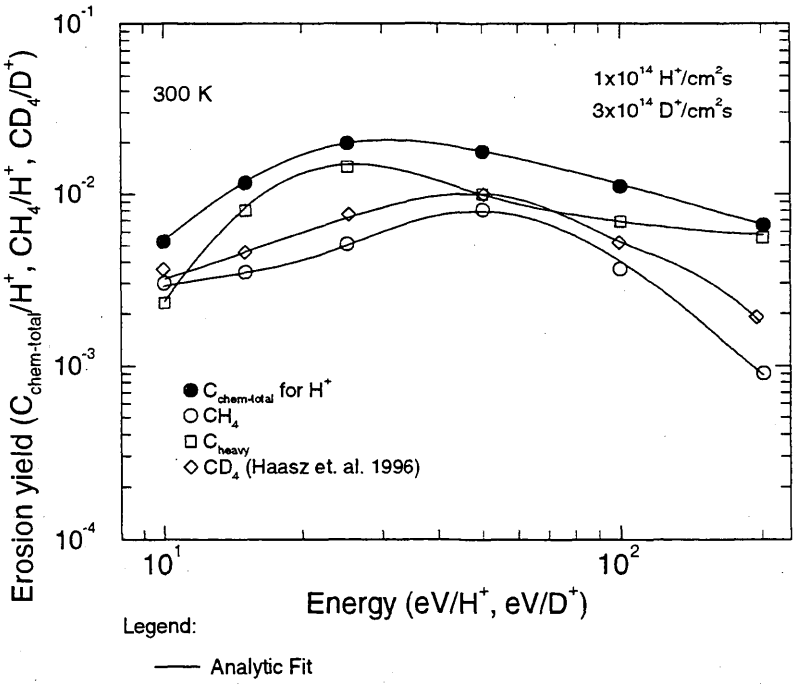

4.2.1.27 H_3^+ + pyrolytic graphite → CH_4, CD_4, C_{heavy}, C

Source: B. V. Mech, A. A. Haasz, and J. W. Davis, J. Nucl. Mater. **241-243**, 1147 (1997).

Accuracy: Yield: ±20%; T: ±25K.

Comments: (1) Steady-state hydrocarbon yield.
(2) Specimen: pyrolytic graphite (HPG99).
(3) Incident ions were mass-analyzed.
(4) Reaction products measured by QMS-RGA.
(5) Yield for total chemical erosion, $Y_{chem-total} = [CH_4 + 2(C_2H_2 + C_2H_4 + C_2H_6) + 3(C_3H_6 + C_3H_8)]/H^+$.
(6) Y_{heavy} is the hydrocarbon contribution excluding methane = $[2(C_2H_2 + C_2H_4 + C_2H_6) + 3(C_3H_6 + C_3H_8)]/H^+$.
(7) CD_4 data from A. A. Haasz, B. V. Mech and J. W. Davis, J. Nucl. Mater. **231**, 170 (1996).

Analytic fitting function:

Erosion yield:

$$Y = A_1 \exp\left[-\left(\frac{E - A_2}{A_3 E + 1}\right)^2 / A_4\right] E^{A_5} + A_6 \exp(-A_7 E) E^{A_8} \quad [\text{molecules/H}^+]$$

where E is in eV. The rms deviation of analytic fits for reactions A (•), B (○), C (□) and D (◇) are 3.0%, 0.6%, 1.7% and 0.9%, respectively. Data for curve D were fitted with EYIELD7A.

Fitting parameters A_1-A_8

A	9.8661E-01	2.7170E+02	2.1804E-02	1.9008E+04	-7.2224E-01	1.4698E-11	2.4909E-01
	8.2721E+00						
B	3.2463E-03	4.9218E+01	2.0453E-02	7.7061E+02	3.8938E-01	1.8014E-04	2.3175E-01
	2.4008E+00						
C	2.5289E-03	2.9667E+01	3.8754E+00	2.5747E-02	6.8317E-01	9.5568E-04	1.3677E-01
	1.6614E+00						
D	9.5225E+02	-2.8174E+02	3.7916E+03	5.1060E+00	3.2247E-01	3.5542E-03	4.5442E-01

ALADDIN evaluation function for erosion yield: EYIELD7A, EYIELD8A

ALADDIN hierarchical labelling:

A: SATM H{3} [+1] GRAPHITE T=HPG99 C [+0]
B: SATM H{3} [+1] GRAPHITE T=HPG99 CH{4} [+0]
C: SATM H{3} [+1] GRAPHITE T=HPG99 C{X}H{Y} [+0]
D: SATM D{3} [+1] GRAPHITE T=HPG99 CD{4} [+0]

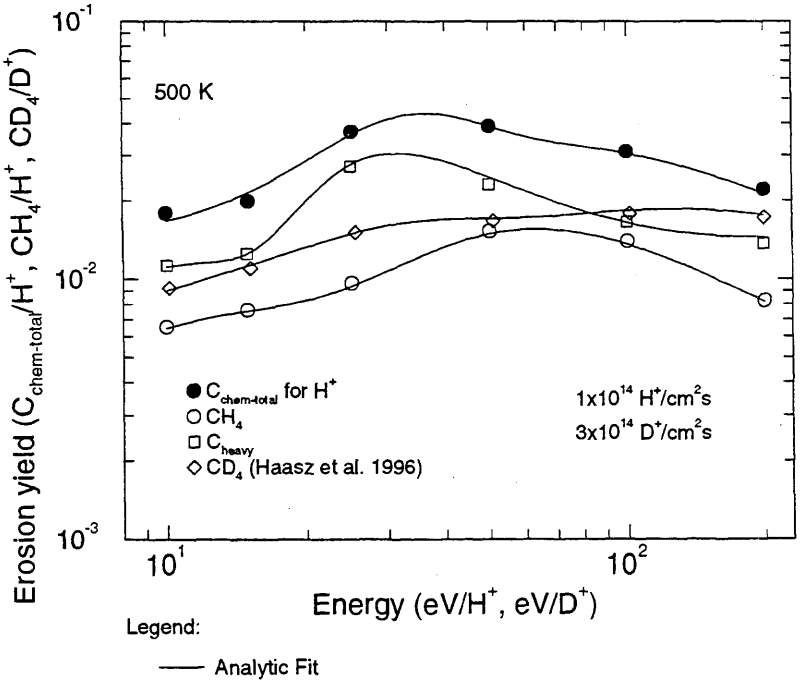

4.2.1.28 H_3^+ + pyrolytic graphite → CH_4, CD_4, C_{heavy}, C

Source: B. V. Mech, A. A. Haasz, and J. W. Davis, J. Nucl. Mater. **241-243**, 1147 (1997).

Accuracy: Yield: ±20%; T: ±25K.

Comments: (1) Steady-state hydrocarbon yield.
(2) Specimen: pyrolytic graphite (HPG99).
(3) Incident ions were mass-analyzed.
(4) Reaction products measured by QMS-RGA.
(5) Yield for total chemical erosion, $Y_{chem-total} = [CH_4 + 2(C_2H_2 + C_2H_4 + C_2H_6) + 3(C_3H_6 + C_3H_8)]/H^+$.
(6) Y_{heavy} is the hydrocarbon contribution excluding methane = $[2(C_2H_2 + C_2H_4 + C_2H_6) + 3(C_3H_6 + C_3H_8)]/H^+$.
(7) CD_4 data from A. A. Haasz, B. V. Mech and J. W. Davis, J. Nucl. Mater. **231**, 170 (1996).

Analytic fitting function:

Erosion yield:

$$Y = A_1 \exp\left[-\left(\frac{E - A_2}{A_3 E + 1}\right)^2 / A_4\right] E^{A_5} + A_6 \exp(-A_7 E) E^{A_8} \quad [\text{molecules/H}^+]$$

where E is in eV. The rms deviation of analytic fits for reactions A (•), B (○), C (□) and D (◇) are 0.7%, 2.2%, 0.5% and 2.4%, respectively.

Fitting parameters A_1-A_8

A	4.5809E-03	3.3830E+01	8.7802E-02	4.1733E+02	4.2741E-01	9.4459E-09	2.0532E-01
	5.6781E+00						
B	2.1999E-04	1.7681E+01	1.6535E+00	2.4838E-01	1.1237E+00	-9.9404E-07	7.8074E-02
	2.8235E+00						
C	5.3545E-02	2.7489E+02	1.3589E+00	3.6541E+02	-2.8454E-01	-6.6456E-08	4.5379E-01
	6.7221E+00						
D	2.6094E-05	4.2362E+01	1.1827E-01	3.4837E+01	1.5989E+00	1.2969E-04	4.7156E-02
	1.4464E+00						

ALADDIN evaluation function for erosion yield: EYIELD8A

ALADDIN hierarchical labelling:

A: SATM H{3} [+1] GRAPHITE T=HPG99 C [+0]
B: SATM H{3} [+1] GRAPHITE T=HPG99 CH{4} [+0]
C: SATM H{3} [+1] GRAPHITE T=HPG99 C{X}H{Y} [+0]
D: SATM D{3} [+1] GRAPHITE T=HPG99 CD{4} [+0]

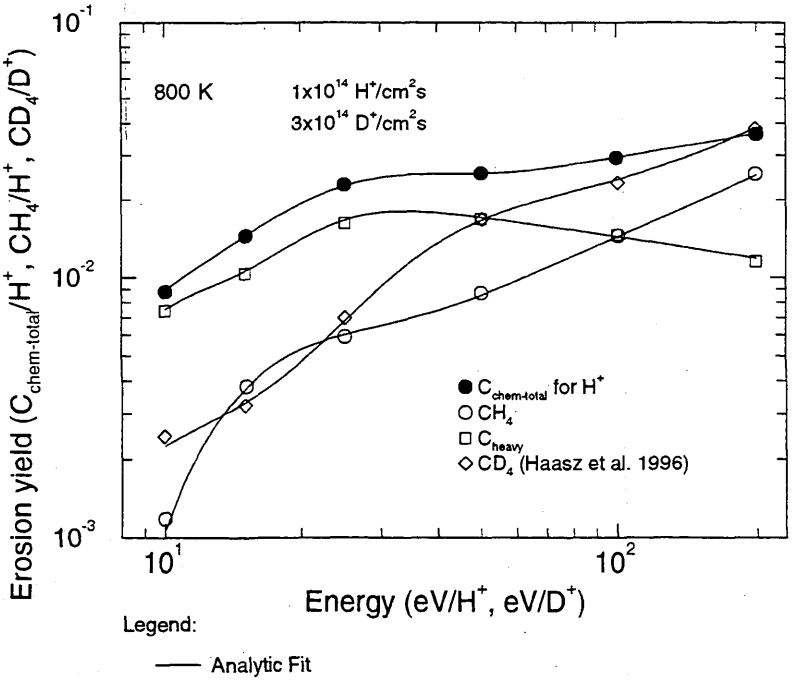

4.2.1.29 H_3^+ + pyrolytic graphite → CH_4, CD_4, C_{heavy}, C

Source: B. V. Mech, A. A. Haasz, and J. W. Davis, J. Nucl. Mater. **241-243**, 1147 (1997).

Accuracy: Yield: ±20%; T: ±25K.

Comments: (1) Steady-state hydrocarbon yield.
(2) Specimen: pyrolytic graphite (HPG99).
(3) Incident ions were mass-analyzed.
(4) Reaction products measured by QMS-RGA.
(5) Yield for total chemical erosion, $Y_{chem-total} = [CH_4 + 2(C_2H_2 + C_2H_4 + C_2H_6) + 3(C_3H_6 + C_3H_8)]/H^+$.
(6) Y_{heavy} is the hydrocarbon contribution excluding methane = $[2(C_2H_2 + C_2H_4 + C_2H_6) + 3(C_3H_6 + C_3H_8)]/H^+$.
(7) CD_4 data from A. A. Haasz, B. V. Mech and J. W. Davis, J. Nucl. Mater. **231**, 170 (1996).

Analytic fitting function:

Erosion yield:

$$Y = A_1(\log E)^3 + A_2(\log E - A_3)^2 + A_4 \quad [\text{molecules}/H^+]$$

where E is in eV. The rms deviation of analytic fits for reactions A (•), B (○), C (□) and D (◇) are 34.3%, 34.5%, 41.4% and 30.1%, respectively. Data for curves B and C were fitted with EYIELD5A and EYIELD4A, respectively.

Fitting parameters A_1-A_5

A	-1.0046e-04	-4.8686e-05	8.1911e+01	3.1109e-01	
B	3.7220e-03	3.6924e-06	1.6784e+00	-3.7160e-03	1.6785e+00
C	5.6014e-03	5.1596e-05	9.9956e-01	-5.5056e-03	
D	-1.7060e-03	1.7566e-02	1.5534e+00	1.2216e-01	

ALADDIN evaluation function for erosion yield: EYIELD4A, EYIELD4C, EYIELD5A

ALADDIN hierarchical labelling:

A: SATM H{3} [+1] GRAPHITE T=HPG99 C [+0]
B: SATM H{3} [+1] GRAPHITE T=HPG99 CH{4} [+0]
C: SATM H{3} [+1] GRAPHITE T=HPG99 C{X}H{Y} [+0]
D: SATM D{3} [+1] GRAPHITE T=HPG99 CD{4} [+0]

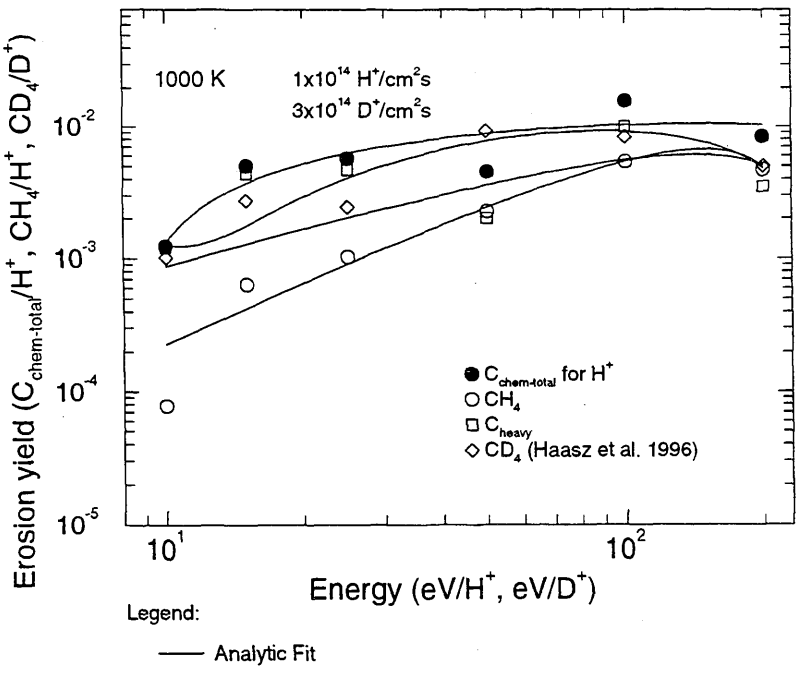

4.2.1.30 H_3^+ + pyrolytic graphite → CH_4, C

Source: B. V. Mech, A. A. Haasz, B. V. Mech and J. W. Davis, J. Nucl. Mater. **241-243**, 1147 (1997).

Accuracy: Yield: ±20%; T: ±25K.

Comments: (1) Steady-state hydrocarbon yield.
(2) Specimen: pyrolytic graphite (HPG99).
(3) Incident ions were mass-analyzed.
(4) Reaction products measured by QMS-RGA.
(5) Yield for total chemical erosion, $Y_{chem-total} = [CH_4 + 2(C_2H_2 + C_2H_4 + C_2H_6) + 3(C_3H_6 + C_3H_8)]/H^+$.
(6) Sub-eV impact results are from J. W. Davis, A. A. Haasz and P. C. Stangeby, J. Nucl. Mater. **155-157**, 234 (1988).

Analytic fitting function:

Erosion yield:

$$Y = A_1 \exp\left[-\left(\frac{E - A_2}{A_3 E + 1}\right)^2 / A_4\right] E^{A_5} + A_6 \exp(-A_7 E) E^{A_8} \quad [\text{molecules/H}^+]$$

where E is in eV. The rms deviation of analytic fits for reactions A (▽, △), B (○, ●) are 11.1% and 17.9%, respectively. Data for curve A were fitted with EYIELD5A.

Fitting parameters A_1-A_8

A	6.8636E-05	5.0934E-02	2.1361E+00	7.3228E-03	2.0695E-01	
B	4.7655E+02	2.9972E+01	-7.1189E-03	1.0535E-01	-4.0927E+00	1.1887E-03
	1.0712E-02	7.6986E-01				

ALADDIN evaluation function for erosion yield: EYIELD5A, EYIELD8A

ALADDIN hierarchical labelling:

A: SATM H{3} [+1] GRAPHITE T=HPG99 C [+0]
B: SATM H{3} [+1] GRAPHITE T=HPG99 CH{4} [+0]

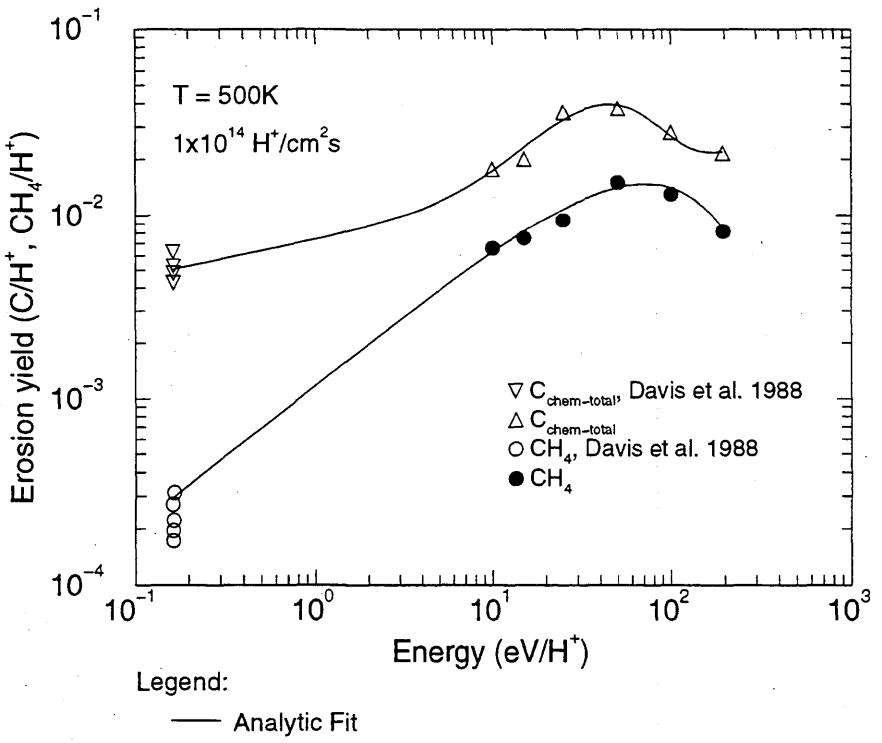

4.2.1.31 H_3^+ + pyrolytic graphite → C_xH_y, C

Source: B. V. Mech, A. A. Haasz, and J. W. Davis, J. Nucl. Mater. **241-243**, 1147 (1997).

Accuracy: Yield: ±20%; T: ±25K.

Comments: (1) Steady-state hydrocarbon yield.
(2) Specimen: pyrolytic graphite (HPG99).
(3) Incident ions were mass-analyzed.
(4) Reaction products measured by QMS-RGA.
(5) Yield for total chemical erosion, $Y_{chem-total} = [CH_4 + 2(C_2H_2 + C_2H_4 + C_2H_6) + 3(C_3H_6 + C_3H_8)]/H^+$.

Analytic fitting function:

Erosion yield:

$$Y = A_1 \exp(-(T - A_2)^2/A_3)T^{A_4} + A_5 \exp(-A_6 T)T^{A_7} \quad [\text{molecules/H}^+]$$

where T is in Kelvin. The rms deviation of analytic fits for reactions A (∗), B (•), C (○), D (△), E (▽), F (□) and G (◇) are 3.3%, 27.3%, 21.7%, 14.8%, 34.7%, 54.7% and 25.3%, respectively. Data for curve C were fitted with EYIELD4B.

Fitting parameters A_1-A_7

A	2.5252e+00	6.1855e+02	5.8856e+04	-7.5716e-01	-2.9911e+02	2.491 8e-02	-9.9931e-01
B	6.3237e+00	5.4913e+02	7.5691e+04	-1.0451e+00	-1.6428e+00	1.9621e-04	-1.0360e+00
C	4.9888e+00	7.8315e+02	8.1618e+04	-1.4159e+00			
D	4.8491e-03	6.7700e+02	4.9600e+04	-1.6439e-01	-5.7057e-03	-1.5683e-03	-8.7528e-01
E	5.8575e-03	6.2819e+02	4.5333e+04	-2.2906e-01	-3.4117e-17	4.8694e-03	4.7241e+00
F	6.2786e-03	5.4467e+02	5.0130e+04	-2.0568e-01	3.2568e-06	5.4475e-04	4.1681e-01
G	2.5163e-01	6.9355e+02	8.0101e+04	-8.7359e-01	-1.0432e-05	2.8738e-02	1.9807e+00

ALADDIN evaluation function for erosion yield: EYIELD4B, EYIELD7A

ALADDIN hierarchical labelling:

A: SATM H{3} [+1] GRAPHITE T=HPG99 C [+0]
B: SATM H{3} [+1] GRAPHITE T=HPG99 CH{4} [+0]
C: SATM H{3} [+1] GRAPHITE T=HPG99 C{2}H{2} [+0]
D: SATM H{3} [+1] GRAPHITE T=HPG99 C{2}H{4} [+0]
E: SATM H{3} [+1] GRAPHITE T=HPG99 C{2}H{6} [+0]
F: SATM H{3} [+1] GRAPHITE T=HPG99 C{3}H{6} [+0]
G: SATM H{3} [+1] GRAPHITE T=HPG99 C{3}H{8} [+0]

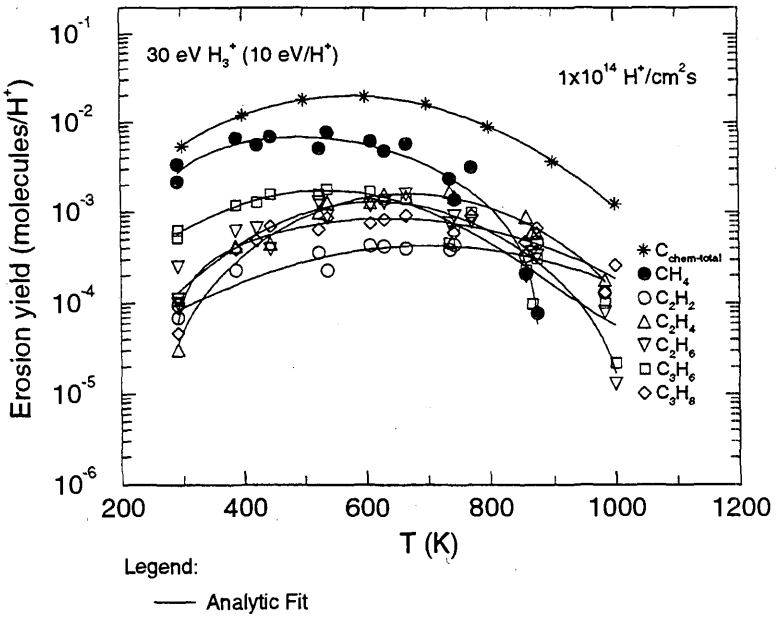

4.2.1.32 H_3^+ + pyrolytic graphite → C_xH_y, C

Source: B. V. Mech, A. A. Haasz, and J. W. Davis, J. Nucl. Mater. **241-243**, 1147 (1997).

Accuracy: Yield: ±20%; T: ±25K.

Comments: (1) Steady-state hydrocarbon yield.
(2) Specimen: pyrolytic graphite (HPG99).
(3) Incident ions were mass-analyzed.
(4) Reaction products measured by QMS-RGA.
(5) Yield for total chemical erosion, $Y_{chem-total} = [CH_4 + 2(C_2H_2 + C_2H_4 + C_2H_6) + 3(C_3H_6 + C_3H_8)]/H^+$.
(6) Only total yields were shown in the original publication.

Analytic fitting function:

Erosion yield:

$$Y = A_1 \exp(-(T - A_2)^2/A_3)T^{A_4} + A_5 \exp(-A_6T)T^{A_7} \quad [\text{molecules}/H^+]$$

where T is in Kelvin. The rms deviation of analytic fits for reactions A (∗), B (•), C (∘), D (△), E (▽), F (□) and G (◇) are 3.1%, 11.1%, 6.3%, 42.7%, 78.8%, 11.5% and 15.1%, respectively. Data for curve E were fitted with EYIELD5A.

Fitting parameters A_1-A_7

A	1.3811e-04	5.6224e+02	1.1367e+05	7.2072e-01	1.7398e-09	7.5552e-03	3.0778e+00
B	1.1206e-04	4.6523e+02	1.0688e+05	6.8451e-01	-9.9468e-08	7.7480e-03	1.9862e+00
C	1.8971e+00	7.9466e+02	1.3764e+04	-1.2791e+00	7.8195e-07	1.1634e-03	9.5828e-01
D	1.1546e-08	6.5077e+02	3.4578e+04	1.6639e+00	1.1899e-02	-9.1248e-04	-7.4068e-01
E	4.2865e-03	1.5636e-03	2.5651e-01	-2.7159e-01	-5.8753e-01		
F	1.3218e-04	4.7638e+02	1.1028e+05	3.4647e-01	2.2655e-07	9.1987e-04	1.2243e+00
G	7.1843e-05	6.4987e+02	6.5633e+04	2.7414e-01	4.0288e-04	-1.9194e-04	-4.0634e-02

ALADDIN evaluation function for erosion yield: EYIELD5A, EYIELD7A

ALADDIN hierarchical labelling:

A: SATM H{3} [+1] GRAPHITE T=HPG99 C [+0]
B: SATM H{3} [+1] GRAPHITE T=HPG99 CH{4} [+0]
C: SATM H{3} [+1] GRAPHITE T=HPG99 C{2}H{2} [+0]
D: SATM H{3} [+1] GRAPHITE T=HPG99 C{2}H{4} [+0]
E: SATM H{3} [+1] GRAPHITE T=HPG99 C{2}H{6} [+0]
F: SATM H{3} [+1] GRAPHITE T=HPG99 C{3}H{6} [+0]
G: SATM H{3} [+1] GRAPHITE T=HPG99 C{3}H{8} [+0]

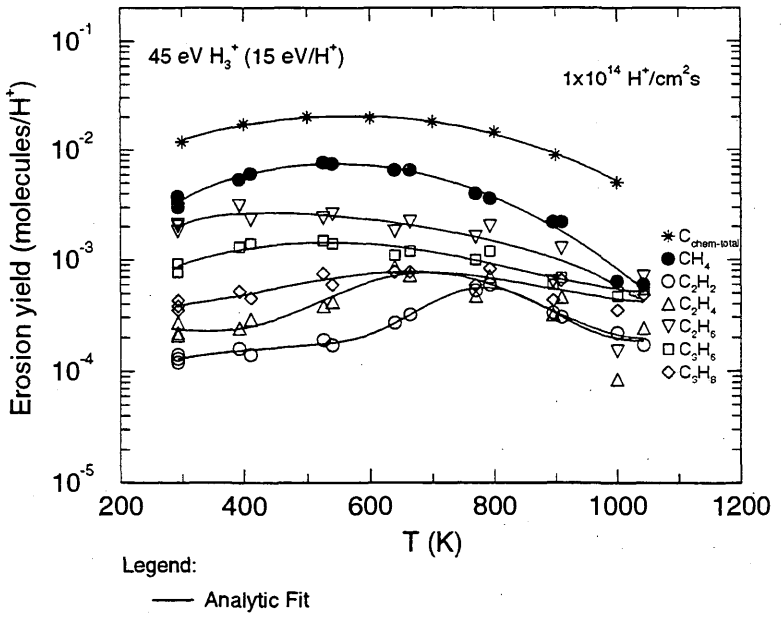

4.2.1.33 H_3^+ + pyrolytic graphite → C_xH_y, C

Source: B. V. Mech, A. A. Haasz, and J. W. Davis, J. Nucl. Mater. **241-243**, 1147 (1997).

Accuracy: Yield: ±20%; T: ±25K.

Comments: (1) Steady-state hydrocarbon yield.
(2) Specimen: pyrolytic graphite (HPG99).
(3) Incident ions were mass-analyzed.
(4) Reaction products measured by QMS-RGA.
(5) Yield for total chemical erosion, $Y_{chem-total} = [CH_4 + 2(C_2H_2 + C_2H_4 + C_2H_6) + 3(C_3H_6 + C_3H_8)]/H^+$.
(6) Only total yields were shown in the original publication.

Analytic fitting function:

Erosion yield:

$$Y = A_1 \exp[-(\frac{T - A_2}{A_3 T + 1})^2 / A_4] T^{A_5} + A_6 \exp(-A_7 T) T^{A_8} \quad [\text{molecules/H}^+]$$

where T is in Kelvin. The rms deviation of analytic fits for reactions A (∗), B (•), C (○), D (△), E (▽), F (□) and G (◇) are 1.3%, 44.8%, 17.9%, 25.1%, 23.4%, 12.0% and 7.6%, respectively. Data for curves E and G were fitted with EYIELD9A and EYIELD7A, respectively.

Fitting parameters A_1-A_9

A	2.8404e-03	5.7683e+02	6.8440e+04	4.0121e-01	1.5793e+00	7.0998e-04	-8.3148e-01
B	1.3841e-03	5.9417e+02	6.4902e+04	3.0185e-01	5.1304e+00	1.4624e-03	-1.2235e+00
C	5.6389e-05	6.2400e+02	7.5638e+04	4.3203e-01	2.5143e+03	-2.8373e-03	-3.0097e+00
D	1.5670e-04	5.9670e+02	4.3721e+04	5.6658e-01	2.9617e+01	-7.4697e-04	-1.7544e+00
E	1.7603e-03	5.3149e+02	8.5541e+03	6.0135e-02	6.9281e-08	9.4258e-03	1.4712e+00
	4.8395e-04	2.2376e+00					
F	1.8631e-03	7.2709e+02	3.5674e+04	-1.7582e-02	9.6169e-10	6.2517e-03	2.6573e+00
G	1.0397e-03	5.1883e+02	5.7100e-03	2.9622e+04	6.7699e-02	-2.6407e-04	-1.8367e-03
	-8.6537e-02						

ALADDIN evaluation function for erosion yield: EYIELD7A, EYIELD8A, EYIELD9A

ALADDIN hierarchical labelling:

A: SATM H{3} [+1] GRAPHITE T=HPG99 C [+0]
B: SATM H{3} [+1] GRAPHITE T=HPG99 CH{4} [+0]
C: SATM H{3} [+1] GRAPHITE T=HPG99 C{2}H{2} [+0]
D: SATM H{3} [+1] GRAPHITE T=HPG99 C{2}H{4} [+0]
E: SATM H{3} [+1] GRAPHITE T=HPG99 C{2}H{6} [+0]
F: SATM H{3} [+1] GRAPHITE T=HPG99 C{3}H{6} [+0]
G: SATM H{3} [+1] GRAPHITE T=HPG99 C{3}H{8} [+0]

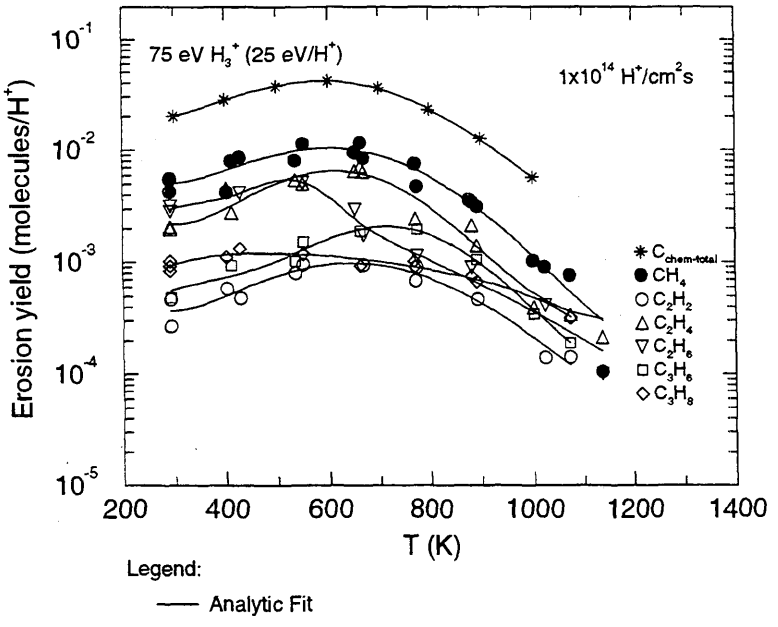

4.2.1.34 H_3^+ + pyrolytic graphite → C_xH_y, C

Source: B. V. Mech, A. A. Haasz, and J. W. Davis, J. Nucl. Mater. **241-243**, 1147 (1997).

Accuracy: Yield: ±20%; T: ±25K.

Comments: (1) Steady-state hydrocarbon yield.
(2) Specimen: pyrolytic graphite (HPG99).
(3) Incident ions were mass-analyzed.
(4) Reaction products measured by QMS-RGA.
(5) Yield for total chemical erosion, $Y_{chem-total} = [CH_4 + 2(C_2H_2 + C_2H_4 + C_2H_6) + 3(C_3H_6 + C_3H_8)]/H^+$.

Analytic fitting function:

Erosion yield:

$$Y = A_1 \exp(-(T - A_2)^2/A_3)T^{A_4} + A_5 \exp(-A_6T)T^{A_7} \quad [\text{molecules}/H^+]$$

where T is in Kelvin. The rms deviation of analytic fits for reactions A (∗), B (•), C (○), D (△), E (▽), F (□) and G (◇) are 0.6%, 20.5%, 81.5%, 41.6%, 104.7%, 36.6% and 57.6%, respectively. Data for curves F and G were fitted with EYIELD9A.

Fitting parameters A_1-A_9

A	8.4982e-03	6.3662e+02	4.6840e+04	2.1630e-01	7.0541e-11	9.4306e-03	3.8656e+00
B	3.1583e-03	5.6229e+02	9.1805e+04	2.5381e-01	9.4405e+00	4.7008e-02	8.9895e-01
C	7.9611e-04	6.8957e+02	5.4264e+04	2.0072e-02	3.9758e-08	2.3302e-03	1.4519e+00
D	1.3479e-07	-1.1302e+03	6.1934e+05	2.3702e+00	-1.2745e-14	-9.6100e-03	2.1765e+00
E	2.3709e-07	-1.5367e+03	6.4125e+05	2.8494e+00	-3.6265e-09	7.3078e-03	3.0389e+00
F	1.5281e-03	6.9591e+02	2.5631e+03	3.6694e-02	2.1173e-18	1.9386e-02	5.2460e+00
	3.3010e-14	6.7853e+00					
G	1.8620e-02	6.6020e+02	4.5912e+04	-4.9267e-01	6.8255e-10	1.4177e-02	3.5665e+00
	-2.0835e+01	-5.5636e-01					

ALADDIN evaluation function for erosion yield: EYIELD7A, EYIELD9A

ALADDIN hierarchical labelling:

A: SATM H{3} [+1] GRAPHITE T=HPG99 C [+0]
B: SATM H{3} [+1] GRAPHITE T=HPG99 CH{4} [+0]
C: SATM H{3} [+1] GRAPHITE T=HPG99 C{2}H{2} [+0]
D: SATM H{3} [+1] GRAPHITE T=HPG99 C{2}H{4} [+0]
E: SATM H{3} [+1] GRAPHITE T=HPG99 C{2}H{6} [+0]
F: SATM H{3} [+1] GRAPHITE T=HPG99 C{3}H{6} [+0]
G: SATM H{3} [+1] GRAPHITE T=HPG99 C{3}H{8} [+0]

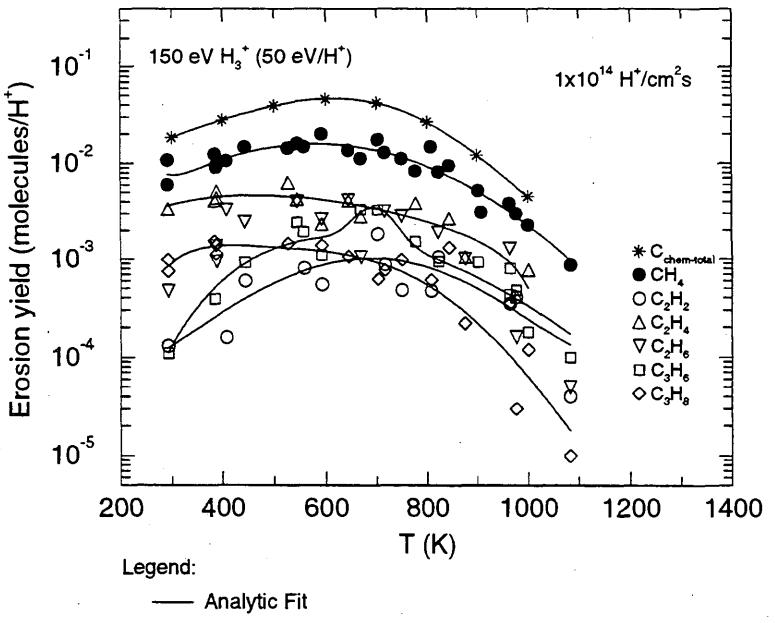

4.2.1.35 H_3^+ + pyrolytic graphite → C_xH_y, C

Source: B. V. Mech, A. A. Haasz, and J. W. Davis, J. Nucl. Mater. **241-243**, 1147 (1997).

Accuracy: Yield: ±20%; T: ±25K.

Comments: (1) Steady-state hydrocarbon yield.
(2) Specimen: pyrolytic graphite (HPG99).
(3) Incident ions were mass-analyzed.
(4) Reaction products measured by QMS-RGA.
(5) Yield for total chemical erosion, $Y_{chem-total} = [CH_4 + 2(C_2H_2 + C_2H_4 + C_2H_6) + 3(C_3H_6 + C_3H_8)]/H^+$.
(6) Only total yields were shown in the original publication.

Analytic fitting function:

Erosion yield:

$$Y = A_1 \exp(-A_2 T) T^{A_3} + A_4 T^{A_5} \quad [\text{molecules}/H^+]$$

where T is in Kelvin. The rms deviation of analytic fits for reactions A (∗), B (•), C (○), D (△), E (▽), F (□) and G (◇) are 4.3%, 0.4%, 14.6%, 32.3%, 16.0%, 2.5% and 26.8%, respectively. Data for curves A and C were fitted with EYIELD4B, data for curves B and F with EYIELD7A.

Fitting parameters A_1-A_7

A	2.0260e-05	5.8825e+02	1.0935e+05	1.1779e+00			
B	2.1492E-01	6.9483E+02	2.7036E+04	3.2009E-01	8.8435E-06	2.8511E-03	2.0093E+00
C	2.2725e+11	1.0186e+03	7.3466e+04	-4.7986e+00			
D	1.3926e-15	7.3050e-03	5.1445e+00	-4.8667e-05	4.8930e-01		
E	1.8294e-11	7.1600e-03	3.5137e+00	-7.4654e+00	-1.7416e+00		
F	2.8996E-02	4.3202E+02	9.6198E+03	2.0167E-01	1.2507E-09	5.5878E-03	3.3167E+00
G	1.8478e-06	2.0468e-04	1.5595e+00	-3.4956e-06	1.4364e+00		

ALADDIN evaluation function for erosion yield: EYIELD4B, EYIELD5A, EYIELD7A

ALADDIN hierarchical labelling:

A: SATM H{3} [+1] GRAPHITE T=HPG99 C [+0]
B: SATM H{3} [+1] GRAPHITE T=HPG99 CH{4} [+0]
C: SATM H{3} [+1] GRAPHITE T=HPG99 C{2}H{2} [+0]
D: SATM H{3} [+1] GRAPHITE T=HPG99 C{2}H{4} [+0]
E: SATM H{3} [+1] GRAPHITE T=HPG99 C{2}H{6} [+0]
F: SATM H{3} [+1] GRAPHITE T=HPG99 C{3}H{6} [+0]
G: SATM H{3} [+1] GRAPHITE T=HPG99 C{3}H{8} [+0]

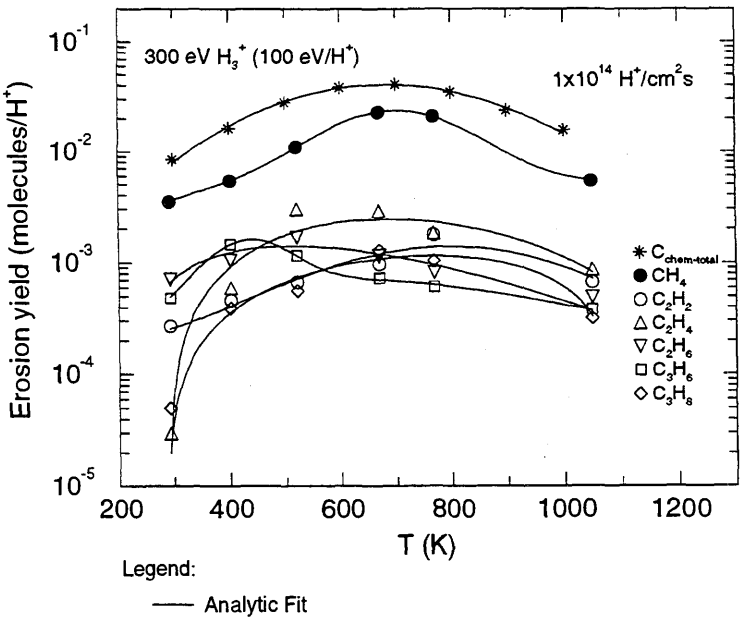

4.2.1.36 H_3^+ + pyrolytic graphite → C_xH_y, C

Source: B. V. Mech, A. A. Haasz, and J. W. Davis, J. Nucl. Mater. **241-243**, 1147 (1997).

Accuracy: Yield: ±20%; T: ±25K.

Comments: (1) Steady-state hydrocarbon yield.
(2) Specimen: pyrolytic graphite (HPG99).
(3) Incident ions were mass-analyzed.
(4) Reaction products measured by QMS-RGA.
(5) Yield for total chemical erosion, $Y_{chem-total} = [CH_4 + 2(C_2H_2 + C_2H_4 + C_2H_6) + 3(C_3H_6 + C_3H_8)]/H^+$.

Analytic fitting function:

Erosion yield:

$$Y = A_1 \exp[-(\frac{T - A_2}{A_3 T + 1})^2 / A_4] T^{A_5} + A_6 \exp(-A_7 T) T^{A_8} \quad [\text{molecules/H}^+]$$

where T is in Kelvin. The rms deviation of analytic fits for reactions A (∗), B (•), C (○), D (△), E (▽), F (□) and G (◇) are 2.8%, 35.4%, 13.5%, 14.3%, 24.5%, 17.6% and 15.7%, respectively. Data for curves A and C were fitted with EYIELD7A; data for curves B and D with EYIELD9A.

Fitting parameters A_1-A_9

A	4.3240e-03	6.8332e+02	2.9754e+04	3.4231e-01	1.4335e-09	4.9650e-03	2.9518e+00
B	4.0994e-03	7.0579e+02	1.8744e+04	3.2011e-01	6.4089e-10	7.8601e-03	1.8408e+00
	5.3105e-06	3.2128e+00					
C	4.9461E-09	-1.9579E+02	3.5731E+05	2.7031E+00	4.1098E+03	5.1409E-03	-3.9353E+00
D	1.3586e-03	6.9383e+02	1.9543e+04	8.2092e-02	2.5346e-07	5.3440e-03	7.7801e-01
	9.6349e-04	2.1309e+00					
E	1.3940e-03	6.2024e+02	2.2314e-03	8.6293e+03	5.7676e-02	4.8044e-05	1.3716e-02
	9.8863e-01						
F	1.2008e-03	5.0003e+02	8.6839e-03	1.6638e+03	4.1696e-02	2.5445e-05	9.2024e-03
	9.7260e-01						
G	4.1954e-04	4.3729e+02	2.4448e-01	1.2312e+01	1.1301e-01	-1.8570e-09	-9.1527e-03
	3.2747e-01						

ALADDIN evaluation function for erosion yield: EYIELD7A, EYIELD9A

ALADDIN hierarchical labelling:

A: SATM H{3} [+1] GRAPHITE T=HPG99 C [+0]
B: SATM H{3} [+1] GRAPHITE T=HPG99 CH{4} [+0]
C: SATM H{3} [+1] GRAPHITE T=HPG99 C{2}H{2} [+0]
D: SATM H{3} [+1] GRAPHITE T=HPG99 C{2}H{4} [+0]
E: SATM H{3} [+1] GRAPHITE T=HPG99 C{2}H{6} [+0]
F: SATM H{3} [+1] GRAPHITE T=HPG99 C{3}H{6} [+0]
G: SATM H{3} [+1] GRAPHITE T=HPG99 C{3}H{8} [+0]

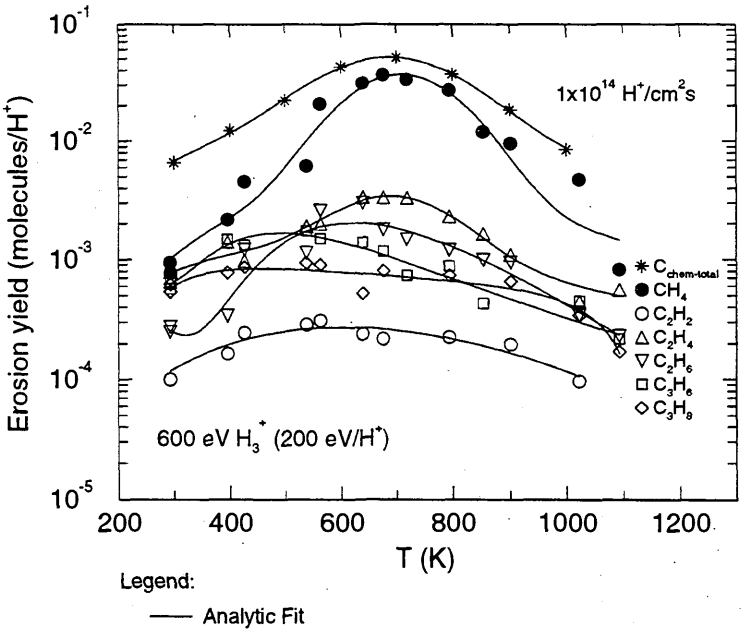

4.2.1.37 H_3^+ + pyrolytic graphite → CH_4, C_{heavy}, C

Source: B. V. Mech, A. A. Haasz and J. W. Davis, J. Nucl. Mater., in press (1998).

Accuracy: Yield: ±20%; T: ±25K.

Comments: (1) Steady-state hydrocarbon yield.
(2) Specimen: pyrolytic graphite (HPG99).
(3) Incident ions were mass-analyzed.
(4) Reaction products measured by QMS-RGA.
(5) Y_{heavy} is the hydrocarbon yield excluding methane = $[2(C_2H_2 + C_2H_4 + C_2H_6) + 3(C_3H_6 + C_3H_8)]/H^+$.
(6) Yield for total chemical erosion, $Y_{chem-total} = [CH_4 + 2(C_2H_2 + C_2H_4 + C_2H_6) + 3(C_3H_6 + C_3H_8)]/H^+$.

Analytic fitting function:

Erosion yield:

$$Y = A_1 \exp(-A_2/E)/(1 + A_3 \exp(-A_4/E)) \quad [\text{molecules/H}^+]$$

where E is in eV. The rms deviation of analytic fits for reactions A (•), B (○), and C (□) are 23.4%, 18.1% and 18.2%, respectively. Data for curve C were fitted with EYIELD4C, and curve B with EYIELD8A.

Fitting parameters A_1-A_8

A	6.4037e-03	-1.5474e+02	5.1686e-01	-1.7134e+02		
B	7.5386e-13	-6.0083e+02	1.68743e-03	1.7671e+04	4.1591e+01	2.0875e-19
	2.3833e-01	1.2519e+01				
C	-1.2130e-03	-1.2174e-03	6.1010e+00	3.4175e-02		

ALADDIN evaluation function for erosion yield: EYIELD4C, EYIELD4D, EYIELD8A

ALADDIN hierarchical labelling:

A: SATM H{3} [+1] GRAPHITE T=HPG99 C [+0]
B: SATM H{3} [+1] GRAPHITE T=HPG99 C{X}H{Y} [+0]
C: SATM H{3} [+1] GRAPHITE T=HPG99 CH{4} [+0]

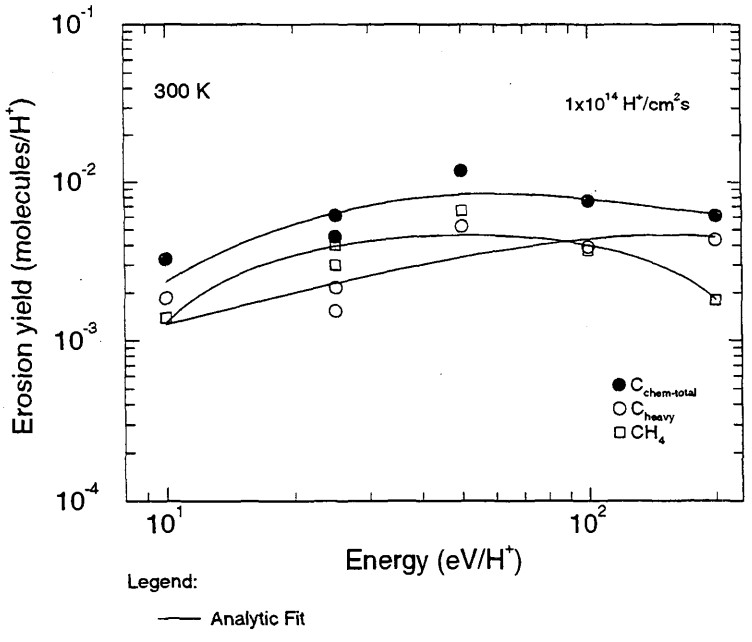

4.2.1.38 H_3^+ + pyrolytic graphite → CH_4, C_{heavy}, C

Source: B. V. Mech, A. A. Haasz and J. W. Davis, J. Nucl. Mater., in press (1998).

Accuracy: Yield: ±20%; T: ±25K.

Comments: (1) Steady-state hydrocarbon yield.
(2) Specimen: pyrolytic graphite (HPG99).
(3) Incident ions were mass-analyzed.
(4) Reaction products measured by QMS-RGA.
(5) Y_{heavy} is the hydrocarbon yield excluding methane = $[2(C_2H_2 + C_2H_4 + C_2H_6) + 3(C_3H_6 + C_3H_8)]/H^+$.
(6) Yield for total chemical erosion, $Y_{chem-total} = [CH_4 + 2(C_2H_2 + C_2H_4 + C_2H_6) + 3(C_3H_6 + C_3H_8)]/H^+$.

Analytic fitting function:

Erosion yield:

$$Y = A_1 \exp(-A_2/E)/(1 + A_3 \exp(-A_4/E)) \quad [\text{molecules}/H^+]$$

where E is in eV. The rms deviation of analytic fits for reactions A (•), B (○), and C (□) are 6.6%, 3.7% and 12.0%, respectively. Data for curve A were fitted with EYIELD4A.

Fitting parameters A_1-A_4

A	1.7791e-03	4.0822e+00	-9.2427e-01	2.3551e-01
B	1.6449e-03	1.7676e-02	6.4953e-01	6.0001e-05
C	3.7161e-02	-9.3818e+01	3.2397e+00	-1.0222e+02

ALADDIN evaluation function for erosion yield: EYIELD4A, EYIELD4D

ALADDIN hierarchical labelling:

A: SATM H{3} [+1] GRAPHITE T=HPG99 C [+0]
B: SATM H{3} [+1] GRAPHITE T=HPG99 C{X}H{Y} [+0]
C: SATM H{3} [+1] GRAPHITE T=HPG99 CH{4} [+0]

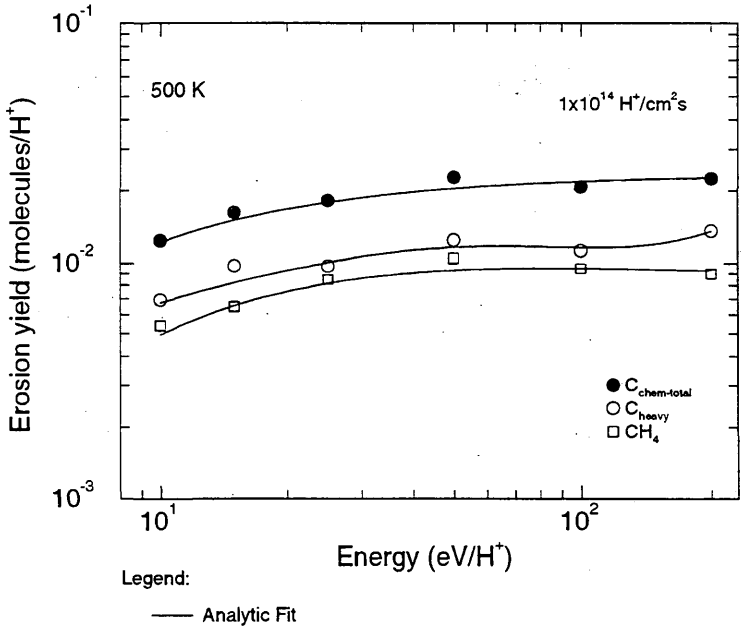

4.2.1.39 H_3^+ + pyrolytic graphite → CH_4, C_{heavy}, C

Source: B. V. Mech, A. A. Haasz and J. W. Davis, J. Nucl. Mater., in press (1998).

Accuracy: Yield: ±20%; T: ±25K.

Comments: (1) Steady-state hydrocarbon yield.
(2) Specimen: pyrolytic graphite (HPG99).
(3) Incident ions were mass-analyzed.
(4) Reaction products measured by QMS-RGA.
(5) Y_{heavy} is the hydrocarbon yield excluding methane = $[2(C_2H_2 + C_2H_4 + C_2H_6) + 3(C_3H_6 + C_3H_8)]/H^+$.
(6) Yield for total chemical erosion, $Y_{chem-total} = [CH_4 + 2(C_2H_2 + C_2H_4 + C_2H_6) + 3(C_3H_6 + C_3H_8)]/H^+$.

Analytic fitting function:

Erosion yield:

$$Y = A_1 \exp(-A_2 E) E^{A_3} + A_4 E \quad [\text{molecules}/H^+]$$

where E is in eV. The rms deviation of analytic fits for reactions A (•), B (○), and C (□) are 12.8%, 6.2% and 27.8%, respectively.

Fitting parameters A_1-A_4

A	5.5699e-03	2.0323e-03	3.9959e-01	1.2266e-04
B	5.7669e-03	4.6909e-03	2.5321e-01	5.3672e-05
C	3.4874e-04	1.0803e-02	9.3713e-01	1.5091e-04

ALADDIN evaluation function for erosion yield: EYIELD4A

ALADDIN hierarchical labelling:

A: SATM H{3} [+1] GRAPHITE T=HPG99 C [+0]
B: SATM H{3} [+1] GRAPHITE T=HPG99 C{X}H{Y} [+0]
C: SATM H{3} [+1] GRAPHITE T=HPG99 CH{4} [+0]

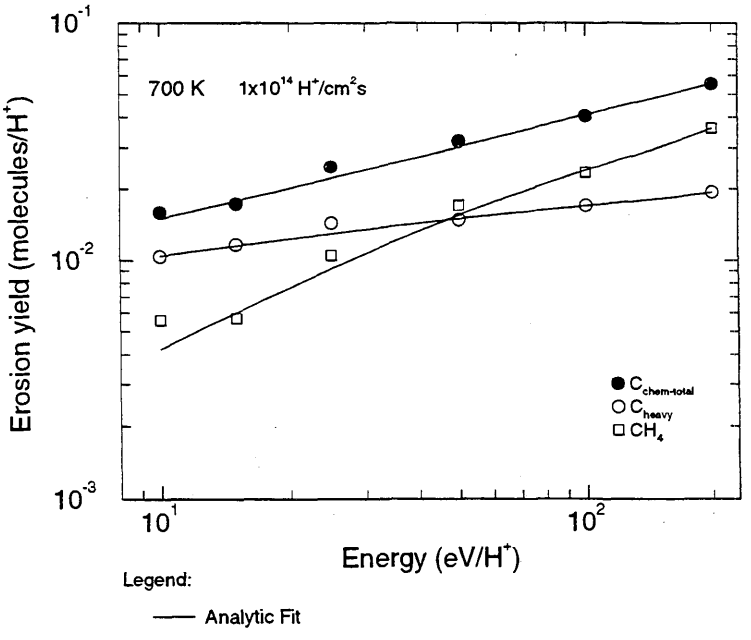

4.2.1.40 H_3^+ + pyrolytic graphite → CH_4, C_{heavy}, C

Source: B. V. Mech, A. A. Haasz and J. W. Davis, J. Nucl. Mater., in press (1998).

Accuracy: Yield: ±20%; T: ±25K.

Comments: (1) Steady-state hydrocarbon yield.
(2) Specimen: pyrolytic graphite (HPG99).
(3) Incident ions were mass-analyzed.
(4) Reaction products measured by QMS-RGA.
(5) Y_{heavy} is the hydrocarbon yield excluding methane = $[2(C_2H_2 + C_2H_4 + C_2H_6) + 3(C_3H_6 + C_3H_8)]/H^+$.
(6) Yield for total chemical erosion, $Y_{chem-total} = [CH_4 + 2(C_2H_2 + C_2H_4 + C_2H_6) + 3(C_3H_6 + C_3H_8)]/H^+$.

Analytic fitting function:

Erosion yield:

$$Y = A_1(\log E)^3 + A_2(\log E - A_3)^2 + A_4 \quad [\text{molecules}/H^+]$$

where E is in eV. The rms deviation of analytic fits for reactions A (•), B (○), and C (□) are 19.4%, 33.1% and 12.0%, respectively. Data for curve C were fitted with EYIELD4A.

Fitting parameters A_1-A_4

A	-1.2208E-02	5.4333E-02	6.6551E-01	7.6263E-03
B	-5.5669E-03	2.2715E-02	5.8191E-01	2.3524E-03
C	7.9516E-04	2.2406E-04	9.9101E-01	-7.1237E-04

ALADDIN evaluation function for erosion yield: EYIELD4A, EYIELD4C

ALADDIN hierarchical labelling:

A: SATM H{3} [+1] GRAPHITE T=HPG99 C [+0]
B: SATM H{3} [+1] GRAPHITE T=HPG99 C{X}H{Y} [+0]
C: SATM H{3} [+1] GRAPHITE T=HPG99 CH{4} [+0]

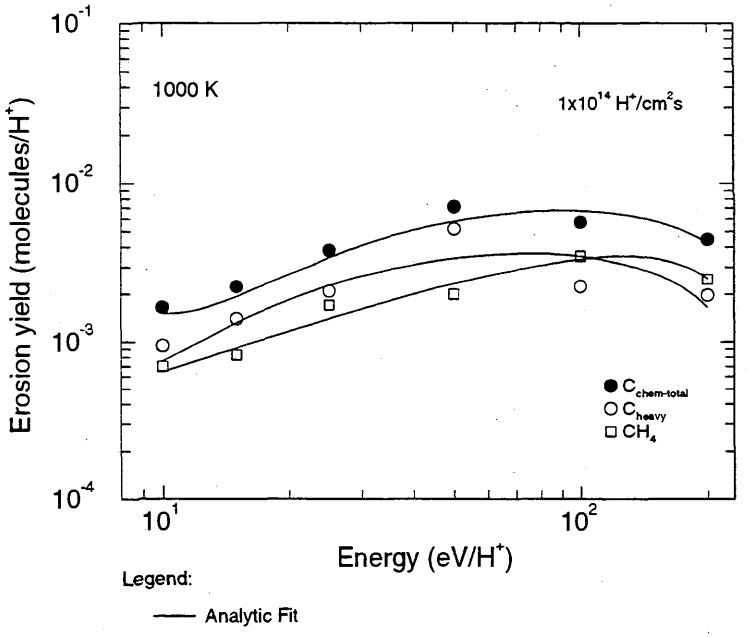

4.2.1.41 H_3^+ + pyrolytic graphite → C_xH_y, C

Source: B. V. Mech, A. A. Haasz and J. W. Davis, J. Nucl. Mater., in press (1998).

Accuracy: Yield: ±20%; T: ±25K.

Comments: (1) Steady-state hydrocarbon yield.
(2) Specimen: pyrolytic graphite (HPG99).
(3) Incident ions were mass-analyzed.
(4) Reaction products measured by QMS-RGA.
(5) Yield for total chemical erosion, $Y_{chem-total} = [CH_4 + 2(C_2H_2 + C_2H_4 + C_2H_6) + 3(C_3H_6 + C_3H_8)]/H^+$.

Analytic fitting function:

Erosion yield:

$$Y = A_1 \exp(-(Y - A_2)^2/A_3)Y^{A_4} + A_5 \exp(-A_6 Y)Y^{A_7}(1 + A_8 Y^{A_9}) \quad [\text{molecules/H}^+]$$

where T is in Kelvin. The rms deviation of analytic fits for reactions A (∗), B (•), C (○), D (△), E (▽), F (□) and G (◇) are 4.8%, 14.7%, 18.4%, 23.2%, 23.1%, 10.7% and 25.9%, respectively. Data for curves A, F and G were fitted with EYIELD7A.

Fitting parameters A_1-A_9

A	2.2123e-07	6.0297e+02	2.7118e+04	1.6944e+00	3.2014e-15	1.0154e-02	5.3807e+00
B	9.9001e-08	5.7186e+02	3.4920e+04	1.7335e+00	5.6813e+00	-1.1058e-04	-1.0639e+00
	-1.6549e+00	-1.0429e-01					
C	2.4453e-09	5.9775e+02	1.8740e+04	1.6925e+00	2.0535e-23	1.3875e-02	8.0566e+00
	1.1370e+09	-3.7261e+00					
D	6.0025e-09	6.4656e+02	1.7353e+04	1.8609e+00	4.7189e-23	1.3730e-02	8.1013e+00
	1.4498e+04	-1.8326e+00					
E	4.2733e-09	6.5462e+02	1.4843e+04	1.8823e+00	4.8391e-23	1.5626e-02	8.4567e+00
	-7.9192e+00	-5.1961e-01					
F	1.0207e-09	6.1304e+02	2.8408e+04	2.0791e+00	1.6847e-15	9.7210e-03	5.0416e+00
G	8.1316e-10	5.9961e+02	2.3158e+04	1.8849e+00	1.3672e-18	1.3406e-02	6.2401e+00

ALADDIN evaluation function for erosion yield: EYIELD7A, EYIELD9A

ALADDIN hierarchical labelling:

A: SATM H{3} [+1] GRAPHITE T=HPG99 C [+0]
B: SATM H{3} [+1] GRAPHITE T=HPG99 CH{4} [+0]
C: SATM H{3} [+1] GRAPHITE T=HPG99 C{2}H{2} [+0]
D: SATM H{3} [+1] GRAPHITE T=HPG99 C{2}H{4} [+0]
E: SATM H{3} [+1] GRAPHITE T=HPG99 C{2}H{6} [+0]
F: SATM H{3} [+1] GRAPHITE T=HPG99 C{3}H{6} [+0]
G: SATM H{3} [+1] GRAPHITE T=HPG99 C{3}H{8} [+0]

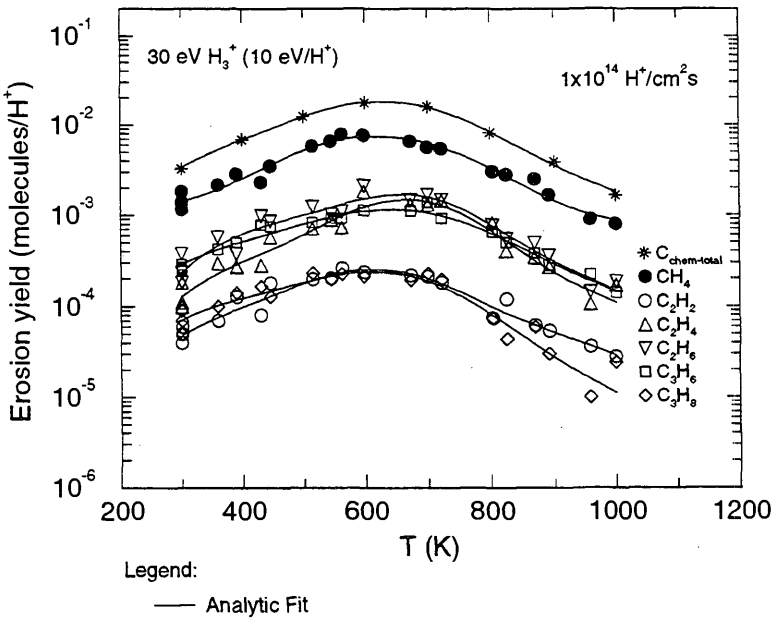

4.2.1.42 H_3^+ + pyrolytic graphite → C_xH_y, C

Source: B. V. Mech, A. A. Haasz and J. W. Davis, J. Nucl. Mater., in press (1998).

Accuracy: Yield: ±20%; T: ±25K.

Comments: (1) Steady-state hydrocarbon yield.
(2) Specimen: pyrolytic graphite (HPG99).
(3) Incident ions were mass-analyzed.
(4) Reaction products measured by QMS-RGA.
(5) Yield for total chemical erosion, $Y_{chem-total} = [CH_4 + 2(C_2H_2 + C_2H_4 + C_2H_6) + 3(C_3H_6 + C_3H_8)]/H^+$.

Analytic fitting function:

Erosion yield:

$$Y = A_1 \exp[-(\frac{T - A_2}{A_3 T + 1})^2 / A_4] T^{A_5} + A_6 \exp(-A_7 T) T^{A_8} \quad [\text{molecules}/H^+]$$

where T is in Kelvin. The rms deviation of analytic fits for reactions A (∗), B (•), C (∘), D (△), E (▽), F (□) and G (◇) are 3.3%, 10.7%, 34.4%, 31.4%, 13.5%, 15.5% and 32.9%, respectively.

Fitting parameters A_1-A_8

A	5.1092E-05	6.0122E+02	2.3783E-01	3.9374E-01	6.0214E-01	2.9303E-16	1.1435E-02
	5.8511E+00						
B	1.1997e-03	6.0234e+02	1.0032e-03	1.2011e+04	1.6833e-01	1.2581e-13	1.0043e-02
	4.7156e+00						
C	1.55512e-05	6.53932e+02	3.00612e+00	3.80608e-03	4.32441e-01	6.89840e-62	5.52098e-02
	2.56870e+01						
D	7.5630e-03	5.7046e+02	1.9914e-03	8.8926e+03	-2.4694e-01	1.8899e-10	-1.3004e-03
	1.7526e+00						
E	4.1010e-03	6.5020e+02	-4.6869e-04	8.3004e+04	-1.0876e-01	4.2881e-12	3.2030e-03
	3.0618e+00						
F	9.6440e-04	6.2365e+02	-2.5037e-04	6.6981e+04	5.0670e-02	1.6133e-13	3.8880e-03
	3.5047e+00						
G	1.7683e-04	6.1224e+02	-4.0977e-06	3.0650e+04	3.9493e-02	3.9705e-10	6.3333e-03
	2.1968e+00						

ALADDIN evaluation function for erosion yield: EYIELD8A

ALADDIN hierarchical labelling:

A: SATM H{3} [+1] GRAPHITE T=HPG99 C [+0]
B: SATM H{3} [+1] GRAPHITE T=HPG99 CH{4} [+0]
C: SATM H{3} [+1] GRAPHITE T=HPG99 C{2}H{2} [+0]
D: SATM H{3} [+1] GRAPHITE T=HPG99 C{2}H{4} [+0]
E: SATM H{3} [+1] GRAPHITE T=HPG99 C{2}H{6} [+0]
F: SATM H{3} [+1] GRAPHITE T=HPG99 C{3}H{6} [+0]
G: SATM H{3} [+1] GRAPHITE T=HPG99 C{3}H{8} [+0]

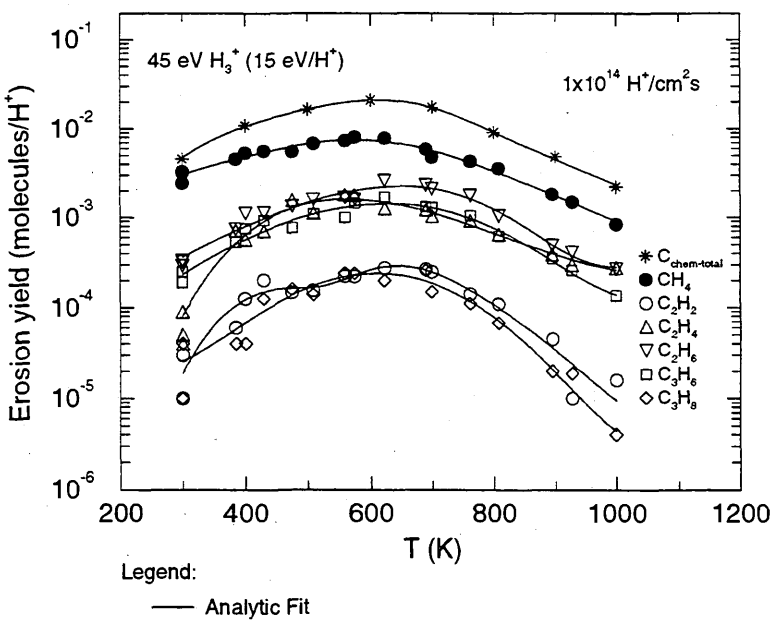

4.2.1.43 H_3^+ + pyrolytic graphite → C_xH_y, C

Source: B. V. Mech, A. A. Haasz and J. W. Davis, J. Nucl. Mater., in press (1998).

Accuracy: Yield: ±20%; T: ±25K.

Comments: (1) Steady-state hydrocarbon yield.
(2) Specimen: pyrolytic graphite (HPG99).
(3) Incident ions were mass-analyzed.
(4) Reaction products measured by QMS-RGA.
(5) Yield for total chemical erosion, $Y_{chem-total} = [CH_4 + 2(C_2H_2 + C_2H_4 + C_2H_6) + 3(C_3H_6 + C_3H_8)]/H^+$.

Analytic fitting function:

Erosion yield:

$$Y = A_1 \exp(-(Y - A_2)^2/A_3)Y^{A_4} + A_5 \exp(-A_6 Y)Y^{A_7}(1 + A_8 Y^{A_9}) \quad [\text{molecules/H}^+]$$

where T is in Kelvin. The rms deviation of analytic fits for reactions A (∗), B (•), C (○), D (△), E (▽), F (□) and G (◇) are 2.8%, 13.8%, 23.5%, 14.3%, 14.0%, 15.8% and 35.1%, respectively. Data for curves A and B were fitted with EYIELD7A, data for curve F with EYIELD8B, data for curve G with EYIELD8A.

Fitting parameters A_1-A_9

A	2.3751e-02	6.4665e+02	3.4194e+04	-2.8312e-02	1.4837e-08	4.994 5e-03	2.5120e+00
B	5.4680e-02	6.5707e+02	4.8976e+04	-2.6775e-01	1.2509e+01	-1.288 1e-03	-1.5269e+00
C	4.6747e-08	6.3833e+02	1.5643e+04	1.3213e+00	9.4282e-05	5.884 0e-03	1.0382e+00
	-1.5919e+00	-8.3580e-02					
D	8.3992e-08	6.3626e+02	1.0913e+04	1.4435e+00	3.4073e-05	4.381 0e-03	1.3014e+00
	-1.5797e+00	-8.3560e-02					
E	7.9326e-09	6.0922e+02	2.5107e+04	1.8966e+00	3.2782e-10	8.173 0e-03	3.5105e+00
	-1.5394e+00	-7.8950e-02					
F	1.5643e-03	6.3868e+02	2.5468e+04	-3.8164e-02	3.0012e-02	-2.517 2e-01	7.6960e-03
	-4.8828e+00						
G	3.5657e-04	6.5804e+02	-5.5782e-4	7.0196e+04	-8.3390e-02	5.5943e-7	4.9870e-03
	1.1403e+00						

ALADDIN evaluation function for erosion yield: EYIELD7A, EYIELD8A, EYIELD8B, EYIELD9A

ALADDIN hierarchical labelling:

A: SATM H{3} [+1] GRAPHITE T=HPG99 C [+0]
B: SATM H{3} [+1] GRAPHITE T=HPG99 CH{4} [+0]
C: SATM H{3} [+1] GRAPHITE T=HPG99 C{2}H{2} [+0]
D: SATM H{3} [+1] GRAPHITE T=HPG99 C{2}H{4} [+0]
E: SATM H{3} [+1] GRAPHITE T=HPG99 C{2}H{6} [+0]
F: SATM H{3} [+1] GRAPHITE T=HPG99 C{3}H{6} [+0]
G: SATM H{3} [+1] GRAPHITE T=HPG99 C{3}H{8} [+0]

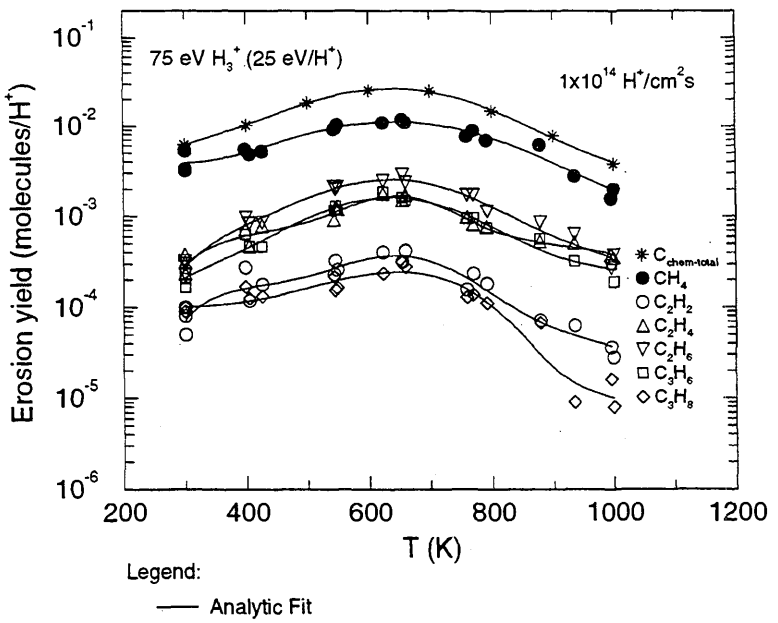

4.2.1.44 H_3^+ + pyrolytic graphite → C_xH_y, C

Source: B. V. Mech, A. A. Haasz and J. W. Davis, J. Nucl. Mater., in press (1998).

Accuracy: Yield: ±20%; T: ±25K.

Comments: (1) Steady-state hydrocarbon yield.
(2) Specimen: pyrolytic graphite (HPG99).
(3) Incident ions were mass-analyzed.
(4) Reaction products measured by QMS-RGA.
(5) Yield for total chemical erosion, $Y_{chem-total} = [CH_4 + 2(C_2H_2 + C_2H_4 + C_2H_6) + 3(C_3H_6 + C_3H_8)]/H^+$.

Analytic fitting function:

Erosion yield:

$$Y = A_1 \exp(-(Y - A_2)^2/A_3)Y^{A_4} + A_5 \exp(-A_6 Y)Y^{A_7}(1 + A_8 Y^{A_9}) \quad [\text{molecules/H}^+]$$

where T is in Kelvin. The rms deviation of analytic fits for reactions A (∗), B (•), C (○), D (△), E (▽), F (□) and G (◇) are 0.7%, 10.2%, 10.1%, 8.3%, 6.3%, 12.2% and 42.3%, respectively. Data for curves A and G were fitted with EYIELD7A, data for curves B and C with EYIELD8B, data for curve F with EYIELD8A.

Fitting parameters A_1-A_9

A	1.4861e-07	6.1823e+02	4.9124e+04	1.8382e+00	2.7962e-07	4.8891e-03	2.1153e+00
B	7.3460e-03	6.9480e+02	3.5254e+04	9.6680e-02	5.3534e+00	-3.4227e-01	1.0640e-02
	-5.4719e+00						
C	1.6543e-03	6.5046e+02	2.5692e+04	-2.6998e-01	4.4273e+05	-8.8631e-02	-1.2256e-02
	-2.1175e+00						
D	1.7451e-05	5.7982e+02	1.5759e+04	5.6993e-01	1.8563e-07	6.7660e-03	1.6786e+00
	8.9461e-09	3.1982e+00					
E	2.6943e-08	5.0153e+02	1.0234e+05	1.7483e+00	2.4565e-07	3.9022e-03	6.3204E-01
	4.9097E-05	2.4778E+00					
F	1.3065e-03	6.4370e+02	-2.7257e-04	1.6956e+05	4.1340e-02	1.1290e-05	2.7443e-03
	5.4624e-01						
G	4.3808e-04	6.0816e+02	3.1259e+04	-4.2060e-02	9.4200e-06	-1.1859e-03	2.0815e-01

ALADDIN evaluation function for erosion yield: EYIELD7A, EYIELD8A, EYIELD8B, EYIELD9A

ALADDIN hierarchical labelling:

A: SATM H{3} [+1] GRAPHITE T=HPG99 C [+0]
B: SATM H{3} [+1] GRAPHITE T=HPG99 CH{4} [+0]
C: SATM H{3} [+1] GRAPHITE T=HPG99 C{2}H{2} [+0]
D: SATM H{3} [+1] GRAPHITE T=HPG99 C{2}H{4} [+0]
E: SATM H{3} [+1] GRAPHITE T=HPG99 C{2}H{6} [+0]
F: SATM H{3} [+1] GRAPHITE T=HPG99 C{3}H{6} [+0]
G: SATM H{3} [+1] GRAPHITE T=HPG99 C{3}H{8} [+0]

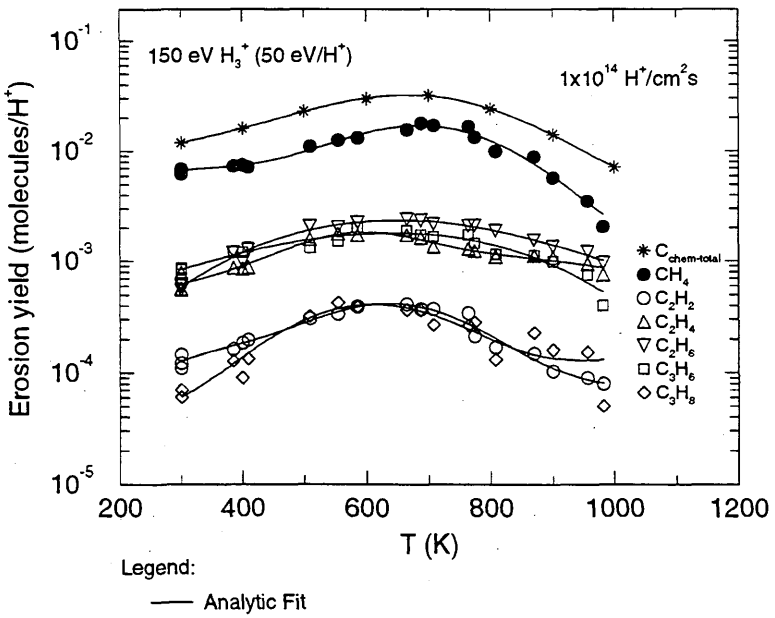

4.2.1.45 H_3^+ + pyrolytic graphite → C_xH_y, C

Source: B. V. Mech, A. A. Haasz and J. W. Davis, J. Nucl. Mater., in press (1998).

Accuracy: Yield: ±20%; T: ±25K.

Comments: (1) Steady-state hydrocarbon yield.
(2) Specimen: pyrolytic graphite (HPG99).
(3) Incident ions were mass-analyzed.
(4) Reaction products measured by QMS-RGA.
(5) Yield for total chemical erosion, $Y_{chem-total} = [CH_4 + 2(C_2H_2 + C_2H_4 + C_2H_6) + 3(C_3H_6 + C_3H_8)]/H^+$.

Analytic fitting function:

Erosion yield:

$$Y = A_1 \exp(-(T - A_2)^2/A_3)T^{A_4} + A_5 \exp(-A_6T)T^{A_7} \quad [\text{molecules/H}^+]$$

where T is in Kelvin. The rms deviation of analytic fits for reactions A (∗), B (•), C (○), D (△), E (▽), F (□) and G (◇) are 3.4%, 10.2%, 17.5%, 24.7%, 13.9%, 18.2% and 55.1%, respectively. Data for curve B were fitted with EYIELD9A, data for curves D and E with EYIELD8B.

Fitting parameters A_1-A_9

A	7.3680e-03	7.1238e+02	1.5727e+04	1.7962e-01	1.1135e-17	1.1603e-02	6.5754e+00
B	1.3355e-02	7.2915e+02	1.8950e+04	5.7910e-02	6.7688e+01	2.4103e-03	-6.2826e-01
	-1.1623e+00	-2.7055e-02					
C	3.4363e-08	6.8503e+02	9.7992e+03	1.3998e+00	1.8494e-13	7.4890e-03	3.9205e+00
D	4.6049e+01	6.9805e+02	4.3475e+04	-1.5431e+00	6.7507e-07	2.4268e-03	-2.1139e-04
	1.2808e+00						
E	4.9545e+01	6.9520e+02	5.0910e+04	-1.5589e+00	2.0983e-06	2.2657e-03	-3.3528e-04
	1.0731e+00						
F	1.6111e-03	6.8475e+02	1.4924e+04	-3.6410e-02	7.3193e-12	6.8070e-03	3.5181e+00
G	5.6571e-04	6.9955e+02	1.3487e+04	-7.6800e-02	1.6344e-10	4.7370e-03	2.4632e+00

ALADDIN evaluation function for erosion yield: EYIELD7A, EYIELD8B, EYIELD9A

ALADDIN hierarchical labelling:

A: SATM H{3} [+1] GRAPHITE T=HPG99 C [+0]
B: SATM H{3} [+1] GRAPHITE T=HPG99 CH{4} [+0]
C: SATM H{3} [+1] GRAPHITE T=HPG99 C{2}H{2} [+0]
D: SATM H{3} [+1] GRAPHITE T=HPG99 C{2}H{4} [+0]
E: SATM H{3} [+1] GRAPHITE T=HPG99 C{2}H{6} [+0]
F: SATM H{3} [+1] GRAPHITE T=HPG99 C{3}H{6} [+0]
G: SATM H{3} [+1] GRAPHITE T=HPG99 C{3}H{8} [+0]

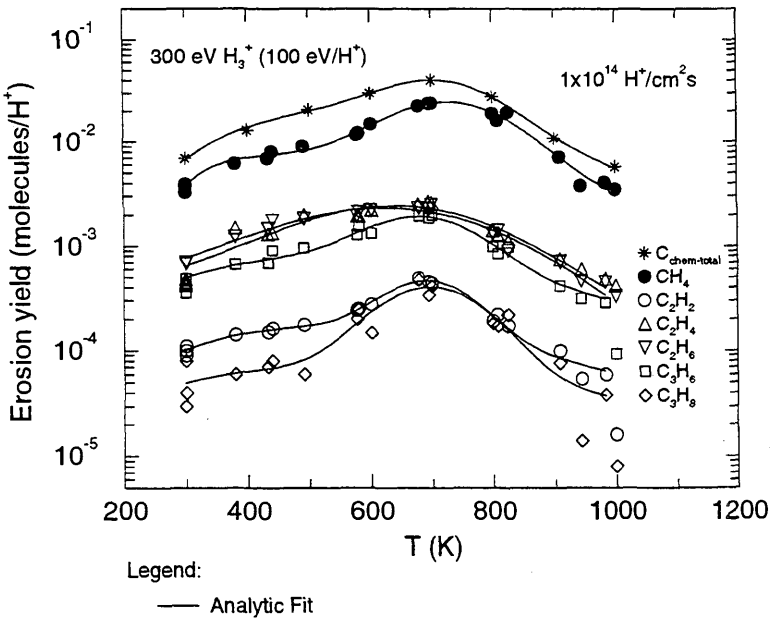

4.2.1.46 H_3^+ + pyrolytic graphite → C_xH_y, C

Source: B. V. Mech, A. A. Haasz and J. W. Davis, J. Nucl. Mater., in press (1998).

Accuracy: Yield: ±20%; T: ±25K.

Comments: (1) Steady-state hydrocarbon yield.
(2) Specimen: pyrolytic graphite (HPG99).
(3) Incident ions were mass-analyzed.
(4) Reaction products measured by QMS-RGA.
(5) Yield for total chemical erosion, $Y_{chem-total} = [CH_4 + 2(C_2H_2 + C_2H_4 + C_2H_6) + 3(C_3H_6 + C_3H_8)]/H^+$.

Analytic fitting function:

Erosion yield:

$$Y = A_1 \exp(-(F - A_2)^2/A_3)F^{A_4} + A_5 \exp(-A_6 F)F^{A_7}(1 + A_8 F^{A_9}) \quad [\text{molecules/H}^+]$$

where T is in Kelvin. The rms deviation of analytic fits for reactions A (∗), B (•), C (○), D (△), E (▽), F (□) and G (◇) are 8.8%, 15.4%, 32.8%, 22.9%, 13.6%, 16.8% and 24.3%, respectively. Data for curves A and C were fitted with EYIELD7A.

Fitting parameters A_1-A_9

A	3.0694e-02	7.1197e+02	1.7376e+04	3.0433e-02	7.5256e-20	1.3046e-02	7.4995e+00
B	1.7616e-02	7.2611e+02	2.2985e+04	9.6680e-02	4.3276e+05	1.0974e-04	-2.3221e+00
	-1.1659e+00	-2.7337e-02					
C	3.0168e-07	6.8075e+02	1.3076e+04	1.0873e+00	5.9086e-19	1.2542e-02	6.4949e+00
D	8.0889e+00	7.2673e+02	2.7160e+03	-1.2889e+00	1.0052e-06	1.5874e-02	1.6073e+00
	9.6442e-19	7.5261e+00					
E	6.2454e+00	7.2140e+02	1.4352e+03	-1.3235e+00	7.5929e-06	1.5634e-02	1.1692e+00
	1.9186e-18	7.5497e+00					
F	5.9376e+00	7.2542e+02	7.4175e+03	-1.3585e+00	3.2457e-11	1.9763e-02	3.8503e+00
	2.0673e-19	7.5227e+00					
G	3.8963e+00	7.4406e+02	2.3920e+03	-1.4051e+00	2.5994e-11	1.7485e-02	3.5251e+00
	5.4861e-17	6.5063e+00					

ALADDIN evaluation function for erosion yield: EYIELD7A, EYIELD9A

ALADDIN hierarchical labelling:

A: SATM H{3} [+1] GRAPHITE T=HPG99 C [+0]
B: SATM H{3} [+1] GRAPHITE T=HPG99 CH{4} [+0]
C: SATM H{3} [+1] GRAPHITE T=HPG99 C{2}H{2} [+0]
D: SATM H{3} [+1] GRAPHITE T=HPG99 C{2}H{4} [+0]
E: SATM H{3} [+1] GRAPHITE T=HPG99 C{2}H{6} [+0]
F: SATM H{3} [+1] GRAPHITE T=HPG99 C{3}H{6} [+0]
G: SATM H{3} [+1] GRAPHITE T=HPG99 C{3}H{8} [+0]

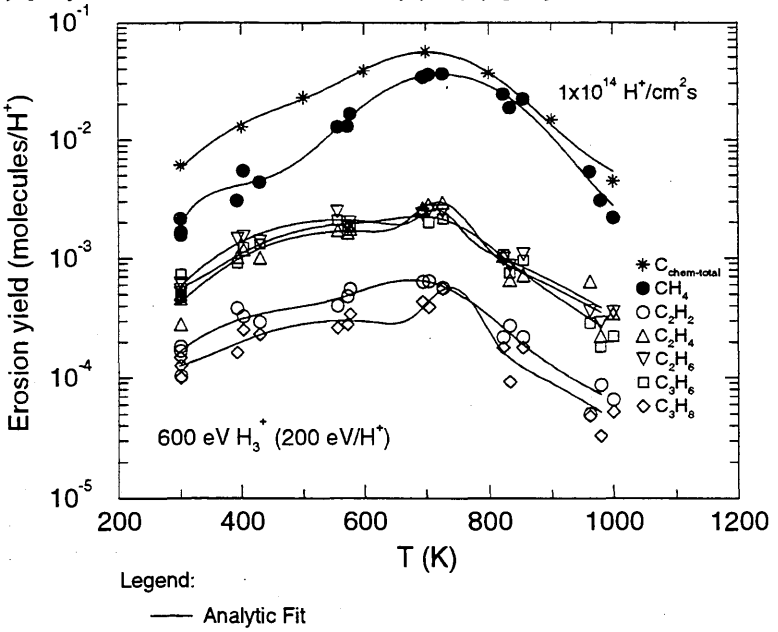

4.2.1.47 H_3^+ + PG-A graphite → CH_4

Source: R. Yamada, K. Nakamura and M. Saidoh, J. Nucl. Mater. **98**, 167 (1981).

Accuracy: Indeterminate.

Comments: (1) Steady-state hydrocarbon yield.
(2) Specimen: graphite (pyrolytic, PG-A basal plane (Nippon Carbon)).
(3) H^+ ions: mass analyzed accelerator.
(4) Methane measured via QMS.

Analytic fitting function:

Methane yield:

$$Y = 1.0 \times 10^{-4}[A_1 \exp(-(T - A_2)^2/A_3)T^{A_4} + A_5 \exp(-A_6 T)T^{A_7}] \quad [CH_4/H^+]$$

where T is in ^{0}C. The rms deviation of the analytic fits for reactions A (•) and B (×) are 2.3% and 2.8%, respectively.

Fitting parameters A_1-A_7

A	6.2799E+02	5.1422E+02	1.1298E+04	-1.0318E-02	5.7572E+02	-3.3186E-03
	-4.7539E-01					
B	3.2224E+00	5.1080E+02	1.8172E+04	8.3134E-01	4.0243E+02	-2.9941E-03
	-4.5489E-01					

ALADDIN evaluation function for methane yield: EYIELD7A

ALADDIN hierarchical labelling:

A, B: SATM H{3} [+1] GRAPHITE T=PGA O=BASAL-PL CH{4} [+0]

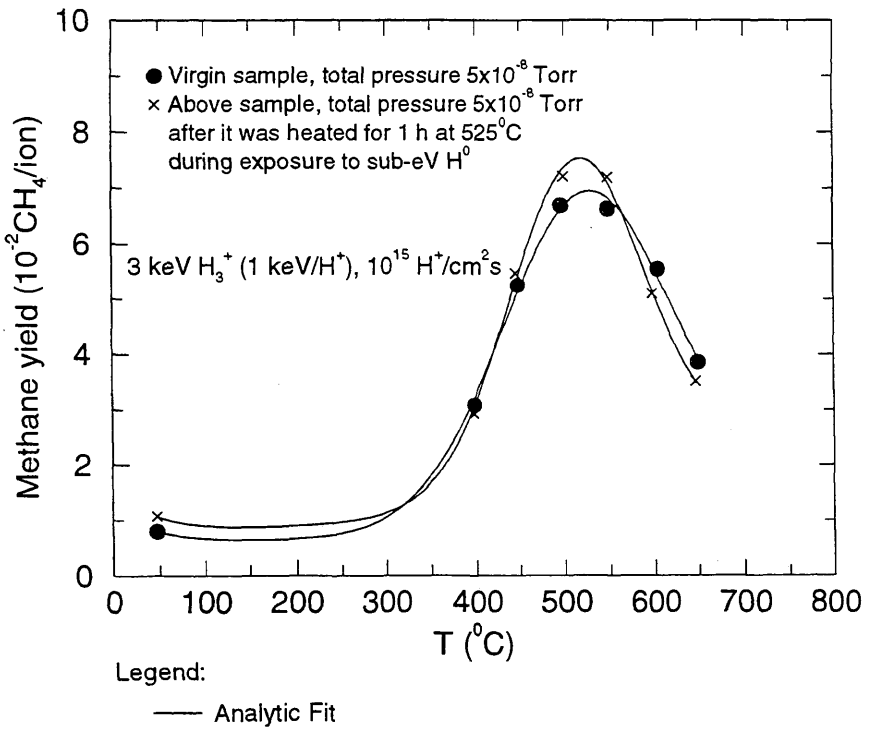

4.2.1.48 H_3^+ + a-C:H film → CH_4

Source: J. W. Davis and A. A. Haasz, J. Nucl. Mater. **149**, 349 (1987).

Accuracy: Yield: ±15%; T: ±25K.

Comments: (1) Steady-state methane yield.
(2) Specimen: graphite (pyrolytic), a-C:H film produced in a plasma discharge in TEXTOR at KFA-Jülich.
(3) H^+ ions: mass analyzed accelerator.
(4) Methane measured via QMS-RGA.

Analytic fitting function:

Methane yield:

$$Y = 1.0 \times 10^{-2}[A_1 \exp(-(T - A_2)^2/A_3)T^{A_4} + A_5 \exp(-A_6 T)T^{A_7}] \quad [CH_4/H^+]$$

where T is in Kelvin. The rms deviation of the analytic fits for reactions A (•), B (□), C (△) and D (○) are 1.2%, 15.9%, 10.4% and 6.6%, respectively. Data for curves C and D were fitted with EYIELD8A.

Fitting parameters A_1-A_8

A	2.6776E+01	1.9116E+02	1.5277E+05	2.6928E-01	-6.4975E+01	1.1535E-02
	1.0757E+00					
B	1.5646E+01	6.9011E+02	1.1185E+04	-4.6614E-02	3.3514E-01	-1.0510E-03
	2.4374E-02					
C	6.0868E-03	7.2359E+02	2.2134E-04	1.1687E+04	4.0402E-01	2.2732E-13
	9.3502E-03	4.5762E+00				
D	4.4706E-03	7.2781E+02	-4.4493E-04	3.1502E+04	4.0806E-01	1.0353E-16
	1.6119E-02	6.3589E+00				

ALADDIN evaluation function for methane yield: EYIELD7A, EYIELD8A

ALADDIN hierarchical labelling:

A-D: SATM H{3} [+1] GRAPHITE T=A-CH-FILM CH{4} [+0]

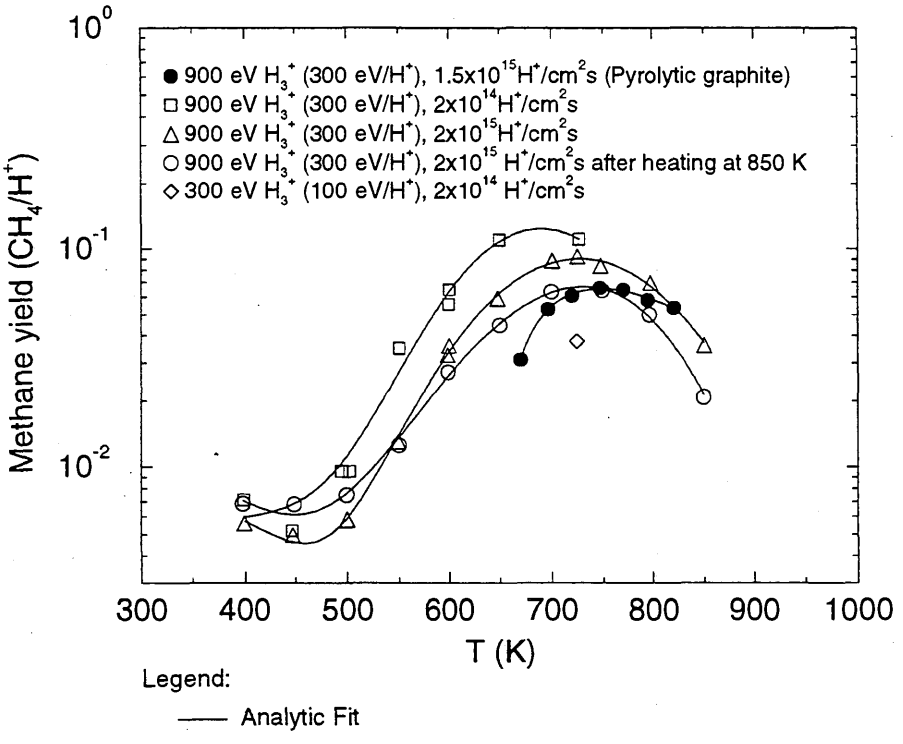

4.2.1.49 H_3^+ + pyrolytic graphite → C_xH_y, C

Source: J. W. Davis and A. A. Haasz, J. Nucl. Mater. **175**, 84 (1990).

Accuracy: Yield: ±15%; T: ±25K.

Comments: (1) Hydrocarbon yield: steady-state.
(2) Specimen: graphite (HPG99).
(3) H^+ ions: mass-analyzed accelerator.
(4) Hydrocarbon products measured via QMS-RGA.
(5) Yield for total chemical erosion, $Y_{chem-total} = [CH_4 + 2(C_2H_2 + C_2H_4 + C_2H_6) + 3(C_3H_6 + C_3H_8)]/H^+$.

Analytic fitting function:

Erosion yield:

$$Y = 1.0 \times 10^{-2}[A_1 \exp(-(T - A_2)^2/A_3)T^{A_4} + A_5 \exp(-A_6T)T^{A_7}] \quad [\text{molecules/H}^+]$$

where T is in Kelvin. The rms deviation of the analytic fits for reactions A (∗), B (•), C (△), D (□), E (◇), F (▽) and G (+) are 21.6%, 28.3%, 15.2%, 34.5%, 15.8%, 29.1% and 10.8%, respectively.

Fitting parameters A_1-A_7

A	4.8790E-01	8.1606E+02	2.0207E+04	4.2003E-01	1.7001E-01	-2.7361E-03	-3.5728E-02
B	1.3922E-01	8.1237E+02	1.6316E+04	5.8930E-01	1.9130E-03	-3.0071E-03	5.2579E-01
C	1.2042E-02	7.6557E+02	2.0756E+04	3.9415E-01	2.7731E-02	-2.0806E-03	-2.6473E-04
D	2.4385E-02	8.5252E+02	8.8562E+04	2.5656E-01	2.9600E-03	-1.1969E-03	-7.5751E-06
E	1.8916E-03	9.0568E+02	3.7987E+04	4.9147E-01	3.8851E-02	-2.0088E-04	3.5626E-05
F	1.7089E-02	7.8378E+02	1.6663E+04	3.0523E-01	2.2962E-03	-3.1396E-03	1.0510E-02
G	2.1237E-02	3.3754E+03	-7.5676E+05	-3.3002E+01	7.8318E+00	-2.0520E-03	-1.1981E+00

ALADDIN evaluation function for erosion yield: EYIELD7A

ALADDIN hierarchical labelling:

A: SATM H{3} [+1] GRAPHITE T=HPG99 C [+0]
B: SATM H{3} [+1] GRAPHITE T=HPG99 CH{4} [+0]
C: SATM H{3} [+1] GRAPHITE T=HPG99 C{2}H{4} [+0]
D: SATM H{3} [+1] GRAPHITE T=HPG99 C{2}H{2} [+0]
E: SATM H{3} [+1] GRAPHITE T=HPG99 C{3}H{6} [+0]
F: SATM H{3} [+1] GRAPHITE T=HPG99 C{2}H{6} [+0]
G: SATM H{3} [+1] GRAPHITE T=HPG99 C{3}H{8} [+0]

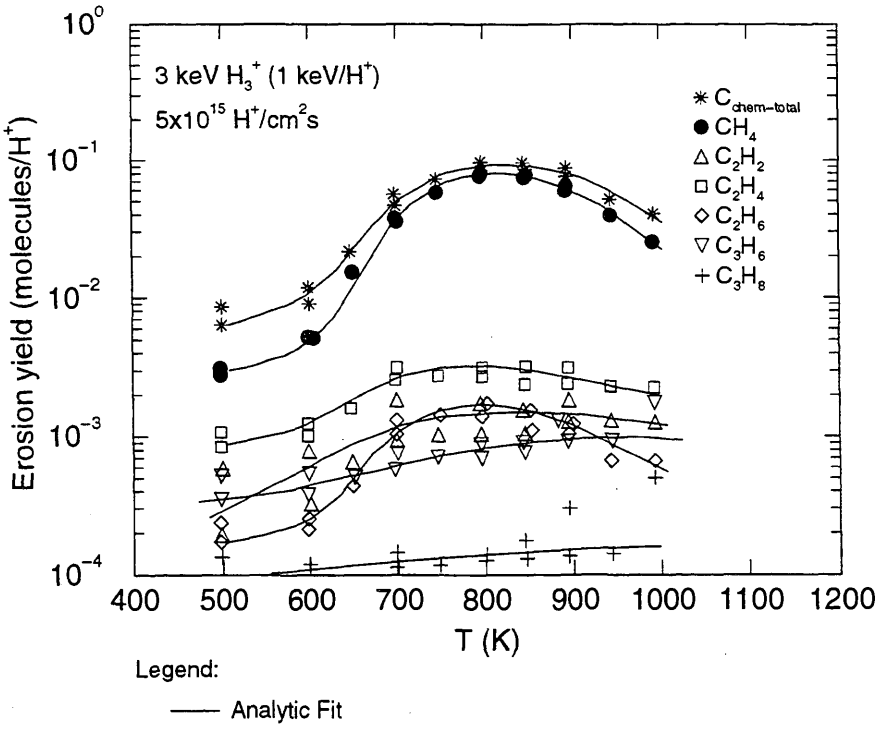

4.2.1.50 H_3^+ + pyrolytic graphite → C_xH_y, C

Source: J. W. Davis and A. A. Haasz, J. Nucl. Mater. **175**, 84 (1990).

Accuracy: Yield: ±15%; T: ±25K.

Comments: (1) Hydrocarbon yield: steady-state.
(2) Specimen: graphite (pyrolytic, HPG99 - Union Carbide).
(3) H^+ ions: mass-analyzed accelerator.
(4) Hydrocarbon products measured via QMS-RGA.
(5) Yield for total chemical erosion, $Y_{chem-total} = [CH_4 + 2(C_2H_2 + C_2H_4 + C_2H_6) + 3(C_3H_6 + C_3H_8)]/H^+$.

Analytic fitting function:

Erosion yield:

$$Y = A_1 \exp[-(\frac{T - A_2}{A_3 T + 1})^2 / A_4] T^{A_5} + A_6 \exp(-A_7 T) T^{A_8} \quad [\text{molecules}/H^+]$$

where T is in Kelvin. The rms deviation of the analytic fits for reactions A (∗), B (•), C (□) and D (△) are 8.9%, 5.0%, 19.5% and 12.8%, respectively.

Fitting parameters A_1-A_8

A	1.8057E-01	8.1363E+02	-1.5856E-02	1.8123E+02	-9.0467E-02	4.1191E-13
	8.4059E-03	4.4892E+00				
B	4.4607E-06	7.9715E+02	2.1732E-03	2.6475E+03	1.4777E+00	6.0649E+00
	1.5264E-04	-1.2219E+00				
C	3.6456E-02	7.7450E+02	0.0	2.2382E+04	4.6430E-01	7.0247E-02
	-2.4604E-03	-2.9581E-03				
D	3.9173E-03	9.0227E+02	0.0	1.4678E+05	6.5123E-01	5.8620E+00
	1.0116E-02	1.2964E-01				

ALADDIN evaluation function for erosion yield: EYIELD8A

ALADDIN hierarchical labelling:

A: SATM H{3} [+1] GRAPHITE T=HPG99 C [+0]
B: SATM H{3} [+1] GRAPHITE T=HPG99 CH{4} [+0]
C: SATM H{3} [+1] GRAPHITE T=HPG99 C{2}H{2} [+0] C{2}H{4} [+0] C{2}H{6} [+0]
D: SATM H{3} [+1] GRAPHITE T=HPG99 C{3}H{6} [+0] C{3}H{8} [+0]

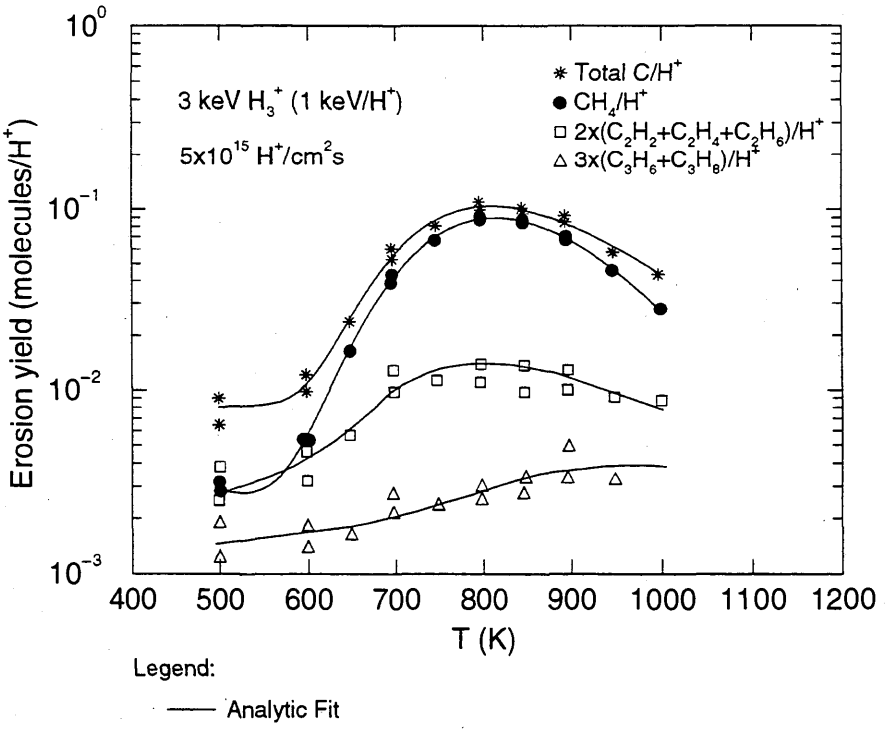

4.2.1.51 H_3^+ + pyrolytic graphite → C_xH_y, C

Source: J. W. Davis and A. A. Haasz, J. Nucl. Mater. **175**, 84 (1990).

Accuracy: Absolute yield: ±15%; T: ±25K.

Comments: (1) Hydrocarbon yield: steady-state.
(2) Specimen: graphite (pyrolytic, HPG99 - Union Carbide).
(3) H^+ ions: mass-analyzed accelerator.
(4) Hydrocarbon products measured via QMS-RGA.
(5) Yield for total chemical erosion, $Y_{chem-total} = [CH_4 + 2(C_2H_2 + C_2H_4 + C_2H_6) + 3(C_3H_6 + C_3H_8)]/H^+$.

Analytic fitting function:

Erosion yield:

$$Y = 1.0 \times 10^{-2}[A_1 \exp(-(T - A_2)^2/A_3)T^{A_4} + A_5 \exp(-A_6T)T^{A_7}] \quad [\text{molecules/H}^+]$$

where T is in Kelvin. The rms deviation of the analytic fits for reactions A (∗), B (•), C (⋄), D (□), E (▽), F (△) and G (+) are 7.9%, 7.1%, 17.2%, 13.0%, 7.9%, 15.4% and 38.0%, respectively.

Fitting parameters A_1-A_7

A	7.4890E-01	7.6681E+02	3.4540E+04	4.0802E-01	1.1316E+00	7.5213E-03	5.4524E-01
B	2.3981E-01	7.7762E+02	3.1234E+04	5.2844E-01	2.5749E+01	4.1399E-02	2.6496E+00
C	1.1004E-01	8.0448E+02	1.3441E+05	1.7538E-01	-1.8094E-01	-1.4290E-03	-1.8500E-01
D	1.6818E-01	7.1666E+02	3.7852E+04	2.2689E-01	-1.0000E-01	1.0000E-01	1.0000E-01
E	9.1722E-02	7.3351E+02	1.2210E+04	2.8993E-01	1.3029E-01	8.6552E-04	-1.0647E-01
F	3.8718E-01	7.5543E+02	1.9146E+04	-1.6360E-01	2.3253E-01	1.3940E-03	-1.5211E-02
G	2.4345E-02	7.2556E+02	7.4483E+03	6.2532E-03	1.2317E-02	-1.1775E-03	-5.4570E-04

ALADDIN evaluation function for reaction yield: EYIELD7A

ALADDIN hierarchical labelling:

A: SATM H{3} [+1] GRAPHITE T=HPG99 C [+0]
B: SATM H{3} [+1] GRAPHITE T=HPG99 CH{4} [+0]
C: SATM H{3} [+1] GRAPHITE T=HPG99 C{2}H{2} [+0]
D: SATM H{3} [+1] GRAPHITE T=HPG99 C{2}H{4} [+0]
E: SATM H{3} [+1] GRAPHITE T=HPG99 C{2}H{6} [+0]
F: SATM H{3} [+1] GRAPHITE T=HPG99 C{3}H{6} [+0]
G: SATM H{3} [+1] GRAPHITE T=HPG99 C{3}H{8} [+0]

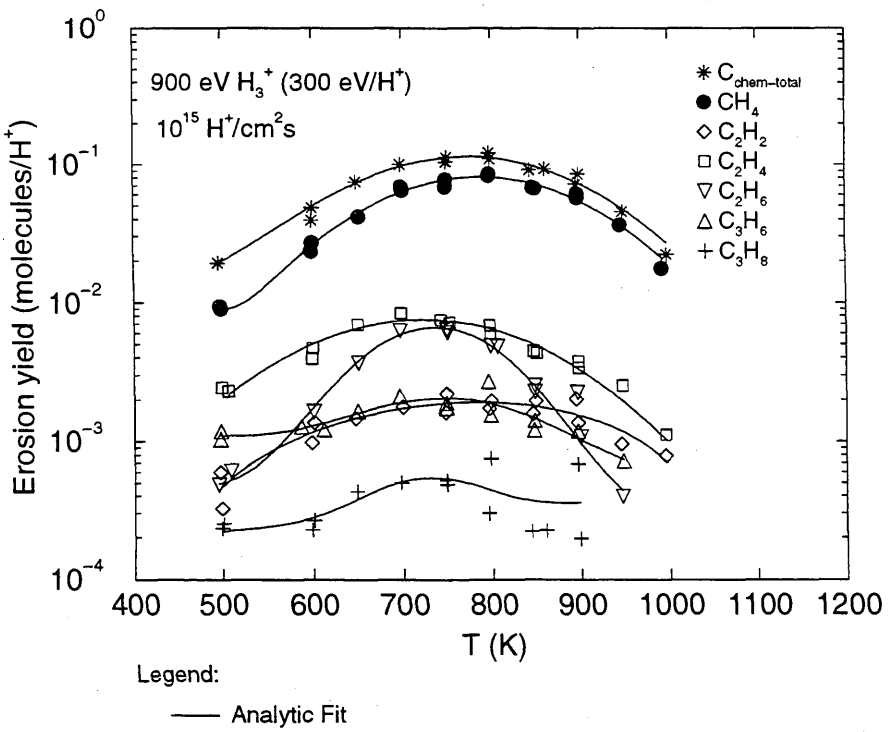

4.2.1.52 H_3^+ + pyrolytic graphite → C_xH_y, C

Source: J. W. Davis and A. A. Haasz, J. Nucl. Mater. **175**, 84 (1990).

Accuracy: Yield: ±15%; T: ±25K.

Comments: (1) Hydrocarbon yield: steady-state.
(2) Specimen: graphite (pyrolytic, HPG99 - Union Carbide).
(3) H^+ ions: mass-analyzed accelerator.
(4) Hydrocarbon products measured via QMS-RGA.
(5) Yield for total chemical erosion, $Y_{chem-total} = [CH_4 + 2(C_2H_2 + C_2H_4 + C_2H_6) + 3(C_3H_6 + C_3H_8)]/H^+$.

Analytic fitting function:

Erosion yield:

$$Y = 1.0 \times 10^{-2}[A_1 \exp(-(T - A_2)^2/A_3)T^{A_4} + A_5 \exp(-A_6T)T^{A_7}] \quad [\text{molecules/H}^+]$$

where T is in Kelvin. The rms deviation of the analytic fits for reactions A (∗), B (•), C (□) and D (△) are 7.5%, 5.4%, 17.9% and 12.4%, respectively.

Fitting parameters A_1-A_7

A	3.1899E-01	7.6302E+02	3.2661E+04	5.4194E-01	3.8172E+00	3.9774E-02
	2.9643E+00					
B	2.0780E-01	7.7714E+02	3.0550E+04	5.5206E-01	1.1173E+01	3.7384E-02
	2.4550E+00					
C	2.7304E-01	7.3222E+02	2.1516E+04	3.5510E-01	6.0617E-01	7.6889E-04
	-1.4691E-03					
D	1.2074E-02	7.2930E+02	2.0899E+04	5.5273E-01	6.1656E-01	1.9695E-03
	7.4118E-02					

ALADDIN evaluation function for erosion yield: EYIELD7A

ALADDIN hierarchical labelling:

A: SATM H{3} [+1] GRAPHITE T=HPG99 C [+0]
B: SATM H{3} [+1] GRAPHITE T=HPG99 CH{4} [+0]
C: SATM H{3} [+1] GRAPHITE T=HPG99 C{2}H{2} [+0] C{2}H{4} [+0] C{2}H{6} [+0]
D: SATM H{3} [+1] GRAPHITE T=HPG99 C{3}H{6} [+0] C{3}H{8} [+0]

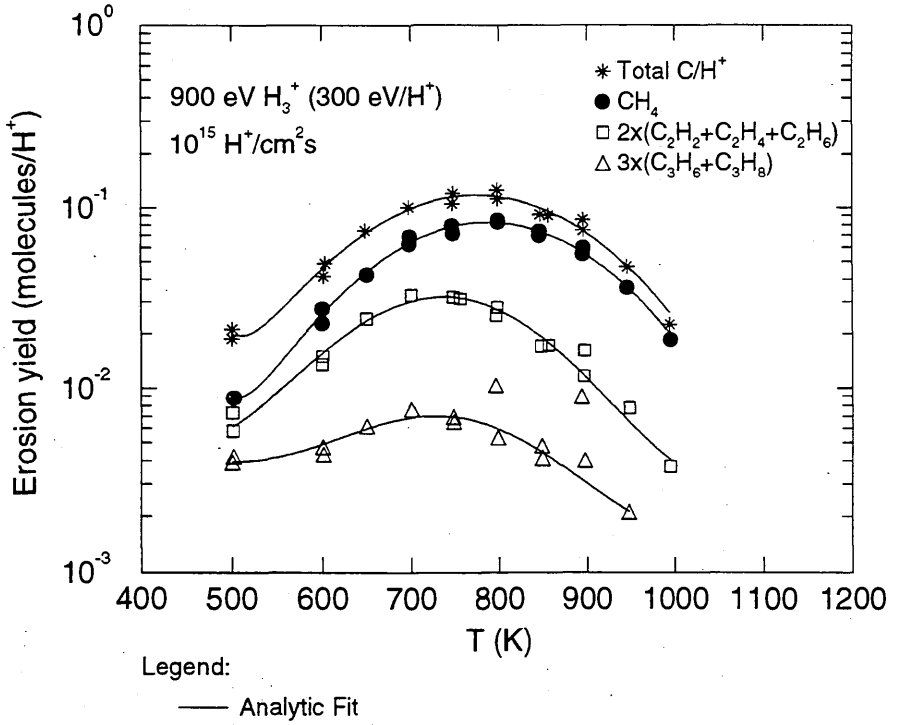

4.2.1.53 H^0, H^+, H_3^+ + pyrolytic graphite → C_xH_y, C

Source: A. A. Haasz and J. W. Davis, J. Nucl. Mater. **175**, 84 (1990).

Accuracy: Yield: ±15%; E: ±5eV.

Comments: (1) Hydrocarbon yield: steady-state.
(2) Specimen: graphite (pyrolytic, HPG99 - Union Carbide).
(3) H^+, H_3^+ ions: mass-analyzed accelerator; H^0 (sub-eV) is produced via dissociation of H_2 on a hot W ribbon.
(4) Hydrocarbon products measured via QMS-RGA.
(5) Yield for total chemical erosion, $Y_{chem-total} = [CH_4 + 2(C_2H_2 + C_2H_4 + C_2H_6) + 3(C_3H_6 + C_3H_8)]/H^+$.

Analytic fitting function:

Erosion yield:

$$Y = 1.0 \times 10^{-2}[A_1 \exp(-(E - A_2)^2/A_3)E^{A_4} + A_5 \exp(-A_6E)E^{A_7}] \quad [\text{molecules}/H^+]$$

where E is in eV. The rms deviation of analytic fits for reactions A (∗, ×), B (•, ○), C (■, □) and D (▲, △) are 0.8%, 1.3%, 1.3% and 0.9%, respectively.

Fitting parameters A_1-A_7

A	6.1713E-01	-1.2446E+04	6.5101E+08	-2.1985E-01	-2.7641E-01	7.5574E-03
	-1.1774E-02					
B	3.2125E-01	-1.5755E+04	2.7518E+08	-4.7335E-02	-8.1655E-02	8.3596E-03
	1.4140E-01					
C	1.7263E+02	5.5166E+03	1.8001E+07	-1.2132E+00	-1.5189E+01	5.1200E-03
	-9.5631E-01					
D	2.9485E+01	1.1115E+04	7.7867E+07	-1.0885E+00	-4.9203E+00	3.6380E-03
	-9.9796E-01					

ALADDIN evaluation function for erosion yield: EYIELD7A

ALADDIN hierarchical labelling:

A: SATM H [+1] GRAPHITE T=HPG99 C [+0]
B: SATM H [+1] GRAPHITE T=HPG99 CH{4} [+0]
C: SATM H [+1] GRAPHITE T=HPG99 C{2}H{X} [+0]
D: SATM H [+1] GRAPHITE T=HPG99 C{3}H{X} [+0]

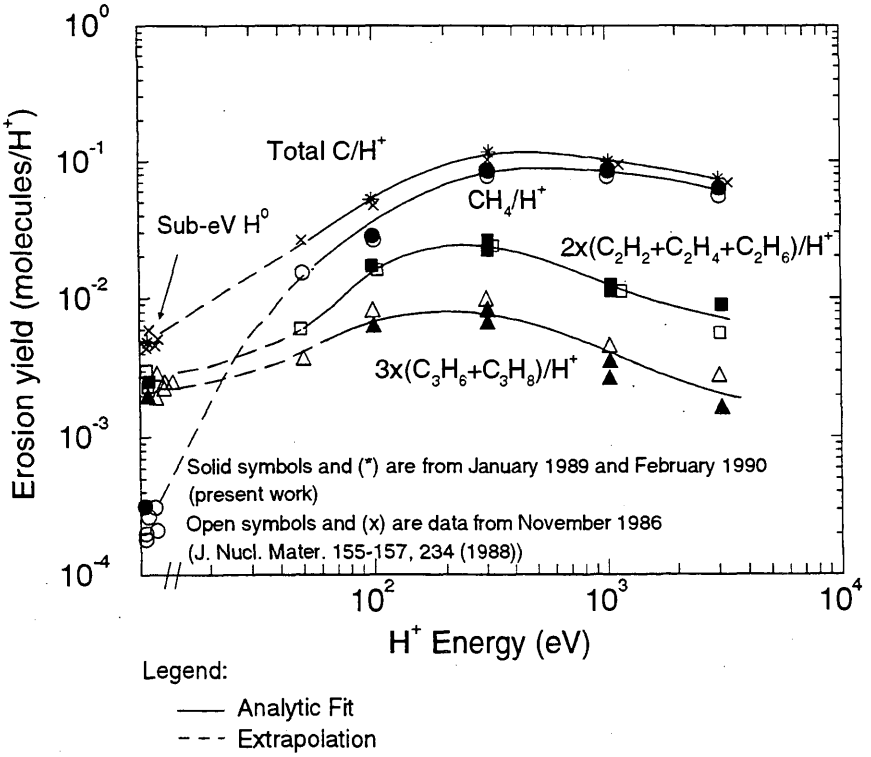

4.2.1.54 H_3^+ + AEROLOR carbon/carbon composite (end cut) → C_xH_y, C

Source: J. W. Davis and A. A. Haasz, J. Nucl. Mater. **175**, 84 (1990).

Accuracy: Yield: ±15%; T: ±25K.

Comments: (1) Hydrocarbon yield: steady-state.
(2) Specimen: carbon/carbon composite (AEROLOR A05G: random planar distribution of fibers), end cut.
(3) H^+ ions: mass-analyzed accelerator.
(4) Hydrocarbon products measured via QMS-RGA.
(5) Yield for total chemical erosion, $Y_{chem-total} = [CH_4 + 2(C_2H_2 + C_2H_4 + C_2H_6) + 3(C_3H_6 + C_3H_8)]/H^+$.

Analytic fitting function:

Erosion yield:

$$Y = 1.0 \times 10^{-2}[A_1 \exp(-(T - A_2)^2/A_3)T^{A_4} + A_5 \exp(-A_6T)T^{A_7}] \quad [\text{molecules/H}^+]$$

where T is in Kelvin. The rms deviation of the analytic fits for reactions A (∗), B (•), C (△), D (□), E (◇), F (▽) and G (+) are 10.2%, 6.2%, 9.8%, 13.6%, 15.5%, 26.5% and 14.1%, respectively.

Fitting parameters A_1-A_7

A	1.4403E+00	7.6167E+02	2.7884E+04	3.0223E-01	5.1485E-02	-3.9654E-03	7.3183E-03
B	2.6677E+00	7.8818E+02	2.9177E+04	1.5309E-01	2.5092E-02	-4.1540E-03	-1.0098E-02
C	1.5054E-01	7.4216E+02	2.5035E+04	-8.9457E-03	3.3347E-02	-1.0660E-03	-9.8075E-03
D	5.1534E-01	7.2313E+02	2.1313E+04	5.4792E-02	2.5531E-02	-2.0598E-03	3.0515E-02
E	6.2996E-02	7.4952E+02	1.1776E+04	3.6226E-01	8.7475E-03	-1.2945E-03	1.0915E-01
F	5.1207E-02	6.8760E+02	7.6637E+04	2.5824E-01	-5.4977E-01	5.0811E-03	1.7730E-01
G	4.2750E-03	7.0958E+02	1.1772E+04	3.8622E-01	6.3989E-04	-4.0697E-03	-2.9620E-02

ALADDIN evaluation function for erosion yield: EYIELD7A

ALADDIN hierarchical labelling:

A: SATM H{3} [+1] CC-COM-END T=AEROLOR C [+0]
B: SATM H{3} [+1] CC-COM-END T=AEROLOR CH{4} [+0]
C: SATM H{3} [+1] CC-COM-END T=AEROLOR C{2}H{2} [+0]
D: SATM H{3} [+1] CC-COM-END T=AEROLOR C{2}H{4} [+0]
E: SATM H{3} [+1] CC-COM-END T=AEROLOR C{2}H{6} [+0]
F: SATM H{3} [+1] CC-COM-END T=AEROLOR C{3}H{6} [+0]
G: SATM H{3} [+1] CC-COM-END T=AEROLOR C{3}H{8} [+0]

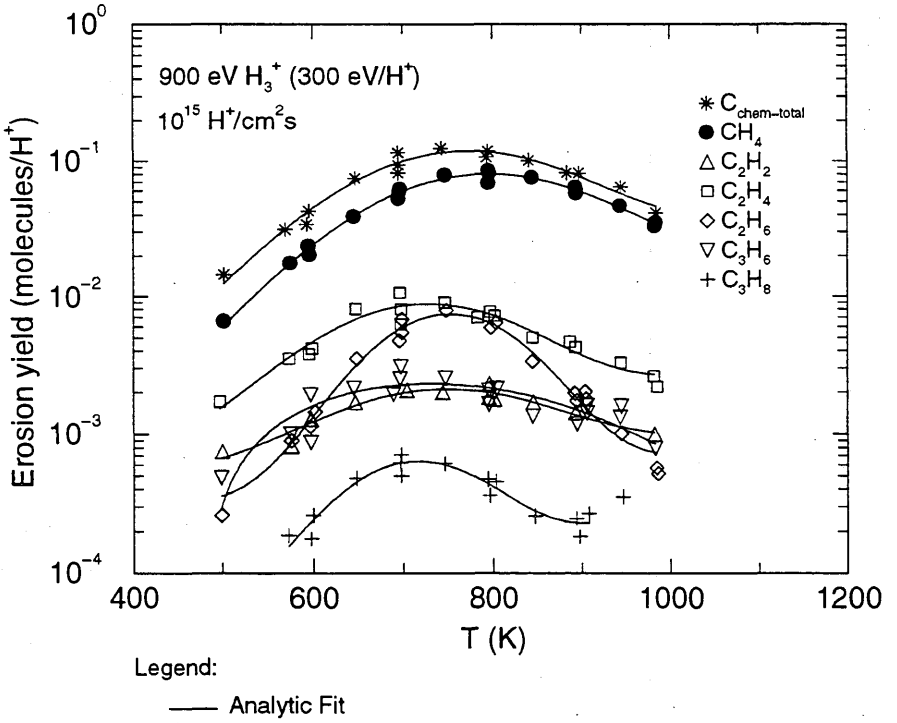

4.2.1.55 H_3^+ + AEROLOR carbon/carbon composite (top cut) → C_xH_y, C

Source: J. W. Davis and A. A. Haasz, J. Nucl. Mater. **175**, 84 (1990).

Accuracy: Yield: ±15%; T: ±25K.

Comments: (1) Hydrocarbon yield: steady-state.
(2) Specimen: carbon/carbon composite (AEROLOR A05G: random planar distribution of fibers), top cut.
(3) H^+ ions: mass-analyzed accelerator.
(4) Hydrocarbon products measured via QMS-RGA.
(5) Yield for total chemical erosion, $Y_{chem-total} = [CH_4 + 2(C_2H_2 + C_2H_4 + C_2H_6) + 3(C_3H_6 + C_3H_8)]/H^+$.

Analytic fitting function:

Erosion yield:

$$Y = 1.0 \times 10^{-2}[A_1 \exp(-(T - A_2)^2/A_3)T^{A_4} + A_5 \exp(-A_6T)T^{A_7}] \quad [\text{molecules}/H^+]$$

where T is in Kelvin. The rms deviation of the analytic fits for reactions A (∗), B (•), C (◇), D (□), E (▽), F (△) and G (+) are 8.7%, 7.8%, 13.6%, 11.3%, 11.1%, 14.0% and 26.2%, respectively.

Fitting parameters A_1-A_7

A	1.0248E-01	7.6463E+02	2.5832E+04	6.9200E-01	1.9497E-01	-1.6354E-03	8.7934E-02
B	6.1737E-02	7.8262E+02	2.4395E+04	6.9891E-01	5.3406E-02	-1.5313E-03	2.5592E-01
C	1.8942E-03	7.3325E+02	3.1155E+04	6.4411E-01	5.7250E-05	-3.4748E-03	5.2822E-01
D	1.7404E-02	7.2619E+02	2.0958E+04	5.6012E-01	8.8652E-02	-2.4275E-04	5.4076E-02
E	6.4319E-03	7.4941E+02	1.1107E+04	6.8490E-01	7.6599E-04	-6.5010E-04	5.5081E-01
F	1.4263E-03	7.2295E+02	1.2132E+04	6.8260E-01	5.5908E-02	-7.2588E-04	1.1947E-03
G	3.3068E-04	7.3106E+02	9.9591E+03	7.2539E-01	4.5102E-04	1.2076E-03	6.6915E-01

ALADDIN evaluation function for erosion yield: EYIELD7A

ALADDIN hierarchical labelling:

A: SATM H{3} [+1] CC-COM-TOP T=AEROLOR C [+0]
B: SATM H{3} [+1] CC-COM-TOP T=AEROLOR CH{4} [+0]
C: SATM H{3} [+1] CC-COM-TOP T=AEROLOR C{2}H{2} [+0]
D: SATM H{3} [+1] CC-COM-TOP T=AEROLOR C{2}H{4} [+0]
E: SATM H{3} [+1] CC-COM-TOP T=AEROLOR C{2}H{6} [+0]
F: SATM H{3} [+1] CC-COM-TOP T=AEROLOR C{3}H{6} [+0]
G: SATM H{3} [+1] CC-COM-TOP T=AEROLOR C{3}H{8} [+0]

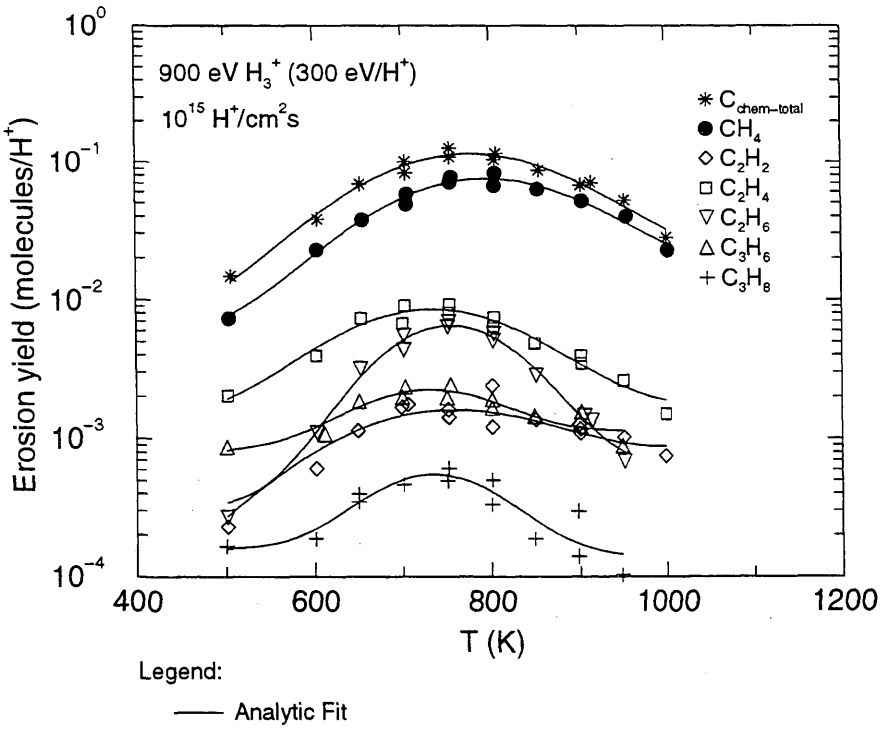

4.2.1.56 H_3^+ + AEROLOR carbon/carbon composite (end cut) → C_xH_y, C

Source: J. W. Davis and A. A. Haasz, J. Nucl. Mater. **175**, 84 (1990).

Accuracy: Absolute yield: ±15%; T: ±25K.

Comments: (1) Hydrocarbon yield: steady-state.
(2) Specimen: carbon/carbon composite (AEROLOR A05G: random planar distribution of fibers), end cut.
(3) H^+ ions: mass-analyzed accelerator.
(4) Hydrocarbon products measured via QMS-RGA.
(5) Yield for total chemical erosion, $Y_{chem-total} = [CH_4 + 2(C_2H_2 + C_2H_4 + C_2H_6) + 3(C_3H_6 + C_3H_8)]/H^+$.

Analytic fitting function:

Erosion yield:

$$Y = 1.0 \times 10^{-2}[A_1 \exp(-(T - A_2)^2/A_3)T^{A_4} + A_5 \exp(-A_6T)T^{A_7}] \quad [\text{molecules/H}^+]$$

where T is in Kelvin. The rms deviation of the analytic fits for reactions A (∗), B (•), C (△), D (□), E (◇), F (▽) and G (+) are 11.1%, 24.3%, 9.0%, 8.7%, 21.1%, 12.2% and 8.1%, respectively.

Fitting parameters A_1-A_7

A	3.1377E-01	8.3916E+02	2.7451E+04	5.1212E-01	5.1159E+00	5.6717E-03	1.2326E-01
B	3.1567E-01	8.4200E+02	2.4368E+04	4.7730E-01	3.2480E+00	5.9935E-03	4.0452E-02
C	7.5081E-02	8.0364E+02	5.1871E+04	9.7105E-02	1.2306E-02	-1.9676E-03	-2.4192E-04
D	1.0083E-01	7.5698E+02	1.8298E+04	1.3406E-01	3.3246E-02	-1.9492E-03	1.8759E-04
E	8.8334E-02	7.9541E+02	1.5261E+04	1.2322E-01	2.4813E-03	-3.0959E-03	2.3938E-02
F	2.0641E-02	7.4931E+02	8.3173E+03	3.8745E-02	1.9152E-02	-1.6589E-03	4.5559E-03
G	3.3166E-03	7.3730E+02	2.5549E+03	3.1142E-02	6.7567E-03	-8.8048E-04	-7.8430E-04

ALADDIN evaluation function for erosion yield: EYIELD7A

ALADDIN hierarchical labelling:

A: SATM H{3} [+1] CC-COM-END T=AEROLOR C [+0]
B: SATM H{3} [+1] CC-COM-END T=AEROLOR CH{4} [+0]
C: SATM H{3} [+1] CC-COM-END T=AEROLOR C{2}H{2} [+0]
D: SATM H{3} [+1] CC-COM-END T=AEROLOR C{2}H{4} [+0]
E: SATM H{3} [+1] CC-COM-END T=AEROLOR C{2}H{6} [+0]
F: SATM H{3} [+1] CC-COM-END T=AEROLOR C{3}H{6} [+0]
G: SATM H{3} [+1] CC-COM-END T=AEROLOR C{3}H{8} [+0]

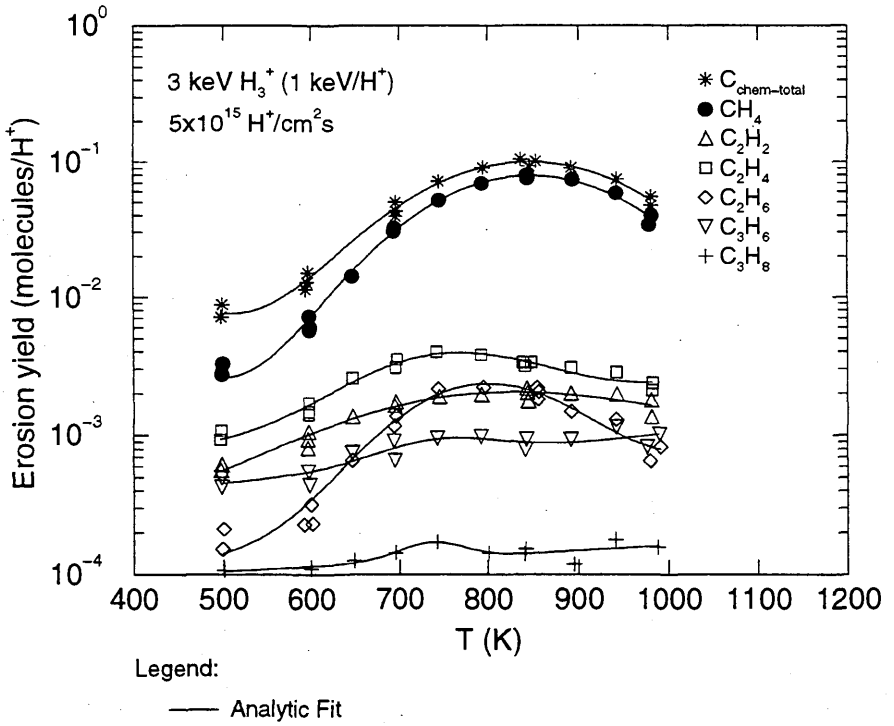

4.2.1.57 H_3^+ + AEROLOR carbon/carbon composite (top cut) → C_xH_y, C

Source: J. W. Davis and A. A. Haasz, J. Nucl. Mater. **175**, 84 (1990).

Accuracy: Yield: ±15%; T: ±25K.

Comments: (1) Hydrocarbon yield: steady-state.
(2) Specimen: carbon/carbon composite (AEROLOR A05G: random planar distribution of fibers), top cut.
(3) H^+ ions: mass-analyzed accelerator.
(4) Hydrocarbon products measured via QMS-RGA.
(5) Yield for total chemical erosion, $Y_{chem-total} = [CH_4 + 2(C_2H_2 + C_2H_4 + C_2H_6) + 3(C_3H_6 + C_3H_8)]/H^+$.

Analytic fitting function:

Erosion yield:

$$Y = 1.0 \times 10^{-2}[A_1 \exp(-(T - A_2)^2/A_3)T^{A_4} + A_5 \exp(-A_6T)T^{A_7}] \quad [\text{molecules/H}^+]$$

where T is in Kelvin. The rms deviation of the analytic fits for reactions A (∗), B (•), C (△), D (□), E (◇), F (▽) and G (+) are 8.9%, 18.0%, 12.8%, 7.3%, 45.0%, 13.4% and 10.1%, respectively.

Fitting parameters A_1-A_7

A	3.4819E-01	8.4987E+02	2.7164E+04	5.0120E-01	9.0370E+00	9.1982E-03	3.0823E-01
B	1.4470E-01	8.4495E+02	2.0743E+04	5.9369E-01	1.2827E+00	-3.0711E-03	-5.1697E-01
C	4.5525E-03	8.6273E+02	7.2779E+04	5.4298E-01	3.8294E-01	6.9656E-03	8.8517E-04
D	1.3771E-02	7.7750E+02	2.0225E+04	4.3019E-01	2.6344E-02	-2.1704E-03	-1.0878E-03
E	1.0453E-01	8.0110E+02	1.5629E+04	9.2265E-02	1.9006E-03	-2.5393E-03	9.9906E-02
F	-5.3015E-03	1.0864E+03	3.4436E+04	5.0254E-01	5.2683E-03	-3.7607E-03	-1.1361E-04
G	2.6681E-03	7.2130E+02	6.5349E+04	2.0770E-02	3.2431E-03	-1.5392E-03	-6.3356E-07

ALADDIN evaluation function for erosion yield: EYIELD7A

ALADDIN hierarchical labelling:

A: SATM H{3} [+1] CC-COM-TOP T=AEROLOR C [+0]
B: SATM H{3} [+1] CC-COM-TOP T=AEROLOR CH{4} [+0]
C: SATM H{3} [+1] CC-COM-TOP T=AEROLOR C{2}H{2} [+0]
D: SATM H{3} [+1] CC-COM-TOP T=AEROLOR C{2}H{4} [+0]
E: SATM H{3} [+1] CC-COM-TOP T=AEROLOR C{2}H{6} [+0]
F: SATM H{3} [+1] CC-COM-TOP T=AEROLOR C{3}H{6} [+0]
G: SATM H{3} [+1] CC-COM-TOP T=AEROLOR C{3}H{8} [+0]

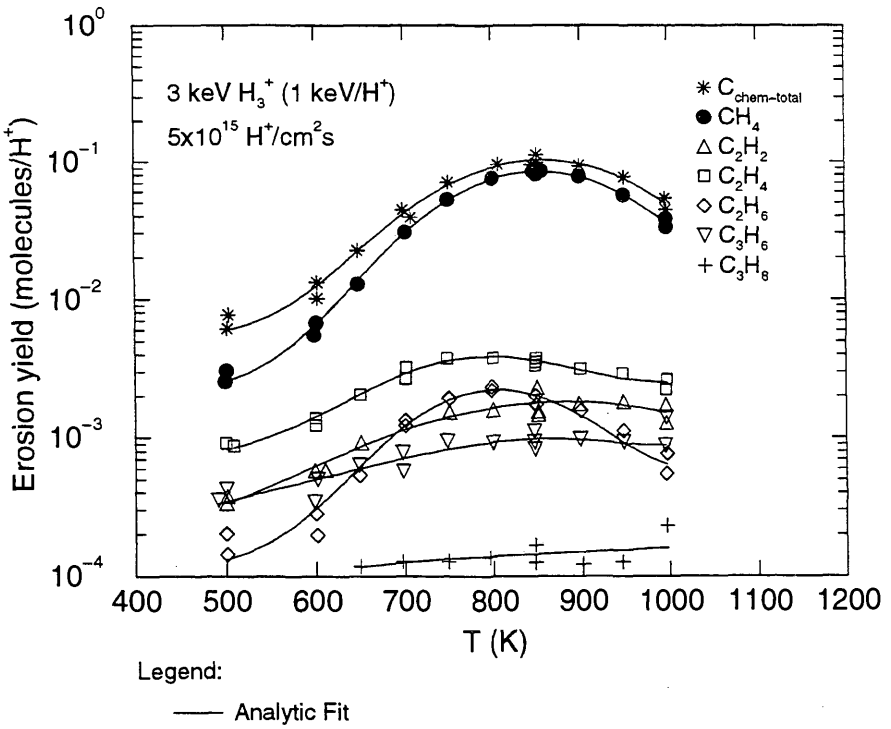

4.2.1.58 H_3^+ + ALCAN carbon/carbon composite → C_xH_y, C

Source: J. W. Davis and A. A. Haasz, J. Nucl. Mater. **195**, 166 (1992).

Accuracy: Yield: Total ±20%; CH_4 ±15%, C_xH_y ±30%; T: ±25K.

Comments: (1) Specimens are C/C composites, no dopants.
(2) H^+ beam produced by mass-selecting ion accelerator.
(3) Hydrocarbon products measured via QMS-RGA, steady-state.
(4) 3 keV H_3^+ (1 keV/H^+); flux: 5×10^{15} H^+/cm^2s; fluence: 3×10^{18} H^+/cm^2.
(5) Yield for total chemical erosion, $Y_{chem-total} = [CH_4 + 2(C_2H_2 + C_2H_4 + C_2H_6) + 3(C_3H_6 + C_3H_8)]/H^+$.

Analytic fitting function:

Erosion yield:

$$Y = 1.0 \times 10^{-2}[A_1 \exp(-(T - A_2)^2/A_3)T^{A_4} + A_5 \exp(-A_6T)T^{A_7}] \quad [\text{molecules/H}^+]$$

where T is in Kelvin. The rms deviation of the analytic fits for reactions A (∗), B (•), C (△), D (□), E (◇), F (▽) and G (+) are 2.0%, 5.7%, 5.7%, 4.8%, 20.9%, 6.6% and 15.7%, respectively.

Fitting parameters A_1-A_7

A	4.6161E+00	7.7448E+02	1.3546E+04	5.9946E-02	9.3752E-04	-8.3782E-04	1.0361E+00
B	6.4370E+00	7.8591E+02	1.1892E+04	-1.5051E-02	1.2095E-01	-2.5540E-03	1.1723E-02
C	9.5038E-02	7.4401E+02	1.9530E+04	7.0377E-02	1.2430E-02	-2.6375E-03	5.3203E-04
D	4.0332E-01	7.4297E+02	1.5403E+04	-1.5477E-02	8.4826E-02	-3.9106E-04	1.5331E-04
E	2.2292E-01	7.5354E+02	8.0555E+03	-7.4806E-03	6.9022E-03	-2.1897E-03	4.3693E-04
F	6.2478E-02	7.6018E+02	2.0476E+04	-2.5872E-02	2.9065E-02	-7.8169E-04	-3.1819E-04
G	1.1916E-01	3.4240E+03	3.6737E+05	2.1991E+00	5.4097E-03	-7.3028E-04	2.1833E-04

ALADDIN evaluation function for erosion yield: EYIELD7A

ALADDIN hierarchical labelling:

A: SATM H{3} [+1] CC-COM T=ALCAN C [+0]
B: SATM H{3} [+1] CC-COM T=ALCAN CH{4} [+0]
C: SATM H{3} [+1] CC-COM T=ALCAN C{2}H{2} [+0]
D: SATM H{3} [+1] CC-COM T=ALCAN C{2}H{4} [+0]
E: SATM H{3} [+1] CC-COM T=ALCAN C{2}H{6} [+0]
F: SATM H{3} [+1] CC-COM T=ALCAN C{3}H{6} [+0]
G: SATM H{3} [+1] CC-COM T=ALCAN C{3}H{8} [+0]

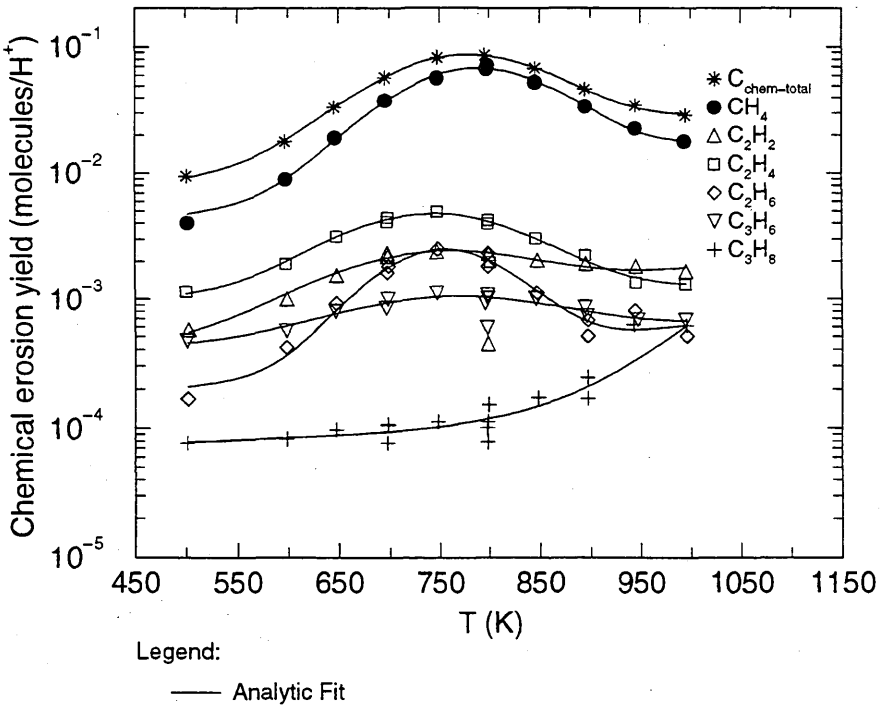

4.2.1.59 H_3^+ + ALCAN carbon/carbon composite (B doped) → C_xH_y, C

Source: J. W. Davis and A. A. Haasz, J. Nucl. Mater. **195**, 166 (1992).

Accuracy: Yield: Total ±20%; CH_4 ±15%, C_xH_y ±30%; T: ±25K.

Comments: (1) Specimens are C/C composites, B doped (7.3 at% B).
(2) H^+ beam produced by mass-selecting ion accelerator.
(3) Hydrocarbon products measured via QMS-RGA, steady-state.
(4) 3 keV H_3^+ (1 keV/H^+); flux: 5×10^{15} H^+/cm^2s; fluence: 3×10^{18} H^+/cm^2.
(5) Yield for total chemical erosion, $Y_{chem-total} = [CH_4 + 2(C_2H_2 + C_2H_4 + C_2H_6) + 3(C_3H_6 + C_3H_8)]/H^+$.

Analytic fitting function:

Erosion yield:

$$Y = 1.0 \times 10^{-2}[A_1 \exp(-(T - A_2)^2/A_3)T^{A_4} + A_5 \exp(-A_6T)T^{A_7}] \quad [\text{molecules}/H^+]$$

where T is in Kelvin. The rms deviation of the analytic fits for reactions A (∗), B (•), C (△), D (□), E (◇), F (▽), and G (+) are 4.9%, 6.8%, 5.8%, 4.7%, 11.8% and 18.5%, respectively.

Fitting parameters A_1-A_7

A	6.0724E+00	7.7842E+02	1.1999E+04	-2.2083E-02	1.6393E-01	-2.1379E-03	1.0948E-02
B	5.9550E+00	7.8156E+02	1.1420E+04	-3.6214E-02	4.2036E-02	-2.9831E-03	2.8068E-02
C	7.5530E-02	7.7811E+02	1.2918E+05	3.4542E-02	-3.1764E-02	1.1404E-03	4.7589E-06
D	1.2480E-01	7.4248E+02	1.6300E+04	3.7540E-02	2.6952E-02	-1.3704E-03	3.7103E-03
E	1.2226E-01	7.5507E+02	7.4092E+03	-2.5831E-02	5.6889E-03	-1.6527E-03	1.5582E-03
F	2.5821E-02	7.4950E+02	1.6259E+04	-1.3431E-02	4.6054E-03	-1.7891E-03	3.1599E-04
G	1.0728E-01	2.7649E+03	1.1401E+07	-3.6458E-01	-5.4851E-01	1.0203E-02	1.3266E-03

ALADDIN evaluation function for erosion yield: EYIELD7A

ALADDIN hierarchical labelling:

A: SATM H{3} [+1] CC-COM T=ALCAN D=B C [+0]
B: SATM H{3} [+1] CC-COM T=ALCAN D=B CH{4} [+0]
C: SATM H{3} [+1] CC-COM T=ALCAN D=B C{2}H{2} [+0]
D: SATM H{3} [+1] CC-COM T=ALCAN D=B C{2}H{4} [+0]
E: SATM H{3} [+1] CC-COM T=ALCAN D=B C{2}H{6} [+0]
F: SATM H{3} [+1] CC-COM T=ALCAN D=B C{3}H{6} [+0]
G: SATM H{3} [+1] CC-COM T=ALCAN D=B C{3}H{8} [+0]

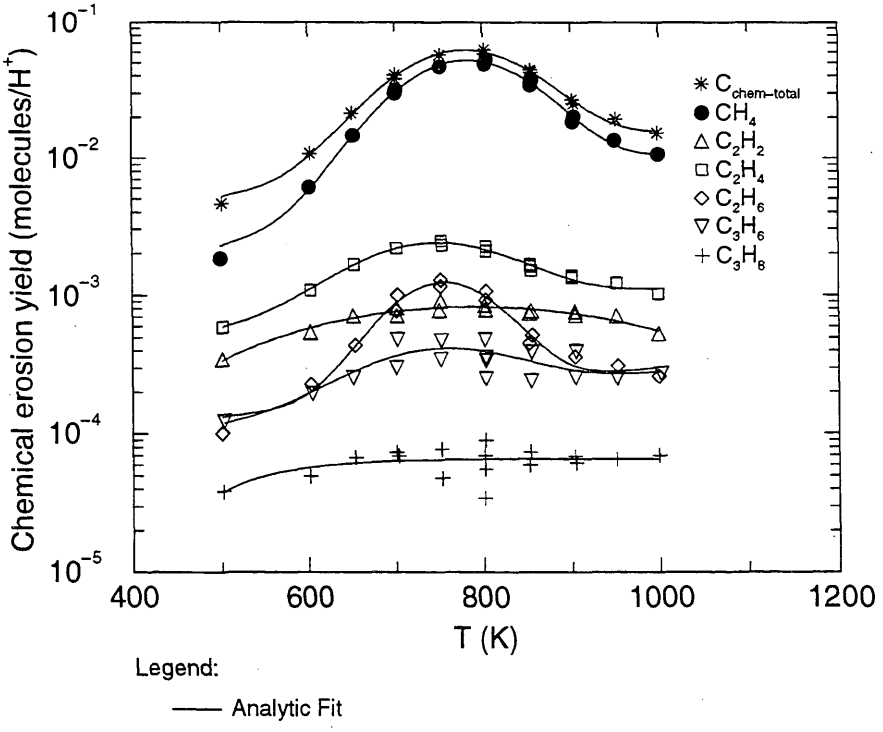

4.2.1.60 H_3^+ + ALCAN carbon/carbon composite (Si doped) → C_xH_y, C

Source: J. W. Davis and A. A. Haasz, J. Nucl. Mater. **195**, 166 (1992).

Accuracy: Yield: Total ±20%; CH_4 ±15%, C_xH_y ±30%; T: ±25K.

Comments: (1) Specimens are C/C composites, Si doped (6.2 at% Si).
(2) H^+ beam produced by mass-selecting ion accelerator.
(3) Hydrocarbon products measured via QMS-RGA, steady-state.
(4) 3 keV H_3^+ (1 keV/H^+); flux: 5×10^{15} H^+/cm^2s; fluence: 3×10^{18} H^+/cm^2.
(5) Yield for total chemical erosion, $Y_{chem-total} = [CH_4 + 2(C_2H_2 + C_2H_4 + C_2H_6) + 3(C_3H_6 + C_3H_8)]/H^+$.

Analytic fitting function:

Erosion yield:

$$Y = 1.0 \times 10^{-2}[A_1 \exp(-(T - A_2)^2/A_3)T^{A_4} + A_5 \exp(-A_6T)T^{A_7}] \quad [\text{molecules}/H^+]$$

where T is in Kelvin. The rms deviation of the analytic fits for reactions A (∗), B (•), C (△), D (□), E (◇), F (▽) and G (+) are 8.1%, 19.9%, 4.3%, 5.8%, 11.1% and 13.4%, respectively.

Fitting parameters A_1-A_7

A	6.5830E+00	7.5267E+02	9.3982E+03	-6.9382E-02	4.0434E-06	1.5660E-03	2.0889E+00
B	3.8518E+00	7.5833E+02	7.9045E+03	-5.2407E-03	1.2286E-07	1.3738E-03	2.4727E+00
C	1.2729E-01	8.0702E+02	1.1170E+05	4.2592E-02	-2.2675E-03	-1.7855E-04	-1.7453E-05
D	1.2202E-01	7.1353E+02	3.6917E+04	5.4717E-02	6.6114E-03	-2.5391E-03	-4.0526E-06
E	9.7166E-02	7.3755E+02	7.4904E+03	-3.5720E-02	1.2060E-02	-9.5422E-04	2.1606E-03
F	5.5591E-02	6.6642E+02	2.7227E+04	-2.4572E-02	4.2817E-03	-2.6417E-03	3.3497E-05
G	2.5457E-03	6.8900E+02	1.5588E+03	3.3048E-03	4.8719E-03	-9.0446E-04	-1.6387E-05

ALADDIN evaluation function for erosion yield: EYIELD7A

ALADDIN hierarchical labelling:

A: SATM H{3} [+1] CC-COM T=ALCAN D=Si C [+0]
B: SATM H{3} [+1] CC-COM T=ALCAN D=Si CH{4} [+0]
C: SATM H{3} [+1] CC-COM T=ALCAN D=Si C{2}H{2} [+0]
D: SATM H{3} [+1] CC-COM T=ALCAN D=Si C{2}H{4} [+0]
E: SATM H{3} [+1] CC-COM T=ALCAN D=Si C{2}H{6} [+0]
F: SATM H{3} [+1] CC-COM T=ALCAN D=Si C{3}H{6} [+0]
G: SATM H{3} [+1] CC-COM T=ALCAN D=Si C{3}H{8} [+0]

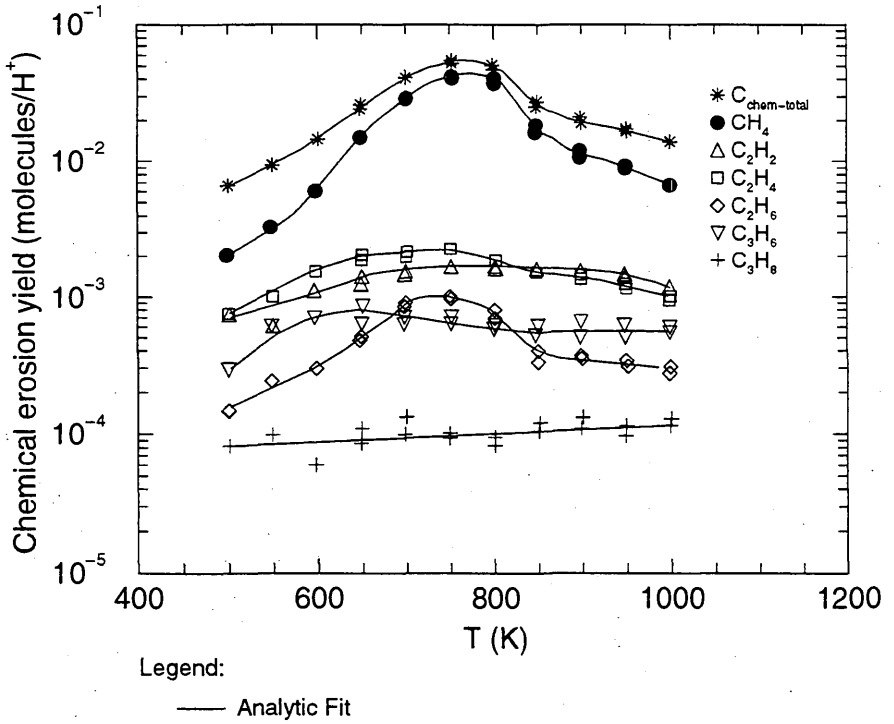

4.2.1.61 H_3^+ + ALCAN carbon/carbon composite (Si and B doped) → C_xH_y, C

Source: J. W. Davis and A. A. Haasz, J. Nucl. Mater. **195**, 166 (1992).

Accuracy: Yield: Total ±20%; CH_4 ±15%, C_xH_y ±30%; T: ±25K.

Comments: (1) Specimens are C/C composites, B and Si doped (6.2 at% Si and 4.0 at% B).
(2) H^+ beam produced by mass-selecting ion accelerator.
(3) Hydrocarbon products measured via QMS-RGA, steady-state.
(4) 3 keV H_3^+ (1 keV/H^+); flux: 5×10^{15} H^+/cm^2s; fluence: 3×10^{18} H^+/cm^2.
(5) Yield for total chemical erosion, $Y_{chem-total} = [CH_4 + 2(C_2H_2 + C_2H_4 + C_2H_6) + 3(C_3H_6 + C_3H_8)]/H^+$.

Analytic fitting function:

Erosion yield:

$$Y = 1.0 \times 10^{-2}[A_1 \exp(-(T - A_2)^2/A_3)T^{A_4} + A_5 \exp(-A_6T)T^{A_7}] \quad [\text{molecules/H}^+]$$

where T is in Kelvin. The rms deviation of the analytic fits for reactions A (∗), B (•), C (△), D (□), E (◇), F (▽) and G (+) are 10.8%, 14.0%, 4.2%, 4.8%, 11.6% and 10.8%, respectively.

Fitting parameters A_1-A_7

A	4.0688E+00	7.4355E+02	8.7085E+03	-3.5774E-02	1.7389E-01	-1.4203E-03	4.8766E-02
B	3.5303E+00	7.4727E+02	8.0816E+03	-2.9794E-02	6.7567E-02	-1.9764E-03	8.0849E-03
C	6.9731E-02	7.7837E+02	1.3711E+05	2.6476E-02	-3.9378E-02	2.0571E-03	-4.1689E-06
D	6.4296E-02	7.2116E+02	1.5807E+04	7.1482E-02	2.4995E-02	-1.3864E-03	1.7330E-03
E	7.8103E-02	7.1060E+02	1.0793E+04	-5.9444E-02	4.9219E-03	-1.1109E-03	3.1047E-05
F	1.0374E+01	4.9056E+03	8.9381E+06	-5.9131E-01	-1.6114E+01	2.5526E-02	9.1292E-01
G	2.0833E-03	1.0372E+03	2.7816E+04	-5.9658E-02	4.7918E-03	-2.8815E-04	1.9213E-06

ALADDIN evaluation function for erosion yield: EYIELD7A

ALADDIN hierarchical labelling:

A: SATM H{3} [+1] CC-COM T=ALCAN D=B,Si C [+0]
B: SATM H{3} [+1] CC-COM T=ALCAN D=B,Si CH{4} [+0]
C: SATM H{3} [+1] CC-COM T=ALCAN D=B,Si C{2}H{2} [+0]
D: SATM H{3} [+1] CC-COM T=ALCAN D=B,Si C{2}H{4} [+0]
E: SATM H{3} [+1] CC-COM T=ALCAN D=B,Si C{2}H{6} [+0]
F: SATM H{3} [+1] CC-COM T=ALCAN D=B,Si C{3}H{6} [+0]
G: SATM H{3} [+1] CC-COM T=ALCAN D=B,Si C{3}H{8} [+0]

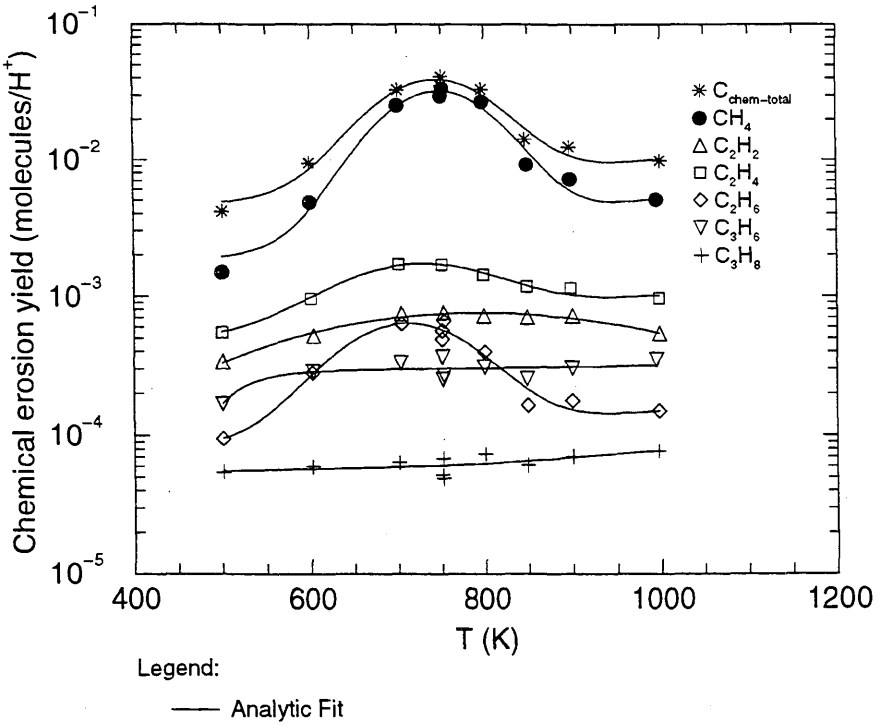

4.2.1.62 H_3^+ + CKC graphite → CH_4

Source: A. Y. K. Chen, A. A. Haasz and J. W. Davis, J. Nucl. Mater. **227**, 66 (1995).

Accuracy: Yield: ±15%; T: ±25K.

Comments: (1) Data is for undoped reference graphite CKC-Ref_{edge} and CKC-Ref_{base}.
(2) Incident ion energy: 3 keV H_3^+ (1 keV/H^+). Flux: 3×10^{15} H^+/cm^2s.
(3) The reaction products emitted from the target are detected via QMS-RGA, steady-state.
(4) H^+ ions produced by a mass-analyzed ion accelerator.

Analytic fitting function:

Methane yield:

$$Y = 1.0 \times 10^{-2}[A_1 \exp(-(T - A_2)^2/A_3)T^{A_4} + A_5 \exp(-A_6 T)T^{A_7}] \quad [\text{molecules/H}^+]$$

where T is in Kelvin. The rms deviation of the analytic fits for reactions A (•) and B (○) are 11% and 9.2%, respectively.

Fitting parameters A_1-A_7

A	2.8922E+00	7.8570E+02	1.3303E+04	1.3816E-01	2.0451E-02	-3.5547E-03
	1.0413E-04					
B	1.5006E+00	7.9374E+02	1.4279E+04	2.2299E-01	5.3361E-03	-4.8360E-03
	4.1453E-05					

ALADDIN evaluation function for methane yield: EYIELD7A

ALADDIN hierarchical labelling:

A: SATM H{3} [+1] GRAPHITE T=CKC O=BASE-PL CH{4}
B: SATM H{3} [+1] GRAPHITE T=CKC O=EDGE-PL CH{4}

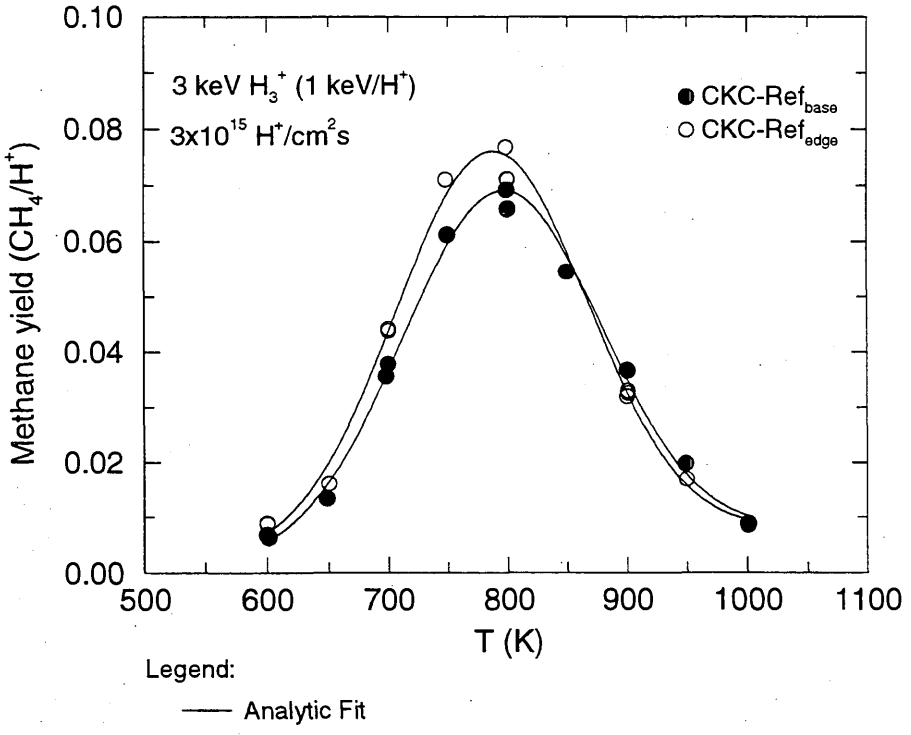

4.2.1.63 H_3^+ + CKC-B2 (B doped) graphite → CH_4

Source: A. Y. K. Chen, A. A. Haasz and J. W. Davis, J. Nucl. Mater. **227**, 66 (1995).

Accuracy: Yield: ±15%; T: ±25K.

Comments: (1) Data is for B-doped graphite (2.0 at%B).
(2) Incident ion energy: 3 keV H_3^+ (1 keV/H^+). Flux: 3×10^{15} H^+/cm^2s.
(3) The reaction products emitted from the target are detected via QMS-RGA, steady-state.
(4) H^+ ions produced by a mass-analyzed ion accelerator.

Analytic fitting function:

Methane yield:

$$Y = 1.0 \times 10^{-2}[A_1 \exp(-(T - A_2)^2/A_3)T^{A_4} + A_5 \exp(-A_6 T)T^{A_7}] \quad [\text{molecules}/H^+]$$

where T is in Kelvin. The rms deviation of the analytic fits for reactions A (•) and B (○) are 8.7% and 5.2%, respectively.

Fitting parameters A_1-A_7

A	1.5421E+00	7.5712E+02	1.4112E+04	1.2720E-01	1.8068E-02	-3.3074E-03
	1.3928E-03					
B	3.7512E+00	7.8439E+02	1.6216E+04	1.7927E-02	4.6496E-03	-4.5204E-03
	2.2010E-03					

ALADDIN evaluation function for methane yield: EYIELD7A

ALADDIN hierarchical labelling:

A: SATM H{3} [+1] GRAPHITE T=CKC D=B O=BASE-PL CH{4}
B: SATM H{3} [+1] GRAPHITE T=CKC D=B O=EDGE-PL CH{4}

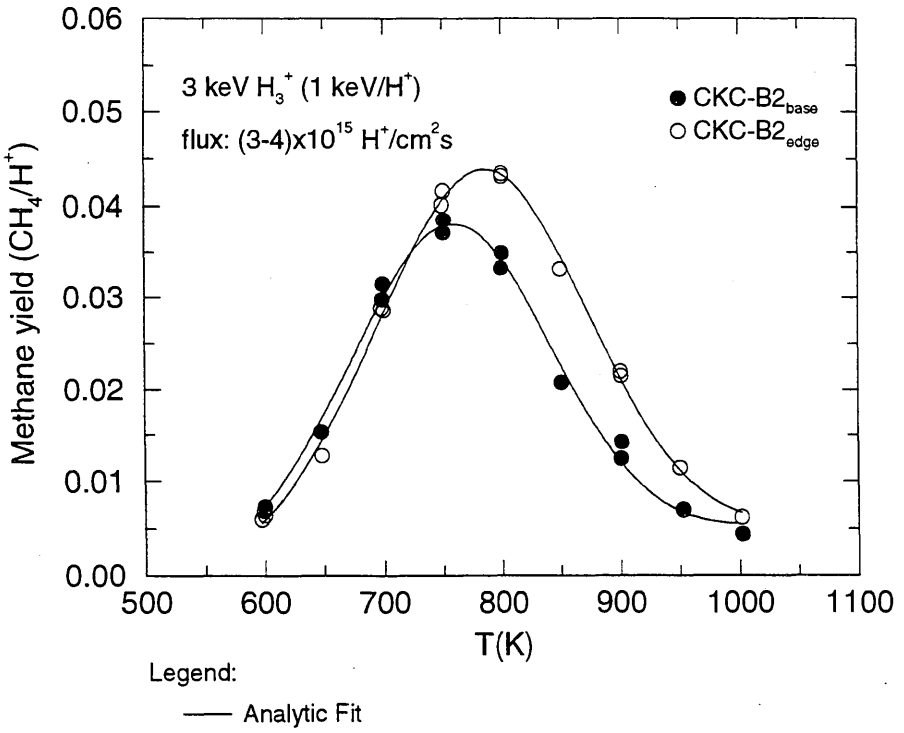

4.2.1.64 H_3^+ + CKC-B10 (B doped) graphite → CH_4

Source: A. Y. K. Chen, A. A. Haasz and J. W. Davis, J. Nucl. Mater. **227**, 66 (1995).

Accuracy: Yield: ±15%; T: ±25K.

Comments: (1) Data is for B-doped graphite (9.4 at%B).
(2) Incident ion energy: 3 keV H_3^+ (1 keV/H^+). Flux: 3×10^{15} H^+/cm^2s.
(3) The reaction products emitted from the target are detected via QMS-RGA, steady-state.
(4) H^+ ions produced by a mass-analyzed ion accelerator.

Analytic fitting function:

Methane yield:

$$Y = 1.0 \times 10^{-2}[A_1 \exp(-(T - A_2)^2/A_3)T^{A_4} + A_5 \exp(-A_6 T)T^{A_7}] \quad [\text{molecules/H}^+]$$

where T is in Kelvin. The rms deviation of the analytic fits for reactions A (•) and B (○) are 4.2% and 6.0%, respectively.

Fitting parameters A_1-A_7

A	6.1787E-01	7.6034E+02	1.3253E+04	1.4623E-01	4.5556E-04	-6.8409E-03
	-9.2270E-04					
B	9.2339E-01	7.6745E+02	1.6942E+04	1.4272E-01	4.2318E-03	-4.3761E-03
	2.4866E-05					

ALADDIN evaluation function for methane yield: EYIELD7A

ALADDIN hierarchical labelling:

A: SATM H{3} [+1] GRAPHITE T=CKC D=B O=BASE-PL CH{4}
B: SATM H{3} [+1] GRAPHITE T=CKC D=B O=EDGE-PL CH{4}

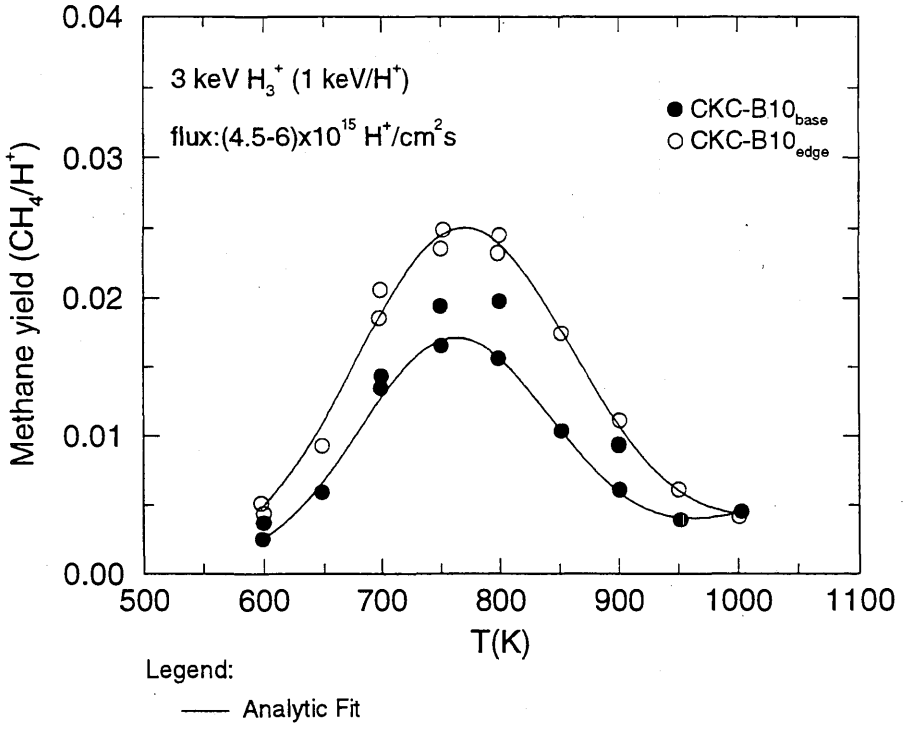

4.2.1.65 H_3^+ + CKC-B20 (B doped) graphite → CH_4

Source: A. Y. K. Chen, A. A. Haasz and J. W. Davis, J. Nucl. Mater. **227**, 66 (1995).

Accuracy: Yield: Total ±20%; CH_4 ±15%, C_xH_y ±30%; T: ±25K.

Comments: (1) Data is for B-doped graphite (20.1 at%B).
(2) Incident ion energy: 3 keV H_3^+ (1 keV/H^+). Flux: 3×10^{15} H^+/cm^2s.
(3) The reaction products emitted from the target are detected via QMS-RGA, steady-state.
(4) H^+ ions produced by a mass-analyzed ion accelerator.

Analytic fitting function:

Methane yield:

$$Y = 1.0 \times 10^{-2}[A_1 \exp(-(T - A_2)^2/A_3)T^{A_4} + A_5 \exp(-A_6T)T^{A_7}] \quad [\text{molecules}/H^+]$$

where T is in Kelvin. The rms deviation of the analytic fits for reactions A (•) and B (○) are 4.5% and 8.4%, respectively.

Fitting parameters A_1-A_7

A	4.5532E-01	7.6534E+02	1.5550E+04	1.9110E-01	1.6632E-01	-3.6959E-04
	1.2815E-02					
B	1.8186E+00	7.5256E+02	1.4096E+04	6.0885E-02	4.5439E-03	-4.4091E-03
	-7.1894E-04					

ALADDIN evaluation function for methane yield: EYIELD7A

ALADDIN hierarchical labelling:

A: SATM H{3} [+1] GRAPHITE T=CKC D=B O=BASE-PL CH{4}
B: SATM H{3} [+1] GRAPHITE T=CKC D=B O=EDGE-PL CH{4}

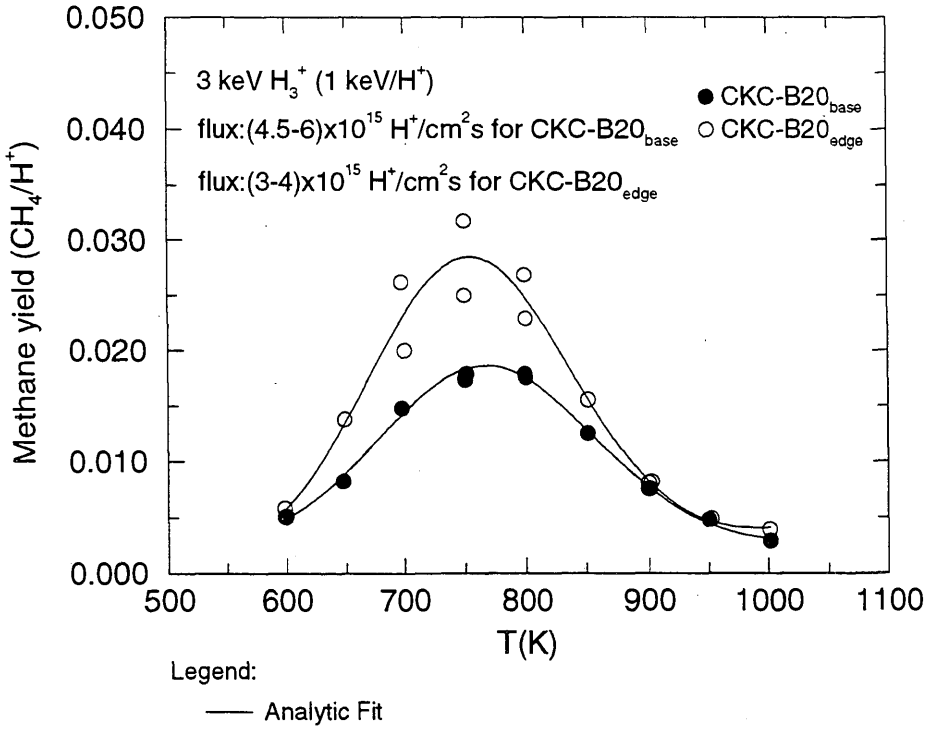

4.2.1.66 H_3^+ + CKC-Si3 (Si doped) graphite → CH_4

Source: A. Y. K. Chen, A. A. Haasz and J. W. Davis, J. Nucl. Mater. **227**, 66 (1995).

Accuracy: Yield: ±15%; T: ±25K.

Comments: (1) Data is for Si-doped graphite (3 at%Si).
(2) Incident ion energy: 3 keV H_3^+ (1 keV/H^+). Flux: $(1.5-6) \times 10^{15}$ H^+/cm^2s.
(3) The reaction products emitted from the target are detected via QMS-RGA, steady-state.
(4) H^+ ions produced by a mass-analyzed ion accelerator.

Analytic fitting function:

Methane yield:

$$Y = 1.0 \times 10^{-2}[A_1 \exp(-(T-A_2)^2/A_3)T^{A_4} + A_5 \exp(-A_6 T)T^{A_7}] \quad [\text{molecules}/H^+]$$

where T is in Kelvin. The rms deviation of the analytic fits for reactions A (•) and B (○) are 8.7% and 3.7%, respectively.

Fitting parameters A_1-A_7

A	3.0085E+00	7.9542E+02	1.6551E+04	1.0924E-01	4.4814E-03	-4.5035E-03
	1.3518E-03					
B	3.2543E+00	8.2060E+02	1.4639E+04	1.1486E-01	6.4046E-01	-4.9695E-04
	-3.5787E-03					

ALADDIN evaluation function for methane yield: EYIELD7A

ALADDIN hierarchical labelling:

A: SATM H{3} [+1] GRAPHITE T=CKC D=Si O=BASE-PL CH{4}
B: SATM H{3} [+1] GRAPHITE T=CKC D=Si O=EDGE-PL CH{4}

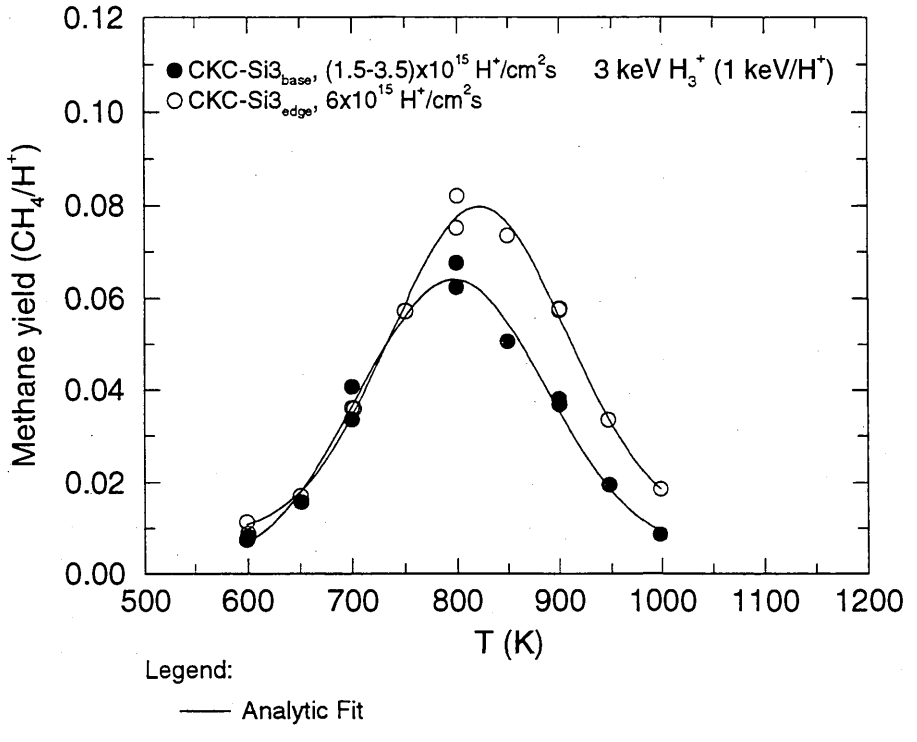

4.2.1.67 H_3^+ + CKC-Si8 (Si doped) graphite → CH_4

Source: A. Y. K. Chen, A. A. Haasz and J. W. Davis, J. Nucl. Mater. **227**, 66 (1995).

Accuracy: Yield: ±15%; T: ±25K.

Comments: (1) Data is for Si-doped graphite (7.5 at%Si).
(2) Incident ion energy: 3 keV H_3^+ (1 keV/H^+). Flux: $(1.5 - 6) \times 10^{15}$ H^+/cm^2s.
(3) The reaction products emitted from the target are detected via QMS-RGA, steady-state.
(4) H^+ ions produced by a mass-analyzed ion accelerator.

Analytic fitting function:

Methane yield:

$$Y = 1.0 \times 10^{-2}[A_1 \exp(-(T - A_2)^2/A_3)T^{A_4} + A_5 \exp(-A_6 T)T^{A_7}] \quad [\text{molecules}/H^+]$$

where T is in Kelvin. The rms deviation of the analytic fits for reactions A (•) and B (◦) are 6.8% and 5.2%, respectively.

Fitting parameters A_1-A_7

A	2.1863E+00	7.9562E+02	1.3058E+04	1.5009E-01	1.4182E-01	-1.7928E-03
	1.3833E-02					
B	1.4795E+00	8.2782E+02	1.8502E+04	1.7610E-01	6.9096E-02	-2.6966E-03
	-8.9209E-03					

ALADDIN evaluation function for methane yield: EYIELD7A

ALADDIN hierarchical labelling:

A: SATM H{3} [+1] GRAPHITE T=CKC D=Si O=BASE-PL CH{4}
B: SATM H{3} [+1] GRAPHITE T=CKC D=Si O=EDGE-PL CH{4}

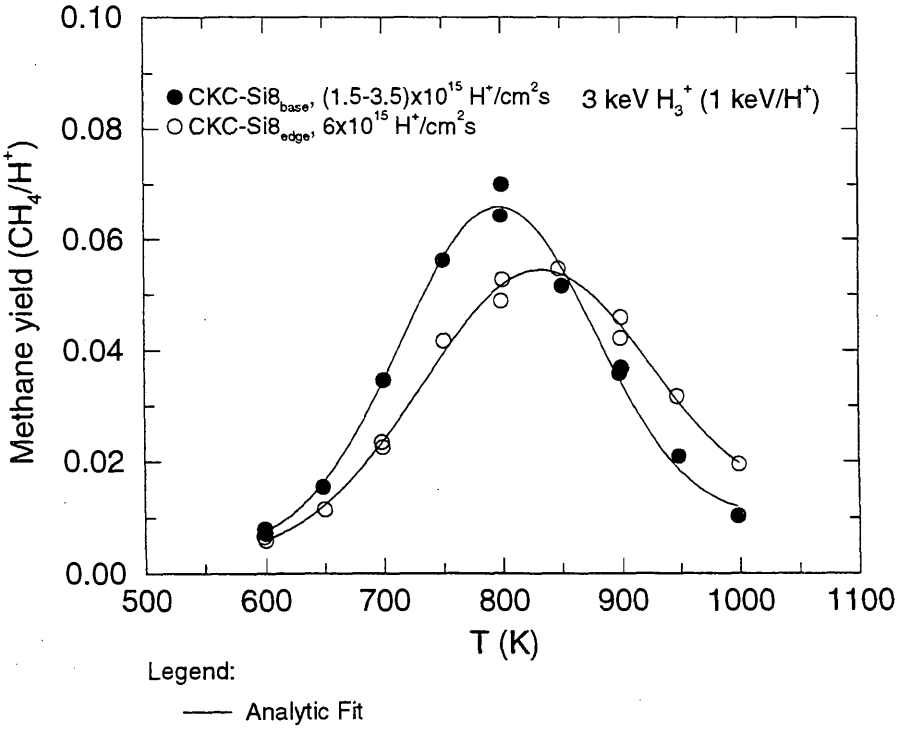

4.2.1.68 H_3^+ + CKC-Si14 (Si doped) graphite → CH_4

Source: A. Y. K. Chen, A. A. Haasz and J. W. Davis, J. Nucl. Mater. **227**, 66 (1995).

Accuracy: Yield: ±15%; T: ±25K.

Comments: (1) Data is for Si-doped graphite (14 at%Si).
(2) Incident ion energy: 3 keV H_3^+ (1 keV/H^+). Flux: $(1.5 - 3.5) \times 10^{15}$ H^+/cm^2s.
(3) The reaction products emitted from the target are detected via QMS-RGA, steady-state.
(4) H^+ ions produced by a mass-analyzed ion accelerator.

Analytic fitting function:

Methane yield:

$$Y = 1.0 \times 10^{-2}[A_1 \exp(-(T - A_2)^2/A_3)T^{A_4} + A_5 \exp(-A_6 T)T^{A_7}] \quad [\text{molecules/H}^+]$$

where T is in Kelvin. The rms deviation of the analytic fits for reactions A (•) and B (○) are 7.9% and 8.9%, respectively.

Fitting parameters A_1-A_7

A	9.7926E-01	7.8534E+02	1.0638E+04	2.2198E-01	3.7013E-01	4.3084E-04
	8.3463E-02					
B	1.3385E+00	7.9633E+02	1.5654E+04	1.9976E-01	5.5508E-02	-2.0458E-03
	1.7705E-03					

ALADDIN evaluation function for methane yield: EYIELD7A

ALADDIN hierarchical labelling:

A: SATM H{3} [+1] GRAPHITE T=CKC D=Si O=BASE-PL CH{4}
B: SATM H{3} [+1] GRAPHITE T=CKC D=Si O=EDGE-PL CH{4}

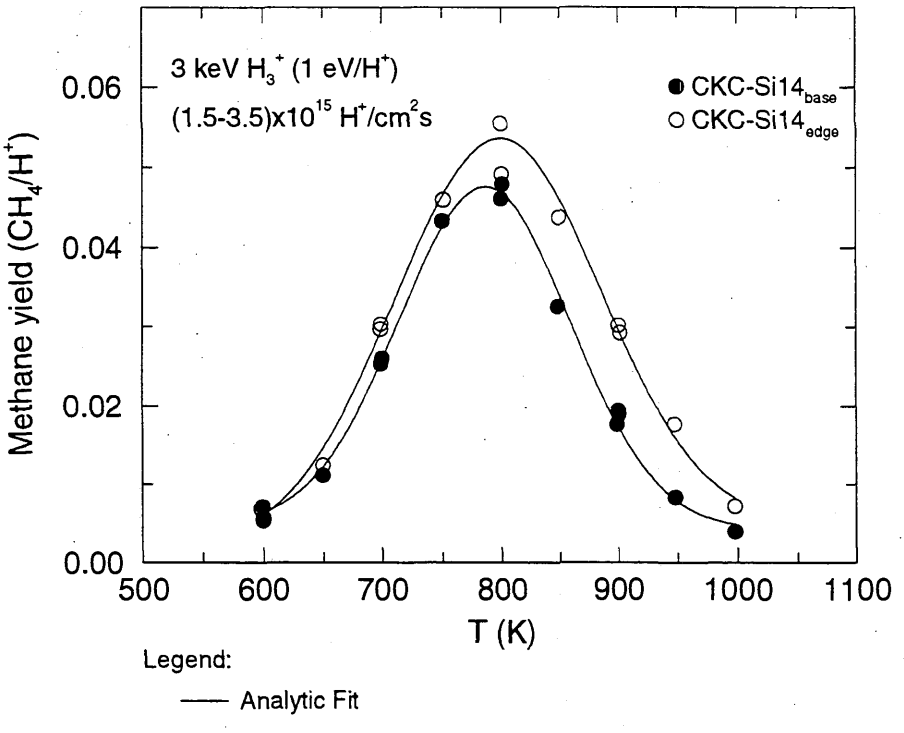

4.2.1.69 H_3^+ + CKC-Ti2 (Ti doped) graphite → CH_4

Source: A. Y. K. Chen, A. A. Haasz and J. W. Davis, J. Nucl. Mater. **227**, 66 (1995).

Accuracy: Yield: ±15%; T: ±25K.

Comments: (1) Data is for Ti-doped graphite (2.0 at%Ti).
(2) Incident ion energy: 3 keV H_3^+ (1 keV/H^+). Flux: $(2.5 - 7.5) \times 10^{15}$ H^+/cm^2s.
(3) The reaction products emitted from the target are detected via QMS-RGA, steady-state.
(4) H^+ ions produced by a mass-analyzed ion accelerator.

Analytic fitting function:

Methane yield:

$$Y = 1.0 \times 10^{-2}[A_1 \exp(-(T - A_2)^2/A_3)T^{A_4} + A_5 \exp(-A_6 T)T^{A_7}] \quad [\text{molecules/H}^+]$$

where T is in Kelvin. The rms deviation of the analytic fits for reactions A (•) and B (○) are 11.1% and 6.1%, respectively.

Fitting parameters A_1-A_7

A	1.2882E+00	8.2712E+02	1.6756E+04	2.2897E-01	3.6423E-01	-2.4222E-03
	-1.6664E-01					
B	7.5569E-01	7.8843E+02	1.3529E+04	3.2041E-01	9.9084E-02	-1.0487E-03
	8.0357E-02					

ALADDIN evaluation function for methane yield: EYIELD7A

ALADDIN hierarchical labelling:

A: SATM H{3} [+1] GRAPHITE T=CKC D=Ti O=BASE-PL CH{4}
B: SATM H{3} [+1] GRAPHITE T=CKC D=Ti O=EDGE-PL CH{4}

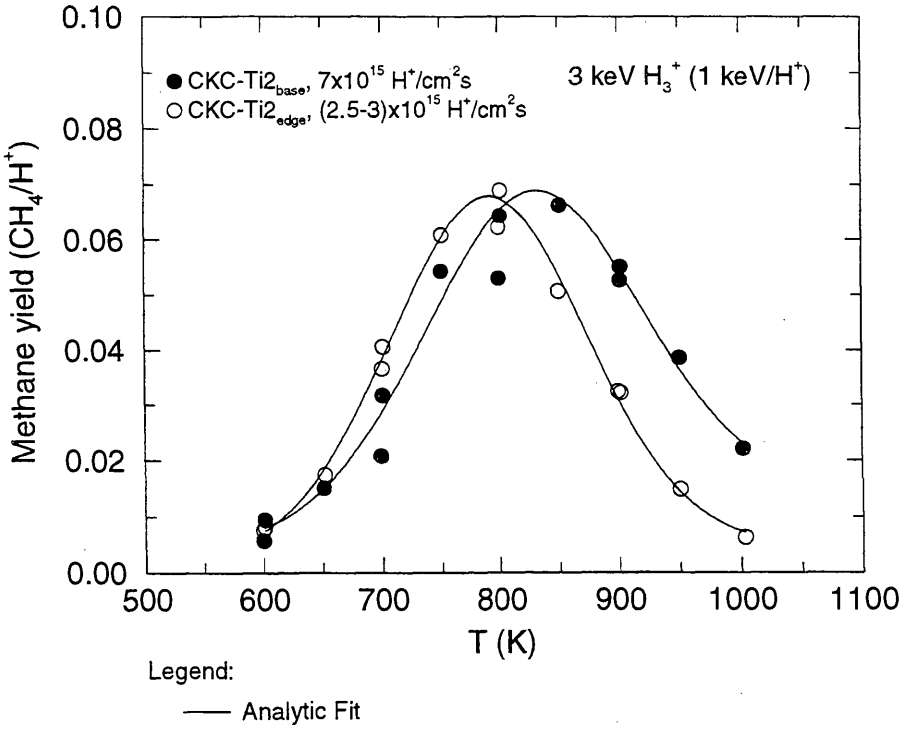

4.2.1.70 H_3^+ + CKC-Ti8 (Ti doped) graphite → CH_4

Source: A. Y. K. Chen, A. A. Haasz and J. W. Davis, J. Nucl. Mater. **227**, 66 (1995).

Accuracy: Yield: ±15%; T: ±25K.

Comments: (1) Data is for Ti-doped graphite (8.5 at%Ti).
(2) Incident ion energy: 3 keV H_3^+ (1 keV/H^+). Flux: $(2.5 - 3.0) \times 10^{15}$ H^+/cm^2s.
(3) The reaction products emitted from the target are detected via QMS-RGA, steady-state.
(4) H^+ ions produced by a mass-analyzed ion accelerator.

Analytic fitting function:

Methane yield:

$$Y = 1.0 \times 10^{-2}[A_1 \exp(-(T - A_2)^2/A_3)T^{A_4} + A_5 \exp(-A_6 T)T^{A_7}] \quad [\text{molecules}/H^+]$$

where T is in Kelvin. The rms deviation of the analytic fits for reactions A (•) and B (○) are 8.5% and 6.6%, respectively.

Fitting parameters A_1-A_7

A	2.5293E+00	8.0407E+02	1.4224E+04	1.0502E-01	5.9377E-02	-2.1996E-03
	8.4318E-04					
B	1.5501E+00	7.8690E+02	1.4789E+04	1.9191E-01	8.1014E-02	-1.4129E-03
	5.4414E-03					

ALADDIN evaluation function for methane yield: EYIELD7A

ALADDIN hierarchical labelling:

A: SATM H{3} [+1] GRAPHITE T=CKC D=Ti O=BASE-PL CH{4}
B: SATM H{3} [+1] GRAPHITE T=CKC D=Ti O=EDGE-PL CH{4}

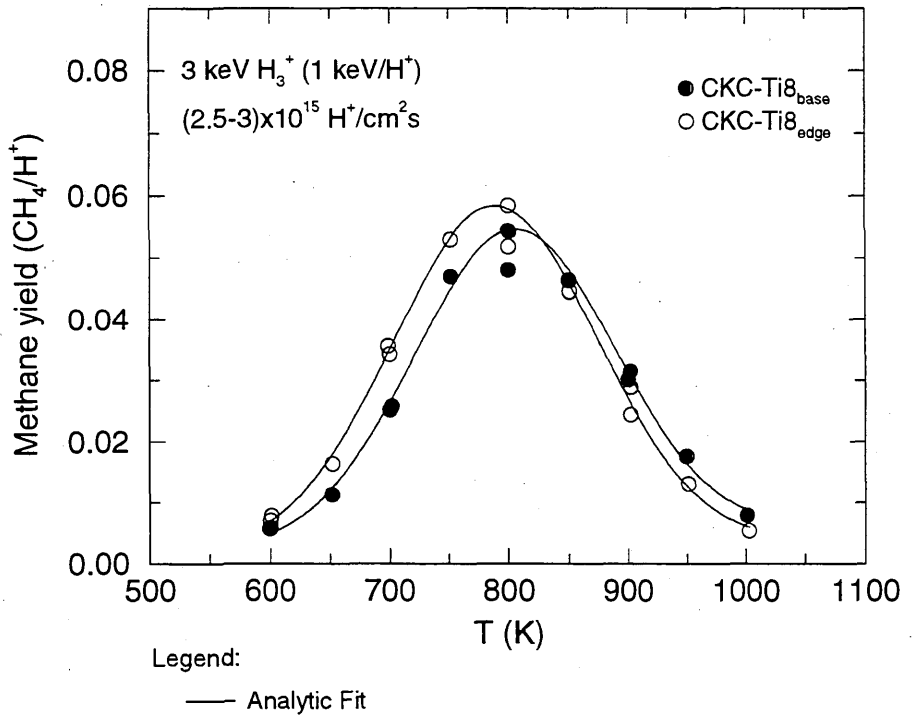

4.2.1.71 H_3^+ + CKC-Ti16 (Ti doped) graphite → CH_4

Source: A. Y. K. Chen, A. A. Haasz and J. W. Davis, J. Nucl. Mater. **227**, 66 (1995).

Accuracy: Yield: ±15%; T: ±25K.

Comments: (1) Data is for Ti-doped graphite (16 at%Ti).
(2) Incident ion energy: 3 keV H_3^+ (1 keV/H^+). Flux: $(2.5 - 3.0) \times 10^{15}$ H^+/cm^2s.
(3) The reaction products emitted from the target are detected via QMS-RGA, steady-state.
(4) H^+ ions produced by a mass-analyzed ion accelerator.

Analytic fitting function:

Methane yield:

$$Y = 1.0 \times 10^{-2}[A_1 \exp(-(T - A_2)^2/A_3)T^{A_4} + A_5 \exp(-A_6T)T^{A_7}] \quad [\text{molecules/H}^+]$$

where T is in Kelvin. The rms deviation of the analytic fits for reactions A (•) and B (○) are 4.0% and 7.6%, respectively.

Fitting parameters A_1-A_7

A	2.2450E+00	7.8609E+02	1.6330E+04	8.6811E-02	7.1228E-02	-1.3199E-03
	2.5675E-03					
B	9.0407E-01	7.7482E+02	1.2072E+04	2.5071E-01	2.9561E-01	-5.7001E-05
	4.4050E-02					

ALADDIN evaluation function for methane yield: EYIELD7A

ALADDIN hierarchical labelling:

A: SATM H{3} [+1] GRAPHITE T=CKC D=Ti O=BASE-PL CH{4}
B: SATM H{3} [+1] GRAPHITE T=CKC D=Ti O=EDGE-PL CH{4}

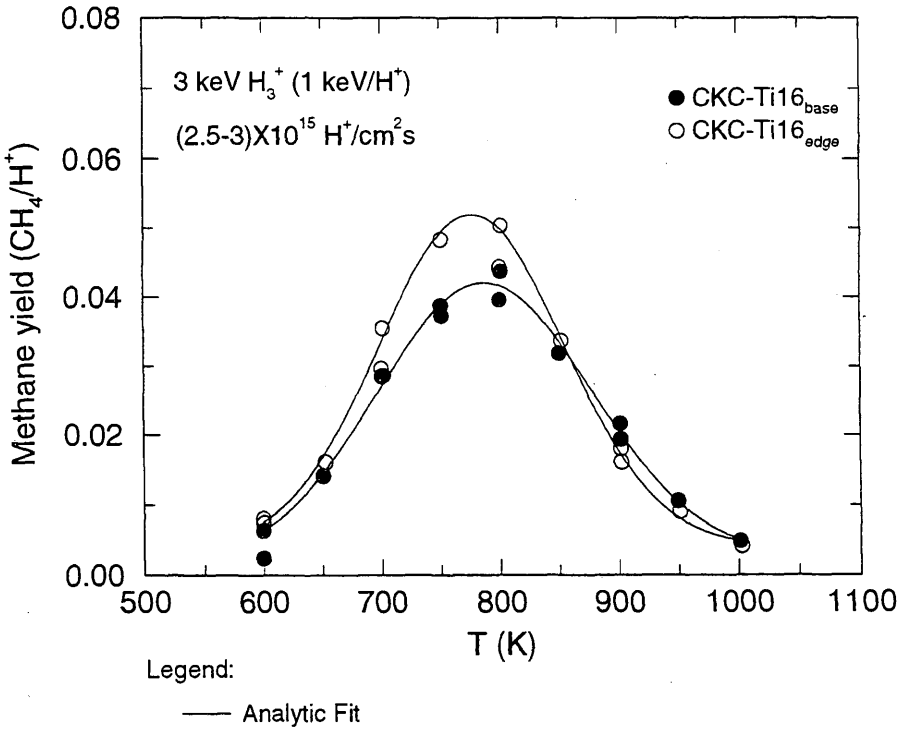

4.2.1.72 H_3^+ + CKC W doped graphite → CH_4

Source: A. Y. K. Chen, A. A. Haasz and J. W. Davis, J. Nucl. Mater. **227**, 66 (1995).

Accuracy: Yield: ±15%; T: ±25K.

Comments: (1) Data is for W-doped graphite (10 at%W).
(2) Incident ion energy: 3 keV H_3^+ (1 keV/H^+). Flux: $(2.5 - 3.0) \times 10^{15}$ H^+/cm^2s.
(3) The reaction products emitted from the target are detected via QMS-RGA, steady-state.
(4) H^+ ions produced by a mass-analyzed ion accelerator.

Analytic fitting function:

Methane yield:

$$Y = 1.0 \times 10^{-2}[A_1 \exp(-(T - A_2)^2/A_3)T^{A_4} + A_5 \exp(-A_6T)T^{A_7}] \quad [\text{molecules/H}^+]$$

where T is in Kelvin. The rms deviation of the analytic fits for reactions A (•) and B (○) are 7.3% and 8.1%, respectively.

Fitting parameters A_1-A_7

A	1.5128E+00	7.7247E+02	1.4031E+04	1.7704E-01	5.6257E-03	-4.4194E-03
	-4.6981E-04					
B	2.0809E+00	7.9784E+02	1.5654E+04	1.6638E-01	1.0688E-02	-4.3639E-03
	4.2474E-03					

ALADDIN evaluation function for methane yield: EYIELD7A

ALADDIN hierarchical labelling:

A: SATM H{3} [+1] GRAPHITE T=CKC D=W O=BASE-PL CH{4}
B: SATM H{3} [+1] GRAPHITE T=CKC D=W O=EDGE-PL CH{4}

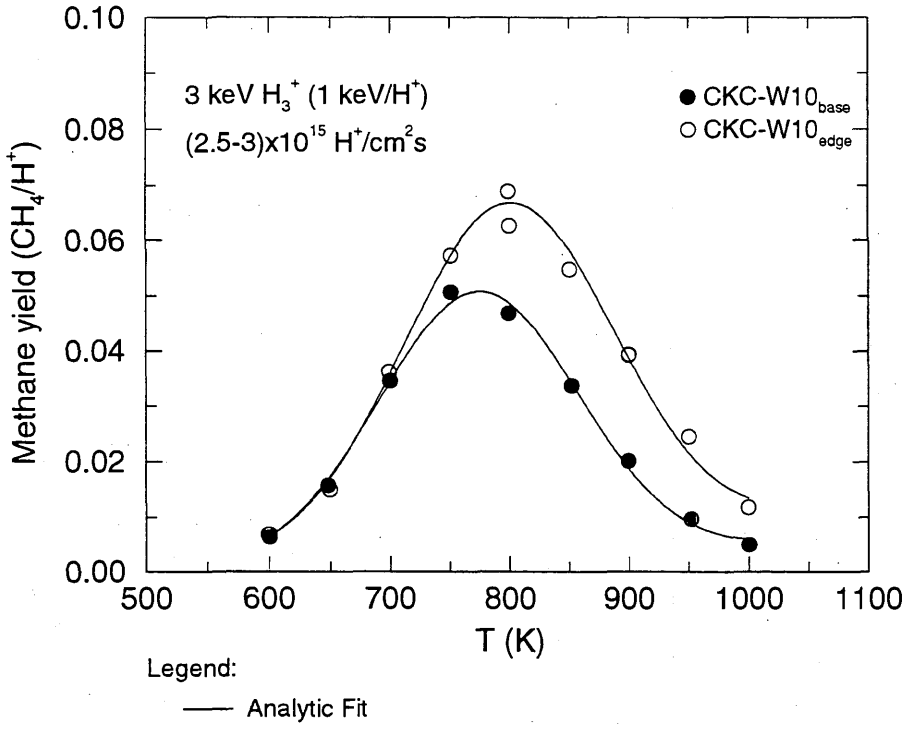

4.2.1.73 H_3^+ + pyrolytic graphite → CH_4

Source: J. W. Davis and A. A. Haasz, J. Nucl. Mater., in press (1998).

Accuracy: Yield: ±20%; T: ±25K.

Comments: (1) Steady-state methane yield.
(2) Specimen: pyrolytic graphite (HPG99).
(3) Incident ions were mass-analyzed.
(4) Reaction products measured by QMS-RGA.

Analytic fitting function:

Erosion yield:

$$Y = A_1 \exp[-(\frac{T - A_2}{A_3 T + 1})^2 / A_4] T^{A_5} + A_6 \exp(-A_7 T) T^{A_8} \quad [\text{molecules/H}^+]$$

where T is in Kelvin. The rms deviation of analytic fits for reactions A (•), B (○), C (□) and D (△) are 16.8%, 10.3%, 7.2% and 5.8%, respectively. Data for curve A were fitted with EYIELD9A.

Fitting parameters A_1-A_9

A	8.0224e-02	8.4836e+02	1.7501e+04	-3.1447e-02	1.1809e-08	-2.5187e-03
	6.2465e-01	2.0655e-03	1.7118e+00			
B	1.5001e-02	7.9666e+02	3.8666e-04	1.6295e+04	1.9035e-01	1.6138e-14
	5.7273e-04	3.6158e+00				
C	9.1155e-03	7.0314e+02	2.1480e-03	6.7106e+03	1.0968e-01	-1.7167e-21
	-1.8245e-02	3.0076e+00				
D	6.1253E-02	6.4659E+02	2.4623E-04	3.2339E+04	-3.4592E-01	4.2824E-04
	1.0616E-03	3.2700E-01				

ALADDIN evaluation function for erosion yield: EYIELD8A, EYIELD9A

ALADDIN hierarchical labelling:

A-D: SATM H{3} [+1] GRAPHITE T=HPG99 CH{4} [+0]

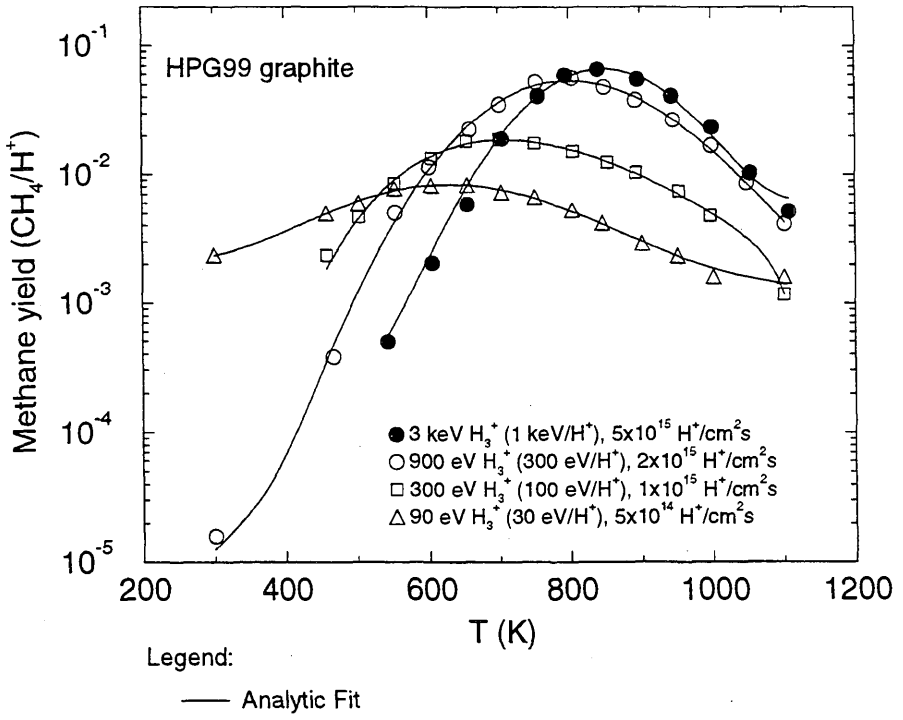

4.2.1.74 H_3^+ + pyrolytic graphite → C

Source: J. W. Davis and A. A. Haasz, J. Nucl. Mater., in press (1998).

Accuracy: Yield: ±20%; T: ±25K.

Comments: (1) Steady-state hydrocarbon yield.
(2) Specimen: pyrolytic graphite (HPG99).
(3) Incident ions were mass-analyzed.
(4) Reaction products measured by QMS-RGA.
(5) Yield for total chemical erosion, $Y_{chem-total} = [CH_4 + 2(C_2H_2 + C_2H_4 + C_2H_6) + 3(C_3H_6 + C_3H_8)]/H^+$.

Analytic fitting function:

Erosion yield:

$$Y = A_1 \exp[-(\frac{T - A_2}{A_3 T + 1})^2 / A_4] T^{A_5} + A_6 \exp(-A_7 T) T^{A_8} \quad [\text{eroded C/H}^+]$$

where T is in Kelvin. The rms deviation of analytic fits for reactions A (•), B (○), C (□) and D (△) are 20.9%, 35.6%, 20.6% and 10.5%, respectively.

Fitting parameters A_1-A_8

A	1.7149e-02	8.4219e+02	8.4641e-04	6.8513e+03	2.1097e-01	1.9390e-15
	2.0985e-03	4.3578e+00				
B	1.6539e-02	7.7464e+02	3.1365e-03	2.0630e+03	2.2325e-01	7.0015e-14
	6.1244e-03	4.4394e+00				
C	8.8778E+02	7.0449E+02	8.1944E-03	6.3190E+02	-1.5679E+00	1.3154E-09
	3.5514E-03	2.6856E+00				
D	2.9550E+06	7.0080E+02	3.3340E-04	2.3491E+04	-2.8974E+00	5.4395E+06
	-6.8257E-03	-4.1016E+00				

ALADDIN evaluation function for erosion yield: EYIELD8A

ALADDIN hierarchical labelling:

A-D: SATM H{3} [+1] GRAPHITE T=HPG99 C [+0]

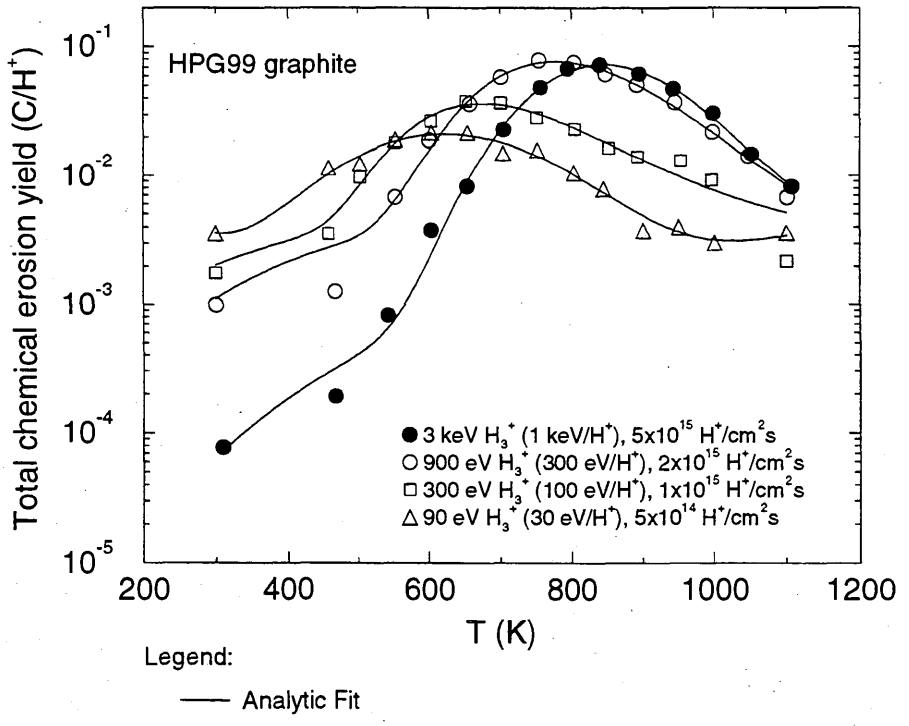

4.2.1.75 H_3^+ + CKC graphite → CH_4

Source: J. W. Davis and A. A. Haasz, J. Nucl. Mater., in press (1998).

Accuracy: Yield: ±20%; T: ±25K.

Comments: (1) Steady-state methane yield.
(2) Specimen: CKC undoped reference graphite. Specimens were cut in two orientations, 'edge' and 'base'.
(3) Incident ions were mass-analyzed.
(4) Reaction products measured by QMS-RGA.

Analytic fitting function:

Erosion yield:

$$Y = A_1 \exp[-(\frac{T - A_2}{A_3 T + 1})^2 / A_4] T^{A_5} + A_6 \exp(-A_7 T) T^{A_8} \quad [\text{molecules/H}^+]$$

where T is in Kelvin. The rms deviation of analytic fits for reactions A (•), B (○), C (□) and D (△) are 13.7%, 6.2%, 22.1% and 5.1%, respectively. Data for curve D were fitted with EYIELD7A.

Fitting parameters A_1-A_8

A	1.4651e-02	8.3802e+02	3.7420e-04	9.8781e+03	2.0694e-01	2.1 870e-15
	3.8995e-03	4.6503e+00				
B	5.7894e-03	7.9854e+02	2.0739e-04	1.8681e+04	3.2195e-01	3.6 946e-05
	-1.1682e-03	4.7666e-01				
C	9.5256e-04	7.2015e+02	5.2672e+04	4.3739e-01	1.4746e-12	5.8 900e-03
	2.3678e+00	5.8288e-08	4.0011e+00			
D	5.0013E-09	-2.2289E+02	3.1864E+05	3.2897E+00	4.9718E-47	-4.4400E-03
	1.4217E+01					

ALADDIN evaluation function for erosion yield: EYIELD7A, EYIELD8A

ALADDIN hierarchical labelling:

A-D: SATM H{3} [+1] GRAPHITE T=CKC O=EDGE-PL CH{4} [+0]

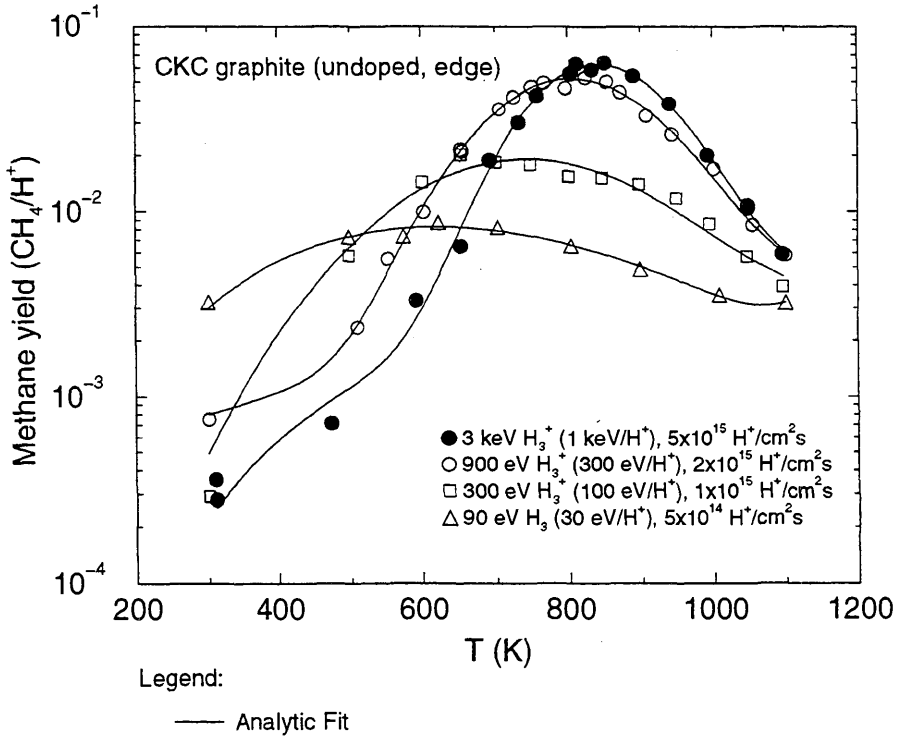

4.2.1.76 H_3^+ + CKC graphite → C

Source: J. W. Davis and A. A. Haasz, J. Nucl. Mater., in press (1998).

Accuracy: Yield: ±20%; T: ±25K.

Comments: (1) Steady-state hydrocarbon yield.
(2) Specimen: CKC undoped reference graphite. Specimens were cut in two orientations, 'edge' and 'base'.
(3) Incident ions were mass-analyzed.
(4) Reaction products measured by QMS-RGA.
(5) Yield for total chemical erosion, $Y_{chem-total} = [CH_4 + 2(C_2H_2 + C_2H_4 + C_2H_6) + 3(C_3H_6 + C_3H_8)]/H^+$.

Analytic fitting function:

Erosion yield:

$$Y = A_1 \exp[-(\frac{T - A_2}{A_3 T + 1})^2 / A_4] T^{A_5} + A_6 \exp(-A_7 T) T^{A_8} \quad [\text{eroded C/H}^+]$$

where T is in Kelvin. The rms deviation of analytic fits for reactions A (•), B (○), C (□) and D (△) are 7.8%, 6.0%, 10.6% and 6.2%, respectively. Data for curves C and D were fitted with EYIELD7A.

Fitting parameters A_1-A_8

A	6.6450e-03	8.3279e+02	5.4517e-04	9.1549e+03	3.4461e-01	3.9358e-08
	1.2589e-03	1.9330e+00				
B	6.8038e-03	7.8021e+02	1.7815e-03	4.6389e+03	3.4814e-01	3.2982e-03
	4.5189e-05	2.9423e-02				
C	2.8805E-10	6.3646E+02	6.2961E+03	3.4945E+00	2.5076E-28	1.5279E-02
	1.1471E+01					
D	3.6998E-04	-1.2485E+03	1.8554E+06	1.5380E+00	3.7592E-69	4.8214E-02
	2.9162E+01					

ALADDIN evaluation function for erosion yield: EYIELD7A, EYIELD8A

ALADDIN hierarchical labelling:

A-D: SATM H{3} [+1] GRAPHITE T=CKC O=EDGE-PL C [+0]

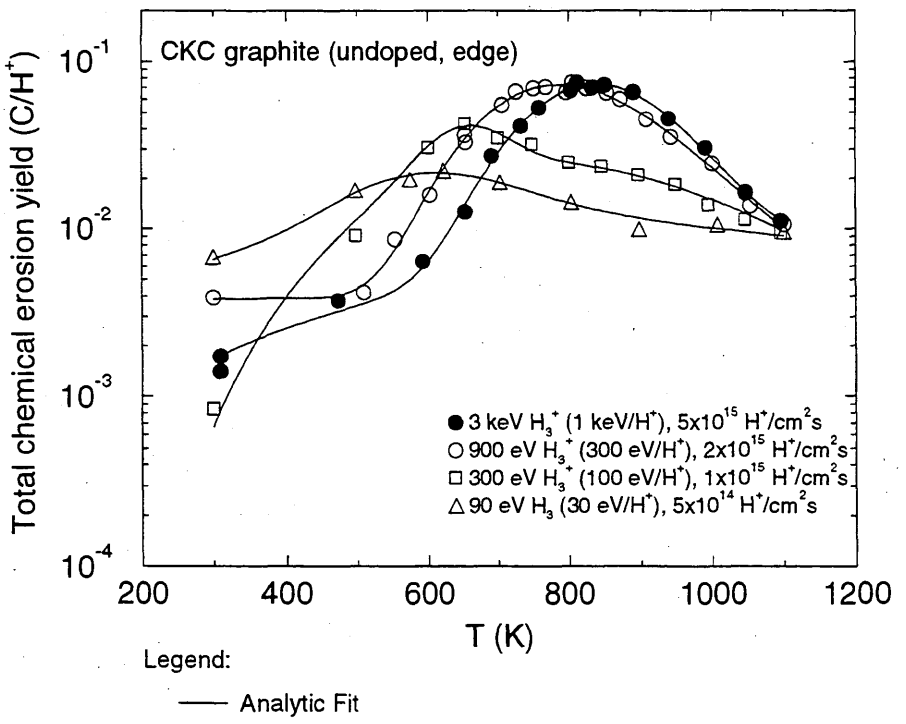

4.2.1.77 H_3^+ + CKC graphite → CH_4

Source: J. W. Davis and A. A. Haasz, J. Nucl. Mater., in press (1998).

Accuracy: Yield: ±20%; T: ±25K.

Comments: (1) Steady-state methane yield.
(2) Specimen: CKC undoped reference graphite. Specimens were cut in two orientations, 'edge' and 'base'.
(3) Incident ions were mass-analyzed.
(4) Reaction products measured by QMS-RGA.

Analytic fitting function:

Erosion yield:

$$Y = A_1 \exp[-(\frac{T - A_2}{A_3 T + 1})^2 / A_4] T^{A_5} + A_6 \exp(-A_7 T) T^{A_8} \quad [\text{molecules/H}^+]$$

where T is in Kelvin. The rms deviation of analytic fits for reactions A (•), B (○), C (□) and D (△) are 22.9%, 3.9%, 7.8% and 7.0%, respectively. Data for curves B and D were fitted with EYIELD7A.

Fitting parameters A_1-A_8

A	5.9337e-03	8.2737e+02	5.7254e-05	1.4998e+04	3.2970e-01	5.4248e-07
	-2.7841e-03	8.1147e-01				
B	1.2052E-02	7.8931E+02	4.8848E+03	7.1571E-01	3.7035E-90	4.6072E-02
	3.6531E+01					
C	1.1907E+02	7.0377E+02	7.7537E-01	5.1483E-02	-1.5902E+00	9.6074E-39
	2.0367E-02	1.4891E+01				
D	1.6453E-01	6.2535E+02	2.4201E+04	1.5058E-01	4.4877E-06	4.1442E-03
	2.1304E+00					

ALADDIN evaluation function for erosion yield: EYIELD7A, EYIELD8A

ALADDIN hierarchical labelling:

A-D: SATM H{3} [+1] GRAPHITE T=CKC O=BASE-PL CH{4} [+0]

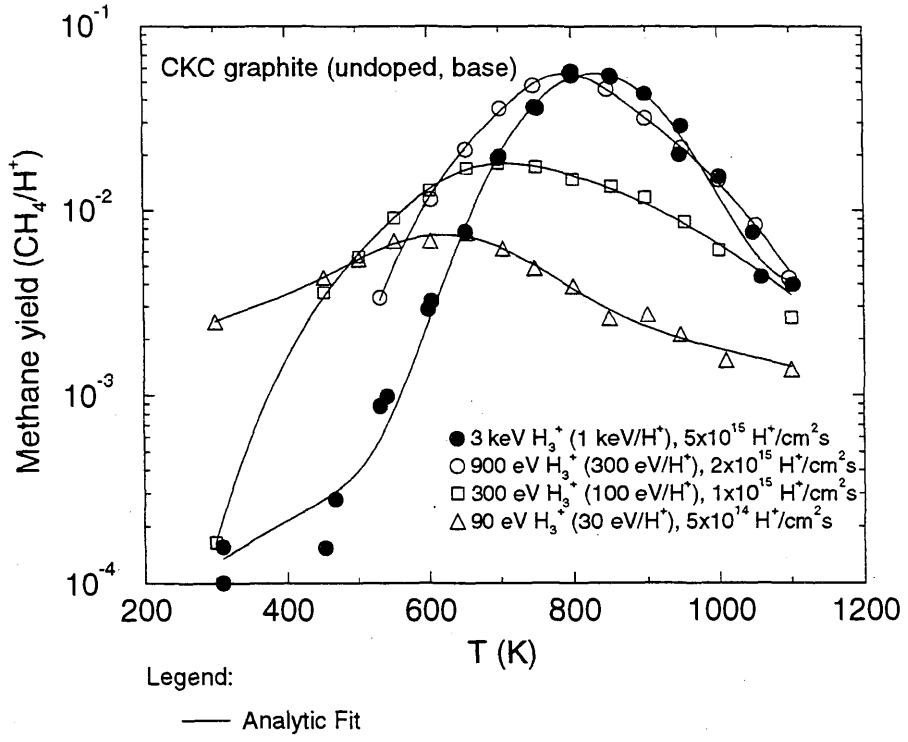

4.2.1.78 H_3^+ + CKC graphite → C

Source: J. W. Davis and A. A. Haasz, J. Nucl. Mater., in press (1998).

Accuracy: Yield: ±20%; T: ±25K.

Comments: (1) Steady-state hydrocarbon yield.
(2) Specimen: CKC undoped reference graphite. Specimens were cut in two orientations, 'edge' and 'base'.
(3) Incident ions were mass-analyzed.
(4) Reaction products measured by QMS-RGA.
(5) Yield for total chemical erosion, $Y_{chem-total} = [CH_4 + 2(C_2H_2 + C_2H_4 + C_2H_6) + 3(C_3H_6 + C_3H_8)]/H^+$.

Analytic fitting function:

Erosion yield:

$$Y = A_1 \exp[-(\frac{T - A_2}{A_3 T + 1})^2 / A_4] T^{A_5} + A_6 \exp(-A_7 T) T^{A_8} \quad [\text{eroded C/H}^+]$$

where T is in Kelvin. The rms deviation of analytic fits for reactions A (•), B (○), C (□) and D (△) are 12.4%, 4.4%, 7.5% and 14.0%, respectively. Data for curve D were fitted with EYIELD7A.

Fitting parameters A_1-A_8

A	6.2864e-03	8.2331e+02	2.9188e-04	1.1798e+04	3.3663e-01	2.8083e-03
	-2.6964e-03	-3.3050e-01				
B	1.9035E+03	7.9592E+02	3.1505E-03	2.1002E+03	-1.5293E+00	1.4057E-11
	4.3211E-03	3.4482E+00				
C	8.3579E+02	6.8680E+02	-4.5200E-03	4.4251E+03	-1.6351E+00	1.7667E-23
	1.2468E-02	8.6996E+00				
D	1.1186E+02	6.3102E+02	2.0284E+04	-6.7094E-01	7.5846E+02	-1.8064E-03
	-1.3222E+00					

ALADDIN evaluation function for erosion yield: EYIELD7A, EYIELD8A

ALADDIN hierarchical labelling:

A-D: SATM H{3} [+1] GRAPHITE T=CKC O=BASE-PL C [+0]

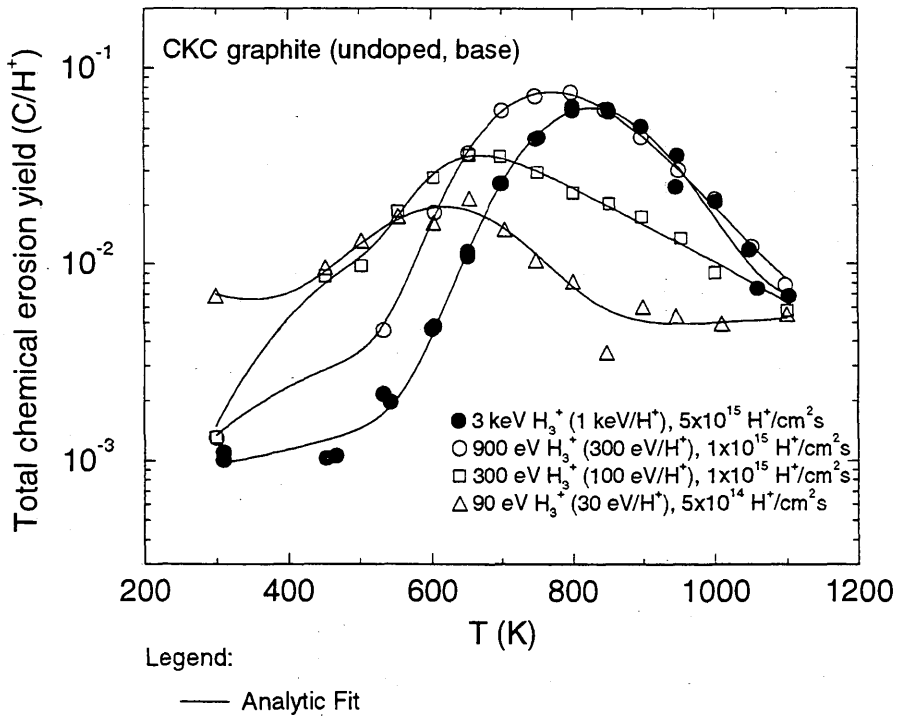

4.2.1.79 H_3^+ + CKC (TiB_2 doped) graphite → CH_4

Source: J. W. Davis and A. A. Haasz, J. Nucl. Mater., in press (1998).

Accuracy: Yield: ±20%; T: ±25K.

Comments: (1) Steady-state methane yield.
(2) Specimens were cut in two orientations, 'edge' and 'base', and doped with 10 at% TiB_2.
(3) Incident ions were mass-analyzed.
(4) Reaction products measured by QMS-RGA.

Analytic fitting function:

Erosion yield:

$$Y = A_1 \exp[-(\frac{T - A_2}{A_3 T + 1})^2 / A_4] T^{A_5} + A_6 \exp(-A_7 T) T^{A_8} \quad [\text{molecules/H}^+]$$

where T is in Kelvin. The rms deviation of analytic fits for reactions A (•), B (○), C (□) and D (△) are 16.5%, 9.7%, 5.0% and 30.5%, respectively.

Fitting parameters A_1-A_8

A	3.1850e-03	7.7399e+02	1.1732e+04	2.7023e-01	5.1213e-04	-8.0226e-02
	4.9147e-03	-1.7692e+00				
B	8.0086E+02	7.4336E+02	4.2670E-04	8.8221E+03	-1.6024E+00	4.7669E-12
	3.5803E-03	3.3846E+00				
C	4.9023E-05	6.4072E+02	5.2283E-04	2.0757E+04	8.2149E-01	2.1459E-06
	1.4639E-03	1.0774E+00				
D	9.0961E-01	1.6593E+03	5.5100E-03	5.3703E+03	-5.2414E+01	4.6650E-21
	1.3682E-02	7.7771E+00				

ALADDIN evaluation function for erosion yield: EYIELD8A

ALADDIN hierarchical labelling:

A-D: SATM H{3} [+1] GRAPHITE T=CKC O=EDGE-PL D=TiB{2} CH{4} [+0]

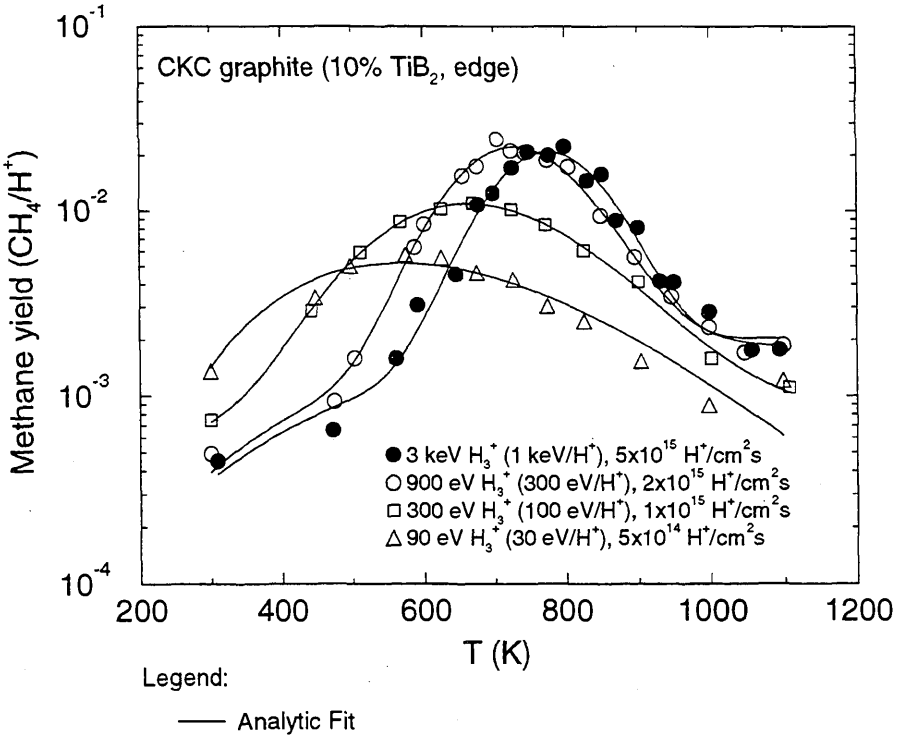

4.2.1.80 H_3^+ + CKC (TiB_2 doped) graphite → C

Source: J. W. Davis and A. A. Haasz, J. Nucl. Mater., in press (1998).

Accuracy: Yield: ±20%; T: ±25K.

Comments: (1) Steady-state hydrocarbon yield.
(2) Specimens were cut in two orientations, 'edge' and 'base', and doped with 10 at% TiB_2.
(3) Incident ions were mass-analyzed.
(4) Reaction products measured by QMS-RGA.
(5) Yield for total chemical erosion, $Y_{chem-total} = [CH_4 + 2(C_2H_2 + C_2H_4 + C_2H_6) + 3(C_3H_6 + C_3H_8)]/H^+$.

Analytic fitting function:

Erosion yield:

$$Y = A_1 \exp[-(\frac{T - A_2}{A_3 T + 1})^2 / A_4] T^{A_5} + A_6 \exp(-A_7 T) T^{A_8} \quad [\text{eroded/H}^+]$$

where T is in Kelvin. The rms deviation of analytic fits for reactions A (•), B (○), C (□) and D (△) are 11.8%, 13.2%, 5.2% and 11.5%, respectively.

Fitting parameters A_1-A_8

A	3.2628e-03	7.6736e+02	1.2552e+04	2.7681e-01	1.9240e-03	-9.4899e-02
	5.3337e-03	-2.0332e+00				
B	1.0505E-02	7.1510E+02	3.2785E-03	1.0876E+03	1.3242E-01	5.8129E-12
	4.5234E-03	3.6354E+00				
C	2.6717E-03	6.3633E+02	5.7005E-03	1.1629E+03	2.9689E-01	3.5460E-06
	3.4771E-03	1.3650E+00				
D	-3.9955E+01	4.8623E+03	2.1652E-01	3.1963E+02	-6.9818E-01	2.1838E-18
	4.4303E-03	6.2248E+00				

ALADDIN evaluation function for erosion yield: EYIELD8A

ALADDIN hierarchical labelling:

A-D: SATM H{3} [+1] GRAPHITE T=CKC O=EDGE-PL D=TiB{2} C [+0]

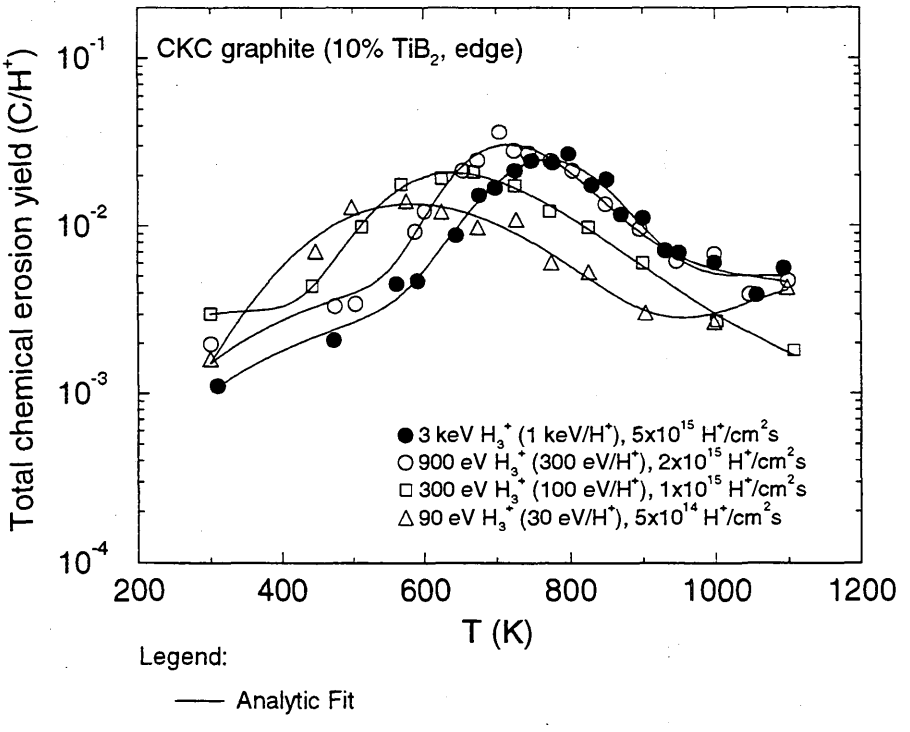

4.2.1.81 H_3^+ + CKC (TiB_2 doped) graphite → CH_4

Source: J. W. Davis and A. A. Haasz, J. Nucl. Mater., in press (1998).

Accuracy: Yield: ±20%; T: ±25K.

Comments: (1) Steady-state methane yield.
(2) Specimens were cut in two orientations, 'edge' and 'base', and doped with 10 at% TiB_2.
(3) Incident ions were mass-analyzed.
(4) Reaction products measured by QMS-RGA.

Analytic fitting function:

Erosion yield:

$$Y = A_1 \exp\left[-\left(\frac{T - A_2}{A_3 T + 1}\right)^2 / A_4\right] T^{A_5} + A_6 \exp(-A_7 T) T^{A_8} \quad [\text{molecules/H}^+]$$

where T is in Kelvin. The rms deviation of analytic fits for reactions A (•), B (○), C (□) and D (△) are 12.8%, 17.0%, 8.1% and 7.8%, respectively.

Fitting parameters A_1-A_8

A	3.9631e-03	7.8597e+02	4.4071e-04	6.2663e+03	2.4916e-01	9.0035e-06
	-3.8940e-04	6.9156e-01				
B	8.7593E+02	7.5219E+02	8.8561E-05	1.3314E+04	-1.6025E+00	4.6123E-18
	7.7043E-03	5.9703E+00				
C	4.7831E+02	6.9304E+02	1.3495E-03	4.9954E+03	-1.6893E+00	2.7923E-23
	1.3447E-02	8.5587E+00				
D	1.6269E-08	5.9365E+02	9.5822E-04	7.8209E+03	1.9340E+00	2.9184E-12
	8.0995E-03	4.0473E+00				

ALADDIN evaluation function for erosion yield: EYIELD8A

ALADDIN hierarchical labelling:

A-D: SATM H{3} [+1] GRAPHITE T=CKC O=BASE-PL D=TiB{2} CH{4} [+0]

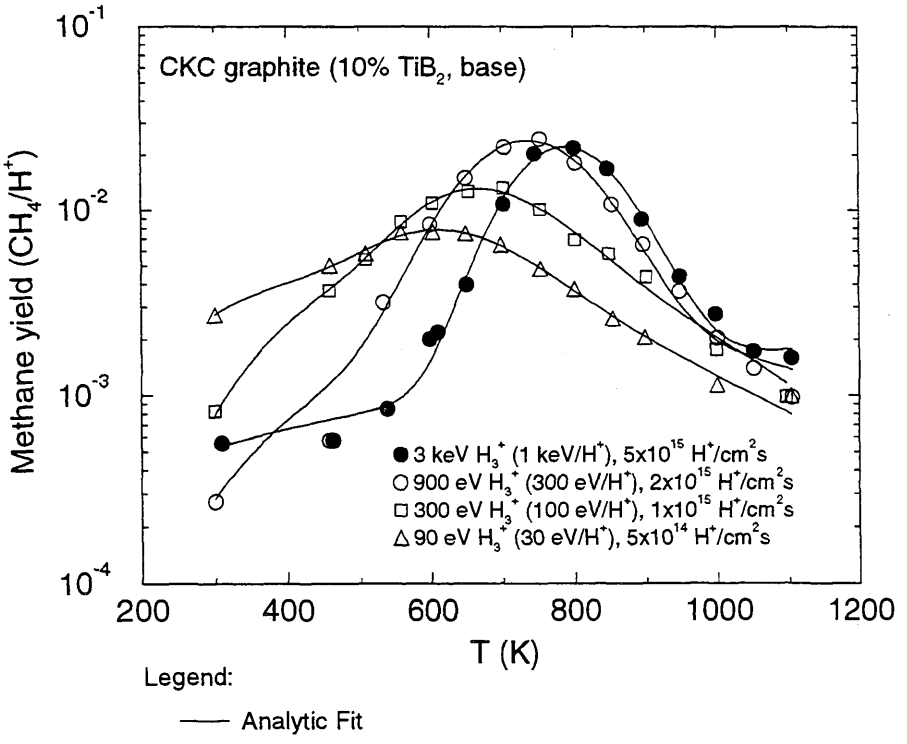

4.2.1.82 H_3^+ + CKC (TiB_2 doped) graphite → C

Source: J. W. Davis and A. A. Haasz, J. Nucl. Mater., in press (1998).

Accuracy: Yield: ±20%; T: ±25K.

Comments: (1) Steady-state hydrocarbon yield.
(2) Specimens were cut in two orientations, 'edge' and 'base', and doped with 10 at% TiB_2.
(3) Incident ions were mass-analyzed.
(4) Reaction products measured by QMS-RGA.
(5) Yield for total chemical erosion, $Y_{chem-total} = [CH_4 + 2(C_2H_2 + C_2H_4 + C_2H_6) + 3(C_3H_6 + C_3H_8)]/H^+$.

Analytic fitting function:

Erosion yield:

$$Y = A_1 \exp[-(\frac{T - A_2}{A_3 T + 1})^2 / A_4] T^{A_5} + A_6 \exp(-A_7 T) T^{A_8} \quad [\text{molecules}/H^+]$$

where T is in Kelvin. The rms deviation of analytic fits for reactions A (•), B (○), C (□) and D (△) are 16.6%, 13.1%, 13.9% and 12.5%, respectively.

Fitting parameters A_1-A_8

A	2.5185e-03	7.7750e+02	6.4636e-03	2.7176e+02	3.3151e-01	3.5190e-07
	1.3049e-03	1.5308e+00				
B	2.9441e-03	7.1560e+02	1.1492e-03	5.3949e+03	3.5400e-01	2.7671e-03
	-1.1151e-03	-2.1123e-01				
C	6.6639E+02	6.6753E+02	3.7250E-03	9.6430E+02	-1.6377E+00	2.0876E-16
	9.2404E-03	5.7677E+00				
D	2.4330e-03	6.1274e+02	-5.0842e-04	7.8790e+04	2.7313e-01	2.2245e-05
	1.7158e-03	9.1856e-01				

ALADDIN evaluation function for erosion yield: EYIELD8A

ALADDIN hierarchical labelling:

A-D: SATM H{3} [+1] GRAPHITE T=CKC O=BASE-PL D=TiB{2} C [+0]

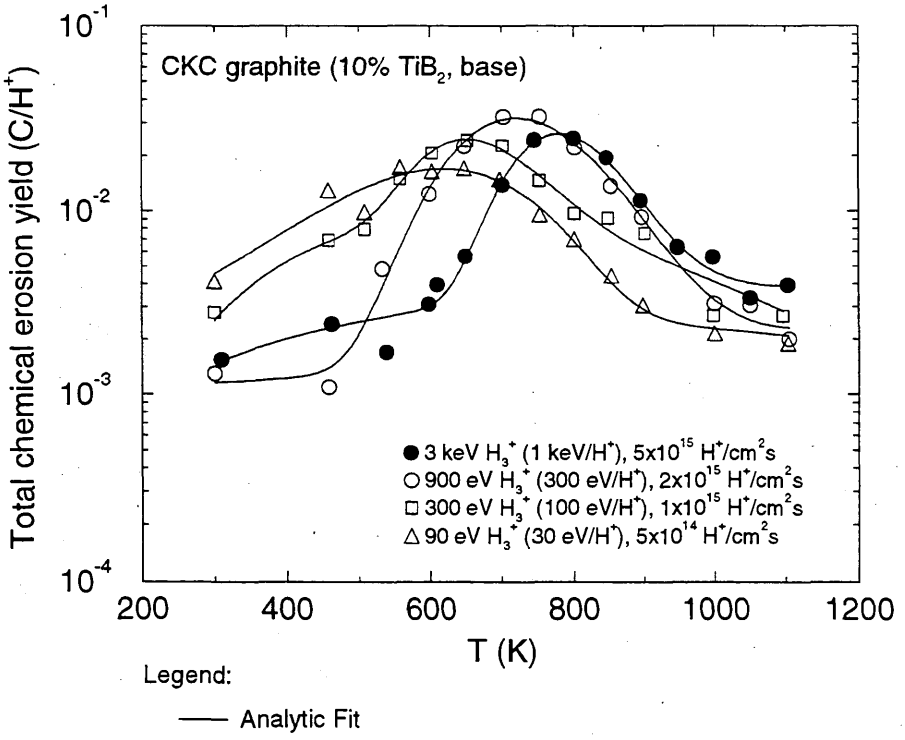

4.2.1.83 H_3^+ + CKC (TiB_2 doped) graphite → CH_4

Source: J. W. Davis and A. A. Haasz, J. Nucl. Mater., in press (1998).

Accuracy: Yield: ±20%; T: ±25K.

Comments: (1) Steady-state methane yield.
(2) Specimens were cut in two orientations, 'edge' and 'base', and doped with 20 at% TiB_2.
(3) Incident ions were mass-analyzed.
(4) Reaction products measured by QMS-RGA.

Analytic fitting function:

Erosion yield:

$$Y = 1.0 \times 10^{-2}[A_1 \exp(-(T - A_2)^2/A_3)T^{A_4} + A_5 \exp(-A_6 T)T^{A_7}] \quad [\text{molecules/H}^+]$$

where T is in Kelvin. The rms deviation of analytic fits for reactions A (•), B (○), C (□) and D (△) are 10.7%, 13.2%, 7.5% and 14.7%, respectively. Data for curves A and D were fitted with EYIELD8A.

Fitting parameters A_1-A_8

A	3.2095e-03	7.6099e+02	1.1862e+04	2.1600e-01	3.8242e-07	4.1261e-03
	1.2841e+00	3.1173e-08	2.9320e+00			
B	4.2126E-01	7.2639E+02	1.3404E+04	2.1908E-01	2.4022E-10	5.1965E-03
	3.6596E+00					
C	4.4878E-02	6.5410E+02	3.0228E+04	4.6661E-01	2.4579E-02	3.6934E-04
	2.1530E-01					
D	-1.3871E-12	8.0296E+02	2.1954E+01	1.8739E-04	3.3390E+00	6.1905E-13
	4.1205E-03	3.9967E+00				

ALADDIN evaluation function for erosion yield: EYIELD7A, EYIELD8A

ALADDIN hierarchical labelling:

A-D: SATM H{3} [+1] GRAPHITE T=CKC O=EDGE-PL D=TiB{2} CH{4} [+0]

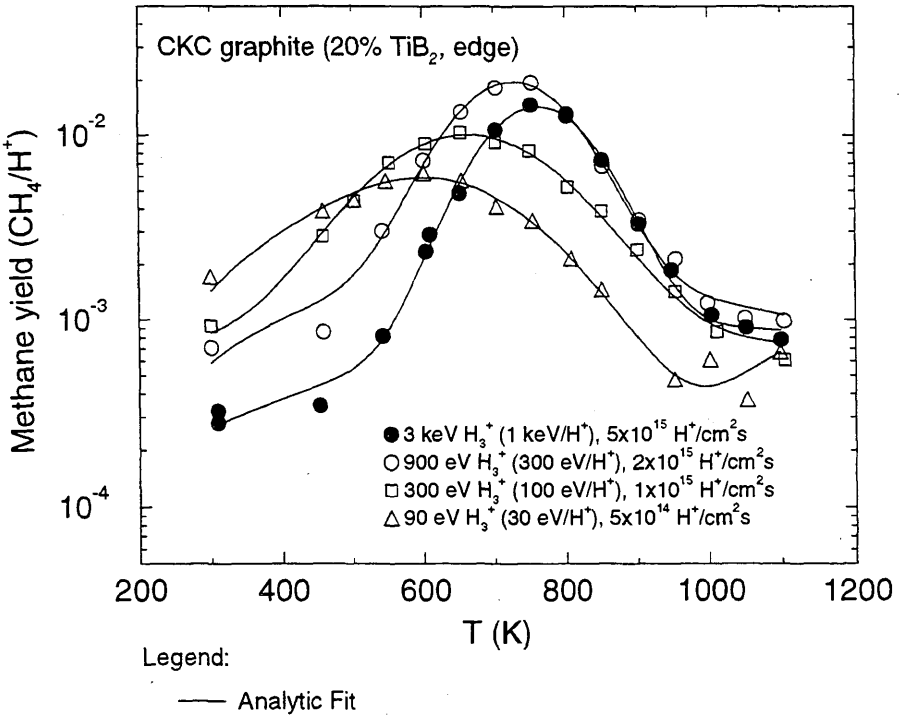

4.2.1.84 H_3^+ + CKC (TiB_2 doped) graphite → C

Source: J. W. Davis and A. A. Haasz, J. Nucl. Mater., in press (1998).

Accuracy: Yield: ±20%; T: ±25K.

Comments: (1) Steady-state hydrocarbon yield.
(2) Specimens were cut in two orientations, 'edge' and 'base', and doped with 20 at% TiB_2.
(3) Incident ions were mass-analyzed.
(4) Reaction products measured by QMS-RGA.
(5) Yield for total chemical erosion, $Y_{chem-total} = [CH_4 + 2(C_2H_2 + C_2H_4 + C_2H_6) + 3(C_3H_6 + C_3H_8)]/H^+$.

Analytic fitting function:

Erosion yield:

$$Y = 1.0 \times 10^{-2}[A_1 \exp(-(T - A_2)^2/A_3)T^{A_4} + A_5 \exp(-A_6T)T^{A_7}] \quad [\text{eroded C/H}^+]$$

where T is in Kelvin. The rms deviation of analytic fits for reactions A (•), B (○), C (□) and D (△) are 8.7%, 27.7%, 16.4% and 20.9%, respectively. Data for curves B and C were fitted with EYIELD9A.

Fitting parameters A_1-A_9

A	1.3296E-01	7.5684E+02	1.1561E+04	3.6668E-01	3.5207E-05	6.3551E-04
	1.3981E+00					
B	1.1684e-07	7.0939e+02	1.0820e+04	1.8622e+00	6.9568e-08	5.1324e-03
	9.2136e-01	1.8530e-05	2.9801e+00			
C	1.0668e-07	6.1558e+02	2.1392e+04	1.8450e+00	2.9220e-04	9.0608e-03
	8.4973e-01	1.0664e-16	6.1508e+00			
D	1.3314E-01	5.6145E+02	4.3271E+04	3.8800E-01	5.4527E-14	-1.5528E-03
	3.9840E+00					

ALADDIN evaluation function for erosion yield: EYIELD7A, EYIELD9A

ALADDIN hierarchical labelling:

A-D: SATM H{3} [+1] GRAPHITE T=CKC O=EDGE-PL D=TiB{2} C [+0]

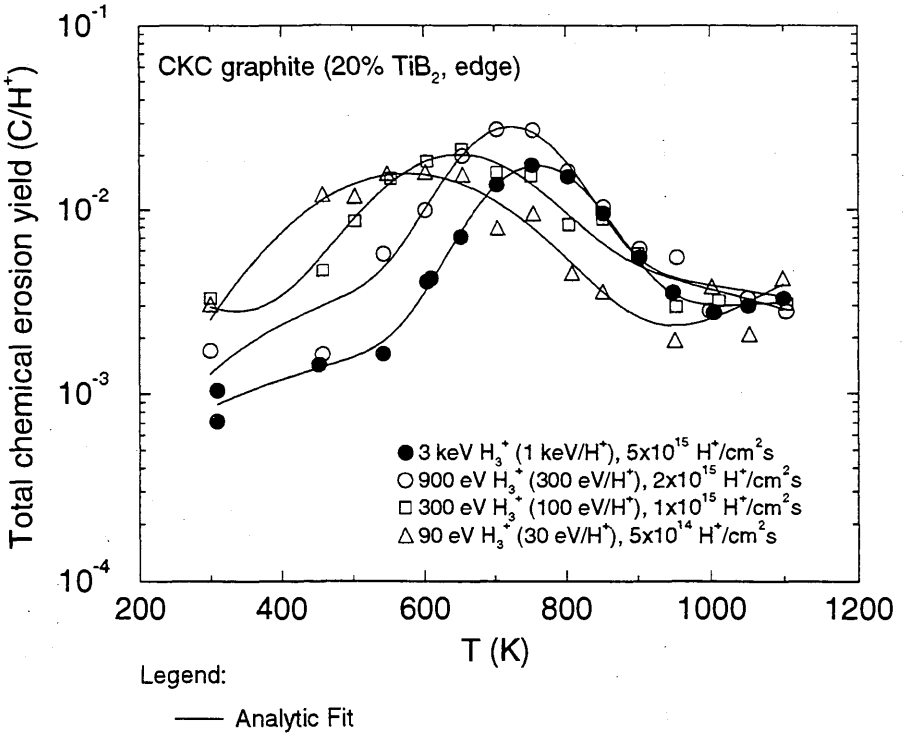

4.2.1.85 H_3^+ + CKC (TiB_2 doped) graphite → CH_4

Source: J. W. Davis and A. A. Haasz, J. Nucl. Mater., in press (1998).

Accuracy: Yield: ±20%; T: ±25K.

Comments: (1) Steady-state methane yield.
(2) Specimens were cut in two orientations, 'edge' and 'base', and doped with 20 at% TiB_2.
(3) Incident ions were mass-analyzed.
(4) Reaction products measured by QMS-RGA.

Analytic fitting function:

Erosion yield:

$$Y = A_1 \exp[-(\frac{T - A_2}{A_3 T + 1})^2 / A_4] T^{A_5} + A_6 \exp(-A_7 T) T^{A_8} \quad [\text{molecules/H}^+]$$

where T is in Kelvin. The rms deviation of analytic fits for reactions A (•), B (○), C (□) and D (△) are 14.9%, 6.1%, 7.1% and 8.8%, respectively. Data for curve C were fitted with EYIELD7A.

Fitting parameters A_1-A_8

A	7.2566E+02	7.9162E+02	2.7682E-04	1.0828E+04	-1.6270E+00	8.2897E-10
	1.7078E-03	2.2388E+00				
B	1.4798E-06	7.1579E+02	2.8555E-04	1.2495E+04	1.3941E+00	3.1643E-09
	2.7549E-03	2.2929E+00				
C	2.0974e-05	6.4356e+02	4.3286e+04	9.1311e-01	1.1970e+02	-3.9856e-03
	-2.4047e+00					
D	1.5950e-03	5.7688e+02	2.4198e+01	5.0000e-05	1.0030e-01	1.1354e-13
	8.5400e-03	4.5631e+00				

ALADDIN evaluation function for erosion yield: EYIELD7A, EYIELD8A

ALADDIN hierarchical labelling:

A-D: SATM H{3} [+1] GRAPHITE T=CKC O=BASE-PL D=TiB{2} CH{4} [+0]

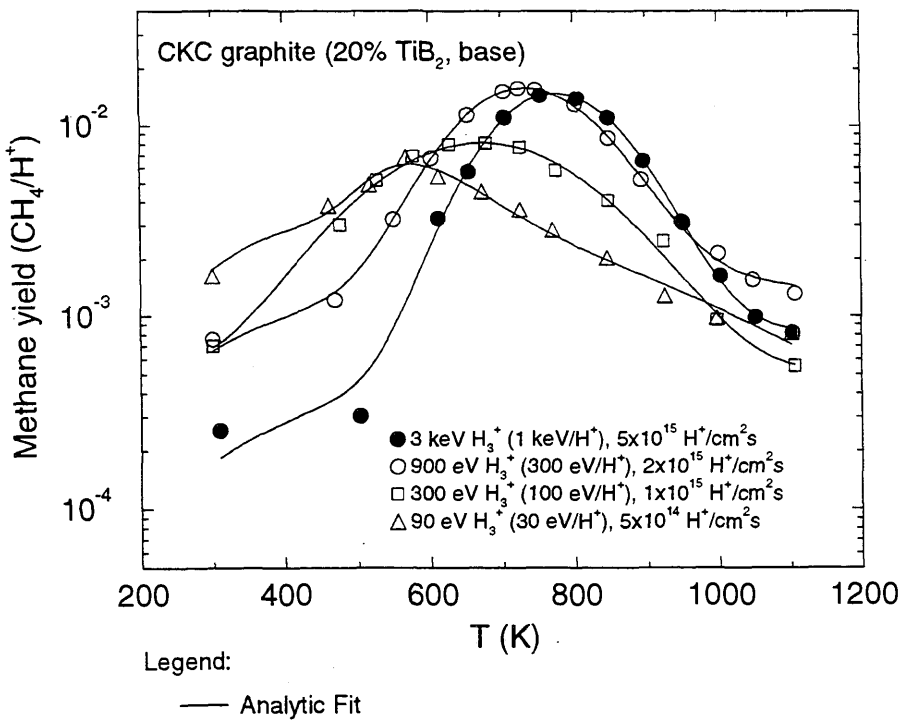

4.2.1.86 H_3^+ + CKC (TiB_2 doped) graphite → C

Source: J. W. Davis and A. A. Haasz, J. Nucl. Mater., in press (1998).

Accuracy: Yield: ±20%; T: ±25K.

Comments: (1) Steady-state hydrocarbon yield.
(2) Specimens were cut in two orientations, 'edge' and 'base', and doped with 20 at% TiB_2.
(3) Incident ions were mass-analyzed.
(4) Reaction products measured by QMS-RGA.
(5) Yield for total chemical erosion, $Y_{chem-total} = [CH_4 + 2(C_2H_2 + C_2H_4 + C_2H_6) + 3(C_3H_6 + C_3H_8)]/H^+$.

Analytic fitting function:

Erosion yield:

$$Y = A_1 \exp\left[-\left(\frac{T - A_2}{A_3 T + 1}\right)^2 / A_4\right] T^{A_5} + A_6 \exp(-A_7 T) T^{A_8} \quad [\text{eroded C/H}^+]$$

where T is in Kelvin. The rms deviation of analytic fits for reactions A (•), B (○), C (□) and D (△) are 6.7%, 5.3%, 35.7% and 14.9%, respectively. Data for curves C and D were fitted with EYIELD9A.

Fitting parameters A_1-A_9

A	1.7462E-07	7.5053E+02	7.0606E-04	6.7754E+03	1.7167E+00	4.2486E-08
	1.1107E-03	1.7011E+00				
B	1.3136E-06	7.0629E+02	1.3676E-03	4.1566E+03	1.4581E+00	3.9480E-10
	3.1652E-03	2.7229E+00				
C	2.5515e-03	6.4484e+02	2.6261e+04	2.4144e-01	6.4826e-09	5.0732e-03
	1.3512e+00	3.0084e-05	2.7309e+00			
D	1.5127e-03	5.9012e+02	1.2026e+04	2.1061e-01	5.4337e-11	1.1056e-02
	2.4584e+00	3.0518e-07	3.8606e+00			

ALADDIN evaluation function for erosion yield: EYIELD8A, EYIELD9A

ALADDIN hierarchical labelling:

A-D: SATM H [+1] GRAPHITE T=CKC O=BASE-PL D=TiB{2} C [+0]

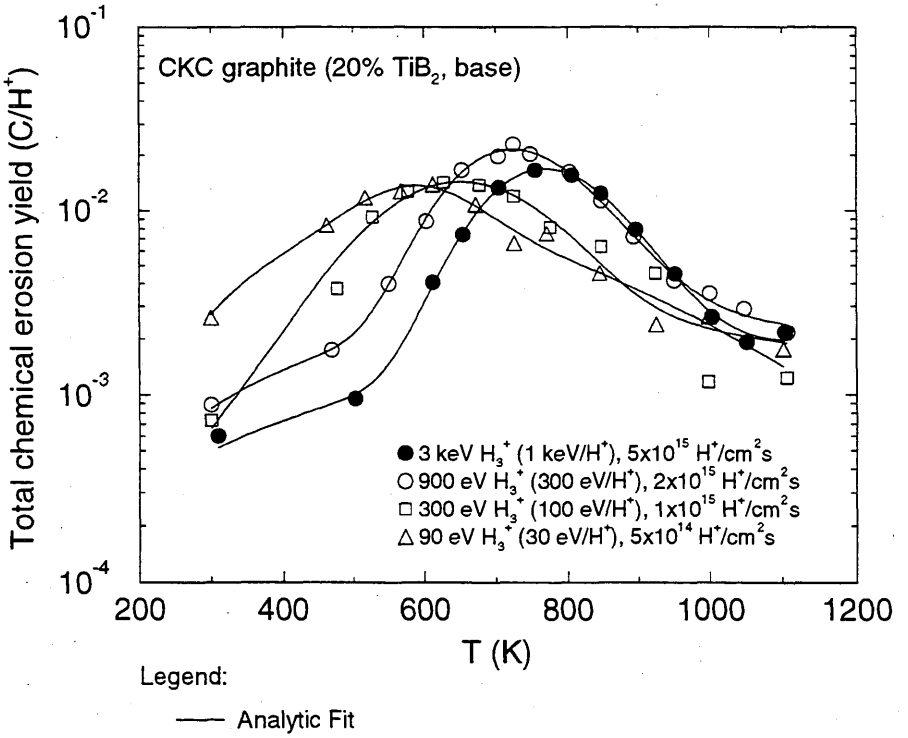

4.2.1.87 H_3^+ + TiC(CVD)/Mo → C

Source: R. Yamada, K. Nakamura, and M. Saidoh, J. Nucl. Mater. **111&112**, 744 (1982).

Accuracy: Yield (rel.): 20%.

Comments: (1) Steady-state methane yield.
(2) Specimen: CVD of titanium carbide on Mo, 20μm thick coating.
(3) H^+ ions: mass analyzed accelerator.
(4) Products measured via QMS-RGA.
(5) H^+ fluence > 10^{19} H^+/cm^2 required to reach steady state.

Analytic fitting function:

Chemical sputtering yield:

$$Y = 1.0 \times 10^{-3}[A_1 \exp(-A_2 E)E^{A_3} + A_4 E^{A_5}] \quad [\text{molecules}/H^+]$$

where E is in keV. The rms deviation of the analytic fit is 3.8%.

Fitting parameters A_1-A_5

3.4330e+00	3.1529e-01	3.9010e-01	7.4158e-01	4.2485e-01

ALADDIN evaluation function for chemical sputtering yield: EYIELD5A

ALADDIN hierarchical labelling:

SATM H{3} [+1] Mo T=CVD-TiC C [+0]

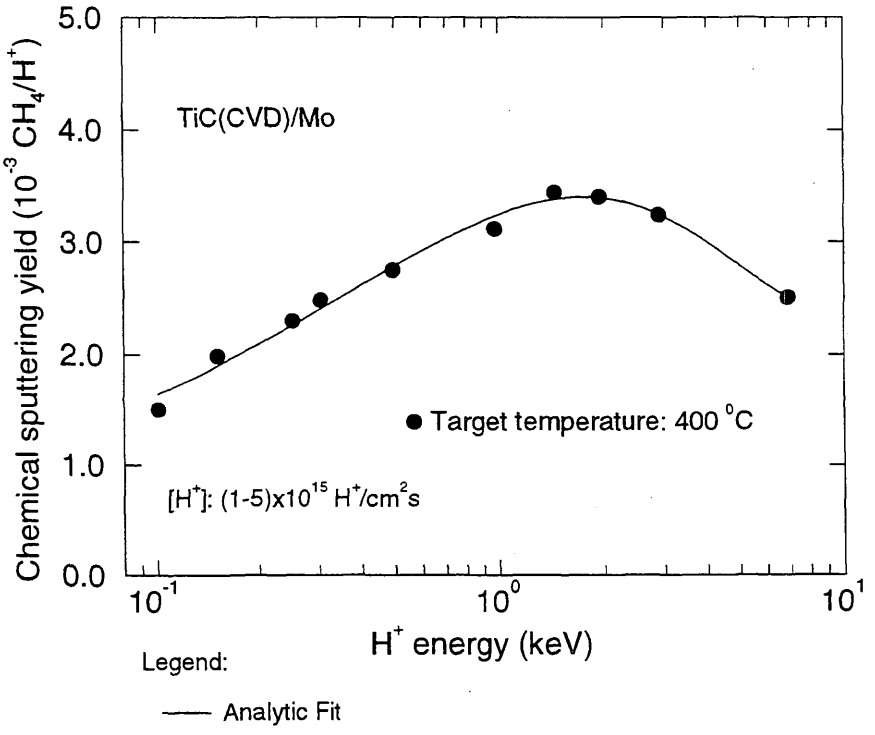

4.2.1.88 H_3^+ + TiC(CVD)/Mo → CH_4

Source: R. Yamada, K. Nakamura, and M. Saidoh, J. Nucl. Mater. **111&112**, 744 (1982).

Accuracy: Yield (rel.): 20%.

Comments: (1) Steady-state methane yield.
(2) Specimen: CVD of titanium carbide on Mo, 20μm thick coating.
(3) H_3^+ ions: mass analyzed accelerator.
(4) Methane measured via QMS-RGA.
(5) H^+ fluence > 10^{19} H^+/cm^2 was required to reach steady state.
(6) Flux density ranged from 1×10^{15} to 5×10^{15} H^+/cm^2s depending on ion energy.

Analytic fitting function:

Methane yield:

$$Y = 1.0 \times 10^{-3}[A_1 \exp[-(\frac{T - A_2}{A_3 T + 1})^2 / A_4] T^{A_5} + A_6 \exp(-A_7 T) T^{A_8}] \quad [\text{molecules/H}^+]$$

where T is in ^{0}C. The rms deviation of the analytic fits for reaction A (•) and B (□) are 0.7% and 1.2%, respectively.

Fitting parameters A_1-A_8

A	6.1844e+04	5.5079e+02	-7.0142e-04	2.4073e+04	-1.8095e+00	5.2551e+00
	-5.3551e-04	-1.3078e-01				
B	3.1647e+01	9.1072e+02	9.0700e-02	6.1360e+01	-5.3513e-01	1.8275e+00
	5.1403e-04	-1.9661e-02				

ALADDIN evaluation function for methane yield: EYIELD8A

ALADDIN hierarchical labelling:

A, B: SATM H{3} [+1] Mo T=CVD-TiC CH{4} [+0]

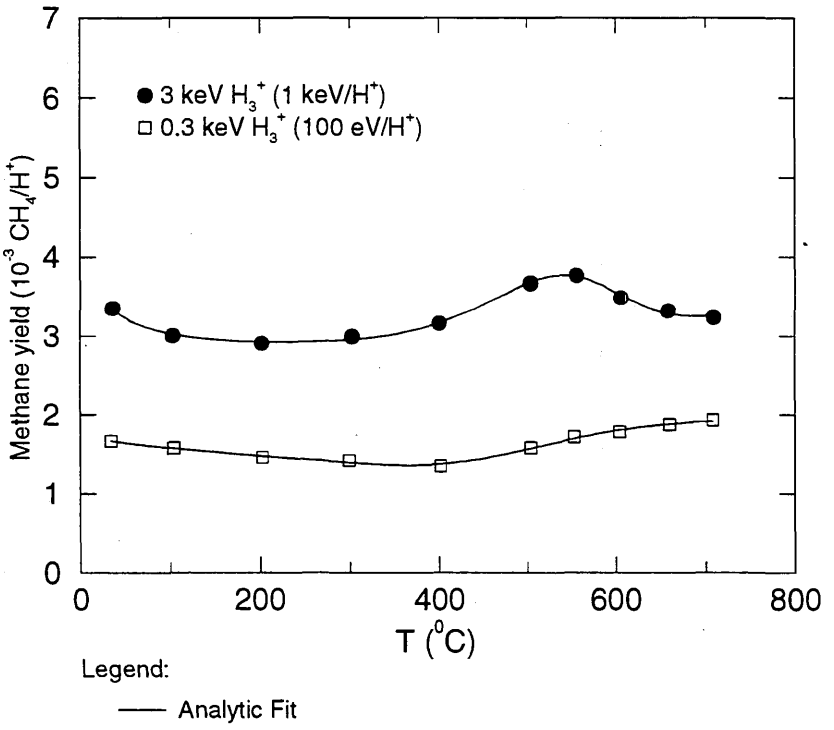

4.2.1.89 H_3^+ + TiC(CVD, PVD)/Mo, POCO graphite → CH_4

Source: R. Yamada, K. Nakamura, and M. Saidoh, J. Nucl. Mater. **111&112**, 744 (1982).

Accuracy: Yield (rel.): 20%.

Comments: (1) Steady-state methane yield.
(2) Specimens: CVD and PVD of titanium carbide on Mo, 20μm thick coating. CVD of TiC on Poco graphite (AXF-5Q), 20μm thick coating. Sintered TiC.
(3) H_3^+ ions: mass analyzed accelerator.
(4) Methane measured via QMS-RGA.
(5) H^+ fluence > 10^{19} H^+/cm^2 was required to reach steady state.

Analytic fitting function:

Methane yield:

$$Y = 1.0 \times 10^{-3}[A_1 \exp(-(T - A_2)^2/A_3)T^{A_4} + A_5 \exp(-A_6 T)T^{A_7}] \quad [\text{molecules/H}^+]$$

where T is in ^{0}C. The rms deviation of the analytic fit for reactions A(•), B (○), C (□) and D (△) are 2.3%, 1.1%, 0.9% and 1.0%, respectively.

Fitting parameters A_1-A_7

A	5.6954e-05	6.4610e+02	1.6824e+04	1.3676e+00	9.6211e+00	-3.5830e-04
	-2.4789e-01					
B	1.8546e+14	6.2953e+02	2.2679e+04	-5.2014e+00	4.5357e+00	-2.4960e-04
	-7.0120e-02					
C	1.7512e+29	6.2153e+02	9.6907e+03	-1.0646e+01	5.2912e+00	-4.8722e-04
	-1.2834e-01					
D	3.7406e+03	6.0382e+02	4.3054e+04	-1.3264e+00	2.6182e+00	-1.7191e-05
	-2.2911e-02					

ALADDIN evaluation function for methane yield: EYIELD7A

ALADDIN hierarchical labelling:

A: SATM H{3} [+1] Mo T=CVD-TiC CH{4} [+0]
B: SATM H{3} [+1] Mo T=PVD-TiC CH{4} [+0]
C: SATM H{3} [+1] GRAPHITE T=CVD-TiC CH{4} [+0]
D: SATM H{3} [+1] TiC CH{4} [+0]

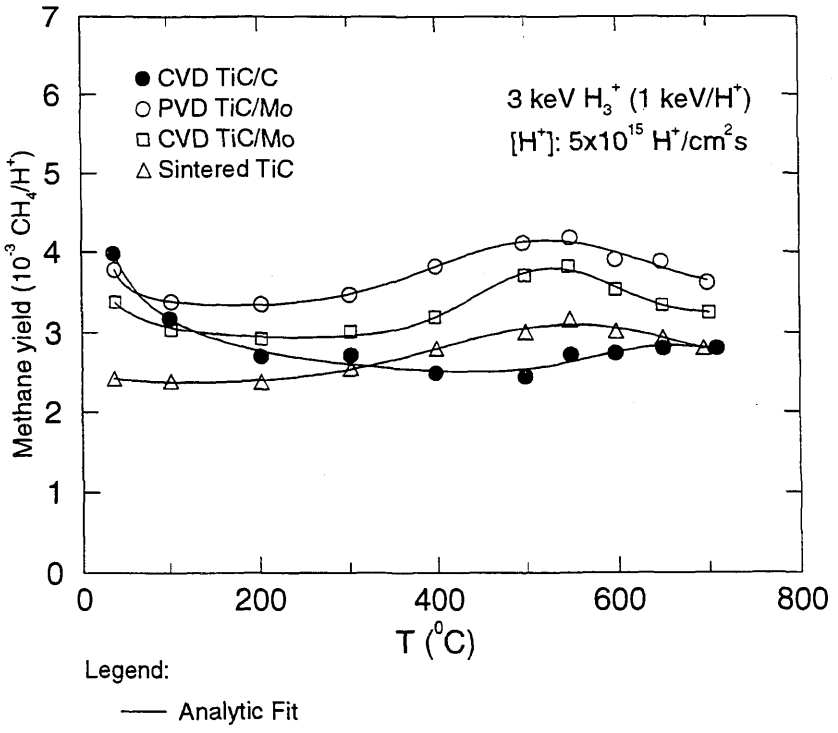

4.2.1.90 H_3^+ + isotropic graphite (B doped) → C

Source: T. Hino, K. Ishio, Y. Hirohata, T. Yamashina, T. Sogabe, M. Okada and K. Kuroda, J. Nucl. Mater. **211**, 30 (1994).

Accuracy: Yield: Indeterminate.

Comments: (1) Yield for total erosion measured by mass loss.
(2) Experiments used an electron cyclotron resonance hydrogen ion apparatus.
(3) Specimen: Boron-doped isotropic graphite (GB-series, Toyo Tanso).
(4) H_3^+ ions: mass analyzed accelerator.

Analytic fitting function:

Erosion yield:

$$Y = A_1 \exp[-(\frac{T - A_2}{A_3 T + 1})^2 / A_4] T^{A_5} + A_6 \exp(-A_7 T) T^{A_8} \quad [\mathrm{C/H^+}]$$

where T is in ^{0}C. The rms deviation of analytic fits for reactions A and B (○), and C (◇, △, □) are 6.8% and 3.3%, respectively. Data for 0 wt%B (curves A and B) were represented by two fits: 300-500 ^{0}C, parameter set A; 500-1800 ^{0}C, parameter set B. Points at 0 ^{0}C were not included in the fits.

Fitting parameters A_1-A_8

A	5.6451e-03	5.2628e+02	-2.6095e-03	3.6165e+05	2.8693e-01	1.3284e-08
	-2.7253e-03	2.3089e+00				
B	4.5564e+10	6.2090e+02	2.6217e-04	1.3870e+04	-4.1789e+00	1.1788e-01
	-2.8819e-03	-6.1292e-01				
C	1.1896e-02	5.5170e+02	-2.8195e-04	1.0510e+05	1.5191e-01	1.5293e-10
	-1.3820e-03	2.4970e+00				

ALADDIN evaluation function for erosion yield: EYIELD8A

ALADDIN hierarchical labelling:

A, B: SATM H{3} [+1] GRAPHITE T=HPG-ISO C [+0]
C: SATM H{3} [+1] GRAPHITE T=HPG-ISO D=B C [+0]

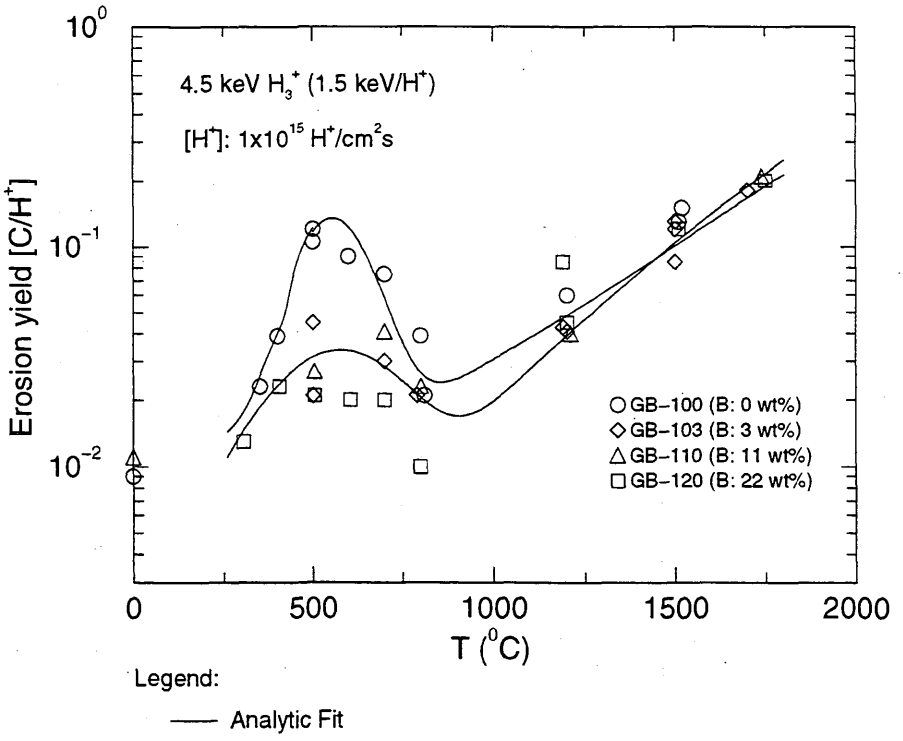

4.2.1.91 H_3^+ + isotropic graphite (V doped) → C

Source: T. Hino, K. Ishio, Y. Hirohata, T. Yamashina, T. Sogabe, M. Okada and K. Kuroda, J. Nucl. Mater. **211**, 30 (1994).

Accuracy: Yield: Indeterminate.

Comments: (1) Yield for total erosion measured by mass loss.
(2) Experiments used an electron cyclotron resonance hydrogen ion apparatus.
(3) Specimen: Vanadium-doped isotropic graphite (GC-series, Toyo Tanso).
(4) H_3^+ ions: mass analyzed accelerator.

Analytic fitting function:

Erosion yield:

$$Y = A_1 \exp\left[-\left(\frac{T - A_2}{A_3 T + 1}\right)^2 / A_4\right] T^{A_5} + A_6 \exp(-A_7 T) T^{A_8} \quad [\mathrm{C/H^+}]$$

where T is in ^{0}C. The rms deviation of analytic fits for reactions A (○, ◇), and B (□, △, •, ×) are 16.3% and 2.2%, respectively.

Fitting parameters A_1-A_8

A	1.7857e+04	5.8427e+02	6.9150e-04	9.2729e+03	-1.8593e+00	1.4576e+00
	-3.4614e-03	-1.0671e+00				
B	5.7909e-03	5.6197e+02	8.0551e-04	1.9246e+04	4.0116e-01	6.0402e-10
	-1.3618e-03	2.3853e+00				

ALADDIN evaluation function for erosion yield: EYIELD8A

ALADDIN hierarchical labelling:

A: SATM H{3} [+1] GRAPHITE T=HPG-ISO C [+0]
B: SATM H{3} [+1] GRAPHITE T=HPG-ISO D=V C [+0]

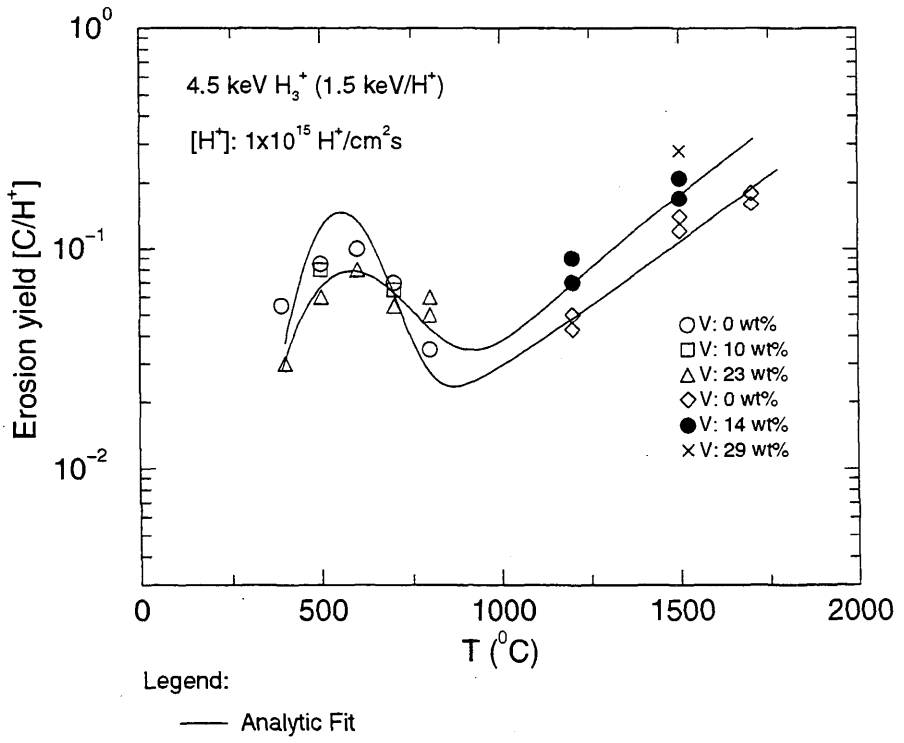

4.2.1.92 H_2^+, H_3^+ + pyrolytic graphite → C

Source: J. Roth, J. Bohdansky, W. Poschenrieder and M. K. Sinha, J. Nucl. Mater. **63**, 222 (1976).

Accuracy: Yield (rel.): ±15%; Yield (abs.): ±30%.

Comments: (1) Weight loss measurement.
(2) Specimen: graphite (pyrolytic).
(3) Mass-analyzed ion beams.

Analytic fitting function:

Sputtering yield:

$$Y = 10^{-2}[A_1 \exp[-(\frac{T - A_2}{A_3 T + 1})^2 / A_4] T^{A_5} + A_6 \exp(-A_7 T) T^{A_8}] \quad \text{[atoms/ion]}$$

where T is in ^{0}C. The rms deviation of the analytic fits for reactions A (•), B (○), C (△) and D (×) are 33.5%, 19.5%, 6.8% and 0.5%, respectively.

Fitting parameters A_1-A_8

A	1.4451E-01	6.2718E+02	1.0342E-02	8.7132E+01	4.2511E-01	1.3518E-18
	1.2417E-02	7.6199E+00				
B	4.9327E-01	6.2542E+02	-6.3272E-04	2.6151E+04	3.7564E-01	1.6684E-13
	4.8613E-03	5.1774E+00				
C	4.6334E-01	6.6695E+02	-7.8242E-04	1.2182E+04	3.1894E-01	1.8748E-12
	4.4681E-03	4.7690E+00				
D	2.5331E-01	6.1313E+02	-4.5355E-05	2.6301E+04	5.4130E-01	1.7765E-11
	5.8358E-02	7.5124E+00				

ALADDIN evaluation function for sputtering yield: EYIELD8A

ALADDIN hierarchical labelling:

A: SATM H{2} [+1] GRAPHITE T=HPG C [+0]
B-D: SATM H{3} [+1] GRAPHITE T=HPG C [+0]

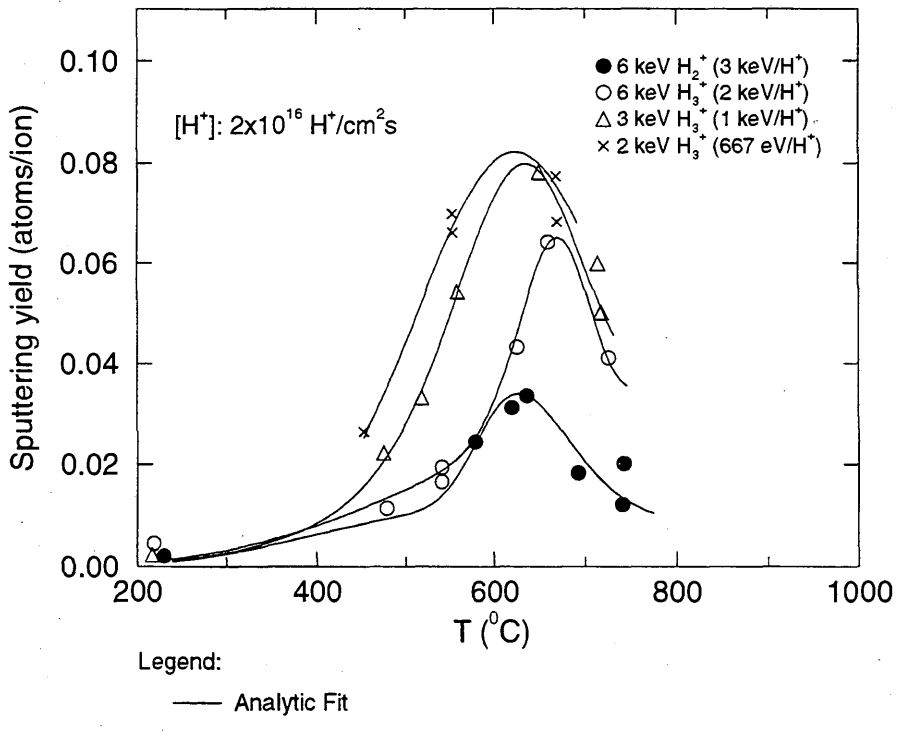

4.2.1.93 H^+, H_3^+ + isotropic graphite → CH_4

Source: R. Yamada, K. Nakamura, K. Sone and M. Saidoh, J. Nucl. Mater. **95**, 278 (1980).

Accuracy: Indeterminate.

Comments: (1) Steady-state methane yield.
(2) Specimen: isotropic graphite (7477PT).
(3) H^+ ions: mass analyzed accelerator.
(4) Methane measured via QMS-RGA.

Analytic fitting function:

Methane yield:

$$Y = 1.0 \times 10^{-4}[A_1 \exp(-(T - A_2)^2/A_3)T^{A_4} + A_5 \exp(-A_6 T)T^{A_7}] \quad [\text{molecules/H}^+]$$

where T is in ^{0}C. The rms deviation of analytic fits for reactions A (×) and B (□) are 6.1% and 3.2%, respectively.

Fitting parameters A_1-A_7

A	5.2647E+02	5.1917E+02	1.3892E+04	-1.7795E-02	5.9208E+01	-1.4670E-03
	-4.7983E-02					
B	2.0871E+02	5.5172E+02	2.0927E+04	-7.1164E-02	1.0366E+00	1.9199E-03
	8.9068E-01					

ALADDIN evaluation function for methane yield: EYIELD7A

ALADDIN hierarchical labelling:

A: SATM H [+1] GRAPHITE T=HPG-ISO CH{4} [+0]
B: SATM H{3} [+1] GRAPHITE T=HPG-ISO CH{4} [+0]

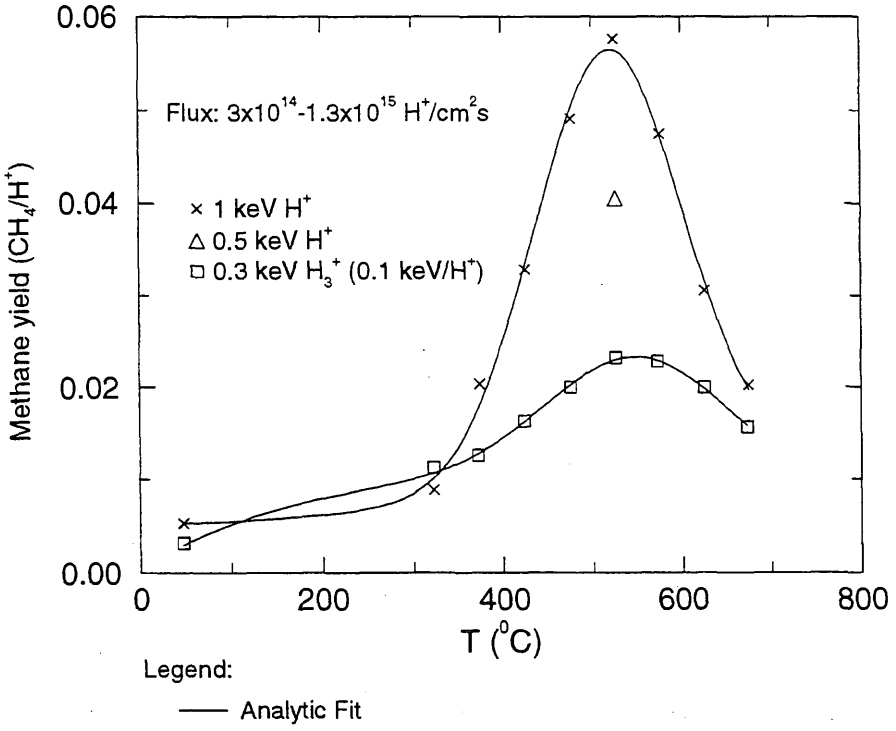

4.2.1.94 H^+, H_2^+, H_3^+ + pyrolytic graphite → CH_4

Source: R. Yamada, K. Nakamura, K. Sone and M. Saidoh, J. Nucl. Mater. **95**, 278 (1980).

Accuracy: Indeterminate.

Comments: (1) Steady-state methane yield.
(2) Specimen: graphite (pyrolytic, HPG, edge plane).
(3) H^+ ions: mass analyzed accelerator.
(4) Methane measured via QMS-RGA.

Analytic fitting function:

Methane yield:

$$Y = 1.0 \times 10^{-4}[A_1 \exp(-(T - A_2)^2/A_3)T^{A_4} + A_5 \exp(-A_6 T)T^{A_7}] \quad [\text{molecules/H}^+]$$

where T is in ^{0}C. The rms deviation of analytic fits for reactions A (×) and B (□) are 2.5% and 2.0%, respectively.

Fitting parameters A_1-A_7

A	3.0954E+03	5.2025E+02	1.2345E+04	-2.7996E-01	4.4960E+02	-2.6830E-03
	-3.7587E-01					
B	6.7249E+02	5.0987E+02	5.3535E+04	-1.9324E-01	1.8610E+01	3.2809E-03
	4.4219E-01					

ALADDIN evaluation function for methane yield: EYIELD7A

ALADDIN hierarchical labelling:

A: SATM H [+1] GRAPHITE T=HPG O=EDGE-PL CH{4} [+0]
B: SATM H{3} [+1] GRAPHITE T=HPG O=EDGE-PL CH{4} [+0]

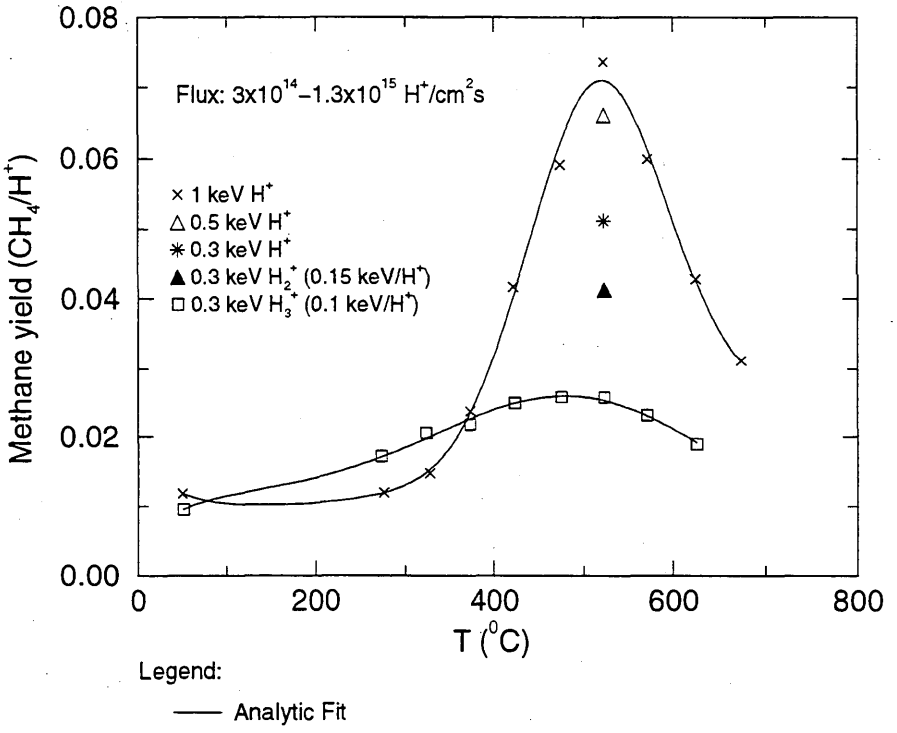

4.2.1.95 H^+, H_2^+, H_3^+ + pyrolytic graphite → CH_4

Source: R. Yamada, K. Nakamura, K. Sone and M. Saidoh, J. Nucl. Mater. **95**, 278 (1980).

Accuracy: Indeterminate.

Comments: (1) Steady-state methane yield.
(2) Specimen: graphite (pyrolytic, HPG, basal plane).
(3) H^+ ions: mass analyzed accelerator.
(4) Methane measured via QMS-RGA.

Analytic fitting function:

Methane yield:

$$Y = 1.0 \times 10^{-4}[A_1 \exp(-(T - A_2)^2/A_3)T^{A_4} + A_5 \exp(-A_6 T)T^{A_7}] \quad [\text{molecules/H}^+]$$

where T is in ^{0}C. The rms deviation of analytic fits for reactions A (×) and B (□) are 1.2% and 1.4%, respectively.

Fitting parameters A_1-A_7

A	1.6121E+03	5.0544E+02	1.3936E+04	-1.6832E-01	2.4312E+02	-1.3056E-03
	-1.3373E-01					
B	4.8605E+02	5.5623E+02	9.8597E+04	-9.2979E-02	8.8662E+01	2.8443E-03
	1.3886E-01					

ALADDIN evaluation function for methane yield: EYIELD7A

ALADDIN hierarchical labelling:

A, B: SATM H [+1] GRAPHITE T=HPG O=BASAL-PL CH{4} [+0]

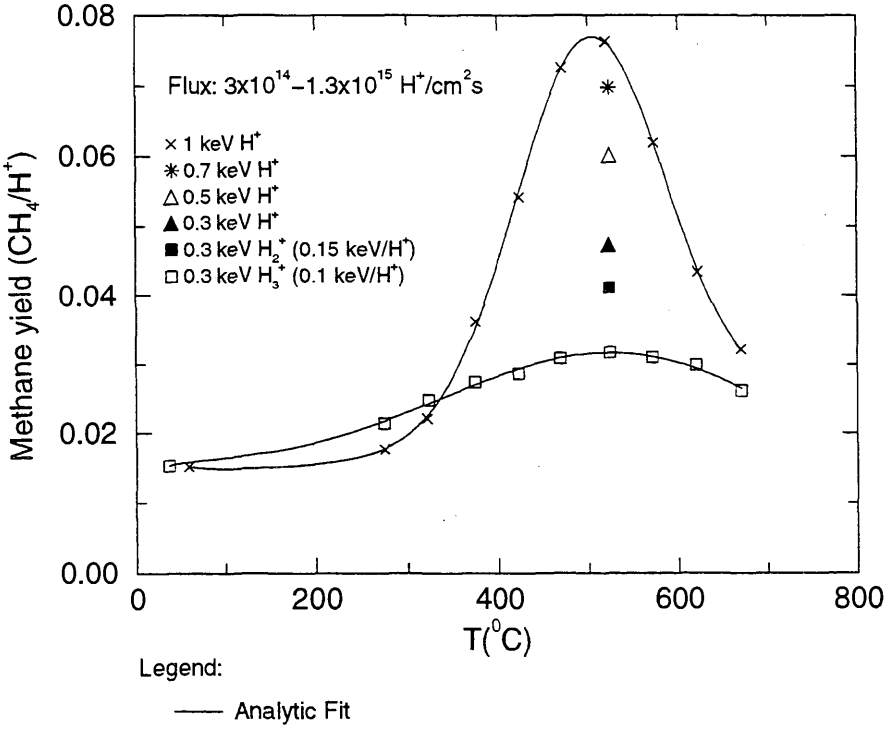

4.2.1.96 H^+, H_3^+ + PG-A graphite → CH_4

Source: R. Yamada, K. Nakamura, K. Sone and M. Saidoh, J. Nucl. Mater. **95**, 278 (1980).

Accuracy: Indeterminate.

Comments: (1) Steady-state methane yield.
(2) Specimen: graphite (pyrolytic, PG-A, basal plane (Nippon Carbon)).
(3) H^+ ions: mass analyzed accelerator.
(4) Methane measured via QMS-RGA.

Analytic fitting function:

Methane yield:

$$Y = 1.0 \times 10^{-4}[A_1 \exp(-(T - A_2)^2/A_3)T^{A_4} + A_5 \exp(-A_6 T)T^{A_7}] \quad [\text{molecules/H}^+]$$

where T is in ^{0}C. The rms deviation of analytic fits for reactions A (×), B (△), C (□) and D (•) are 5.8%, 1.7%, 6.8% and 2.8%, respectively.

Fitting parameters A_1-A_7

A	9.0406E+02	5.1643E+02	1.2099E+04	-9.3459E-02	1.2636E+02	-2.0684E-03
	-1.3319E-01					
B	2.6424E+02	5.1787E+02	8.5407E+03	-1.8765E-02	3.7746E+01	-1.5588E-03
	1.1368E-01					
C	4.4002E+01	5.0775E+02	1.4837E+04	2.2920E-01	2.8215E+02	-4.2607E-03
	-5.1282E-01					
D	2.7152E+02	5.1166E+02	9.6675E+03	-3.7328E-02	8.3509E+00	5.9013E-04
	3.7338E-01					

ALADDIN evaluation function for methane yield: EYIELD7A

ALADDIN hierarchical labelling:

A-D: SATM H [+1] GRAPHITE T=PGA O=BASAL-PL CH{4} [+0]

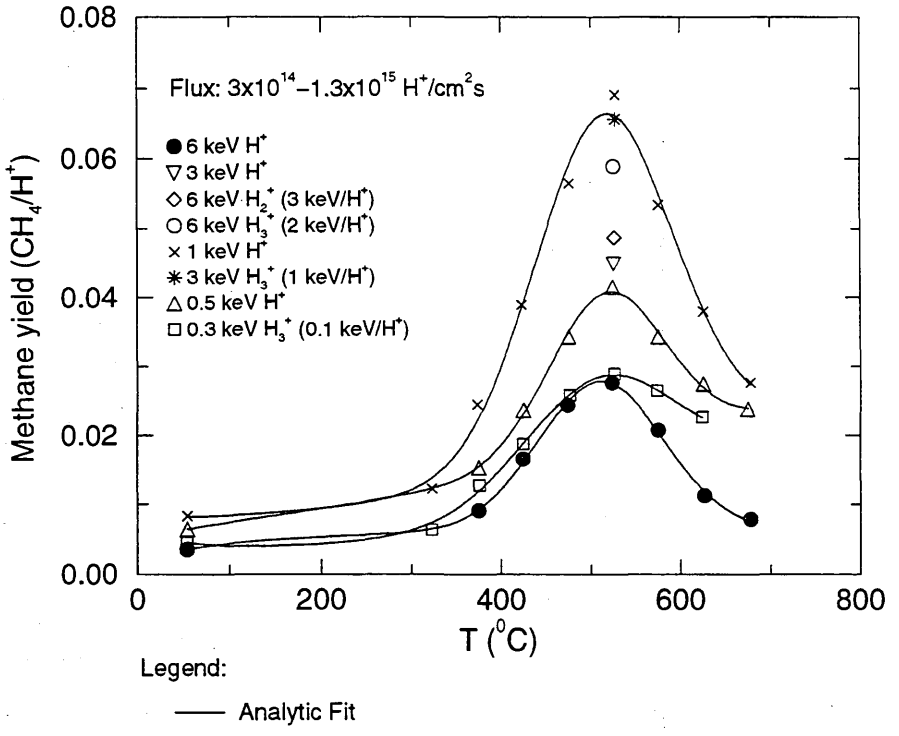

4.2.1.97 H^+, H_3^+ + GC-30 glassy carbon → CH_4

Source: R. Yamada, K. Nakamura and M. Saidoh, J. Nucl. Mater. **95**, 278 (1980).

Accuracy: Indeterminate.

Comments: (1) Steady-state methane yield.
(2) Specimen: glassy carbon (GC-30).
(3) H^+ ions: mass analyzed accelerator.
(4) Methane measured via QMS-RGA.

Analytic fitting function:

Methane yield:

$$Y = 1.0 \times 10^{-4}[A_1 \exp(-(T - A_2)^2/A_3)T^{A_4} + A_5 \exp(-A_6 T)T^{A_7}] \quad \text{[molecules/ion]}$$

where T is in ^{0}C. The rms deviation of the analytic fits for reactions A (×) and B (□) are 6.7% and 1.6%, respectively.

Fitting parameters A_1-A_7

A	1.8734E+00	5.1255E+02	1.5877E+04	9.0991E-01	1.2700E+02	-3.1443E-03
	-1.9791E-01					
B	2.6182E+02	5.3807E+02	2.6919E+04	-3.9363E-02	4.3970E+00	1.1714E-03
	5.9757E-01					

ALADDIN evaluation function for methane yield: EYIELD7A

ALADDIN hierarchical labelling:

A: SATM H [+1] C T=GLASSYC-GC-30 CH{4} [+0]
B: SATM H{3} [+1] C T=HPG-ISO CH{4} [+0]

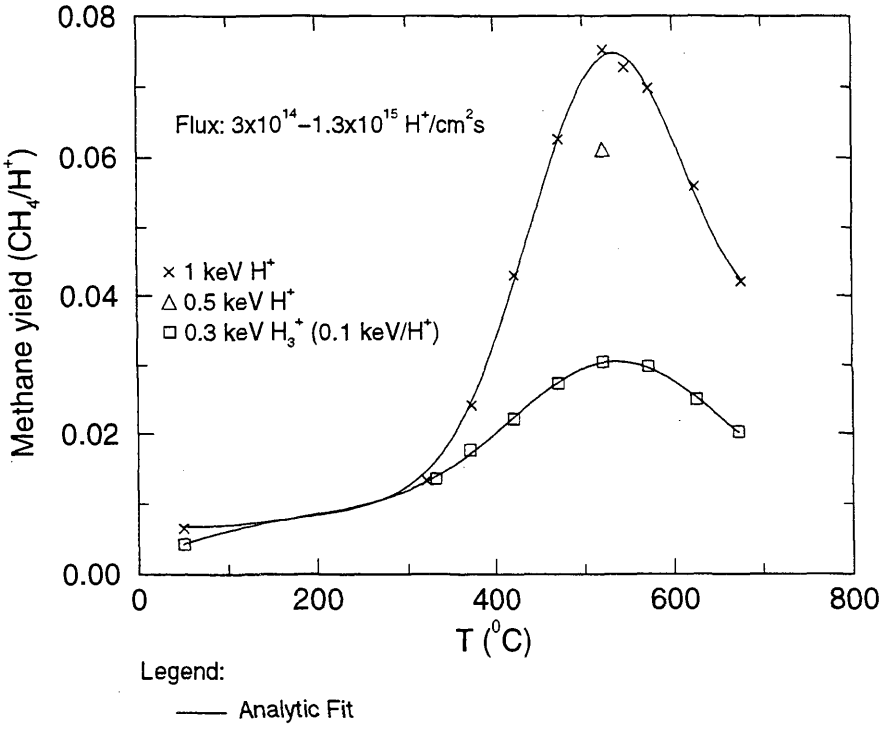

4.2.1.98 H^+, H_3^+ + B_4C → CH_4

Source: J. W. Davis and A. A. Haasz, J. Nucl. Mater. **175**, 117 (1990).

Accuracy: Yield: ±15%; T: ±25%.

Comments: (1) Methane yields: A: (1 keV/H^+) steady-state; B: (3 keV/H^+) steady-state; C: (10 keV H^+) possibly transient.
(2) Specimen: B_4C.
(3) H^+ ions: mass-analyzed accelerator.
(4) Methane measured via QMS-RGA.

Analytic fitting function:

Methane yield:

$$Y = 1.0 \times 10^{-2}[A_1 \exp(-(T - A_2)^2/A_3)T^{A_4} + A_5 \exp(-A_6 T)T^{A_7}] \quad [\text{molecules/H}^+]$$

where T is in Kelvin. The rms deviation of the analytic fits for reactions A (•), B (△) and C (×) are 5.3%, 11.2% and 44.4%, respectively. Data for curve B were fitted with EYIELD8A.

Fitting parameters A_1-A_8

A	2.2554E-02	7.2733E+02	4.2521E+03	4.4509E-02	3.9836E-02	-8.9349E-05
	-2.3115E-03					
B	1.0808E-23	6.5055E+02	6.4688E+01	3.0917E-06	6.9735E+00	4.8389E-01
	-2.7362E-03	-1.4911E+00				
C	2.6327E-01	6.4082E+02	1.8291E+04	-8.8414E-02	2.7921E-03	-1.7910E-03
	-1.3569E-04					

ALADDIN evaluation function for methane yield: EYIELD7A, EYIELD8A

ALADDIN hierarchical labelling:

A, B: SATM H{3} [+1] B{4}C CH{4} [+0]
C: SATM H [+1] B{4}C CH{4} [+0]

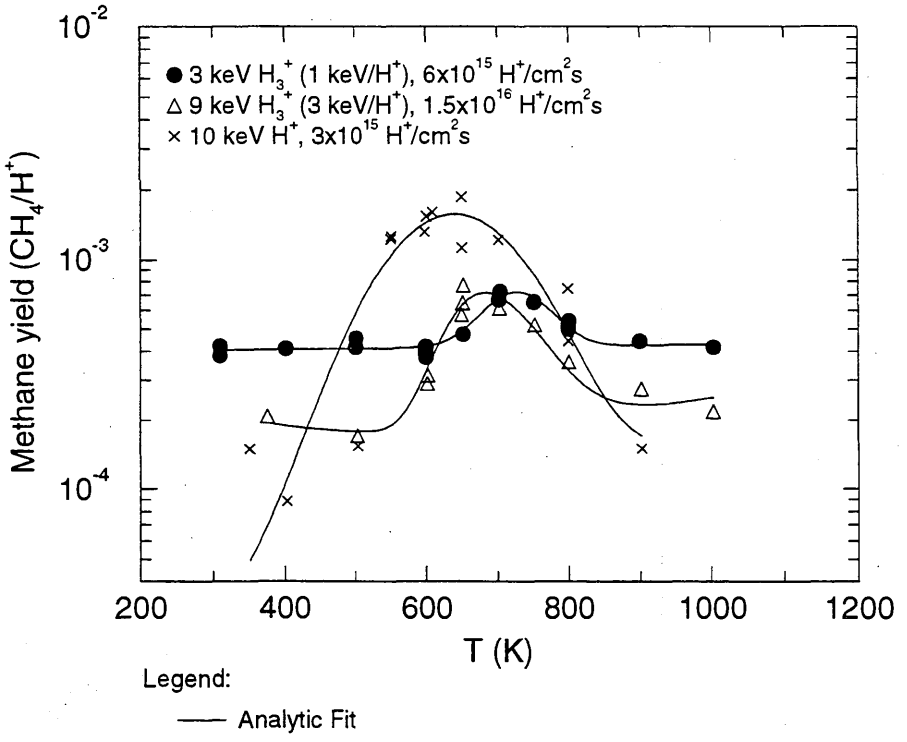

4.2.2.1 D^+ + pyrolytic graphite → CD_4

Source: C. M. Braganza, S. K. Erents and G. M. McCracken, J. Nucl. Mater. **75**, 220 (1978).

Accuracy: Yield: Indeterminate.

Comments: (1) Target bombarded by monoenergetic beam of mass-selected D^+ ions.
(2) Hydrocarbon products measured via QMS.
(3) Specimen: graphite (pyrolytic).
(4) Curves were fitted with an equation of the form derived from a kinetics analysis discussed in the source paper.

Analytic fitting function:

Methane yield:

$$Y = 10^{-2}[A_1 \exp(-A_2/T)/(1 + A_3 \exp(-A_4/T))] \quad \text{[molecules/ion]}$$

where the temperature T is in Kelvin. The rms deviation of analytic fits for reactions A (□), B (△), C (•) and D (×) are 20.1%, 85.6%, 56.4% and 306.4%, respectively.

Fitting parameters A_1-A_4

A	1.7502E+08	1.2774E+04	3.5717E+13	2.3617E+04
B	5.8543E+06	1.0387E+04	4.1485E+12	2.2396E+04
C	7.5247E+04	7.6415E+03	5.3425E+12	2.3739E+04
D	1.9477E+06	1.0407E+04	2.8020E+15	2.9009E+04

ALADDIN evaluation function for methane yield: EYIELD4D

ALADDIN hierarchical labelling:

A-D: SATM D [+1] GRAPHITE T=HPG CD{4} [+0]

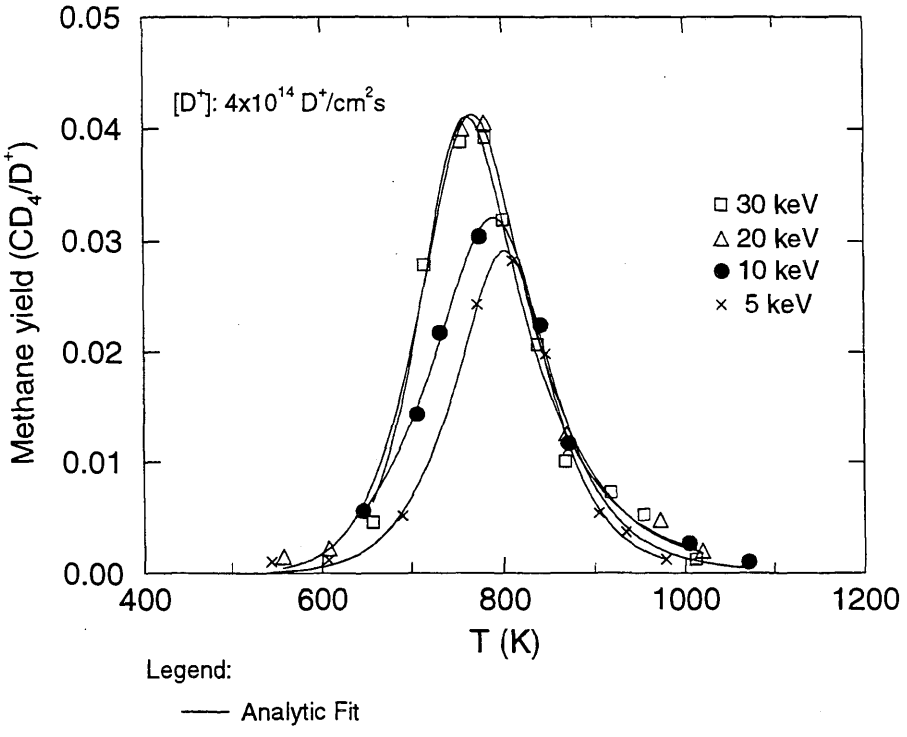

4.2.2.2 D^+ + pyrolytic graphite → CD_4

Source: C. M. Braganza, S. K. Erents and G. M. McCracken, J. Nucl. Mater. **75**, 220 (1978).

Accuracy: Yield: Indeterminate.

Comments: (1) Target is bombarded by monoenergetic beam of mass-selected D^+ ions.
(2) Hydrocarbon products measured via QMS.
(3) Specimen: graphite (pyrolytic).
(4) Curves were fitted with an equation of the form derived from a kinetics analysis discussed in the source paper.

Analytic fitting function:

Methane yield:

$$Y = 10^{-2}[A_1 \exp(-A_2/T)/(1 + A_3 \exp(-A_4/T))] \quad \text{[molecules/ion]}$$

where the temperature T is in Kelvin. The rms deviation of analytic fits for reactions A (△) and and B (×) are 56.2% and 7.6%, respectively.

Fitting parameters A_1-A_4

A	9.1739E+06	1.0636E+04	1.3450E+12	2.1299E+04
B	1.0092E+06	9.5453E+03	2.3962E+11	2.1333E+04

ALADDIN evaluation function for methane yield: EYIELD4D

ALADDIN hierarchical labelling:

A-D: SATM D [+1] GRAPHITE T=HPG CD{4} [+0]

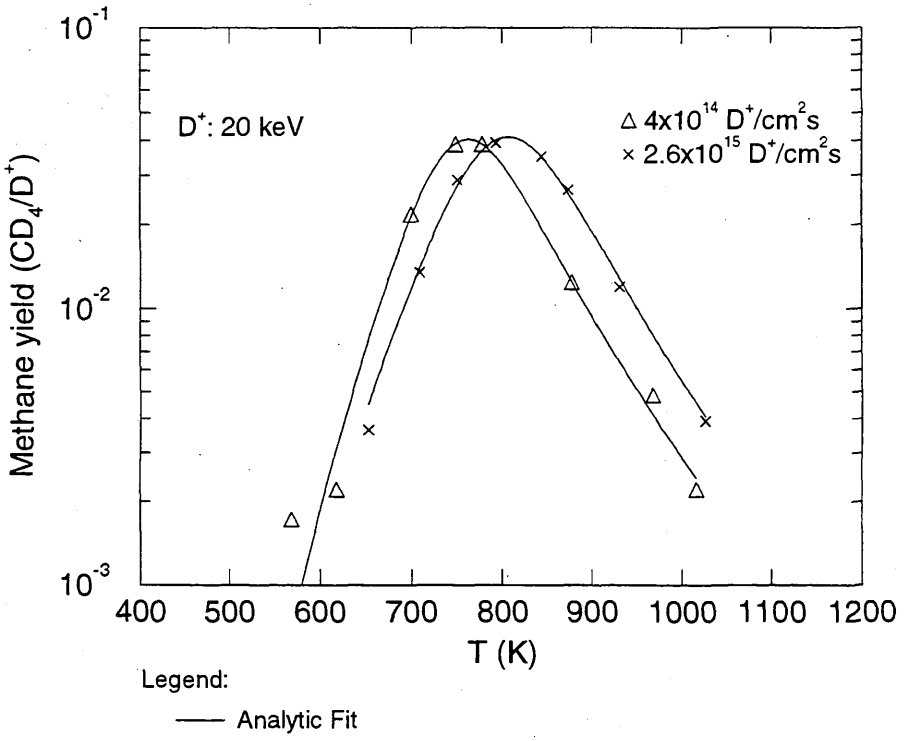

4.2.2.3 D^+ + pyrolytic graphite → CD_4, C_2D_2, C

Source: J. Roth and J. Bohdansky, "Graphite in High Power Fusion Reactors", IEA Workshop Rep., Federal Institute for Reactor Research, Würenlingen (1983).

Accuracy: Yield: Indeterminate.

Comments: (1) Total sputtering (chemical+physical) and chemical erosion yields compared at 580 °C and RT.
(2) Specimen: graphite (pyrolytic).
(3) $[D^+]$: 2×10^{15} D^+/cm^2s.

Analytic fitting function:

Sputtering yield:

$$Y = A_1 \exp(-A_2/E)/(1 + A_3 \exp(-A_4/E)) \quad [\text{particles}/D^+]$$

where E is in keV. The rms deviation of analytic fits for reactions A (•), B (◇), C (△) and D (□) are 3.2%, 8.2%, 7.5% and 3.7%, respectively. Data for curve B were fitted with EYIELD4C.

Fitting parameters A_1-A_4

A	2.1968e-01	3.6170e-02	1.6414e+00	9.9655e-01
B	8.8530e-02	1.7130e-02	1.9229e+00	-2.2010e-02
C	5.9350e-03	-2.5349e+00	2.2912e-01	-2.5716e+00
D	2.6139e-02	-1.8988e+00	4.0064e-01	-2.1334e+00

ALADDIN evaluation function for sputtering yield: EYIELD4D, EYIELD4C

ALADDIN hierarchical labelling:

A: SAT D [+1] GRAPHITE T=PYG C [+0]
B: SATM D [+1] GRAPHITE T=PYG C{2}D{2} [+0]
C: SAT D [+1] GRAPHITE T=PYG C [+0]
D: SATM D [+1] GRAPHITE T=PYG CD{4} [+0]

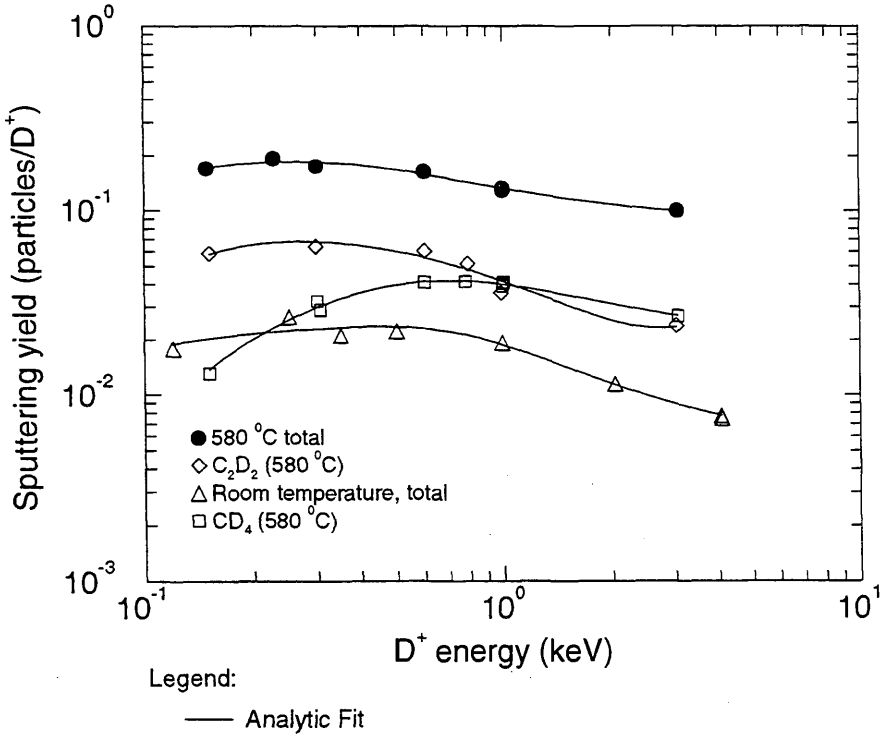

4.2.2.4 D^+ + pyrolytic graphite → CD_4

Source: J. Roth and J. Bohdansky, Nucl. Instrum. Methods B **23**, 549 (1987).

Accuracy: Yield (rel.): ±10%; Yield (abs.): ±30%.

Comments: (1) Steady-state methane yield.
(2) Specimen: graphite (pyrolytic).
(3) Mass analyzed beam.
(4) Methane production measured via QMS-RGA.

Analytic fitting function:

Methane yield:

$$Y = 1.0 \times 10^{-2}[A_1 \exp(-(T - A_2)^2/A_3)T^{A_4} + A_5 \exp(-A_6 T)T^{A_7}] \quad [CD_4/\text{ion}]$$

where T is in Kelvin. The rms deviation of analytic fits for reactions A (•), B (△) and C (□) are 3.2%, 20.1% and 31.5%, respectively.

Fitting parameters A_1-A_7

A	1.8299E+00	7.0364E+02	1.1854E+04	-6.0613E-02	6.8712E-01	-1.7106E-03
	5.7924E-02					
B	8.3847E+00	8.0785E+02	6.0257E+03	-2.8987E-02	3.0939E-10	3.4189E-03
	3.8812E+00					
C	1.2213E+01	8.3611E+02	1.1782E+04	4.1343E-02	-1.1410E+00	2.4735E-03
	1.3542E-01					

ALADDIN evaluation function for methane yield: EYIELD7A

ALADDIN hierarchical labelling:

A-C: SATM D [+1] GRAPHITE T=HPG CD{4} [+0]

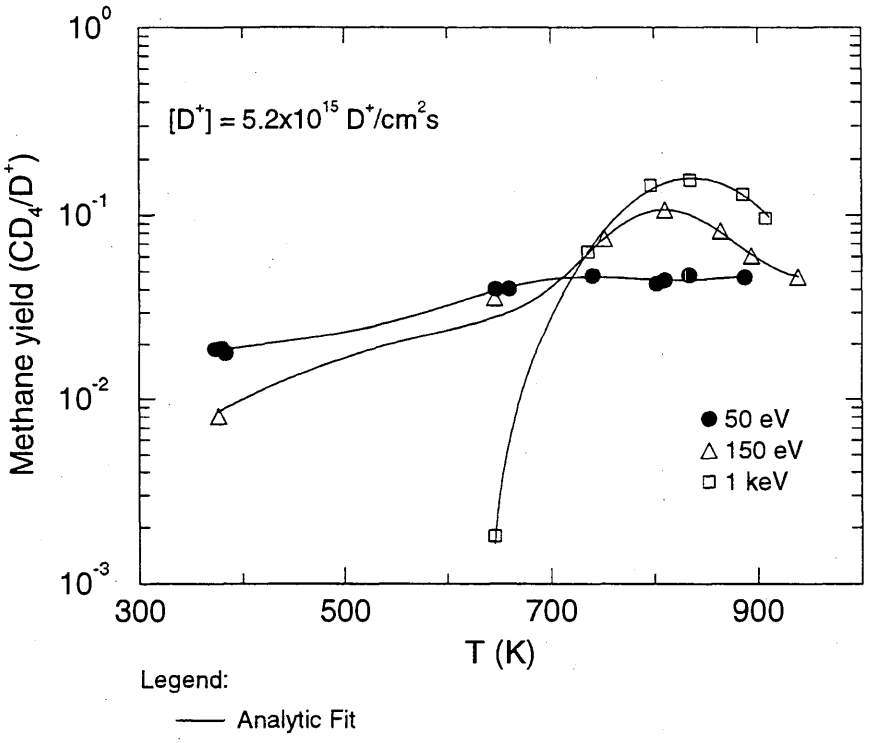

4.2.2.5 D^+, H^+ + pyrolytic graphite $\rightarrow CD_4$, C

Source: J. Roth and J. Bohdansky, Nucl. Instrum. Methods B **23**, 549 (1987).

Accuracy: Yield (rel.): ±10%; Yield (abs.): ±30%.

Comments: (1) Weight loss measurement of total (physical+chemical) sputtering yield.
(2) Specimen: graphite (pyrolytic with various orientations, isotropic fine-grain).
(3) Flux: $5 \times 10^{15} - 1 \times 10^{16}$ H^+ or D^+/cm^2s for H_3^+ and D_3^+. The total target current was 1×10^{-4} A for H_3^+ and D_3^+.
(4) Mass analyzed beam.
(5) Methane production measured via QMS-RGA.

Analytic fitting function:

Erosion yield:

$$Y = A_1(\log E)^3 + A_2(\log E - A_3)^2 + A_4 \quad \text{[atoms/ion or } CD_4\text{/ion]}$$

where ion energy E is in eV. The rms deviation of analytic fits for reactions A (□), B (○), C (◇) and D (•) are 15.5%, 15.3%, 13.1% and 14.3%, respectively.

Fitting parameters A_1-A_4

A	-1.8067E-02	4.8192E-02	-1.2329E+00	-2.1694E-01
B	-2.0080E-03	1.1696E-02	1.2685E+00	3.8303E-02
C	1.1150E-01	-6.7514E-01	9.7561E-01	-1.6944E-01
D	-5.6633E-04	7.7589E-04	-4.2428E+00	-1.8080E-02

ALADDIN evaluation function for erosion yield: EYIELD4C

ALADDIN hierarchical labelling:

A: SATM D [+1] GRAPHITE T=HPG CD{4} [+0]
B: SATM D [+1] GRAPHITE T=HPG C [+0]
C: SATM D [+1] GRAPHITE T=HPG CD{4} [+0]
D: SATM H [+1] GRAPHITE T=HPG C [+0]

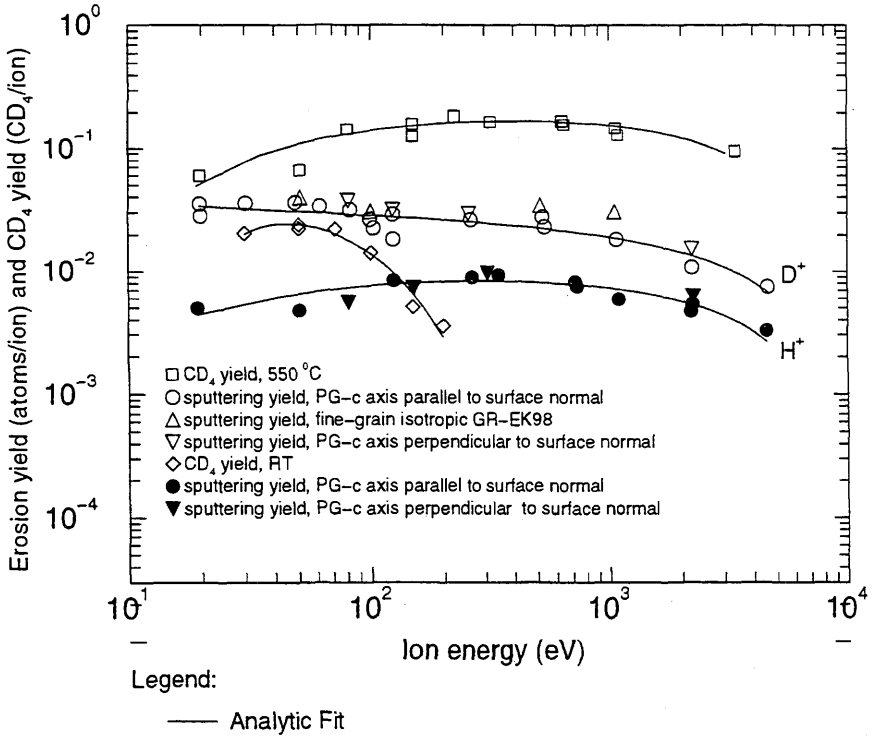

4.2.2.6 D^+ + pyrolytic graphite → C

Source: J. Roth, E. Vietzke and A. A. Haasz, Nucl. Fusion Suppl. **1**, 63 (1991).

Accuracy: Yield: ±20%.

Comments: (1) Weight loss measurements of total (chemical+physical+RES) sputtering yield.
(2) Specimen: graphite (pyrolytic, HPG99).
(3) Mass analyzed beam.
(4) Original data from J. Roth, J. Nucl. Mater. **145-147**, 87 (1987); J. Roth and P. Franzen, unpublished data, 1990.

Analytic fitting function:

Sputtering yield:

$$Y = A_1 \exp\left[-\left(\frac{T - A_2}{A_3 T + 1}\right)^2 / A_4\right] T^{A_5} + A_6 \exp(-A_7 T) T^{A_8} \quad [\mathrm{C/D^+}]$$

where temperature T is in Kelvin. The rms deviation of analytic fits for reactions A (△) and B (□) are 10.4% and 5.9%, respectively. Data for curve A were fitted with EYIELD7A.

Fitting parameters A_1-A_8

A	1.9534E-03	8.1169E+02	1.5387E+04	6.2602E-01	2.5568E+04	-4.6257E-03
	-2.6374E+00					
B	5.2242E-02	7.3750E+02	-3.1023E-04	1.1370E+05	7.7256E-02	7.2497E+07
	-4.7257E-03	-4.0316E+00				

ALADDIN evaluation function for sputtering yield: EYIELD7A, EYIELD8A

ALADDIN hierarchical labelling:

SATM D [+1] GRAPHITE T=HPG99 C [+0]

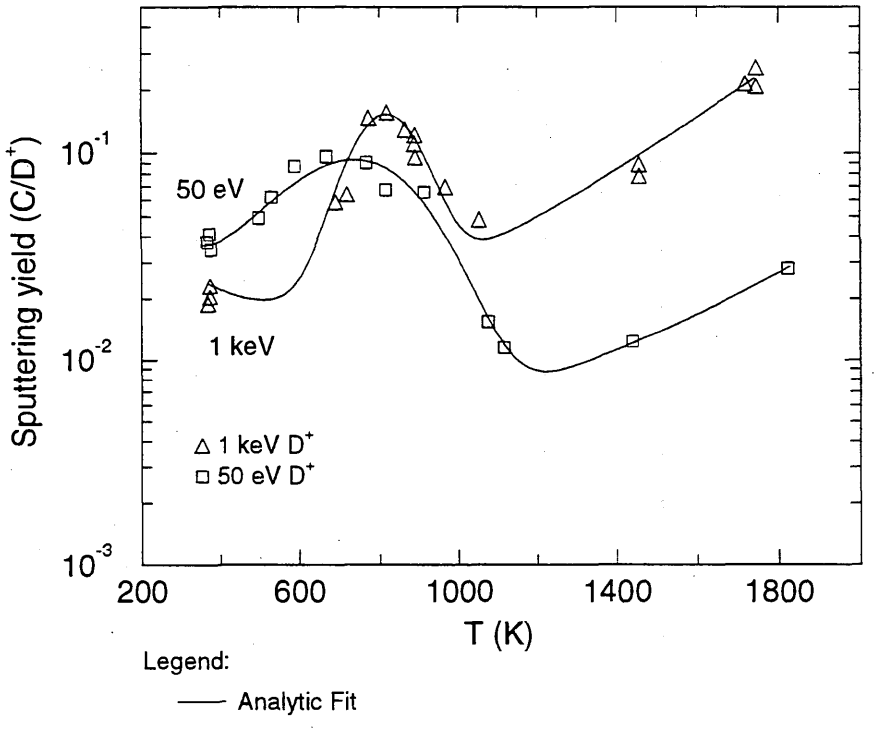

4.2.2.7 D^+ + pyrolytic graphite → CD_4

Source: J. Roth and C. García-Rosales, Nucl. Fusion **36**, 1647 (1996).

Accuracy: Yield: ±20%.

Comments: (1) Steady-state methane yield.
(2) Specimen: pyrolytic graphite.
(3) D^+ ions: Mass-analyzed ion beam.
(4) Methane measured via QMS-RGA.

Analytic fitting function:

Methane yield:

$$Y = A_1 \exp(-(T - A_2)^2/A_3)T^{A_4} + A_5 \exp(-A_6 T)T^{A_7}(1 + A_8 T^{A_9}) \quad [CD_4/D^+]$$

where T is in Kelvin. The rms deviation of analytic fits for reactions A (•) and B (□) are 32.8% and 60.0%, respectively.

Fitting parameters A_1-A_9

A	4.7260e-03	7.6237e+02	3.3796e+04	3.1010e-01	7.1246e-06	8.4140e-03
	8.3093e-01	1.0831e-03	2.1377e+00			
B	5.9770e-03	7.9788e+02	1.0527e+04	4.3480e-01	3.6331e-10	-8.6500e-03
	1.2212e+00	0.0	0.0			

ALADDIN evaluation function for methane yield: EYIELD9A

ALADDIN hierarchical labelling:

A, B: SATM D [+1] GRAPHITE T=HPG CD{4} [+0]

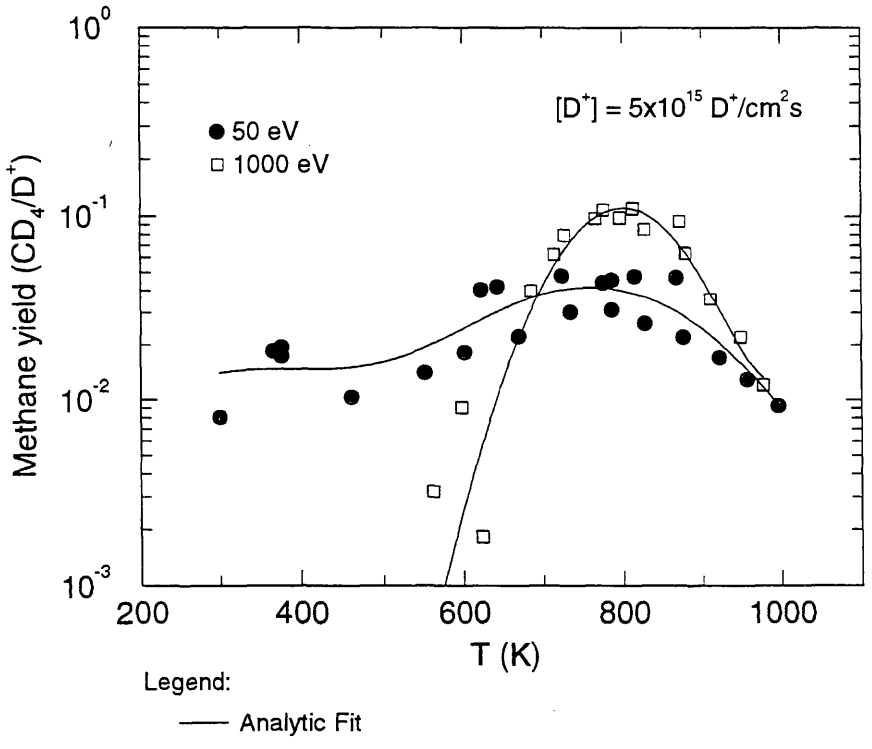

4.2.2.8 D^+ + pyrolytic graphite → C

Source: J. Roth and C. García-Rosales, Nucl. Fusion **36**, 1647 (1996).

Accuracy: Yield: ±20%.

Comments: (1) Weight loss measurement.
(2) Specimen: pyrolytic graphite.
(3) D^+ ions: mass-analyzed ion beam.
(4) Yield is for total (chemical+physical) sputtering.

Analytic fitting function:

Sputtering yield:

$$Y = A_1 \exp(-A_2 E) T^{A_3} + A_4 E \quad [\mathrm{C/D^+}]$$

where E is in eV. The rms deviation of analytic fits for reactions A (•) and B (□) are 34.9% and 55.8%, respectively. Data for curve B were fitted with EYIELD4C.

Fitting parameters A_1-A_4

A	4.0770e-02	-1.1079e-04	-5.0360e-02	-7.1101e-06
B	-1.9376E-02	-3.0419E-03	6.3272E+01	1.1736E+01

ALADDIN evaluation function for sputtering yield: EYIELD4A, EYIELD4C

ALADDIN hierarchical labelling:

A, B: SATM D [+1] GRAPHITE T=HPG C [+0]

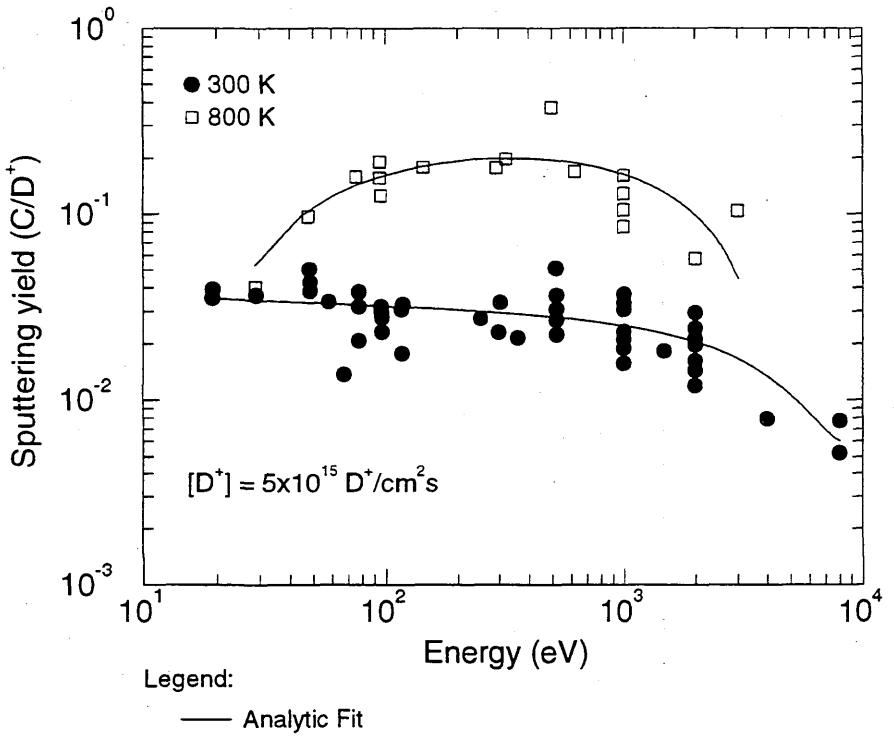

4.2.2.9 D^+, D_3^+ + pyrolytic graphite → CD_4

Source: S. Chiu and A. A. Haasz, J. Nucl. Mater. **208**, 282 (1994).

Accuracy: Yield: Total ±20%; Flux: ±30%.

Comments: (1) D^+ produced by mass-analyzed ion accelerator.
(2) Methane measured via QMS-RGA, steady-state.
(3) Specimens: graphite (pyrolytic, HPG99).
(4) Specimen temperature is fixed at 800 K.

Analytic fitting function:

Methane yield:

$$Y = A_1(\log F)^3 + A_2(\log F - A_3)^2 + A_4 \quad [CD_4/D^+]$$

where the flux F is in D^+/cm^2s. The rms deviation of analytic fits for reactions A (•), B (□) and C (△) are 0.7%, 2.9% and 1.6%, respectively.

Fitting parameters A_1-A_4

A	-1.2340E-02	5.4569E-02	5.9110E-01	6.3440E-02
B	-4.2370E-03	2.2266E-02	6.8879E-01	2.7743E-02
C	-2.0471E-03	9.4460E-03	3.3729E-01	1.6351E-02

ALADDIN evaluation function for methane yield: EYIELD4C

ALADDIN hierarchical labelling:

A-C: SATM D [+1] GRAPHITE T=HPG99 CD{4} [+0]

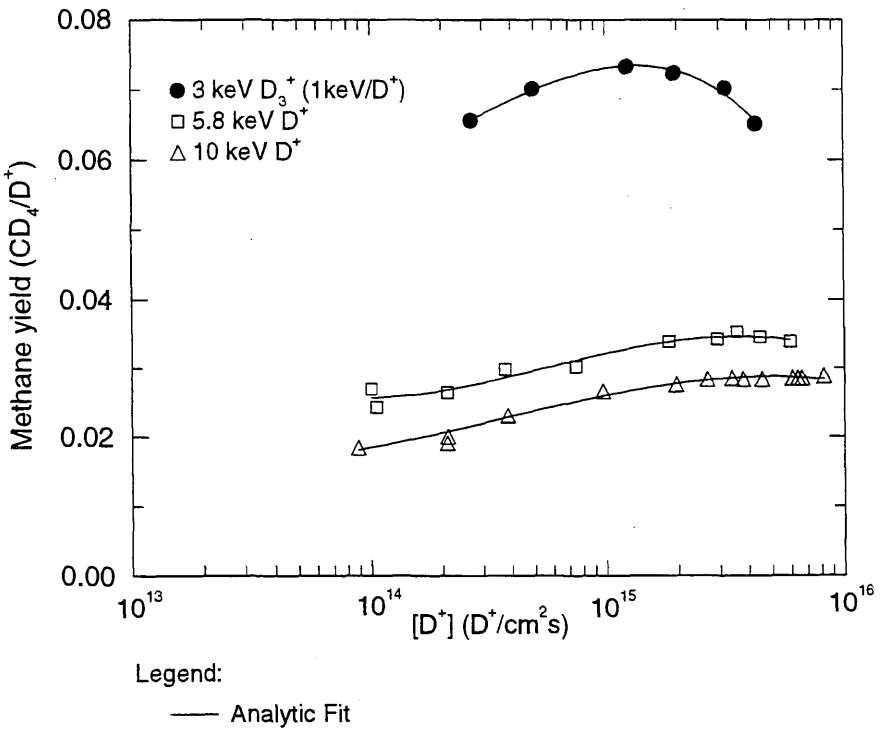

4.2.2.10 D^+ + pyrolytic graphite → CD_4

Source: S. Chiu and A. A. Haasz, J. Nucl. Mater. **208**, 282 (1994).

Accuracy: Yield: Total ±20% (CD_4 calibration based on CH_4); Flux ratio: ±30% (beam spot size, distribution).

Comments: (1) These results are part of a mechanistic study of CH_4 formation; the reader is referred to the paper.
(2) The erosion yield at previously unirradiated beam spots is generally reduced by higher fluence bombardment by D^+ ions.
(3) D^+ produced by mass-selecting ion accelerator.
(4) Methane measured via QMS-RGA, time-dependent.
(5) Specimens: graphite (pyrolytic, HPG99).

Analytic fitting function:

Methane yield:

$$Y = A_1(\log F)^3 + A_2(\log F - A_3)^2 + A_4 \quad [CD_4/D^+]$$

where the flux F is in D^+/cm^2s. The rms deviation of analytic fits for reactions A (×), B (○), C (□), D (△), E (▽), F (◇) and G (•) are 4.9%, 3.0%, 3.2%, 1.6%, 1.4%, 2.7% and 1.6%, respectively.

Fitting parameters A_1-A_4

A	-2.0329E-02	2.3978E-03	-1.0383E+01	-2.3341E-01
B	-9.9790E-03	1.9176E-03	-1.0791E+01	-1.9969E-01
C	-4.8963E-03	1.3861E-03	-9.2856E+00	-9.6294E-02
D	-2.7347E-02	8.1228E-02	4.0908E-01	3.7427E-02
E	-2.3128E-02	7.2880E-02	4.6303E-01	3.6773E-02
F	-9.6747E-03	3.9012E-02	6.1790E-01	3.4306E-02
G	4.8963E-03	-1.8479E-02	6.7024E-01	2.4278E-02

ALADDIN evaluation function for methane yield: EYIELD4C

ALADDIN hierarchical labelling:

A-G: SATM D [+1] GRAPHITE T=HPG99 CD{4} [+0]

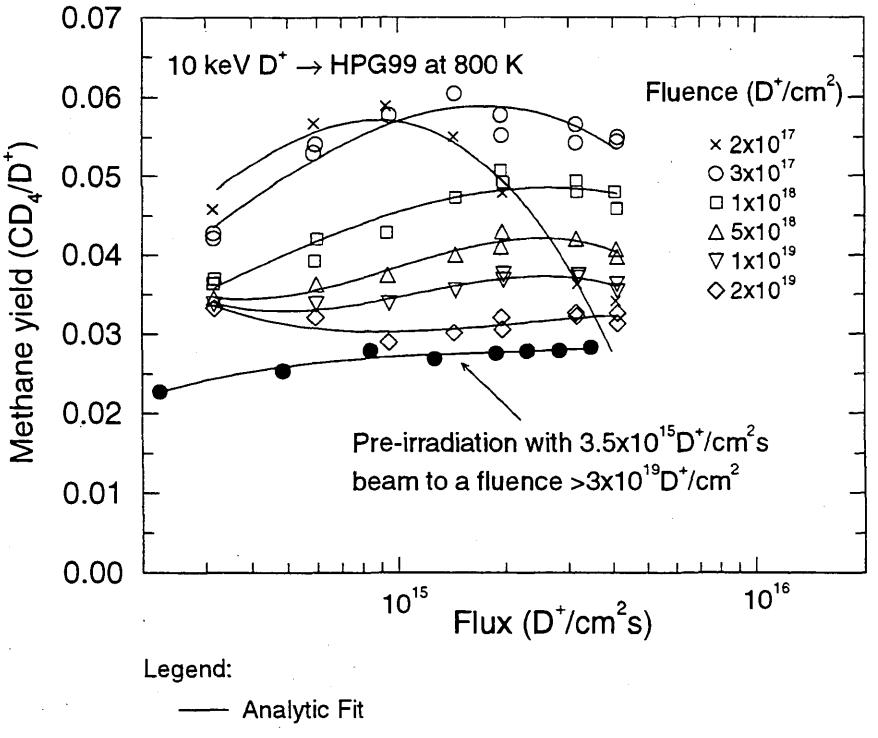

4.2.2.11 D^+ + POCO graphite → C

Source: D. M. Goebel, J. Bohdansky, R. W. Conn, Y. Hirooka, B. LaBombard, W. K. Leung, R. E. Nygren, J. Roth and G. R. Tynan, Nucl. Fusion **28**, 1041 (1988).

Accuracy: Yield: ±20%; T: ±5%.

Comments: (1) High-flux (~10^{18} D^+/cm^2s), steady-state (>10 min.) plasma bombardment.
(2) Specimen: graphite (isotropic, POCO: AXF-5Q).
(3) Total erosion yield (incl. physical and chemical sputtering) estimated from weight loss (>1 mg).
(4) Erosion assumed to be dominated by physical sputtering at 1000 ^{0}C.
(5) Large ionization mean free path, i.e. no redeposition effect (see 4.2.1.15).

Analytic fitting function:

Erosion yield:

$$Y = 1.0 \times 10^{-2}[A_1 \exp(-(T - A_2)^2/A_3)T^{A_4} + A_5 \exp(-A_6 T)T^{A_7}] \quad \text{[atoms/ion]}$$

where T is in ^{0}C. The rms deviation of analytic fits for reactions A (•) and B (△) are 1.7% and 3.9%, respectively. Data for reaction B were fitted using the function EYIELD9A.

Fitting parameters A_1-A_9

A	2.0414E+00	5.3187E+02	4.5250E+04	1.5392E-01	7.0157E-01	8.1747E-04
	1.6618E-01					
B	1.2110E+05	5.9877E+02	2.1438E+04	-2.4438E+00	2.2524E-04	1.5597E-02
	1.2192E+00	1.1274E-09	3.9325E+00			

ALADDIN evaluation function for erosion yield: EYIELD7A, EYIELD9A

ALADDIN hierarchical labelling:

A, B: SAT D [+1] GRAPHITE T=POCO-AXF5Q C [+0]

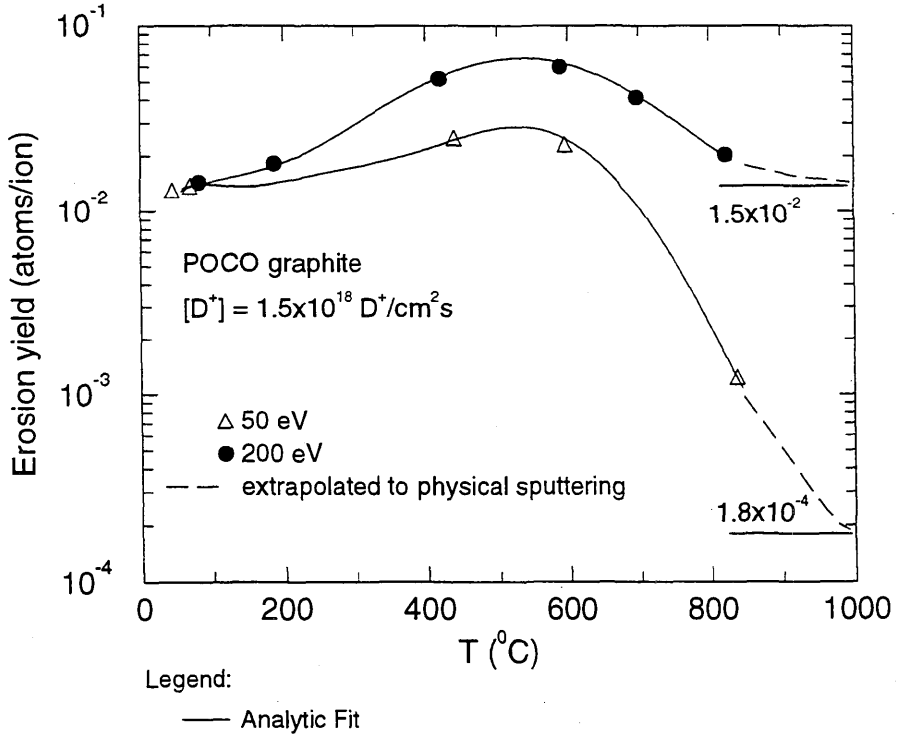

4.2.2.12 D^+ + redeposited carbon, POCO graphite → C

Source: Y. Hirooka, A. Pospieszczyk, R. W. Conn, B. Mills, R. E. Nygren and Y. Ra, J. Vac. Sci. Technol. A **7**, 1070 (1989).

Accuracy: Yield: ±20%; T: ±5%.

Comments: (1) High-flux (10^{18} D^+/cm^2s), temperature ramp at 5 $^0C/s$.
(2) Specimen: isotropic graphite (POCO AXF-5Q): virgin, TFTR redeposited.
(3) D-content in the redeposited carbon estimated by NRA to be $2x10^{18}$ D/cm^2.
(4) Total erosion yield estimated from CH-band spectroscopy calibrated by weight loss measurements.
(5) The erosion data for the "TFTR-eroded" graphite essentially overlaps those for "virgin" graphite.

Analytic fitting function:

Erosion yield:

$$Y = A_1 \exp\left[-\left(\frac{T - A_2}{A_3 T + 1}\right)^2 / A_4\right] T^{A_5} + A_6 \exp(-A_7 T) T^{A_8} \quad [C/D^+]$$

where T is Kelvin. The rms deviation of the analytic fit for reactions A (•) and B(○) are 3.0% and 7.2%, respectively.

Fitting parameters A_1-A_8

A	8.7487E-01	7.9398E+02	7.4973E-03	4.8378E+02	-3.7760E-01	7.0625E-08
	5.5134E-03	2.4876E+00				
B	4.4688E-02	8.6786E+02	-1.4448E-04	8.3359E+04	7.3484E-02	1.7501E-58
	5.9988E-02	2.5555E+01				

ALADDIN evaluation function for erosion yield: EYIELD8A

ALADDIN hierarchical labelling:

A: SAT D [+1] GRAPHITE T=TFTR-REDEP C [+0]
B: SAT D [+1] GRAPHITE T=POCO-AXF5Q C [+0]

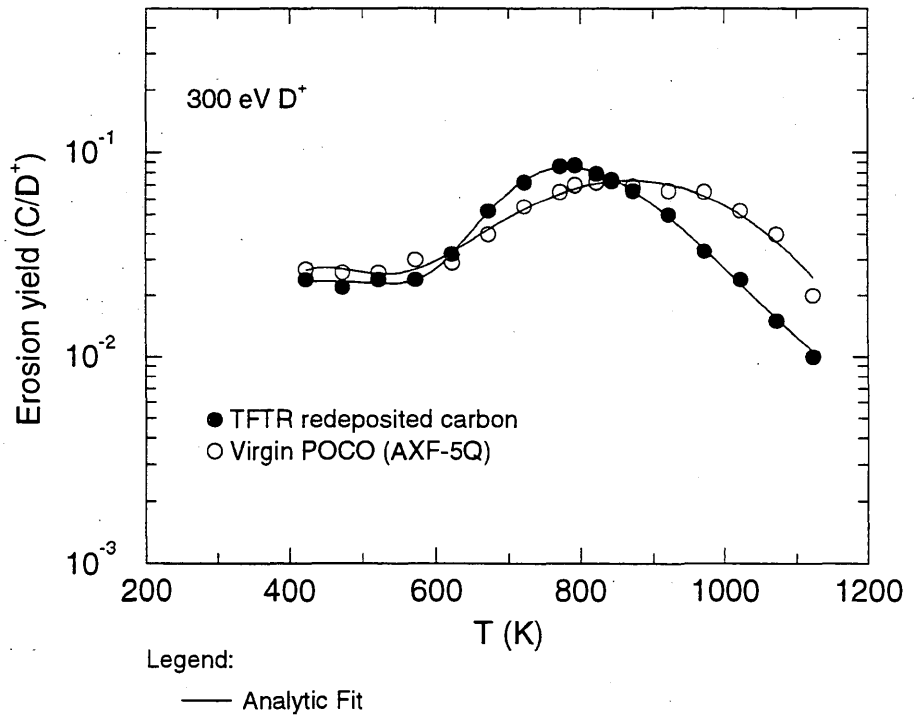

4.2.2.13 D^+ + pyrolytic graphite, B-doped GB graphite → C

Source: Y. Hirooka, R. Conn, R. Causey, D. Croessmann, R. Doerner, D. Holland, M. Khandagle, T. Matsuda, G. Smolik, T. Sogabe, J. Whitley and K. Wilson, J. Nucl. Mater. **176&177**, 473 (1990).

Accuracy: Yield: ±20%; T: ±5%.

Comments: (1) High-flux (~10^{18} D^+/cm^2s), steady-state (>10 min.) plasma bombardment.
(2) Specimen: pyrolytic graphite (Pfizer), bulk-boronized isotropic graphite and C-C composite (Toyo Tanso).
(3) Total erosion yield estimated from weight loss (>1 mg).
(4) Large ionization mean free path, i.e. no redeposition effect (see 4.2.1.15).
(5) Boron and carbon masses are assumed equal for erosion yield calculations.

Analytic fitting function:

Erosion yield:

$$Y = 1.0 \times 10^{-2}[A_1 \exp(-(T - A_2)^2/A_3)T^{A_4} + A_5 \exp(-A_6 T)T^{A_7}] \quad [\text{atoms/D}^+]$$

where temperature T is in ^{0}C. The rms deviation of analytic fits for reactions A (•, ∗, □) and B (△, ◇) are 47.1% and 26.9%, respectively.

Fitting parameters A_1-A_7

A	3.1553E+00	5.7198E+02	1.0471E+05	1.5317E-02	1.0503E-04	-9.3215E-03
	-3.6593E-01					
B	2.5227E-02	4.2882E+02	1.3699E+05	6.6751E-01	3.8563E-02	-1.0051E-02
	-1.4396E+00					

ALADDIN evaluation function for erosion yield: EYIELD7A

ALADDIN hierarchical labelling:

A: SAT D [+1] GRAPHITE T=PFG C [+0]
B: SAT D [+1] GRAPHITE T=GB D=B C [+0]

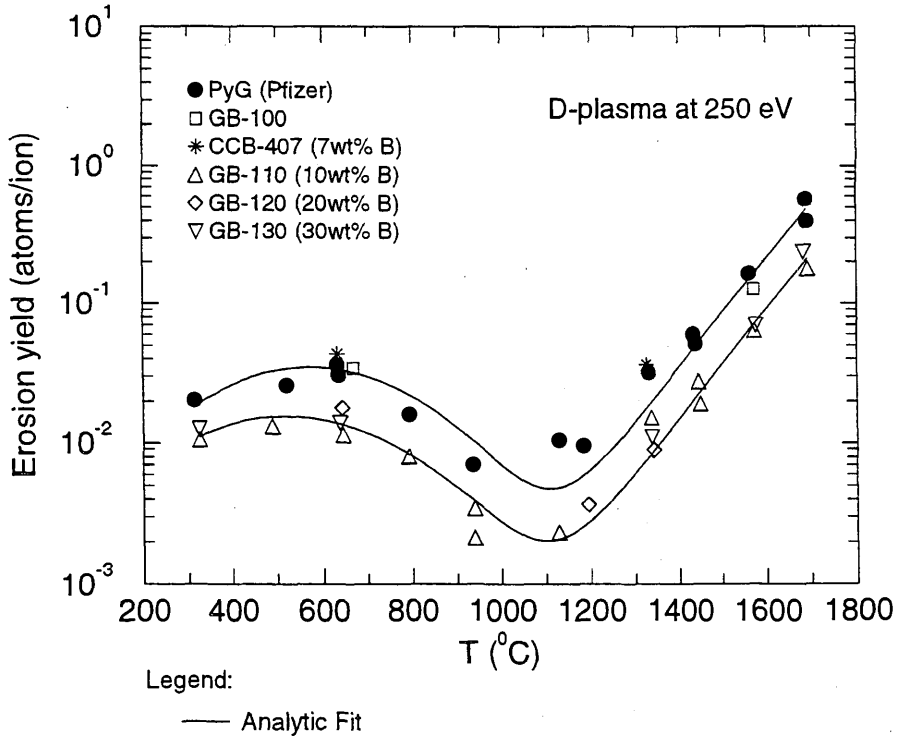

4.2.2.14 D^+ + C-SiC coated graphite → C

Source: D. M. Goebel, J. Bohdansky, R. W. Conn, Y. Hirooka, B. LaBombard, W. K. Leung, R. E. Nygren, J. Roth and G. R. Tynan, Nucl. Fusion **28**, 1041 (1988).

Accuracy: Yield: ±20%; T: ±5%.

Comments: (1) High-flux (~10^{18} D^+/cm^2s), steady-state (>10 min.) plasma bombardment.
(2) Specimen: C+SiC (5%) co-deposited isotropic graphite (ATJ).
(3) Total erosion yield (incl. physical and chemical sputtering) estimated from weight loss (>1 mg).
(4) Large ionization mean free path, i.e. no redeposition effect (see 4.2.1.15).

Analytic fitting function:

Erosion yield:

$$Y = 1.0 \times 10^{-2}[A_1 \exp(-(T - A_2)^2/A_3)T^{A_4} + A_5 \exp(-A_6 T)T^{A_7}] \quad \text{[atoms/ion]}$$

where T is in ^{0}C. The rms deviation of the analytic fit is 1.6%.

Fitting parameters A_1-A_7

1.7411E-01	5.5101E+02	6.7576E+04	3.6151E-01	7.0240E-02	5.7265E-03	5.5680E-01

ALADDIN evaluation function for erosion yield: EYIELD7A

ALADDIN hierarchical labelling:

SAT D [+1] GRAPHITE T=C-SiC C [+0]

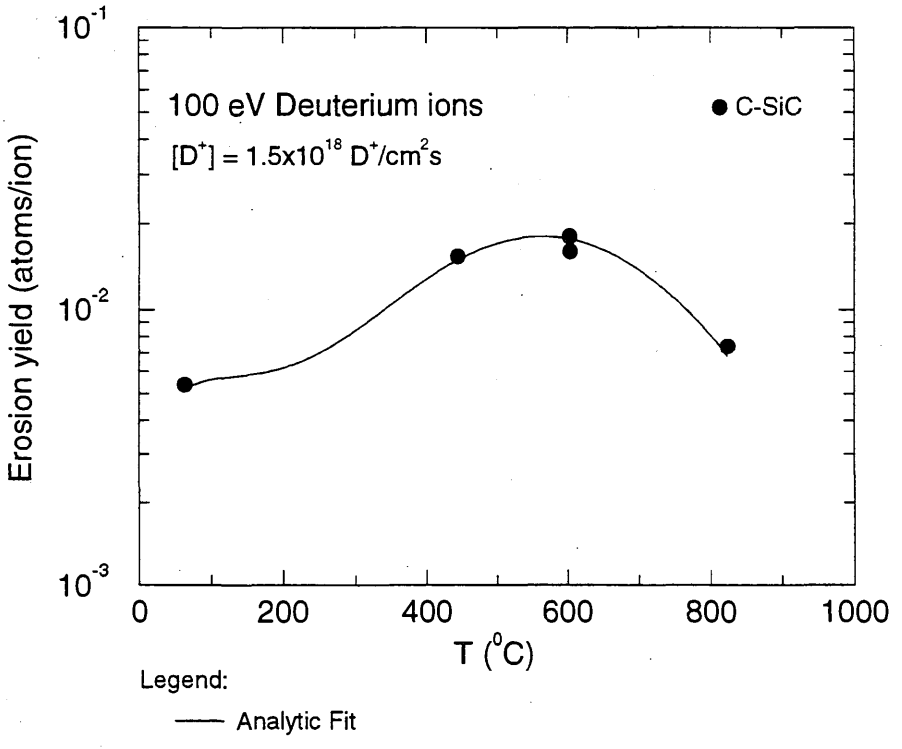

4.2.2.15 D^+ + pyrolytic, B-doped SEP-CFC, Ti-doped graphite, Be/C → CD_4

Source: C. García-Rosales, E. Gauthier, J. Roth, R. Schwörer and W. Eckstein, J. Nucl. Mater. **189**, 1 (1992).

Accuracy: Yield (rel.): ±10%; Yield (abs.): ±30%.

Comments: (1) Methane measured via QMS-RGA.
(2) Specimen: graphite (pyrolytic, B-doped, Ti-doped, deposited C/Be layer from JET).
(3) Mass-analyzed beam.

Analytic fitting function:

Methane yield:

$$Y = 1.0 \times 10^{-2}[A_1 \exp(-(T - A_2)^2/A_3)T^{A_4} + A_5 \exp(-A_6 T)T^{A_7}] \quad [CD_4/D^+]$$

where T is in Kelvin. The rms deviation of analytic fits for reactions A (•), B (○), C (△) and D (◇) are 13.0%, 14.3%, 11.2% and 11.3%, respectively.

Fitting parameters A_1-A_7

A	7.4313E+00	7.9528E+02	1.2662E+04	3.3991E-02	1.1881E-01	-2.6831E-03
	-3.1570E-02					
B	7.5578E+00	7.9761E+02	1.2158E+04	-8.9434E-04	2.9918E-01	1.2290E-03
	3.5856E-02					
C	1.6478E+00	8.0148E+02	1.6114E+04	1.8126E-01	3.8191E+00	-2.6377E-03
	-6.5513E-01					
D	2.3045E+00	7.1223E+02	2.1003E+04	-4.3413E-02	4.7864E+00	1.1397E-02
	5.9043E-02					

ALADDIN evaluation function for methane yield: EYIELD7A

ALADDIN hierarchical labelling:

A: SATM D [+1] GRAPHITE T=HPG CD{4} [+0]
B: SATM D [+1] GRAPHITE T=SEP-CFC D=B CD{4} [+0]
C: SATM D [+1] GRAPHITE T=HPG D=Ti CD{4} [+0]
D: SATM D [+1] GRAPHITE T=HPG D=Be CD{4} [+0]

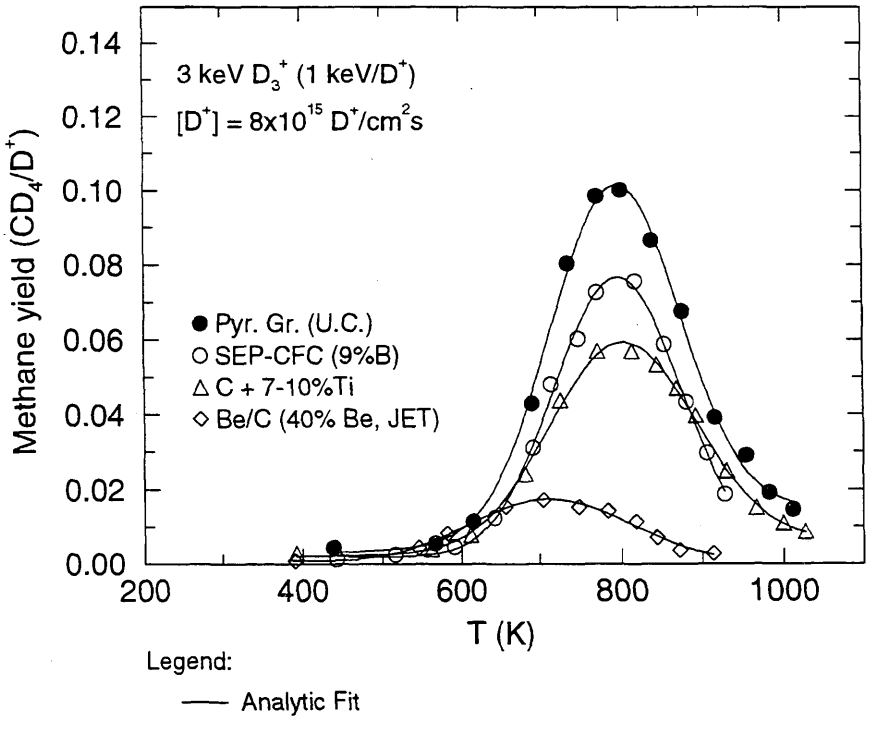

4.2.2.16 D^+ + B-doped S 2508, USB 15, GB graphite, $B_4C \rightarrow CD_4$

Source: C. García-Rosales, E. Gauthier, J. Roth, R. Schwörer and W. Eckstein, J. Nucl. Mater. **189**, 1 (1992).

Accuracy: Yield (rel.): ±10%; Yield (abs.): ±30%.

Comments: (1) Methane measured by QMS-RGA.
(2) Specimen: graphite (pyrolytic, B-doped) and B_4C).
(3) Mass-analyzed beam.

Analytic fitting function:

Methane yield:

$$Y = 1.0 \times 10^{-2}[A_1 \exp(-(T - A_2)^2/A_3)T^{A_4} + A_5 \exp(-A_6 T)T^{A_7}] \quad [CD_4/D^+]$$

where T is in Kelvin. The rms deviation of analytic fits for reactions A (•), B (○), C (△) and D (◇) are 4.2%, 9.7%, 8.5% and 5.4%, respectively. Data for curve D were fitted with EYIELD8A.

Fitting parameters A_1-A_8

A	9.1576E-02	6.7414E+02	4.8416E+03	3.5846E-01	2.8344E-03	3.7685E-04
	7.9442E-01					
B	1.0928E+00	6.9336E+02	5.2190E+03	-1.4737E-02	1.3100E-01	3.8928E-06
	6.1493E-02					
C	8.1421E-01	7.1001E+02	9.3074E+03	-2.5472E-02	6.1473E-02	-1.6137E-03
	2.7616E-03					
D	8.41578e-05	4.92705E+02	-1.65343E-03	2.26043E+05	6.51021E-01	7.25696E-08
	4.34105E-03	1.97493E+00				

ALADDIN evaluation function for methane yield: EYIELD7A, EYIELD8A

ALADDIN hierarchical labelling:

A: SATM D [+1] GRAPHITE T=S2508 D=B CD{4} [+0]
B: SATM D [+1] GRAPHITE T=USB15 D=B CD{4} [+0]
C: SATM D [+1] GRAPHITE T=GB D=B CD{4} [+0]
D: SATM D [+1] B{4}C [+0] CD{4} [+0]

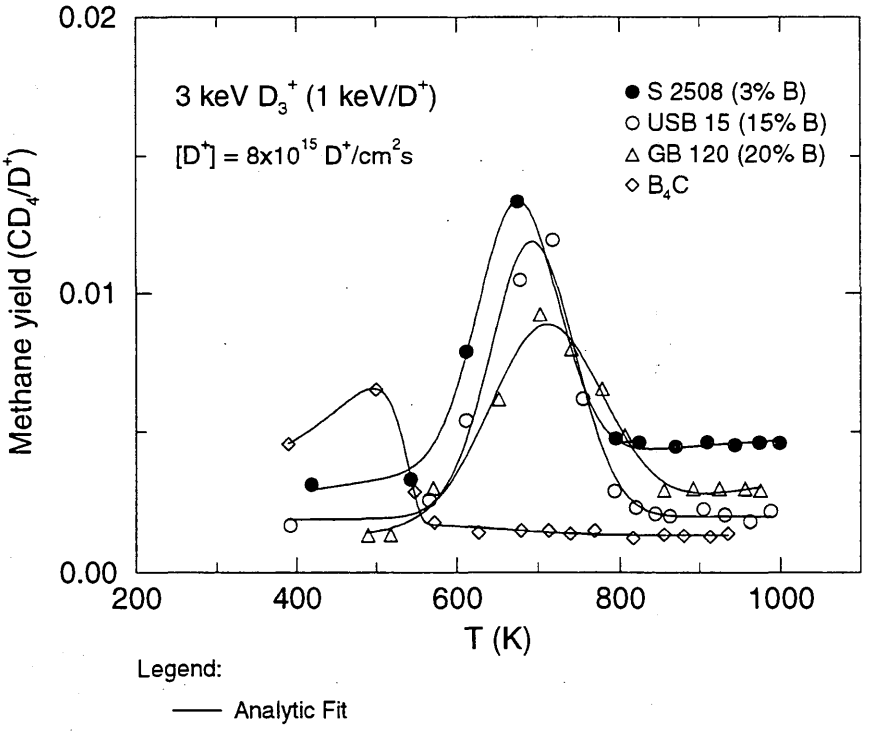

4.2.2.17 D^+ + pure, B-doped graphite, $B_4C \rightarrow C$

Source: C. García-Rosales, E. Gauthier, J. Roth, R. Schwörer and W. Eckstein, J. Nucl. Mater. **189**, 1 (1992).

Accuracy: Yield: ±20%.

Comments: (1) Weight loss measurement at 800 K (physical sputtering subtracted) or methane yield at T_m.
(2) Specimens: graphite (pyrolytic, isotropic, B-doped), diamond, B_4C. Boron content (at%): DPE - 0.5, S 2508 - 3, SEP-CFC - 9, USB 15 - 15, S 1325 - 32, M019 αII - 41, bulk B_4C - 80.
(3) Mass-analyzed beams.
(4) T_m temperature of maximum CD_4 production.

Analytic fitting function:

Chemical sputtering yield:

$$Y = A_1 \exp(-A_2 X) X^{A_3} + A_4 X^{A_5} \quad [\text{atoms/D}^+]$$

where the atomic ratio is $X = B/(C + B)$. The rms deviation of the analytic fit is 13.6%.

Fitting parameters A_1-A_5

2.6060E-03	-2.4446E+00	-5.6233E-01	-5.1406E-02	3.9364E+00

ALADDIN evaluation function for chemical sputtering yield: EYIELD5A

ALADDIN hierarchical labelling:

SATM D [+1] GRAPHITE T=HPG,B{4}C D=B C [+0]

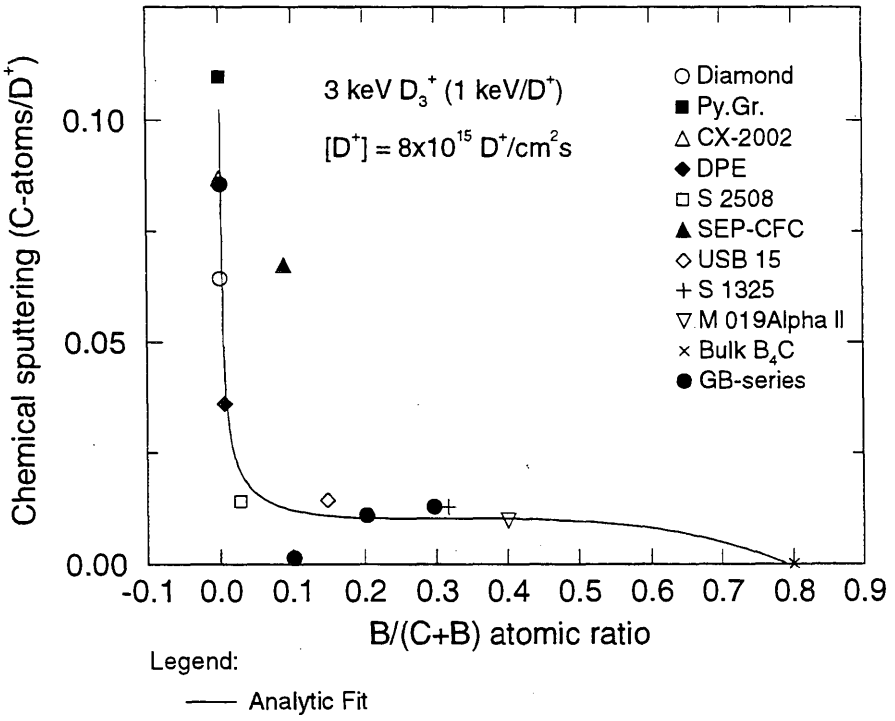

4.2.2.18 D^+ + pyrolytic graphite → CD_4

Source: C. García-Rosales and J. Roth, J. Nucl. Mater. **196-198**, 573 (1992).

Accuracy: Yield (rel.): ±10%; Yield (abs.): ±30%.

Comments: (1) Methane production measured by QMS, calibrated by mass-loss measurements.
(2) Specimen: graphite (pyrolytic).
(3) D_3^+ ions: mass analyzed beam.

Analytic fitting function:

Methane yield:

$$Y = 1.0 \times 10^{-2}[A_1 \exp(-(T - A_2)^2/A_3)T^{A_4} + A_5 \exp(-A_6 T)T^{A_7}] \quad [CD_4/D^+]$$

where T is in Kelvin. The rms deviation of analytic fits for reactions A (□), B (•) and C (△) are 3.0%, 10.2% and 5.7%, respectively.

Fitting parameters A_1-A_7

A	4.1711E-02	7.8005E+02	2.9116E+04	6.0996E-01	2.2197E-06	5.2268E-03
	2.5145E+00					
B	8.8796E+02	8.1335E+02	1.6334E+04	-7.1719E-01	3.7280E-39	2.4159E-02
	1.6129E+01					
C	4.6293E-01	7.9502E+02	1.3357E+04	4.6120E-01	1.5796E-02	-4.1332E-03
	-9.9474E-02					

ALADDIN evaluation function for methane yield: EYIELD7A

ALADDIN hierarchical labelling:

A-C: SATM D [+1] GRAPHITE T=HPG CD{4} [+0]

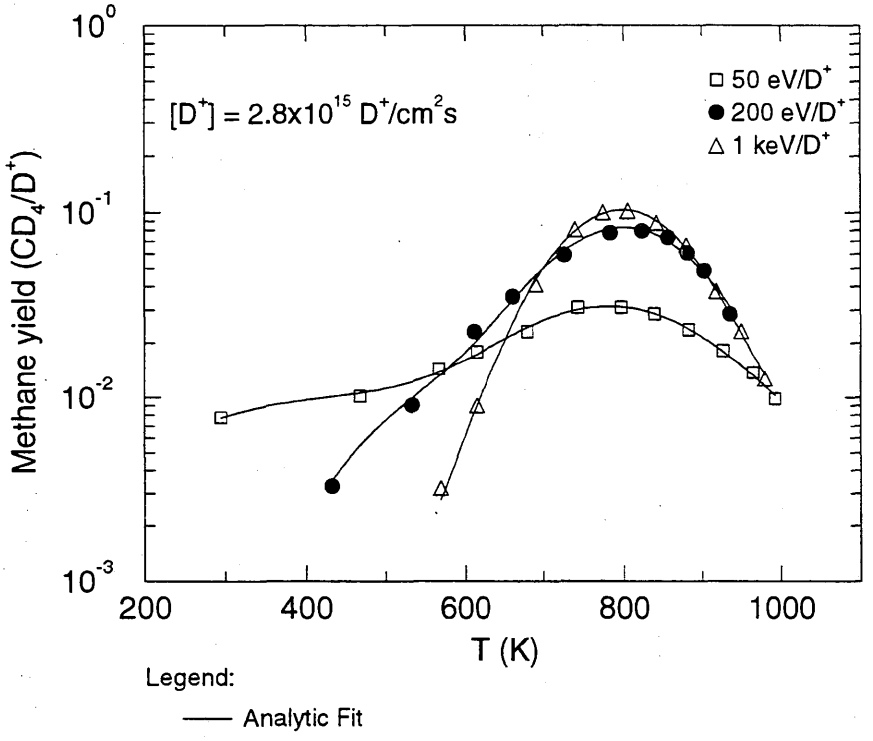

4.2.2.19 D^+ + USB15 graphite → CD_4

Source: C. García-Rosales and J. Roth, J. Nucl. Mater. **196-198**, 573 (1992).

Accuracy: Yield (rel.): ±10%; Yield (abs.): ±30%.

Comments: (1) Methane production measured by QMS, calibrated by mass-loss measurements.
(2) Specimen: USB15 (B-doped graphite, 15 at%B).
(3) D_3^+ ions: mass analyzed beam.

Analytic fitting function:

Methane yield:

$$Y = 1.0 \times 10^{-2}[A_1 \exp(-(T - A_2)^2/A_3)T^{A_4} + A_5 \exp(-A_6 T)T^{A_7}] \quad [CD_4/D^+]$$

where T is in Kelvin. The rms deviation of analytic fits for reactions A (□), B (•) and C (△) are 3.8%, 2.2% and 6.8%, respectively. Data for curves B and C were fitted with EYIELD8A.

Fitting parameters A_1-A_8

A	1.5185E+00	6.1504E+02	1.7560E+04	-6.4989E-02	4.0624E-04	5.0340E-03
	1.6170E+00					
B	1.2290E-02	6.5605E+02	-5.7106E-04	1.9307E+04	1.7538E-02	1.0079e-32
	2.1107E-02	1.2716E+01				
C	3.0476e+06	7.1410E+02	-6.1770E+01	1.1619e-06	-3.0405E+00	4.8536e-170
	1.0544E-01	6.9976E+01				

ALADDIN evaluation function for methane yield: EYIELD7A, EYIELD8A

ALADDIN hierarchical labelling:

A-C: SATM D [+1] GRAPHITE T=USB15 CD{4} [+0]

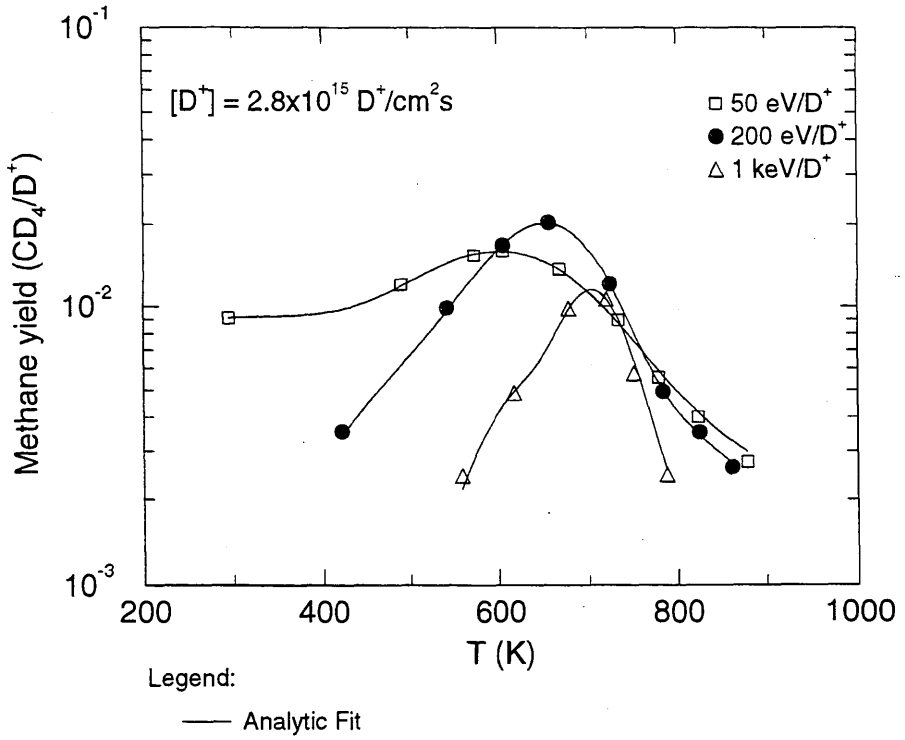

4.2.2.20 D^+ + USB15, B-doped graphite → C, CD_4

Source: C. García-Rosales and J. Roth, J. Nucl. Mater. **196-198**, 573 (1992).

Accuracy: Yield (rel.): ±10%; Yield (abs.): ±30%.

Comments: (1) Weight loss measurement and mass spectroscopy.
(2) Specimen: USB15 (B-doped graphite, 15 at%B).
(3) D_3^+ ions: mass analyzed beam.

Analytic fitting function:

Erosion yield:

$$Y = A_1(\log E)^3 + A_2(\log E - A_3)^2 + A_4 \quad [\text{atoms or molecules}/D^+]$$

where ion energy E is in eV. The rms deviation of analytic fits for reactions A (△), B (□) and C (•) are 11.8%, 0.3% and 9.2%, respectively.

Fitting parameters A_1-A_4

A	-1.1091E-02	6.1238E-02	8.5514E-01	3.6693E-02
B	-7.6050E-02	3.0612E-01	6.6656E-01	5.6241E-02
C	-1.7526E-02	8.4898E-02	7.4464E-01	2.3281E-02

ALADDIN evaluation function for erosion yield: EYIELD4C

ALADDIN hierarchical labelling:

A: SATM D [+1] GRAPHITE T=USB15 D=B C [+0]
B, C: SATM D [+1] GRAPHITE T=USB15 D=B CD{4} [+0]

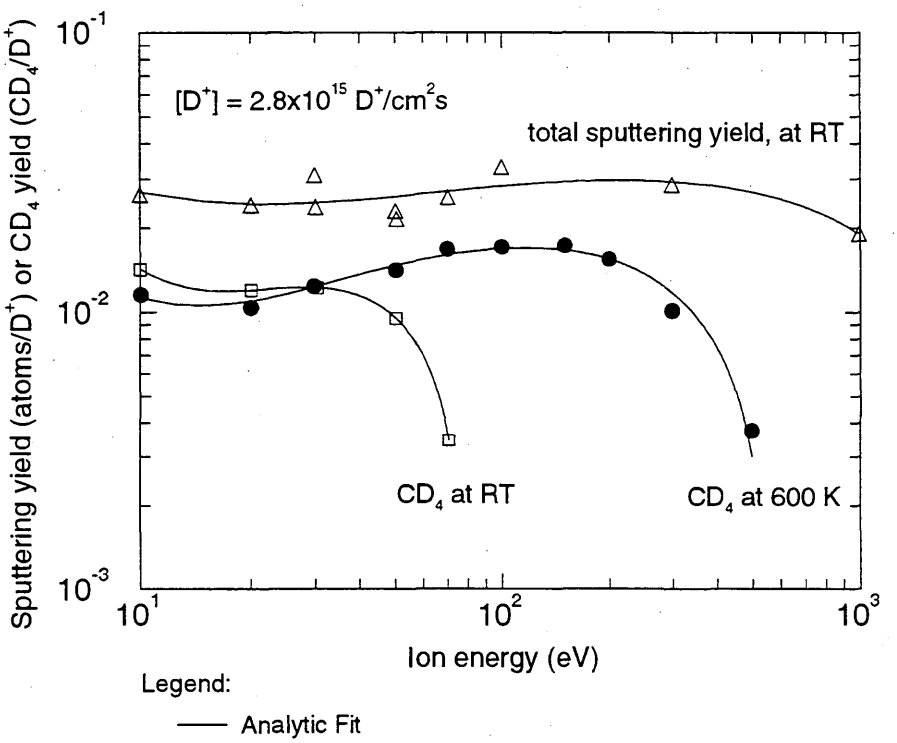

4.2.2.21 D_2^+ + TiC-coated graphite → CH_4

Source: E. Vietzke, K. Flaskamp and V. Philipps, J. Nucl. Mater. **128&129**, 564 (1984).

Accuracy: Yield: 50%.

Comments: (1) Chemical erosion yield due to CH_4 formation by impact of D_2^+ ions.
(2) Specimen: TiC (TiC coated POCO-graphite).
(3) Two-stage differentially pumped QMS-LOS detection of CH_4, steady state.
(4) Mass analyzed ion beam.

Analytic fitting function:

Methane yield:

$$Y = A_1 \exp(-A_2 T) T^{A_3} \quad [CH_4/\text{ion}]$$

where T is in Kelvin. The rms deviation of the analytic fit is 0.0%.

Fitting parameters A_1-A_3

2.4923E-07	8.9353E-03	2.0448E+00

ALADDIN evaluation function methane yield: EYIELD3A

ALADDIN hierarchical labelling:

SATM D{2} [+1] GRAPHITE T=PVD-TiC CH{4} [+0]

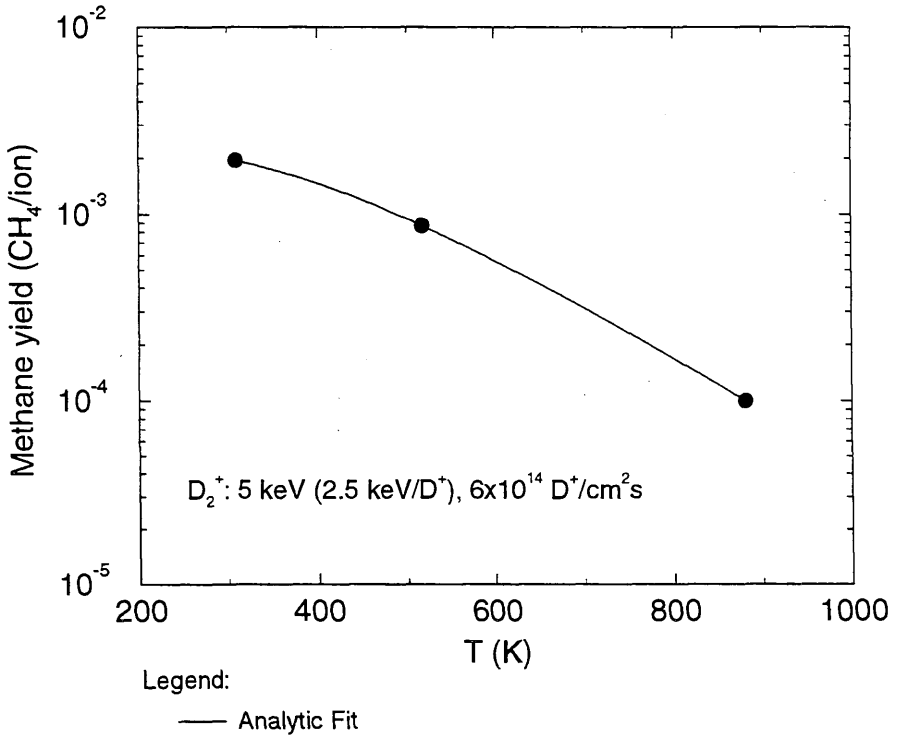

4.2.2.22 D_2^+ + pyrolytic graphite → CD_4

Source: A. A. Haasz, B. V. Mech and J. W. Davis, J. Nucl. Mater. **231**, 170 (1996).

Accuracy: Yield: ±20%.

Comments: (1) Steady-state methane yield.
(2) Specimen: pyrolytic graphite (HPG99).
(3) Incident ions were mass-analyzed.
(4) Reaction products measured by QMS-RGA.

Analytic fitting function:

Methane yield:

$$Y = 1.0 \times 10^{-2}[A_1 \exp(-(E - A_2)^2/A_3)E^{A_4} + A_5 \exp(-A_6 E)E^{A_7}] \quad [CD_4/D^+]$$

where E is in eV. The rms deviation of analytic fits for reactions A (•), B (□), C (△) and D (◇) are 4.5%, 0.9%, 2.4% and 2.5%, respectively. Data for curve C were fitted with EYIELD8A.

Fitting parameters A_1-A_7

A	1.5970E-01	3.3830E+01	1.4799E+03	3.6776E-01	1.4210E-03	2.2217E-02
	1.7469E+00					
B	9.5225E+02	-2.8174E+02	3.7916E+03	5.1060E+00	3.2247E-01	3.5542E-03
	4.5442E-01					
C	2.6094E-05	4.2362E+01	1.1827E-01	3.4837E+01	1.5989E+00	1.2969 E-04
	4.7156E-02	1.4464E+00				
D	8.4787E-02	-3.3345E+02	7.6573E+03	5.3563E+00	1.3069E-02	5.1499E-03
	9.3540E-01					

ALADDIN evaluation function for reaction yield: EYIELD7A, EYIELD8A

ALADDIN hierarchical labelling:

A-D: SATM D{3} [+1] GRAPHITE T=HPG99 CD{4} [+0]

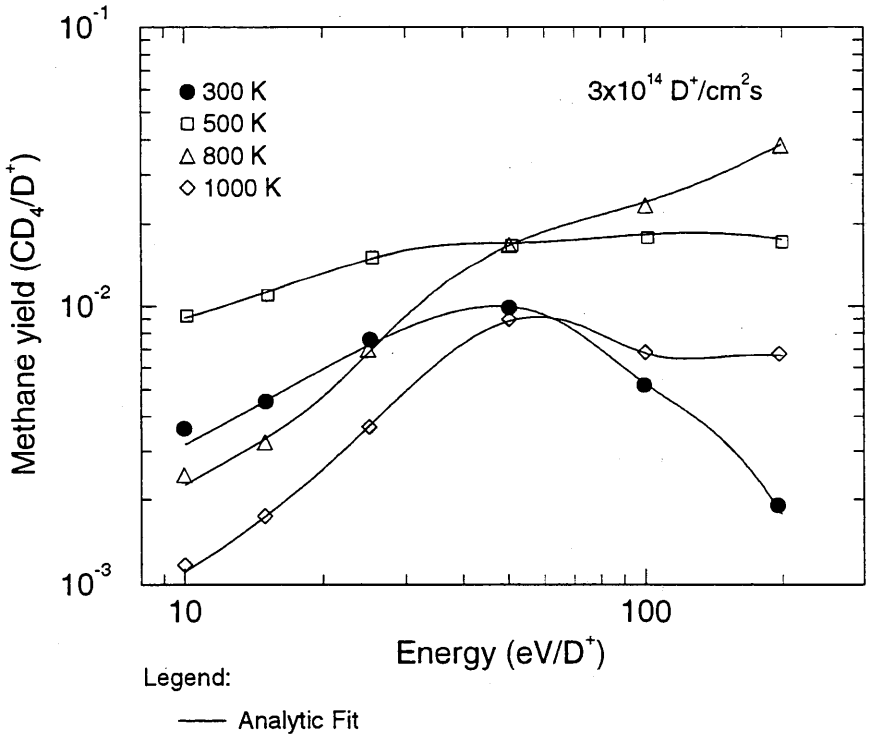

4.2.2.23 D_2^+ + pyrolytic graphite → CD_4

Source: A. A. Haasz, B. V. Mech and J. W. Davis, J. Nucl. Mater. **231**, 170 (1996).

Accuracy: Yield: ±20%; T: ±25K.

Comments: (1) Steady-state methane yield.
(2) Specimen: pyrolytic graphite (HPG99).
(3) Incident ions were mass-analyzed.
(4) Reaction products measured by QMS-RGA.

Analytic fitting function:

Methane yield:

$$Y = A_1 \exp[-(\frac{T - A_2}{A_3 T + 1})^2 / A_4] T^{A_5} + A_6 \exp(-A_7 T) T^{A_8} \quad [CD_4/D^+]$$

where T is in Kelvin. The rms deviation of analytic fits for reactions A (+), B (◇), C (△), D (▽), E (•) and F (□) are 27.6%, 25.7%, 32.5%, 16.5%, 21.3% and 21.0%, respectively.

Fitting parameters A_1-A_8

A	-1.1973E+02	8.3963E+02	1.8156E-02	3.0590E+02	-1.4732E+00	1.8114E-14
	7.7872E-03	4.9525E+00				
B	-2.3525E+02	7.5756E+02	5.7874E-04	1.1183E+04	-1.6862E+00	1.3861E-14
	9.9924E-03	5.1912E+00				
C	8.5817E+05	1.9403E+03	1.9765E-04	-1.3448E+04	-1.5540E+02	1.4694E-13
	9.7308E-03	4.8430E+00				
D	1.3897E+03	8.2539E+02	3.3963E-02	2.7273E+02	-1.7064E+00	2.2609E-11
	1.4463E-02	4.2625E+00				
E	1.9404E+01	6.9777E+02	2.5501E-01	6.5010E-01	-1.0652E+00	5.3787E-18
	1.0875E-02	6.6128E+00				
F	1.0353E+03	7.1297E+02	9.4195E-03	2.7353E+02	-1.5845E+00	1.6718E-32
	1.9093E-02	1.2662E+01				

ALADDIN evaluation function for methane yield: EYIELD8A

ALADDIN hierarchical labelling:

A-F: SATM D{3} [+1] GRAPHITE T=HPG99 CD{4} [+0]

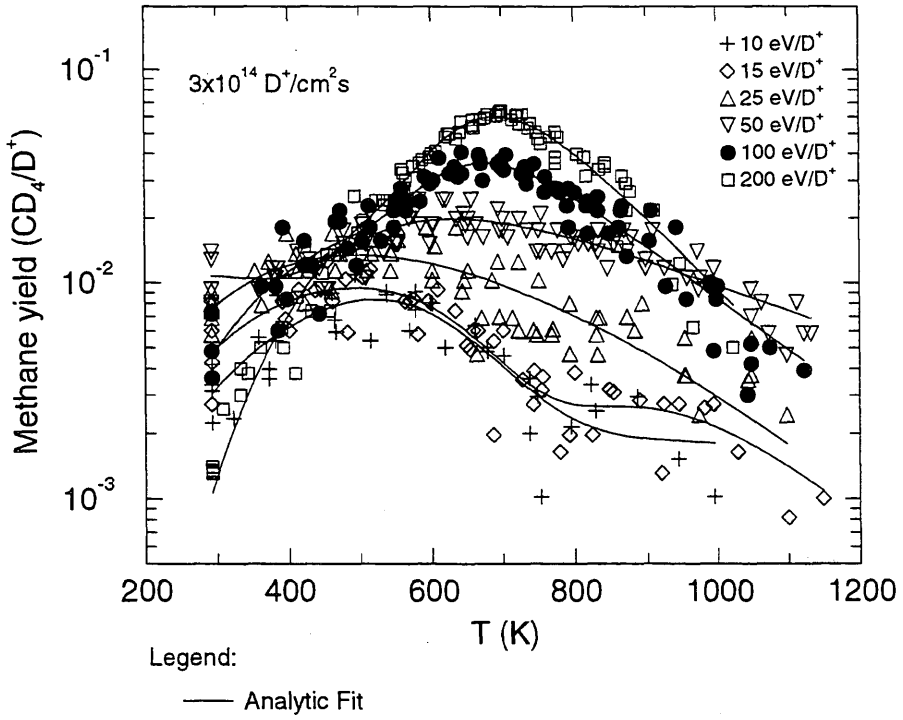

4.2.2.24 D_2^+ + pyrolytic graphite → CD_4, C_{heavy}, C

Source: B. V. Mech, A. A. Haasz and J. W. Davis, J. Nucl. Mater., in press (1998).

Accuracy: Yield: ±20%; T: ±25K.

Comments: (1) Steady-state hydrocarbon yield.
(2) Specimen: pyrolytic graphite (HPG99).
(3) Incident ions were mass-analyzed.
(4) Reaction products measured by QMS-RGA.
(5) Y_{heavy} is the hydrocarbon yield excluding methane = $[2(C_2D_2 + C_2D_4 + C_2D_6) + 3(C_3D_6 + C_3D_8)]/D^+$.
(6) Yield for total chemical erosion, $Y_{chem-total} = [CD_4 + 2(C_2D_2 + C_2D_4 + C_2D_6) + 3(C_3D_6 + C_3D_8)]/D^+$.

Analytic fitting function:

Erosion yield:

$$Y = A_1(\log E)^3 + A_2(\log E - A_3)^2 + A_4 \quad [\text{molecules}/D^+]$$

where E is in eV. The rms deviation of analytic fits for reactions A (•), B (○), and C (□) are 18.7%, 16.1% and 21.9%, respectively. Data for curves A were fitted with EYIELD4D.

Fitting parameters A_1-A_4

A	1.3053e-02	-1.2579e+02	1.0738e+00	-1.3268e+02
B	4.5464e-03	-2.0683e-02	7.2942e-01	1.7703e-04
C	-1.3364e-03	-8.9739e-04	8.2625e+00	5.1689e-02

ALADDIN evaluation function for erosion yield: EYIELD4C, EYIELD4D

ALADDIN hierarchical labelling:

A: SATM D{3} [+1] GRAPHITE T=HPG99 C [+0]
B: SATM D{3} [+1] GRAPHITE T=HPG99 C{X}D{Y} [+0]
C: SATM D{3} [+1] GRAPHITE T=HPG99 CD{4} [+0]

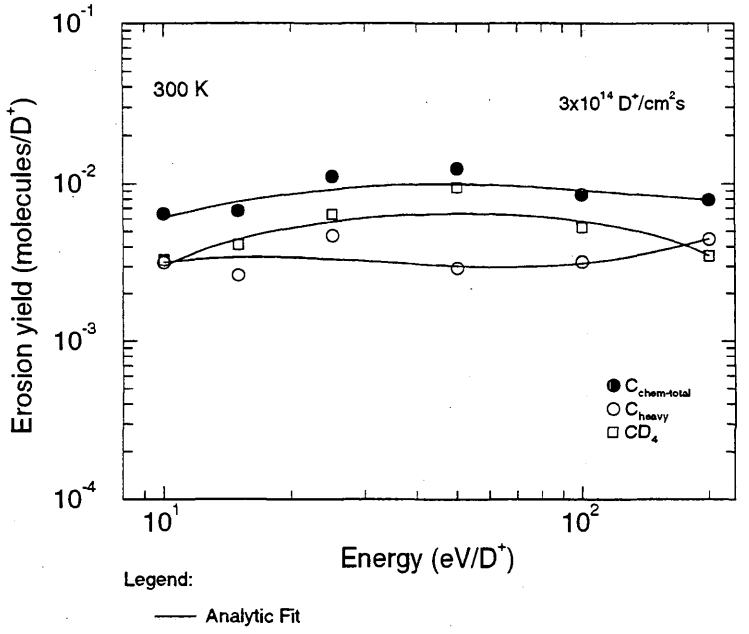

4.2.2.25 D_2^+ + pyrolytic graphite → CD_4, C_{heavy}, C

Source: B. V. Mech, A. A. Haasz and J. W. Davis, J. Nucl. Mater., in press (1998).

Accuracy: Yield: ±20%; T: ±25K.

Comments: (1) Steady-state hydrocarbon yield.
(2) Specimen: pyrolytic graphite (HPG99).
(3) Incident ions were mass-analyzed.
(4) Reaction products measured by QMS-RGA.
(5) Y_{heavy} is the hydrocarbon yield excluding methane = $[2(C_2D_2 + C_2D_4 + C_2D_6) + 3(C_3D_6 + C_3D_8)]/D^+$.
(6) Yield for total chemical erosion, $Y_{chem-total} = [CD_4 + 2(C_2D_2 + C_2D_4 + C_2D_6) + 3(C_3D_6 + C_3D_8)]/D^+$.

Analytic fitting function:

Erosion yield:

$$Y = A_1 \exp(-A_2/E)/(1 + A_3 \exp(-A_4/E)) \quad [\text{molecules}/D^+]$$

where E is in eV. The rms deviation of analytic fits for reactions A (•), B (○), and C (□) are 5.7%, 16.1% and 21.9%, respectively. Data for curve A were fitted with EYIELD4A.

Fitting parameters A_1-A_4

A	6.2590e-03	1.4030e-02	4.7850e-01	1.0000e-04
B	1.7592e-01	2.3009e+01	1.5985e+01	3.1667e+01
C	6.4668e-01	9.3896e+00	4.2233e+01	1.0254e+00

ALADDIN evaluation function for erosion yield: EYIELD4A, EYIELD4D

ALADDIN hierarchical labelling:

A: SATM D{3} [+1] GRAPHITE T=HPG99 C [+0]
B: SATM D{3} [+1] GRAPHITE T=HPG99 C{X}D{Y} [+0]
C: SATM D{3} [+1] GRAPHITE T=HPG99 CD{4} [+0]

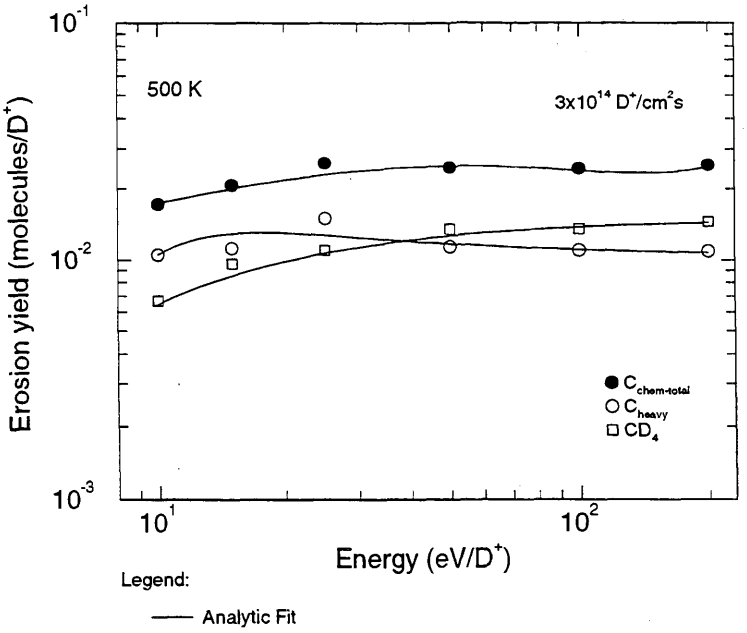

4.2.2.26 D_2^+ + pyrolytic graphite → CD_4, C_{heavy}, C

Source: B. V. Mech, A. A. Haasz and J. W. Davis, J. Nucl. Mater., in press (1998).

Accuracy: Yield: ±20%; T: ±25K.

Comments: (1) Steady-state hydrocarbon yield.
(2) Specimen: pyrolytic graphite (HPG99).
(3) Incident ions were mass-analyzed.
(4) Reaction products measured by QMS-RGA.
(5) Y_{heavy} is the hydrocarbon contribution excluding methane = $[2(C_2D_2 + C_2D_4 + C_2D_6) + 3(C_3D_6 + C_3D_8)]/D^+$.
(6) Yield for total chemical erosion, $Y_{chem-total} = [CD_4 + 2(C_2D_2 + C_2D_4 + C_2D_6) + 3(C_3D_6 + C_3D_8)]/D^+$.

Analytic fitting function:

Erosion yield:

$$Y = A_1 \exp(-A_2 E) E^{A_3} + A_4 E \quad [\text{molecules/D}^+]$$

where E is in eV. The rms deviation of analytic fits for reactions A (•), B (○), and C (□) are 13.2%, 20.8% and 26.8%, respectively. Data for curve C were fitted with EYIELD4D.

Fitting parameters A_1-A_4

A	9.59891e-04	1.93244e-02	1.02558e+00	4.21231e-04
B	1.4492e-03	9.2634e-03	6.3226e-01	1.1092e-04
C	1.2973e-03	-2.6421e+00	-9.9384e-01	3.1675e+00

ALADDIN evaluation function for erosion yield: EYIELD4A, EYIELD4D

ALADDIN hierarchical labelling:

A: SATM D{3} [+1] GRAPHITE T=HPG99 C [+0]
B: SATM D{3} [+1] GRAPHITE T=HPG99 C{X}D{Y} [+0]
C: SATM D{3} [+1] GRAPHITE T=HPG99 CD{4} [+0]

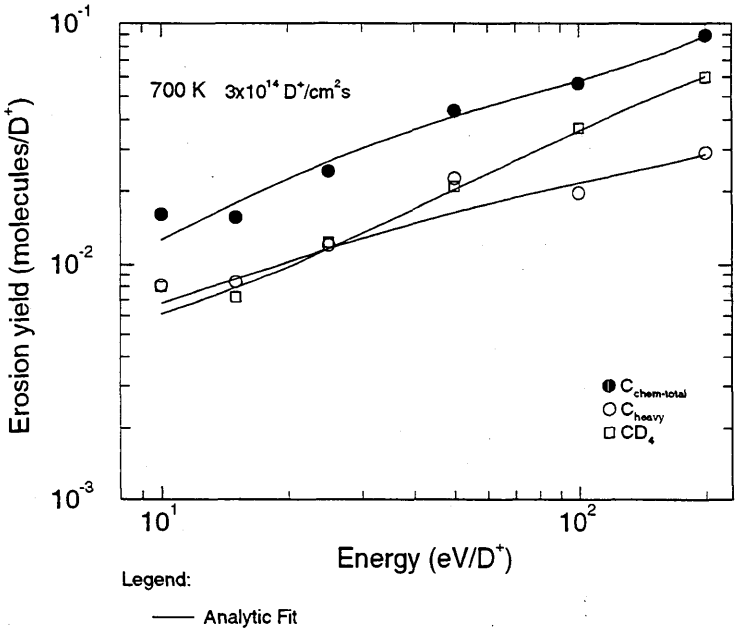

4.2.2.27 D_2^+ + pyrolytic graphite → CD_4, C_{heavy}, C

Source: B. V. Mech, A. A. Haasz and J. W. Davis, J. Nucl. Mater., in press (1998).

Accuracy: Yield: ±20%; T: ±25K.

Comments: (1) Steady-state hydrocarbon yield.
(2) Specimen: pyrolytic graphite (HPG99).
(3) Incident ions were mass-analyzed.
(4) Reaction products measured by QMS-RGA.
(5) Y_{heavy} is the hydrocarbon contribution excluding methane = $[2(C_2D_2 + C_2D_4 + C_2D_6) + 3(C_3D_6 + C_3D_8)]/D^+$.
(6) Yield for total chemical erosion, $Y_{chem-total} = [CD_4 + 2(C_2D_2 + C_2D_4 + C_2D_6) + 3(C_3D_6 + C_3D_8)]/D^+$.

Analytic fitting function:

Erosion yield:

$$Y = A_1 \exp(-A_2 E) E^{A_3} + A_4 E^{A_5} \quad [\text{molecules}/D^+]$$

where E is in eV. The rms deviation of analytic fits for reactions A (•), B (○), and C (□) are 2.4%, 23.3% and 3.2%, respectively.

Fitting parameters A_1-A_5

A	2.90327e-18	2.73927e-01	1.26302e+01	5.63037e-04	4.31397e-01
B	6.56865e-15	1.61908e-01	9.04002e+00	1.25172e-04	4.68461e-01
C	9.56259e-22	3.87056e-01	1.59559e+01	3.75033e-04	4.47891e-01

ALADDIN evaluation function for erosion yield: EYIELD5A

ALADDIN hierarchical labelling:

A: SATM D{3} [+1] GRAPHITE T=HPG99 C [+0]
B: SATM D{3} [+1] GRAPHITE T=HPG99 C{X}D{Y} [+0]
C: SATM D{3} [+1] GRAPHITE T=HPG99 CD{4} [+0]

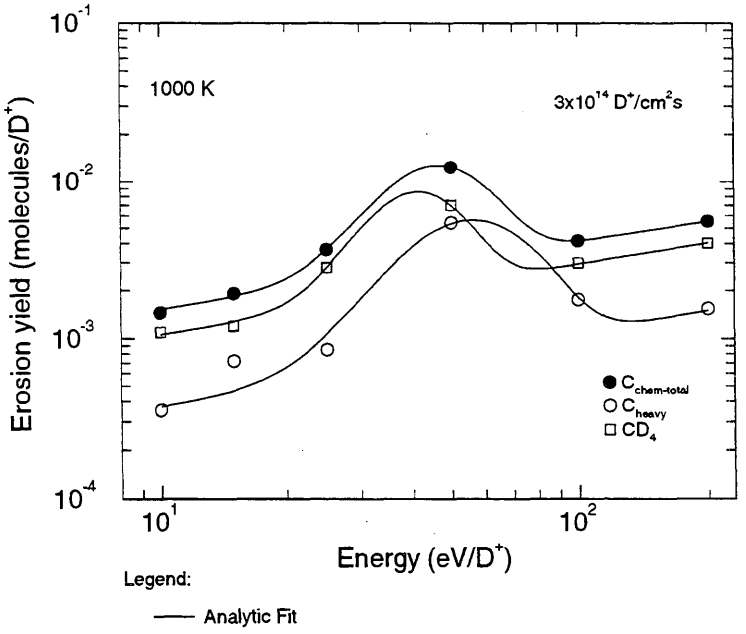

4.2.2.28 D_2^+ + pyrolytic graphite → C_xD_y, C

Source: B. V. Mech, A. A. Haasz and J. W. Davis, J. Nucl. Mater., in press (1998).

Accuracy: Yield: ±20%; T: ±25K.

Comments: (1) Steady-state hydrocarbon yield.
(2) Specimen: pyrolytic graphite (HPG99).
(3) Incident ions were mass-analyzed.
(4) Reaction products measured by QMS-RGA.
(5) Yield for total chemical erosion, $Y_{chem-total} = [CD_4 + 2(C_2D_2 + C_2D_4 + C_2D_6) + 3(C_3D_6 + C_3D_8)]/D^+$.

Analytic fitting function:
Erosion yield:

$$Y = A_1 \exp(-(T - A_2)^2/A_3)T^{A_4} + A_5 \exp(-A_6T)T^{A_7}(1 + A_8T^{A_9}) \quad [\text{molecules/D}^+]$$

where T is in Kelvin. The rms deviation of analytic fits for reactions A (∗), B (•), C (○), D (△), E (▽), F (□) and G (◇) are 15.0%, 13.0%, 21.9%, 20.7%, 21.0%, 24.4% and 33.6%, respectively. Data for curves A, F and G were fitted with EYIELD7A.

Fitting parameters A_1-A_9

A	5.8180e-08	5.5249e+02	3.0296e+04	1.9943e+00	2.0870e-03	2.0369e-03	2.8558e-01
B	7.9403e-07	5.9087e+02	4.6893e+04	1.4371e+00	1.4873e+04	-3.5500e-03	-2.7702e+00
	-1.5036e-01	2.2651e-01					
C	9.3137e-09	5.6909e+02	2.7460e+03	1.7390e+00	2.9021e-22	1.9882e-02	8.4596e+00
	-9.7449e+00	-4.0804e-01					
D	1.9098e-08	5.8738e+02	1.0614e+04	1.8162e+00	6.1861e-22	2.0479e-02	8.5758e+00
	-8.6648e+00	-4.3755e-01					
E	1.0908e-08	5.9016e+02	1.0314e+04	1.7908e+00	1.0678e-22	1.3447e-02	7.9468e+00
	9.1201e+04	-1.9470e+00					
F	2.8872e-10	5.4907e+02	1.7637e+04	2.4238e+00	4.1992e-04	3.3180e-03	1.0764e-01
G	1.2983e-10	5.3906e+02	3.0753e+04	2.2640e+00	6.6541e-09	4.1380e-03	1.7081e+00

ALADDIN evaluation function for erosion yield: EYIELD7A, EYIELD9A

ALADDIN hierarchical labelling:

A: SATM D{3} [+1] GRAPHITE T=HPG99 C [+0]
B: SATM D{3} [+1] GRAPHITE T=HPG99 CD{4} [+0]
C: SATM D{3} [+1] GRAPHITE T=HPG99 C{2}D{2} [+0]
D: SATM D{3} [+1] GRAPHITE T=HPG99 C{2}D{4} [+0]
E: SATM D{3} [+1] GRAPHITE T=HPG99 C{2}D{6} [+0]
F: SATM D{3} [+1] GRAPHITE T=HPG99 C{3}D{6} [+0]
G: SATM D{3} [+1] GRAPHITE T=HPG99 C{3}D{8} [+0]

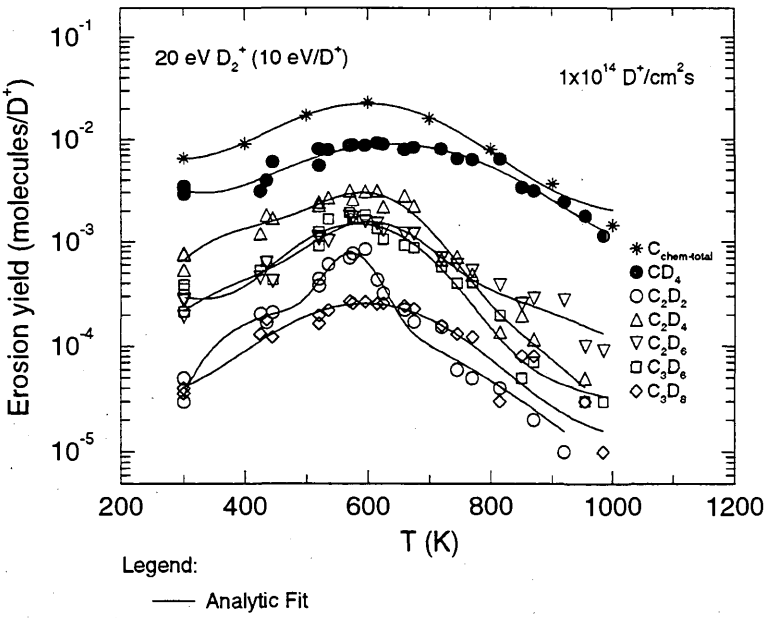

4.2.2.29 D_2^+ + pyrolytic graphite → C_xD_y, C

Source: B. V. Mech, A. A. Haasz and J. W. Davis, J. Nucl. Mater., in press (1998).

Accuracy: Yield: ±20%; T: ±25K.

Comments: (1) Steady-state hydrocarbon yield.
(2) Specimen: pyrolytic graphite (HPG99).
(3) Incident ions were mass-analyzed.
(4) Reaction products measured by QMS-RGA.
(5) Yield for total chemical erosion, $Y_{chem-total} = [CD_4 + 2(C_2D_2 + C_2D_4 + C_2D_6) + 3(C_3D_6 + C_3D_8)]/D^+$.

Analytic fitting function:

Erosion yield:

$$Y = A_1 \exp[-(\frac{T - A_2}{A_3T + 1})^2/A_4]T^{A_5} + A_6 \exp(-A_7T)T^{A_8} \quad [\text{molecules}/D^+]$$

where T is in Kelvin. The rms deviation of analytic fits for reactions A (∗), B (•), C (○), D (△), E (▽), F (□) and G (◇) are 5.7%, 9.4%, 86.3%, 31.3%, 47.0%, 32.0% and 62.3%, respectively. Data for curve A were fitted with EYIELD7A, for curve C with EYIELD9A, and for curve E EYIELD8B.

Fitting parameters A_1-A_9

A	1.0272e-05	5.8150e+02	1.5685e+04	1.1288e+00	1.3326e-16	1.2168e-02	6.1643e+00
B	1.4925e-03	5.7026e+02	1.8481e-03	5.2984e+03	2.0765e-01	1.5560e-11	8.2390e-03
	3.8344e+00						
C	4.2530e-02	5.8994e+02	1.5647e+04	-7.5429e-01	9.7837e-05	5.6840e-03	-7.0260e-02
	1.2344e-02	1.1412e+00					
D	7.3999E-05	5.5074E+02	1.3379E+04	1.3057E+00	2.9166E+02	-4.0381E+00	-3.9526E-01
	1.6285E-01						
E	1.4174e-11	5.2440e+02	3.5415e+04	2.8851e+00	6.3596e+03	-4.7399e+00	-2.7232e-01
	1.0564e-01						
F	3.5150e-03	5.8878e+02	-2.9462e-04	1.5609e+04	-2.1780e-01	7.1102e-14	9.3420e-03
	4.4568e+00						
G	1.7467e-03	5.9021e+02	-3.0382e-04	2.0160e+04	-3.4132e-01	4.6681e-20	1.3508e-02
	6.7869e+00						

ALADDIN evaluation function for erosion yield: EYIELD7A, EYIELD8A, EYIELD8B, EYIELD9A

ALADDIN hierarchical labelling:

A: SATM D{3} [+1] GRAPHITE T=HPG99 C [+0]
B: SATM D{3} [+1] GRAPHITE T=HPG99 CD{4} [+0]
C: SATM D{3} [+1] GRAPHITE T=HPG99 C{2}D{2} [+0]
D: SATM D{3} [+1] GRAPHITE T=HPG99 C{2}D{4} [+0]
E: SATM D{3} [+1] GRAPHITE T=HPG99 C{2}D{6} [+0]
F: SATM D{3} [+1] GRAPHITE T=HPG99 C{3}D{6} [+0]
G: SATM D{3} [+1] GRAPHITE T=HPG99 C{3}D{8} [+0]

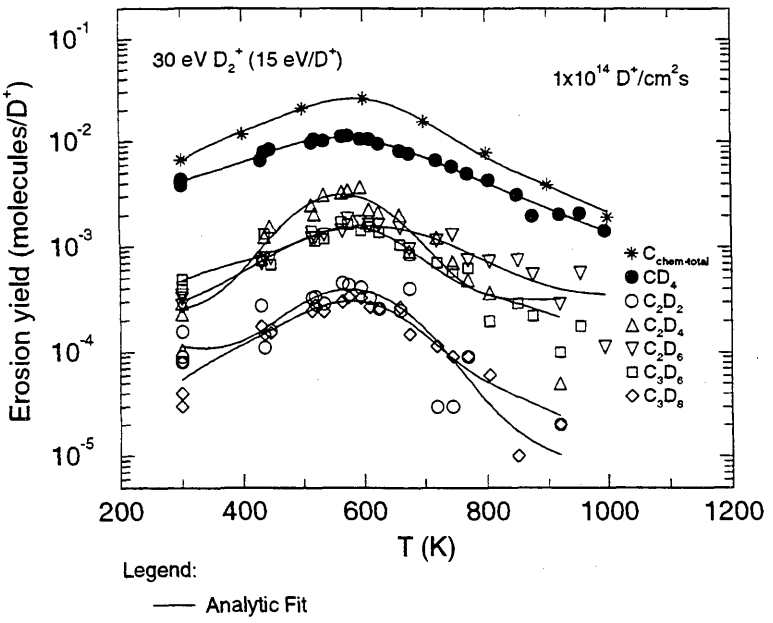

4.2.2.30 D_2^+ + pyrolytic graphite → C_xD_y, C

Source: B. V. Mech, A. A. Haasz and J. W. Davis, J. Nucl. Mater., in press (1998).

Accuracy: Yield: ±20%; T: ±25K.

Comments: (1) Steady-state hydrocarbon yield.
(2) Specimen: pyrolytic graphite (HPG99).
(3) Incident ions were mass-analyzed.
(4) Reaction products measured by QMS-RGA.
(5) Yield for total chemical erosion, $Y_{chem-total} = [CD_4 + 2(C_2D_2 + C_2D_4 + C_2D_6) + 3(C_3D_6 + C_3D_8)]/D^+$.

Analytic fitting function:
Erosion yield:

$$Y = A_1 \exp(-(Y - A_2)^2/A_3)Y^{A_4} + A_5 \exp(-A_6 Y)Y^{A_7}(1 + A_8 Y^{A_9}) \quad [\text{molecules/D}^+]$$

where T is in Kelvin. The rms deviation of analytic fits for reactions A (∗), B (•), C (○), D (△), E (▽), F (□) and G (◇) are 4.4%, 7.5%, 18.1%, 22.2%, 7.5%, 32.9% and 30.6%, respectively. Data for curves A and B were fitted with EYIELD7A.

Fitting parameters A_1-A_9

A	2.0396e-02	6.0418e+02	2.8062e+04	2.2941e-02	4.4642e-06	4.0460e-03	1.5683e+00
B	1.1551e-01	6.3675e+02	3.2459e+04	-3.8825e-01	6.7140e-03	1.0696e-03	3.4660e-02
C	4.2551e-04	5.7230e+02	2.8096e+04	5.5280e-02	3.0792e-03	1.4933e-03	-7.3132e-01
	4.8136e+02	-7.2800e-01					
D	9.3267e-04	5.8344e+02	1.1601e+04	1.9068e-01	3.0774e-04	7.2370e-03	1.0802e+00
	-7.4646e+00	-3.5838e-01					
E	2.3715e-06	6.1910e+02	1.0038e+04	8.2631e-01	1.2733e-18	1.2180e-02	6.7230e+00
	-1.4378e+00	-9.6980e-02					
F	2.0829E-03	6.0203E+02	3.2435E+04	-3.6018E-02	1.0500E-09	1.1537E-02	1.6321E+00
	9.5847E-03	2.1124E+00					
G	2.6489E-04	6.1141E+02	1.7273E+04	7.1480E-03	6.3786E-03	2.7030E-03	-3.5108E-01
	-4.8891E+01	-7.4324E-01					

ALADDIN evaluation function for erosion yield: EYIELD7A, EYIELD9A.

ALADDIN hierarchical labelling:

A: SATM D{3} [+1] GRAPHITE T=HPG99 C [+0]
B: SATM D{3} [+1] GRAPHITE T=HPG99 CD{4} [+0]
C: SATM D{3} [+1] GRAPHITE T=HPG99 C{2}D{2} [+0]
D: SATM D{3} [+1] GRAPHITE T=HPG99 C{2}D{4} [+0]
E: SATM D{3} [+1] GRAPHITE T=HPG99 C{2}D{6} [+0]
F: SATM D{3} [+1] GRAPHITE T=HPG99 C{3}D{6} [+0]
G: SATM D{3} [+1] GRAPHITE T=HPG99 C{3}D{8} [+0]

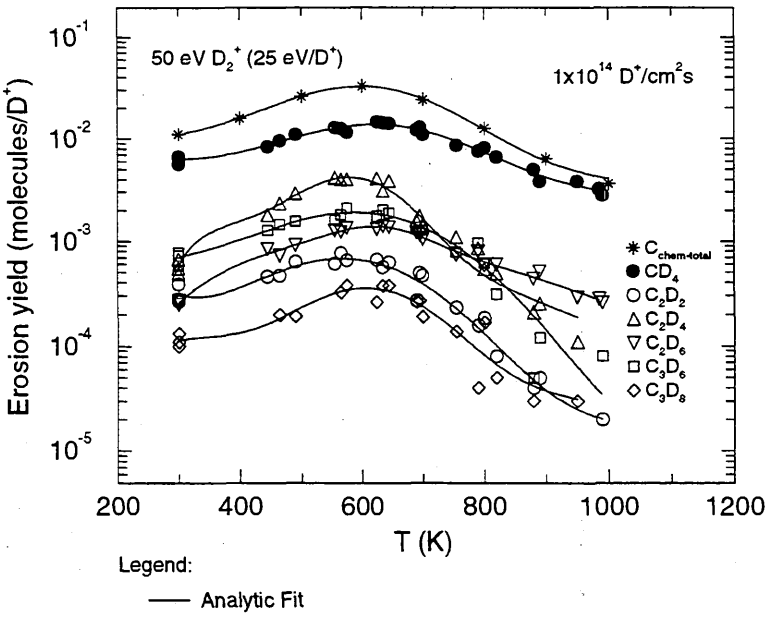

4.2.2.31 D_2^+ + pyrolytic graphite → C_xD_y, C

Source: B. V. Mech, A. A. Haasz and J. W. Davis, J. Nucl. Mater., in press (1998).

Accuracy: Yield: ±20%; T: ±25K.

Comments: (1) Steady-state hydrocarbon yield.
(2) Specimen: pyrolytic graphite (HPG99).
(3) Incident ions were mass-analyzed.
(4) Reaction products measured by QMS-RGA.
(5) Yield for total chemical erosion, $Y_{chem-total} = [CD_4 + 2(C_2D_2 + C_2D_4 + C_2D_6) + 3(C_3D_6 + C_3D_8)]/D^+$.

Analytic fitting function:
Erosion yield:

$$Y = A_1 \exp(-(T - A_2)^2/A_3)T^{A_4} + A_5 \exp(-A_6T)T^{A_7} \quad [\text{molecules/D}^+]$$

where T is in Kelvin. The rms deviation of analytic fits for reactions A (∗), B (•), C (○), D (△), E (▽), F (□) and G (◇) are 3.7%, 9.0%, 24.5%, 17.0%, 10.3%, 16.0% and 17.2%, respectively.

Fitting parameters A_1-A_7

A	1.0218e-07	6.1979e+02	3.6961e+04	1.9538e+00	1.6864e-03	6.7664e-04	3.7827e-01
B	4.6903E-09	6.4935E+02	5.0664E+04	2.2672E+00	6.9416E-05	2.6265E-03	9.9690E-01
C	5.7525e-05	6.5523e+02	1.4578e+04	2.9614e-01	3.6462e-10	4.4760e-03	2.4926e+00
D	2.8027E-09	5.9855E+02	1.1974E+04	2.1840E+00	6.3790E-16	7.4186E-03	5.1399E+00
E	2.2029E-09	6.4057E+02	1.0122E+04	2.0872E+00	6.1367E-14	6.4731E-03	4.3206E+00
F	7.2142e-04	6.6463e+02	1.7842e+04	1.1409e-01	3.0786e-12	4.8660e-03	3.5042e+00
G	2.9492e-04	6.9358e+02	2.5143e+04	1.7637e-02	2.8931e-18	9.5260e-03	5.8322e+00

ALADDIN evaluation function for erosion yield: EYIELD7A

ALADDIN hierarchical labelling:

A: SATM D{3} [+1] GRAPHITE T=HPG99 C [+0]
B: SATM D{3} [+1] GRAPHITE T=HPG99 CD{4} [+0]
C: SATM D{3} [+1] GRAPHITE T=HPG99 C{2}D{2} [+0]
D: SATM D{3} [+1] GRAPHITE T=HPG99 C{2}D{4} [+0]
E: SATM D{3} [+1] GRAPHITE T=HPG99 C{2}D{6} [+0]
F: SATM D{3} [+1] GRAPHITE T=HPG99 C{3}D{6} [+0]
G: SATM D{3} [+1] GRAPHITE T=HPG99 C{3}D{8} [+0]

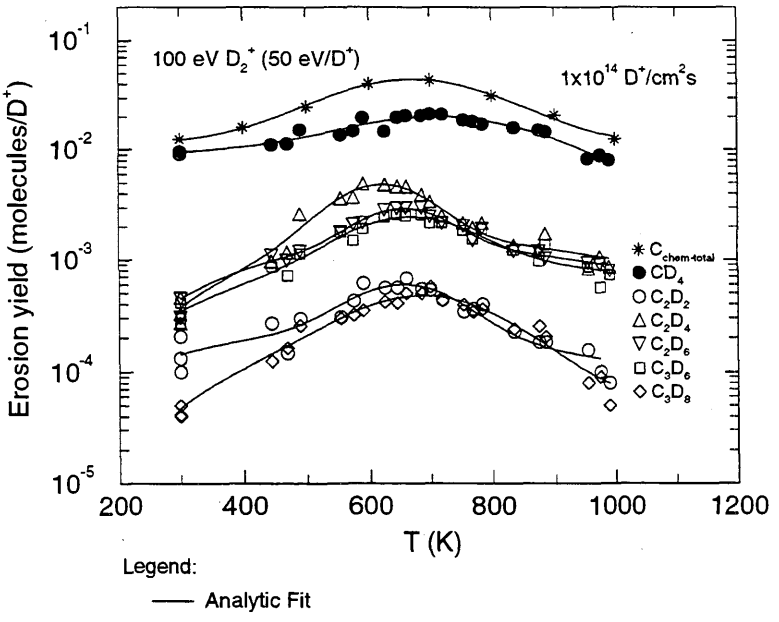

4.2.2.32 D_2^+ + pyrolytic graphite → C_xD_y, C

Source: B. V. Mech, A. A. Haasz and J. W. Davis, J. Nucl. Mater., in press (1998).

Accuracy: Yield: ±20%; T: ±25K.

Comments: (1) Steady-state hydrocarbon yield.
(2) Specimen: pyrolytic graphite (HPG99).
(3) Incident ions were mass-analyzed.
(4) Reaction products measured by QMS-RGA.
(5) Yield for total chemical erosion, $Y_{chem-total} = [CD_4 + 2(C_2D_2 + C_2D_4 + C_2D_6) + 3(C_3D_6 + C_3D_8)]/D^+$.

Analytic fitting function:

Erosion yield:

$$Y = A_1 \exp[-(\frac{T - A_2}{A_3 T + 1})^2 / A_4] T^{A_5} + A_6 \exp(-A_7 T) T^{A_8} \quad [\text{molecules/D}^+]$$

where T is in Kelvin. The rms deviation of analytic fits for reactions A (∗), B (•), C (○), D (△), E (▽), F (□) and G (◇) are 6.6%, 11.1%, 29.5%, 33.6%, 25.0%, 132.9% and 11.8%, respectively. Data for curves A and B were fitted with EYIELD7A and EYIELD9A, respectively.

Fitting parameters A_1-A_9

A	1.6995e+00	6.9624e+02	2.3168e+04	-5.5221e-01	7.2038e-13	8.9900e-03	4.5385e+00
B	5.6870e-02	7.0880e+02	2.3207e+04	-8.6340e-02	8.4637e+00	3.7440e-03	-1.8606e-01
	-1.1609e+00	-2.7153e-02					
C	1.0799e-01	6.4903e+02	-3.4940e-03	2.7854e+03	-9.4208e-01	1.8435e-20	1.3377e-02
	7.1025e+00						
D	3.2335e-01	6.3931e+02	-4.2130e-02	1.4740e+01	-7.3051e-01	3.2946e-20	1.6115e-02
	7.4506e+00						
E	2.2526e-01	6.7651e+02	-2.6662e-02	2.4088e+01	-7.8624e-01	9.9456e-21	1.3034e-02
	7.3610e+00						
F	4.5833e-01	6.5643e+02	-4.7230e-02	1.1004e+01	-8.1557e-01	3.2736e-23	1.7417e-02
	8.6132e+00						
G	2.9170e-03	6.9244e+02	-1.0911e-03	1.2362e+05	-3.1957e-01	3.9490e-13	9.2570e-03
	4.0524e+00						

ALADDIN evaluation function for erosion yield: EYIELD7A, EYIELD8A, EYIELD9A

ALADDIN hierarchical labelling:

A: SATM D{3} [+1] GRAPHITE T=HPG99 C [+0]
B: SATM D{3} [+1] GRAPHITE T=HPG99 CD{4} [+0]
C: SATM D{3} [+1] GRAPHITE T=HPG99 C{2}D{2} [+0]
D: SATM D{3} [+1] GRAPHITE T=HPG99 C{2}D{4} [+0]
E: SATM D{3} [+1] GRAPHITE T=HPG99 C{2}D{6} [+0]
F: SATM D{3} [+1] GRAPHITE T=HPG99 C{3}D{6} [+0]
G: SATM D{3} [+1] GRAPHITE T=HPG99 C{3}D{8} [+0]

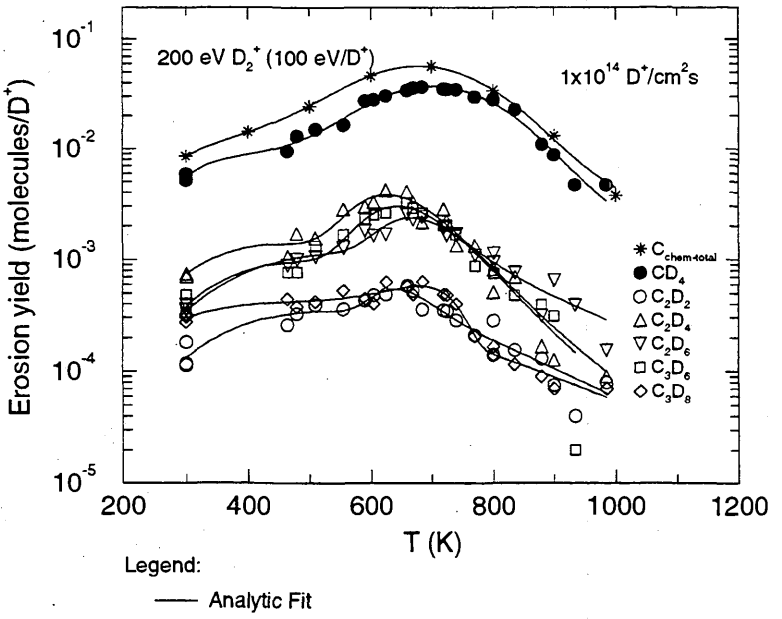

4.2.2.33 D_2^+ + pyrolytic graphite → C_xD_y, C

Source: B. V. Mech, A. A. Haasz and J. W. Davis, J. Nucl. Mater., in press (1998).

Accuracy: Yield: ±20%; T: ±25K.

Comments: (1) Steady-state hydrocarbon yield.
(2) Specimen: pyrolytic graphite (HPG99).
(3) Incident ions were mass-analyzed.
(4) Reaction products measured by QMS-RGA.
(5) Yield for total chemical erosion, $Y_{chem-total} = [CD_4 + 2(C_2D_2 + C_2D_4 + C_2D_6) + 3(C_3D_6 + C_3D_8)]/D^+$.

Analytic fitting function:
Erosion yield:

$$Y = A_1 \exp(-(T - A_2)^2/A_3)T^{A_4} + A_5 \exp(-A_6T)T^{A_7} \quad [\text{molecules/D}^+]$$

where T is in Kelvin. The rms deviation of analytic fits for reactions A (∗), B (•), C (∘), D (△), E (▽), F (□) and G (⋄) are 2.4%, 8.3%, 18.8%, 56.5%, 26.9%, 33.3% and 24.4%, respectively. Data for curves B and D were fitted with EYIELD9A.

Fitting parameters A_1-A_7

A	8.3661e-06	6.7662e+02	2.1011e+04	1.3967e+00	1.7400e-12	8.0940e-03	4.3240e+00
B	2.3290e-02	7.1430e+02	2.4551e+04	1.3667e-01	1.1148e+05	2.7154e-03	-1.7952e+00
	-1.1663e+00	-2.7309e-02					
C	5.2827e-08	6.5395e+02	6.0033e+03	1.3749e+00	4.1352e-16	9.8230e-03	5.1864e+00
D	7.2307e-05	6.6165e+02	7.1525e+03	6.9970e-01	1.0275e-14	8.6540e-03	5.0608e+00
	-1.5472e+00	-1.0253e-01					
E	5.3389e-05	6.6682e+02	1.0177e+04	5.7361e-01	4.4170e-18	1.2496e-02	6.3668e+00
F	1.5881e-05	6.5950e+02	1.3743e+04	7.3194e-01	1.4065e-13	8.3180e-03	4.3090e+00
G	1.2977e-06	6.8530e+02	1.3879e+04	8.6659e-01	4.0118e-13	8.2650e-03	3.9072e+00

ALADDIN evaluation function for erosion yield: EYIELD7A, EYIELD9A

ALADDIN hierarchical labelling:

A: SATM D{3} [+1] GRAPHITE T=HPG99 C [+0]
B: SATM D{3} [+1] GRAPHITE T=HPG99 CD{4} [+0]
C: SATM D{3} [+1] GRAPHITE T=HPG99 C{2}D{2} [+0]
D: SATM D{3} [+1] GRAPHITE T=HPG99 C{2}D{4} [+0]
E: SATM D{3} [+1] GRAPHITE T=HPG99 C{2}D{6} [+0]
F: SATM D{3} [+1] GRAPHITE T=HPG99 C{3}D{6} [+0]
G: SATM D{3} [+1] GRAPHITE T=HPG99 C{3}D{8} [+0]

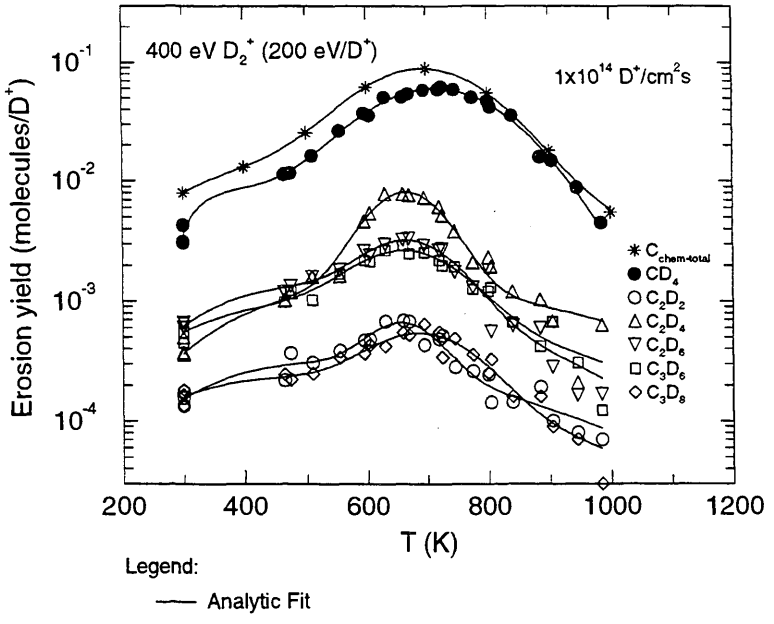

4.2.2.34 D_3^+ + pyrolytic graphite (Ti doped) → C

Source: C. García-Rosales, J. Roth and R. Behrisch, J. Nucl. Mater. **212-215**, 1211 (1994).

Accuracy: Yield: ±20%.

Comments: (1) Total sputtering yield measured by mass loss at room temperature.
(2) Specimen: Ti doped pyrolytic graphite (RG-Ti, 1.7 at%Ti).
(3) D_3^+ ions: mass analyzed accelerator.

Analytic fitting function:

Sputtering yield:

$$Y = A_1 \exp(-A_2 E) E^{A_3} + A_4 E^{A_5} \quad \text{[atoms/ion]}$$

where E is in keV. The rms deviation of the analytic fit is 22.0%.

Fitting parameters A_1-A_5

6.87050e-02	1.84265e+00	1.44433e+00	1.15920e-01	-3.22837e-01

ALADDIN evaluation function for sputtering yield: EYIELD5A

ALADDIN hierarchical labelling:

SATM D{3} [+1] GRAPHITE T=HPG D=Ti C [+0]

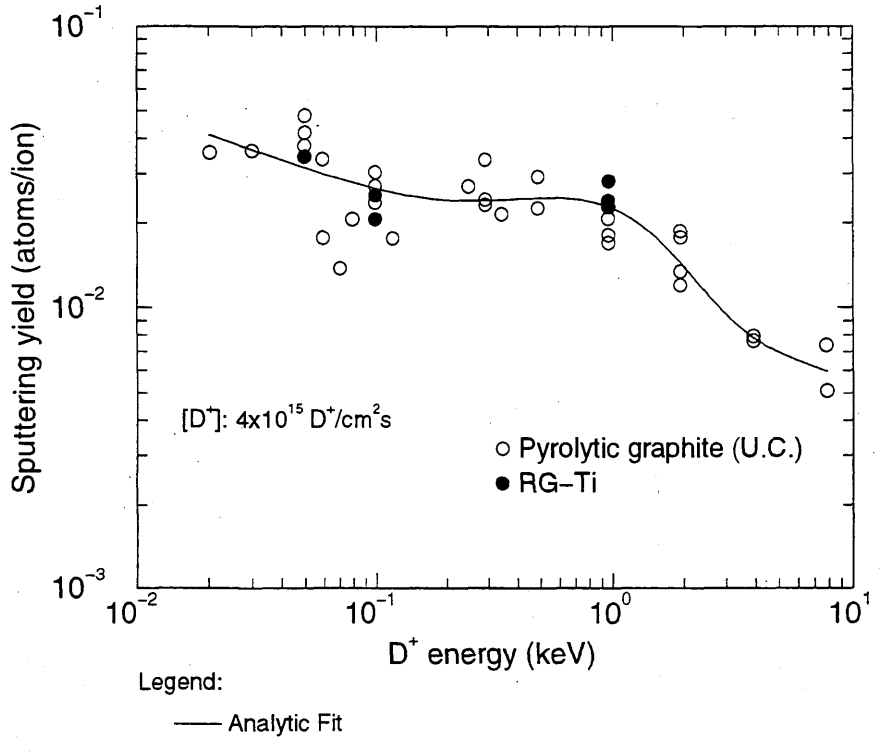

4.2.2.35 D_3^+ + graphite (pyrolytic, Ti, B doped) → CD_4

Source: C. García-Rosales, J. Roth and R. Behrisch, J. Nucl. Mater. **212-215**, 1211 (1994).

Accuracy: Yield: ±20%.

Comments: (1) Steady-state methane production.
(2) Specimen: pyrolytic graphite, RG-Ti (1.7 at%Ti), RG-Ti (1 at%B), USB15 (15 at%B). The RG-Ti was produced at the Efremov Institute, St. Petersburg.
(3) D_3^+ ions: mass analyzed accelerator.

Analytic fitting function:

Methane yield:

$$Y = A_1 \exp[-(\frac{T - A_2}{A_3 T + 1})^2 / A_4] T^{A_5} + A_6 \exp(-A_7 T) T^{A_8} \quad [CD_4/D^+]$$

where T is in Kelvin. The rms deviation of the analytic fits for reactions A (□), B (○), C (•), D (△) are 10.0%, 5.2, 7.0% and 8.8%, respectively.

Fitting parameters A_1-A_8

A	6.2601e-03	7.8625e+02	1.3595e-03	3.0077e+03	4.1211e-01	1.1223e-09
	8.8487e-04	2.3007e+00				
B	3.2814e-03	7.7163e+02	-4.4771e-04	3.1842e+04	3.5000e-01	4.8817e-08
	-1.9227e-04	1.6067e+00				
C	1.9198e-03	7.5334e+02	-2.9289e-04	1.4013e+04	3.7515e-01	3.2129e-28
	1.3260e-02	1.0207e+01				
D	4.9670e-08	7.0101e+02	-1.0709e-03	6.2101e+04	1.8592e+00	1.7282e-10
	4.2064e-03	2.9455e+00				

ALADDIN evaluation function for methane yield: EYIELD8A

ALADDIN hierarchical labelling:

A: SATM D{3} [+1] GRAPHITE T=HPG CD{4} [+0]
B: SATM D{3} [+1] GRAPHITE T=RG-Ti CD{4} [+0]
C: SATM D{3} [+1] GRAPHITE T=RG-Ti D=B CD{4} [+0]
D: SATM D{3} [+1] GRAPHITE T=USB D=B CD{4} [+0]

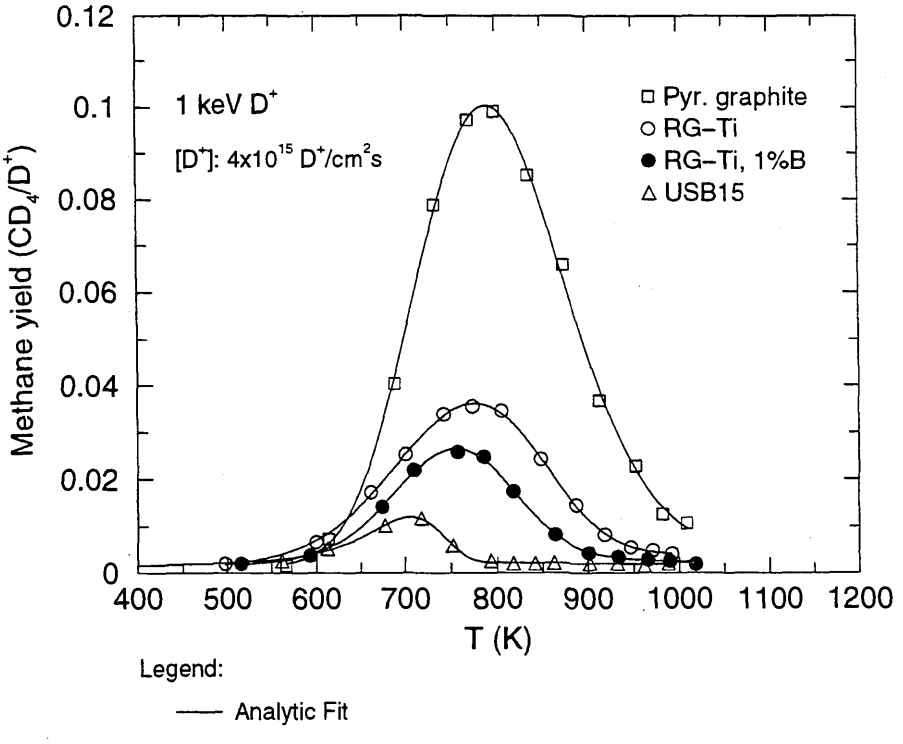

4.2.3.1 H^+, D^+ + pyrolytic graphite → CH_4, CD_4

Source: S. K. Erents, C. M. Braganza and G. M. McCracken, J. Nucl. Mater. **63**, 399 (1976).

Accuracy: Indeterminate.

Comments: (1) Equilibrium hydrocarbon gas release.
(2) Specimen: graphite (pyrolytic).
(3) H^+, D^+ ions: mass analyzed accelerator.
(4) Methane measured via QMS-RGA.

Analytic fitting function:

Methane yield:

$$Y = C \times [A_1 \exp[-(\frac{T - A_2}{A_3 T + 1})^2 / A_4] T^{A_5} + A_6 \exp(-A_7 T) T^{A_8}] \quad \text{[molecules/ion]}$$

where T is in Kelvin. The rms deviation of analytic fits for reactions A (CD_4) and B (CH_4) are 26.5% and 62.5%, respectively. The constant $C = 2.38095 \times 10^{-3}$ and 2.17391×10^{-3} for D^+ and H^+, respectively.

Fitting parameters A_1-A_8

A	3.1443E-01	8.0661E+02	8.7722E-02	8.4808E-01	5.0211E-01	7.1137E-24
	1.2847E-02	9.4309E+00				
B	2.1819E-01	8.6113E+02	2.5672E-01	1.4351E-01	4.8083E-01	8.7013E-38
	1.5922E-02	1.4583E+01				

ALADDIN evaluation function for methane yield: EYIELD8A

ALADDIN hierarchical labelling:

A: SATM D [+1] GRAPHITE T=HPG CD{4} [+0]
B: SATM H [+1] GRAPHITE T=HPG CH{4} [+0]

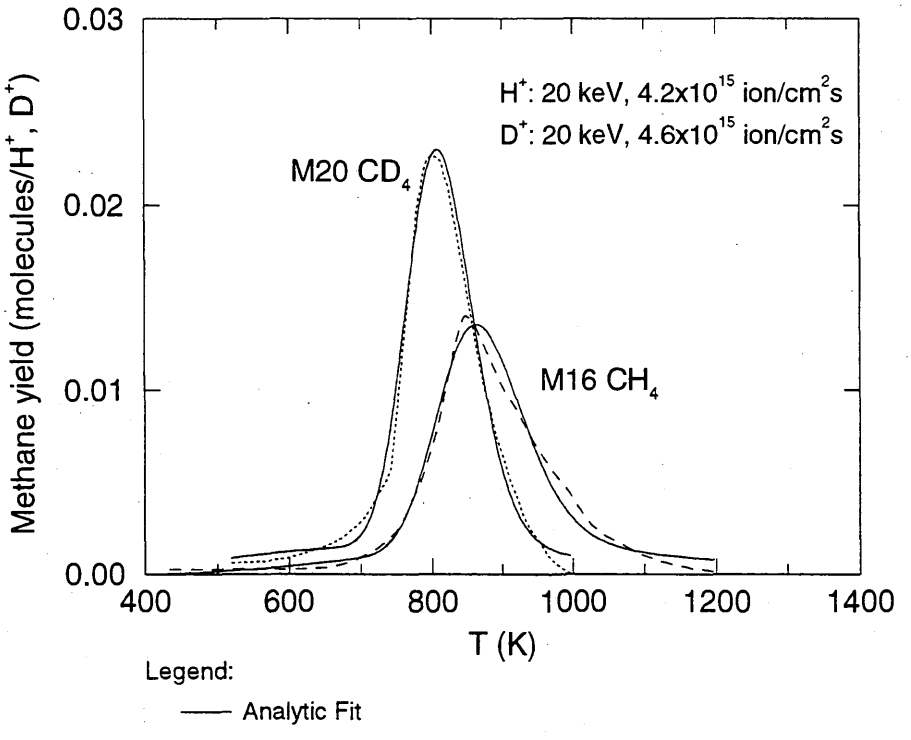

4.2.3.2 H^+, D^+ + pyrolytic graphite → C

Source: J. Roth and C. García-Rosales, Nucl. Fusion **36**, 1647 (1996).

Accuracy: Yield: ±20%.

Comments: (1) Weight loss measurement.
(2) Specimen: pyrolytic graphite.
(3) Mass-analyzed ion beam.
(4) Yield is for total (chemical+physical) sputtering.

Analytic fitting function:

Erosion yield:

$$Y = A_1 \exp(-(T - A_2)^2/A_3)T^{A_4} + A_5 \exp(-A_6 T)T^{A_7} \quad \text{[C/ion]}$$

where T is in Kelvin. The rms deviation of analytic fits for reactions A (•) and B (□) are 24.6% and 27.9%, respectively. Data for curve B were fitted with EYIELD4B.

Fitting parameters A_1-A_7

A	9.9202e-04	7.9602e+02	3.7804e+04	7.4583e-01	5.0595e+02	-2.6492e-03
	-1.8617e+00					
B	1.1899e+43	1.1602e+03	3.6699e+04	-1.4766e+01		

ALADDIN evaluation function for erosion yield: EYIELD4B, EYIELD7A

ALADDIN hierarchical labelling:

A: SATM D [+1] GRAPHITE T=HPG C [+0]
B: SATM H [+1] GRAPHITE T=HPG C [+0]

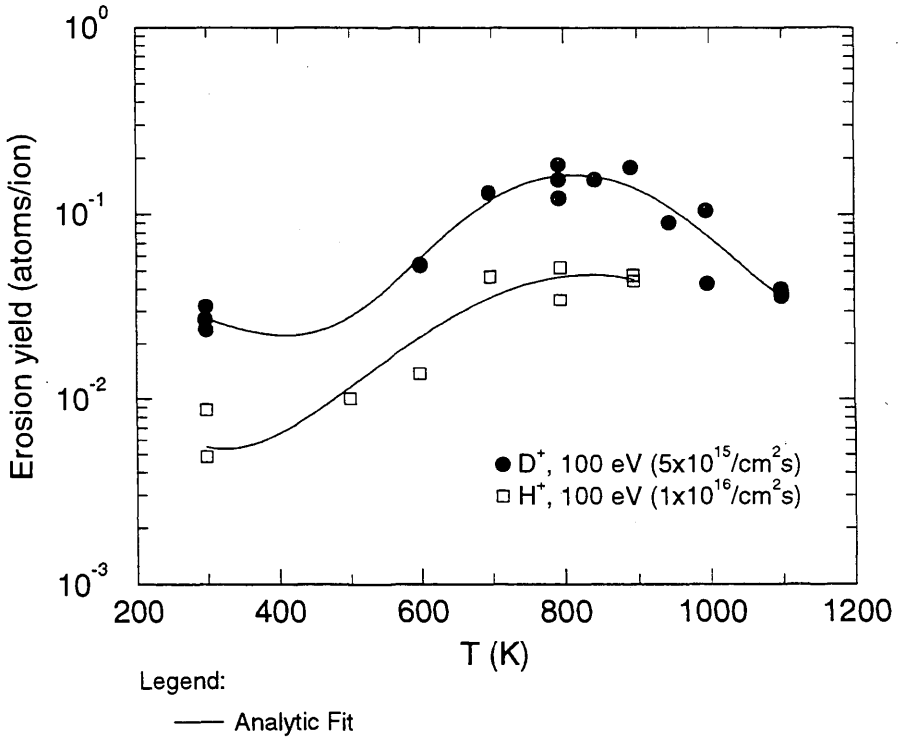

4.2.3.3 H^+, D^+ + POCO graphite → C

Source: D. M. Goebel, J. Bohdansky, R. W. Conn, Y. Hirooka, B. LaBombard, W. K. Leung, R. E. Nygren, J. Roth and G. R. Tynan, Nucl. Fusion **28**, 1041 (1988).

Accuracy: Yield: ±20%; T: ±5%.

Comments: (1) High-flux ($\sim 10^{18}$ D^+/cm^2s), steady-state (>10 min.) plasma bombardment.
(2) Specimen: isotropic graphite (POCO: AXF-5Q).
(3) Total erosion yield estimated from weight loss (>1 mg).
(4) Large ionization mean free path, i.e. no redeposition effect (see 4.2.1.15).
(5) CH-band spectroscopy applied to corroborate weight loss data.

Analytic fitting function:

Erosion yield:

$$Y = 1.0 \times 10^{-2}[A_1 \exp(-(T - A_2)^2/A_3)T^{A_4} + A_5 \exp(-A_6 T)T^{A_7}] \quad \text{[C/ion]}$$

where T is in ^{0}C. The rms deviation of analytic fits for reactions A (□) and B (•) are 7.8% and 14.0%, respectively.

Fitting parameters A_1-A_7

A	5.1306E+00	5.8035E+02	3.8258E+04	-5.4919E-02	6.4135E-01	1.8129E-03
	1.8168E-01					
B	7.9738E-01	5.6422E+02	6.7282E+04	1.5437E-01	7.1423E-02	4.8260E-03
	5.6311E-01					

ALADDIN evaluation function for erosion yield: EYIELD7A

ALADDIN hierarchical labelling:

A: SAT D [+1] GRAPHITE T=POCO-AXF5Q C [+0]
B: SAT H [+1] GRAPHITE T=POCO-AXF5Q C [+0]

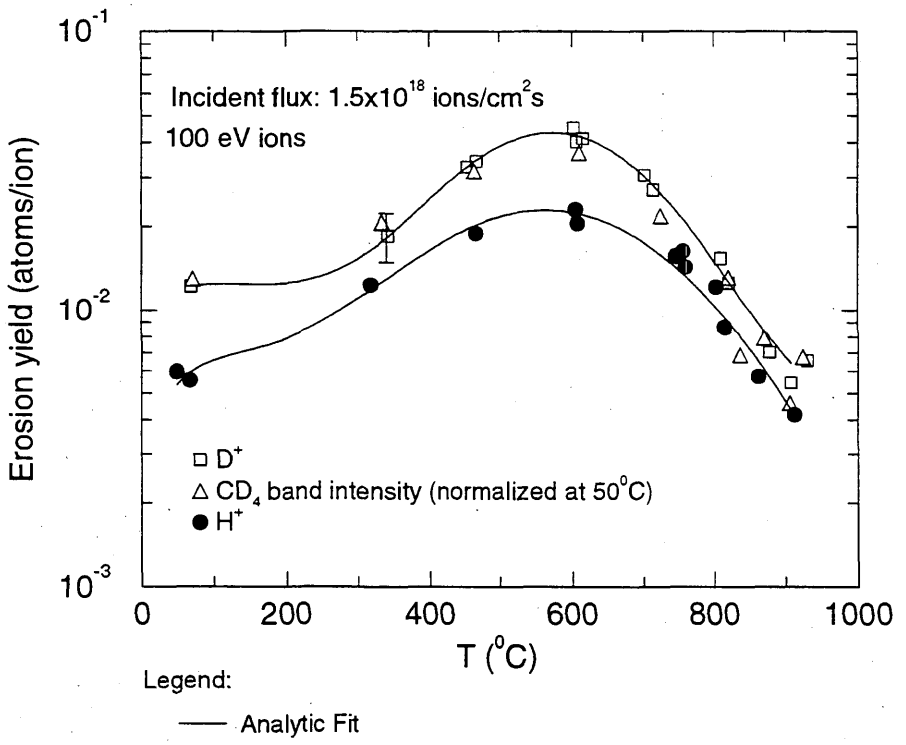

4.3.1.1 $[H^0, H^+]$ + pyrolytic graphite → CH_4

Source: A. A. Haasz, J. W. Davis, O. Auciello, P. C. Stangeby, E. Vietzke, K. Flaskamp and V. Phillips, J. Nucl. Mater. **145-147**, 412 (1987).

Accuracy: Yield: ±15%; T: ±25K.

Comments: (1) Steady-state methane yield, normalized by H^+ flux.
(2) Specimen: graphite (pyrolytic).
(3) H^+ ions: mass analyzed accelerator; H^0 (sub-eV) is produced via dissociation of H_2 on a hot W ribbon.
(4) Methane measured via QMS-RGA.

Analytic fitting function:

Methane yield:

$$Y = A_1 \exp(-(F - A_2)^2/A_3)F^{A_4} + A_5 \exp(-A_6 F)F^{A_7} \quad [CH_4/H^+]$$

where F is the flux ratio $[H^+]/[H^0]$. The rms deviation of analytic fits for reactions A (•, ○) and B (△, ▽) are 13.3% and 12.2%, respectively.

Fitting parameters A_1-A_7

A	8.3718e+03	-3.2261e+00	1.0982e+00	1.6550e-01	2.0122e-01	2.4685e-01
	1.5542e-01					
B	1.3316e+05	-8.6441e-01	6.1360e-02	2.3290e-01	4.6287e-01	1.5982e+00
	2.0051e-01					

ALADDIN evaluation function for methane yield: EYIELD7A

ALADDIN hierarchical labelling:

A-D: SSATM H [+0] H [+1] GRAPHITE T=HPG CH{4} [+0]

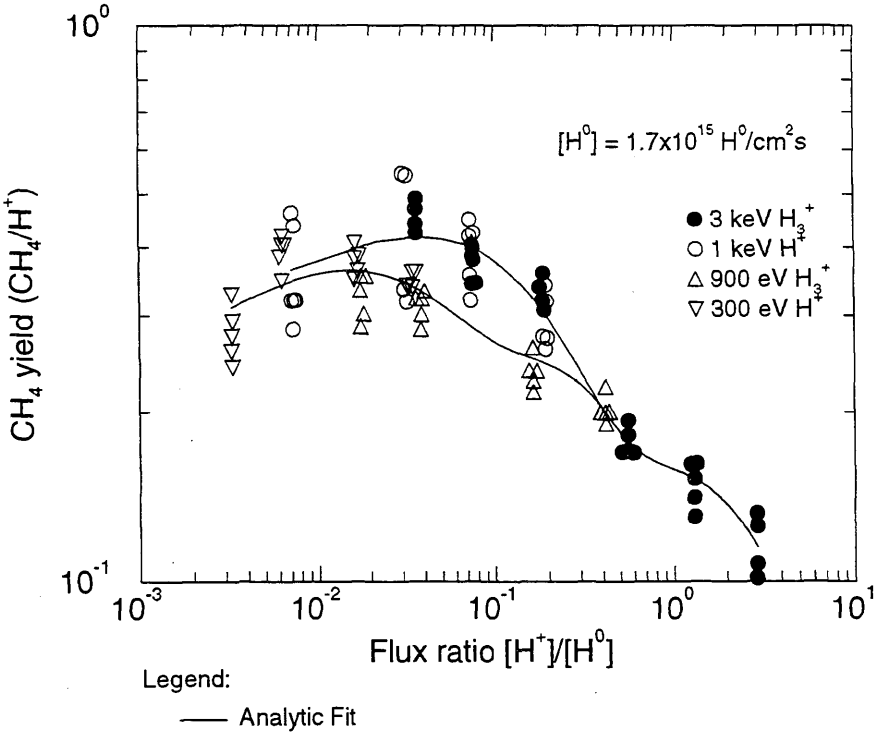

4.3.1.2 $[H^0, H^+]$ + pyrolytic graphite → CH_4, C_2H_x, C_3H_x, C

Source: J. W. Davis, A. A. Haasz and P. C. Stangeby, J. Nucl. Mater. **155-157**, 234 (1988).

Accuracy: Yield: ±35%; E: ±5eV.

Comments: (1) Steady-state hydrocarbon yield, normalized by the total hydrogen flux, $[H] = [H^0] + [H^+]$.
(2) Specimen: graphite (pyrolytic).
(3) H^+ ions: mass analyzed accelerator; H^0 (sub-eV) is produced via dissociation of H_2 on a hot W ribbon.
(4) Hydrocarbon products measured via QMS-RGA.
(5) Yield for total chemical erosion, $Y_{chem-total} = [CH_4 + 2(C_2H_2 + C_2H_4 + C_2H_6) + 3(C_3H_6 + C_3H_8)]/(H^+ + H^0)$.
(6) Yield values correspond to the maximum hydrocarbon yields of the respective temperature dependencies.

Analytic fitting function:

Chemical erosion yield:

$$Y = A_1 \exp(-A_2 E/(A_3 E + A_4))E^{A_5} + A_6 E^{A_7} \quad \text{[molecules/H]}$$

where E is in keV. The rms deviation of analytic fits for reactions A (◇), B (△), C (•) and D (□) are 6.8%, 0.2%, 2.2% and 5.0%, respectively.

Fitting parameters A_1-A_7

A	-1.2943E+01	2.9916E+03	-5.3883E+03	9.9939E-01	3.0155E-01	2.2609E+01
	3.0099E-01					
B	3.7980E-02	2.0805E-01	8.4457E-03	6.3330E-01	3.8268E-01	6.5178E-04
	1.9310E+00					
C	4.3243E+00	4.9920E-01	3.0995E-02	3.5459E-02	3.2017E+00	1.2987E-02
	2.5618E-01					
D	6.5668E+00	7.3806E-01	5.2959E-02	5.7088E-02	2.9860E+00	8.6747E-03
	5.8200E-01					

ALADDIN evaluation function for chemical erosion yield: EYIELD7B

ALADDIN hierarchical labelling:

A: SSATM H [+0] H [+1] GRAPHITE T=HPG C [+0]
B: SSATM H [+0] H [+1] GRAPHITE T=HPG C{3}H{X} [+0]
C: SSATM H [+0] H [+1] GRAPHITE T=HPG C{2}H{X} [+0]
D: SSATM H [+0] H [+1] GRAPHITE T=HPG CH{4} [+0]

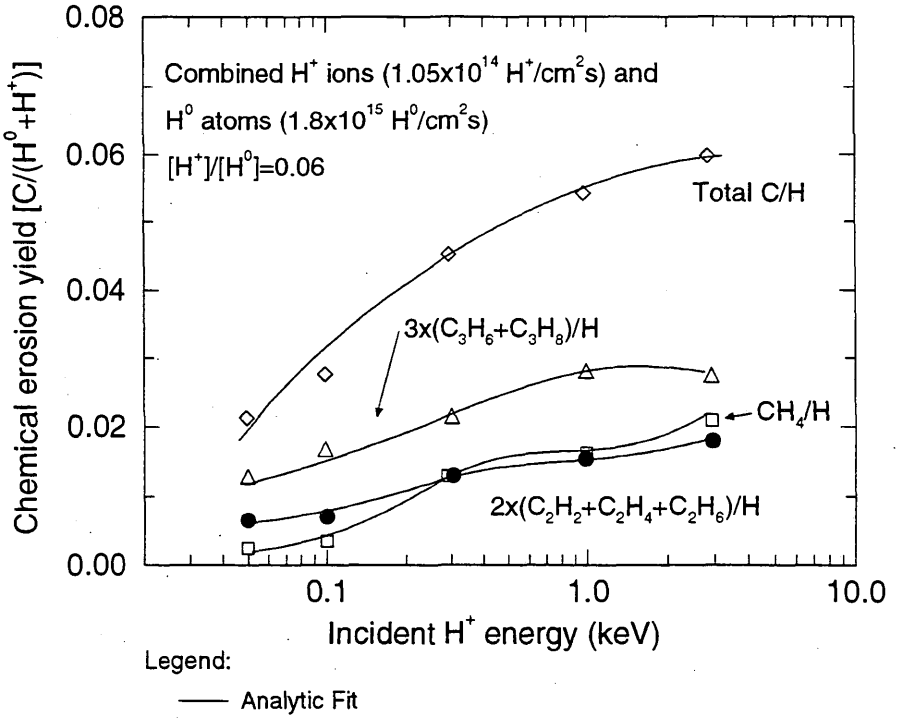

4.3.1.3 $[H^0, H^+]$ + pyrolytic graphite → C_xH_y, C

Source: J. W. Davis, A. A. Haasz, P. C. Stangeby, J. Nucl. Mater. **155-157**, 234 (1988).

Accuracy: Yield: ±35% except for the H^+-only case for which the accuracy is ±15%.

Comments: (1) Steady-state hydrocarbon yield, normalized by the total hydrogen flux, $[H] = [H^0] + [H^+]$.
(2) Specimen: graphite (pyrolytic).
(3) H^+ ions: mass analyzed accelerator; H^0 (sub-eV) is produced via dissociation of H_2 on a hot W ribbon.
(4) H^0 flux: 1.8×10^{15} H^0/cm^2s.
(5) Hydrocarbon products measured via QMS-RGA.
(6) Yield values shown in the figure correspond to the maximum hydrocarbon yield in their respective temperature profiles.
(7) Yield for total chemical erosion, $Y_{chem-total} = [CH_4 + 2(C_2H_2 + C_2H_4 + C_2H_6) + 3(C_3H_6 + C_3H_8)]/(H^+ + H^0)$.

Analytic fitting function:

Erosion yield:

$$Y = A_1 \exp(-A_2 F) F^{A_3} + A_4 F^{A_5} \quad \text{[molecules/H]}$$

where F is the flux ratio $[H^+]/[H^0]$. The rms deviation of analytic fits for reactions A (top group: +, •) and B (bottom group: ○, △) are 4.4% and 3.7%, respectively.

Fitting parameters A_1-A_5

A	1.0435E-01	8.1132E-01	7.3464E-01	2.3392E-02	7.3594E-01
B	1.5348E-01	8.0362E-01	4.6677E-01	5.3679E-02	4.8118E-01

ALADDIN evaluation function for erosion yield: EYIELD5A

ALADDIN hierarchical labelling:

A: SSATM H [+0] H [+1] GRAPHITE T=HPG C [+0]
B: SSATM H [+0] H [+1] GRAPHITE T=HPG CH{4} [+0]

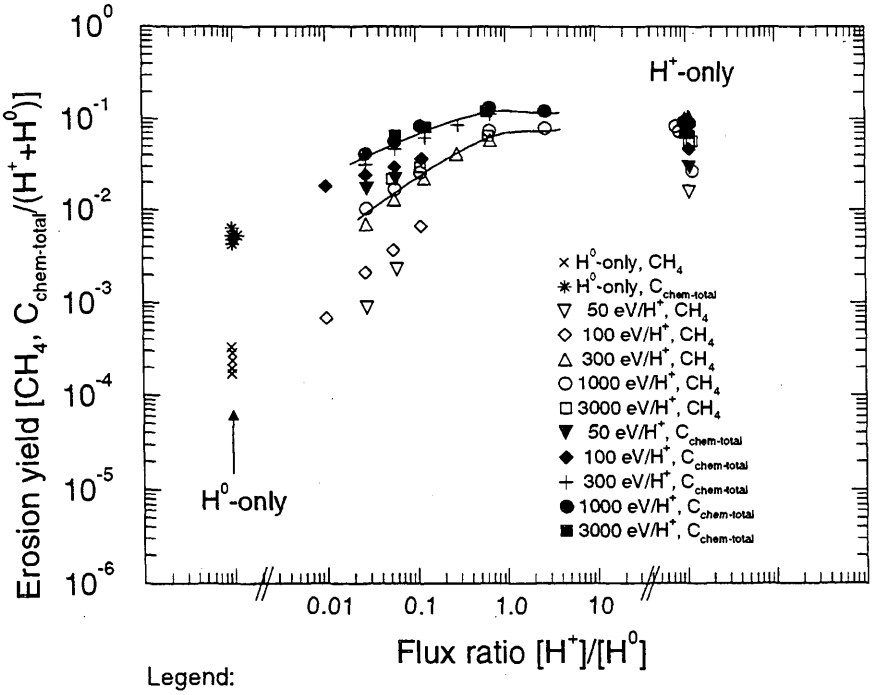

Legend:

—— Analytic Fit (1 keV data)

4.3.1.4 $[H^0, H^+]$ + pyrolytic graphite → C_xH_y, C

Source: J. W. Davis, A. A. Haasz, P. C. Stangeby, J. Nucl. Mater. **155-157**, 234 (1988).

Accuracy: Yield: ±15%.

Comments: (1) Steady-state hydrocarbon yield, normalized by the H^+ flux.
(2) Specimen: graphite (pyrolytic).
(3) H^+ ions: mass analyzed accelerator; H^0 (sub-eV) is produced via dissociation of H_2 on a hot W ribbon.
(4) Hydrocarbon products measured via QMS-RGA.
(5) Yield values shown in the figure correspond to the maximum hydrocarbon yield in their respective temperature profiles.
(6) H^0 flux: 1.8×10^{15} H^0/cm^2s.
(7) Yield for total chemical erosion, $Y_{chem-total} = [CH_4 + 2(C_2H_2 + C_2H_4 + C_2H_6) + 3(C_3H_6 + C_3H_8)]/H^+$.

Analytic fitting function:

Erosion yield:

$$Y = A_1 \exp(-A_2 F) F^{A_3} + A_4 F^{A_5} \quad [\text{molecules}/H^+]$$

where F is the flux ratio $[H^+]/[H^0]$. The rms deviation of analytic fits for reactions A (•) and B (○) are 1.6% and 0.9%, respectively.

Fitting parameters A_1-A_5

A	1.8029E-01	3.4626E-01	-1.6070E-01	1.2791E-02	9.7185E-01
B	8.0476E-02	1.8089E+00	-3.9669E-01	2.3684E-01	-4.2092E-01

ALADDIN evaluation function for erosion yield: EYIELD5A

ALADDIN hierarchical labelling:

A: SSATM H [+0] H [+1] GRAPHITE T=HPG C [+0]
B: SSATM H [+0] H [+1] GRAPHITE T=HPG CH{4} [+0]

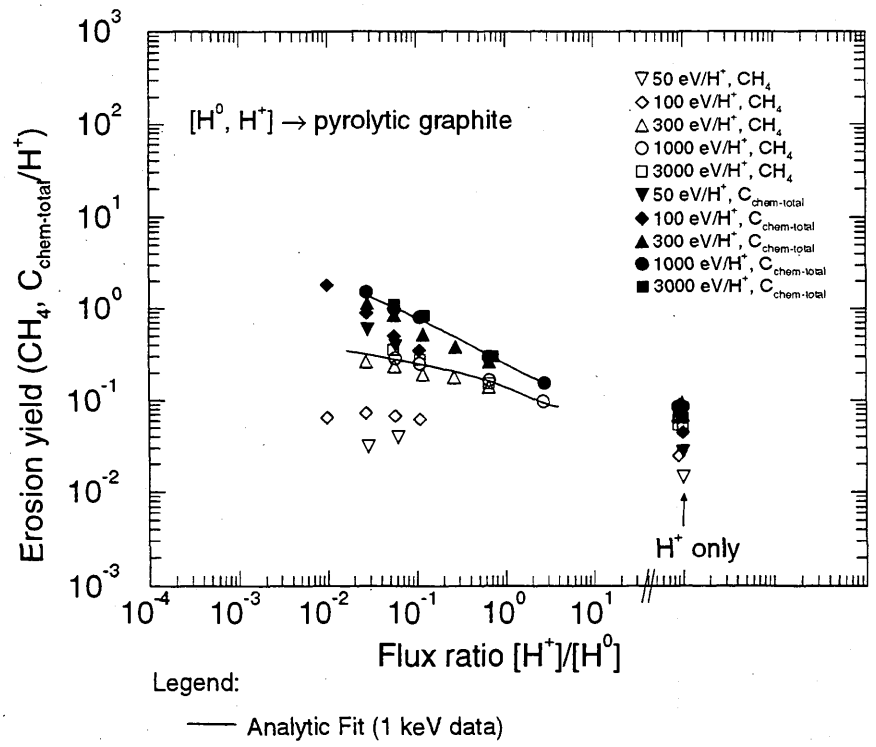

4.3.1.5 $[H^0, H^+]$ + pyrolytic graphite → C_xH_y, C

Source: J. W. Davis, A. A. Haasz and P. C. Stangeby, J. Nucl. Mater. **155-157**, 234 (1988).

Accuracy: Yield: ±35%; T: ±25K.

Comments: (1) Steady-state hydrocarbon yield, normalized by the total hydrogen flux, $[H] = [H^0] + [H^+]$.
(2) Specimen: graphite (pyrolytic).
(3) H^+ ions: mass analyzed accelerator; H^0 (sub-eV) is produced via dissociation of H_2 on a hot W ribbon.
(4) Hydrocarbon products measured via QMS-RGA.
(5) Yield for total chemical erosion, $Y_{chem-total} = [CH_4 + 2(C_2H_2 + C_2H_4 + C_2H_6) + 3(C_3H_6 + C_3H_8)]/(H^+ + H^0)$.

Analytic fitting function:

Erosion yield:

$$Y = 1.0 \times 10^{-2}[A_1 \exp(-(T - A_2)^2/A_3)T^{A_4} + A_5 \exp(-A_6T)T^{A_7}] \quad \text{[molecules/H]}$$

where T is in Kelvin. The rms deviation of analytic fits for reactions A (∗), B (•), C (○), D (△), E (□), F (◇) and G (+) are 5.2%, 11.2%, 2.6%, 202.9% 7.3%, 6.9% and 8.7%, respectively.

Fitting parameters A_1-A_7

A	2.4666E+00	6.5490E+02	4.9773E+04	1.2144E-01	4.5660E-03	-4.3563E-03	3.9673E-03
B	3.1975E+00	8.5960E+02	1.2173E+05	-6.3220E-03	-3.6816E-02	-4.1054E-03	8.4117E-04
C	-2.1270E-05	1.6395E+03	-1.4938E+05	-9.6865E-02	1.9553E-01	2.9490E-03	8.3907E-04
D	1.8074E-01	6.7639E+02	5.9146E+04	2.0847E-02	-7.4301E-03	-2.1489E-03	-3.7050E-06
E	3.8383E+00	7.1665E+02	2.1767E+04	-2.8401E-01	2.3351E+00	5.6815E-03	7.8341E-02
F	2.3724E-01	6.1434E+02	1.1319E+04	4.9874E-02	4.0882E-01	2.7116E-03	1.4215E-03
G	2.0100E-01	6.1025E+02	2.3821E+04	1.4164E-01	2.1990E-02	1.3259E-03	-9.2740E-05

ALADDIN evaluation function for erosion yield: EYIELD7A

ALADDIN hierarchical labelling:

A: SSATM H [+0] H{3} [+1] GRAPHITE T=HPG C [+0]
B: SSATM H [+0] H{3} [+1] GRAPHITE T=HPG CH{4} [+0]
C: SSATM H [+0] H{3} [+1] GRAPHITE T=HPG C{2}H{2} [+0]
D: SSATM H [+0] H{3} [+1] GRAPHITE T=HPG C{2}H{4} [+0]
E: SSATM H [+0] H{3} [+1] GRAPHITE T=HPG C{2}H{6} [+0]
F: SSATM H [+0] H{3} [+1] GRAPHITE T=HPG C{3}H{6} [+0]
G: SSATM H [+0] H{3} [+1] GRAPHITE T=HPG C{3}H{8} [+0]

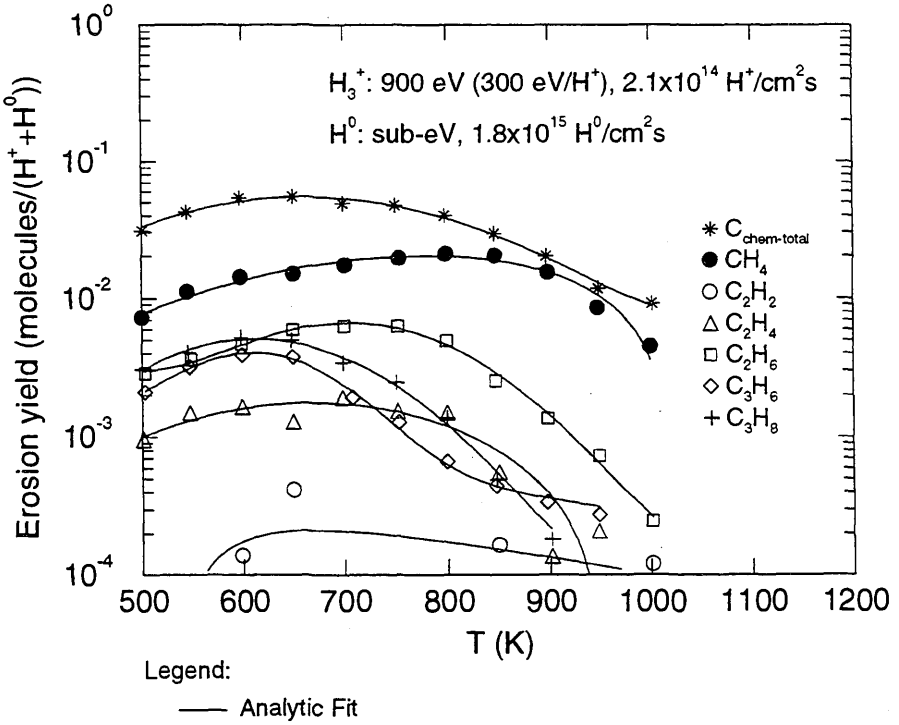

4.3.1.6 $[H^0, H^+]$, H^0, H_3^+ + pyrolytic graphite → CH_4

Source: A. A. Haasz, J. W. Davis, O. Auciello, P. C. Stangeby, E. Vietzke, K. Flaskamp and V. Phillips, J. Nucl. Mater. **145-147**, 412 (1987).

Accuracy: Yield: ±15%; T: ±25K.

Comments: (1) Steady-state methane yield, normalized by the H^+ flux for the H^+-only and H^++H^0 cases; and normalized by the H^0 flux for the H^0-only case.
(2) Specimen: graphite (pyrolytic).
(3) H^+ ions: mass analyzed accelerator; H^0 (sub-eV) is produced via dissociation of H_2 on a hot W ribbon.
(4) Methane measured via QMS-RGA.
(5) H_3^+ energy: 900 eV (300 eV/H^+); flux density 2.8×10^{14} H^+/cm^2s.
(6) Sub-eV H^0 flux density 1.7×10^{15} H^0/cm^2s.

Analytic fitting function:

Methane yield:

$$Y = A_1 \exp(-(T - A_2)^2/A_3)T^{A_4} + A_5 \exp(-A_6T/(A_7T + 1.0))T^{A_8} \quad [CH_4/H^0,\ H^+]$$

where T is in Kelvin. The rms deviation of analytic fits for reactions A (□), B (○) and C (×) are 8.8%, 13.0% and 11.5%, respectively. The fit for reaction C employed the evaluation function EYIELD5A.

Fitting parameters A_1-A_8

A	2.0997E+01	7.9843E+02	4.5615E+04	4.1266E-02	-1.4895E-04	3.6074E+02
	2.5701E+01	3.6030E+00				
B	5.9487E+00	7.7401E+02	1.7447E+04	1.0060E-02	1.9885E+00	-2.6967E+00
	1.3636E-01	-3.0828E+00				
C	1.0694E-05	7.4721E-03	1.2752E+00	8.6028E-50	1.4730E+01	

ALADDIN evaluation function for methane yield: EYIELD5A, EYIELD8B

ALADDIN hierarchical labelling:

A: SSATM H [+0] H [+1] GRAPHITE T=HPG CH{4} [+0]
B: SATM H [+1] GRAPHITE T=HPG CH{4} [+0]
C: SATM H [+0] GRAPHITE T=HPG CH{4} [+0]

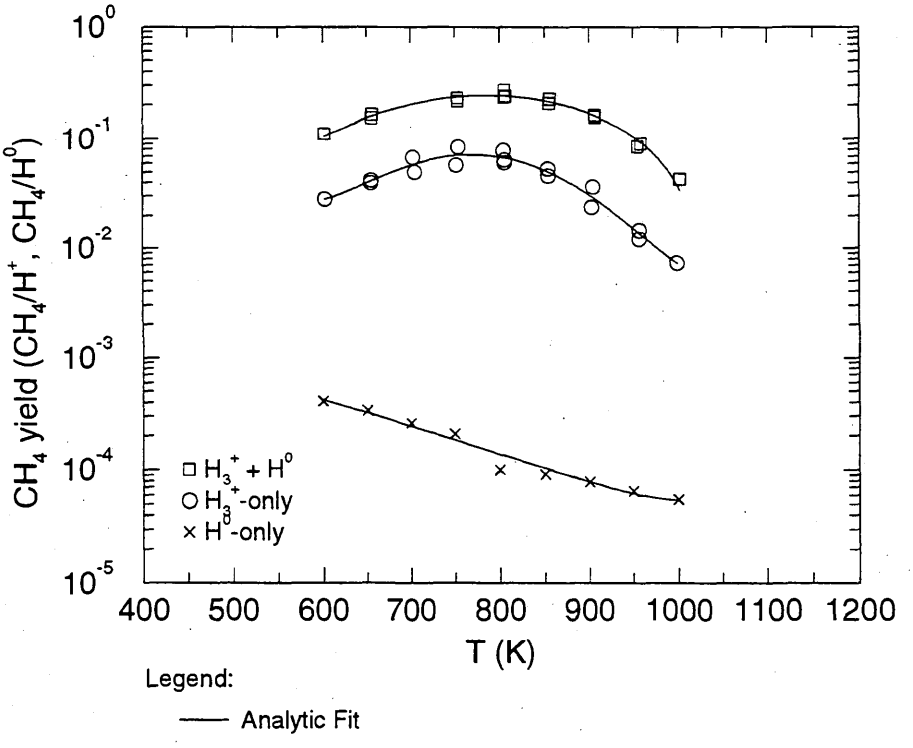

4.3.1.7 $[H^0, H^+]$, H^0, H_3^+ + pyrolytic graphite → CH_4

Source: A. A. Haasz, J. W. Davis, O. Auciello, P. C. Stangeby, E. Vietzke, K. Flaskamp and V. Phillips, J. Nucl. Mater. **145-147**, 412 (1987).

Accuracy: Yield: ±15%; T: ±25K.

Comments: (1) Steady-state methane yield, normalized by the H^+ flux for the H^+-only and H^++H^0 cases; and normalized by the H^0 flux for the H^0-only case.
(2) Specimen: graphite (pyrolytic).
(3) H^+ ions: mass analyzed accelerator; H^0 (sub-eV) is produced via dissociation of H_2 on a hot W ribbon.
(4) Methane measured via QMS-RGA.
(5) H_3^+ energy: 3 keV (1 keV/H^+); flux density 3.3×10^{14} H^+/cm^2s.
(6) Sub-eV H^0 flux density 1.7×10^{15} H^0/cm^2s.

Analytic fitting function:

Methane yield:

$$Y = A_1 \exp(-(T - A_2)^2/A_3)T^{A_4} + A_5 \exp(-A_6T/(A_7T + 1.0))T^{A_8} \quad [CH_4/H^0,\ H^+]$$

where T is in Kelvin. The rms deviation of analytic fits for reactions A (□), B (○) and C (×) are 7.4%, 13.1% and 11.5%, respectively. The fit for reaction C employed the evaluation function EYIELD5A.

Fitting parameters A_1-A_8

A	1.0511E+03	7.8812E+02	1.1787E+04	-5.5479E-01	2.4407E+00	6.8173E+02
	-9.4407E+01	-8.8993E-01				
B	2.1721E+01	7.4956E+02	1.0870E+04	-1.4352E-01	1.1949E-01	6.0743E-01
	2.6173E-01	5.7760E-01				
C	1.0694E-05	7.4721E-03	1.2752E+00	8.6028E-50	1.4730E+01	

ALADDIN evaluation function for methane yield: EYIELD5A, EYIELD8B

ALADDIN hierarchical labelling:

A: SSATM H [+0] H [+1] GRAPHITE T=HPG CH{4} [+0]
B: SATM H [+1] GRAPHITE T=HPG CH{4} [+0]
C: SATM H [+0] GRAPHITE T=HPG CH{4} [+0]

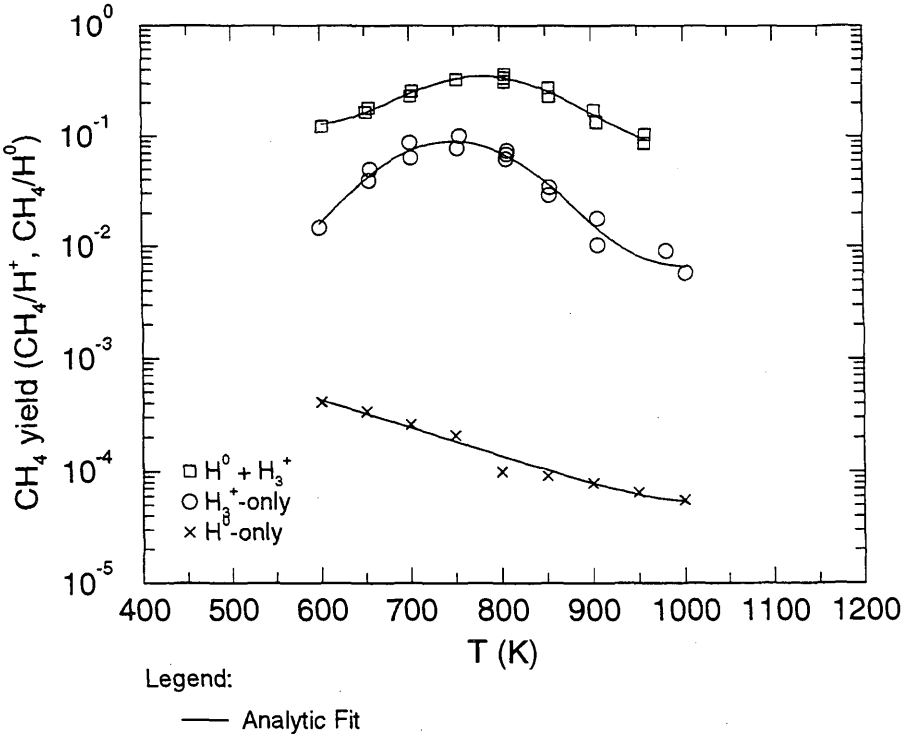

4.3.2.1 $[H^0, C^+]$ + pyrolytic graphite → C

Source: J. W. Davis and A. A. Haasz, Appl. Phys. Lett. **57**, 1976 (1990).

Accuracy: Yield: ±15% (Primarily leak bottles, ±10%); Flux ratio: ±35% (error in H^0 flux).

Comments: . (1) Chemical erosion yield due to C^+ ions in the presence of H^0 atoms.
(2) C^+ beam produced by mass-selecting ion accelerator.
(3) H^0 produced by contact dissociation of H_2 on hot W filament.
(4) Hydrocarbon products measured via QMS-RGA, steady state.
(5) Specimen: graphite (pyrolytic, HPG99).
(6) Yield for total chemical erosion, $Y_{chem-total} = [CH_4 + 2(C_2H_2 + C_2H_4 + C_2H_6) + 3(C_3H_6 + C_3H_8)]/C^+$.

Analytic fitting function:

Erosion yield:

$$Y = A_1 \exp(-(T - A_2)^2/A_3)T^{A_4} + A_5 \exp(-A_6 T)T^{A_7} \quad [C/C^+]$$

where T is in Kelvin. The rms deviation of analytic fits for reactions A (□), B (△) and C (○) are 2.9%, 4.2% and 4.5%, respectively.

Fitting parameters A_1-A_7

A	8.3060e-02	7.5020e+02	4.4772e+04	6.4942e-01	6.0540e-02	6.4930e-03
	1.0114e+00					
B	1.5643e-01	7.6012e+02	3.9195e+04	4.7655e-01	8.3432e-06	8.8360e-03
	2.5586e+00					
C	1.4889e-01	7.5511e+02	3.8772e+04	3.6236e-01	2.3086e-06	9.3290e-03
	2.7210e+00					

ALADDIN evaluation function erosion yield: EYIELD7A

ALADDIN hierarchical labelling:

A-C: SSATM H [+0] C [+1] GRAPHITE T=HPG99 C [+0]

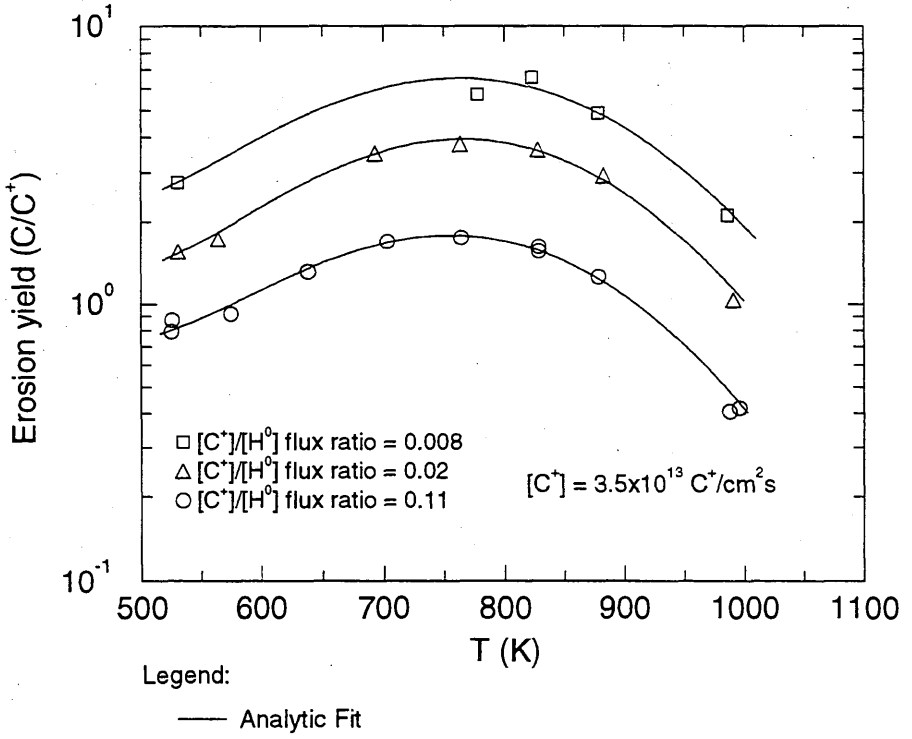

4.3.2.2 $[H^0, C^+]$ + pyrolytic graphite → C

Source: J. W. Davis and A. A. Haasz, Appl. Phys. Lett. **57**, 1976 (1976).

Accuracy: Yield: ±15% (Primarily leak bottles, ±10%); Flux ratio: ±35% (error in H^0 flux).

Comments: (1) Total erosion yield due to C^+ ions in the presence of H^0 atoms.
(2) C^+ beam produced by mass-selecting ion accelerator.
(3) H^0 produced by contact dissociation of H_2 on hot W filament.
(4) Temperatures correspond to location of maximum erosion yield.
(5) Hydrocarbon products measured via QMS-RGA, steady state.
(6) Specimen: graphite (pyrolytic, HPG99).
(7) Yield for total chemical erosion, $Y_{chem-total} = [CH_4 + 2(C_2H_2 + C_2H_4 + C_2H_6) + 3(C_3H_6 + C_3H_8)]/C^+$.

Analytic fitting function:

Erosion yield:

$$Y = A_1 \exp(-A_2 F) F^{A_3} + A_4 F^{A_5} \quad [C/C^+]$$

where F is the flux ratio $[C^+]/[H^0]$. The rms deviation of analytic fits for reactions A (•) and B (◇) are 6.7% and 4.6%, respectively.

Fitting parameters A_1-A_5

A	4.3972E-01	8.7595E-01	-5.4497E-01	1.1727E-01	-1.6920E-01
B	1.3860E+00	2.6814E+01	-1.7765E-01	9.3537E-01	2.0773E-01

ALADDIN evaluation function for erosion yield: EYIELD5A

ALADDIN hierarchical labelling:

A, B: SSATM H [+0] C [+1] GRAPHITE T=HPG99 C [+0]

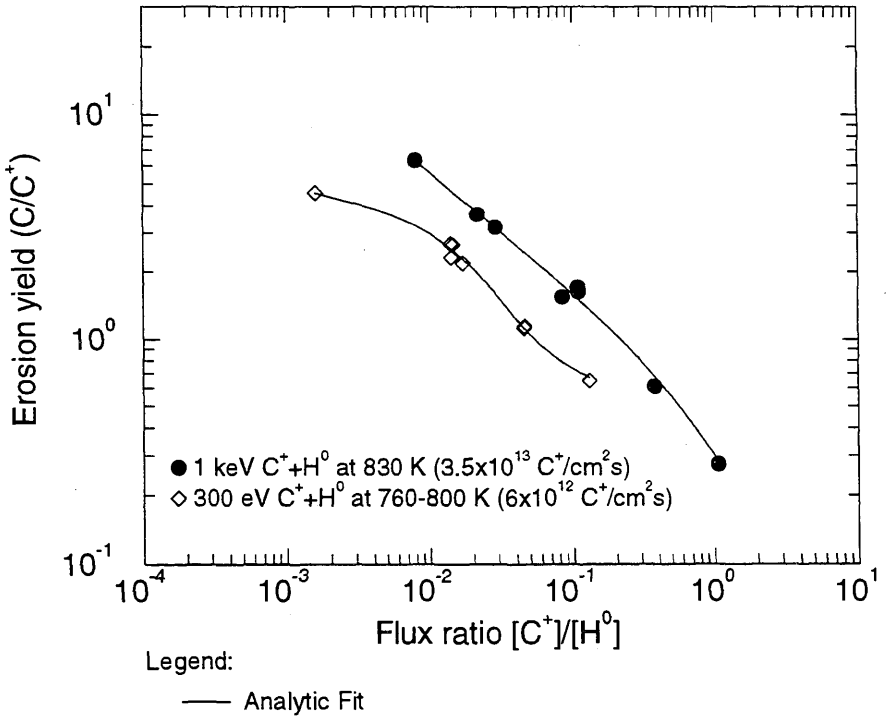

4.3.3.1 $[H^0, O^+]$ + pyrolytic graphite → C

Source: J. Roth and W. Ottenberger, Max Planck Institut für Plasmaphysik, Garching, Germany, unpublished (1990).

Accuracy: Indeterminate.

Comments: (1) Total erosion yield due to simultaneous impact of thermal H atoms and O^+ ions on graphite.
(2) Specimen: graphite (pyrolytic).

Analytic fitting function:

Erosion yield:

$$Y = A_1 \exp(-A_2 F) F^{A_3} + A_4 F^{A_5} \quad [C/O^+]$$

where F is the flux ratio $[H^0]/[O^+]$. The rms deviation of the analytic fit is 7.5%.

Fitting parameters A_1-A_5

9.5989E-01	1.0251E-02	-3.0251E-02	2.2491E-01	5.5710E-01

ALADDIN evaluation function erosion yield: EYIELD5A

ALADDIN hierarchical labelling:

SSATM H [+0] O [+1] GRAPHITE T=HPG C [+0]

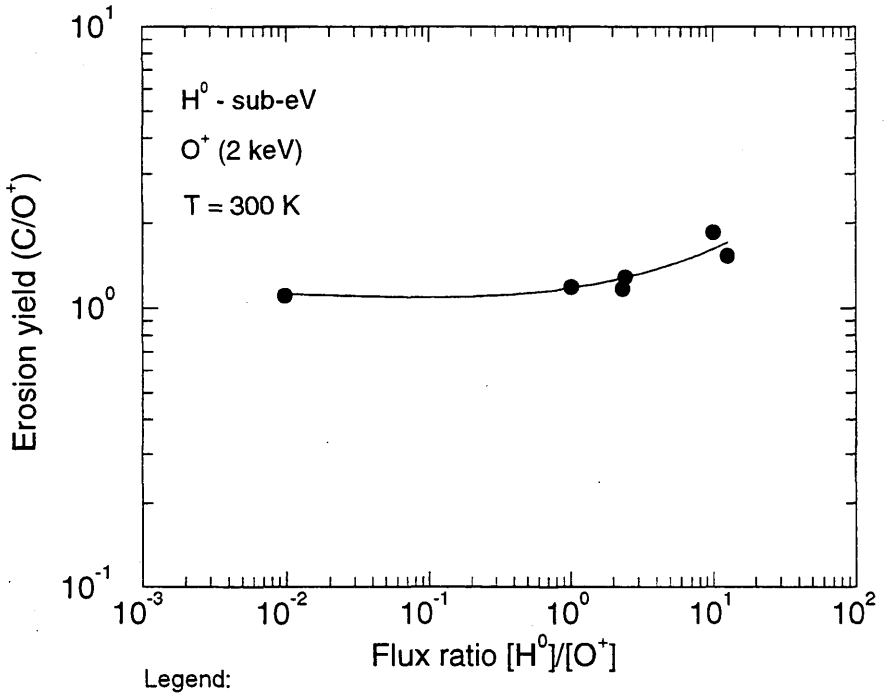

Legend:

4.3.4.1 $[H^0, Ar^+]$ + pyrolytic graphite → CH_3, CH_4, C_2-compounds

Source: E. Vietzke, K. Flaskamp and V. Philipps, J. Nucl. Mater. **111&112**, 763 (1982).

Accuracy: Yield: 50%.

Comments: (1) Reaction of atomic hydrogen with oriented pyrolytic graphite (HPG), with simultaneous bombardment with Ar^+ ions. Products with mass 15 (A, mostly CH_3), mass 16 (B, CH_4), and mass 26 (C_2-compounds) are detected.
(2) Incident ion energy: 5 keV Ar^+. Flux: 1.1×10^{13} ions/cm^{2}s.
(3) Line-of-sight QMS detection.
(4) Published data corrected for Maxwell-Boltzmann distributions with respect to specimen temperature and the pumping of methane. Following this correction, several of the m16 data points became negative. Only the remaining positive yield values were fitted.

Analytic fitting function:

Reaction yield:

$$Y = 1.0 \times 10^{-2}[A_1 \exp(-(T - A_2)^2/A_3)T^{A_4} + A_5 \exp(-A_6 T)T^{A_7}] \quad [\text{molecules}/H^0]$$

where T is in Kelvin. The rms deviation of the analytic fits for products A (•), B (□), C (△) are 14.8%, 15.3% and 115.5%, respectively.

Fitting parameters A_1-A_9

A	1.5115E-03	7.2453E+02	2.3515E+04	8.5502E-01	1.0761E-10	1.1484E-02
	4.3457E+00					
B	5.2169E-11	7.6572E+02	3.6534E+04	3.4980E+00	3.6397E-07	2.0227E-03
	2.3245E+00					
C	-1.6191E-07	8.9436E+02	4.8397E+03	1.4907E+00	3.3836E-07	9.8144E-03
	2.6462E+00					

ALADDIN evaluation function for reaction yield: EYIELD7A

ALADDIN hierarchical labelling:

A: SSATM H [+0] Ar [+1] GRAPHITE T=HPG O=BASAL-PL M{15}
B: SSATM H [+0] Ar [+1] GRAPHITE T=HPG O=BASAL-PL M{16}
C: SSATM H [+0] Ar [+1] GRAPHITE T=HPG O=BASAL-PL M{26}

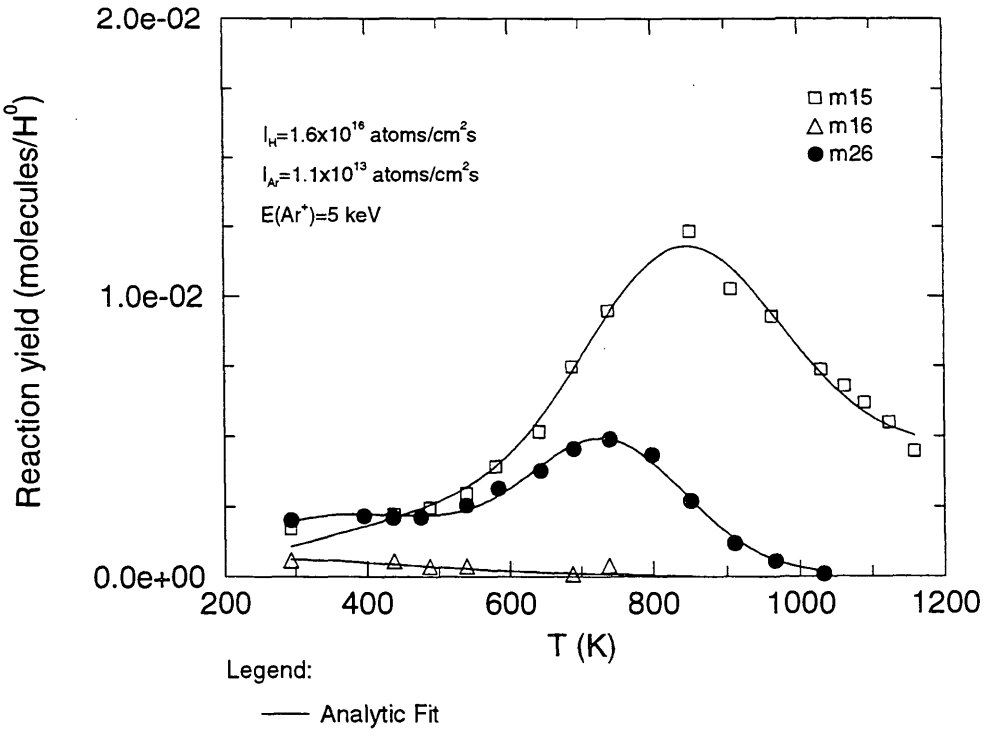

4.3.4.2 $[H^0, Ar^+]$ + pyrolytic graphite → CH_3

Source: E. Vietzke, K. Flaskamp and V. Philipps, J. Nucl. Mater. **111&112**, 763 (1982).

Accuracy: Yield: 50%.

Comments: (1) Data with fitted curve is for continuous irradiation of H-atoms after a simultaneous $Ar^+ + H^0$ irradiation.
(2) Incident ion energy: 5 keV Ar^+. Flux: 1.1×10^{13} ions/cm^{2}s.
(3) Line-of-sight QMS detection.
(4) Masses with m=15 are mostly CH_3.
(5) The analytic fit on the figure is pertinent to the continuous irradiation case.
(6) Original data are corrected for Maxwell-Boltzmann distributions with respect to specimen temperature of 800 K.
(7) Measurements with increasing delay times indicate that the reduction in reactivity is due to H^0 exposure, and not time alone.

Analytic fitting function:

Reaction yield:

$$Y = 1.69 \times 10^{-3} A_1 \exp(-A_2 F) F^{A_3} \quad [\text{molecules}/H^0]$$

where F is in units of 10^{18} atoms/cm^2. The rms deviation of the analytic fit is 18.2%.

Fitting parameters A_1-A_3

2.9010E+00	3.4585E-03	-5.4328E-01

ALADDIN evaluation function for reaction yield: EYIELD3A

ALADDIN hierarchical labelling:

SSATM H [+0] Ar [+1] GRAPHITE T=HPG O=BASAL-PL CH{3}

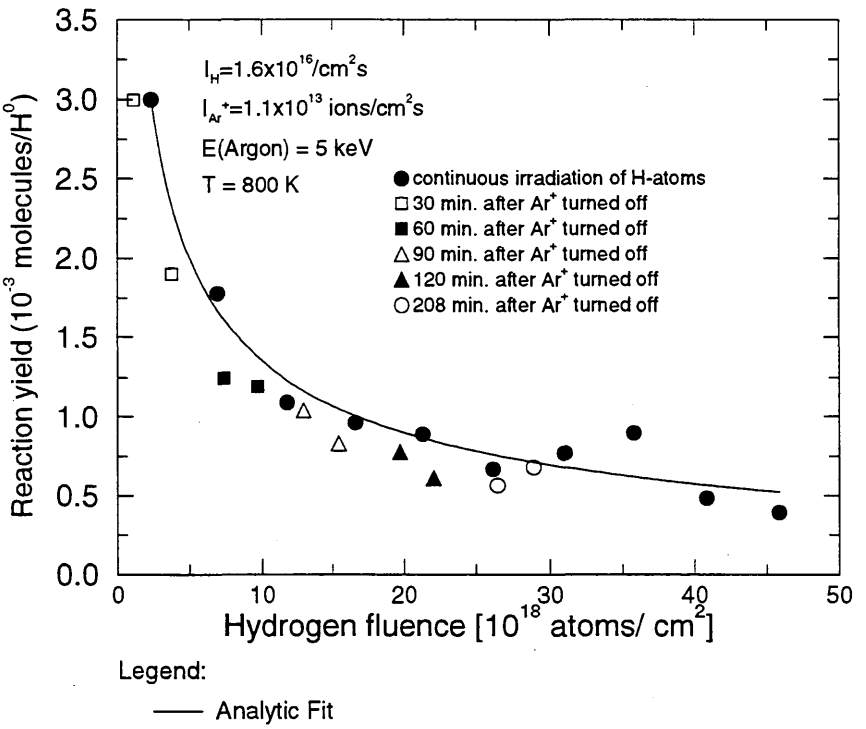

4.3.4.3 $[H^0, Ar^+]$ + pyrolytic graphite → CH_3, CH_4, C_2-compounds

Source: E. Vietzke, K. Flaskamp and V. Philipps, J. Nucl. Mater. **111&112**, 763 (1982).

Accuracy: Yield: 50%.

Comments: (1) Reaction of atomic hydrogen with oriented pyrolytic graphite (HPG), averaged over the first 28 s after the simultaneous H-atom/Ar^+ irradiation is stopped. Products with mass 15 (A, mostly CH_3), mass 26 (B, C_2-compounds), and mass 16 (C, CH_4) are detected.
(2) Hydrogen flux: 1.6×10^{16} atoms/cm^2s.
(3) Line-of-sight QMS detection.
(4) Points at temperatures 441.2, 540.4, 798.1, 966.2, and 1095.1 K from the original data were not included in the fitting of curve 3.
(5) Published data corrected for Maxwell-Boltzmann distributions with respect to specimen temperature. Following this correction, several of the m16 data points became negative. Only the remaining positive yield values were fitted.

Analytic fitting function:

Reaction yield:

$$Y = 1.0 \times 10^{-5}[A_1 \exp(-(T - A_2)^2/A_3)T^{A_4} + A_5 \exp(-A_6T)T^{A_7})] \quad [\text{molecules/H}^0]$$

where T is in Kelvin. The rms deviation of the analytic fits for reactions A (•), B (△) and C (□) are 50.4%, 83.8% and 7.2%, respectively.

Fitting parameters A_1-A_7

A	2.8402E-01	6.4129E+02	5.6030E+04	9.7864E-01	2.3170E-02	1.1191E-01
	-4.1741E+00					
B	5.5399E-01	6.5315E+02	1.4858E+04	7.5542E-01	3.7317E-16	1.3510E-02
	7.2372E+00					
C	5.9223E-07	1.0193E+02	6.7760E+05	1.8259E+00	0.0	0.0

ALADDIN evaluation function for reaction yield: EYIELD7A

ALADDIN hierarchical labelling:

A: SSATM H [+0] Ar [+1] GRAPHITE T=HPG O=BASAL-PL M{15}
B: SSATM H [+0] Ar [+1] GRAPHITE T=HPG O=BASAL-PL M{16}
C: SSATM H [+0] Ar [+1] GRAPHITE T=HPG O=BASAL-PL M{26}

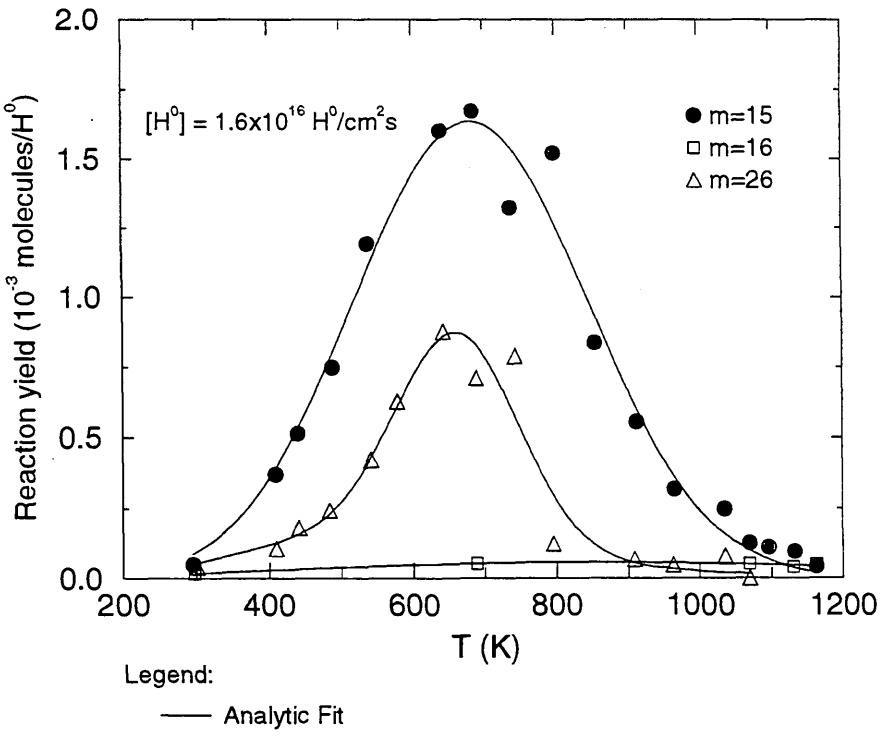

4.3.4.4 $[H^0, Ar^+]$ + pyrolytic graphite → CH_3, CH_4

Source: E. Vietzke, K. Flaskamp and V. Philipps, J. Nucl. Mater. **111&112**, 763 (1982).

Accuracy: Yield: 50%.

Comments: (1) Arrhenius plot of some data from 4.3.4.1, 4.3.4.2, 4.1.1.3.
(2) Specimen: graphite (pyrolytic, HPG).

Analytic fitting function:

Reaction yield:

$$Y = A_1 \exp[-(\frac{X - A_2}{A_3 X + 1})^2 / A_4] X^{A_5} + A_6 \exp(-A_7 X) X^{A_8} \quad [\text{molecules}/H^0]$$

where X = 10^4/T, with T given in Kelvin. The rms deviation of the analytic fits for reactions A (○), B (●) and C (△) are 3.3%, 4.4% and 3.3%, respectively.

Fitting parameters A_1-A_8

A	6.8815E-22	8.4244E+00	3.9519E+00	1.4727E-03	1.8323E+01	8.2236E-01
	5.9131E-01	-1.4037E+00				
B	3.8538E-10	1.2471E+01	1.2917E-01	2.0174E+00	4.9882E+00	1.2578E-12
	3.6048E-01	7.9292E+00				
C	-8.5022E-07	1.5789E-01	-3.8022E-02	1.5072E+03	1.4531E+00	7.3404E-07
	6.2231E-02	1.7427E+00				

ALADDIN evaluation function for reaction yield: EYIELD8A

ALADDIN hierarchical labelling:

A: SSATM H [+0] Ar [+1] GRAPHITE T=HPG O=BASAL-PL CH{3}
B: SATM H [+0] GRAPHITE T=HPG-PI O=BASAL-PL CH{3}
C: SATM H [+0] GRAPHITE T=HPG O=BASAL-PL CH{4}

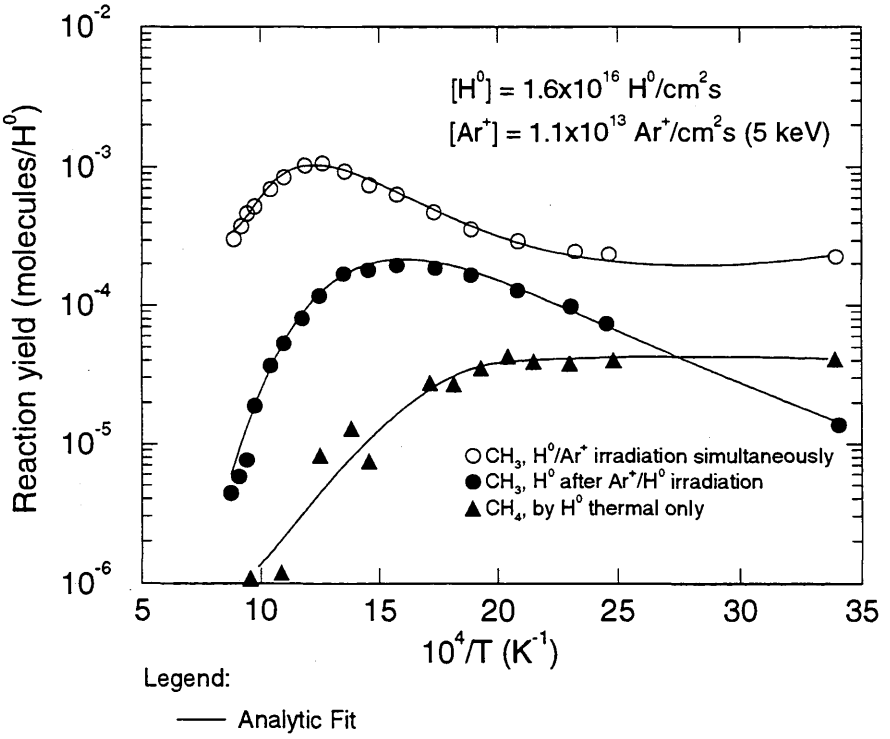

4.3.4.5 $[H^0, Ar^+]$ + pyrolytic graphite → CH_3, CH_4

Source: E. Vietzke, K. Flaskamp and V. Philipps, J. Nucl. Mater. **128&129**, 545 (1984).

Accuracy: Yield: 50%.

Comments: (1) Synergistic reaction of H^0 + Ar^+ on pyrolytic graphite.
(2) Specimen: pyrolytic graphite (machined, HPG, basal plane).
(3) Line-of-sight QMS detection.
(4) H^0 beam produced by thermal dissociation in W oven at 2800 K.
(5) Published data corrected for Maxwell-Boltzmann distributions with respect to specimen temperature.

Analytic fitting function:

Reaction yield:

$$Y = 1.0 \times 10^{-2}[A_1 \exp(-(T - A_2)^2/A_3)T^{A_4} + A_5 \exp(-A_6 T)T^{A_7}] \quad [\text{molecules}/H^0]$$

where T is in Kelvin. The rms deviation of analytic fits for reactions A (□) and B (•) are 36.6% and 10.2%, respectively.

Fitting parameters A_1-A_7

A	4.6760E-03	9.2494E+02	1.9324E+04	2.2197E-01	2.8338E-05	7.5914E-03
	1.7874E+00					
B	7.8175E-09	7.2306E+02	5.5822E+04	2.7770E+00	1.2785E-03	-5.0034E-04
	7.1559E-01					

ALADDIN evaluation function for reaction yield: EYIELD7A

ALADDIN hierarchical labelling:

A: SSATM H [+0] Ar [+1] GRAPHITE T=HPG O=BASAL-PL CH{4} [+0]
B: SSATM H [+0] Ar [+1] GRAPHITE T=HPG O=BASAL-PL CH{3} [+0]

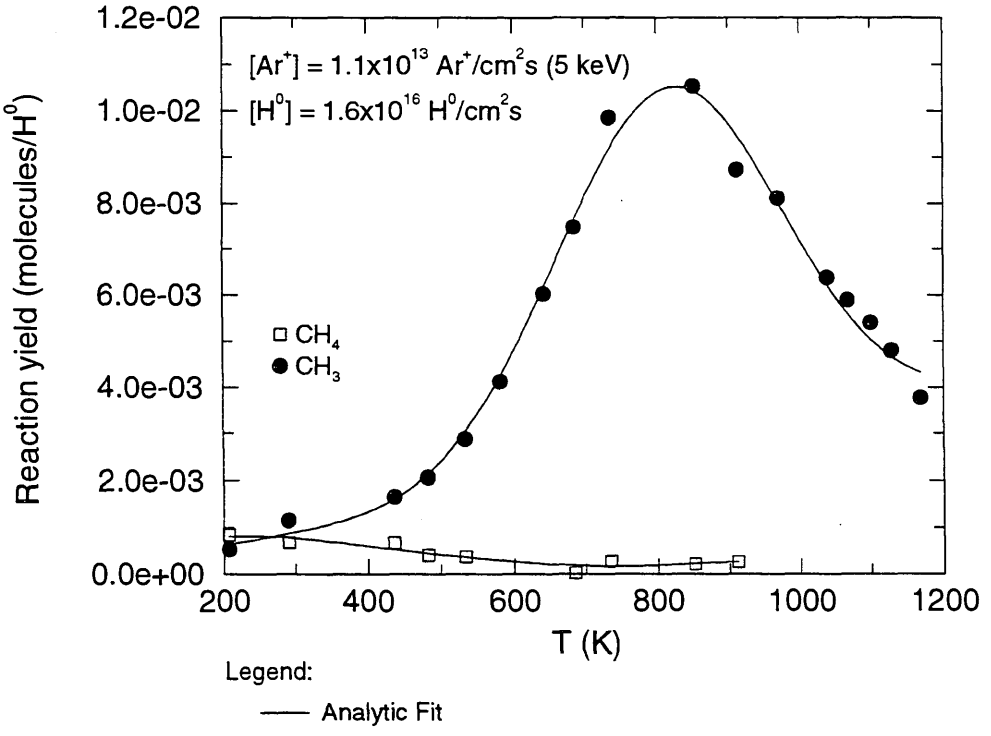

4.3.4.6 [H^0, Ar^+] + CLOR, POCO, pyrolytic, Papyex graphite → CH_3

Source: V. Philipps, K. Flaskamp and E. Vietzke, J. Nucl. Mater. **122&123**, 1440 (1984).

Accuracy: Yield: 50%.

Comments: (1) Comparison of the synergistic reaction H^0+Ar^+ on different graphites.
(2) Specimen: graphites (Carbone Lorraine, Poco, Papyex, pyrolytic).
(3) CH_3 is detected in a line-of-sight QMS.
(4) Published data are corrected for Maxwell-Boltzmann distributions with respect to specimen temperature.
(5) The relative reaction yield is obtained by multiplying the measured QMS signals with $(280/T)^{1/2}$, where T is given in Kelvin.

Analytic fitting function:

Relative reaction yield:

$$Y = 1.0 \times 10^{-2}[A_1 \exp(-(T - A_2)^2/A_3)T^{A_4} + A_5 \exp(-A_6 T)T^{A_7}] \quad \text{[arb. units]}$$

where T is in Kelvin. The rms deviation of analytic fits for reactions A (×), B (•), C (□) and D (△) are 15.2%, 5.9%, 3.9% and 5.0%, respectively. Data for curve A were fitted with EYIELD8A.

Fitting parameters A_1-A_8

A	1.0972E-05	4.0340E+01	-6.3980E-02	6.2216E+00	7.5993E+00	-2.8695E-39
	8.0230E-03	1.4545E+01				
B	1.2231E+03	7.9844E+02	1.9635E+04	-1.8384E-01	3.7106E-10	7.2557E-03
	4.7899E+00					
C	1.5633E+02	7.8433E+02	2.7749E+04	8.5172E-02	3.4252E+02	-6.1211E-04
	-3.3003E-01					
D	2.3594E+02	7.8189E+02	1.5405E+04	5.8254E-02	1.6318E-03	2.3320E-03
	1.9539E+00					

ALADDIN evaluation function for relative reaction yield: EYIELD7A, EYIELD8A

ALADDIN hierarchical labelling:

A: SSATM H [+0] Ar [+1] GRAPHITE T=CLOR CH{3} [+0]
B: SSATM H [+0] Ar [+1] GRAPHITE T=POCO CH{3} [+0]
C: SSATM H [+0] Ar [+1] GRAPHITE T=PAPYEX CH{3} [+0]
D: SSATM H [+0] Ar [+1] GRAPHITE T=HPG CH{3} [+0]

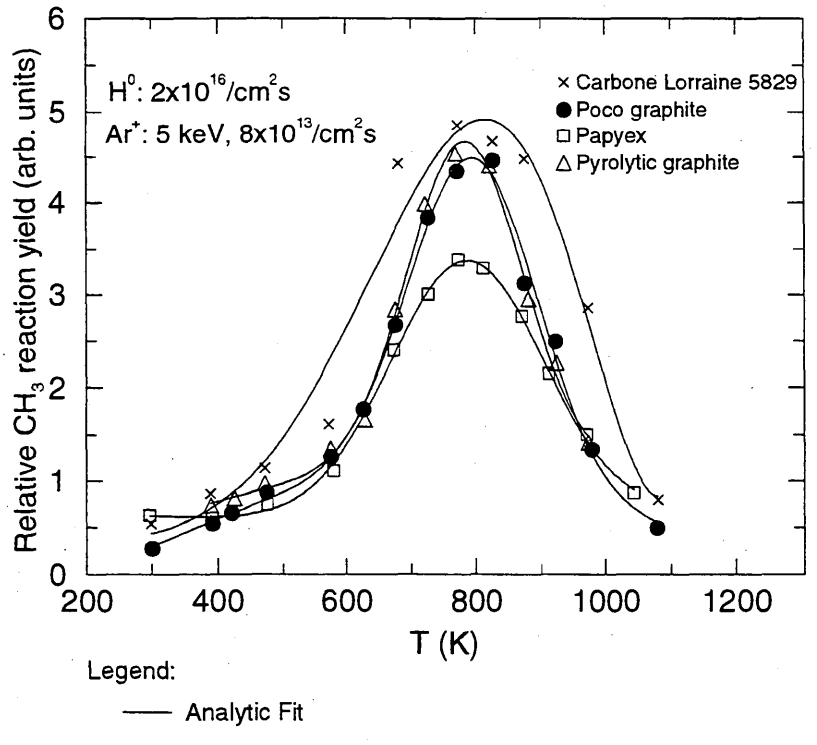

4.3.4.7 $[H^0, Ar^+]$, H^0 + pyrolytic graphite → C_2H_3

Source: E. Vietzke, V. Philipps and K. Flaskamp, J. Nucl. Mater. **162-164**, 898 (1989).

Accuracy: Yield: 50%.

Comments: (1) Relative reaction yields of H^0 atoms on different modified pyrolytic graphite (HPG).
(2) "Peak" means the maximum value after H^0 exposure.
(3) "After 100 s" means the nearly constant value after 100 seconds of H^0 exposure.

Analytic fitting function:

Relative reaction signal:

$$Y = 1.0 \times 10^{-2}[A_1 \exp(-(T - A_2)^2/A_3)T^{A_4} + A_5 \exp(-A_6 T)T^{A_7}] \quad \text{[arb. units]}$$

where T is in Kelvin. The rms deviation of analytic fits for reactions A (•), B (□), C (○), D (◇) and E (△) are 2.5%, 3.2%, 11.4%, 12.9% and 18.2%, respectively.

Fitting parameters A_1-A_7

A	1.2247E+03	7.4829E+02	2.7167E+04	-5.3112E-02	2.8872E-06	6.9497E-03
	3.4776E+00					
B	8.5564E+02	7.0995E+02	1.3966E+04	3.1929E-02	5.8328E+01	-1.8359E-03
	-3.7740E-02					
C	5.2588E+02	6.9579E+02	2.0251E+04	-3.9882E-02	3.8191E-05	7.4297E-04
	2.4504E+00					
D	3.6916E+02	6.5921E+02	1.2902E+04	-4.4551E-02	8.4946E-11	8.0996E-03
	5.0923E+00					
E	4.4697E+02	6.5757E+02	2.1955E+04	-6.4005E-02	4.3138E-10	1.1074E-02
	4.9251E+00					

ALADDIN evaluation function for relative reaction signal: EYIELD7A

ALADDIN hierarchical labelling:

A: SSATM H [+0] Ar [+1] GRAPHITE T=HPG C{2}H{3} [+0]
B-E: SATM H [+0] GRAPHITE T=HPG-PI C{2}H{3} [+0]

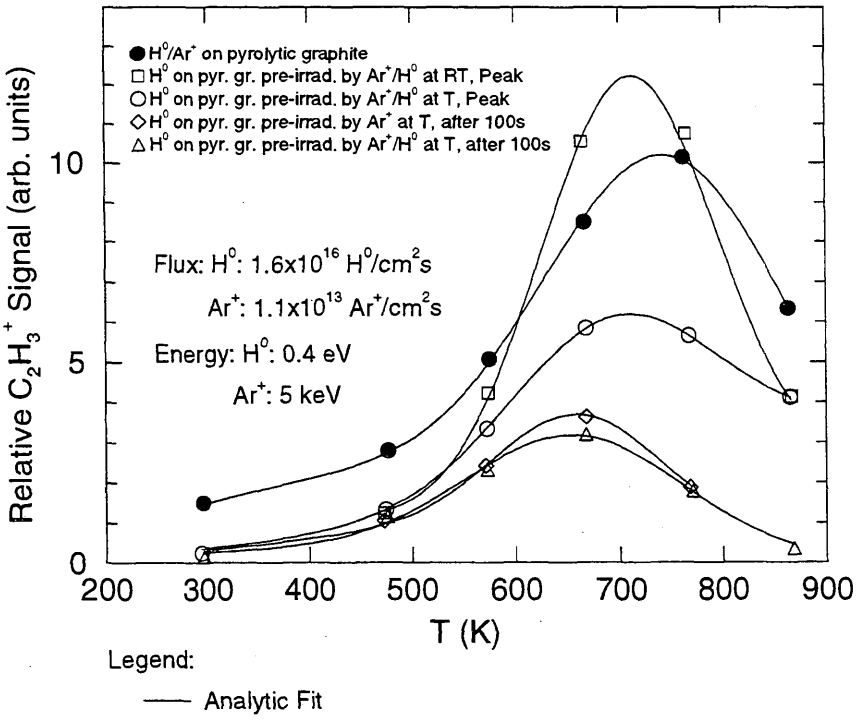

4.3.4.8 $[H^0, Ar^+]$, H^0, H^+ + pyrolytic graphite → CH_3, CH_4

Source: E. Vietzke and V. Philipps, Nucl. Instr. and Meth. B **23**, 449 (1987).

Accuracy: Yield: 50%.

Comments: (1) Comparison of different methyl and methane formation as shown in the figure.
(2) Specimen: pyrolytic graphite (machined, HPG).
(3) Line-of-sight QMS detection.
(4) Data are corrected for Maxwell-Boltzmann distribution with with respect to specimen temperature.
(5) Comparison with H^+ reaction (R. Yamada, J. Nucl. Mater. **145-147**, 359 (1987)).

Analytic fitting function:

Reaction yield:

$$Y = A_1 \exp\left[-\left(\frac{T - A_2}{A_3 T + 1}\right)^2 / A_4\right] T^{A_5} + A_6 \exp(-A_7 T) T^{A_8} \quad [\text{molecules}/H^0]$$

where T is in Kelvin. The rms deviation of analytic fits for reactions A (•), B (□), C (×) and D (∗) are 8.1%, 4.0%, 10.3% and 3.1%, respectively. Data for reaction D were fitted with EYIELD7A.

Fitting parameters A_1-A_8

A	2.8250E-02	8.1716E+02	-5.3568E-01	8.3555E-02	8.0033E-02	1.5810E-13
	5.9446E-03	4.5451E+00				
B	7.7962E+02	8.6464E+02	8.6508E-05	2.6237E+04	-1.7131E+00	1.0586E-07
	5.5223E-04	1.6005E+00				
C	1.6666E+05	2.8548E+03	5.6279E+00	2.0653E+01	-8.1017E+01	5.6840E-04
	2.1821E-03	1.6424E-01				
D	8.7339E-07	5.2004E+02	5.8706E+04	1.4975E+00	8.3397E+01	-2.2702E-03
	-1.9756E+00					

ALADDIN evaluation function for reaction yield: EYIELD7A, EYIELD8A

ALADDIN hierarchical labelling:

A: SATM H [+1] GRAPHITE T=HPG CH{4} [+0]
B: SSATM Ar [+1] H [+0] GRAPHITE T=HPG CH{3} [+0]
C: SSATM Ar [+1] H [+0] GRAPHITE T=HPG CH{4} [+0]
D: SATM H [+0] GRAPHITE T=HPG CH{3} [+0] CH{4} [+0]

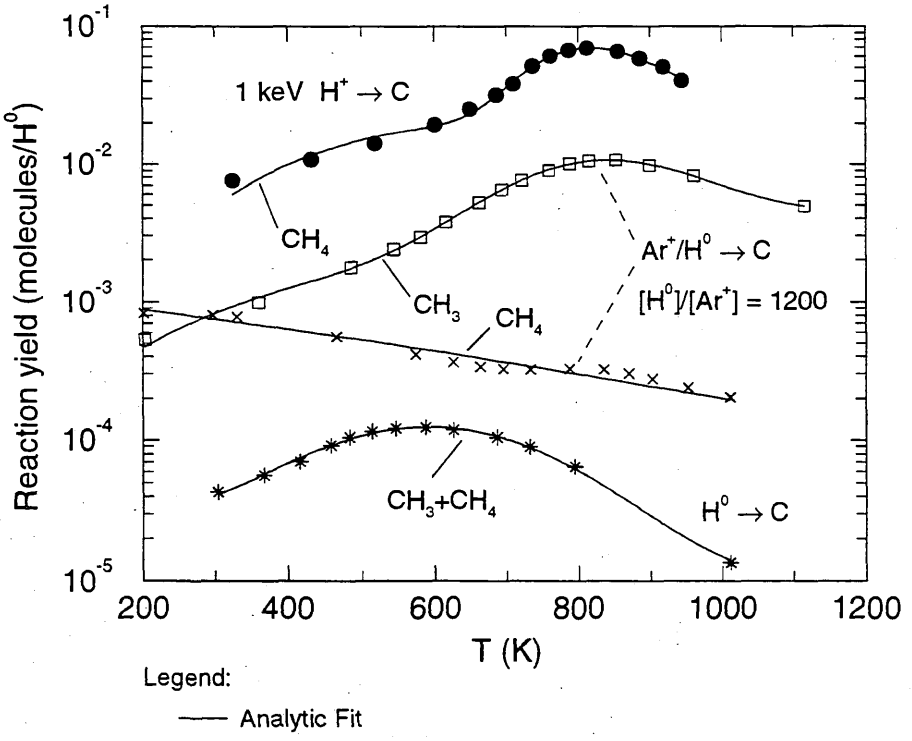

4.3.4.9 $[H^0, Ar^+]$, H^0, H^+ + pyrolytic graphite, a-C:H → CH_3, CH_4

Source: E. Vietzke and V. Philipps, Radiochemica Acta **43**, 75 (1988).

Accuracy: Yield: 50%.

Comments: (1) Steady-state CH_3 and CH_4 formation by H-atom and H^+ impact.
(2) Specimens: pyrolytic graphite and a-C:H film.
(3) Reaction products detected by line-of-sight QMS.
(4) H^+(0.4 keV) + C data from R. Yamada, J. Nucl. Mater. **145-147**, 359 (1987).

Analytic fitting function:

Reaction yield:

$$Y = A_1 \exp\left[-\left(\frac{T - A_2}{A_3 T + 1}\right)^2 / A_4\right] T^{A_5} + A_6 \exp(-A_7 T) T^{A_8} \quad [\text{molecules}/H^0]$$

where T is in Kelvin. The rms deviation of the analytic fits are 0.7% (A: H^+(2.5 keV) + a-C:H), 2.3% (B: H^0 + a-C:H) 3.4% (C: H^+(0.4 keV) + C), 2.5% (D: [H^0, Ar^+(5 keV)] + C) and 3.4% (E: H^0 + C), respectively.

Fitting parameters A_1-A_8

A	1.7045e-01	6.6628e+02	-1.0601e-03	2.9822e+05	1.1656e-02	-7.9642e- 05
	3.3680e-03	1.3506e+00				
B	3.3090e-02	6.6235e+02	-2.6649e-04	1.9935e+04	-4.9280e-02	1.4500e- 05
	-2.6674e-03	7.4834e-01				
C	6.9970e-02	8.0635e+02	-5.3364e-04	7.5833e+04	-2.0859e-02	3.3458e- 05
	-1.0339e-03	6.3634e-01				
D	1.4857e-02	8.2882e+02	-6.7924e-05	3.4424e+04	-9.5630e-02	1.2522e- 06
	-4.6052e-04	1.1098e+00				
E	2.0521e-04	5.5150e+02	5.8718e-04	3.1474e+04	-7.5260e-02	4.4916e- 04
	2.2365e-02	4.9957e-01				

ALADDIN evaluation function for reaction yield: EYIELD8A

ALADDIN hierarchical labelling:

A: SATM H [+1] GRAPHITE T=A-CH-FILM CH{4} [+0]
B: SATM H [+0] GRAPHITE T=A-CH-FILM CH{3} [+0]
C: SATM H [+1] GRAPHITE T=HPG CH{4} [+0]
D: SSATM H [+0] Ar [+1] GRAPHITE T=HPG CH{3} [+0]
E: SATM H [+0] GRAPHITE T=HPG CH{3} [+0] CH{4} [+0]

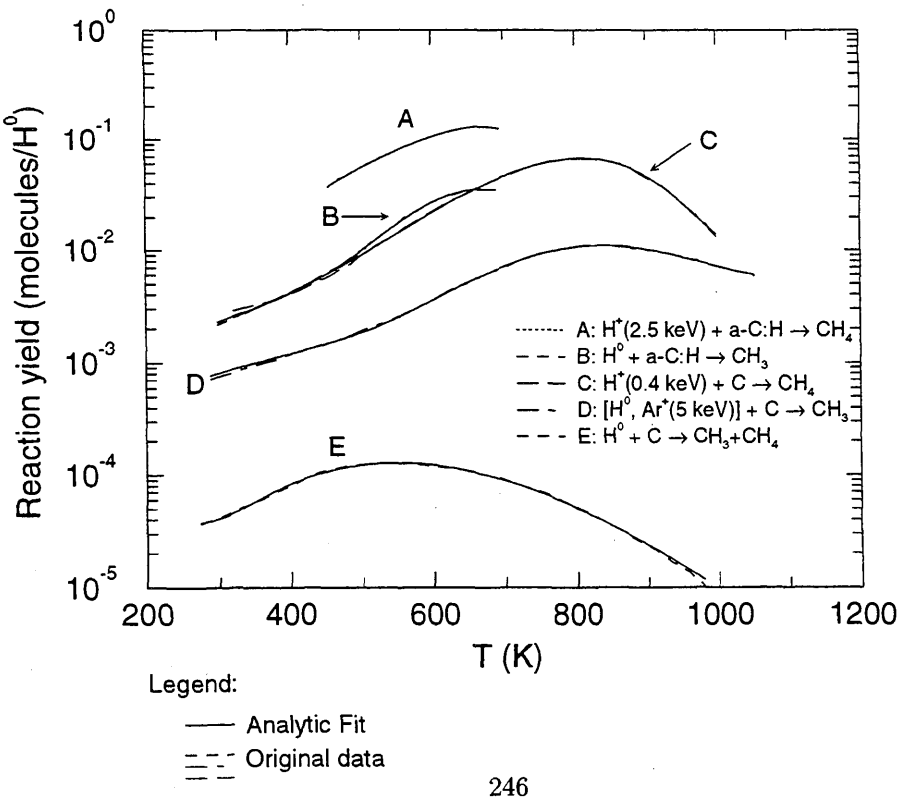

4.3.5.1 $[H^+, He^+]$ + pyrolytic graphite → C_xH_y, C

Source: A. A. Haasz and J. W. Davis, Nucl. Instr. Meth. Phys. Res. B **83**, 117 (1993).

Accuracy: Yield: Total ±20%; CH_4 ±15%, C_2H_2 ±30%; Flux ratio: ±30% (beam stability, beam profile overlap).

Comments: (1) Chemical erosion due to simultaneous bombardment by He^+ and H^+ ions.
(2) He^+ and H^+ ions produced by independent mass-selecting ion accelerators.
(3) Hydrocarbon products measured via QMS-RGA, steady-state.
(4) Specimens: graphite (pyrolytic, HPG99).
(5) Yield for total chemical erosion, $Y_{chem-total} = [CH_4 + 2(C_2H_2 + C_2H_4 + C_2H_6) + 3(C_3H_6 + C_3H_8)]/H^+$.

Analytic fitting function:

Erosion yield:

$$Y = A_1 \exp(-A_2 F) F^{A_3} \quad [\text{molecules}/H^+]$$

where F is the flux ratio $[He^+]/[H^+]$. The rms deviation of analytic fits for reactions A (•), B (△) and C (□) are 5.7%, 7.7% and 6.8%, respectively.

Fitting parameters A_1-A_3

A	1.0381E-01	1.0945E+00	1.0978E-01
B	6.6251E-02	1.4586E+00	1.3691E-01
C	6.6899E-03	-1.6458E-01	2.1142E-01

ALADDIN evaluation function for erosion yield: EYIELD3A

ALADDIN hierarchical labelling:

A: SSATM H{3} [+1] He [+1] GRAPHITE T=HPG99 C [+0]
B: SSATM H{3} [+1] He [+1] GRAPHITE T=HPG99 CH{4} [+0]
C: SSATM H{3} [+1] He [+1] GRAPHITE T=HPG99 C{2}H{2} [+0]

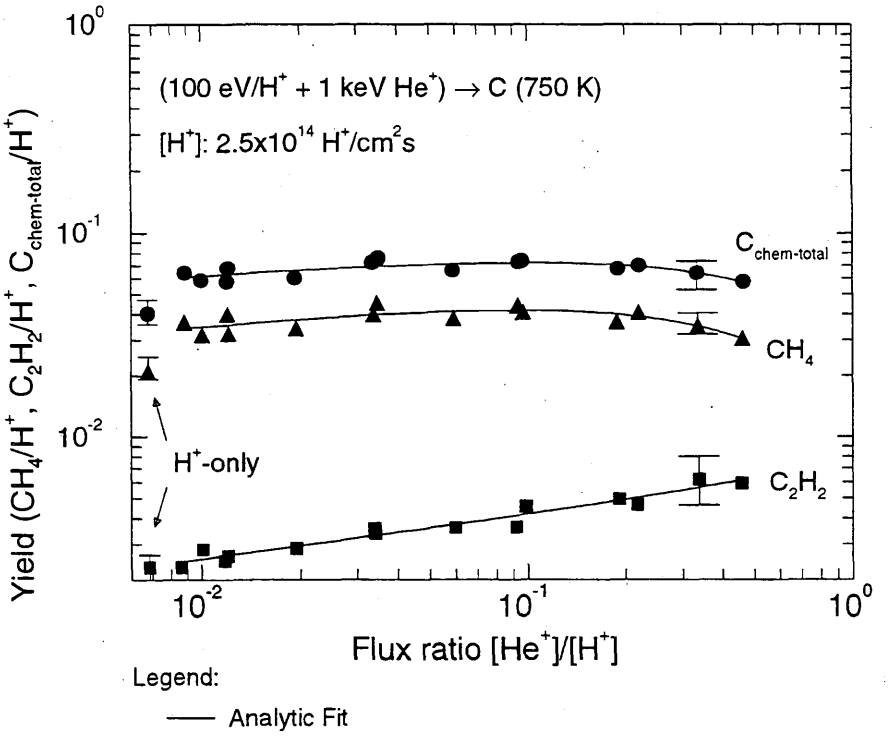

4.3.6.1 $[H^+, C^+]$ + pyrolytic graphite → C_xH_y, C

Source: J. W. Davis, A. A. Haasz and C. H. Wu, J. Nucl. Mater. **196-198**, 581 (1992).

Accuracy: Yield: Total ±20%; CH_4 ±15%, C_2H_2 ±30%; T: ±25K.

Comments: (1) Chemical erosion due to simultaneous bombardment by C^+ and H^+ ions.
(2) C^+ and H^+ ions produced by independent mass-selecting ion accelerators.
(3) Hydrocarbon products measured via QMS-RGA, steady-state.
(4) Specimens: graphite (pyrolytic, HPG99).
(5) Yield for total chemical erosion, $Y_{chem-total} = [CH_4 + 2(C_2H_2 + C_2H_4 + C_2H_6) + 3(C_3H_6 + C_3H_8)]/H^+$.

Analytic fitting function:

Erosion yield:

$$Y = 1.0 \times 10^{-2}[A_1 \exp(-(T - A_2)^2/A_3)T^{A_4} + A_5 \exp(-A_6T)T^{A_7}] \quad [\text{molecules}/H^+]$$

where T is in Kelvin. The rms deviation of analytic fits for reactions A (∗), B (○), C (△), D (▽), E (□) and F (◇) are 5.7%, 8.0%, 1.9%, 2.4%, 4.8% and 5.2%, respectively.

Fitting parameters A_1-A_7

A	8.4600E+00	7.4639E+02	3.7246E+04	-3.9928E-02	1.1369E+00	-4.8613E-04	1.6955E-02
B	5.3552E+00	7.1154E+02	3.9231E+04	-2.5275E-03	8.8977E-01	-5.1212E-04	-1.3721E-02
C	1.3969E+00	7.3693E+02	4.2372E+04	1.0777E-01	5.7399E-01	1.3864E-03	4.3116E-03
D	3.1305E+00	7.5249E+02	3.1283E+04	2.2994E-02	3.0517E-01	-5.5535E-04	2.4318E-03
E	1.1709E+00	8.1853E+02	6.1027E+04	-8.1249E-02	8.2640E-01	2.6186E-03	1.9803E-03
F	3.4382E+00	8.2086E+02	1.1296E+04	-4.8432E-01	4.5497E-04	1.9122E-03	1.1518E+00

ALADDIN evaluation function for erosion yield: EYIELD7A

ALADDIN hierarchical labelling:

A: SSATM H{3} [+1] C [+1] GRAPHITE T=HPG99 C [+0]
B: SATM H{3} [+1] GRAPHITE T=HPG99 C [+0]
C: SATM H{3} [+1] GRAPHITE T=HPG99 CH{4} [+0]
D: SSATM H{3} [+1] C [+1] GRAPHITE T=HPG99 CH{4} [+0]
E: SSATM H{3} [+1] C [+1] GRAPHITE T=HPG99 C{2}H{2} [+0]
F: SATM H{3} [+1] GRAPHITE T=HPG C{2}H{2} [+0]

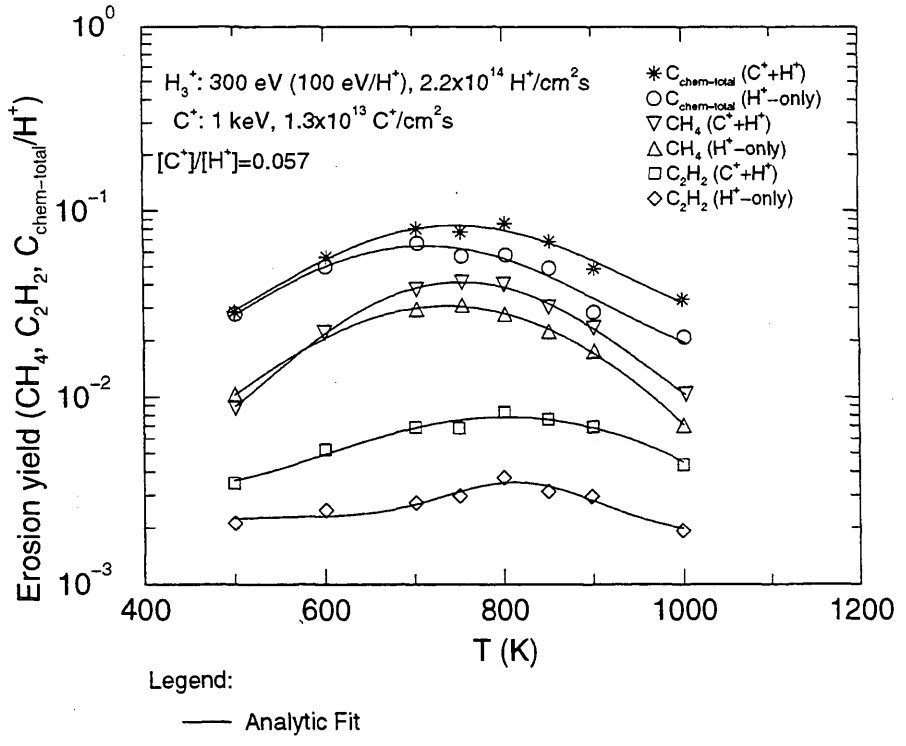

4.3.6.2 $[H^+, C^+]$ + pyrolytic graphite → C_xH_y, C

Source: J. W. Davis, A. A. Haasz and C. H. Wu, J. Nucl. Mater. **196-198**, 581 (1992).

Accuracy: Yield: Total ±20%; CH_4 ±15%, C_2H_2 ±30%; T: ±25K.

Comments: (1) Chemical erosion due to simultaneous bombardment by C^+ and H^+ ions.
(2) C^+ and H^+ ions produced by independent mass-selecting ion accelerators.
(3) Hydrocarbon products measured via QMS-RGA, steady-state.
(4) Specimens: graphite (pyrolytic, HPG99).
(5) Yield for total chemical erosion, $Y_{chem-total} = [CH_4 + 2(C_2H_2 + C_2H_4 + C_2H_6) + 3(C_3H_6 + C_3H_8)]/H^+$.

Analytic fitting function:

Erosion yield:

$$Y = 1.0 \times 10^{-2}[A_1 \exp(-(T - A_2)^2/A_3)T^{A_4} + A_5 \exp(-A_6T)T^{A_7}] \quad [\text{molecules}/H^+]$$

where T is in Kelvin. The rms deviation of analytic fits for reactions A (∗), B (○), C (△), D (▽), E (□) and F (◇) are 8.0%, 0.4%, 1.4%, 3.7%, 2.5% and 8.4%, respectively.

Fitting parameters A_1-A_7

A	1.2746E+01	7.6242E+02	1.2500E+04	-1.2881E-01	3.5806E+01	3.5625E-04	-3.1431E-01
B	1.7307E+01	7.5035E+02	7.0088E+03	-2.5329E-01	1.0836E+02	7.0563E-04	-4.3595E-01
C	2.4368E+00	7.6674E+02	1.2454E+04	-2.3752E-02	4.8739E+00	1.4430E-03	-2.5261E-02
D	3.8022E+00	7.8407E+02	1.0427E+04	-1.1660E-02	2.2907E+00	7.9639E-04	1.0507E-02
E	1.3254E-04	7.4825E+02	8.8604E+03	1.0971E+00	7.9287E-03	2.9841E-03	9.3739E-01
F	1.9724E-01	6.3293E+02	1.2745E+05	-1.4476E-04	4.7141E-02	-6.4991E-04	1.2423E-05

ALADDIN evaluation function for erosion yield: EYIELD7A

ALADDIN hierarchical labelling:

A: SSATM H{3} [+1] C [+1] GRAPHITE T=HPG C [+0]
B: SATM H{3} [+1] GRAPHITE T=HPG C [+0]
C: SATM H{3} [+1] GRAPHITE T=HPG CH{4} [+0]
D: SSATM H{3} [+1] C [+1] GRAPHITE T=HPG CH{4} [+0]
E: SSATM H{3} [+1] C [+1] GRAPHITE T=HPG C{2}H{2} [+0]
F: SATM H{3} [+1] GRAPHITE T=HPG C{2}H{2} [+0]

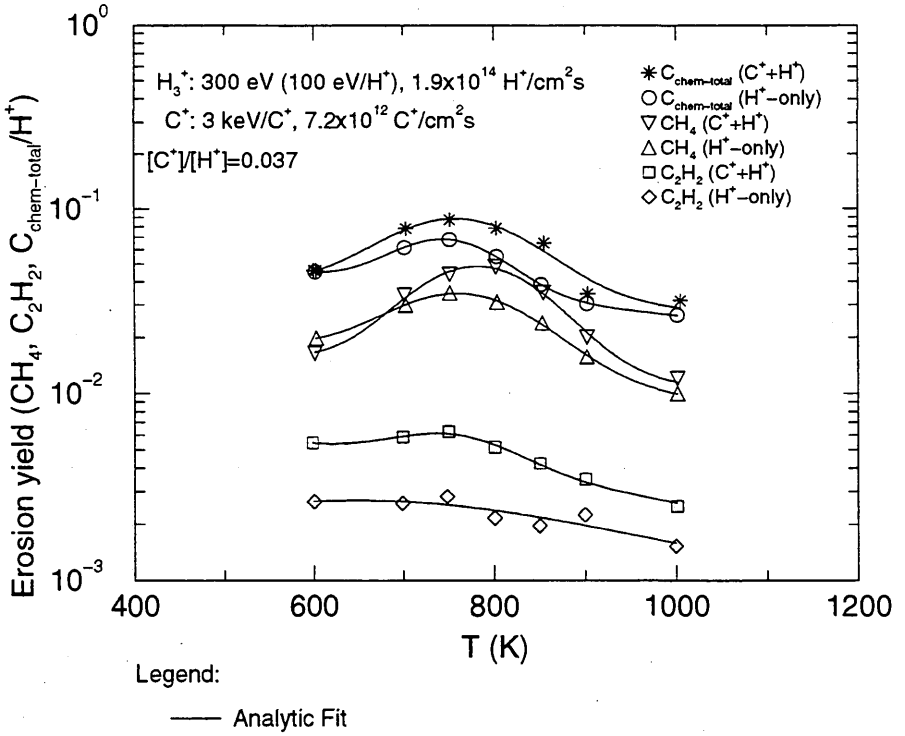

4.3.6.3 $[H^+, C^+]$ + pyrolytic graphite → C_xH_y, C

Source: J. W. Davis, A. A. Haasz and C. H. Wu, J. Nucl. Mater. **196-198**, 581 (1992).

Accuracy: Yield: Total ±20%; CH_4 ±15%, C_2H_2 ±30%; T: ±25K.

Comments: (1) Chemical erosion due to simultaneous bombardment by C^+ and H^+ ions.
(2) C^+ and H^+ ions produced by independent mass-selecting ion accelerators.
(3) Hydrocarbon products measured via QMS-RGA, steady-state.
(4) Specimens: graphite (pyrolytic, HPG99).
(5) Yield for total chemical erosion, $Y_{chem-total} = [CH_4 + 2(C_2H_2 + C_2H_4 + C_2H_6) + 3(C_3H_6 + C_3H_8)]/H^+$.

Analytic fitting function:

Erosion yield:

$$Y = 1.0 \times 10^{-2}[A_1 \exp(-(T - A_2)^2/A_3)T^{A_4} + A_5 \exp(-A_6T)T^{A_7}] \quad [\text{molecules/H}^+]$$

where T is in Kelvin. The rms deviation of analytic fits for reactions A (∗), B (○), C (△), D (▽), E (□) and F (◇) are 1.7%, 1.9%, 6.5%, 3.5%, 5.5% and 5.1%, respectively.

Fitting parameters A_1-A_7

A	8.2096E+00	7.7418E+02	2.7622E+04	1.0806E-02	8.4823E-01	-9.9569E-04	7.8994E-03
B	8.7115E+00	7.8070E+02	2.3979E+04	2.1067E-03	1.0961E+00	-9.4495E-04	-2.6958E-02
C	2.0874E+01	7.8994E+02	2.1110E+04	-2.0065E-01	6.9929E-06	1.8344E-03	1.9868E+00
D	6.2088E+00	7.8374E+02	2.6513E+04	-9.5395E-04	1.4270E-01	-1.3754E-03	-2.4838E-04
E	6.2416E-01	7.8482E+02	8.8485E+04	1.5020E-02	1.9391E-02	-2.3893E-03	-6.9035E-05
F	5.6843E-01	7.6844E+02	1.2592E+05	4.3022E-02	-7.2265E-01	2.5869E-03	2.1909E-03

ALADDIN evaluation function for erosion yield: EYIELD7A

ALADDIN hierarchical labelling:

A: SSATM H{3} [+1] C [+1] GRAPHITE T=HPG C [+0]
B: SATM H{3} [+1] GRAPHITE T=HPG C [+0]
C: SATM H{3} [+1] GRAPHITE T=HPG CH{4} [+0]
D: SSATM H{3} [+1] C [+1] GRAPHITE T=HPG CH{4} [+0]
E: SSATM H{3} [+1] C [+1] GRAPHITE T=HPG C{2}H{2} [+0]
F: SATM H{3} [+1] GRAPHITE T=HPG C{2}H{2} [+0]

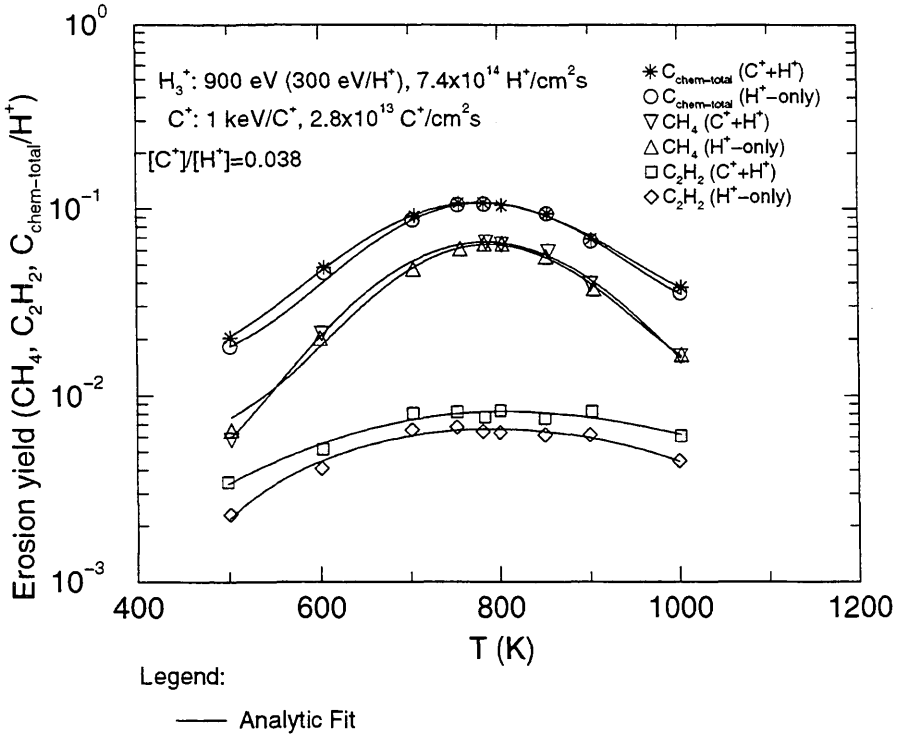

4.3.6.4 $[H^+, C^+]$ + pyrolytic graphite → C_xH_y, C

Source: J. W. Davis, A. A. Haasz and C. H. Wu, J. Nucl. Mater. **196-198**, 581 (1992).

Accuracy: Yield: Total ±20%; CH_4 ±15%, C_2H_2 ±30%; T: ±25K.

Comments: (1) Chemical erosion due to simultaneous bombardment by C^+ and H^+ ions.
(2) C^+ and H^+ ions produced by independent mass-selecting ion accelerators.
(3) Hydrocarbon products measured via QMS-RGA, steady-state.
(4) Specimens: graphite (pyrolytic, HPG99).
(5) Yield for total chemical erosion, $Y_{chem-total} = [CH_4 + 2(C_2H_2 + C_2H_4 + C_2H_6) + 3(C_3H_6 + C_3H_8)]/H^+$.

Analytic fitting function:

Erosion yield:

$$Y = 1.0 \times 10^{-2}[A_1 \exp(-(T - A_2)^2/A_3)T^{A_4} + A_5 \exp(-A_6T)T^{A_7}] \quad [\text{molecules}/H^+]$$

where T is in Kelvin. The rms deviation of analytic fits for reactions A (∗), B (∘), C (△), D (▽), E (□) and F (◇) are 6.0%, 4.5%, 3.5%, 4.1%, 2.7% and 4.8%, respectively.

Fitting parameters A_1-A_7

A	3.9261E+00	7.8236E+02	2.0819E+04	1.1099E-01	1.0714E+01	-2.3469E-03	-4.6167E-01
B	4.6020E+00	7.8197E+02	2.4200E+04	9.8603E-02	6.9134E+00	-2.2433E-03	-4.1165E-01
C	6.6592E+00	7.9736E+02	1.9342E+04	-2.3975E-02	1.9650E-01	-1.9794E-03	1.6850E-03
D	6.5449E+00	7.9592E+02	2.4257E+04	-1.4966E-02	1.1827E-01	-2.6618E-03	-4.7148E-02
E	8.0019E-03	7.1222E+02	6.2380E+04	6.9532E-01	6.1282E-03	-4.1729E-03	2.0849E-02
F	5.9674E-01	7.4104E+02	5.3721E+04	2.8398E-02	4.1654E-03	-4.5454E-03	1.7527E-04

ALADDIN evaluation function for erosion yield: EYIELD7A

ALADDIN hierarchical labelling:

A: SSATM H{3} [+1] C [+1] GRAPHITE T=HPG C [+0]
B: SATM H{3} [+1] GRAPHITE T=HPG C [+0]
C: SATM H{3} [+1] GRAPHITE T=HPG CH{4} [+0]
D: SSATM H{3} [+1] C [+1] GRAPHITE T=HPG CH{4} [+0]
E: SSATM H{3} [+1] C [+1] GRAPHITE T=HPG C{2}H{2} [+0]
F: SATM H{3} [+1] GRAPHITE T=HPG C{2}H{2} [+0]

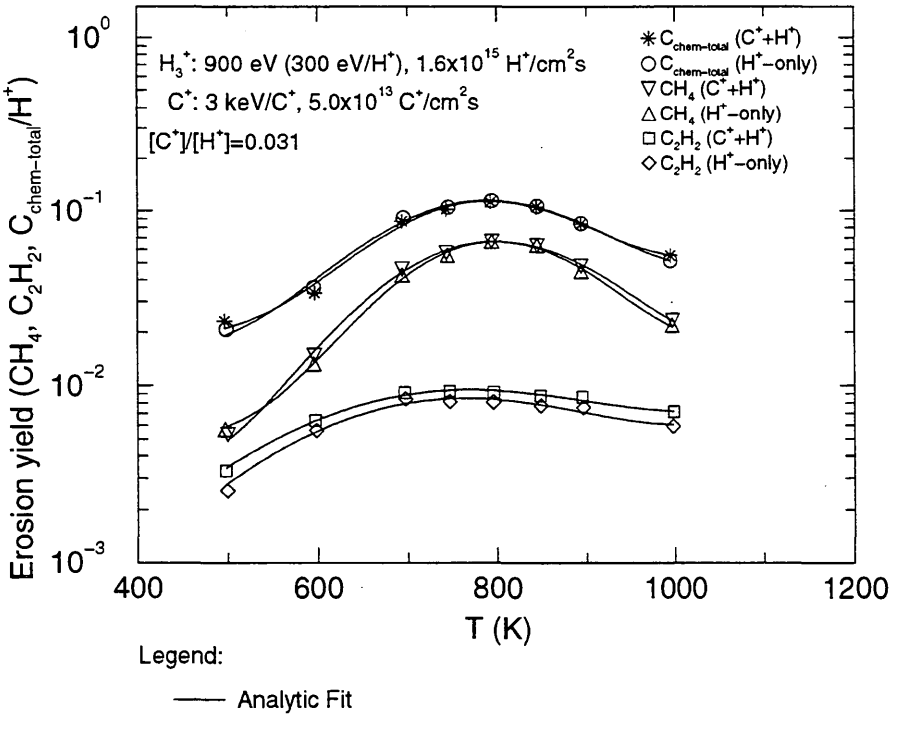

4.3.6.5 $[H^+, C^+]$ + pyrolytic graphite → C_xH_y, C

Source: J. W. Davis, A. A. Haasz and C. H. Wu, J. Nucl. Mater. **196-198**, 581 (1992).

Accuracy: Yield: Total ±20%; CH_4 ±15%, C_2H_2 ±30%; Flux ratio: ±30% (beam stability, beam profile overlap).

Comments: (1) Chemical erosion due to simultaneous bombardment by C^+ and H^+ ions.
(2) C^+ and H^+ ions produced by independent mass-selecting ion accelerators.
(3) Hydrocarbon products measured via QMS-RGA, steady-state.
(4) Specimens: graphite (pyrolytic, HPG99).
(5) Projectile energies: 300 eV H_3^+ (100 eV/H^+), 1 keV C^+, 1 keV He^+. Target temperature: 750-800 K.
(6) Fits are for H_3^+ + C^+ bombardment, compared with data for He^+ + H_3^+.
(7) Yield for total chemical erosion, $Y_{chem-total} = [CH_4 + 2(C_2H_2 + C_2H_4 + C_2H_6) + 3(C_3H_6 + C_3H_8)]/H^+$.

Analytic fitting function:

Erosion yield:

$$Y = A_1 \exp(-A_2 F) F^{A_3} + A_4 F^{A_5} \quad [\text{molecules}/H^+]$$

where F is the flux ratio $[C^+]/[H^+]$ or $[He^+]/[H^+]$. The rms deviation of analytic fits for reactions A (•), B (△) and C (□) are 6.1%, 11.5% and 8.9%, respectively.

Fitting parameters A_1-A_5

A	1.1100E-01	6.1420E-01	1.0550E-01	-2.0415E+00	8.0905E+01
B	5.1124E-02	1.1263E+00	6.6600E-02	-2.2600E+00	8.4146E+01
C	9.6835E-03	-2.2430E+00	1.2006E-01	3.6704E+01	1.6363E+02

ALADDIN evaluation function for erosion yield: EYIELD5A

ALADDIN hierarchical labelling:

A: SSATM H{3} [+1] C [+1] GRAPHITE T=HPG C [+0]
B: SSATM H{3} [+1] C [+1] GRAPHITE T=HPG CH{4} [+0]
C: SSATM H{3} [+1] C [+1] GRAPHITE T=HPG C{2}H{2} [+0]

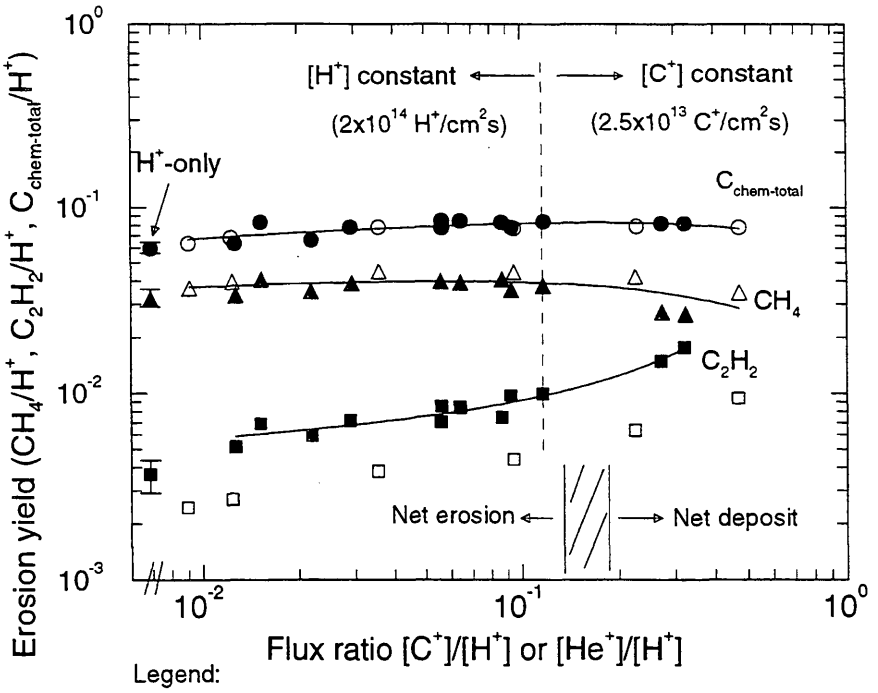

Legend:
—— Analytic Fit
Solid symbols: C^++H_3^+ and H^+ only
Open symbols: 1 keV He^++H_3^+ bombardment

4.3.6.6 $[H^+, C^+]$ + pyrolytic graphite → C_xH_y, C

Source: J. W. Davis, A. A. Haasz and C. H. Wu, J. Nucl. Mater. **196-198**, 581 (1992).

Accuracy: Yield: Total ±20%; CH_4 ±15%, C_2H_2 ±30%; Flux ratio: ±30% (beam stability, beam profile overlap).

Comments: (1) Chemical erosion due to simultaneous bombardment by C^+ and H^+ ions.
(2) C^+ and H^+ ions produced by independent mass-selecting ion accelerators.
(3) Hydrocarbon products measured via QMS-RGA, steady-state.
(4) Specimens: graphite (pyrolytic, HPG99).
(5) Projectile energies: 300 eV H_3^+ (100eV/H^+), 3 keV C^+. Target temperature: 750-800 K.
(6) Yield for total chemical erosion, $Y_{chem-total} = [CH_4 + 2(C_2H_2 + C_2H_4 + C_2H_6) + 3(C_3H_6 + C_3H_8)]/H^+$.

Analytic fitting function:

Erosion yield:

$$Y = A_1 \exp(-A_2 F) F^{A_3} + A_4 F^{A_5} \quad [\text{molecules}/H^+]$$

where F is the flux ratio $[C^+]/[H^+]$. The rms deviation of analytic fits for reactions A (•), B (△) and C (□) are 6.2%, 6.8% and 11.1%, respectively.

Fitting parameters A_1-A_5

A	6.4358E-02	-2.6200E-02	-6.7205E-02	1.3065E-01	9.7362E-01
B	4.2670E-02	1.6606E+00	-4.5645E-02	4.1687E-02	1.1484E+00
C	1.7240E-03	8.4995E+01	-3.7096E-01	3.7305E-02	5.2428E-01

ALADDIN evaluation function for erosion yield: EYIELD5A

ALADDIN hierarchical labelling:

A: SSATM H{3} [+1] C [+1] GRAPHITE T=HPG C [+0]
B: SSATM H{3} [+1] C [+1] GRAPHITE T=HPG CH{4} [+0]
C: SSATM H{3} [+1] C [+1] GRAPHITE T=HPG C{2}H{2} [+0]

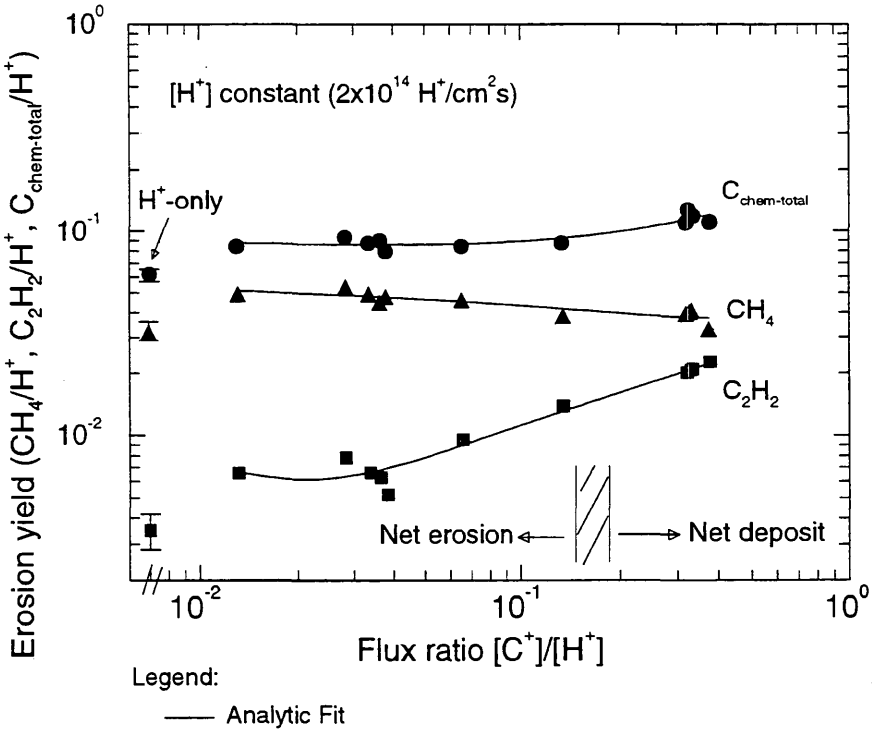

4.3.6.7 $[H^+, C^+]$ + pyrolytic graphite → C_xH_y, C

Source: J. W. Davis, A. A. Haasz and C. H. Wu, J. Nucl. Mater. **196-198**, 581 (1992).

Accuracy: Yield: Total ±20%; CH_4 ±15%, C_2H_2 ±30%; Flux ratio: ±30% (beam stability, beam profile overlap).

Comments: (1) Chemical erosion due to simultaneous bombardment by C^+ and H^+ ions.
(2) C^+ and H^+ ions produced by independent mass-selecting ion accelerators.
(3) Hydrocarbon products measured via QMS-RGA, steady-state.
(4) Specimens: graphite (pyrolytic, HPG99).
(5) Projectile energies: 900 eV H_3^+ (300 eV/H^+), 1 keV C^+, 1 keV He^+. Target temperature: 750-800 K.
(6) Fits are for H_3^+ + C^+ bombardment, compared with data for He^+ + H_3^+.
(7) Yield for total chemical erosion, $Y_{chem-total} = [CH_4 + 2(C_2H_2 + C_2H_4 + C_2H_6) + 3(C_3H_6 + C_3H_8)]/H^+$.

Analytic fitting function:

Erosion yield:

$$Y = A_1 \exp(-A_2 F) F^{A_3} + A_4 F^{A_5} \quad [\text{molecules}/H^+]$$

where F is the flux ratio $[C^+]/[H^+]$ or $[He^+]/[H^+]$. The rms deviation of analytic fits for reactions A (•), B (△) and C (□) are 4.9%, 5.5% and 6.5%, respectively.

Fitting parameters A_1-A_5

A	7.7282E-02	-8.2839E-01	-7.8114E-02	-9.3172E+00	3.7528E+01
B	5.3751E-02	3.0828E-01	-5.4201E-02	3.0575E-01	2.0944E+02
C	8.8812E-03	-1.8390E+00	7.9100E-02	2.6290E+02	1.0062E+03

ALADDIN evaluation function for erosion yield: EYIELD5A

ALADDIN hierarchical labelling:

A: SSATM H{3} [+1] C [+1] GRAPHITE T=HPG C [+0]
B: SSATM H{3} [+1] C [+1] GRAPHITE T=HPG CH{4} [+0]
C: SSATM H{3} [+1] C [+1] GRAPHITE T=HPG C{2}H{2} [+0]

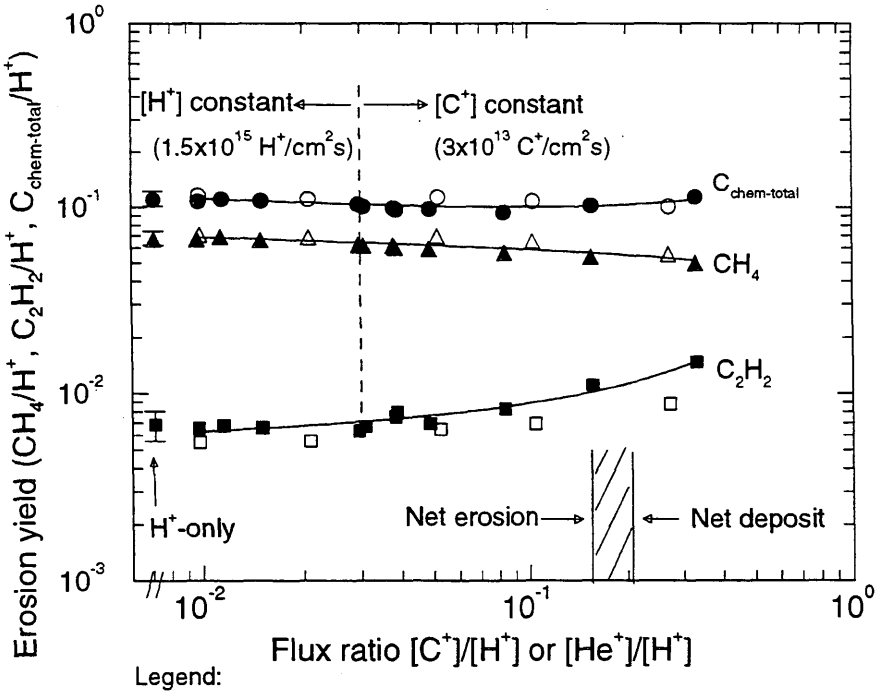

Legend:
—— Analytic Fit
Solid symbols: C^++H_3^+ and H^+ only
Open symbols: 1 keV He^++H_3^+ bombardment

4.3.6.8 $[H^+, C^+]$ + pyrolytic graphite → C_xH_y, C

Source: J. W. Davis, A. A. Haasz and C. H. Wu, J. Nucl. Mater. **196-198**, 581 (1992).

Accuracy: Yield: Total ±20%; CH_4 ±15%, C_2H_2 ±30%; Flux ratio: ±30% (beam stability, beam profile overlap).

Comments: (1) Chemical erosion due to simultaneous bombardment by C^+ and H^+ ions.
(2) C^+ and H^+ ions produced by independent mass-selecting ion accelerators.
(3) Hydrocarbon products measured via QMS-RGA, steady-state.
(4) Specimens: graphite (pyrolytic, HPG99).
(5) Projectile energies: 900 eV H_3^+ (300 eV/H^+), 3 keV C^+. Target temperature: 750-800 K.
(6) Yield for total chemical erosion, $Y_{chem-total} = [CH_4 + 2(C_2H_2 + C_2H_4 + C_2H_6) + 3(C_3H_6 + C_3H_8)]/H^+$.

Analytic fitting function:

Erosion yield:

$$Y = A_1 \exp(-A_2 F) F^{A_3} + A_4 F^{A_5} \quad [\text{molecules}/H^+]$$

where F is the flux ratio $[C^+]/[H^+]$. The rms deviation of analytic fits for reactions A (•), B (△) and C (□) are 6.7%, 5.7% and 8.5%, respectively.

Fitting parameters A_1-A_5

A	1.5300E-01	4.8530E-01	8.2374E-02	-8.4613E+00	3.6646E+01
B	8.5416E-02	2.0656E+00	5.5060E-02	3.5252E+00	3.1007E+02
C	1.9258E-02	-1.3163E+00	2.5046E-01	1.3640E+01	7.0503E+01

ALADDIN evaluation function for erosion yield: EYIELD5A

ALADDIN hierarchical labelling:

A: SSATM H{3} [+1] C [+1] GRAPHITE T=HPG C [+0]
B: SSATM H{3} [+1] C [+1] GRAPHITE T=HPG CH{4} [+0]
C: SSATM H{3} [+1] C [+1] GRAPHITE T=HPG C{2}H{2} [+0]

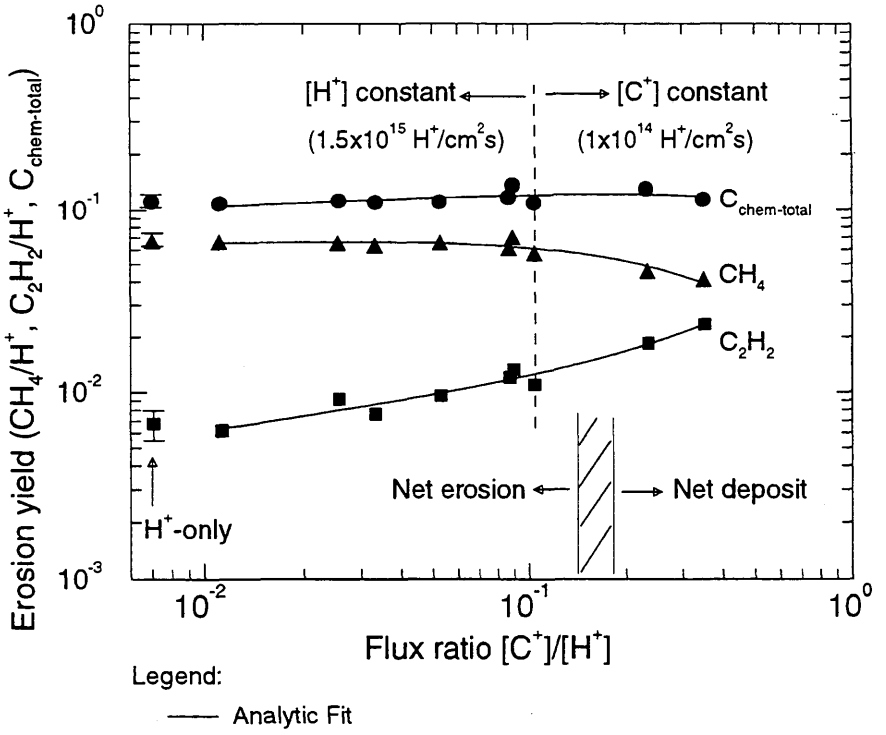

4.3.6.9 $[H^+, C^+]$ + pyrolytic graphite → C_xH_y, C

Source: J. W. Davis, A. A. Haasz and C. H. Wu, J. Nucl. Mater. **196-198**, 581 (1992).

Accuracy: Enhancement yield: ±30%; Flux ratio: ±30%.

Comments: (1) Enhancement (reduction) in the total hydrocarbon production rate due to C^+ ions in the presence of H^+ ions, normalized by C^+ flux.
(2) C^+ and H^+ ions produced by independent mass-selecting ion accelerators.
(3) Hydrocarbon products measured via QMS-RGA, steady-state.
(4) Specimens: graphite (pyrolytic, HPG99).
(5) Projectile energies: 300 eV H_3^+ (100 eV/H^+), 900 eV H_3^+ (300 eV/H^+), 1 and 3 keV C^+. Target temperature: 750-800 K.
(6) Data from Figures 3.6.5-3.6.8.

Analytic fitting function:

Erosion enhancement yield:

$$Y = A_1 \exp(-A_2 F) F^{A_3} + A_4 F^{A_5} \quad [\text{molecules}/H^+]$$

where F is the flux ratio $[C^+]/[H^+]$. The rms deviation of analytic fits for reactions A (■, □), B (•, ○) are 28.8% and 352.0%, respectively.

Fitting parameters A_1-A_5

A	4.7622E-02	4.5271E-01	-8.2306E-01	-1.6631E+01	6.7480E+01
B	-3.5014E+00	1.5591E+01	1.3224E+00	-1.4615E-05	-2.1627E+00

ALADDIN evaluation function for erosion enhancement yield: EYIELD5A

ALADDIN hierarchical labelling:

A, B: SSATM H{3} [+1] C [+1] GRAPHITE T=HPG C [+0]

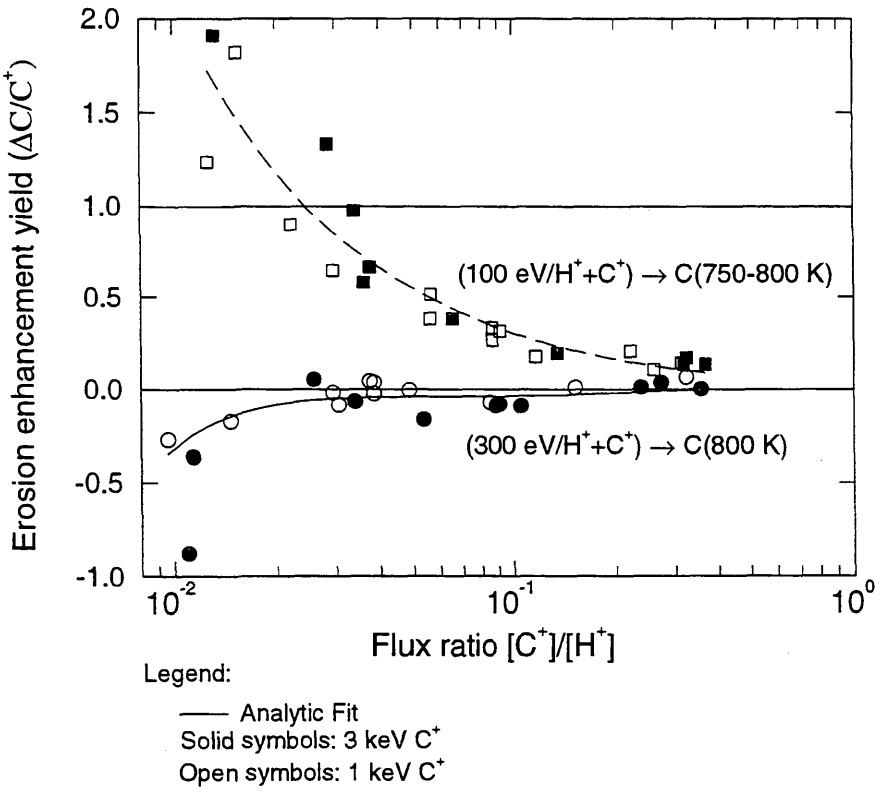

4.3.6.10 $[H^+, C^+]$ + pyrolytic graphite → C_xH_y, C

Source: A. A. Haasz and J. W. Davis, Nucl. Instr. Meth. Phys. Res. B **83**, 117 (1993).

Accuracy: Yield: Total ±20%; CH_4 ±15%, C_2H_2 ±30%; Flux ratio: ±30% (beam stability, beam profile overlap).

Comments: (1) Chemical erosion due to simultaneous bombardment by C^+ and H^+ ions.
(2) C^+ and H^+ ions produced by independent mass-selecting ion accelerators.
(3) Hydrocarbon products measured via QMS-RGA, steady-state.
(4) Specimens: graphite (pyrolytic, HPG99).
(5) Data is from Davis et al., J. Nucl. Mater. **196-198**, 681 (1992), corrected for wall signals.
(6) Yield for total chemical erosion, $Y_{chem-total} = [CH_4 + 2(C_2H_2 + C_2H_4 + C_2H_6) + 3(C_3H_6 + C_3H_8)]/H^+$.

Analytic fitting function:

Erosion yield:

$$Y = A_1 \exp(-A_2 F) F^{A_3} \quad [\text{molecules}/H^+]$$

where F is the flux ratio $[C^+]/[H^+]$. The rms deviation of analytic fits for reactions A (•), B (△) and C (□) are 7.5%, 6.5% and 12.2%, respectively.

Fitting parameters A_1-A_3

A	1.2368E-01	2.9129E+00	1.2211E-01
B	7.7014E-02	4.0336E+00	1.6702E-01
C	6.9762E-03	-1.3071E+00	6.8524E-02

ALADDIN evaluation function for erosion yield: EYIELD3A

ALADDIN hierarchical labelling:

A: SSATM H{3} [+1] C [+1] GRAPHITE T=HPG C [+0]
B: SSATM H{3} [+1] C [+1] GRAPHITE T=HPG CH{4} [+0]
C: SSATM H{3} [+1] C [+1] GRAPHITE T=HPG C{2}H{2} [+0]

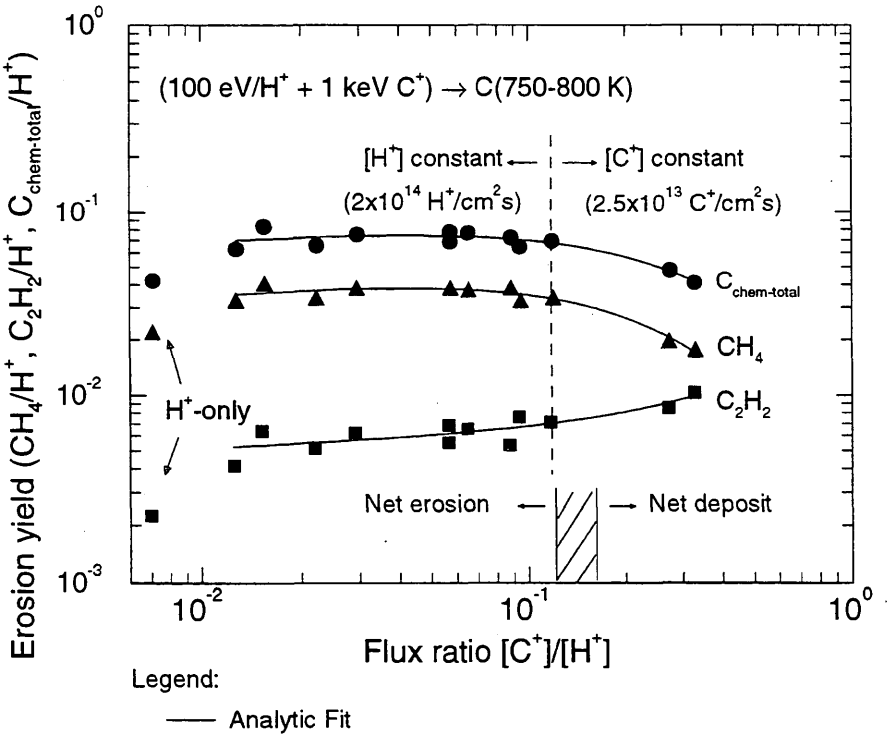

4.3.7.1 [H^+, O^+], O^+ + pyrolytic graphite → CO, CO_2

Source: A. A. Haasz, A. Y. K. Chen, J. W. Davis and E. Vietzke, J. Nucl. Mater. **248**, 19 (1997).

Accuracy: Yield: ±20%; T: ±25K.

Comments: (1) Erosion of graphite studied by simultaneous bombardment by 10 keV O_2^+ (5 keV/O^+) and 3 keV H_3^+ (1 keV/H^+).
(2) Specimen: pyrolytic graphite (HPG99).
(3) Incident ions were mass-analyzed.
(4) Reaction products measured by QMS-RGA.

Analytic fitting function:

Erosion yield:

$$Y = A_1 \exp(-(T - A_2)^2/A_3)T^{A_4} + A_5 \exp(-A_6 T)T^{A_7} \quad [\text{molecules}/O^+]$$

where T is in Kelvin. The rms deviation of analytic fits for reactions A (•), B (○), C (△), D (▽), E (□), F (◇) and G (∗) are 6.7%, 6.8%, 10.4%, 12.4%, 41.8%, 6.8% and 6.5%, respectively. Data for curves A and B were fitted with EYIELD5A, data for curve E with EYIELD8A.

Fitting parameters A_1-A_8

A	-1.3934e-03	4.6147e-04	1.2260e+00	2.7822e-02	7.4664e-01		
B	-2.6202e-04	6.4132e-04	1.4826e+00	1.3633e-02	8.3645e-01		
C	1.6535e+00	1.0730e+03	2.4676e+04	-5.7068e-01	1.0368e-07	5.5850e-03	2.7477e+00
D	2.0448e-01	1.1059e+03	5.4877e+04	-2.0094e-01	4.8851e-13	9.8580e-03	5.0344e+00
E	1.6739E-03	7.1837E+02	1.5007E+00	1.0938E-02	6.1701E-01	9.2253E-51	2.0986E-02
	1.9345E+01						
F	2.3998e-04	1.2298e+03	2.5824e+05	1.1427e+00	8.7277e-10	7.9090e-03	3.9809e+00
G	2.3493e-04	1.2776e+03	7.3725e+05	1.1309e+00	1.1085e-09	7.5870e-03	3.8771e+00

ALADDIN evaluation function for erosion yield: EYIELD5A, EYIELD7A, EYIELD8A

ALADDIN hierarchical labelling:

A: SATM O{2} [+1] GRAPHITE T=HPG99 CO [+0]
B: SSATM H{3} [+1] O{2} [+1] GRAPHITE T=HPG99 CO [+0]
C: SATM O{2} [+1] GRAPHITE T=HPG99 CO{2} [+0]
D: SSATM H{3} [+1] O{2} [+1] GRAPHITE T=HPG99 CO{2} [+0]
E: SSATM H{3} [+1] O{2} [+1] GRAPHITE T=HPG99 H{2}O [+0]
F: SATM O{2} [+1] GRAPHITE T=HPG99 O [+0]
G: SSATM H{3} [+1] O{2} [+1] GRAPHITE T=HPG99 O [+0]

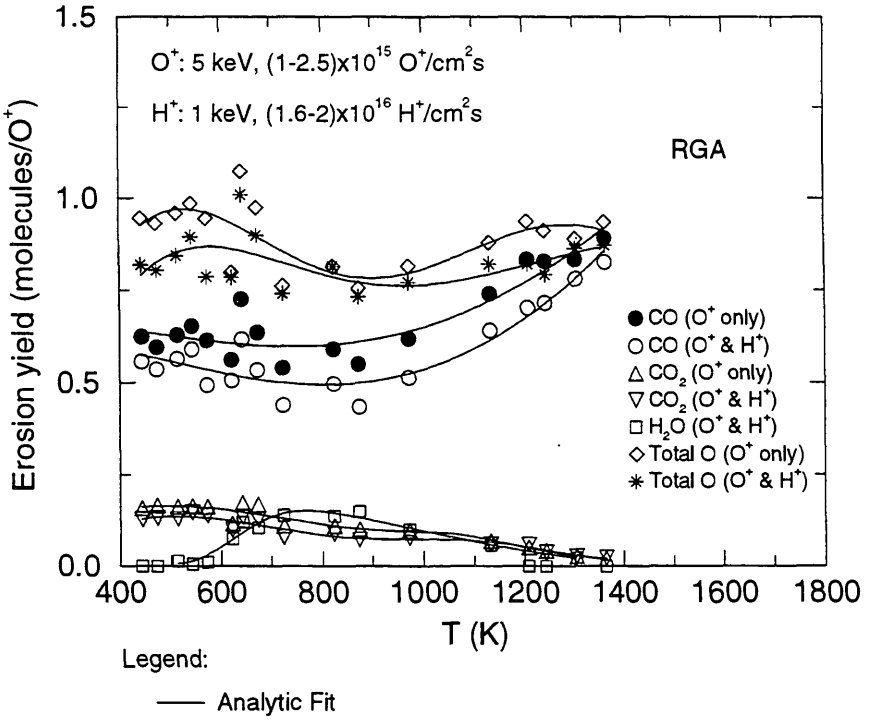

4.3.7.2 $[H^+, O^+]$, O^+ + pyrolytic graphite → CO, CO_2

Source: A. A. Haasz, A. Y. K. Chen, J. W. Davis and E. Vietzke, J. Nucl. Mater. **248**, 19 (1997).

Accuracy: Yield: ±20%; T: ±25K.

Comments: (1) Erosion of graphite studied by simultaneous bombardment by 10 keV O_2^+ (5 keV/O^+) and 3 keV H_3^+ (1 keV/H^+).
(2) Specimen: pyrolytic graphite (HPG99).
(3) Incident ions were mass-analyzed.
(4) Reaction products measured by LOS-QMS.
(5) Oxygen yields $(CO+2CO_2)/H^+$ greater than unity may be due to the non-thermal nature of the CO reaction products which is not taken into consideration in the analysis.

Analytic fitting function:

Erosion yield:

$$Y = A_1 \exp(-A_2 T) T^{A_3} + A_4 T^{A_5} \quad [\text{molecules}/O^+]$$

where T is in Kelvin. The rms deviation of analytic fits for reactions A (•), B (○), C (△), D (▽), E (□), F (◇) and G (∗) are 11.6%, 7.9%, 4.7%, 12.0%, 33.7%, 2.4% and 1.4%, respectively. Data for curves A and B were fitted with EYIELD7B, and data for curve E with EYIELD7A.

Fitting parameters A_1-A_7

A	2.4493e+01	7.7102e-01	9.8069e-01	1.6507e+03	3.3500e-02	-2.7337e+01	2.0000e-04
B	-2.9932E+01	4.4857E+00	-2.7145E+00	-1.4679E+03	-1.1893E-01	5.4947E+00	2.8416E-01
C	9.5560e-02	5.4056e-06	9.3389e-01	-9.5760e-02	9.3239e-01		
D	3.1696e-03	6.9545e-04	5.0164e-01	1.3471e-02	2.9005e-01		
E	1.8442E-01	8.1828E+02	3.9435E+04	6.8579E-01	1.9744E-06	3.2741E-04	2.0385E+00
F	1.1781e-03	-4.9569e-04	8.9065e-01	1.6573e+02	-9.7402e-01		
G	3.2446e-09	-1.2347e-02	4.3097e-01	5.5750e-02	4.3020e-01		

ALADDIN evaluation function for erosion yield: EYIELD5A, EYIELD7A, EYIELD7B

ALADDIN hierarchical labelling:

A: SATM O{2} [+1] GRAPHITE T=HPG99 CO [+0]
B: SSATM H{3} [+1] O{2} [+1] GRAPHITE T=HPG99 CO [+0]
C: SATM O{2} [+1] GRAPHITE T=HPG99 CO{2} [+0]
D: SSATM H{3} [+1] O{2} [+1] GRAPHITE T=HPG99 CO{2} [+0]
E: SSATM H{3} [+1] O{2} [+1] GRAPHITE T=HPG99 H{2}O [+0]
F: SATM O{2} [+1] GRAPHITE T=HPG99 O [+0]
G: SSATM H{3} [+1] O{2} [+1] GRAPHITE T=HPG99 O [+0]

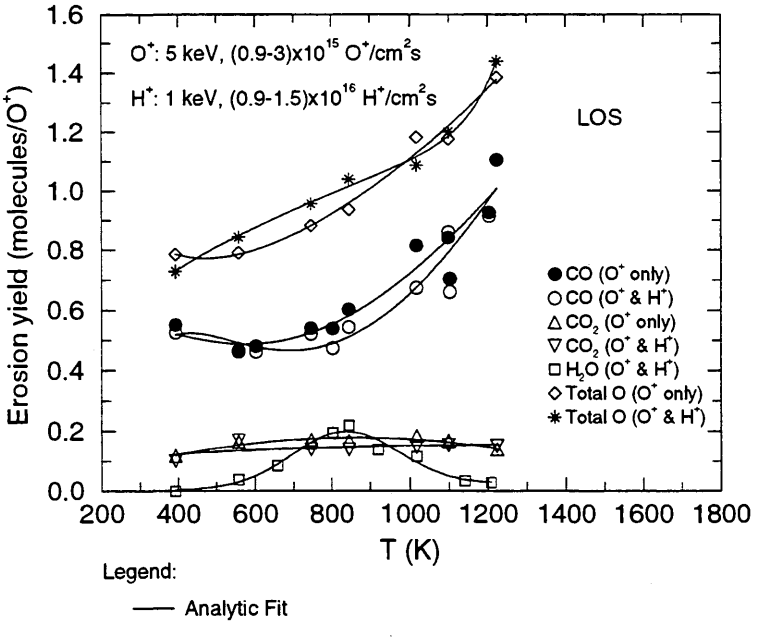

4.3.7.3 $[H^+, O^+]$, O^+ + pyrolytic graphite → CH_4

Source: A. A. Haasz, A. Y. K. Chen, J. W. Davis and E. Vietzke, J. Nucl. Mater. **248**, 19 (1997).

Accuracy: Yield: ±20%; T: ±25K.

Comments: (1) Erosion of graphite studied by simultaneous bombardment by 10 keV O_2^+ (5 keV/O^+) and 3 keV H_3^+ (1 keV/H^+).
(2) Specimen: pyrolytic graphite (HPG99).
(3) Incident ions were mass-analyzed.
(4) Reaction products measured by RGA.

Analytic fitting function:

Erosion yield:

$$Y = A_1 \exp(-(T - A_2)^2/A_3)T^{A_4} + A_5 \exp(-A_6 T)T^{A_7} \quad [CH_4/H^+]$$

where T is in Kelvin. The rms deviation of analytic fits for reactions A (•) and B (○) are 11.4% and 13.3%, respectively.

Fitting parameters A_1-A_7

A	7.1577E-06	8.0885E+02	1.6900E+04	2.0561E+00	2.3715E-02	-1.7428E-03	6.9927E-02
B	4.4111E-06	8.0744E+02	1.6320E+04	2.1179E+00	1.1805E-02	-1.7728E-03	1.6634E-01

ALADDIN evaluation function for erosion yield: EYIELD7A

ALADDIN hierarchical labelling:

A: SATM O{2} [+1] GRAPHITE T=HPG99 CH{4} [+0]
B: SSATM H{3} [+1] O{2} [+1] GRAPHITE T=HPG99 CH{4} [+0]

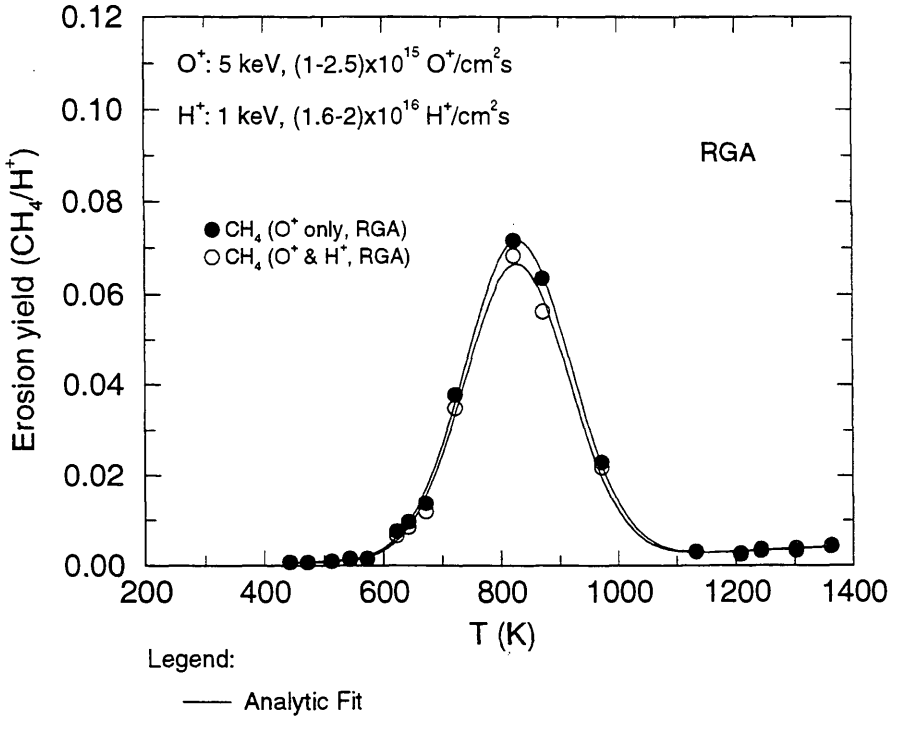

4.3.8.1 $[H^+, Ne^+]$ + pyrolytic graphite → C_xH_y, C

Source: A. A. Haasz and J. W. Davis, Nucl. Instr. Meth. Phys. Res. B **83**, 117 (1993).

Accuracy: Yield: Total ±20%; CH_4 ±15%, C_2H_2 ±30%; Flux ratio: ±30% (beam stability, beam profile overlap).

Comments: (1) Chemical erosion due to simultaneous bombardment by Ne^+ and H^+ ions.
(2) Ne^+ and H^+ ions produced by independent mass-selecting ion accelerators.
(3) Hydrocarbon products measured via QMS-RGA, steady-state.
(4) Specimens: graphite (pyrolytic, HPG99).
(5) Yield for total chemical erosion, $Y_{chem-total} = [CH_4 + 2(C_2H_2 + C_2H_4 + C_2H_6) + 3(C_3H_6 + C_3H_8)]/H^+$.

Analytic fitting function:

Erosion yield:

$$Y = A_1 \exp(-A_2 F) F^{A_3} \quad [\text{molecules}/H^+]$$

where F is the flux ratio $[Ne^+]/[H^+]$. The rms deviation of analytic fits for reactions A (•), B (△) and C (□) are 18.0%, 11.0% and 19.0%, respectively.

Fitting parameters A_1-A_3

A	8.5563E-02	2.1941E+00	1.2184E-01
B	5.2052E-02	2.7674E+00	1.5635E-01
C	1.2956E-02	-5.7153E-01	2.5339E-01

ALADDIN evaluation function for erosion yield: EYIELD3A

ALADDIN hierarchical labelling:

A: SSATM H{3} [+1] He [+1] GRAPHITE T=HPG C [+0]
B: SSATM H{3} [+1] He [+1] GRAPHITE T=HPG CH{4} [+0]
C: SSATM H{3} [+1] He [+1] GRAPHITE T=HPG C{2}H{2} [+0]

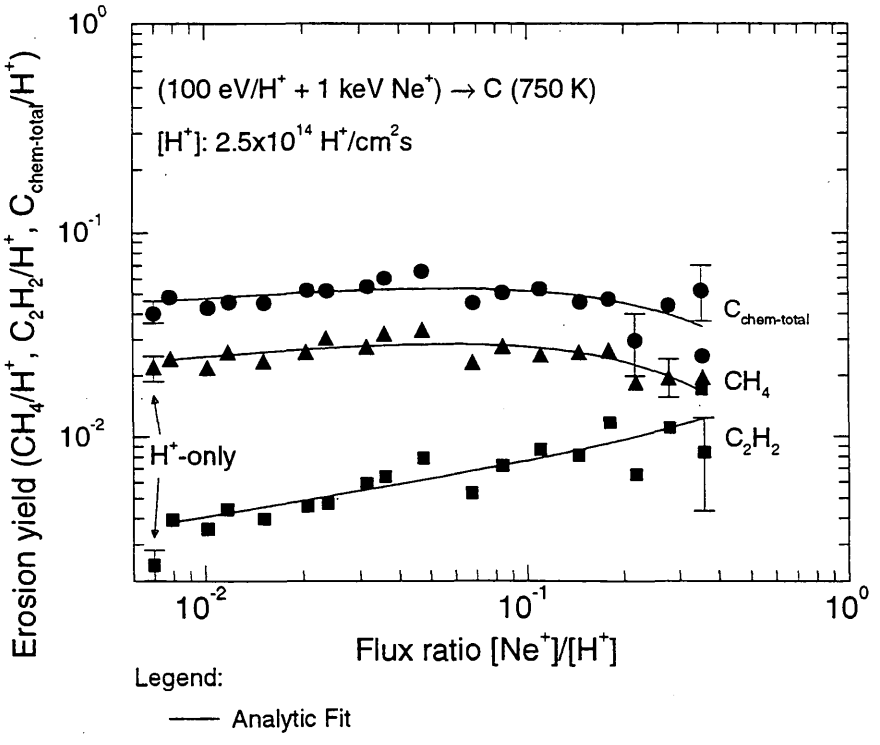

4.3.9.1 $[H^+, Ar^+]$ + pyrolytic graphite → C_xH_y, C

Source: A. A. Haasz and J. W. Davis, Nucl. Instr. Meth. Phys. Res. B **83**, 117 (1993).

Accuracy: Yield: Total ±20%; CH_4 ±15%, C_2H_2 ±30%; Flux ratio: ±30% (beam stability, beam profile overlap).

Comments: (1) Chemical erosion due to simultaneous bombardment by Ar^+ and H^+ ions.
(2) Ar^+ and H^+ ions produced by independent mass-selecting ion accelerators.
(3) Hydrocarbon products measured via QMS-RGA, steady-state.
(4) Specimens: graphite (pyrolytic, HPG99).
(5) Yield for total chemical erosion, $Y_{chem-total} = [CH_4 + 2(C_2H_2 + C_2H_4 + C_2H_6) + 3(C_3H_6 + C_3H_8)]/H^+$.

Analytic fitting function:

Erosion yield:

$$Y = A_1 \exp(-A_2 F) F^{A_3} \quad [\text{molecules}/H^+]$$

where F is the flux ratio $[Ar^+]/[H^+]$. The rms deviation of analytic fits for reactions A (•), B (△) and C (□) are 10.8%, 7.3% and 14.8%, respectively.

Fitting parameters A_1-A_3

A	5.9007E-02	1.5911E-03	5.3625E-02
B	3.2633E-02	8.1563E-01	6.9958E-02
C	1.2663E-02	-5.6274E-01	2.7360E-01

ALADDIN evaluation function for erosion yield: EYIELD3A

ALADDIN hierarchical labelling:

A: SSATM H{3} [+1] Ar [+1] GRAPHITE T=HPG C [+0]
B: SSATM H{3} [+1] Ar [+1] GRAPHITE T=HPG CH{4} [+0]
C: SSATM H{3} [+1] Ar [+1] GRAPHITE T=HPG C{2}H{2} [+0]

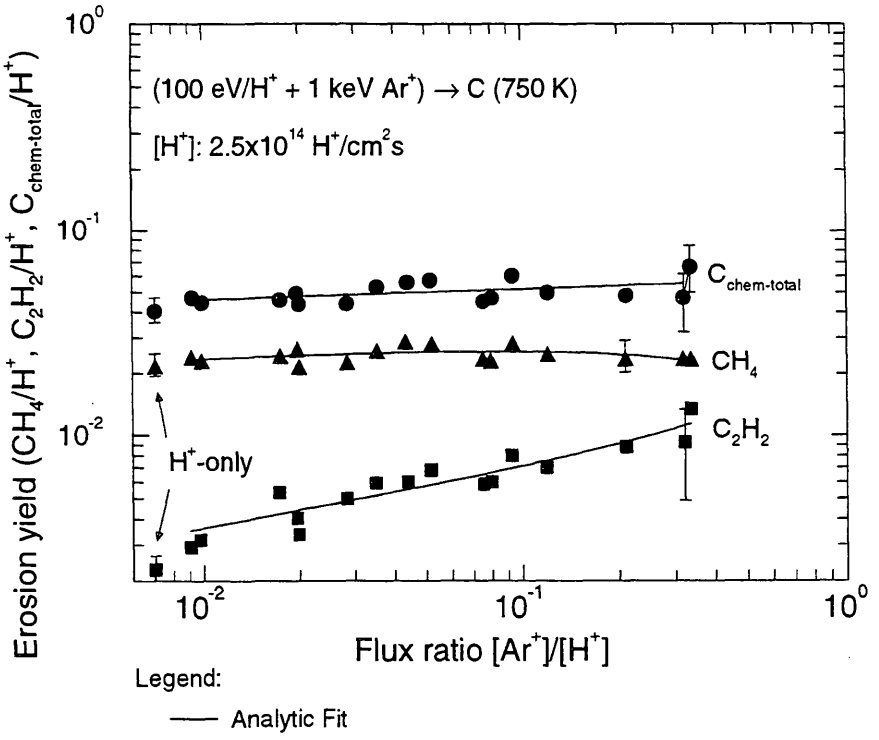

4.3.10.1 $[D^+, He^+]$ + pyrolytic graphite → CD_4

Source: S. Chiu, A. A. Haasz and P. Franzen, J. Nucl. Mater. **218**, 319 (1995).

Accuracy: Relative yield: < 10%; He^+ energy: ±10eV.

Comments: (1) Erosion yield reduction due to cobombardment with D^+ and He^+ ions; the greater the He^+ energy, the more effective it is at suppressing CD_4 formation.
(2) D^+ and He^+ ions produced by independent mass-selecting ion accelerators.
(3) Methane measured via QMS-RGA, steady-state.
(4) Specimens: graphite (pyrolytic, HPG99).

Analytic fitting function:

Reaction yield ratio:

$$Y_R = A_1 E + A_2$$

where Y_R is the yield ratio $(CD_4)_{He^+on}/(CD_4)_{He^+off}$, and E is the energy in keV. The rms deviations of analytic fits for reactions A (•), B (○), C (□), D (◇) and E (△) are 1.1%, 2.8%, 1.3%, 1.1% and 1.8%, respectively.

Fitting parameters A_1-A_2

A	-4.0263E-02	1.0590E+00
B	-5.5138E-02	1.0623E+00
C	-4.6750E-02	1.0094E+00
D	-5.5401E-02	8.9715E-01
E	-4.8043E-02	7.6749E-01

ALADDIN evaluation function for reaction yield ratio: EYIELD2A

ALADDIN hierarchical labelling:

A-D: SSATM D [+1] He [+1] GRAPHITE T=HPG CD{4} [+0]
E: SSATM D{+3} [+1] He [+1] GRAPHITE T=HPG CD{4} [+0]

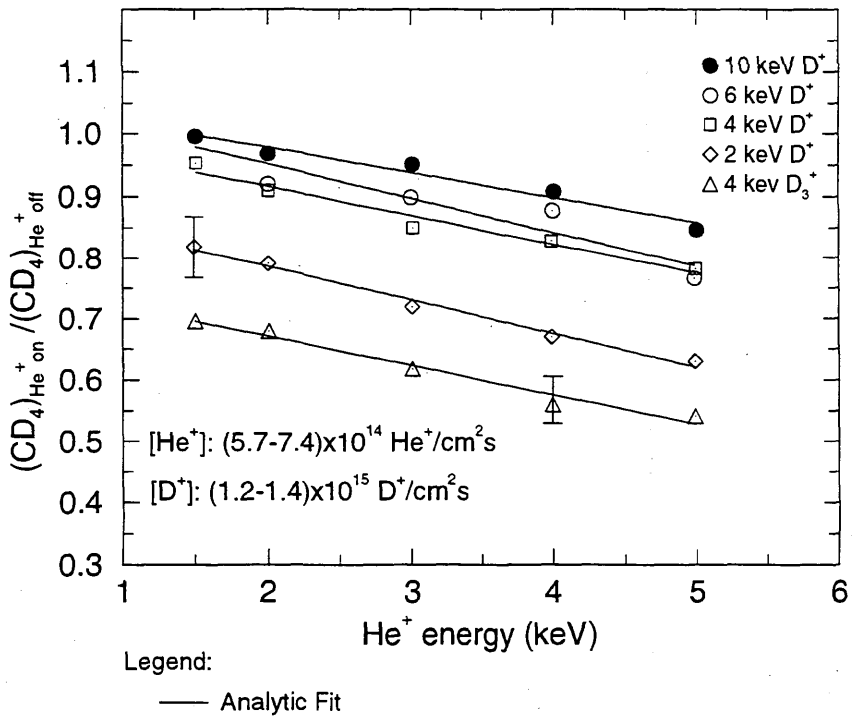

Sec4.1

4.4.1.1 O^0 + pyrolytic graphite → CO

Source: D. Rosner and H. D. Allendorf, *Heterogeneous Kinetics at Elevated Temperatures*, Proc. Int. Conf. Univ. Pennsylvania 1969, Plenum, New York (1970), p.231.

Accuracy: Indeterminate.

Comments: (1) Chemical erosion yield due to sub-eV O atoms.
(2) Specimen: graphite (pyrolytic).
(3) QMS measurement of CO, steady state.

Analytic fitting function:

Erosion yield:

$$Y = 1.0 \times 10^{-2}[A_1 \exp(-(T - A_2)^2/A_3)T^{A_4} + A_5 \exp(-A_6 T)T^{A_7}] \quad [\mathrm{CO/O^0}]$$

where T is in Kelvin. The rms deviation of the analytic fit is 5.9%.

Fitting parameters A_1-A_7

2.0155E-01	1.5027E+03	2.9820E+05	8.1204E-01	1.1780E+00	6.9676E-03
8.6177E-01					

ALADDIN evaluation function erosion yield: EYIELD7A

ALADDIN hierarchical labelling:

SATM O [+0] GRAPHITE T=HPG CO [+0]

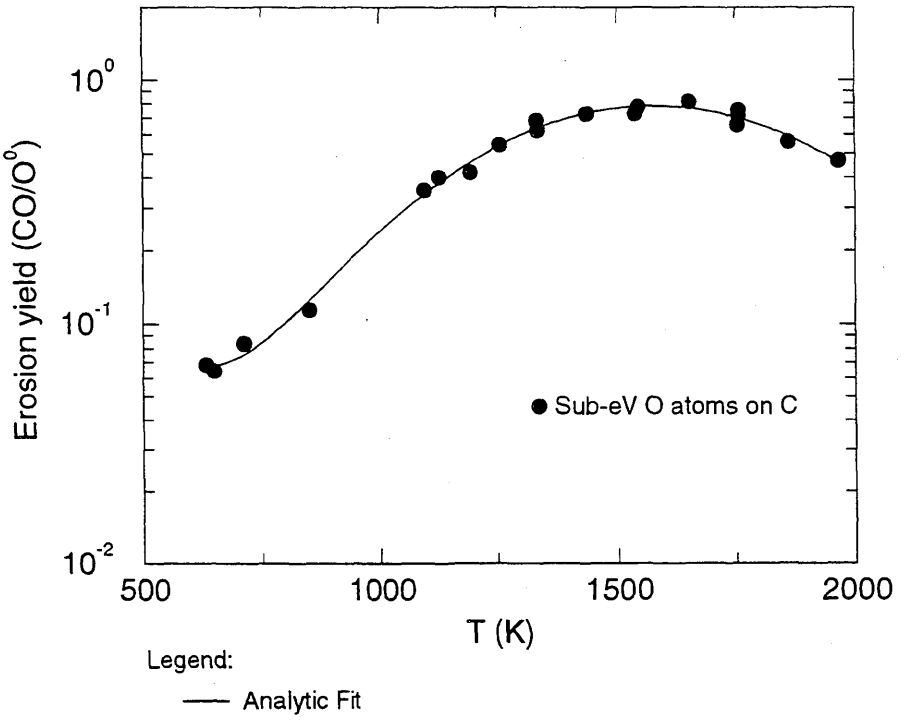

4.4.1.2 O_2 + pyrolytic graphite → CO, CO_2

Source: E. Vietzke, T. Tanabe, V. Philipps, M. Erdweg and K. Flaskamp, J. Nucl. Mater. **145-147**, 425 (1987).

Accuracy: Yield: 50%.

Comments: (1) Steady state CO, CO_2 formation by O_2 and O_2+Ar^+ impact.
(2) Specimen: graphite (pyrolytic).
(3) Reaction products detected by line-of-sight QMS.

Analytic fitting function:

Reaction yield:

$$Y = 1.0 \times 10^{-2}[A_1 \exp(-(T - A_2)^2/A_3)T^{A_4} + A_5 \exp(-A_6 T)T^{A_7}] \quad [\text{molecules}/O_2]$$

where T is in Kelvin. The rms deviation of analytic fits for reactions A (□), B (△) and C (dashed line) are 12.3%, 7.8% and 2.3%, respectively.

Fitting parameters A_1-A_7

A	1.1066E+00	1.3051E+03	1.2984E+05	-1.8433E-01	2.7526E+01	3.2561E-03
	-5.4860E-01					
B	7.8390E-02	-2.5219E+01	1.3765E+06	4.2311E-01	-3.5567E+00	2.9147E-03
	1.6899E-01					
C	1.8467E-02	8.3966E+01	6.4948E+04	2.0927E-01	9.5993E-04	-2.2619E-03
	3.2356E-06					

ALADDIN evaluation function for reaction yield: EYIELD7A

ALADDIN hierarchical labelling:

A: SSATM O{2} [+0] Ar [+1] GRAPHITE T=HPG CO [+0]
B: SATM O{2} [+0] GRAPHITE T=HPG O{2} [+0] CO [+0]
C: SSATM O{2} [+0] Ar [+1] GRAPHITE T=HPG CO{2} [+0]

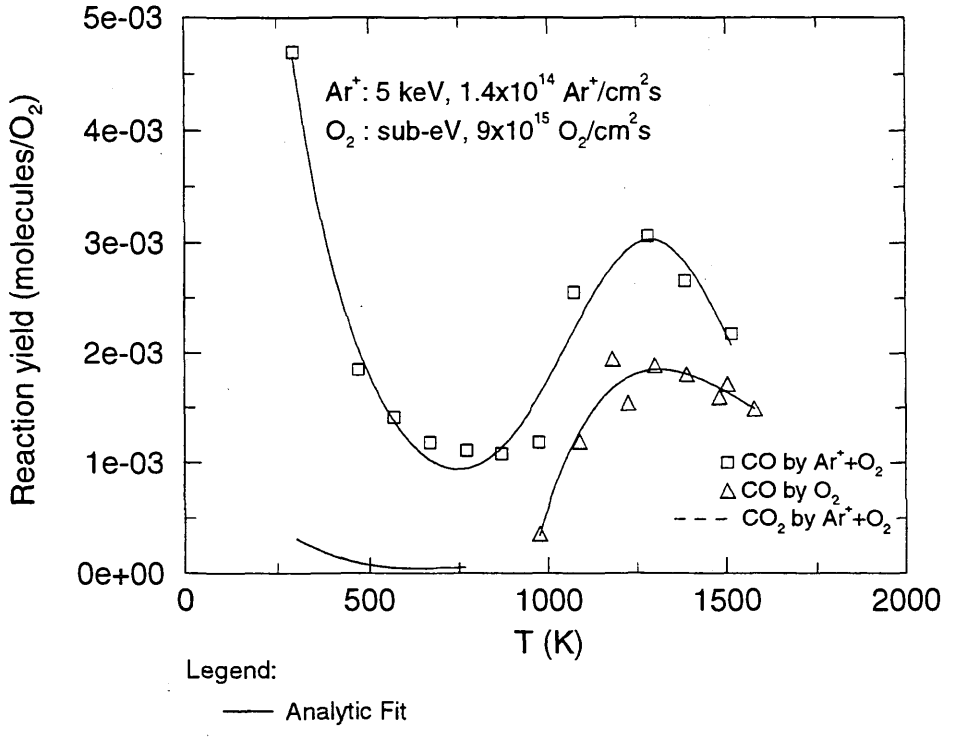

4.4.2.1 O^+ + pyrolytic graphite → C

Source: E. Hechtl and J. Bohdansky, J. Nucl. Mater. **122&123**, 1431 (1984).

Accuracy: Yield: ±10%.

Comments: (1) Weight loss measurement.
(2) Specimen: graphite (pyrolytic, with two orientations).
(3) The flux density of ions on the sample was $\sim 6 \times 10^{14}/\mathrm{cm}^2\mathrm{s}$.
(4) Mass analyzed beam.
(5) Physical sputtering by Ne^+ ions shown for comparison.

Analytic fitting function:

Sputtering yield:

$$Y = A_1 \exp(-A_2 E) E^{A_3} + A_4 E^{A_5} \quad \text{[atoms/ion]}$$

where the ion energy E is in eV. The rms deviation of analytic fits for reactions A (•, ○) and B (□) and C (△) are 6.8%, 0.6% and 2.4%, respectively.

Fitting parameters A_1-A_5

A	-1.0720E-01	2.2609E-03	4.0700E-01	2.0008E+00	-6.3843E-02
B	-1.3171E+00	3.8852E-04	-3.4015E-02	1.1447E+00	-1.0214E-03
C	-1.6848E-01	8.0928E-04	1.6596E-01	1.8816E-01	1.4322E-01

ALADDIN evaluation function for sputtering yield: EYIELD5A

ALADDIN hierarchical labelling:

A: SAT O [+1] GRAPHITE T=HPG O=PERP-PL C [+0]
B: SAT Ne [+1] GRAPHITE T=HPG O=PARA-PL C [+0]
C: SAT Ne [+1] GRAPHITE T=HPG O=PERP-PL C [+0]

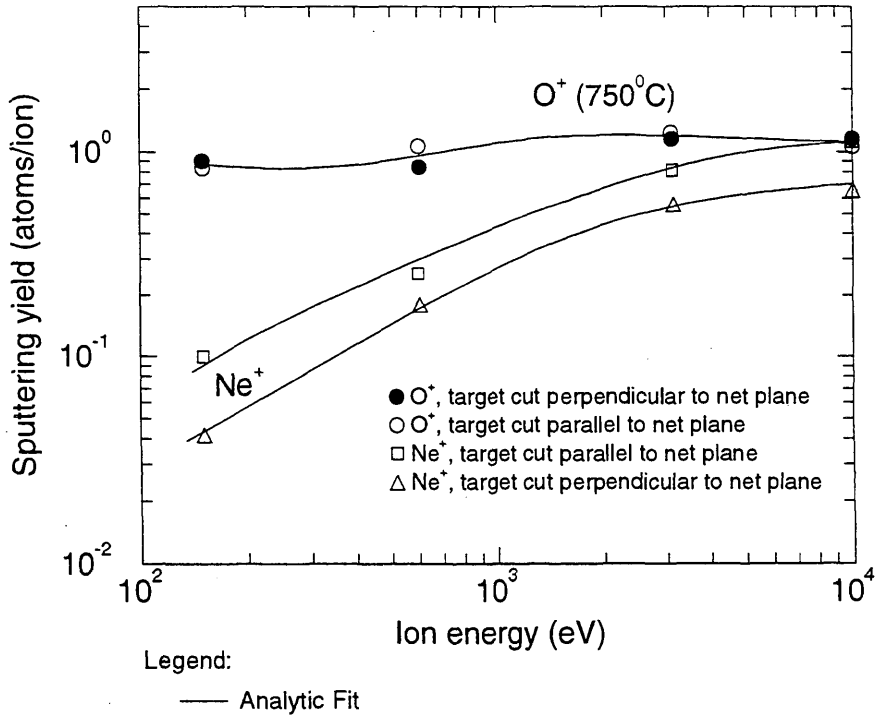

4.4.2.2 O^+ + pyrolytic graphite → CO, CO_2, C

Source: E. Vietzke, T. Tanabe, V. Philipps, M. Erdweg and K. Flaskamp, J. Nucl. Mater. **145-147**, 425 (1987).

Accuracy: Yield: ±10%.

Comments: (1) Reaction products, sputtered atoms detected by line-of-sight QMS.
(2) Specimen: graphite (pyrolytic).
(3) The flux density of ions on the sample was $\sim 10^{15}$ O^+/cm^2s.
(4) Mass analyzed beam.

Analytic fitting function:

Reaction yield:

$$Y = 1.0 \times 10^{-2}[A_1 \exp(-(T - A_2)^2/A_3)T^{A_4} + A_5 \exp(-A_6 T)T^{A_7}] \quad [\text{particles}/O^+]$$

where T is in Kelvin. The rms deviation of analytic fits for reactions A (dashed line), B (□), C (△) and CO_2 (•) are 0.7%, 1.8%, 2.2% and 0.9%, respectively.

Fitting parameters A_1-A_7

A	1.3468E+01	1.0846E+03	9.2273E+04	7.5575E-03	3.4485E+03	-1.1818E-03
	-6.5979E-01					
B	5.4342E+01	1.3578E+03	4.1224E+05	7.5902E-02	6.3949E-04	8.8353E-03
	2.4066E+00					
C	-1.6806E+01	1.2364E+03	2.7938E+04	-5.1266E-02	2.4481E+03	-1.2522E-03
	-7.3195E-01					
D	2.0337E+01	-4.1902E+03	6.3016E+06	6.8503E-01	-7.2484E+01	-2.4614E-07
	-1.6428E-01					

ALADDIN evaluation function for reaction yield: EYIELD7A

ALADDIN hierarchical labelling:

A: SAT O [+1] GRAPHITE T=HPG C [+0]
B: SATM O [+1] GRAPHITE T=HPG CO [+0]
C: SATM O [+1] GRAPHITE T=HPG C [+0]
D: SATM O [+1] GRAPHITE T=HPG CO{2} [+0]

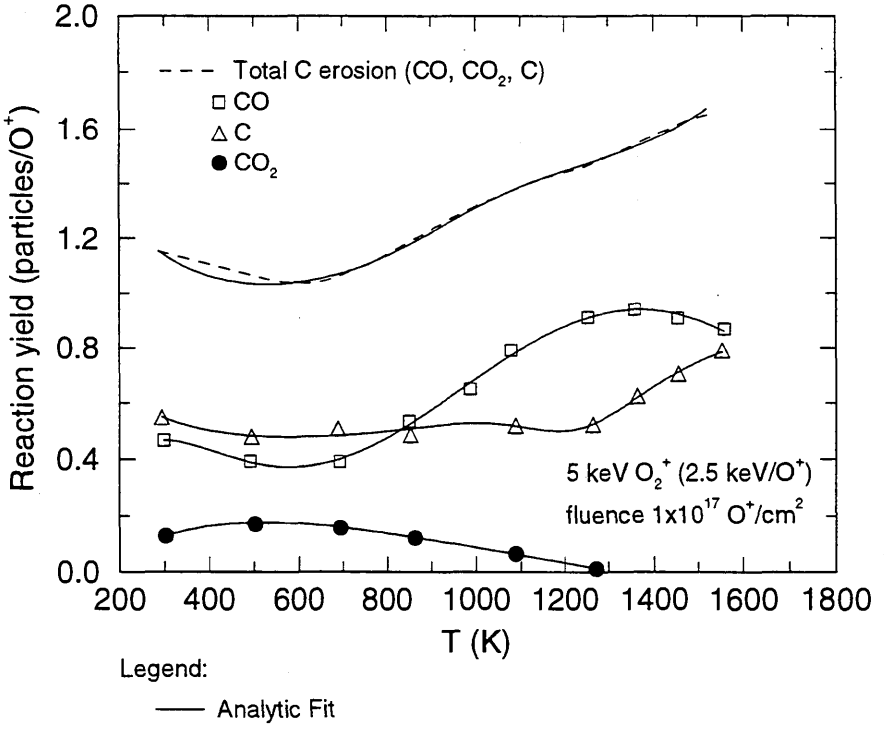

4.4.2.3 O_2^+ + pyrolytic graphite, $B_4C \rightarrow$ BO, CO

Source: E. Vietzke, A. Refke, V. Philipps and M. Hennes, J. Nucl. Mater. **220-222**, 249 (1995).

Accuracy: Energy distribution: Indeterminate.

Comments: (1) Energy distribution of BO, CO by time-of-flight.
(2) Specimen: graphite (pyrolytic), B_4C.
(3) O_2^+: mass selected ion beam.
(4) The CO curve were fitted to the original data by a combined Maxwell-Boltzmann and Thompson distribution function as in the source paper. The BO curve were fitted to the original data with a Thompson distribution alone.

Analytic fitting function:

Energy distributions:

$$CO: I = A_1 E \exp(-EA_2) + A_3 E/(E + A_4) \quad [\text{flux/eV}]$$

$$BO: I = A_1 E/(E + A_2) \quad [\text{flux/eV}]$$

where E is the kinetic energy in eV. The rms deviation of analytic fits for reactions A (solid curve) and B (dashed curve) are 8.5% and 5.5%, respectively. Original curves are not shown.

Fitting parameters A_1-A_4

A	8.9793E+02	3.7843E+01	3.1479E-01	3.4253E-01
B	5.4773E-01	2.7435E-01		

ALADDIN evaluation function for energy distributions: EMAXTHOM, ETHOM

ALADDIN hierarchical labelling:

A: SATM O{2} [+1] GRAPHITE T=HPG CO [+0]
B: SATM O{2} [+1] B{4}C [+0] BO [+0]

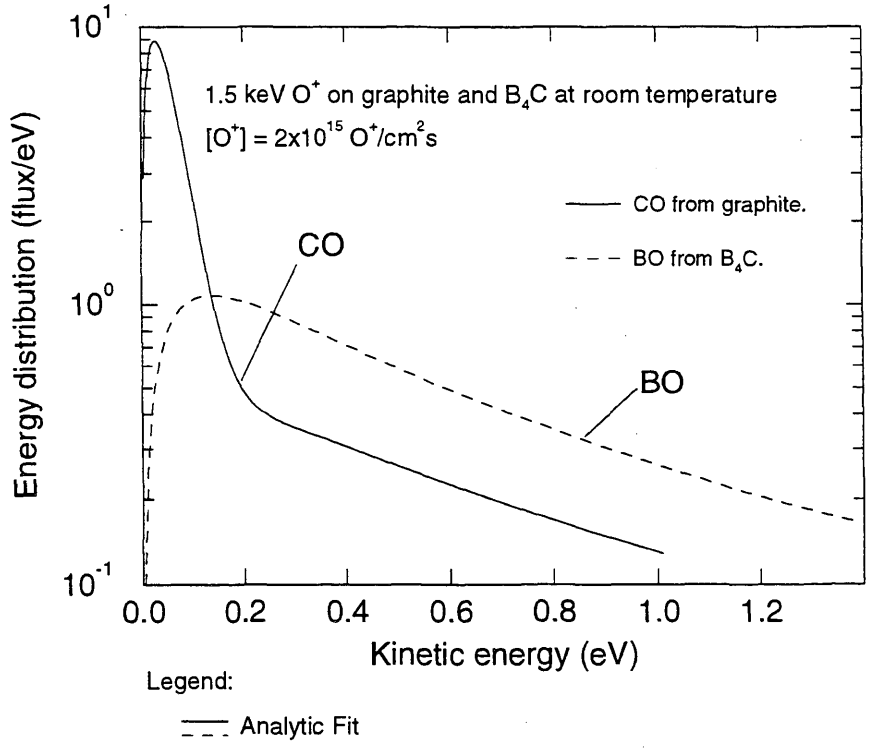

4.4.2.4 O_2^+ + pyrolytic graphite → CO, CO_2

Source: E. Vietzke, A. Refke, V. Philipps and M. Hennes, J. Nucl. Mater. **220-222**, 249 (1995).

Accuracy: Yield: 20%.

Comments: (1) CO, CO_2 steady state formation by O_2^+ impact.
(2) Specimen: graphite (pyrolytic).
(3) O_2^+ ion beam (mass selected).
(4) Reaction products detected by line-of-sight QMS.
(5) CO energy distribution have been taken into account.
(6) Earlier results were published in J. Nucl. Mater. **145-147**, 425 (1987).

Analytic fitting function:

Erosion yield:

$$Y = 1.0 \times 10^{-2}[A_1 \exp(-(T - A_2)^2/A_3)T^{A_4} + A_5 \exp(-A_6 T)T^{A_7}] \quad [\text{molecules/O}^+]$$

where T is in Kelvin. The rms deviation of analytic fits for reactions A (□), B (×) and C (∗) are 2.5%, 2.6% and 24.1%, respectively. Data for curve C was fitted with EYIELD8A.

Fitting parameters A_1-A_8

A	1.5960E-06	8.9049E+02	2.3242E+05	2.3500E+00	8.5583E+02	-6.4291E-04
	-4.9577E-01					
B	1.9685E-01	8.5525E+02	2.1477E+06	8.3084E-01	1.0639E+02	9.1503E-03
	2.8080E-01					
C	1.9772E-05	-1.6181E+07	-6.0262E-04	1.8676E+15	1.2373E+00	3.6740E-08
	5.4066E-03	2.8398E+00				

ALADDIN evaluation function for erosion yield: EYIELD7A, EYIELD8A

ALADDIN hierarchical labelling:

A: SATM O{2} [+1] GRAPHITE T=HPG C [+0]
B: SATM O{2} [+1] GRAPHITE T=HPG CO [+0]
C: SATM O{2} [+1] GRAPHITE T=HPG CO{2} [+0]

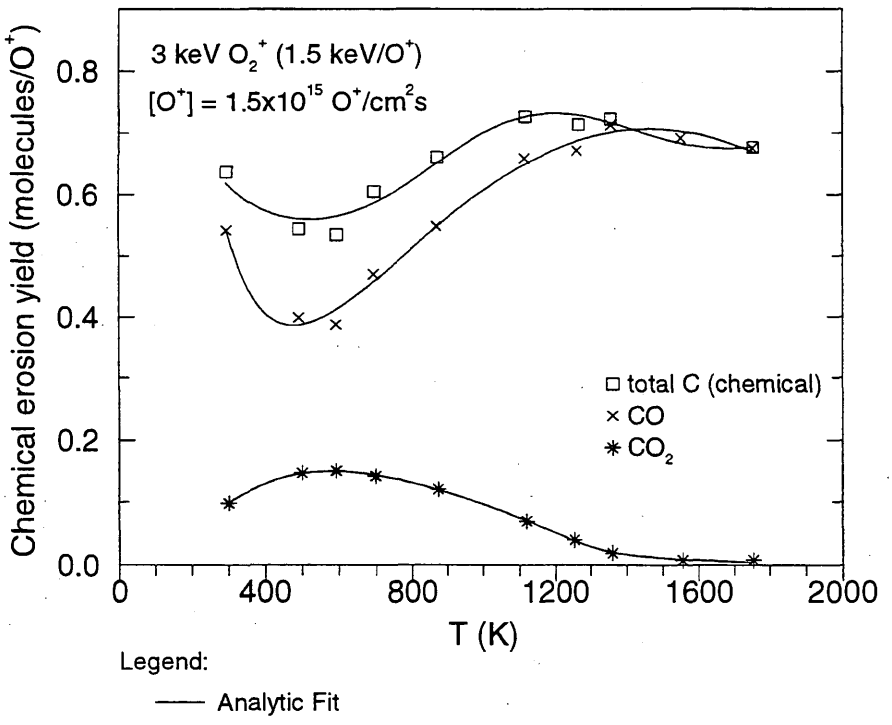

4.4.2.5 $O_2^+ + B_4C \rightarrow BO, CO, B_2O_2$

Source: E. Vietzke, A. Refke, V. Philipps and M. Hennes, J. Nucl. Mater. **220-222**, 249 (1995).

Accuracy: Yield: 20%.

Comments: (1) CO, BO, B_2O_2 steady state formation by O_2^+ impact.
(2) Specimen: B_4C.
(3) O_2^+: mass selected ion beam.
(4) Reaction products detected by line-of-sight QMS.
(5) CO, BO, B_2O_2 energy distributions have been taken into account.

Analytic fitting function:

Erosion yield:

$$Y = 1.0 \times 10^{-2}[A_1 \exp(-(T - A_2)^2/A_3)T^{A_4} + A_5 \exp(-A_6 T)T^{A_7}] \quad [\text{molecules}/O^+]$$

where T is in Kelvin. The rms deviation of analytic fits for reactions A (•), B (×), C (∗) and D (□) are 1.5%, 1.0%, 4.6% and 4.3%, respectively.

Fitting parameters A_1-A_7

A	6.5167E+00	1.5226E+03	7.7811E+04	1.9243E-01	1.4674E+02	-9.6274E-04
	-3.6503E-01					
B	5.9365E+00	1.5961E+03	5.7776E+04	1.5826E-01	2.1096E-01	1.2203E-03
	7.6787E-01					
C	3.0703E-18	1.4082E+03	1.4631E+05	5.9773E+00	2.0030E-02	1.5719E-03
	1.1120E+00					
D	1.6055E-01	1.2973E+03	2.7588E+04	5.1711E-01	3.6203E+01	-1.0355E-03
	-6.6648E-01					

ALADDIN evaluation function for erosion yield: EYIELD7A

ALADDIN hierarchical labelling:

A: SATM O{2} [+1] B{4}C [+0] C [+0] B [+0]
B: SATM O{2} [+1] B{4}C [+0] CO [+0]
C: SATM O{2} [+1] B{4}C [+0] BO [+0]
D: SATM O{2} [+1] B{4}C [+0] B{2}O{2} [+0]

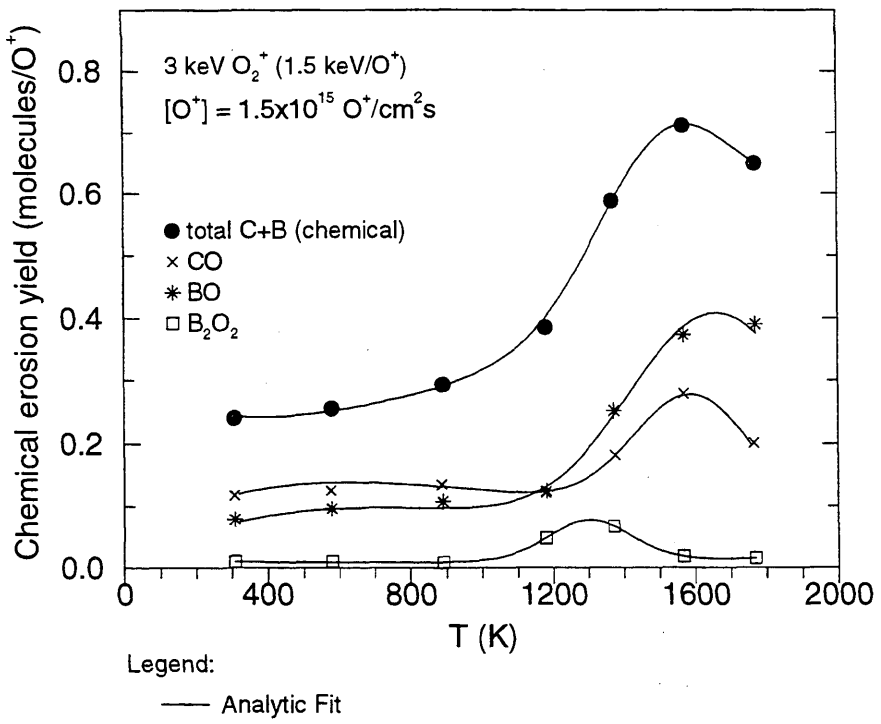

4.4.2.6 O_2^+ + SiC/C/Si → CO, CO_2, SiO, O, O_2

Source: A. Refke, V. Philipps, and E. Vietzke, J. Nucl. Mater. **241-243**, 1103 (1997).

Accuracy: Yield: 20%.

Comments: (1) Steady state formation or reemission by O_2^+ impact (mass selected ion beam).
(2) Specimen: SiC30 (Schunk Company). Composition: C/SiC/pure Si = 67/30/3 at.%.
(3) Reaction products detected by line-of-sight QMS.
(4) Thermal energy distribution assumed for all products except for Si and C.
(5) Si: only physical sputtering is assumed (0.16 Si/O^+) up to 1000 K; above 1000 K thermal evaporation is also included. This yield was not included in the original paper.

Analytic fitting function:

Reemission yield:

$$Y = A_1 \exp(-(T - A_2)^2/A_3)T^{A_4} + A_5 \exp(-A_6 T)T^{A_7} \quad [\text{molecules}/O^+]$$

where T is in Kelvin. The rms deviation of the analytic fits for reactions A (•), B (○), C (□), D (△), E (▽) and F (∗) are 4.6%, 5.9%, 2.6%, 1.4%, 2.0% and 5.0%, respectively. Data for curves A were fitted with EYIELD8A.

Fitting parameters A_1-A_8

A	8.1070e-03	6.9671e+02	7.9013e-04	6.6411e+04	1.0295e-01	1.2781e- 03	-5.4662e-04
	3.2822e-01						
B	1.6640E-03	1.4097E+03	1.5040E+05	2.2327E-01	2.2801E-05	1.4324E-03	
	9.9041E-01						
C	3.2479E-03	1.7241E+03	2.5640E+04	1.0858E+00	2.0859E-01	-2.0339E-0 4	-5.9859E-02
D	3.6630e-03	1.0016e+03	1.3663e+06	6.5695e-01	1.0734e-02	6.4530e- 03	8.3016e-01
E	4.9720e-02	7.1518e+02	2.2933e+05	-1.9185e-01	3.6520e-04	1.3213e- 03	7.7890e-01
F	2.7785E-03	1.4569E+03	1.4916E+05	4.4466E-01	3.0974E-02	-2.9179E-03	-4.8503E-01

ALADDIN evaluation function for reemission yield: EYIELD7A, EYIELD8A.

ALADDIN hierarchical labelling:

A: SAT O{2} [+1] GRAPHITE T=SiC30 O [+0]
B: SATM O{2} [+1] GRAPHITE T=SiC30 O{2} [+0]
C: SAT O{2} [+1] GRAPHITE T=SiC30 Si [+0]
D: SATM O{2} [+1] GRAPHITE T=SiC30 CO [+0]
E: SATM O{2} [+1] GRAPHITE T=SiC30 CO{2} [+0]
F: SATM O{2} [+1] GRAPHITE T=SiC30 SiO [+0]

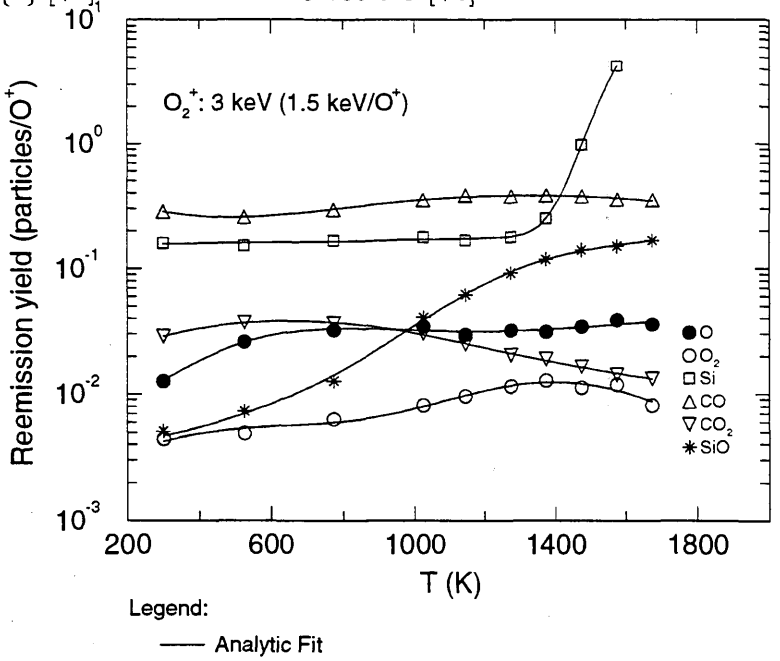

4.4.2.7 O_2^+ + a-Si/C:H → C, CO, CO_2, SiO, O, O_2

Source: A. Refke, V. Philipps, and E. Vietzke, J. Nucl. Mater. **241-243**, 1103 (1997).

Accuracy: Yield: 20%.

Comments: (1) Steady state formation or reemission by O_2^+ impact (mass selected ion beam).
(2) Specimen: a-Si/C:H film from TEXTOR.
(3) Reaction products detected by line-of-sight QMS.
(4) Thermal energy distribution assumed for all products except for Si and C.
(5) Si, C: physical sputtering is assumed up to 1000 K (E_B^{Si} = 4.7 eV; E_B^C = 7.4 eV); above 1000 K thermal emission is also included. These yields were not included in the original paper.

Analytic fitting function:

Reemission yield:

$$Y = A_1 \exp(-A_2 T) T^{A_3} + A_4 T^{A_5} \quad [\text{particles}/O^+]$$

where T is in Kelvin. The rms deviation of the analytic fits for reactions A (•), B (○), C (□), D (△), E (▽), F (∗) and G (+) are 4.7%, 1.5%, 6.7%, 19.7%, 2.8%, 9.3% and 18.6%, respectively.

Fitting parameters A_1-A_5

A	6.3188e-07	3.4836e-04	1.8467e+00	1.1929e+02	-1.1398e+00
B	2.5285e-06	2.5967e-03	1.6277e+00	3.8334e+00	-1.2062e+00
C	9.2092e-22	3.7979E-03	6.9062E+00	2.4099E-02	-3.5309E-01
D	8.2550e-02	-7.7669e-06	9.9635e-01	-7.8250e-02	1.0050e+00
E	9.6821e+02	-3.3334e-05	-4.8346e-01	-9.1221e+02	-4.7237e-01
F	-1.7374e+01	-7.0681e-05	-2.1191e-01	1.3997e+01	-1.6864e-01
G	1.5063e-138	4.2202E-02	5.1595E+01	8.0608E-03	-1.4252E-02

ALADDIN evaluation function for reemission yield: EYIELD5A

ALADDIN hierarchical labelling:

A: SAT O{2} [+1] GRAPHITE T=A-SiCH-FILM C [+0]
B: SAT O{2} [+1] GRAPHITE T=A-SiCH-FILM O [+0]
C: SATM O{2} [+1] GRAPHITE T=A-SiCH-FILM O{2} [+0]
D: SAT O{2} [+1] GRAPHITE T=A-SiCH-FILM Si [+0]
E: SATM O{2} [+1] GRAPHITE T=A-SiCH-FILM CO [+0]
F: SATM O{2} [+1] GRAPHITE T=A-SiCH-FILM CO{2} [+0]
G: SATM O{2} [+1] GRAPHITE T=A-SiCH-FILM SiO [+0]

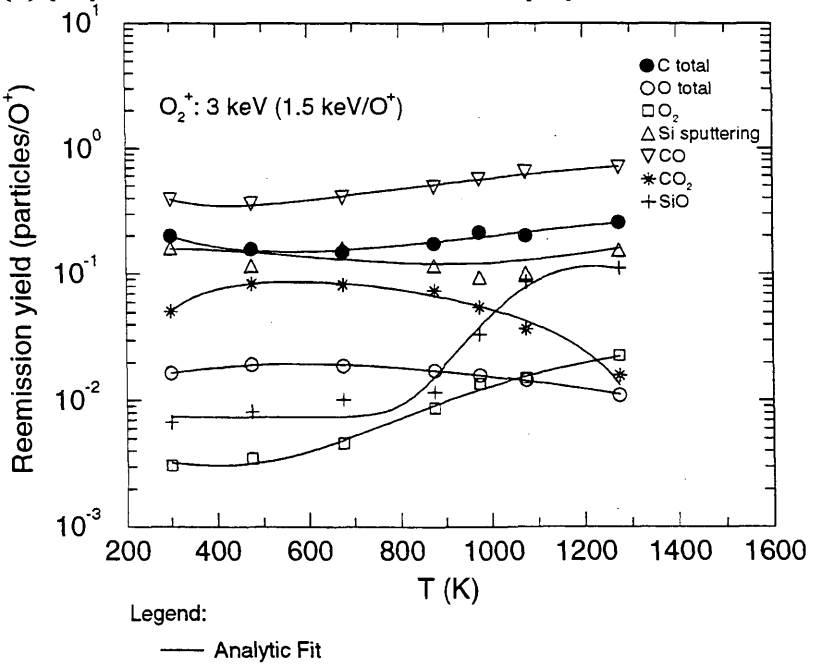

Appendix A: List of Abbreviations

Abbreviations used for experimental techniques:

AES - Auger electron spectroscopy
CVD - chemical vapor deposition
HREELS - high resolution electron energy loss spectroscopy
JET - Joint European Torus
LOS - line of sight detection
NRA - nuclear reaction analysis
PISCES - Plasma Interactive Surface Component Experimental Station
PVD - physical vapor deposition
RGA - residual gas analysis
TDS - thermal desorption spectroscopy
TEXTOR - Tokamak Experiment for Technology Oriented Research
TFTR - Tokamak Fusion Test Reactor
QMS - quadrupole mass spectrometer

Abbreviations used in graph labels:

C - generic erosion yield (physical sputtering, chemical erosion, or the sum of both)
$C_{sputt-total}$ - total erosion yield or sputtering yield (physical sputtering+chemical erosion)
$C_{chem-total}$ - total chemical erosion yield
C_{heavy} - chemical erosion yield for hydrocarbons heavier than CH_4
RT - room temperature
T - target temperature
T_m - target temperature at which erosion yield is a maximum
[A, B] - synergistic reaction involving particles A and B
[A] - incident flux density of species A (e.g. H^0/cm^2s, etc.) [A]/[B] - flux ratio of incident particles A and B
$[A_xB_y]$ - production rate of molecules A_xB_y (e.g. CH_4/cm^2s, etc.)

Abbreviations used for material descriptions and ALADDIN hierarchical labels:

AEROLOR - C/C composite, A05G
ALCAN - ALACAN C/C composite
A-CH-FILM - a-C:H (amorphous hydrogenated carbon film)
A-CB-FILM - a-C/B:H, (amorphous hydrogenated carbon film)
A-SiCH-FILM - a-Si/C:H plasma deposited amorphous film
ATJ - isotropic graphite, 4D C/C composite, Fiber Materials Incorporated (USA)
B{4}C - graphite, high-density material, 80% Boron
BASAL-PL - basal-plane orientation
BASE-PL - base-plane orientation
BASAL-PL-CL - basal-plane orientation, cleaved
BASAL-PL-MI - milled-plane orientation, milled
CC-COM - C/C composite
CC-COM-WE - C/C composite, weave
CC-COM-TOP - C/C composite, top cut
CC-COM-END - C/C composite, end cut
CFC - Carbon fiber composite
C-SiC - C-SiC coated graphite
CKC - Ceramics Kingston Ceramiques, Inc.
CLOR - 5829 graphite, Carbone Lorraine (France)
CVD-TiC - chemical vapor deposited TiC on a substrate
D - dopant material
DIAM-FILM - diamond film deposited on a substrate

DPE - boronized isotropic graphite, 0.5% Boron, UKAEA (United Kingdom)
EDGE-PL - edge-plane orientation
GB - boronized graphite, structure: As GB 100, Toyo Tanso (Japan)
GLASSYC-GC-30 - GC-30 glassy carbon
HPG - pyrolytic graphite, anisotropic, Union Carbide (USA)
HPG99 - polycrystalline pyrolytic graphite, Union Carbide (USA)
HPG-REDEP - pyrolytic graphite, redeposited carbon
HPG-PI - pyrolytic graphite, preirradiated
HPG-ISO - pyrolytic graphite, isotropic
GRAPHITE - graphite material, generic
MPG-8 - MPg-8 graphite
O - sample orientation
PAPYEX - compressed graphite tape
PARA-PL - parallel to reference plane
PERP-PL - perpendicular to reference plane
PGA - pyrolytic graphite, PG-A, Nippon Carbon (Japan)
POCO - low-impurity, high-density (low-porosity) isotropic graphite
POCO-AXF5Q - POCO graphite (product number AXF5Q)
PFG - pyrolytic graphite, Pfizer (USA)
PYG - pyrolytic graphite, generic
PRISM-PL - prism-plane orientation
PRISM-PL-CL - prism-plane orientation, cleaved
PRISM-PL-MI - prism-plane orientation, milled
PVD-TiC - physical vapor deposited TiC on a substrate
RG-Ti - Recrystallized graphite containing 1.7 at%Ti
SATM - sputtering by atoms leading to molecule emission (chemical erosion)
SSATM - synergistic sputtering by atoms leading to molecule emission (chemical erosion)
SAT - sputtering by atoms leading to molecule and atom emission (physical + chemical erosion)
SEP-CFC - carbon fiber composite, SEP (France)
S2508 - anisotropic graphite, 3% Boron, Carbone Lorraine (France)
SiC30 - bulk Si doped graphite
T - material type
TFTR-REDEP - TFTR redeposited graphite
TiC - titanium carbide, bulk
USB - boronized isotropic graphite, NII Grafit (Russia)

Appendix B: List of Analytic Fitting Functions

The following analytic functions are used to represent chemical erosion data as functions of the variable X. In this work X may represent target temperature, incident particle kinetic energy, or incident particle flux (or flux ratio). The function names EYIELD2A, EYIELD2B, etc., refer to the relevant ALADDIN evaluation function.

$$Y = A_1 X + A_2 \qquad \text{[EYIELD2A]}$$

$$Y = A_1 \exp(A_2 X) \qquad \text{[EYIELD2B]}$$

$$Y = A_1 X^{A_2} \qquad \text{[EYIELD2C]}$$

$$Y = A_1 \exp(-A_2 X) X^{A_3} \qquad \text{[EYIELD3A]}$$

$$Y = A_1 \exp(-A_2 X) X^{A_3} + A_4 X \qquad \text{[EYIELD4A]}$$

$$Y = A_1 \exp(-(X - A_2)^2 / A_3) X^{A_4} \qquad \text{[EYIELD4B]}$$

$$Y = A_1 (\log X)^3 + A_2 (\log X - A_3)^2 + A_4 \qquad \text{[EYIELD4C]}$$

$$Y = A_1 \exp(-A_2/X)/(1 + A_3 \exp(-A_4/X)) \qquad \text{[EYIELD4D]}$$

$$Y = A_1 \exp(-A_2 X) X^{A_3} + A_4 X^{A_5} \qquad \text{[EYIELD5A]}$$

$$Y = A_1 \exp(-(X - A_2)^2 / A_3) X^{A_4} + A_5 \exp(-A_6 X) X^{A_7} \qquad \text{[EYIELD7A]}$$

$$Y = A_1 \exp(-A_2 X/(A_3 X + A_4)) X^{A_5} + A_6 \exp(-A_7 X) \qquad \text{[EYIELD7B]}$$

$$Y = A_1 \exp(-\left(\tfrac{X - A_2}{A_3 X + 1}\right)^2 / A_4) X^{A_5} + A_6 \exp(-A_7 X) X^{A_8} \qquad \text{[EYIELD8A]}$$

$$Y = A_1 \exp(-(X - A_2)^2 / A_3) X^{A_4} + A_5 \exp(-A_6 X/(A_7 X + 1)) X^{A_8} \qquad \text{[EYIELD8B]}$$

$$Y = A_1 \exp(-(X - A_2)^2 / A_3) X^{A_4} + A_5 \exp(-A_6 X) X^{A_7} (1 + A_8 X^{A_9}) \qquad \text{[EYIELD9A]}$$

$$Y = A_1 X \exp(-X A_2) + A_3 X/(X + A_4) \qquad \text{[EMAXTHOM]}$$

$$Y = A_1 X/(X + A_2) \qquad \text{[ETHOM]}$$

Acknowledgements

We wish to acknowledge contributions from several people who aided in the preparation and support of this data compendium project. Dr. Igor Komarov, Dr. Yuri Ralchenko and Dr. Dahai Wang performed a substantial number of analytic fits of the data presented in Section 4. Dr. Wang also numerically digitized a large amount of data from collected experimental papers. Professor Ratko Janev suggested this project, and provided important guidance throughout the course of the work. His critical remarks on the final manuscript are also gratefully acknowledged.

Contents of previous volumes of Atomic and Plasma–Material Interaction Data for Fusion

Volume 1 (1991)

Volume 2 (1992)

Volume 3 (1992)

Volume 4 (1993)

Volume 5 (1994)

Volume 6 (1995)

INFORMATION FOR AUTHORS

General

Atomic and Plasma-Material Interaction Data for Fusion (APMIDF) publishes papers, letters and reviews which deal with elementary atomic collision processes in fusion plasmas, collision processes of plasma particles with surfaces and plasma-material interaction phenomena, including the thermophysical and thermomechanical response of candidate fusion reactor plasma facing materials. Each contribution submitted to APMIDF should be highly fusion relevant and should contain a significant amount of quantitative data information in one of the above fields. Review articles are normally prepared on the invitation by the Editor or with his prior consent. APMIDF is a regular IAEA publication and its abbreviation for the purpose of referencing is: At. Plasma-Mater. Interact. Data Fusion.

Manuscripts, which may be submitted in Chinese, English, French, Russian or Spanish, will be published in English. For a manuscript submitted in a language other than English, a translation into English of technical terms should be provided. Manuscripts must be submitted in triplicate and typewritten double spaced on good quality standard size paper. All copies should include the main text, an abstract, tables, references, figures, captions and appendices, as appropriate. One set of glossy prints or reproducible transparencies of the figures should also be provided. *Final manuscript versions may be submitted in camera ready form or on diskettes.*

Every manuscript submitted must be accompanied by a disclaimer stating that the paper has not been published and is not being considered for publication elsewhere. If no copyright is claimed by the authors, the IAEA automatically owns the copyright of the paper.

Authors will receive proofs of the text of accepted manuscripts. Proofs of figures are sent only if requested. Rejected manuscripts will not be returned unless this is expressly requested within six weeks of rejection.

Manuscripts and correspondence should be addressed to: The Editor, ATOMIC AND PLASMA-MATERIAL INTERACTION DATA FOR FUSION, International Atomic Energy Agency, Wagramer Strasse 5, P.O. Box 100, A-1400 Vienna, Austria.

Manuscript preparation

Authors are referred to any recent issues of APMIDF or the IAEA journal NUCLEAR FUSION (NF) for examples of *format* and *style*.

All submitted articles should be *concise* and written in a *clear style*. The description of the methods used for obtaining the presented original data information should be kept to a reasonable minimum. The review papers should provide a critical analysis of a broader class (or classes) of data or processes together with a set of recommended data of specified accuracy.

Titles should be as concise as possible but sufficiently informative to describe the subject of the paper.

Abstracts must briefly summarize the contents of the article. They should state the principal objectives, mention the methodology employed, summarize the results (emphasizing the new findings) and present the main conclusions. They should be concise and self-contained so that they can be used by the International Nuclear Information System (INIS) and other abstracting systems without changes. General, well known information should be avoided in the abstract and accommodated in the introduction.

Letters to APMIDF are short communications of net sets of data obtained with a standard, highly accurate method. As a rule, they should be not longer than ten typewritten double spaced standard pages, including references and figures.

Guidelines for *bibliographical citations* can be found in issues 2, 3 and 4 of NF **28** (1988). In short, references should be accurately described in sufficient detail for easy identification. In the text, they should be indicated consecutively by Arabic numerals in square brackets. All references should be listed on a separate page at the end of the text. In this list, the names of all authors (or, if there are more than six, of the first three authors plus 'et al.') should be given. All unpublished material, e.g. laboratory reports, doctoral theses or papers in proceedings that have not yet been published, should be cited with full titles, place and year; citations of reports should also contain the laboratory prefix and number, date of issue, etc. References to periodicals should contain the name of the journal, volume number, page number and year of publication; the title of the article is not needed. References to books should contain the full title of the book, names of editors (if any), name and location of the publisher, year of publication and page number (if appropriate). References to personal communications should be avoided if possible. For journal citations use the list of abbreviations given in "IAEA-INIS-11, INIS: Authority List for Journal Titles". Russian names should be transliterated according to "IAEA-INIS-10, INIS: Transliteration Rules for Selected Non-Roman Characters". Examples of the style for references are:

REFERENCES

[1] SHAH, M.B., GILBODY, H.B., J. Phys., B (Lond.). At. Mol. Phys. **14** (1981) 2361.

[2] WILSON, K.L., BASTASZ, R.A., CAUSEY, R.A., et al., At. Plasma-Mater. Interact. Data Fusion **1** (1991) 31.

[3] BRANSDEN, B.H., Atomic Collision Theory, 2nd edn., Benjamin, New York (1982).

[4] MÄRK, T.D., DUNN, G.H. (Eds), Electron Impact Ionization, Springer-Verlag, Berlin, Heidelberg, New York, London (1985).

[5] MÖLLER, W., ROTH, J., in Physics of Plasma-Wall Interactions in Controlled Fusion (POST, D.E., BEHRISCH, R., Eds), Plenum Press, New York (1986) 45.

[6] McGRATH, R.T., Thermal Loads on Tokamak Plasma Facing Components During Normal Operation and Disruptions, Rep. SAND89-2064, Sandia National Laboratories, Albuquerque, NM (1990).

[7] TRUBNIKOV, B.A., in Problems of Plasma Theory, Vol. 1 (LEONTOVICH, M.A., Ed.), Gosatomizdat, Moscow (1963) 98 (in Russian). (English translation: Reviews of Plasma Physics, Vol. 1, Consultants Bureau, New York (1965) 105.)

[8] HUBER, B.A., Zum Elektronentransfer zwischen mehrfach geladenen Ionen und Atomen oder Molekülen, PhD Thesis, Ruhr-Universität, Bochum (1981).

[9] de HEER, F.J., HOEKSTRA, R., KINGSTON, A.E., SUMMERS, H.P., Excitation of neutral helium by electron impact, to be published in At. Plasma-Mater. Interact. Data Fusion.

[10] MOORES, D.L., Electron impact ionisation of Be and B atoms and ions, submitted to At. Plasma-Mater. Interact. Data Fusion.

All figures should be on separate sheets and numbered consecutively with Arabic numerals, e.g. Fig. 1. A separate list of captions must be provided (see also *General* above).

Tables must carry a heading and be numbered consecutively with Roman numerals in the order in which they are mentioned in the text, e.g. Table II. Footnotes to tables should be indicated by raised letters (not numbers or asterisks) and set immediately below the table itself. Tables should be typed clearly for possible direct reproduction.

Footnotes to the text should be numbered consecutively with raised Arabic numerals; excessive use of footnotes should be avoided.

All *equations* should be typed as carefully as possible, with unavailable Greek letters and other symbols clearly inserted by hand. Specifically:

(1) To eliminate confusion between symbols with similar appearance (e.g. between ones, ells and primes), make them as distinct as possible, if necessary marking them clearly by hand. In manuscripts with handwritten formulas, all further sources of confusion (such as n's and u's, u's and v's, c's and l's, J's and I's) should also be marked.

(2) Indicate a vector by an arrow on top rather than by bold face lettering.

(3) Tensors of second rank should bear two arrows on top; if higher rank tensors are required, choose an appropriate symbol and explain it.

(4) Indicate the normal algebraic product by simple juxtaposition of symbols, i.e. without multiplication sign.

(5) Write scalar products of vectors with a raised point, e.g. $\vec{A} \cdot \vec{B}$.

(6) Use the multiplication sign ($\times$) solely to designate: (i) a vector product, (ii) an algebraic (but not a scalar) product in the case where an equation has to be split over two lines, and (iii) in expressions like 3 cm $\times$ 3 cm or 2 $\times$ 10^6 cm.

(7) The nabla operator (∇) does not carry an arrow.

(8) When equations are split over two or more lines, place operational signs only at the beginning of each new line, not at the end of the preceding line. For direct reproduction of an equation, the length of the lines should not exceed 9 cm.

(9) Where it is impossible to split long fractions over two lines, use negative exponents: similarly, replace root signs by fractional exponents where appropriate.

(10) Do not use symbols, abbreviations and formulations that are recognizable only in a particular language.

Use *SI units* as far as possible; where this is not possible, please give the appropriate conversion factor.